ELSEVIER

World Journal of Gastroenterology®

Supported by NSFC 2005-2006

Volume 11 Number 15
April 21, 2005

National Journal Award 2005

Contents

World Journal of Gastroenterology®
Volume 11 **Number** 15 **April** 21, 2005

Contents

World Journal of Gastroenterology®
Volume 11 **Number** 15 **April** 21, 2005

Contents

Editorial Coordinator for this issue: Anitha Kumaran

World Journal of Gastroenterology (*World J Gastroenterol , WJG*), a leading international journal in gastroenterology and hepatology, has an established reputation for publishing first class research on esophageal cancer, gastric cancer, liver cancer, viral hepatitis, colorectal cancer, and *Helicobacter pylori* infection, providing a forum for both clinicians and scientists, and has been indexed and abstracted in Index Medicus, MEDLINE, PubMed, Chemical Abstracts, EMBASE, Abstracts Journals, Nature Clinical Practice Gastroenterology and Hepatology, CAB Abstracts and Global Health. Impact factor of ISI JCR during 2000-2003 is 0.993, 1.445, 2.532 and 3.318 respectively. *WJG* is a weekly journal published jointly by The *WJG* Press and Elsevier Inc. The publication date is on 7th, 14th, 21st, and 28th every month. The *WJG* is supported by The National Natural Science Foundation of China, No. 30224801 and No.30424812, which was founded with a name of *China National Journal of New Gastroenterology* on October 1,1995, and renamed as *WJG* on January 25, 1998.

PUBLISHED JOINTLY BY
The WJG Press and Elsevier Inc

PRINTING GROUP
Printed in Beijing on acid-free paper by Beijing Kexin Printing House

 Print ISSN 1007-9327
CN 14-1219/R.

SPECIAL STATEMENT
All articles published in this journal represent the viewpoints of the authors except where indicated otherwise.

EDITORIAL OFFICE
Editor: *World Journal of Gastroenterology*,
The WJG Press, Apartment 1066 Yishou Garden, 58 North Langxinzhuang Road, PO Box 2345, Beijing 100023, China
Telephone: +86-(0)10-85381901-1023
Fax:+86-10-85381893
E-mail: wjg@wjgnet.com
http://www.wjgnet.com

Public Relationship Manager
Shi-Yu Guo
The WJG Press, Apartment 1066 Yishou Garden, 58 North Langxinzhuang Road, PO Box 2345, Beijing 100023, China
Telephone: +86-(0)10-85381901-1023
Fax: +86-10-8538 1893
E-mail: s.y.guo@wjgnet.com
http://www.wjgnet.com

SUBSCRIPTION INFORMATION
Foreign
Elsevier (Singapore) Pte Ltd, 3 Killiney Road #08-01, Winsland House I, Singapore 239519
Telephone: +65-6349 0200
Fax: +65-6733 1817
E-mail: r.garcia@elsevier.com
http://asia.elsevierhealth.com
Institutional Rates Print-2005 rates: USD1 500.00
Personal Rates Print-2005 rates: USD700.00

Domestic
Local Post Offices Code No. BM 82-261

Author Reprints and Commercial Reprints
The WJG Press, Apartment 1066 Yishou Garden, 58 North Langxinzhuang Road, PO Box 2345, Beijing 100023, China
Telephone: +86-(0)10-85381901-1023
Fax:+86-10-85381893
E-mail: wjg@wjgnet.com
http://www.wjgnet.com

ADVERTISING
Rosalia Da Carcia
Elsevier Science
Journals Marketing & Society Relations Health Science Asia
3 Killiney Road #08-01, Winsland House 1
Singapore 239519
Telephone: +65-6349 0200
Fax +65- 6733 1817
E-mail: r.garcia@elsevier.com
http://asia.elsevierhealth.com

INSTRUCTIONS TO AUTHORS
Full instructions are available online at http://www.wjgnet.com/wjg/help/instructions.jsp If you do not have web access please contact the editorial office.

World Journal of Gastroenterology®

Editorial Board

2004-2006

Published by The WJG Press and Elsevier Inc., PO Box 2345, Beijing 100023, China
Fax: +86-(0)10-85381893 E-mail: wjg@wjgnet.com http://www.wjgnet.com

Bulgaria
Zahariy Alexandrov Krastev, *Sofia*

Canada
Wang-Xue Chen, *Ottawa*
Richard N Fedorak, *Edmonton*
Hugh James Freeman, *Vancouver*
Samuel S Lee, *Calgary*
Philip Martin Sherman, *Toronto*
Alan BR Thomson, *Edmonton*
Eric M Yoshida, *Vancouver*

China
Francis KL Chan, *Hong Kong*
Xiao-Ping Chen, *Wuhan*
Jun Cheng, *Beijing*
Chi-Hin Cho, *Hong Kong*
Zong-Jie Cui, *Beijing*
Da-Jun Deng, *Beijing*
Er-Dan Dong, *Beijing*
Sheung-Tat Fan, *Hong Kong*
Xue-Gong Fan, *Changsha*
Jin Gu, *Beijing*
De-Wu Han, *Taiyuan*
Shao-Heng He, *Shantou*
Fu-Lian Hu, *Beijing*
Wayne HC Hu, *Hong Kong*
Ching Lung Lai, *Hong Kong*
Kam Chuen Lai, *Hong Kong*
Wai-Keung Leung, *Hong Kong*
Zhi-Hua Liu, *Beijing*
Ai- Ping Lu, *Beijing*
Jing-Yun Ma, *Beijing*
Lun-Xiu Qin, *Shanghai*
Yu-Gang Song, *Guangzhou*
Peng Shang, *Xi'an*
Qin Su, *Beijing*
Yuan Wang, *Shanghai*
Benjamin Wong, *Hong Kong*
Wai-Man Wong, *Hong Kong*
Hong Xiao, *Shanghai*
Dong-Liang Yang, *Wuhan*
Xue-Biao Yao, *Hefei*
Yuan Yuan, *Shenyang*
Man-Fung Yuen, *Hong Kong*
Jian-Zhong Zhang, *Beijing*
Zhi-Rong Zhang, *Chengdu*
Xiao-Hang Zhao, *Beijing*
Shu Zheng, *Hangzhou*

Costa Rica
Edgar M Izquierdo, *San José*

Croatia
Marko Duvnjak, *Zagreb*

Denmark
Flemming Burcharth, *Herlev*
Peter Bytzer, *Copenhagen*
Hans Gregersen, *Aalborg*
Jens H Henriksen, *Hvidovre*
Fin Stolze Larsen, *Copenhagen*
Søren Møller, *Hvidovre*

Egypt
Abdel-Rahman El-Zayadi, *Giza*

Finland
Pentti Sipponen, *Espoo*

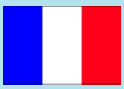

France
Charles Paul Balabaud, *Bordeaux*
Jacques Belghiti, *Clichy*
Pierre Brissot, *Rennes*
Franck Carbonnel, *Besancon*
Bruno Clément, *Rennes*
Jacques Cosnes, *Paris*
Francoise Degos, *Clichy*
Francoise Lunel Fabian, *Angers*
Gérard Feldmann, *Paris*
Jean Fioramonti, *Toulouse*
Rene Lambert, *Lyon*
Didier Lebrec, *Clichy*
Francis Mégraud, *Bordeaux*
Richard Moreau, *Clichy*
Jose Sahel, *Marseille*
Jean-Yves Scoazec, *Lyon*
Jean-Pierre Henri Zarski, *Grenoble*

Germany
HD Allescher, *Garmisch-Partenkirchen*
Rudolf Arnold, *Marburg*
Hubert Blum, *Freiburg*
Peter Born, *Muchen*
Heinz J Buhr, *Berlin*
Haussinger Dieter, *Düsseldorf*
Dietrich CF, *Bad Mergentheim*
Wolfram W Domschke, *Muenster*
Ulrich Robert Fölsch, *Kiel*
Peter R Galle, *Mainz*
Burkhard Göke, *Munich*
Axel M Gressner, *Aachen*
Eckhart Georg Hahn, *Erlangen*
Werner Hohenberger, *Erlangen*
RG Jakobs, *Ludwigshafen*
Joachim Labenz, *Siegen*
Ansgar W Lohse, *Hamburg*
Peter Malfertheiner, *Magdeburg*
Andrea Dinah May, *Wiesbaden*
Stephan Miehlke, *Dresden*
Gustav Paumgartner, *Munich*
Ulrich Ks Peitz, *Magdeburg*
Giuliano Ramadori, *Göttingen*
Tilman Sauerbruch, *Bonn*
Hans Seifert, *Oldenburg*
J Ruediger Siewert, *Munich*
Manfred V Singer, *Mannheim*
Jurgen M Stein, *Frankfurt*
Manfred Stolte, *Bayreuth*
Wolfgang R Stremmel, *Heidelberg*
Hans Ludger Tillmann, *Leipzig*
Siegfried Wagner, *Deggendorf*
Bertram Wiedenmann, *Berlin*

Greece
Arvanitakis C, *Thessaloniki*
Elias A Kouroumalis, *Heraklion*

Hungary
Simon A László, *Szekszárd*
János Papp, *Budapest*

Iceland
Hallgrimur Gudjonsson, *Reykjavik*

India
Sujit Kumar Bhattacharya, *Kolkata*
Chawla YK, *Chandigarh*
Radha Dhiman K, *Chandigarh*
Sri Prakash Misra, *Allahabad*
Kartar Singh, *Lucknow*

Iran
Reza Malekzadeh, *Tehran*

Israel
Abraham Rami Eliakim, *Haifa*
Yaron Niv, *Pardesia*

Italy
Giovanni Addolorato, *Roma*
Alfredo Alberti, *Padova*
Annese V, *San Giovanni Rotondo*
Giovanni Barbara, *Bologna*
Gabrio Bassotti, *Perugia*
Franco Bazzoli, *Bologna*
Adolfo Francesco Attili, *Roma*
Antomio Benedetti, *Ancona*
Giovanni Cammarota, *Roma*
Antonino Cavallari, *Bologna*
Dario Conte, *Milano*
Gino Roberto Corazza, *Pavia*
Guido Costamagua, *Roma*
Antonio Craxi, *Palermo*
Fabio Farinati, *Padua*
Giovanni Gasbarrini, *Roma*
Paolo Gentilini, *Florence*
Edoardo G Giannini, *Genoa*

Paolo Gionchetti, *Bologna*
Roberto De Giorgio, Bologna
Mario Guslandi, *Milano*
Giovanni Maconi, *Milan*
Giulio Marchesini, *Bologna*
Giuseppe Montalto, *Palermo*
Luisi Pagliaro, *Palermo*
Fabrizio R Parente, *Milan*
Perri F, *San Giovanni Rotondo*
Raffaele Pezzilli, *Bologna*
Pilotto A, *San Giovanni Rotondo*
Massimo Pinzani, *Firenze*
Gabriele Bianchi Porro, *Milano*
Piero Portincasa, *Bari*
Giacomo Laffi, *Firenze*
Enrico Roda, *Bologna*
Massimo Rugge, *Padova*
Vincenzo Savarino, *Genova*
Vincenzo Stanghellini, *Bologna*
Calogero Surrenti, *Florence*
Roberto Testa, *Genoa*
Dino Vaira, *Bologna*

Japan

Kyoichi Adachi, *Izumo*
Takashi Aikou, *Kagoshima*
Taiji Akamatsu, *Matsumoto*
Takafumi Ando, *Nagoya*
Akira Andoh, *Otsu*
Taku Aoki, *Tokyo*
Masahiro Arai, *Tokyo*
Tetsuo Arakawa, *Osaka*
Yasuji Arase, *Tokyo*
Masahiro Asaka, *Sapporo*
Hitoshi Asakura, *Tokyo*
Yutaka Atomi, *Tokyo*
Takeshi Azuma, *Fukui*
Nobuyuki Enomoto, *Yamanashi*
Kazuma Fujimoto, *Saga*
Toshio Fujioka, *Oita*
Yoshihide Fujiyama, *Otsu*
Hiroyuki Hanai, *Hamamatsu*
Kazuhiro Hanazaki, *Nagano*
Naohiko Harada, *Fukuoka*
Makoto Hashizume, *Fukuoka,*
Tetsuo Hayakawa, *Nagoya*
Kazuhide Higuchi, *Osaka*
Ichiro Hirata, *Osaka*
Keiji Hirata, *Kitakyushu*
Takafumi Ichida, *Shizuoka*
Kenji Ikeda, *Tokyo*
Kohzoh Imai, *Sapporo*
Fumio Imazeki, *Chiba*
Masayasu Inoue, *Osaka*
Hiromi Ishibashi, *Nagasaki*
Shunji Ishihara, *Izumo*
Toru Ishikawa, *Niigata*
Kei Ito, *Sendai*
Masayoshi Ito, *Tokyo*
Hiroaki Itoh, *Akita*
Hiroshi Kaneko, *Aichi-Gun*
Shuichi Kaneko, *Kanazawa*
Takashi Kanematsu, *Nagasaki*
Junji Kato, *Sapporo*
Mototsugu Kato, *Sapporo*
Shinzo Kato, *Tokyo*
Sunao Kawano, *Osaka*
Yoshikazu Kinoshita, *Izumo*
Masaki Kitajima, *Tokyo*
Tsuneo Kitamura, *Chiba*
Seigo Kitano, *Oita*
Hironori Koga, *Kurume*
Satoshi Kondo, *Sapporo*
Shoji Kubo, *Osaka*
Shigeki Kuriyama, *Kagawa*
Masato Kusunoki, *Mie*
Takashi Maeda, *Fukuoka*
Shin Maeda, *Tokyo*
Osamu Matsui, *Kanazawa*
Yasushi Matsuzaki, *Tsukuba*
Hiroto Miwa, *Hyogo*
Masashi Mizokami, *Nagoya*
Motowo Mizuno, *Hiroshima*
Morito Monden, *Suita*
Hisataka S Moriwaki, *Gifu*
Yoshiharu Motoo, *Kanazawa*
Akihiro Munakata, *Hirosaki*
Kazunari Murakami, *Oita*
Kunihiko Murase, *Tusima*
Masato Nagino, *Nagoya*
Yujl Naito, *Kyoto*
Hisato Nakajima, *Tokyo*
Hiroki Nakamura, *Yamaguchi*
Shotaro Nakamura, *Fukuoka*
Akimasa Nakao, *Nagoya*
Mikio Nishioka, *Niihama*
Susumu Ohmada, *Maebashi*
Masayuki Ohta, *Oita*
Tetsuo Ohta, *Kanazawa*
Susumu Okabe, *Kyoto*
Katsuhisa Omagari, *Nagasaki*
Saburo Onishi, *Nankoku*
Morikazu Onji, *Ehime*
Hiromitsu Saisho, *Chiba*
Hidetsugu Saito, *Tokyo*
Takafumi Saito, *Yamagata*
Isao Sakaida, *Yamaguchi*
Michiie Sakamoto, *Tokyo*
Iwao Sasaki, *Sendai*
Motoko Sasaki, *Kanazawa*
Chifumi Sato, *Tokyo*
Shuichi Seki, *Osaka*
Hiroshi Shimada, *Yokohama*
Mitsuo Shimada, *Tokushima*
Hiroaki Shimizu, *Chiba*
Tooru Shimosegawa, *Sendai*
Tadashi Shimoyama, *Hirosaki*
Ken Shirabe, *Iizuka City*
Yoshio Shirai, *Niigata*
Katsuya Shiraki, *Mie*
Yasushi Shiratori, *Okayama*
Yasuhiko Sugawara, *Tokyo*
Toshiro Sugiyama, *Toyama*
Kazuyuki Suzuki, *Morioka*
Hidekazu Suzuki, *Tokyo*
Tadatoshi Takayama, *Tokyo*
Tadashi Takeda, *Osaka*
Koji Takeuchi, *Kyoto*
Kiichi Tamada, *Tochigi*
Akira Tanaka, *Kyoto*
Eiji Tanaka, *Matsumoto*
Noriaki Tanaka, *Okayama*
Shinji Tanaka, *Hiroshima*
Kyuichi Tanikawa, *Kurume*
Tadashi Terada, *Shizuoka*
Akira Terano, *Shimotsugagun*
Kazunari Tominaga, *Osaka*
Hidenori Toyoda, *Ogaki*
Akihito Tsubota, *Chiba*
Shingo Tsuji, *Osaka*
Takato Ueno, *Kurume*
Shinichi Wada, *Tochigi*
Hiroyuki Watanabe, *Kanazawa*
Sumio Watanabe, *Akita*
Toshio Watanabe, *Osaka*
Yuji Watanabe, *Ehime*
Chun-Yang Wen, *Nagasaki*
Koji Yamaguchi, *Fukuoka*
Takayuki Yamamoto, *Yokkaichi*
Takashi Yao, *Fukuoka*
Hiroshi Yoshida, *Tokyo*
Masashi Yoshida, *Tokyo*
Norimasa Yoshida, *Kyoto*
Kentaro Yoshika, *Toyoake*
Masahide Yoshikawa, *Kashihara*

Lithuania

Sasa Markovic, *Japljeva*

Macedonia

Vladimir Cirko Serafimoski, *Skopje*

Malaysia

Andrew Seng Boon Chua, *Ipoh*
Jayaram Menon, *Sabah*
Khean-Lee Goh, *Kuala Lumpur*

Monaco

Patrick Rampal, *Monaco*

Netherlands

Louis MA Akkermans, *Utrecht*
Karel Van Erpecum, *Utrecht*
Albert K Groen, *Amsterdam*
Dirk Joan Gouma, *Amsterdam*
Jan BMJ Jansen, *Nijmegen*
Evan Anthony Jones, *Abcoude*
Ernst Johan Kuipers, *Rotterdam*
Chris JJ Mulder, *Amsterdam*
Michael Müller, *Wageningen*

Pena AS, *Amsterdam*
Andreas Smout, *Utrecht*
RW Stockbrugger, *Maastricht*
GP Vanberge-Henegouwen, *Utrecht*

New Zealand
Ian David Wallace, *Auckland*

Norway
Trond Berg, *Oslo*
Helge Lyder Waldum, *Trondheim*

Pakistan
Muhammad S Khokhar, *Lahore*

Philippines
Eulenia Rasco Nolasco, *Manila*

Poland
Tomasz Brzozowski, *Cracow*
Andrzej Nowak, *Katowice*

Portugal
Miguel Carneiro De Moura, *Lisbon*

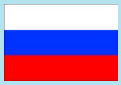

Russia
Vladimir T Ivashkin, *Moscow*
Leonid Lazebnik, *Moscow*
Vasiliy I Reshetnyak, *Moscow*

Singapore
Bow Ho, *Kent Ridge*
Francis Seow-Choen, *Singapore*

Slovakia
Anton Vavrecka, *Bratislava*

South Africa
Michael C Kew, *Parktown*

South Korea
Jin-Hong Kim, *Suwon*
Myung-Hwan Kim, *Seoul*
Yun-Soo Kim, *Seoul*
Yung-Il Min, *Seoul*
Jae-Gahb Park, *Seoul*
Dong Wan Seo, *Seoul*

Spain
Abraldes JG, *Barcelona*
Fernando Azpiroz, *Barcelona*
Ramon Bataller, *Barcelona*
Josep M Bordas, *Barcelona*
Maria Buti, *Barcelon*
Xavier Calvet, *Sabadell*
Antoni Castells, *Barcelona*
Manuel Daz-Rubio, *Madrid*
Juan C Garcia-Pagán, *Barcelona*
Genover JB, *Barcelona*
Javier P Gisbert, *Madrid*
Jaime Guardia, *Barcelona*
Angel Lanas, *Zaragoza*
Ricardo Moreno-Otero, *Madrid*
Julian Panes, *Barcelona*
Miguel Perez-Mateo, *Alicante*
Josep M Pique, *Barcelona*
Jesus Prieto, *Pamplona*
Luis Rodrigo, *Oviedo*

Sri Lanka
Janaka De Silva, *Ragama*

Swaziland
Gerd Kullak-Ublick, *Zurich*

Sweden
Lars Christer Olbe, *Molndal*
Curt Einarsson, *Huddinge*
Lars R Lundell, *Stockholm*
Xiao-Feng Sun, *Linkoping*

Switzerland
Christoph Beglinger, *Basel*
Michael W Fried, *Zurich*
Bruno Stieger, *Zurich*
Arthur Zimmermann, *Berne*

Turkey
Yusuf Bayraktar, *Ankara*
Figen Gurakan, *Ankara*
Cihan Yurdaydin, *Ankara*

United Kingdom
Axon ATR, *Leeds*
Paul Jonathan Ciclitira, *London*
Amar Paul Dhillon, *London*
Stuarts Forbes
Subrata Ghosh, *London*
Brian T Johnston, *Belfast*
David EJ Jones, *Newcastle*
Michael A Kamm, *Harrow*
Hong-Xiang Liu, Cambridge
Giorgina Mieli-Vergani, *London*
Nikolai V Naoumov, *London*
John P Neoptolemos, *Liverpool*
James Neuberger, *Birmingham*
Colm Antoine O'Morain, *Dublin*
Simon D Taylor-Robinson, *London*
Frank Ivor Tovey, *Basingstoke*
Min Zhao, *Foresterhill*

United States
Firas H Ac-Kawas, *Washington*
Gianfranco D Alpini, *Temple*
Paul Angulo, *Rochester*
Jamie S Barkin, *Miami Beach*
Todd Baron, *Rochester*
Kim Elaine Barrett, *San Diego*
Jennifer D Black, *Buffalo*
Xu Cao, *Birmingham*
David L Carr-Locke, *Boston*
Marc F Catalano, *Milwaukee*
Xian-Ming Chen, *Rochester*
James M Church, *Cleveland*
Vincent Coghlan, *Beaverton*
James R Connor, *Hershey*
Pelayo Correa, *New Orleans*
John Cuppoletti, *Cincinnati*
Peter V Danenberg, *Los Angeles*
Kiron Moy Das, *New Brunswick*
Hala El-Zimaity, *Houston*
Ronnie Fass, *Tucson*
Emma E Furth, *Pennsylvania*
John Geibel, *New Haven*
Graham DY, *Houston*
Joel S Greenberger, *Pittsburgh*
Anna S Gukovskaya, *Los Angeles*
Gavin Harewood, *Rochester*
Atif Iqbal, *Omaha*
Hajime Isomoto, *Rochester*
Dennis M Jensen, *Los Angeles*
Leonard R Johnson, *Memphis*
Peter James Kahrilas, *Chicago*
Anthony Nicholas Kalloo, *Baltimore*
Neil Kaplowitz, *Los Angeles*
Emmet B Keeffe, *Palo Alto*
Joseph B Kirsner, *Chicago*
Burton I Korelitz, *New York*
Robert J Korst, *New York*
Richard A Kozarek, *Seattle*
Shiu-Ming Kuo, *Buffalo*
Frederick H Leibach, *Augusta*
Andreas Leodolter, *La Jolla*
Ming Li, *New Orleans*
Lenard M Lichtenberger, *Houston*
Gary R Lichtenstein, *Philadelphia*
Josep M Llovet, *New York*
Martin Lipkin, *New York*

Manuscript reviewers of *World Journal of Gastroenterology*

PO Box 2345, Beijing 100023, China
www.wjgnet.com
wjg@wjgnet.com

ELSEVIER

World J Gastroenterol 2005;11(15):2211-2212
World Journal of Gastroenterology ISSN 1007-9327

• *REVIEW* •

Surgical resection for esophageal carcinoma: Speaking the language

Robert J. Korst

Robert J. Korst, Division of Thoracic Surgery, Department of Cardiothoracic Surgery, and Department of Genetic Medicine, Weill Medical College of Cornell University, New York, NY, USA
Correspondence to: Robert J. Korst, MD, Weill Medical College of Cornell University, Room M404, 525 East 68th Street, New York, NY 10021, USA. rjk2002@med.cornell.edu
Telephone: +1-212-7465104 Fax: +1-212-7468426
Received: 2004-07-17 Accepted: 2004-07-21

Abstract

The terminology used to describe esophagectomy for carcinoma can be confusing, even for specialists in gastrointestinal disease. As a result, specific terms are often used out of their intended context. To simplify the nomenclature, two points regarding procedures for surgical resection of the esophagus are critical: the extent of resection (radical *vs* standard) and the operative approach (choice of incisions). It is important to understand that the radicality of the resection may have little to do with the operative approach, with the exception of esophagectomy without thoracotomy (transhiatal esophagectomy), which mandates the performance of a standard or non-radical resection. Esophagectomy has emerged as the standard curative treatment option for patients with esophageal carcinoma; however, unlike the surgical resection of other types of solid tumors, many different surgical options and/or approaches exist for these patients. This heterogeneity of care may result from the fact that the esophagus is accessible through more than one body cavity (left hemithorax, right hemithorax, abdomen). In addition, and partially as a result of its accessibility, different types of surgical specialists harbor this operation in their armamentarium, including general surgeons, thoracic surgeons, and surgical oncologists. Despite this enthusiasm amongst surgeons, little consensus exists as to which option is most oncologically sound. Further, the details of the various surgical approaches and procedures for resection of the esophagus are often difficult to comprehend, even for specialists in gastrointestinal disease, with much of the relevant terminology used out of its intended context. To facilitate the understanding of the surgical options for esophageal carcinoma, it is useful to view the operation from two angles: the extent of resection (Aradical@ *vs* Astandard@) and the operative approach (choice of incisions).

Key words: Esophageal carcinoma; Terminology

Korst RJ. Surgical resection for esophageal carcinoma: Speaking the language. *World J Gastroenterol* 2005; 11 (15): 2211-2212
http://www.wjgnet.com/1007-9327/11/2211.asp

STANDARD *VS* RADICAL RESECTION

Esophagectomy for carcinoma can be viewed as being comprised of two components: resection of the esophagus itself and resection of the enveloping lymphatics. Controversy exists regarding how radical, or extensive these two components should be. Standard resection of the esophagus involves simple extirpation of the organ, leaving behind adjacent peritumoral tissues and organs. However, unlike the intra-abdominal gastrointestinal tract, the esophagus is not separated from the surrounding mediastinal organs and fat by a serosal covering, suggesting that simply removing the organ itself may leave behind microscopic tumor in the surrounding tissues, particularly with deeply penetrating lesions. Surgeons performing radical, or en bloc esophagectomy, as initially described by Skinner[1], attempt to address this issue by removing all peritumoral tissues in addition to the esophagus. For the intrathoracic esophagus, this includes all posterior mediastinal fat and lymphatics, the thoracic duct, as well as the posterior pericardium and bilateral parietal pleurae: a Aposterior mediastinectomy@. For a tumor at the gastroesophageal junction, a cuff of normal diaphragm is removed surrounding the tumor. In both cases the goal is to never actually for visualizing the tumor in the gross specimen.

The extent of lymphadenectomy performed during esophagectomy is also highly variable, ranging from minimal to radical. With regard to the esophageal lymphatics, three distinct lymphatic regions, or fields, have been described[2]. The abdominal field represents the lymph node areas below the diaphragm, from the crura to the celiac axis. The mediastinal field generally refers to the lower aspect of the mediastinum, from the carina down to the diaphragm. Strictly speaking, the cervical field encompasses the deep lateral nodes accompanying the accessory nerve, the deep external nodes lateral to the carotid sheath, which includes the scalene, or supraclavicular nodes, and the deep internal nodes, which accompany the recurrent laryngeal nerves down into the chest. Of the three cervical areas, however, it is this latter group that has received the greatest attention due to the relatively high frequency of metastases encountered in this area, reported to be as high as 35% in patients with tumors of the tubular esophagus[3]. A Aradical@ esophagectomy, therefore, refers to a procedure by which the esophagus and its enveloping tissues are

removed as a single specimen (en bloc), combined with either two-field (abdominal and mediastinal) or three-field (abdominal, mediastinal, cervical) lymphadenectomy.

OPERATIVE APPROACH

While terms such as Aradical@ and Astandard@ describe the extent of resection and lymphadenectomy, a separate set of terms describe the operative approach and the choice of incisions used by the surgeon to perform the procedure. These operative approaches can be simply viewed as either transthoracic (involving a thoracotomy) or transhiatal (not involving a thoracotomy). A standard esophagectomy can technically be performed using either of these operative approaches; however, a radical operation mandates the transthoracic approach to directly access the posterior mediastinum. The transhiatal esophagectomy, popularized in the recent past by Orringer[4], involves a laparotomy for mobilization of the gastric replacement conduit, dissection of the thoracic esophagus through the diaphragmatic hiatus, and a cervical esophagogastrostomy through a cervical incision. Transthoracic approaches include: (1) The combination of a laparotomy and a right thoracotomy with an intrathoracic esophagogastrostomy (Ivor Lewis esophagectomy[5]). (2) A right thoracotomy, laparotomy and neck incision with a cervical anastomosis (McKeown esophagectomy[6]). This technique is sometimes incorrectly confused with the three-field lymphadenectomy by virtue of its three incisions. While it is correct that three incisions may be popular for performing a radical esophagectomy with a three-field lymphadenectomy, many surgeons perform a standard esophagectomy using this operative approach as well. (3) Left thoracic approaches may involve thoracotomy alone, with the abdominal portion of the procedure performed through the diaphragm, or thoracoabdominal incisions where the costal margin is divided to facilitate access to the abdomen. For these left thoracic approaches, the anastomosis between the remaining esophagus and the replacement conduit may be placed either in the superior mediastinum or in the neck through a cervical incision.

ONCOLOGIC CONSIDERATIONS

Although it is generally agreed that the accuracy of staging is enhanced by a radical procedure, debate currently exists regarding whether or not any oncologic benefits are provided over standard esophagectomy. While cure rates in the range of 10-15% are consistently seen after standard esophagectomy alone for stage III esophageal carcinoma[4,7,8], multiple series now demonstrate long-term survival figures of 25-45% after radical procedures for similarly staged disease[9,10]. Despite these data, the answer to this controversy should ideally come from prospective, randomized trials, since the phenomenon of stage migration may occur in comparison with non-randomized series of patients. In this regard, the only published phase III trial till this date compared transhiatal resection with a radical, transthoracic esophagectomy and two-field lymphadenectomy for patients with adenocarcinoma of the esophagus[11]. The overall 5-year survival with the radical approach was 39%, compared with 29% for the patients undergoing the transhiatal, standard resection. Although not statistically significant, this trial was powered to detect a survival increase of 50%. However, many esophageal cancer specialists would consider less of an increase in survival to be clinically relevant.

SUMMARY

The terminology concerning surgical resection for esophageal carcinoma tends to be somewhat confusing and is often used out of its proper context. The extent of resection and lymphadenectomy is best described as either Aradical@ or Astandard@, and with the exception of the transhiatal esophagectomy has little to do with the operative approach, which mainly refers to the surgeons=choice of incisions.

REFERENCES

1 **Skinner DB.** En bloc resection of neoplasms for the esophagus and cardia. *J Thorac Cardiovasc Surg* 1983; **85**: 59-71
2 **Altorki NK,** Lerut T. Three-field lymph node dissection for cancer of the esophagus. In: Pearson FG, Cooper JD, Deslauriers J, Ginsberg RJ, Hiebert CA, Patterson GA, Urschel HC, eds. Esophageal surgery. *New York: Churchill Livingstone,* 2002: 866-870
3 **Altorki NK,** Skinner DB. Occult cervical nodal metastasis in esophageal cancer: preliminary results of three-field lymphadenectomy. *J Thorac Cardiovasc Surg* 1997; **113**: 540-544
4 **Orringer MB,** Marshall B, Stirling MC. Transhiatal esophagectomy for benign and malignant disease. *J Thorac Cardiovasc Surg* 1993; **105**: 265-276; discussion 276-277
5 **Lewis I.** The surgical treatment of carcinoma of the oesophagus with special reference to a new operation for growths of the middle third. *Br J Surg* 1946; **34**: 18-31
6 **McKeown KC.** Total three-stage oesophagectomy for cancer of the oesophagus. *Br J Surg* 1976; **63**: 259-262
7 **Killinger WA,** Rice TW, Adelstein DJ, Medendorp SV, Zuccaro G, Kirby TJ, Goldblum JR. Stage II esophageal carcinoma: the significance of T and N. *J Thorac Cardiovasc Surg* 1996; **111**: 935-940
8 **Visbal AL,** Allen MS, Miller DL, Deschamps C, Trastek VF, Pairolero PC. Ivor Lewis esophagogastrectomy for esophageal cancer. *Ann Thorac Surg* 2001; **71**: 1803-1808
9 **Altorki NK,** Girardi L, Skinner DB. En bloc esophagectomy improves survival for stage III esophageal cancer. *J Thorac Cardiovasc Surg* 1997; **114**: 948-955; discussion 955-956
10 **Akiyama H,** Tsurumaru M, Udagawa H, Kajiyama Y. Radical lymph node dissection for cancer of the thoracic esophagus. *Ann Surg* 1994; **220**: 364-372; discussion 372-373
11 **Hulscher JB,** van Sandick JW, de Boer AG, Wijnhoven BP, Tijssen JG, Fockens P, Stalmeier PF, ten Kate FJ, van Dekken H, Obertop H, Tilanus HW, van Lanschot JJ. Extended transthoracic resection compared with limited transhiatal resection for adenocarcinoma of the esophagus. *N Engl J Med* 2002; **347**: 1662-1669

Science Editor Wang XL and Li WZ **Language Editor** Elsevier HK

PO Box 2345, Beijing 100023, China
www.wjgnet.com
wjg@wjgnet.com

ELSEVIER

World J Gastroenterol 2005;11(15):2213-2217
World Journal of Gastroenterology ISSN 1007-9327

• *GASTRIC CANCER* •

Transcription factor Sp1 expression in gastric cancer and its relationship to long-term prognosis

Jun Zhang, Zheng-Gang Zhu, Jun Ji, Fei Yuan, Ying-Yan Yu, Bing-Ya Liu, Yan-Zhen Lin

Jun Zhang, Zheng-Gang Zhu, Jun Ji, Ying-Yan Yu, Bing-Ya Liu, Yan-Zhen Lin, Department of Surgery, Rui Jin Hospital, Shanghai Institute of Digestive Surgery, Shanghai Second Medical University, Shanghai 200025, China
Fei Yuan, Department of Pathology, Rui Jin Hospital, Shanghai Institute of Digestive Surgery, Shanghai Second Medical University, Shanghai 200025, China
Supported by the "211" Project sponsored by Ministry of Education, China
Correspondence to: Jun Zhang, Department of Surgery, Rui Jin Hospital, Shanghai Institute of Digestive Surgery, Shanghai Second Medical University, Shanghai 200025, China. jun_zj@sina.com
Telephone: +86-21-64370045-611018 Fax: +86-21-64373909
Received: 2004-06-30 Accepted: 2004-07-11

Abstract

AIM: To explore the expression of Sp1 in gastric carcinoma as well as its association with other clinicopathologic features, and to evaluate the role of Sp1 as a prognostic indicator of gastric carcinoma.

METHODS: By using immunohistochemistry, we examined the Sp1 expression patterns in 65 cases of human gastric cancer, and 40 normal gastric mucosa specimens. Simultaneously, the correlation between Sp1 expression and clinical outcome or clinicopathologic features was investigated.

RESULTS: The percentage of Sp1 expression was 12.5% (5/40) in normal gastric mucosa, and the Sp1 protein was mainly expressed in the nuclei of cells located in the mucous neck region. In sharp contrast, strong Sp1 expression was detected in tumor cells, whereas no or faint Sp1 staining was detected in stromal cells and normal glandular cells surrounding the tumors. The expression rate of Sp1 in gastric cancer lesions was 53.85% (35/65). The medium survival duration in patients who had a tumor with negative, weak and strong Sp1 expressions was 1 700, 1 560 and 1 026 d, respectively ($P<0.05$). Sp1 protein expression was closely related to the depth of tumor infiltration ($\chi^2 = 13.223$, $P<0.01$) and TNM stage ($\chi^2 = 11.009$, $P<0.05$), but had no relationship with the number of lymph nodes and Lauren's classification ($P>0.05$). Cox regression model for multivariate analysis revealed that high Sp1 expression ($P<0.05$) and advanced stage ($P<0.01$) were independent predictors of poor survival.

CONCLUSION: Normal and malignant gastric tissues have unique Sp1 expression patterns. Sp1 might serve as an independent prognostic factor, by influencing the tumor infiltration and progression.

Key words: Sp1; Gastric carcinoma

Zhang J, Zhu ZG, Ji J, Yuan F, Yu YY, Liu BY, Lin YZ. Transcription factor Sp1 expression in gastric cancer and its relationship to long-term prognosis. *World J Gastroenterol* 2005; 11(15): 2213-2217
http://www.wjgnet.com/1007-9327/11/2213.asp

INTRODUCTION

Gastric carcinoma is currently one of the leading causes of cancer-related death in mainland of China. Despite improvement in early diagnosis, surgical technique and chemotherapy, the majority of gastric cancer patients die of the physiological effects of local recurrence and/or distant metastasis[1]. The overall 5-year survival rate is 30-40%. Studies over the past half century have tried to explore the mechanism of tumor metastasis on the histopathologic, cytologic and molecular biology[2-4]. Although a few critical factors such as TNM stage have been indicated to be prognostic parameters, the precise molecular parameters to predict the risk of metastasis and evaluate the outcome of gastric cancer patients remain to be defined[5,6].

The aggressive nature of gastric cancer is related to various abnormalities in oncogenes, tumor suppressor genes, growth factors and their receptors, which in turn confer growth advantages to gastric cancer cells. Increasing evidence suggests that such molecular changes are regulated by a plethora of external and internal factors[7,8]. Sp1 is a well-characterized, sequence-specific, DNA-binding protein that is important in the transcription of many cellular and viral genes containing GC boxes in their promoters[9]. Previous studies have shown that abnormal Sp1 activation might augment the growth and metastatic potential of tumor cells through over-expression of many Sp1 downstream genes. The role of Sp1 as an essential transcription factor for many genes regulating cell growth, angiogenesis and survival has been proved in pancreatic cancer[10,11]. Yet, the expression of Sp1 and its impact on the outcome of gastric cancer patients are still unknown.

In the present study, we examined Sp1 expression in human gastric cancer by using immunohistochemistry, and studied its relationship with the length of survival and clinicopathologic features.

MATERIALS AND METHODS

Patients and specimens

Sixty-five patients (45 men and 20 women, medium age 65 years) with gastric cancer undergoing radical gastrectomy (D2 or D3) in the Department of Surgery, Rui Jin Hospital, from March 1997 to September 2001, were enrolled in this study. The eligibility criteria were histologically proven gastric adenocarcinoma, no hematogenous metastatic lesions, no previous systemic chemotherapy before operation, with well-documented clinical histories and follow-up information. Distant peritoneal metastatic foci, fixed lymph nodes with a positive frozen biopsy in nodes around the middle coliac artery and/or para-aortic nodes, or involvement of the rectal shelf were considered as distant metastases and were excluded from the study.

All of the patients were observed and followed up in the same institute. At the end of March 2004, 42 patients were still alive, whereas 23 patients died of tumor recurrence and/or distant metastasis. Patients who were killed in accidents, or died of surgical-related postoperative complications as well as other cancers were excluded. All of the resected primary tumors and regional lymph nodes were histopathologically evaluated by hematoxylin and eosin staining according to the 5th UICC TNM classification published in 1997[12]. Forty normal gastric tissue specimens obtained from patients who underwent partial gastrectomy for benign gastric diseases were also collected in this study.

Immunohistochemistry

Formalin-fixed gastric cancer specimens were embedded in paraffin, and 4-μm thick sections were obtained. These sections were mounted on salinized glass slides and heated at 60 ℃ for 30 min. After deparaffinization in xylene, the sections were rehydrated in graded alcohol, and washed in water. Endogenous peroxidase activity was blocked by incubation with 3% hydrogen peroxide in methanol for 30 min at room temperature. Antigen retrieval was accomplished by 1 mmol/L EDTA solution. After being washed with phosphate-buffered saline (PBS) and exposed to 10% normal goat serum for 10 min to reduce non-specific binding, the slides were incubated for 12 h with rabbit monoclonal antibody against Sp1 (Santa Cruz Biotechnology, Inc., USA, Code No.: SC-59), which was diluted at 1:200 in PBS. Primary antibodies were visualized with an Envision system (DAKO, Denmark, Code No.: K4003). After further being washed with PBS, slides were incubated with substrate diaminobenzidine and hydrogen peroxide for 10 min. Finally, sections were counterstained with hematoxylin[13].

The specificity of Sp1 staining was confirmed using parallel negative control sections, which were processed immunohistochemically after the primary antibody was replaced with PBS, and positive control sections from a colonic adenocarcinoma previously were shown to express high levels of Sp1 by immunohistochemistry. Simultaneously, the samples from normal gastric mucosa were also stained according to the procedures described above.

Evaluation of immunohistochemical staining

In each specimen, immunoreactivity was examined under light microscopy and scored independently by two assessors who were blinded to patient outcomes. A positive reaction was indicated by reddish-brown precipitates in the nuclei. Only nuclear staining was considered as positive reaction. In scoring the sections, an assessment of the proportion of cell staining and the staining intensity was made. Specifically, the percentage of positive cells was divided into five grades (percentage scores): <10% (0), 10-25% (1), 25-50% (2), 50-75% (3) and >75% (4). The intensity of staining was divided into four grades (intensity scores): no staining (0), weak staining (1), moderate staining (2) and strong staining (3). Sp1 staining positivity was determined by the following formula: overall score = percentage score×intensity score. The overall score ≤3 was defined as negative, 3-6 as weak positive, and >6 as strong positive[14,15]. The concordance between the blinded reviewers was 93.3% (98/105). In the seven cases of discordance, a final evaluation was determined by consensus after reexamination.

Patient observation and follow-up

Postoperatively, the patients received chemotherapy with LV/FP (5-FU+LV+CDDP) or FM (5-FU+LV+MMC) regimen for at least 6 mo during the period of follow-up[15]. The selection of chemotherapeutic regimen was based on the histologic type and cancer stage, individually. The patients were reevaluated regularly with a physical examination and biochemical laboratory studies. Image diagnostic assessment, including computed tomography and/or ultrasonography was carried out every 6 mo.

All the enrolled patients had well-documented clinical histories and follow-up information. The epidemiological information including the age, gender and clinicopathological data including tumor type, TNM stage as well as Lauren's classification were registered. For dead patients, the precise date and cause of death were recorded[16].

Duration of survival was defined as the time from the date of operation to the time of death. Patients who were still alive would be censored until March 31, 2004. The average follow-up period for the 65 patients was 1 472 d for all patients and 1 787 d for patients alive in March 2004 (range 619-2 478 d). The overall survival rate was 64.6% (42/65).

Statistical analysis

Two-tailed χ^2 test was performed to determine the significance of the difference between Sp1 positivity and other variables. Survival curve was calculated with the Kaplan-Meier method. Log-rank test was used to assess the statistical differences in survival. For multivariate analysis, the Cox regression model was used. In all of the tests, probability values from two-tailed test less than 0.05 were considered statistically significant. SPSS 11.0 statistic software for Windows was used for analyses.

RESULTS

Sp1 expression in human gastric cancer tissues

Expression of Sp1 in human gastric cancer tissues and its localization patterns were evaluated immunohistochemically. Moderate to strong Sp1 staining was seen in the nuclei of tumor cells of various types of gastric cancer, whereas no or

weak Sp1 staining was detected in stromal cells and normal glandular cells surrounding the tumor lesions (Figure 1A). Of the 65 patients, 35 (53.85%) had Sp1 nuclear staining, while 30 (46.15%) were negative.

According to the overall Sp1 staining score based on percentage and intensity, the weak and strong staining gastric cancer cases accounted for 13.85% (9/65) and 37.68% (26/65), respectively. In the 13 cases of early gastric cancer, the percentage of Sp1 expression was 15.38% (2/13), and most of them were weak staining.

Sp1 expression in normal human gastric tissues

In most of the normal gastric mucosae, no or faint nuclear staining of Sp1 was shown. Positive staining was predominantly observed in the nuclei of cells localized in the mucous neck region. There was no Sp1 protein expression in the cells of the glandular epithelial cells or cells located towards the gastric pit (foveolar) (Figure 1B). The overall percentage of Sp1 expression was only 12.5% (5/40) in normal human gastric mucosa.

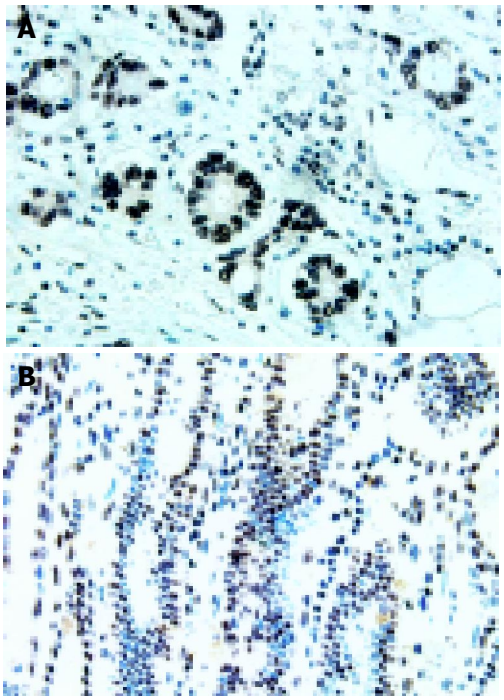

Figure 1 Sp1 protein expression and its localization in human gastric cancer tissue (**A**) and in normal human gastric tissue (**B**), IHC staining ×400 (**A**), ×200 (**B**).

Relationship between Sp1 expression and clinicopathologic features

The relationship between Sp1 expression and clinicopathologic features is summarized in Table 1. Sp1 expression was more frequently found in tumors with serosal invasion than in those without serosal invasion ($\chi^2 = 13.223$, $P<0.01$). Sp1 expression was also closely related to advanced TNM stage ($\chi^2 = 11.009$, $P<0.05$). However, no significant correlation was found between Sp1 expression and age at surgery, gender, tumor location, number of metastatic lymph nodes and Lauren's classification ($P>0.05$).

Sp1 immunohistochemical staining revealed that 13 of 19 well-differentiated gastric cancer tissues (including papillary adenocarcinoma, tubular adenocarcinoma and moderately differentiated adenocarcinoma) and 22 of 46 poorly differentiated gastric cancer tissues (including poorly differentiated adenocarcinoma, signet ring cell carcinoma and mucous adenocarcinoma) were positive. There was no relationship between Sp1 expression and histopathologic differentiation.

Table 1 **Sp1 expression in human gastric cancer tissues and its relationship with clinicopathologic features**

Clinicopathological parameters	Sp1 negative $n = 30$	Sp1 weak $n = 9$	Sp1 strong $n = 26$	χ^2	P
Age (yr)					
⩾60	15	3	19	5.396	0.067
<60	15	6	7		
Gender					
Male	18	6	21	2.583	0.240
Female	12	3	5		
Location					
Upper third	6	2	9	4.660	0.324
Middle third	3	2	6		
Lower third	21	5	11		
Histopathologic type					
Well differentiated	6	4	9	2.607	0.272
Poorly differentiated	24	5	17		
Depth of infiltration					
T1–2	19	4	4	13.223	0.001
T3–4	11	5	22		
LN metastasis					
No	19	5	9	4.819	0.306
⩽6	6	2	10		
>6	5	2	7		
TNM stage					
I	16	3	3	11.009	0.026
II, III	10	4	17		
IV	4	2	6		
Lauren's classification					
Intestinal type	9	4	10	0.811	0.667
Diffuse type	21	5	16		

Sp1 protein expression and survival in gastric cancer patients

The median survival duration in patients who had a tumor with negative, weak and strong Sp1 expressions was 1 700, 1 560 and 1 026 d, respectively. The elevated Sp1 expression was associated with a poor tumor prognosis ($P<0.05$, Figure 2).

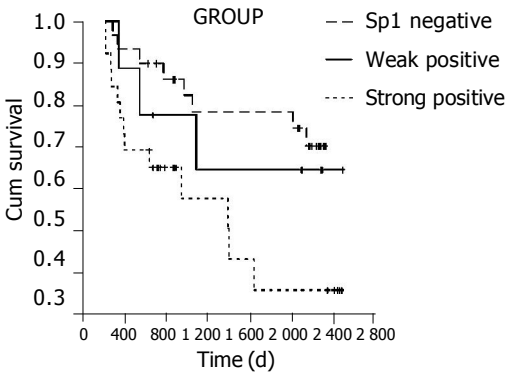

Figure 2 Correlation of Sp1 expression with long-term survival in gastric cancer patients.

Sp1 expression, age at surgery, gender, histologic differentiation, depth of infiltration, number of metastatic lymph nodes, TNM stage and Lauren's classification were entered into a Cox regression model for multivariate analysis. High Sp1 expression ($P<0.05$) and advanced stage ($P<0.01$) were independent predictors of poor survival. Age at surgery, gender, histologic differentiation, depth of infiltration, number of metastatic lymph nodes and Lauren's classification did not have a statistically significant effect on survival in multivariate analysis.

DISCUSSION

Metastasis is the most devastating aspect of gastric cancer. In fact, at the time of diagnosis, patients usually had locally advanced diseases or metastasis involving the lymph nodes, liver or peritoneum[17]. Understanding the critical determinants of cancer, metastasis is helpful in designing potential preventive and therapeutic strategies. Studies over the past several decades have indicated that the process of cancer metastasis consists of a series of conceptual and sequential steps[18]. Malignant neoplasm consists of multiple cell populations that exhibit a wide range of biologic characteristics, including antigenicity, chemosensitivity, growth rate, karyotype as well as metastatic potential[19,20]. The development of multiple growth signaling pathways could render tumor cells a tremendous growth advantage[2,19,20]. A number of molecular events are being recognized to play a part in metastatic process.

Sp1 is a sequence-specific DNA-binding protein, which is important in the transcription of many cellular and viral genes that contain GC elements within the proximal region of their promoter[21]. Recently, additional transcription factors such as Sp2, Sp3 and Sp4, which are similar to Sp1 in their structures and transcriptional properties, have been cloned[22,23]. Sp1 is essential for many genes that regulate the cell survival, growth and angiogenesis. Earlier studies have established that Sp1 protein can regulate many tumor-related genes, including FGFR1, insulin-like growth factor receptor1, insulin-like growth factor-binding protein 2, VEGF and thymidine kinase[24,25]. The relevance of these factors to tumor growth and metastasis has been evaluated. Abnormal Sp1 protein activation and expression might up-regulate the production of these genes, thus creating a microenvironment, which favors tumor cell growth, metastasis and angiogenesis. Sp1 signaling pathway may contribute to tumor development and progression.

It was reported that Sp1 involved apoptosis by altering the expression and function of multiple apoptosis-related proteins, including Bcl-2 and Bax[26].

The mechanism underlying in different levels of Sp1 is currently unknown. Investigations indicated that Sp1 expression was influenced by many stimuli, and varied in different tumor origins. Kumar and Butler[27] revealed that the DNA-binding activity of Sp1 was significantly higher in human epithelium-derived cancer than in human skin papilloma. A recent study showed that Sp1 activity could be modulated by stress factors such as hypoxia, acidosis and over-expression of free radicals, thus activating the p42/p42 mitogen-activated protein kinase and c-JunNH2-terminal kinase-related signal pathways[28]. It may also involve many other cellular factors, including the functional status of oncogenes and tumor suppressor genes.

In agreement with a previous study, we did not find strong expression of Sp1 in nuclei of normal gastric mucosa cells. The normal gastric mucosa not displayed or little staining for Sp1, and the positive cells were located in the mucous neck region in normal gastric mucosa, suggesting that Sp1 is mainly expressed in dividing cells, and not in differentiated cells. In contrast, our results showed that expression of Sp1 was a prominent feature of advanced gastric cancer, regardless of its histologic type. In the present study, we identified nuclear expression of Sp1 in 63.46% (33/52) of advanced gastric carcinoma cases, and 15.38% (2/13) of early gastric cancer cases. Shi *et al*[29], studied the relationship between constitutive Sp1 activity and constitutive expression of VEGF in human pancreatic adenocarcinomas, and found that the level of Sp1 activity was directly correlated with the VEGF promoter activity, the steady-state level of mRNA, and VEGF secretion. These results suggested that altered expression of Sp1 in human pancreatic cancer might lead to the over-expression of multiple Sp1 downstream genes, which in turn could enhance the tumor angiogenesis and contribute to the aggressive biology of human gastric cancer. In the present study, we also found that the expression of Sp1 protein was correlated with increasing gastric cancer stage and depth of invasion. There was no significant difference in Sp1 expression between tumors with more or less lymph node metastasis. These data suggest that Sp1 might contribute to the progression and dissemination of human gastric caner via other pathways except lymph node metastasis. Sp1 expression was inversely correlated with patient long-term survival, suggesting that Sp1 could serve as an independent and sensitive prognostic marker for gastric cancer.

In summary, Sp1 is aberrantly over-expressed in gastric adenocarcinoma. Sp1 expression is closely related to the advanced stage, depth of tumor infiltration as well as poor outcome of the patients. A further understanding of the molecular basis of Sp1 will have functional implications in suppressing gastric cancer progression and ultimately lead to the design of new therapeutic strategies. On the basis of this study, we propose that increasing Sp1 expression may augment the metastatic potential of tumor cells, and may be a reliable tumor progression marker and/or effective therapeutic target for gastric cancer.

ACKNOWLEDGMENTS

We are grateful to all of the individuals described here for their contribution to this study.

REFERENCES

1 **Lu JB,** Sun XB, Dai DX, Zhu SK, Chang QL, Liu SZ, Duan WJ. Epidemiology of gastroenterologic cancer in Henan Province, China. *World J Gastroenterol* 2003; **9**: 2400-2403

2 **Chau I,** Norman AR, Cunningham D, Waters JS, Oates J, Ross PJ. Multivariate prognostic factor analysis in locally advanced and metastatic esophago-gastric cancer-pooled analysis from three multicenter, randomized, controlled trials using individual patient data. *J Clin Oncol* 2004; **22**: 2395-2403

3 **Ajisaka H,** Yonemura Y, Miwa K. Correlation of lymph node metastases and expression of matrix metalloproteinase-7 in patients with gastric cancer. *Hepatogastroenterology* 2004; **51**: 900-905

4 **Miyachi K,** Sasaki K, Onodera S, Taguchi T, Nagamachi M, Kaneko H, Sunagawa M. Correlation between survivin mRNA expression and lymph node metastasis in gastric cancer. *Gastric Cancer* 2003; **6**: 217-224

5 **Klein Kranenbarg E,** Hermans J, van Krieken JH, van de Velde CJ. Evaluation of the 5th edition of the TNM classification for gastric cancer: improved prognostic value. *Br J Cancer* 2001; **84**: 64-71

6 **Fondevila C,** Metges JP, Fuster J, Grau JJ, Palacin A, Castells A, Volant A, Pera M. p53 and VEGF expression are independent predictors of tumour recurrence and survival following curative resection of gastric cancer. *Br J Cancer* 2004; **90**: 206-215

7 **Lim JW,** Kim H, Kim KH. Expression of Ku70 and Ku80 mediated by NF-kappa B and cyclooxygenase-2 is related to proliferation of human gastric cancer cells. *J Biol Chem* 2002; **277**: 46093-46100

8 **Wang J,** Chen S. Screening and identification of gastric adenocarcinoma metastasis-related genes using cDNA microarray coupled to FDD-PCR. *J Cancer Res Clin Oncol* 2002; **128**: 547-553

9 **Roder K,** Kim KH, Sul HS. Induction of murine H-rev107 gene expression by growth arrest and histone acetylation: involvement of an Sp1/Sp3-binding GC-box. *Biochem Biophys Res Commun* 2002; **294**: 63-70

10 **Wei D,** Wang L, He Y, Xiong HQ, Abbruzzese JL, Xie K. Celecoxib inhibits vascular endothelial growth factor expression in and reduces angiogenesis and metastasis of human pancreatic cancer via suppression of Sp1 transcription factor activity. *Cancer Res* 2004; **64**: 2030-2038

11 **Zhao S,** Venkatasubbarao K, Li S, Freeman JW. Requirement of a specific Sp1 site for histone deacetylase-mediated repression of transforming growth factor beta Type II receptor expression in human pancreatic cancer cells. *Cancer Res* 2003; **63**: 2624-2630

12 **de Manzoni G,** Verlato G, Roviello F, Morgagni P, Di Leo A, Saragoni L, Marrelli D, Kurihara H, Pasini F. The new TNM classification of lymph node metastasis minimises stage migration problems in gastric cancer patients. *Br J Cancer* 2002; **87**: 171-174

13 **Wang L,** Wei D, Huang S, Peng Z, Le X, Wu TT, Yao J, Ajani J, Xie K. Transcription factor Sp1 expression is a significant predictor of survival in human gastric cancer. *Clin Cancer Res* 2003; **9**: 6371-6380

14 **Chen F,** Zhang F, Rao J, Studzinski GP. Ectopic expression of truncated Sp1 transcription factor prolongs the S phase and reduces the growth rate. *Anticancer Res* 2000; **20**: 661-667

15 **Van Cutsem E,** Haller D, Ohtsu A. The role of chemotherapy in the current treatment of gastric cancer. *Gastric Cancer* 2002; **5** Suppl 1: 17-22

16 **Ruo L,** Coit DG, Brennan MF, Guillem JG. Long-term follow-up of patients with familial adenomatous polyposis undergoing pancreaticoduodenal surgery. *J Gastrointest Surg* 2002; **6**: 671-675

17 **Kobayashi O,** Sugiyama Y, Cho H, Tsuburaya A, Sairenji M, Motohashi H, Yoshikawa T. Clinical and pathological study of gastric cancer with ovarian metastasis. *Int J Clin Oncol* 2003; **8**: 67-71

18 **Yokota J,** Nishioka M, Tani M, Kohno T. Genetic alterations responsible for metastatic phenotypes of lung cancer cells. *Clin Exp Metastasis* 2003; **20**: 189-193

19 **Yasui W,** Oue N, Ito R, Kuraoka K, Nakayama H. Search for new biomarkers of gastric cancer through serial analysis of gene expression and its clinical implications. *Cancer Sci* 2004; **95**: 385-392

20 **Koide N,** Nishio A, Hiraguri M, Shimada K, Shimozawa N, Hanazaki K, Kajikawa S, Adachi W, Amano J. Cell proliferation, apoptosis and angiogenesis in gastric cancer and its hepatic metastases. *Hepatogastroenterology* 2002; **49**: 869-873

21 **Suzuki T,** Muto S, Miyamoto S, Aizawa K, Horikoshi M, Nagai R. Functional interaction of the DNA-binding transcription factor Sp1 through its DNA-binding domain with the histone chaperone TAF-I. *J Biol Chem* 2003; **278**: 28758-28764

22 **Koutsodontis G,** Moustakas A, Kardassis D. The role of Sp1 family members, the proximal GC-rich motifs, and the upstream enhancer region in the regulation of the human cell cycle inhibitor p21WAF-1/Cip1 gene promoter. *Biochemistry* 2002; **41**: 12771-12784

23 **Mao X,** Moerman AM, Barger SW. Neuronal kappa B-binding factors consist of Sp1-related proteins. Functional implications for autoregulation of N-methyl-D- aspartate receptor-1 expression. *J Biol Chem* 2002; **277**: 44911-44919

24 **Patel SG,** DiMario JX. Two distal Sp1-binding cis-elements regulate fibroblast growth factor receptor 1 (FGFR1) gene expression in myoblasts. *Gene* 2001; **270**: 171-180

25 **Li T,** Chen YH, Liu TJ, Jia J, Hampson S, Shan YX, Kibler D, Wang PH. Using DNA microarray to identify Sp1 as a transcriptional regulatory element of insulin-like growth factor 1 in cardiac muscle cells. *Circ Res* 2003; **93**: 1202-1209

26 **Trisciuoglio D,** Iervolino A, Candiloro A, Fibbi G, Fanciulli M, Zangemeister-Wittke U, Zupi G, Del Bufalo D. bcl-2 induction of urokinase plasminogen activator receptor expression in human cancer cells through Sp1 activation: involvement of ERK1/ERK2 activity. *J Biol Chem* 2004; **279**: 6737-6745

27 **Kumar AP,** Butler AP. Enhanced Sp1 DNA-binding activity in murine keratinocyte cell lines and epidermal tumors. *Cancer Lett* 1999; **137**: 159-165

28 **Yoshida S,** Harada H, Nagai H, Fukino K, Teramoto A, Emi M. Head-to-head juxtaposition of Fas-associated phosphatase-1 (FAP-1) and c-Jun NH2-terminal kinase 3 (JNK3) genes: genomic structure and seven polymorphisms of the FAP-1 gene. *J Hum Genet* 2002; **47**: 614-619

29 **Shi Q,** Le X, Abbruzzese JL, Peng Z, Qian CN, Tang H, Xiong Q, Wang B, Li XC, Xie K. Constitutive Sp1 activity is essential for differential constitutive expression of vascular endothelial growth factor in human pancreatic adenocarcinoma. *Cancer Res* 2001; **61**: 4143-4154

Science Editor Wang XL and Li WZ **Language Editor** Elsevier HK

PO Box 2345, Beijing 100023, China
www.wjgnet.com
wjg@wjgnet.com

ELSEVIER

World J Gastroenterol 2005;11(15):2218-2223
World Journal of Gastroenterology ISSN 1007-9327

• *GASTRIC CANCER* •

Expression of *p16* gene and Rb protein in gastric carcinoma and their clinicopathological significance

Xiu-Sheng He, Ying-Hui Rong, Qi Su, Qiao Luo, Dong-Mei He, Yan-Lan Li, Yan Chen

Xiu-Sheng He, Ying-Hui Rong, Qi Su, Qiao Luo, Dong-Mei He, Yan-Lan Li, Yan Chen, Oncology Institute, Nanhua University, Hengyang 421001, Hunan Province, China
Supported by the Grant From the Education Committee of Hunan Province, No. 97B095, No. 01B016 and the grant from the Health Bureau of Hunan Province, No. 9301, the Key Programs during the 8th 5-Year Plan Period, the Bureau of Health, Hunan Province, China
Correspondence to: Dr. Qi Su, Institute of Oncology, Nanhua University, Changsheng Xilu, Hengyang 421001, Hunan Province, China. suqil@hotmail.com
Telephone: +86-734-8281075 Fax: +86-734-8281547
Received: 2003-11-26 Accepted: 2004-02-18

Abstract

AIM: To analyze the correlation between the protein expression of *p16* and *Rb* genes in gastric carcinoma (GC), to investigate the role of *p16* gene in invasion and lymph node metastasis of GC, and to examine the deletion and mutation in exon 2 of *p16* gene in GC.

METHODS: The protein expression of *p16* and *Rb* genes was examined by streptavidin-peroxidase conjugated method (S-P) in normal gastric mucosa, dysplastic gastric mucosa and GC. The deletion and mutation of *p16* gene were examined by polymerase chain reaction (PCR) and polymerase chain reaction single strand conformation polymorphism (PCR-SSCP) respectively in normal gastric mucosa and GC.

RESULTS: The positive rates of P16 and Rb protein expression respectively were 96% (77/80) and 99% (79/80) in normal gastric mucosa, 92% (45/50) and 80% (40/50) in dysplastic gastric mucosa, 48% (58/122) and 60% (73/122) in GC. The positive rates of P16 and Rb protein expression in GC were significantly lower than that in normal gastric mucosa and dysplastic gastric mucosa ($P<0.05$). The positive rate of P16 protein expression in mucoid carcinoma (10%, 1/10) was significantly lower than that in poorly differentiated carcinoma (51%, 21/41), undifferentiated carcinoma (58%, 15/26) and signet ring cell carcinoma (62%, 10/16) ($P<0.05$). The positive rates of P16 protein in 30 cases of paired primary and lymph node metastatic GC were 47% (14/30) and 17% (5/30) respectively, being significantly lower in the later than in the former ($P<0.05$). There was no mutation in exon 2 of *p16* gene in the 25 freshly resected primary GCs. But five cases in the 25 freshly resected primary GCs displayed deletion in exon 2 of *p16* gene. The positive rate of both P16 and Rb proteins was 16% (14/90), and the negative rate of both P16 and Rb proteins was 8% (7/90) in 90 GCs. The rate of positive P16 protein with negative Rb protein was 33% (30/90). The rate of negative P16 protein with positive Rb protein was 43% (39/90). There was reverse correlation between P16 and Rb expression in 90 GCs ($P<0.05$).

CONCLUSION: The loss protein expression of *p16* and *Rb* genes is related to GC. The loss expression of P16 protein is related to the histopathologic subtypes and lymph node metastasis of GC. Expression of P16 and Rb proteins in GC is reversely correlated. The deletion but not mutation in exon 2 of *p16* gene may be involved in GC.

Key words: *p16* gene; Gastric carcinoma

He XS, Rong YH, Su Q, Luo Q, He DM, Li YL, Chen Y. Expression of *p16* gene and Rb protein in gastric carcinoma and their clinicopathological significance. *World J Gastroenterol* 2005; 11(15): 2218-2223
http://www.wjgnet.com/1007-9327/11/2218.asp

INTRODUCTION

It is now widely accepted that carcinogenesis and progression of human Gastric carcinoma are related to the activation of proto-oncogenes and/or the inactivation of anti-oncogenes, and they are the results of genetic alteration accumulation. The *p16* and *Rb* genes are tumor suppressor genes and participate in regulating the proliferation of normal cell negatively[1,2]. There were abnormal expressions of P16 and Rb proteins in a variety of cancer cell lines and primary tumors, such as osteosarcoma cell lines, renal cancer cell lines, lung cancer, brain tumor, esophageal cancer, breast cancer, hepatocellular carcinoma[3] and leukemogenesis[4]. In recent years, studies have revealed homozygous deletion and mutation of *p16* gene, predominantly in exon 2, in various malignant tumors[5]. The frequency of *p16* gene deletion and mutation is up to 75% in all kinds of human neoplasm, higher than that of the well-known *p53* gene[1]. GC is one of the most common malignant tumors in China[6]. As with many other tumors, development of GC also involves multiple genes and stages, including some oncogenes and antioncogenes. However, till now, its carcinogenic molecular mechanism is not well clarified. In this paper, S-P immunohistochemical staining was used to detect the expression of P16 and Rb proteins in GC, dysplastic gastric mucosa and normal gastric mucosa. PCR and PCR-SSCP

methods were used to detect deletion and mutation in exon 2 of *p16* gene. We aimed at investigating the role of P16 protein in the carcinogenesis, progression, histologic types as well as biological behaviors of GC, to find a new marker for early diagnosis of GC, to discover the role of deletion and mutation in exon 2 of *p16* gene in the carcinogenesis and progression of GC, and also to analyze the correlation of P16 and Rb proteins expression in GC.

MATERIALS AND METHODS

Specimens and treatment

All specimens were confirmed by pathological examination. Paraffin-embedded tissue specimens were collected from the pathology department and freshly resected specimens were collected from the surgery department of the First Affiliated Hospital of Nanhua University, among which there were 50 cases of dysplastic gastric mucosa, 80 cases of normal gastric mucosa (including 25 freshly resected specimens far away from cancer) and 122 GC (including 25 freshly resected specimens). In the 122 cases of GC, 29 were well-differentiated adenocarcinoma, 41 poorly-differentiated adenocarcinoma, 26 undifferentiated carcinoma, 16 signet ring cell carcinoma and 10 mucoid carcinoma. There were 81 men and 41 women, including 22 aged below 40 years, 69 aged from 41 to 59 years, and 31 older than 60 years (range 15-79, mean 56 years). Superficial muscles were invaded in 50 cases, deep muscles and the full layer in 72 cases. Sixty-nine cases had lymph node metastasis. The other 53 cases had no lymph node metastasis. Thirty cases of primary cancer and lymph node metastatic cancer respectively, were randomly selected and compared. According to Borrmann's classification[7], 15 GCs were type I, 43 type II 47 type III and 17 type IV. The 25 freshly resected specimens, each containing cancer, cancer adjacent tissues and normal mucosa far away from cancer, were cut into 2-4 blocks under sterile conditions. Each block was 2-3 mm^3 in size and stored at -70 ℃ for PCR and PCR-SSCP analyses. The rest of the tissues were fixed in 100 mL/L neutral formalin, resected, dehydrated, cleaned and paraffin-embedded. All paraffin-embedded tissues were cut into sequential slices at 5 μm thickness and mounted on to the glass slides that had been processed by poly-lys previously.

Reagents and instruments

Rabbit-anti-human P16 protein polyclonal antibody, rabbit-anti-human Rb protein polyclonal antibody, streptavidin-peroxidase immunozator kit (S-P kit), and DAB were all purchased from Maxim Company, USA. Protease K (Merk, USA), SmaI, agarose gel, propylene acrylamide, *N-N*-sulmethyl bipropylene acrylamide, ammonium persulfate, xylene nitrile, bromophenol blue were purchased from Shanghai Sangon Company. PCR primers were synthesized by Shanghai Sangon. Primer sequences in exon 2 of p16 gene: sense 5'-TCT GAC CAT TCT GTT CTC TC-3', antisense 5'-CTC AGC TTT GGA AGC TCT CA-3', were used for PCR and PCR-SSCP. The fragment length of amplification was 384 bp. Primer sequences of β-actin served as an internal control for PCR: sense 5'-GCG GGG CGC CCC AGG CAC CA-3', antisense 5'-CTC CTT AAT GTC ACG CAC GAT TTC-3'. The fragment length of amplification was 548 bp. Experimental instruments included ultra low refrigerator of -70 ℃ (Japan), rotary sector (Germany), microscope (Japan), type 480 DNA amplificatory (PE, USA), type 901 ultraviolet spectrophotometer (PE, USA), type DYB vertical electrophoresis and various kinds of centrifuges (Liuyi, Beijing).

Methods

S-P immunohistochemical staining According to the specification of S-P kit: paraffin-embedded tissue slices were deparaffinized and hydrated for 20 min, endogenous peroxidase was blocked for 10 min, first antibody was added (rabbit-anti-human P16 protein polyclonal antibody or rabbit-anti-human Rb protein polyclonal antibody) for 8 h at 4 ℃, bridge antibody was added for 15 min, enzyme labeled S-P reagents were added for 10 min, and was colored with DAB for 5 min, nucleolus was stained with hematoxylin for 3 min, dehydrated for 15 min, cleaned for 10 min, later was covered and observed under a microscope.

Genomic DNA extraction[8] Frozen tissue of 0.5 g was put into liquid nitrogen and powdered immediately, followed by addition of 10× buffer (10 mmol/L Tris-HCl, pH 8.0, 0.1 mol/L EDTA, pH 8.0, 5 g/L SDS) in 37 ℃ water for 1 h. At the same time, protease K was added to the mixture at a final concentration of 100 mg/L in 50 ℃ water for 3 h. After the mixtures were dissolved completely, the mixtures were reacted with 20 mg/L Rnase in 37 ℃ water for 1 h. It was mixed with saturated phony and bugged slightly for 10 min, then centrifuged and supernatant was extracted, and transferred to a cleaned plastic tube. The above processes were repeated thrice. The supernatant was added with 1/10 volume 3 mol/L NaAc and 2-2.5 times cold ethyl, and centrifuged. DNA was precipitated, ethyl removed. DNA was washed by 700 mL/L ethyl and centrifuged thrice, dried, resolved with TE and stored at -20 ℃ for use.

PCR amplification PCR was performed according to the reference[8] in 50 μL reaction mixture containing 0.1 μg of DNA template, 200 μmol/L each of dCTP, dATP, dGTP, dTTP, 0.25 μmol/L primer, PCR buffer (10 mmol/L Tris-HCl, pH 8.3, 1.5 μmol/L $MgCl_2$, 50 mmol/L KCl, 100 mg/L gelatin). Then the reaction mixture was pre-denatured at 95 ℃ for 5 min and added with 1.5 μL of Taq DNA polymerase and 75 μL of mineral oil. These samples were subjected to 30 amplification cycles, each consisting of denaturation at 95 ℃ for 1 min, primer annealing at 60 ℃ for 1 min, and extension at 72 ℃ for 1 min. Finally, the samples were subjected to a further extension at 72 ℃ for 5 min. A 5 μL of PCR product was electrophoresed on agarose gel (20 g/L), then observed and photographed under ultraviolet light. No products of PCR amplification suggested loss of homozygosis of *p16* gene.

PCR-SSCP analysis[8] A 5 μL of PCR product digested by *SmaI* was mixed with 5 μL of denatured dissolution (950 mL/L formamide, 20 mmol/L EDTA, 0.05% bromophenol blue, 0.5 g/L xylene nitrile) and denatured at 95 ℃ for 5 min, and then cooled on ice. Solution processed as above was added to the gel containing 80 g/L polypropylene acrylamide, vertically electrophoresed at 100 V for 4 h. The gel stained with silver was fixed in 100 mL/L alcohol for 10 min, oxidized in 100 g/L nitric acid for 3 min, drip washed for 1 min with double distilled water, stained in 12 mmol/L silver nitric acid for 20 min, again drip washed

Table 1 **P16 protein expression, *p16* gene mutation and deletion in GC**

Histologic types	*n*	P16 protein					*p16* gene	
		–	+	++	+++	Positive rate (%)	Mutation	Deletion
Normal gastric mucosa[a]	80	3	41	20	16	96	0/25	0/25
Dysplastic gastric mucosa[a]	50	5	12	19	14	92	0/25	0/25
GC	122	64	13	20	25	48	0/25	5/25

[a]$P<0.05$ *vs* GC.

for 1 min with double distilled water, showed appropriately colored in 0.028 moL anhydrous sodium carbonate and 0.19 mL/L formalin, reduction response was ended by 100 mL/L glacial acetic acid, drip washed with double distilled water. The results were analyzed and photographed. The abnormal traces found in PCR-SSCP were considered gene mutation.

Immunohistochemical determination The brown-yellow staining of nucleus or nucleus and cytoplasm was considered positive; (-) indicates no positively stained cell or only plasma stained or the number of nuclear stained positive cells less than 1; (+) indicates the cells stained weakly or the number of stained cells less than 25%; (++) indicates the cells stained moderately or the stained cells about 26-50%; (+++) indicates cells stained strongly or the number of stained cells more than 50%. Positive nuclear staining in more than two cells (under high power microscope) was considered to be positive. No folding, and edging-effect fields were chosen during calculation of 100 cells per five fields. The assessment was performed by two observers. P16 protein expression in positively confirmed cervical carcinoma served as positive control. The first antibody was replaced with PBS for negative control.

Statistical analysis

χ^2 test was used to analyze the data. *P* value less than 0.05 was considered statistically significant.

RESULTS

Expression of P16 protein in GC

P16 protein expression could only be seen in particular adenoepithelial cells. We did not find positive staining in mucosal epithelial cells, matrix fibrocytes, lymphocytes and smooth myocytes. The positive rate of P16 protein expression was 96% (77/80) in normal gastric mucosa (Figure 1A) and 90% (45/50) in dysplastic gastric mucosa (Figure 1B). There was no significant difference in these mucosa. But in GC, the positive rate of P16 protein expression was 48% (58/122) (Figures 1C-F), lower than that in normal and dysplastic mucosa ($P<0.05$, Table 1). The positive rate of P16 protein expression was 38%, 51%, 58%, 62% and 10% in well-differentiated adenocarcinoma, poorly-differentiated adenocarcinoma, undifferentiated carcinoma, signet ring cell carcinoma and mucoid carcinoma, respectively. The P16 protein expression in mucoid carcinoma was significantly lower than that in signet ring cell carcinoma, undifferentiated carcinoma and poorly-differentiated adenocarcinoma ($P<0.05$, Table 2). The positive rate of P16 protein expression was 48% (24/50) in GC with superficial muscle layer invasion and 47% (34/72) in GC with deep muscle and full layer invasion. There was no apparent relevance between P16 protein expression and the depth of invasion (Table 2). In 30 cases of paired primary and lymph node metastatic GC, the rate of P16 protein expression in lymph node metastatic cancer (17%, 5/30) was significantly lower than that of primary cancer (47%, 14/30) ($P<0.05$, Table 3).

Deletion and mutation in exon 2 of p16 gene in GC

Among 25 freshly resected GCs, there were seven well-differentiated adenocarcinoma, 13 poorly-differentiated adenocarcinoma, three undifferentiated carcinoma, one signet ring cell carcinoma and one mucoid carcinoma. Cancer adjacent tissue and normal gastric mucosa were taken at the same time. The PCR amplification showed no product in one case of well-differentiated adenocarcinoma, one case of poorly-differentiated adenocarcinoma and one case of mucoid carcinoma. Few products found in one case of well-differentiated adenocarcinoma and one case of poorly-differentiated adenocarcinoma. But the remaining 20 cases of GC, cancer adjacent gastric mucosa and normal gastric mucosa showed products of PCR amplification. All experiments were repeated thrice. The results were identical. No product of PCR amplification could indicate the loss of homozygosis of *p16* gene, few products of PCR amplification showed possible loss of heterozygosis or homozygosis of *p16* gene contaminated with normal mucosa (Figure 2). Four of these five cases showed negative expression for P16 protein and one case showed weak expression detected with immunohistochemical staining. No gene mutation was observed by PCR-SSCP analysis after the PCR amplification products were cut with *SmaI* (Figure 3 and Table 1).

Table 2 **P16 protein expression in various histologic types of GC**

Histologic types	*n*	Positive	Negative	Positive rate (%)
Well-differentiated adenocarcinoma[a]	29	11	18	38
Poorly-differentiated adenocarcinoma[a]	41	21	20	51
Undifferentiated carcinoma[a]	26	15	11	58
Signet ring cell carcinoma[a]	16	10	6	62
Mucoid carcinoma	10	1	9	10

[a]$P<0.05$ *vs* mucoid carcinoma.

Table 3 **P16 protein expression in primary GC and lymph node metasatic GC**

Types	*n*	Positive	Positive rate (%)
Primary GC[a]	30	14	47
Lymph node metasatic GC	30	5	17

[a]$P<0.05$ *vs* lymph node metasatic GC.

Table 4 **Rb protein expression in GC**

Types	*n*	Negative		Positive		Positive rate (%)
		–	+	++	+++	
Normal gastric mucosa[a]	80	1	10	20	49	99
Dysplastic gastric mucosa[a]	50	10	8	17	15	80
GC	122	49	17	30	26	60

[a]$P<0.05$ *vs* GC.

Table 5 **Correlation between expression of P16 and Rb proteins in GC**

	n	Positive Rb		Negative Rb	
		n	(%)	*n*	(%)
Positive P16[a]	44	14	16	30	33
Negative P16	46	39	43	7	8

[a]$P<0.05$ *vs* negative P16.

Expression of Rb protein in GC

The positive rate of Rb protein expression in normal gastric mucosa was 99% (79/80), 80% (40/50) in dysplastic gastric mucosa, and 60% (73/122) in GC (Figure 4). The positive rate of Rb protein expression in GC was significantly lower than that in normal gastric mucosa and dysplastic mucosa ($P<0.05$, Table 4). There was no significant difference between the normal gastric mucosa and dysplastic gastric mucosa ($P>0.05$, Table 4).

Correlation between the expression of P16 and Rb proteins in GC

Ninety paired GCs were selected from 122 cases of GC to make a comparison analysis. The positive expression of both P16 and Rb proteins was 16% (14/90), the negative expression of both P16 and Rb proteins was 8% (7/90). The positive expression of P16 with negative expression of Rb was 33% (30/90). The negative expression of P16 with positive expression of Rb was 43% (39/90). The results suggested negative correlation between P16 and Rb proteins expression in GC ($P<0.05$, Table 5).

DISCUSSION

The development of human cancers including GC is a multi-step process and phenotypic changes during cancer progression reflect the sequential accumulation of genetic alterations in cells[9]. Both *p16* and *Rb* genes are tumor suppressor genes. They play important roles in the regulation of the cell cycle. The proteins of these two genes, P16 and pRb respectively, inhibit cell progression from G_1 to S phase[1,2]. Dephosphorylation retinoblastoma protein (Rb) inactivates the transcription factors such as E2F1, an important factor for the transition from G_1 to S phase, thereby arrests cells in G_0/G_1 phase, resulting in suppressed cell division and proliferation. When Rb protein is phosphorylated, several transcription factors are released, which induce the cell from G_1 to S phase rapidly, resulting in excessive proliferation of cell. P16 has been shown to exert its function through

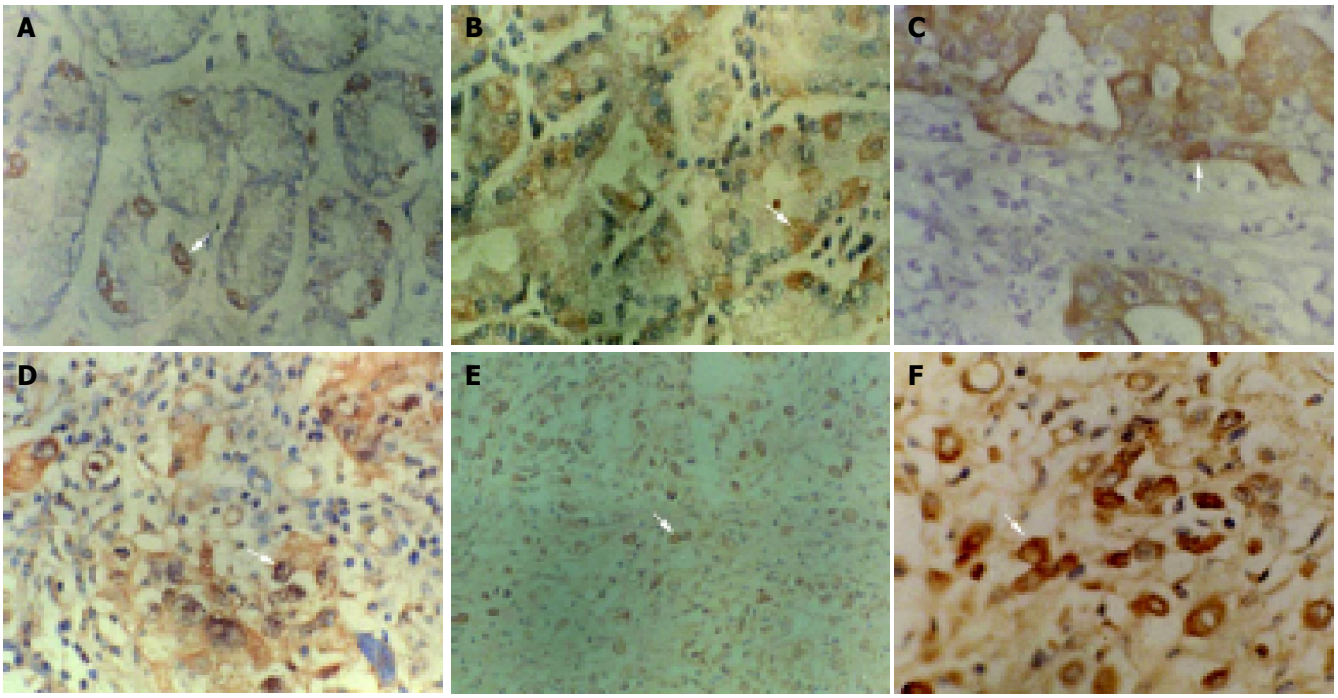

Figure 1 Immunohistochemical staining of P16 protein expression. Arrow shows positive cell. **A**: Normal gastric mucosa SP ×400; **B**: dysplastic gastric mucosa SP ×400; **C**: well-differentiated adenocarcinoma SP ×400; **D**: poorly-differentiated adenocarcinoma SP ×400; **E**: undifferentiated carcinoma SP ×200; **F**: undifferentiated carcinoma SP ×400.

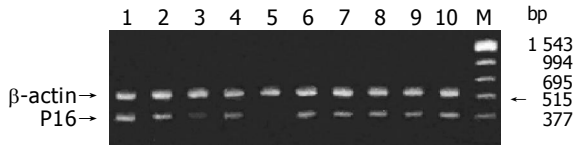

Figure 2 PCR amplification products in exon 2 of *p16* gene. Lanes 1-3, 5-6, 8-10: GC; Lane 4 : normal gastric mucosa; Lane 7: cancer adjacent tissue; Lane M: marker; Few PCR products in lane 3 and no PCR product in lane 5.

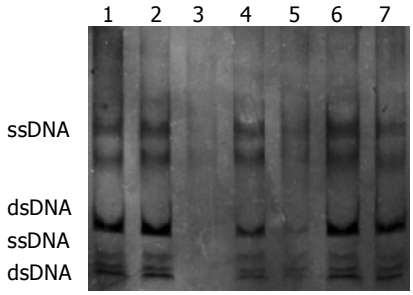

Figure 3 Exon 2 of *p16* gene analyzed by SSCP, Lanes 2, 3, 5, 6, 7: GC; Lane 4: cancer adjacent tissue; Lane 1: normal gastric mucosa. No electrophoresis band in lane 3; weak electrophoresis band in lane 5; no abnormal electrophoresis band in all lanes.

inhibition of cyclin-dependent kinase 4(CDK4) mediated phosphorylation of pRb. Functional loss of *p16* might result in nonregulation of CDK4 activity, leading to persistent pRb phosphorylation and uncontrolled cellular proliferation[1,2]. Abnormalities of *p16* and *Rb* genes are frequent molecular events in human cancer[10-13]. Some investigations demonstrated increased cell cycle arrest, growth inhibition and apoptosis after adenovirus-mediated transduction of *p16* gene in gliomas, lung, pancreas, liver, head and neck tumor cell lines[1,2]. All these findings indicate that *p16* and *Rb* are important tumor suppressor genes.

In human GC, loss of *p16* expression is common. Our result showed that the positive rate of P16 protein expression in GC was remarkably lower than that in dysplastic gastric mucosa and normal gastric mucosa. This is in accordance with observations by others[1-3]. These results indicated that P16 loss expression was characteristically associated with tumor progression in GC. Several other studies have shown that re-expression of *p16* in various tumor cell lines was sufficient to cause arrest of the cells in G_1 phase[14,15]. In our study, there was no significant difference between the normal mucosa and the dysplastic mucosa of stomach in P16 protein expression. Interestingly, the expression quantity of P16 protein increased from normal mucosa to precancerous lesions and GC. Nguyen *et al*[16], found that the level of *p16* mRNA in part of prostate carcinoma was higher than that in prostate tissues. They also showed that P16 protein expression increased with the progression of the pathologic lesion. This change might inhibit cell proliferation. Our results showed that the positive rate of P16 protein expression was significantly lower in mucoid carcinoma than that in poorly-differentiated adenocarcinoma, undifferentiated carcinoma and signet cell carcinoma. It suggested that the alteration of *p16* gene was different between various histologic types of GC. The discrepancy of P16 protein

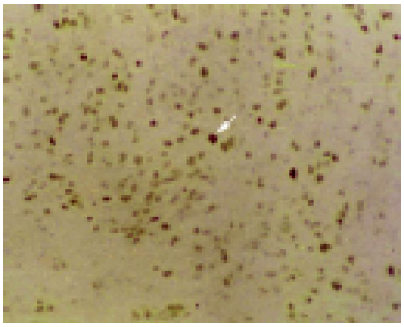

Figure 4 Rb protein expression in undifferentiated carcinoma, SP×200.

expression also existed between various histologic types of lung cancer, esophageal cancer and gliomas[10,17]. In our investigation, P16 protein expression was not significantly related to sex, age, the depth of invasion and Borrmann's classification. However, decreased expression of *p16* was found more frequently in lymph node metasatic GC than in primary GC. It was demonstrated that the loss of expression of P16 protein contributed to tumor progression with lymph node metastasis, which is in agreement with previous reports[6]. Some studies indicated that the loss of *p16* expression was associated with aggressive phenotype and poor prognosis of several tumors[18]. The positive expression of P16 protein could merely be observed in partial adeno-epithelial cells of normal and dysplastic gastric mucosa, and were weakly positive or undetectable in gastric mucosa epithelium cells, interstitial lymphocytes, fibroblasts and smooth muscle cells, which were contrary to some published reports[19]. Nevertheless, P16 protein expression was undetectable in neoplasmic stroma[20], normal lung tissue[21] and normal urethral epithelium cells[19]. This might attribute to a paucity of P16 molecule in G_0/G_1 phase cells[22] or a short half-life of P16 protein[23].

Some studies have shown that deletion and mutation of *p16* gene are important mechanisms responsible for the dysfunction of tumor suppressor genes[24]. In our present study, deletion in exon 2 of *p16* gene was detected in five GC tissues. But PCR amplification products appeared in the rest of the 20 cases of GC, normal gastric mucosa and cancer adjacent gastric mucosa, suggesting an association between deletion of *p16* gene and GC. Previous studies have shown that deletion of *p16* gene is associated with the degree of differentiation and metastasis of GC. Our observation failed to demonstrate the similar trend. It was likely that only exon 2 was examined due to inadequate specimens or other unknown factors. The mutation of *p16* gene was not found by SSCP analysis of digestion product of PCR amplification. The results revealed that point mutation of *p16* gene was rare during gastric carcinogenesis. It coincides with previous findings[25,26]. It was also implied that the frequency of *p16* gene deletion was lower than that of loss of P16 protein expression. Some other uncertain mechanisms might exist in the regulation of *p16* gene expression. Many studies suggested that hypermethylation of *p16* gene was the major process for its inactivation in GC and an important mechanism in gastric carcinogenesis[27]. Further studies are needed to prove this.

Immunohistochemical analysis showed that the positive rate of pRb was significantly lower in GC than in normal

gastric mucosa and dysplastic gastric mucosa. The result indicated GC carcinogenesis was probably related with the loss of pRb expression, which was consistent with other reports[28]. Serrano *et al*[1], have proposed that physiological inactivation of *Rb* during G_1 phase leads to increased *p16* expression in order to limit CDK4 activity. Genetic inactivation of *Rb* would also stimulate cell to increase *p16* expression in an ultimately unnecessary attempt to inhibit CDK4. This negative feedback model predicts that Rb-negative tumors would have high levels of *p16*, while Rb-positive tumors might require decreased amounts of functional *p16* in order to achieve a level of CDK4 activity sufficient for *Rb* inactivation. Shapiro *et al*[21], also confirmed the inverse reciprocity between *Rb* inactivation and *p16* expression in lung cancer. We therefore sought to determine whether there was a specific correlation between *p16* gene and *Rb* gene in GC. We analyzed the relationship between P16 and pRb expression in GC. The result indicated that there was not only loss of P16 and Rb proteins expression, but also negative correlation between P16 and Rb expression in human GC which is consistent with others[29]. These support the hypothesis that *p16* and *Rb* genes adjust with each other by negative feedback in cell cycle regulation and indicate that the alteration of *p16* and *Rb* gene expression may be involved in carcinogenesis and progression of human GC.

REFERENCES

1 **Serrano M,** Hannon GJ, Beach D. A new regulatory motif in cell-cycle control causing specific inhibition of cyclin D/CDK4. *Nature* 1993; **366**: 704-707
2 **Kamb A,** Gruis NA, Weaver-Feldhaus J, Liu Q, Harshman K, Tavtigian SV, Stockert E, Day RS, Johnson BE, Skolnick MH. A cell cycle regulator potentially involved in genesis of many tumor types. *Science* 1994; **264**: 436-440
3 **Peng CY,** Chen TC, Hung SP, Chen MF, Yeh CT, Tsai SL, Chu CM, Liaw YF. Genetic alterations of INK4alpha/ARF locus and p53 in human hepatocellular carcinoma. *Anticancer Res* 2002; **22**: 1265-1271
4 **Mitani K.** Molecular mechanisms in leukemogenesis. *Gan To Kagaku Ryoho* 2002; **29**: 1107-1112
5 **Sasaki S,** Kitagawa Y, Sekido Y, Minna JD, Kuwano H, Yokota J, Kohno T. Molecular processes of chromosome 9p21 deletions in human cancers. *Oncogene* 2003; **22**: 3792-3798
6 **He XS,** Su Q, Chen ZC, He XT, Che SY. Expression, Mutation and Deletion of p16 Gene in gastric carcinoma. *Aizheng* 2001; **20**: 468-473
7 **Borrman R.** Geschwülste des Magens und Duodenums. In Henke F. Lubarsch O. eds: Handbuch der Speziellen Pathologischen Anatomie und Histologie. *Berlin Julius Springer* 1926: 864-871
8 **Sambrook J,** Frisch EF, Maniatis T. Molecular Cloning, A Laboratory Manual 2nded, *Cold Spring Harbor Laboratory Press* 1989
9 **Yasui W,** Yokozaki H, Fujimoto J, Naka K, Kuniyasu H, Tahara E. Genetic and epigenetic alterations in multistep carcinogenesis of the stomach. *J Gastroenterol* 2000; **35 Suppl 12**: 111-115
10 **Kratzke RA,** Greatens TM, Rubins JB, Maddaus MA, Niewoehner DE, Niehans GA, Geradts J. Rb and p16INK4a expression in resected non-small cell lung tumors. *Cancer Res* 1996; **56**: 3415-3420
11 **Jarrard DF,** Modder J, Fadden P, Fu V, Sebree L, Heisey D, Schwarze SR, Friedl A. Alterations in the p16/pRb cell cycle checkpoint occur commonly in primary and metastatic human prostate cancer. *Cancer Lett* 2002; **185**: 191-199
12 **Mobley SR,** Liu TJ, Hudson JM, Clayman GL. *In vitro* growth suppression by adenoviral transduction of p21 and p16 in squamous cell carcinoma of the head and neck: a research model for combination gene therapy. *Arch Otolaryngol Head Neck Surg* 1998; **124**: 88-92
13 **Tsujie M,** Yamamoto H, Tomita N, Sugita Y, Ohue M, Sakita I, Tamaki Y, Sekimoto M, Doki Y, Inoue M, Matsuura N, Monden T, Shiozaki H, Monden M. Expression of tumor suppressor gene p16(INK4) products in primary gastric cancer. *Oncology* 2000; **58**: 126-136
14 **Arap W,** Nishikawa R, Furnari FB, Cavenee WK, Huang HJ. Replacement of the p16/CDKN2 gene suppresses human glioma cell growth. *Cancer Res* 1995; **55**: 1351-1354
15 **Frizelle SP,** Grim J, Zhou J, Gupta P, Curiel DT, Geradts J, Kratzke RA. Re-expression of p16INK4a in mesothelioma cells results in cell cycle arrest, cell death, tumor suppression and tumor regression. *Oncogene* 1998; **16**: 3087-3095
16 **Nguyen TT,** Nguyen CT, Gonzales FA, Nichols PW, Yu MC, Jones PA. Analysis of cyclin-dependent kinase inhibitor expression and methylation patterns in human prostate cancers. *Prostate* 2000; **43**: 233-242
17 **Nishikawa R,** Furnari FB, Lin H, Arap W, Berger MS, Cavenee WK, Su Huang HJ. Loss of P16INK4 expression is frequent in high grade gliomas. *Cancer Res* 1995; **55**: 1941-1945
18 **Kawabuchi B,** Moriyama S, Hironaka M, Fujii T, Koike M, Moriyama H, Nishimura Y, Mizuno S, Fukayama M. p16 inactivation in small-sized lung adenocarcinoma: its association with poor prognosis. *Int J Cancer* 1999; **84**: 49-53
19 **Reznikoff CA,** Yeager TR, Belair CD, Savelieva E, Puthenveettil JA, Stadler WM. Elevated p16 at senescence and loss of p16 at immortalization in human papillomavirus 16 E6, but not E7, transformed human uroepithelial cells. *Cancer Res* 1996; **56**: 2886-2890
20 **Geradts J,** Hruban RH, Schutte M, Kern SE, Maynard R. Immunohistochemical p16INK4a analysis of archival tumors with deletion, hypermethylation, or mutation of the CDKN2/MTS1 gene. A comparison of four commercial antibodies. *Appl Immunohistochem Mol Morphol* 2000; **8**: 71-79
21 **Shapiro GI,** Edwards CD, Kobzik L, Godleski J, Richards W, Sugarbaker DJ, Rollins BJ. Reciprocal Rb inactivation and p16INK4 expression in primary lung cancers and cell lines. *Cancer Res* 1995; **55**: 505-509
22 **Tam SW,** Shay JW, Pagano M. Differential expression and cell cycle regulation of the cyclin-dependent kinase 4 inhibitor p16Ink4. *Cancer Res* 1994; **54**: 5816-5820
23 **Shapiro GI,** Park JE, Edwards CD, Mao L, Merlo A, Sidransky D, Ewen ME, Rollins BJ. Multiple mechanisms of p16INK4A inactivation in non-small cell lung cancer cell lines. *Cancer Res* 1995; **55**: 6200-6209
24 **Giroux MA,** Audrezet MP, Metges JP, Lozac'h P, Volant A, Nousbaum JB, Labat JP, Gouerou H, Ferec C, Robaszkiewicz M. Infrequent p16/CDKN2 alterations in squamous cell carcinoma of the oesophagus. *Eur J Gastroenterol Hepatol* 2002; **14**: 15-18
25 **Gunther T,** Schneider-Stock R, Pross M, Manger T, Malfertheiner P, Lippert H, Roessner A. Alterations of the p16/MTS1-tumor suppressor gene in gastric cancer. *Pathol Res Pract* 1998; **194**: 809-813
26 **Sakata K,** Tamura G, Maesawa C, Suzuki Y, Terashima M, Satoh K, Eda Y, Suzuki A, Sekiyama S, Satodate R. Loss of heterozygosity on the short arm of chromosome 9 without p16 gene mutation in gastric carcinomas. *Jpn J Cancer Res* 1995; **86**: 333-335
27 **Ficorella C,** Cannita K, Ricevuto E, Toniato E, Fusco C, Sinopoli NT, De Galitiis F, Di Rocco ZC, Porzio G, Frati L, Gulino A, Martinotti S, Marchetti P. P16 hypermethylation contributes to the characterization of gene inactivation profiles in primary gastric cancer. *Oncol Rep* 2003; **10**: 169-173
28 **Ogawa M,** Maeda K, Chung YS, Onoda N, Kato Y, Nakata B, Sowa M. Correlation between expression of RB protein and prognosis of gastric cancer. *Gan To Kagaku Ryoho* 1996; **23** Suppl 2: 148-150
29 **Lee WA,** Woo DK, Kim YI, Kim WH. p53, p16 and RB expression in adenosquamous and squamous cell carcinomas of the stomach. *Pathol Res Pract* 1999; **195**: 747-752

Science Editor Kumar M and Zhu LH **Language Editor** Elsevier HK

PO Box 2345, Beijing 100023, China
www.wjgnet.com
wjg@wjgnet.com

ELSEVIER

World J Gastroenterol 2005;11(15):2224-2229
World Journal of Gastroenterology ISSN 1007-9327

• *GASTRIC CANCER* •

Suppression of gastric cancer growth by adenovirus-mediated transfer of the PTEN gene

Ying Hang, Yong-Chen Zheng, Yan Cao, Qing-Shan Li, Yu-Jie Sui

Ying Hang, Yong-Chen Zheng, Yan Cao, Yu-Jie Sui, Central Laboratory, The Second Hospital of Jilin University, Chuangchun 130041, Jilin Province, China
Qing-Shan Li, Department of Biochemistry and Molecular Biology, Life Science School of Jilin University, Chuangchun 130021, Jilin Province, China
Supported by the National Natural Science Foundation of China, No. 39970229
Correspondence to: Dr. Ying Hang, Central Laboratory, The Second Hospital of Jilin University, 18 Zi Qiang Street, Chuangchun 130041, Jilin Province, China. angelah622000@yahoo.com.cn
Telephone: +86-431-8796575 Fax: +86-431-8934741
Received: 2004-04-27 Accepted: 2004-07-11

Abstract

AIM: To investigate the tumor-suppressive effect of the phosphatase and tensin homologue deleted from chromosome (PTEN) in human gastric cancer cells that were wild type for PTEN.

METHODS: Adenoviruses expressing PTEN or luciferase as a control were introduced into gastric cancer cells. The effect of exogenous PTEN gene on the growth and apoptosis of gastric cancer cells that are wtPTEN were examined *in vitro* and *in vivo*.

RESULTS: Adenovirus-mediated transfer of PTEN (Ad-PTEN) suppressed cell growth and induced apoptosis significantly in gastric cancer cells (MGC-803, SGC-7901) carrying wtPTEN in comparison with that in normal gastric epithelial cells (GES-1) carrying wtPTEN. This suppression was induced through downregulation of the Akt/PKB pathway, dephosphorylation of focal adhesion kinase and mitogen-activated protein kinase and cell-cycle arrest at the G2/M phase but not at the G1 phase. Furthermore, treatment of human gastric tumor xenografts (MGC-803, SGC-7901) with Ad-PTEN resulted in a significant (P<0.01) suppression of tumor growth.

CONCLUSION: These results indicate a significant tumor-suppressive effect of Ad-PTEN against human gastric cancer cells. Thus, Ad-PTEN may be used as a potential therapeutic strategy for treatment of gastric cancers.

Key words: PTEN; Gastric cancer

Hang Y, Zheng YC, Cao Y, Li QS, Sui YJ. Suppression of gastric cancer growth by adenovirus-mediated transfer of the PTEN gene. *World J Gastroenterol* 2005; 11(15): 2224-2229
http://www.wjgnet.com/1007-9327/11/2224.asp

INTRODUCTION

Phosphatase and tensin homolog deleted from chromosome 10 (PTEN) gene is a tumor-suppressor gene located on human chromosome 10q23.3[1,2]. Frequent deletions and somatic mutations of PTEN have been reported in glioblastoma, endometrial cancer, prostate cancer, and small cell lung cancer[3-7]. Furthermore, germline mutations of PTEN are the cause of Cowden disease and Bannayan-Zonana syndrome, which are autosomal dominant cancer predisposition disorders[8-10]. PTEN functions both as a protein and as a lipid phosphatase in cells that are genotypically wild type for PTEN[11,12]. PTEN also modulates the phosphatidylinositol 3-kinase (PI3K) pathway by catalyzing degradation of PtdIns (3, 4, 5) P3 generated by PI3K. This mechanism inhibits downstream functions mediated by the PI3K pathway, such as activation of Akt/protein kinase B (PKB), cell survival, and cell proliferation[13]. Thus, overexpression of PTEN in cancer cells carrying mutant- or deletion-type PTEN can inhibit cell proliferation and tumorigenicity via induction of cell-cycle arrest at G1 phase and apoptosis[14-17]. Although studies demonstrating the inhibitory function of PTEN in tumor cell mutants for PTEN exist, very little information is available on the effect of PTEN in tumor cells that are wild type for PTEN (wtPTEN). More recently, studies using melanoma cells, ovarian and thyroid cancer cells that are wtPTEN demonstrated ectopic expression of PTEN resulting in growth inhibition and cell death[18-20]. Based on these reports, we investigated the tumor-suppressive effect of PTEN on gastric cancer cells that were wtPTEN.

In the present study, we demonstrated that adenovirus mediated overexpression of PTEN (Ad-PTEN) in gastric cancer cells and in normal gastric epithelial cells that were wtPTEN resulted in selective induction of G2 cell-cycle arrest and apoptosis in tumor cells, but not in normal cells. Furthermore, treatment of gastric tumor xenografts with Ad-PTEN resulted in tumor inhibition. These results indicate that Ad-PTEN can be used as a gene therapeutic strategy for the treatment of gastric cancers.

MATERIALS AND METHODS

Cell lines and cell culture

Human gastric carcinoma metastatic lymph node cell line, SGC-7901, and normal gastric epithelial cell line, GES-1, were obtained from Cancer Research Institute of Beijing,

China. Human gastric mucinous adenocarcinoma cell line, MGC-803, was obtained from the Cell Bank of Shanghai Institute of Cell Biology, Chinese Academy of Sciences (Shanghai, China). The derived cell lines were grown in IMDM medium supplemented with 10% heat-inactivated fetal calf serum, 50 U/mL penicillin and 50 μg/mL streptomycin. The cells were maintained at 37 ℃ in a humidified atmosphere containing 50 mL/L CO_2. Viability of the cells used in these experiments was consistently more than 95% when evaluated by the trypan blue exclusion method.

Construction of recombinant adenoviral vector

To construct adenoviruses carrying PTEN (Ad-PTEN), cDNA of PTEN was cloned by RT-PCR using placental mRNA as a template and the following primers: 5'-CTTCA-GCCACAGGCTCCCA-3' and 5'-TGGTGTTTTATCCC-TCTTGATA-3'. A 1.2-kb blunt-ended fragment of PTEN cDNA was inserted into the SwaI site of the cosmid pAxCAwt (TaKaRa) that contained the CAG promoter and an entire genome of type 5 adenoviruses except for E1 and E3 regions. This procedure generated pAxCAPTEN. The pAxCAPTEN was cotransfected with pJM17 (Microbix Biosystems Inc., Canada) into 293 cells to obtain Ad-PTEN viruses. As a control, Ad-Luc viruses were constructed. Viruses were propagated in the 293 cells lines and purified by two rounds of CsCl density centrifugation. Viral titers were measured in a limiting-dilution bioassay using the 293 cells. Recombinant adenovirus infections of the cell lines were carried out by dilution of viral stock to certain concentrations, addition of viral solution to cell monolayers, and incubation at room temperature for 30 min with agitation every 10 min. This was followed by addition of culture medium and the return of the infected cells to the 37 ℃ incubator.

Transduction and cell proliferation assay

All the cell lines were plated in six-well tissue culture plates at a density of 1×10^5 cells/well. Tumor cells and normal cells were then treated with Ad-PTEN or Ad-Luc, or treated with PBS as a mock control. Cells in each treatment group were plated in triplicate and cultured for 5 d. Then, at designated time points, cells were harvested and stained with 0.4% trypan blue (GIBCO BRL, Grand Island, NY, USA) to reveal dead cells. Viable cells were then counted using a hemocytometer.

Apoptotic staining

Cells were seeded in six-well tissue culture dishes at a density of 1×10^5 cells/well and treated with Ad-PTEN or Ad-Luc. At 72 h after treatment, cells were analyzed for apoptosis using Hoechst 33 258 staining (Sigma Chemicals, St. Louis, MO, USA). Apoptotic cells were determined via apoptotic body and/or chromosome condensation.

Cell-cycle analysis

Cells were seeded in 10-cm culture dishes ($5\text{-}10\times10^5$ cells/dish) and treated with Ad-PTEN or Ad-Luc, or treated with PBS, 20 μmol/L LY294002 (Cell Signaling Technology, Beverly, MA, USA). At specific time points after treatment, cells were harvested, washed once with ice-cold PBS, fixed with 70% ethanol, and stored at -20 ℃. Cells were then washed twice with ice-cold PBS and treated with RNase (for 30 min at 37 ℃, 500 U/mL; Sigma Chemicals), and DNA was stained with propidium iodide (50 mg/mL; Boehringer Mannheim, Indianapolis, IN, USA). The cell cycle phase and apoptotic rate (cells at sub-G0/G1 phase) were analyzed using a FACScan (Beckman Coulter Inc., Fullerton, CA, USA).

Antibody and Western blotting analysis

Following antibodies were used as primary antibodies: PTEN (Santa Cruz, CA, USA), β-actin (Sigma Chemicals), p27Kip1, Akt, phospho-Akt, p44/42MAPK, and phospho-p44/42MAPK (Cell Signaling Technology Inc., Beverly, MA, USA), phospho-FAK (Pharmingen, San Diego, CA, USA). To perform Western blotting analysis, cells were harvested by centrifugation. After being washed with ice-cold PBS, cells were lysed with EBC buffer (120 mmol/L NaCl, 10 mmol/L Tris at pH 8.0, 0.1 mmol/L EDTA, 1 mmol/L DTT) containing 0.5%NP-40 (Sigma), and protease inhibitors (Roche, Indianapolis, IN, USA). Cell lysates were normalized before loading onto 4-20% SDS-PAGE gradient gels (Invitrogen, Carlsbad, CA, USA). Proteins were subsequently transferred to a nitrocellulose membrane (Invitrogen) and probed with primary and secondary antibodies. The proteins were visualized on an enhanced chemiluminescence (ECL) film (Amersham) using the ECL Western blot detection regent (Amersham).

In vivo tumor xenograft studies

Subcutaneous tumor xenografts (MGC803, SGC7901) were established in nude mice by injecting tumor cells (1×10^6 cells/animal) in the right dorsal flank. When the tumor reached a size of 50-100 mm^3, animals were randomized into three groups (n = 9, animals/group) and treatment was initiated as follows. Group 1 received no treatment, group 2 received Ad-Luc (2×10^{10} vp/dose), and group 3 received Ad-PTEN (2×10^{10} vp/dose). All treatments were given on alternate days for a total of six doses. Intratumoral injections were performed under anesthesia.

Experiments were terminated when tumors showed signs of necrosis. The therapeutic effect was determined by statistical analysis using Student's t-test.

RESULTS

Inhibition of cell proliferation in gastric cancer due to overexpression of PTEN

Tumor cells (MGC-803, SGC-7901) and normal cells (GES-1) were treated with PBS, Ad-Luc, or Ad-PTEN and examined for exogenous PTEN expression and cell proliferation at various time points. Treatment with Ad-PTEN resulted in exogenous PTEN expression in all the cell lines tested (Figure 1A). However, no endogenous PTEN protein could be detected by Western blotting in tumor cells, suggesting that additional epigenetic mechanisms might compromise the expression of PTEN, consistent with tumor suppressor role of PTEN. Endogenous PTEN expression was observed in normal cells, indicating that they were wild type for PTEN. Furthermore, analysis for cell viability daily on days 1-5 demonstrated significant inhibition of cell proliferation

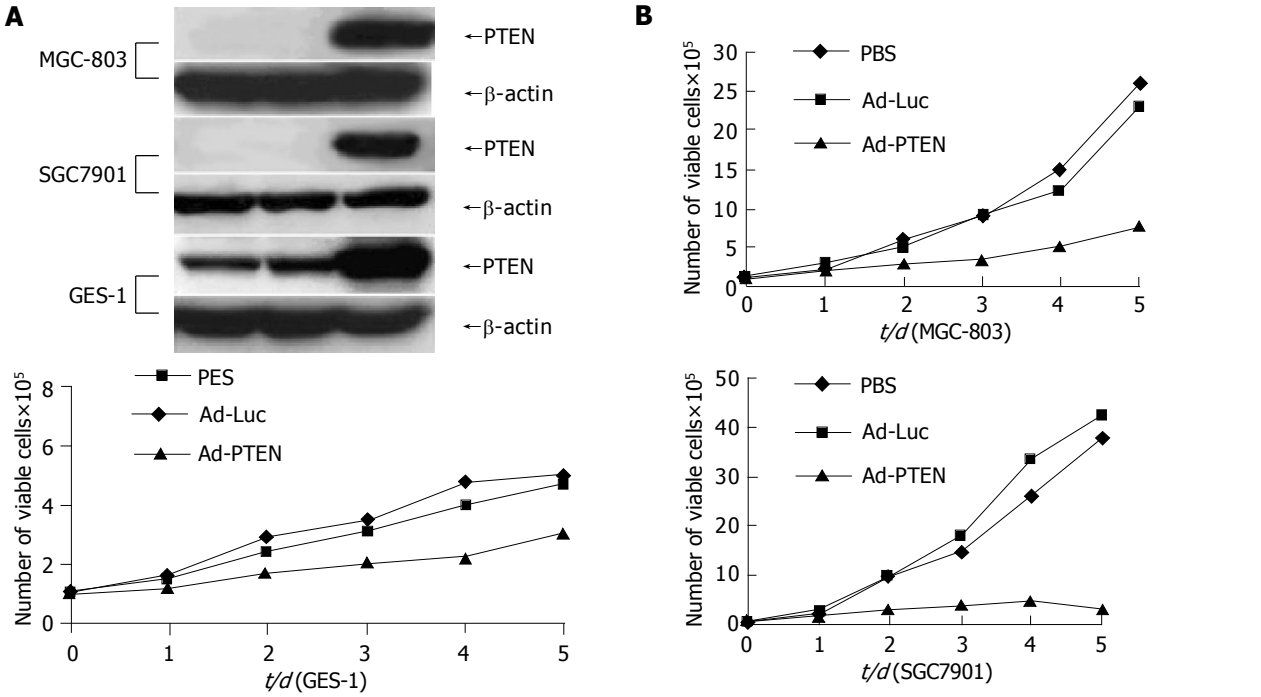

Figure 1 Inhibition of cell proliferation in gastric cancer cells due to overexpression of PTEN. **A**: Cells analyzed for PTEN protein expression by Western blot analysis; **B**: Measurement of cell proliferation as determined by viability assay on d 1, 2, 3, 4, and 5.

($P<0.01$) in all the cancer cell lines treated with Ad-PTEN, when compared with that in control cells treated with Ad-Luc or PBS (Figure 1B). In normal cells (GES-1), Ad-PTEN treatment resulted in moderate inhibition of cell growth compared to cells treated with Ad-Luc and PBS (Figure 1B). However, Ad-PTEN-mediated inhibitory effect on tumor cell proliferation was greater and more pronounced than that observed in normal cells. Minimal to no inhibitory effect on cell proliferation was also observed in normal human fibroblast cell line when treated with Ad-PTEN (data not shown). These results suggested that Ad-PTEN might selectively and more effectively inhibit tumor cells than normal cells.

Induction of apoptosis in gastric cancer cells due to overexpression of PTEN

After treatment with Ad-PTEN, tumor cells (MGC-803, SGC-7901) and normal cells (GES-1) were analyzed for apoptotic changes using a fluorescence-activated cell sorter (FACS) and/or Hoechst 33258 staining. At 72 h after Ad-PTEN treatment, an increase in the number of cells in the sub-G0/G1 phase, an indicator of apoptotic changes, was observed in the two cancer cell lines by FACS analysis (Figure 2A). The percent increase in apoptotic cells was 20-30%, depending on the tumor cell type. However, no changes were observed in tumor cells treated with Ad-Luc or PBS. In contrast, no significant induction of apoptosis was observed in normal cells treated with Ad-PTEN compared to cells treated with PBS and Ad-Luc (Figure 2A). To confirm these results further, Hoechst 33 258 staining was performed 72 h after treatment. Tumor cells underwent apoptosis following Ad-PTEN treatment, but normal cells did not. No changes were observed in any of the cells treated with Ad-Luc (Figure 2B).

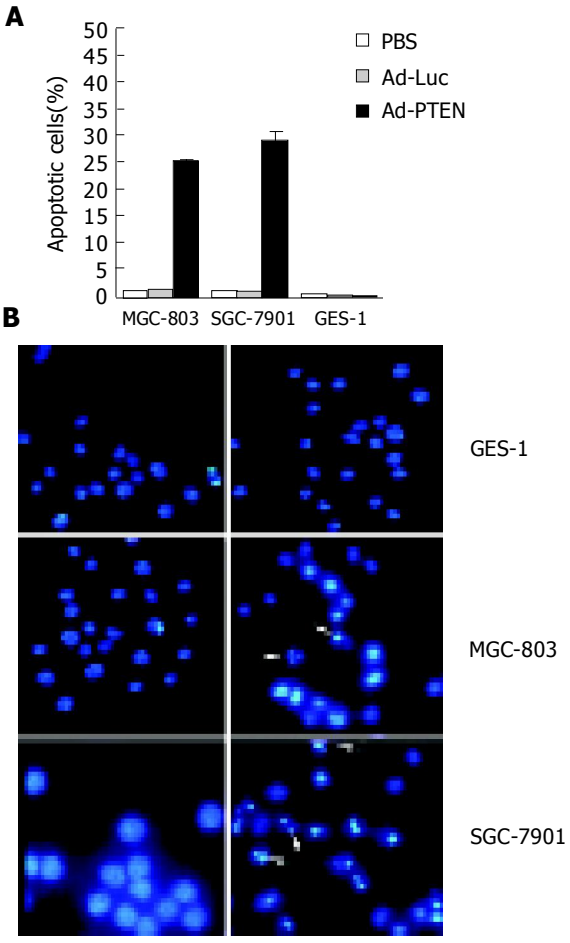

Figure 2 Induction of apoptosis due to overexpression of PTEN. **A**: Tumor cells (MGC-803, SGC-7901) and normal cells (GES-1) treated with PBS, Ad-Luc, or Ad-PTEN and harvested at 72 h after treatment; **B**: Analysis of tumor cells (MGC-803, SGC-7901) and normal cells (GES-1) by Hoechst 33258 staining 72 h after treatment with Ad-Luc and Ad-PTEN. Arrows indicate apoptotic cells. Magnification ×40 for all cell lines.

Induction of G2/M cell-cycle arrest due to overexpression of PTEN

To determine whether Ad-PTEN was capable of inducing G1 cell-cycle arrest as previously reported[19-22], cell-cycle phases were analyzed using a FACS. Cell-cycle analysis demonstrated an increase in the percentage (10-25%) of tumor cells (MGC-803, SGC-7901) in the G2/M population 72 h after treatment with Ad-PTEN (Figure 3) when compared to control cells treated with Ad-Luc, PBS, or exposed to 20 μmol/L LY294002. However, tumor cells treated with LY294002 were arrested at the G1 phase since LY294002 was a PI3K inhibitor. Although one of the PTEN functions was PI3K inhibition, like LY294002[15,20,23], Ad-PTEN did not induce G1 arrest in cancer cells carrying wtPTEN.

Signaling pathways modulated by PTEN overexpression in gastric cancer cells

To investigate if PI3K downstream signaling was involved in PTEN-mediated growth suppression, we examined the expression of Akt which was downstream of the Akt kinase pathway and transcriptional regulators leading to apoptotic cell death[24], in tumor cells (SGC-7901) and normal cells (GES-1) by Western blot analysis (Figure 4). In SGC-7901 cells, phospho-Akt was strongly dephosphorylated by Ad-PTEN and LY294002 (PI3K inhibitor). The reduction in Akt phosphorylation signal was not due to the decrease of phosphorylated and unphosphorylated forms of Akt (Figure 4A). In contrast, no significant change in pAkt was observed in Ad-PTEN-treated GES-1 cells compared to control cells (Figure 4B). These results demonstrated that PTEN downregulated the Akt-kinase pathway and suppressed cell growth and proliferation in cancer cells, but not in normal cells carrying wtPTEN.

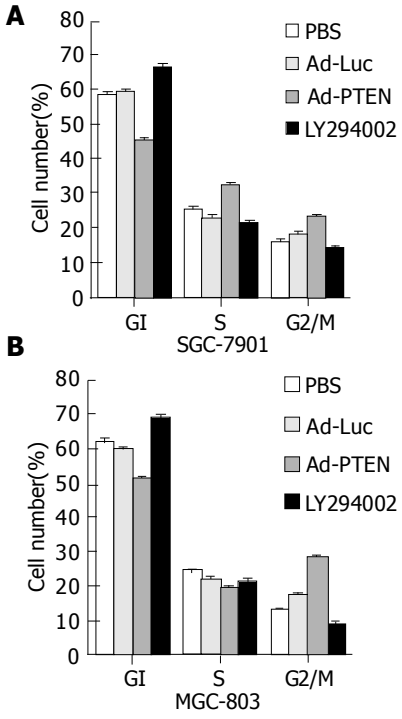

Figure 3 Induction of G2/M cell-cycle arrest due to overexpression of PTEN. (**A**: SGC-7901 cells; **B**: MGC-803 cells.) Bars denote standard error (SE).

We also examined the phosphorylation status of focal adhesion kinase (pFAK) and p44/42MAPK associated with cell migration and/or focal adhesions in SGC-7901 and GES-1 cells 72 h after infection[25-28]. In SGC-7901 cells, pFAK and p44/42MAPK were dephosphorylated by Ad-PTEN, but not by Ad-Luc or PBS (Figure 5A). Ly126, an MEK 1/2 inhibitor, also inhibited p44/42MAPK and served as a positive control. No changes in pFAK and p44/42MAPK expression were observed in Ad-PTEN-treated GES-1 cells compared to cells treated with Ad-Luc and PBS (Figure 5B). These results demonstrated that PTEN could selectively inhibit cell migration and adhesion through downregulation of the FAK and mitogen-activated protein kinase (MAPK) pathways in cancer cells carrying wtPTEN, but not in normal cells.

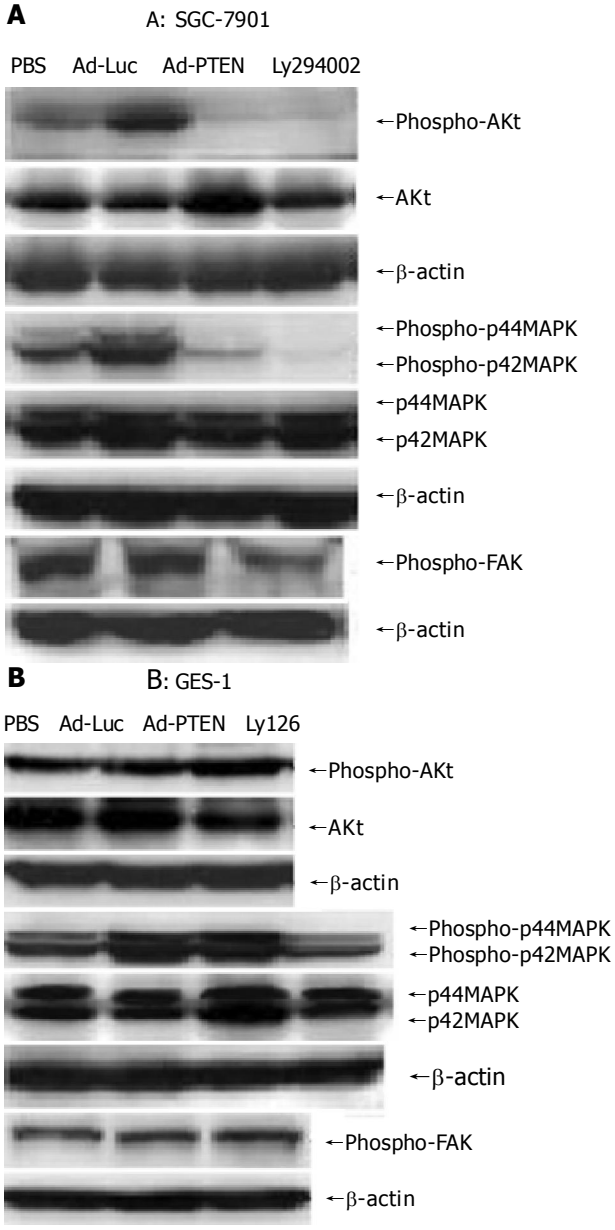

Figure 4 Signaling pathways regulated by PTEN overexpression. **A**: Downregulation of phospho-Akt, phospho-FAK, and inhibition of phospho-p44/42MAPK in SGC-7901 cells after Ad-PTEN treatment compared to Ad-Luc- and PBS-treated cells; **B**: No change in the expression levels of phospho-Akt, phospho-FAK, and phospho-p44/42MAPK observed in GES-1 cells after Ad-PTEN treatment compared to Ad-Luc- and PBS-treated cells.

Inhibition of gastric tumor xenografts by PTEN

The ability of Ad-PTEN to inhibit subcutaneous tumor xenografts was evaluated next. Subcutaneous colorectal tumor xenografts established in nude mice were divided into groups (n = 9/group) and treated as follows. Group 1 received PBS, group 2 received Ad-Luc, and group 3 received Ad-PTEN. Intratumoral injections of Ad-PTEN on SGC-7901 and MGC-803 tumor xenografts resulted in a significant (P<0.01) growth inhibition compared to control tumors that were treated with PBS or treated with Ad-Luc (Figures 5A and B). However, no complete tumor regression and no treatment-related toxicity were observed during the course of the experiment.

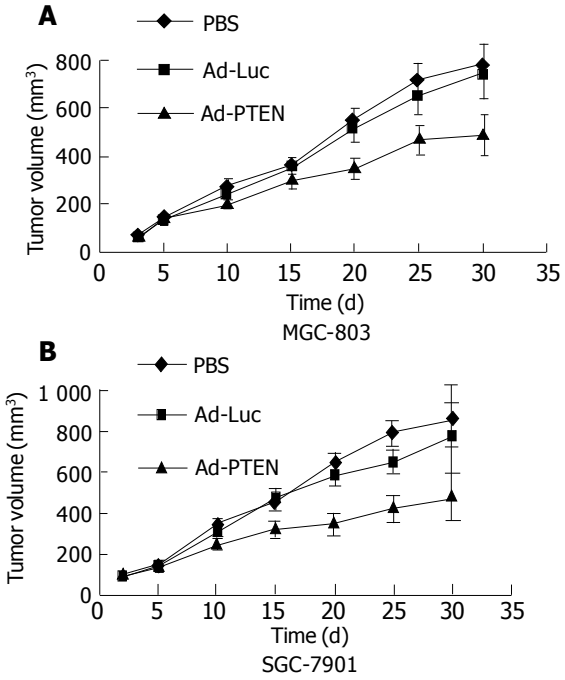

Figure 5 Therapeutic effect of Ad-PTEN on subcutaneous human gastric tumor xenografts. Bars represent standard error (SE). **A**: MGC-803 cells; **B**: SGC-7901 cells.

DISCUSSION

In the present study, we investigated the effects of overexpressing PTEN proteins in gastric cancer cells that were wtPTEN. Prior to the start of the study, we examined the mutational status of PTEN gene in the cancer cell lines used in the study. Genetic alterations were determined by sequencing the coding region using exon-specific primers. Both cancer cell lines were sequenced and found to contain no mutations in this gene. Furthermore, we showed that overexpression of PTEN suppressed the growth of cancer cells and induced apoptosis in gastric cancer cell lines significantly compared to normal cells. These results are similar to the findings previously reported in ovarian and thyroid cancers that were wtPTEN[18,19]. However, one major difference observed in our results from others is that we observed that gastric tumor cells that were wtPTEN were arrested in G2/M phase after Ad-PTEN treatment. In contrast, previous studies reported that ectopic expression of PTEN in cancer cells resulted in G1 arrest that was associated with an increase in p27 expression[15,16,19,29-31]. Analysis of p27 expression in gastric cancer cells after Ad-PTEN treatment demonstrated no change in expression levels (data not shown). In support of our findings, the recent report by Stewart *et al*[20], demonstrated that enforced expression of PTEN inhibited growth of melanoma cells that were wtPTEN. The discrepancy in the results is not clear. However, one possibility is that the induction of cell-cycle arrest by PTEN may be cell-type-dependent. Alternatively, differences in the mutational changes in different cancers may contribute to the determination of cell-cycle phases. In fact, as demonstrated in the present study, overexpression of PTEN in gastric cancers that were wtPTEN underwent G2 arrest, while tumor cells that were mutants for PTEN underwent G1 arrest. These results indicate that the endogenous status of PTEN may play a role in the cell cycle arrest and warrants further investigation. Whatever the underlying mechanism, it is evident from the present study that the ability of PTEN to inhibit tumor growth is independent of the mutational status of PTEN in cancer cells and is in agreement with the findings previously reported by Li *et al*[32].

The mechanism by which PTEN suppresses cell growth and induces apoptosis appears to be dependent upon its phosphatase activity. Requirement of the PTEN phosphatase activity to downregulate the Akt, FAK, and p44/42MAPK pathways has been previously demonstrated in tumor cells that were mutants or null for PTEN[25,26,28,33-35]. The results from the present study agree with these reports. Treatment of gastric cancer cells with Ad-PTEN resulted in the inhibition of Akt, FAK, and p44/42MAPK pathways. However, Ad-PTEN treatment in normal cells did not result in the regulation of these pathways, which may explain their inability to undergo apoptotic cell death, thereby achieving tumor-selective killing. The ability of tumor cells, but not normal cells that are wtPTEN, to undergo apoptotic cell death is in agreement with the findings of Li *et al*[32], who demonstrated that colorectal cancer cells that were wtPTEN were sensitive to PTEN, but not normal cells. It is also possible that tumor cells have other signaling pathways that are defective, result in triggering of apoptotic cell death upon PTEN expression. An alternate explanation can be that the endogenous PTEN expressed in tumor cell lines, but not in normal cells, is not functional. To gain an insight into this possibility, further investigation is warranted.

Finally, the ability of Ad-PTEN to suppress the growth of xenograft tumors (MGC-803, SGC-7901) was investigated. Ad-PTEN treatment inhibited tumor growth significantly, supporting our *in vitro* findings presented here. The ability of Ad-PTEN to inhibit human gastric tumor growth that wtPTEN has not been previously documented. In conclusion, Ad-PTEN inhibits gastric cancer growth, both *in vitro* and *in vivo*. Thus, adenovirus-mediated transfer of the PTEN gene may be a promising therapeutic strategy for the treatment of patients with gastric cancer.

REFERENCES

1 **Steck PA,** Pershouse MA, Jasser SA, Yung WK, Lin H, Ligon AH, Langford LA, Baumgard ML, Hattier T, Davis T, Frye C, Hu R, Swedlund B, Teng DH, Tavtigian SV. Identification of a candidate tumour suppressor gene, MMAC1, at chromo-

some 10q23.3 that is mutated in multiple advanced cancers. *Nat Genet* 1997; **15**: 356–362

2 **Li J,** Yen C, Liaw D, Podsypanina K, Bose S, Wang SI, Puc J, Miliaresis C, Rodgers L, McCombie R, Bigner SH, Giovanella BC, Ittmann M, Tycko B, Hibshoosh H, Wigler MH, Parsons R. PTEN, a putative protein tyrosine phosphatase gene mutated in human brain, breast, and prostate cancer. *Science* 1997; **275**: 1943–1947

3 **Rasheed BK,** Stenzel TT, McLendon RE, Parsons R, Friedman AH, Friedman HS, Bigner DD, Bigner SH. PTEN gene mutations are seen in high-grade but not in low-grade gliomas. *Cancer Res* 1997; **57**: 4187–4190

4 **Wang SI,** Puc J, Li J, Bruce JN, Cairns P, Sidransky D, Parsons R. Somatic mutations of PTEN in glioblastoma multiforme. *Cancer Res* 1997; **57**: 4183–4186

5 **Tashiro H,** Blazes MS, Wu R, Cho KR, Bose S, Wang SI, Li J, Parsons R, Ellenson LH. Mutations in PTEN are frequent in endometrial carcinoma but rare in other common gynecological malignancies. *Cancer Res* 1997; **57**: 3935–3940

6 **Cairns P,** Okami K, Halachmi S, Halachmi N, Esteller M, Herman JG, Jen J, Isaacs WB, Bova GS, Sidransky D. Frequent inactivation of PTEN/MMAC1 in primary prostate cancer. *Cancer Res* 1997; **57**: 4997–5000

7 **Yokomizo A,** Tindall DJ, Drabkin H, Gemmill R, Franklin W, Yang P, Sugio K, Smith DI, Liu W. PTEN/MMAC1 mutations identified in small cell, but not in non-small cell lung cancers. *Oncogene* 1998; **17**: 475–479

8 **Nelen MR,** van Staveren WC, Peeters EA, Hassel MB, Gorlin RJ, Hamm H, Lindboe CF, Fryns JP, Sijmons RH, Woods DG, Mariman EC, Padberg GW, Kremer H. Germline mutations in the PTEN/MMAC1 gene in patients with Cowden disease. *Hum Mol Genet* 1997; **6**: 1383–1387

9 **Liaw D,** Marsh DJ, Li J, Dahia PL, Wang SI, Zheng Z, Bose S, Call KM, Tsou HC, Peacocke M, Eng C, Parsons R. Germline mutations of the PTEN gene in Cowden disease, an inherited breast and thyroid cancer syndrome. *Nat Genet* 1997; **16**: 64–67

10 **Marsh DJ,** Dahia PL, Zheng Z, Liaw D, Parsons R, Gorlin RJ, Eng C. Germline mutations in PTEN are present in Bannayan–Zonana syndrome. *Nat Genet* 1997; **16**: 333–334

11 **Maehama T,** Dixon JE. The tumor suppressor, PTEN/MMAC1, dephosphorylates the lipid second messenger, phosphatidylinositol 3, 4,5-trisphosphate. *J Biol Chem* 1998; **273**: 13375–13378

12 **Myers MP,** Stolarov JP, Eng C, Li J, Wang SI, Wigler MH, Parsons R, Tonks NK. P-TEN, the tumor suppressor from human chromosome 10q23, is a dual-specificity phosphatase. *Proc Natl Acad Sci USA* 1997; **94**: 9052–9057

13 **Stambolic V,** Suzuki A, de la Pompa JL, Brothers GM, Mirtsos C, Sasaki T, Ruland J, Penninger JM, Siderovski DP, Mak TW. Negative regulation of PKB/Akt-dependent cell survival by the tumor suppressor PTEN. *Cell* 1998; **95**: 29–39

14 **Cheney IW,** Johnson DE, Vaillancourt MT, Avanzini J, Morimoto A, Demers GW, Wills KN, Shabram PW, Bolen JB, Tavtigian SV, Bookstein R. Suppression of tumorigenicity of glioblastoma cells by adenovirus-mediated MMAC1/PTEN gene transfer. *Cancer Res* 1998; **58**: 2331–2334

15 **Li DM,** Sun H. PTEN/MMAC1/TEP1 suppresses the tumorigenicity and induces G1 cell cycle arrest in human glioblastoma cells. *Proc Natl Acad Sci USA* 1998; **95**: 15406–15411

16 **Furnari FB,** Huang HJ, Cavenee WK. The phosphoinositol phosphatase activity of PTEN mediates a serum-sensitive G1 growth arrest in glioma cells. *Cancer Res* 1998; **58**: 5002–5008

17 **Davies MA,** Lu Y, Sano T, Fang X, Tang P, LaPushin R, Koul D, Bookstein R, Stokoe D, Yung WK, Mills GB, Steck PA. Adenoviral transgene expression of MMAC/PTEN in human glioma cells inhibits Akt activation and induces anoikis. *Cancer Res* 1998; **58**: 5285–5290

18 **Minaguchi T,** Mori T, Kanamori Y, Matsushima M, Yoshikawa H, Taketani Y, Nakamura Y. Growth suppression of human ovarian cancer cells by adenovirus-mediated transfer of the PTEN gene. *Cancer Res* 1999; **59**: 6063-6067

19 **Weng LP,** Gimm O, Kum JB, Smith WM, Zhou XP, Wynford-Thomas D, Leone G, Eng C. Transient ectopic expression of PTEN in thyroid cancer cell lines induces cell cycle arrest and cell type-dependent cell death. *Hum Mol Genet* 2001; **10**: 251–258

20 **Stewart AL,** Mhashilkar AM, Yang XH, Ekmekcioglu S, Saito Y, Sieger K, Schrock R, Onishi E, Swanson X, Mumm JB, Zumstein L, Watson GJ, Snary D, Roth JA, Grimm EA, Ramesh R, Chada S. PI3 kinase blockade by Ad-PTEN inhibits invasion and induces apoptosis in RGP and metastatic melanoma cells. *Mol Med* 2002; **8**: 451-461

21 **Gottschalk AR,** Basila D, Wong M, Dean NM, Brandts CH, Stokoe D, Haas-Kogan DA. p27Kip1 is required for PTEN-induced G1growth arrest. *Cancer Res* 2001; **61**: 2105–2111

22 **Weng LP,** Brown JL, Eng C. PTEN coordinates G(1) arrest by down-regulating cyclin D1 via its protein phosphatase activity and up-regulating p27 via its lipid phosphatase activity in a breast cancer model. *Hum Mol Genet* 2001; **10**: 599–604

23 **Taylor V,** Wong M, Brandts C, Reilly L, Dean NM, Cowsert LM, Moodie S, Stokoe D. 5′ phospholipid phosphatase SHIP-2 causes protein kinase B inactivation and cell cycle arrest in glioblastoma cells. *Mol Cell Biol* 2000; **20**: 6860–6871

24 **Lu Y,** Lin YZ, LaPushin R, Cuevas B, Fang X, Yu SX, Davies MA, Khan H, Furui T, Mao M, Zinner R, Hung MC, Steck P, Siminovitch K, Mills GB. The PTEN/MMAC1/TEP tumor suppressor gene decreases cell growth and induces apoptosis and anoikis in breast cancer cells. *Oncogene* 1999; **18**: 7034–7045

25 **Tamura M,** Gu J, Matsumoto K, Aota S, Parsons R, Yamada KM. Inhibition of cell migration, spreading, and focal adhesions by tumor suppressor PTEN. *Science* 1998; 280: 1614–1617

26 **Gu J,** Tamura M, Yamada KM. Tumor suppressor PTEN inhibits integrin- and growth factor-mediated mitogen-activated protein (MAP) kinase signaling pathways. *J Cell Biol* 1998; **143**: 1375–1383

27 **Tamura M,** Gu J, Takino T, Yamada KM. Tumor suppressor PTEN inhibition of cell invasion, migration, and growth: differential involvement of focal adhesion kinase and p130Cas. *Cancer Res* 1999; **59**: 442–449

28 **Gu J,** Tamura M, Pankov R, Danen EH, Takino T, Matsumoto K, Yamada KM. Shc and FAK differentially regulate cell motility and directionality modulated by PTEN. *J Cell Biol* 1999; **146**: 389–403

29 **Furnari FB,** Lin H, Huang HS, Cavenee WK. Growth suppression of glioma cells by PTEN requires a functional phosphatase catalytic domain. *Proc Natl Acad Sci USA* 1997; **94**: 12479–12484

30 **Robertson GP,** Furnari FB, Miele ME, Glendening MJ, Welch DR, Fountain JW, Lugo TG, Huang HJ, Cavenee WK. *In vitro* loss of heterozygosity targets the PTEN/MMAC1 gene in melanoma. *Proc Natl Acad Sci USA* 1998; **95**: 9418–9423

31 **Cheney IW,** Neuteboom ST, Vaillancourt MT, Ramachandra M, Bookstein R. Adenovirus-mediated gene transfer of MMAC1/PTEN to glioblastoma cells inhibits S phase entry by the recruitment of p27Kip1 into cyclin E/CDK2 complexes. *Cancer Res* 1999; **59**: 2318–2323

32 **Li J,** Simpson L, Takahashi M, Miliaresis C, Myers MP, Tonks N, Parsons R. The PTEN/MMAC1 tumor suppressor induces cell death that is rescued by the AKT/ protein kinase B oncogene. *Cancer Res* 1998; **58**: 5667-5672

33 **Nakamura N,** Ramaswamy S, Vazquez F, Signoretti S, Loda M, Sellers WR. Forkhead transcription factors are critical effectors of cell death and cell cycle arrest downstream of PTEN. *Mol Cell Biol* 2000; **20**: 8969–8982

34 **Dijkers PF,** Medema RH, Pals C, Banerji L, Thomas NS, Lam EW, Burgering BM, Raaijmakers JA, Lammers JW, Koenderman L, Coffer PJ. Forkhead transcription factor FKHR-L1 modulates cytokine-dependent transcriptional regulation of p27 (KIP1). *Mol Cell Biol* 2000; **20**: 9138–9148

35 **Lu Y,** Lin YZ, LaPushin R, Cuevas B, Fang X, Yu SX, Davies MA, Khan H, Furui T, Mao M, Zinner R, Hung MC, Steck P, Siminovitch K, Mills GB. The PTEN/MMAC1/TEP tumor suppressor gene decreases cell growth and induces apoptosis and anoikis in breast cancer cells. *Oncogene* 1999; **18**: 7034–7045

Science Editor Wang XL and Li WZ **Language Editor** Elsevier HK

PO Box 2345, Beijing 100023, China
www.wjgnet.com
wjg@wjgnet.com

ELSEVIER

World J Gastroenterol 2005;11(15):2230-2237
World Journal of Gastroenterology ISSN 1007-9327

• *GASTRIC CANCER* •

Inhibitory effect of human telomerase antisense oligodeoxyribonucleotides on the growth of gastric cancer cell lines in variant tumor pathological subtype

Jing Ye, Yun-Lin Wu, Shu Zhang, Zi Chen, Li-Xia Guo, Ruo-Yu Zhou, Hong Xie

Jing Ye, Yun-Lin Wu, Shu Zhang, Department of Gastroenterology, Ruijin Hospital, Shanghai Second Medical University, Shanghai 200025, China
Zi Chen, Department of Hematology, Huashan Hospital, Fudan University, Shanghai 200040, China
Li-Xia Guo, Ruo-Yu Zhou, Hong Xie, Department of Biotherapy, Institute of Biochemistry and Cell biology, Shanghai Institutes for Biological Sciences, the Chinese Academy of Sciences, Shanghai 200031, China
Supported by the Key Laboratory Open Fund, Ministry of Public Health, No. WKL 200010
Correspondence to: Professor Hong Xie, Department of Biotherapy, Institute of Biochemistry and Cell Biology, Shanghai Institutes for Biological Sciences, Chinese Academy of Sciences, Shanghai 200031, China. xiehong@sunm.shcnc.ac.cn
Telephone: +86-21-64735609 Fax: +86-21-34010138
Received: 2004-03-26 Accepted: 2004-06-07

Abstract

AIM: To investigate the inhibitory effect of specialized human telomerase antisense oligodeoxyribonucleotides on the growth of well (MKN-28), moderately (SGC-7901) and poorly (MKN-45) differentiated gastric cancer cell lines under specific conditions and its inhibition mechanism, and to observe the correlation between the growth inhibition ratio and the tumor pathologic subtype of gastric cancer cells.

METHODS: Telomerase activity in three gastric cancer cell lines of variant tumor pathologic subtype was determined by modified TRAP assay before and after the specialized human telomerase antisense oligodeoxyribonucleotides were dealt with under specific conditions. Effect of antisense oligomer under specific conditions of the growth and viability of gastric cancer cell lines was explored by using trypan blue dye exclusion assay, and cell apoptosis was detected by cell morphology observation, flow cytometry and TUNEL assay.

RESULTS: Telomerase activity was detected in well, moderately and poorly differentiated gastric cancer cell lines (the quantification expression of telomerase activity was 43.7TPG, 56.5TPG, 76.7TPG, respectively). Telomerase activity was controlled to 30.2TPG, 36.3TPG and 35.2TPG for MKN-28, SGC-7901 and MKN-45 cell lines respectively after treatment with human telomerase antisense oligomers at the concentration of 5 μmol/L, and was entirely inhibited at 10 μmol/L, against the template region of telomerase RNA component, whereas no inhibition effect was detected in missense oligomers (P<0.05). After treatment with antisense oligomers at different concentrations under specific conditions for 96 h, significant growth inhibition effects were found in MKN-45 and SGC-7901 gastric cancer cell lines (the inhibition ratio was 40.89% and 71.28%), but not in MKN-28 cell lines (15.86%). The ratio of inactive SGC-7901 cells increased according to the prolongation of treatment from 48 to 96 h. Missense oligomers could not lead to the same effect (P<0.05). Apoptosis of SGC-7901 and MKN-45 cells was detected not only by morphology and TUNEL assay but also by flow cytometry. The apoptotic rate reached 33.56% for SGC-7901 cells and 44.75% for MKN-45 cells.

CONCLUSION: The viability and proliferation of gastric cancer cells can be inhibited by antisense telomerase oligomers. The growth inhibition of gastric cancer cells is correlated with concentration, time and sequence specialty of antisense oligomers. The inhibition mechanism of antisense human telomerase oligomers depends not only on the sequence specialty but also on the biological characteristics of gastric cancer cell lines.

Key words: MKN-28; SGC-7901; MKN-45

Ye J, Wu YL, Zhang S, Chen Z, Guo LX, Zhou RY, Xie H. Inhibitory effect of human telomerase antisense oligodeoxyribonucleotides on the growth of gastric cancer cell lines in variant tumor pathological subtype. *World J Gastroenterol* 2005; 11(15): 2230-2237
http://www.wjgnet.com/1007-9327/11/2230.asp

INTRODUCTION

Telomere, a complex structure present at the ends of eukaryotic chromosomes, is regarded as a mitotic clock, eventually signaling the senescence of programed cell death in aged cells, and thus preventing further accumulated genetic changes and chromosome instability that can lead to pathologic lesions such as cancer. So maintenance of telomeres is essential to the proliferation of tumor cells[1]. Telomerase, a ribonucleoprotein, is actually a reverse transcriptase consisting of RNA and protein, the function of which is to add hexameric repeats of 5'-TTAGGG-3' to the end of telomeres to compensate for the progressive loss of telomeres[2]. It has been approved that telomerase is

an enzyme associated with cellular immortality and tumorigenesis, and strangely repressed in most normal somatic cells, but is reactivated in malignant tumor cells or immortal cells. Without the activation of telomerase, oncogene alone is not sufficient to make human cells become malignant phenotypes[3]. Studies have confirmed that telomerase activity is generally undetectable in normal gastric tissue, but is expressed in approximately 85-100% of human gastric cancers[4]. These facts strongly support the idea that telomerase has a promising potential, not only as a useful predictive diagnostic marker for gastric cancer, but also as a novel targeting approach of gastric cancer therapy.

Gastric cancer is one of the most common malignancies and the major cause of cancer-related death in many countries, including China, where it accounts for 15.4 out of 100 000 persons[5]. Much has been done to improve the earlier diagnosis and survival rate of gastric cancer through telomerase activity detection and telomerase activity inhibition by anticancer chemotherapy, but according to MEDLINE searches up to the year of 2004, little is known about the effect of antisense human telomerase oligodeoxyribonucleotides on the growth inhibition of gastric cancer cell lines of variant pathologic differentiations and their inhibition mechanism, and the relationship between the inhibition effect of telomerase antisense oligomers and tumor pathologic subtype. The strategy we performed here was to investigate the inhibitory effect of specialized human telomerase antisense oligodeoxyribonucleotides on the growth of well-, moderately- and poorly-differentiated gastric cancer cell lines under specific conditions and the possible mechanism of antisense oligodeoxyribonucleotides, to observe the correlation between the inhibition ratio and tumor pathologic differentiation of tumor cells, or other factors that might affect the inhibition effect of antisense oligodeoxyribonucleotides.

MATERIALS AND METHODS

Cell culture

Human gastric cancer tissue and normal gastric tissue were obtained from Shanghai Ruijin Hospital. MKN-28, the well-differentiated human gastric cancer cells and MKN-45, the poorly-differentiated human gastric cancer cells were kindly provided by Japanese Foundation of Cancer Research, Tokyo, Japan. SGC-7901, the moderately-differentiated human gastric cancer cells were present as a gift from No. 6 People's Hospital, Shanghai, China. All tumor cells were cultured in RPMI-1640 median (Gibco) supplemented with 10% heat-inactivated fetal calf serum at 37 ℃ in a modified CO_2 incubator containing 50 mL/L CO_2 and 95% air.

Synthesis of oligomers

Fifteen-mer specific human telomerase antisense oligodeoxyribonucleotides (AS-ODN, 5'-GTT AGG GTT AGA CAA-3') and missense oligodeoxyribonucleotides (N-ODN, 5'-ACG TCG ATC TGA GCA-3') were synthesized by β-cyanoethyl-phospharamidite chemistry using a model 381, an automated DNA synthesizer (Applied Biosystems). The assay procedure and precautions were in accordance with the instructions. Briefly, each basic group was synthesized including deblocking DMT at a controlled pore glass by trichloroacetic acids, then activated, couple purified, condensed, oxidized and aminolyzed according to the protocol of the user's manual (Applied Biosystems). Electrophoresis in a polyacrylamide gel under denaturing conditions was used for the purification of oligomers. The oligomers were added to cell culture medium containing stable modifications with phosphorothiodate residues.

Telomerase activity assay modified quantitative TRAP (telomeric repeat amplification protocol) assay

A highly sensitive method was developed with some modifications for quantification analysis of telomerase activity according to Zhang *et al*[6,7] in our research center.

Reagent

CHAPS lysis buffer: 10 mmol/L Tris–HCl (pH 7.5), 1 mmol/L $MgCl_2$, 1 mmol/L EGTA, 0.1 mmol/L PMSF, 5 mmol/L β-mercaptoethanol, 0.5% CHAPS (Sigma), 10% glycerol. TRAP reaction buffer: 20 mmol/L Tris-HCl (pH 8.3), 1.5 mmol/L $MgCl_2$, 63 mmol/L KCl, 0.005% Tween-20, 1 mmol/L EGTA, 50 μmol/L dNTPs (Promega), 0.1 μg TS primer 5'-AATCCGTCGAGCAGAGTT-3' (All the primers used were synthesized by Shanghai Department of Sangon, Canada). ACX, the return primer: 5'-GCGCGG [CTTACC]$_3$CTAACC-3'. NT, internal control primer: 5'-ATCGCTTCTCGGCCTTTT-3'. TSNT, internal control template: 5'-AATCCGTCGAGCAGAGTTAAAAGG CCGAGAAGCGAT-3'. R_8, the quantification standard of oligodeoxyribonucleotide: 5'-AATCCGTCGAGCAGAGT TAG[GGTTAG]$_7$-3'. Taq DNA polymerase (Promega). SYBR Green I (FCM Bioproducts).

Preparation of telomerase extracts

All cells and tissues were washed twice with phosphate-buffered saline (0.05 mol/L, pH 7.0), centrifuged (1 000 r/min, 5 min) suspended in ice-cold CHAPS-lysis buffer (0 ℃, 30 min), centrifuged once again (BECKMAN, 4 ℃, 12 000 *g*, 30 min). The supernatant was rapidly frozen and stored at -70 ℃.

Bradford protein assay[5]

The concentration of proteins was measured by using the Bradford protein assay, an aliquot of extract containing 1 μg of proteins was used for each telomerase assay.

Quantification analysis of telomerase activity

One microgram protein of telomerase extracts was added into 50 μL TRAP reaction, after 30 min of incubation at 30 ℃, 0.1 μg ACX, 0.1 μg NT 0.003 amol TSNT and 2U Taq DNA polymerase were added. The reaction mixture was then subjected to polymerase chain reaction (PCR) amplification in a thermal cycler (Perkin-Elmer 2400) with 30 cycles at 94 ℃ for 30 s, at 60 ℃ for 30 s. The PCR products were resolved by electrophoresis in a 12% polyacrylamide gel under nondenaturing conditions. The gel was then stained with SYBR Green I (FCM bioproducts) for 15 min, visualized by the UVP system and analyzed by Gelworks 1D advanced software. In each experiment, negative control (1 μL CHAPS lysis buffer or 1 μg extracts incubated with

5 g/L RNase for 20 min at 37 ℃) and positive control (0.1 amol of R_8) were included. Telomerase quantification was calculated with the formulation: TPG={[(TP-B/TI)/[R_8-B/RI]]×100}. TP, B, R_8, TI and RI were telomerase products in fluorescent counts from the test extract, blank lysis buffer only, R_8 quantification standard, and internal controls of the test extract and that of the R_8 quantification standard, respectively.

Cell viability assay

The cytotoxic effect of antisense oligomers on tumor cells was determined using the trypan blue dye exclusion assay. Tumor cells in logarithmic phase were seeded at 10^4 cells/well (100 μL) in 96-well plates and incubated overnight at 37 ℃, then the oligomers were added to the appropriate wells (the final concentrations of 5, 10, 15, 20 and 25 μmol/L were revised for antisense and 10 μmol/L for missense). Cells were harvested after 96 h after administration of oligomers, and cell suspension was diluted to 10^6/L and cell viability was determined by trypan blue dye.

Then SGC-7901 gastric cancer cell line, the most sensitive to the inhibition effect of antisense oligomers of the three cell lines, was chosen for the next assay to observe whether the cytotoxic effect of antisense oligomers at 48, 72, 96 h was time dependent.

Cell cycle analysis by flow cytometry

Three gastric cancer cell lines were seeded at 10^6 cells/L in a six-well microplate. Following a 12-h incubation at 37 ℃, 50 mL/L CO_2, antisense and missense oligomers were added at a final concentration of 10 μmol/L. Additional controls contained 10 μmol/L missense oligomers and culture medium alone respectively. Cells were harvested 96 h later and resuspended in the solution containing sodium citrate 40 mmol/L, sucrose 250 mmol/L and 5% dimethyl sulfoxide. The suspension was stored at -20 ℃ for 20 min, then thawed rapidly at room temperature and centrifuged to collect the cells. The cells were then resuspended in a solution containing RNase A (5×10^4 unit/g, 50 mg/L) and propidium iodide (PI, 20 mg/L). PI-stained cells were analyzed by flow cytometry (Becton-Dickson).

Electron microscope observation of gastric cancer cell lines

Electron microscope observation was used to determine whether tumor cells displayed an apoptotic morphology. Gastric cancer cells were fixed with 2.5% glutaraldehyde in advance, after being fixed with 2% osmic acid, washed with phosphate-buffered saline, dehydrated in alcohol of different grades, and embedded with Epon 812 to form ultrathin sections. After having dyed in both sodium acetate and lead citrate, the ultrathin sections were observed under an electron microscope.

TUNEL assay of apoptosis analysis (Roche molecular biochemicals)

The increased apoptosis of gastric cancer cells was also evaluated using the TUNEL (TDT-mediated dUTP nick end labeling) assay. DNA fragments were detected with FITC-labeled dUTP and terminal deoxynucleotidyl transferase as described by the supplier of reagents.

Cells (1×10^5/well) were seeded on four-well plates and treated with oligomers in the same manner as described above at the final concentration of 10 μmol/L for 96 h. Cell samples were air dried. A fresh paraformaldehyde solution (4% in PBS, pH 7.4) was prepared for 1 h at room temperature, slides were rinsed with PBS and incubated in a permeability solution (0.1% Triton X-100, 0.1% sodium citrate) for 2 min on ice, then labeled and analyzed by rinsing slides twice with PBS and adding 50 μL TUNEL reaction mixture to sample. Each experiment should include negative controls containing terminal transferase instead of TUNEL reaction and positive controls containing fixed and permeabilized cells incubated with micrococcal nuclease or DNase I (1 μg/mL in 50 mmol/L Tris-HCl, pH 7.5, 1 mmol/L $MgCl_2$, 1 mg/mL BSA, for 10 min at room temperature) to induce DNA strand breaks. The results were observed and photographed via fluorescence microscopy.

Statistical analysis

Data were expressed as mean±SD. Comparison between means was tested by Student's *t* test, Friedman's ANOVA and Duncan test in SAS. $P<0.05$ was considered statistically significant.

RESULTS

Quantification analysis of telomerase activity in three gastric cancer cell lines of variant tumor pathologic subtype

Telomerase activity was detected with the modified TRAP assay. As shown in Figure 1, internal standard bands were detected in all samples starting from 36 bp, by using lysis buffer and normal gastric mucosa as negative controls, human gastric cancer tissue and 0.1 amol R8 as positive controls, which excluded the possibility of false-negative results due to Taq polymerase inhibitor.

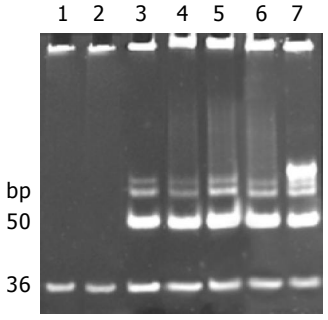

Figure 1 Results of quantification determination of telomerase activity. Lane 1: negative control of lysis buffer; lane 2: normal human tissue of gastric mucosa; lane 3: gastric cancer; lane 4: MKN-28 cell line; lane 5: SGC-7901 cell line; lane 6: MKN-45 cell line; lane 7: positive control of 0.1 amol R8.

Telomerase activity, starting at 50 bp and producing a characteristic 6-bp ladder periodically, was clearly detected in poorly, moderately and well-differentiated gastric cancer cell lines and human gastric cancer tissue, but not detected in normal gastric mucosae. The quantification expression of telomerase activity in poorly-, moderately- and well-differentiated gastric cancer cell lines was MKN-45 76.7TPG, SGC-7901 56.5TPG, MKN-28 43.7TPG. According to the statistical analysis, though the tumor pathologic differentiation

and malignancy of these gastric cancer cell lines varied, no significant difference in telomerase activity was observed, which confirmed that the expression of telomerase activity was not correlated with the pathologic differentiation of tumor cells (P>0.05). All of the experiments were repeated for not less than five times.

Effect of antisense oligomers on telomerase activity in three human gastric cancer cell lines of variant pathologic differentiation

Telomerase activity in well-, moderately-, and poorly-differentiated gastric cancer cell lines was significantly inhibited after having been cultured with antisense human telomerase oligonucleotides for 96 h at the concentrations of 5 and 10 μmol/L, compared to the missense oligomers as contrasts. As shown in Figure 2, telomerase activity was controlled to 30.2TPG, 36.3TPG and 35.2TPG for MKN-28, SGC-7901 and MKN-45 cell lines respectively at the concentration of 5 μmol/L, and was entirely inhibited at 10 μmol/L, while 10 μmol/L missense oligomers could not inhibit telomerase activity.

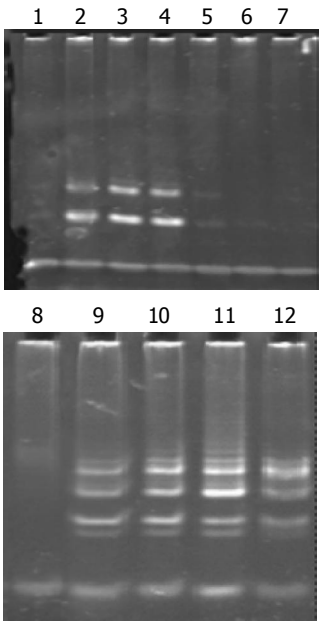

Figure 2 Effect of antisense oligomers on telomerase activity. Lane 1: negative control of lysis buffer; lanes 2-4: 5 μmol/L ASODN* on MKN-28, SGC-7901 and MKN-45 cell lines; lanes 5–7: 10 μmol/L ASODN on MKN-28, SGC-7901 and MKN-45 cell lines; lane 8: negative control of dealing with RNase A; lanes 9–11: 10 μmol/L NODN* on MKN-28, SGC-7901 and MKN-45 cell lines; lane 12: positive control of 0.1 amol R8. *ASODN: antisense oligomer and NODN: missense oligomer.

Effect of antisense oligomers on the growth and viability of three gastric cancer cell lines

As controls of blank group and missense oligomer group, the antitumor effect of antisense oligomers was remarkable in MKN-45, the poorly-differentiated cells and SGC-7901, the moderately-differentiated cells (P<0.05) at the specified conditions. In both kinds of cell lines, the addition of anticancer agents was associated with concentration-dependent reductions in cell growth inhibition from 5, 10, 15, 20-25 μmol/L. As shown in Figure 3, the slope of curve was a severe slant at the concentration of 10 μmol/L, suggesting that the antitumor effect was even more critical at this point of concentration. Thus, it was a prompt for us to detect the antisense effect on cell apoptosis at this circumstance (10 μmol/L, 96 h). Substantial decrease in cell growth was not seen in MKN-28 groups when analyzed at 96 h (P>0.05).

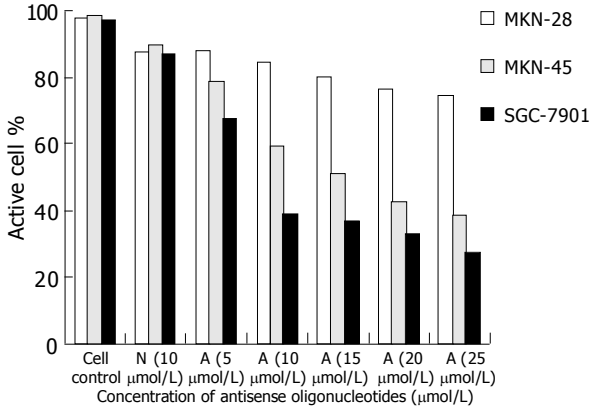

Figure 3 Effect of oligomers on viability of MKN-28, SGC-7901 and MKN-45 cells.

A represents antisense telomerase oligodeoxyribonucleotides (ASOND) and N represents missense oligodeoxyribonucleotides (NOND)

However, the missense control group did show a decrease in viability (10%), which was not statistically different from the antisense group, and this might represent a nonspecific antisense effect.

Since SGC-7901, the moderately-differentiated cells, was more sensitive to antitumor effect of antisense oligomers than any other two cell lines, we then chose it to investigate cell viability after incubation with oligomers at 48, 72, 96 h at different concentrations. As shown in Figure 4, when the reaction time was extended from 48 to 96 h, the antisense oligomers displayed a more effective way to inhibit the viability of tumor cells, compared to the missense oligomers as controls (P<0.05). The IC_{50} of antisense oligomers on growth inhibition of SGC-7901 cancer cells at 48, 72 and 96 h was 15, 10 and 8 μmol/L or so. In this study, the effect of antisense oligomers on gastric cancer cells was not only sequence-specific but also concentration-dependent and time-dependent in cell growth inhibition.

Effect of antisense oligomers on cell apoptosis

Morphologic observation of cell apoptosis under light microscopy After treatment with 10 μmol/L of antisense oligomers for 96 h, the growth rate of SGC-7901 and MKN-45 declined. When cells stopped proliferating, they showed the morphologic characteristics associated with crisis, such as larger cells with a flattened appearance, membrane blebbing, contact inhibition and adhesion decline (Figure 5), but these changes did not occur to MKN-28, the well-differentiated cells, which had almost the same effect as missense group. Three cell lines in blank group grew exuberantly with bright cell membranes and perfect clear culture solution. All these cells in missense group also grew actively, but not as well as the blank group.

Morphologic observation of cell apoptosis under electron microscopy We investigated whether these cells had the phenotypic hallmarks of apoptosis under electron microscope. Morphologic changes under electron microscope during apoptosis after treatment with 10 μmol/L of antisense oligomers for 96 h were characterized as membrane blebbing instead of microvillus growth, chromatin condensation and margination to the nuclear membrane, nuclear fragmentation and disintegration to form apoptosis corpus (Figure 6). But the MKN-28, the well-differentiated cells, did not have the effect after the same treatment.

Investigating apoptotic rate by flow cytometry To determine whether the cells were undergoing apoptosis, and to examine the apoptotic ratio after treatment of oligomers at 10 μmol/L for 96 h, we performed analysis of cells labeled with PI. Flow cytometric analysis of DNA content demonstrated the accumulation of a sub-G1 peak with the apoptotic rate reaching 33.56% for SGC-7901 cells and 44.75% for MKN-45 cells in antisense group, which was significantly higher than those in missense group (Table 1).

Examining apoptosis by TUNEL assay To further confirm whether gastric cancer cells underwent apoptosis, we performed TUNEL assay. Similar results were obtained by TUNEL assay conforming DNA fragmentation under fluorescence microscopy. Cells in logarithmic phase infiltrating with DNase I (50 μg/mL) were used as a positive contrast and cells in logarithmic phase without any treatment and reagent as a negative contrast, the results showed SGC-7901 and MKN-45 cells of antisense group were fluoresced and turned to green, rounder, larger, and even polykaryon, which was a characteristic sign of apoptosis. Cells in missense group were not found to have changes under fluorescence microscopy (Figure 7).

DISCUSSION

The antisense human telomerase oligomers used were sequence specific and complementary to telomerase RNA, which is absolutely required for telomerase reverse transcription and therefore a natural target for anti-telomerase agents. Another strongpoint that we designed for the antisense oligmers was modification of DNA oligomers with phosphorothioate (PS) linkages. The modifications of sugar phosphodiester backbone in these molecules were intended to confer certain desirable characteristics of properties, such as superior binding affinity and therefore specificity to the hTR RNA template, intracellular penetration and importantly, to enable the intact delivery to their targets[8]. Compared to other modifications, such as ribozyme, 2',5'-oligoadenylate[9], peptide nucleotide acid[10], and RNA interference[11], phosphorothioate oligonucleotides are the current gold standard for antisense therapy and have a bright future in clinical study, because they have acceptable physical and chemical properties and show reasonable resistance to

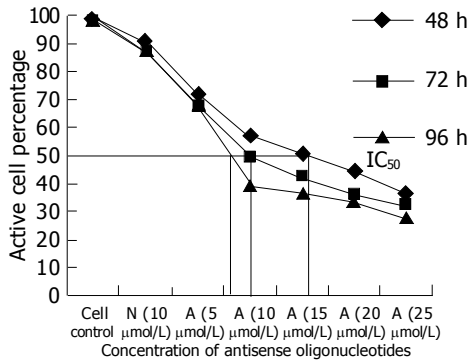

Figure 4 Effect of oligomers on viability of SGC-7901 cells at different time points and concentrations. A represents antisense telomerase oligodeoxyribonucleotides (ASOND) and N represents missense oligodeoxyribonucleotides (NOND).

Table 1 **Apoptosis of three gastric cancer cell lines after treatment with oligomers (10 μmol/L, 96 h) (mean±SD)**

	Group	% Apoptosis	P^a
MKN-28	Control	2.68±1.05	
	AS-ODN	17.56±2.57	P>0.05
	N-ODN	12.37±4.79	
SGC-7901	Control	2.59±0.94	
	AS-ODN	33.56±3.56	P<0.05
	N-ODN	8.46±0.76	
MKN-45	Control	6.77±2.16	
	AS-ODN	44.75±9.93	P<0.05
	N-ODN	15.97±4.01	

% Apoptosis, percentage of cells in a sub-G1 peak, quantified by flow cytometric DNA analysis. P^a represents the statistical comparison in columns between antisense group and missense group.

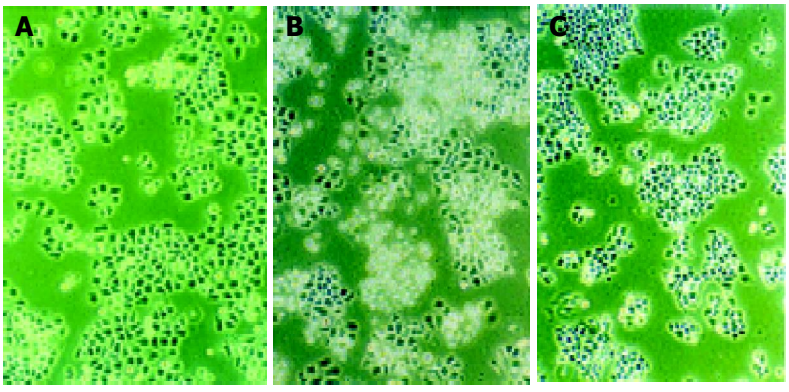

Figure 5 Light microscopy investigation of MKN-45 and SGC-7901 cells after *in vitro* treatment with different oligomers (10 μmol/L, 96 h). **A**: contrast group (10×15); **B**: antisense oligomer group (10×15); **C**: non-antisense oligomer group (10×15).

nucleases[12].

Our research confirmed that telomerase activity of well-, moderately-, and poorly-differentiated gastric cancer cells was significantly inhibited by antisense oligomers of sequence specificity at 10 μmol/L for 96 h, and the degree of inactivity had no correlation with tumor pathologic differentiation. They had almost consistent expression of telomerase activity before and after the suppression of antisense oligomers, indicating that the suppression mechanism of antisense oligomers is related to the telomerase activity, and antisense oligomers inhibit telomerase and cell growth via sequence specificity against human telomerase RNA components.

In our research, antisense oligomers of sequence specificity inhibited cell proliferation, especially moderately-differentiated gastric cancer cells (SGC-7901), in a concentration- and time-dependent manner. But our findings also had no significant correlation between the reduction in telomerase activity and cell counts or viability. After having been treated with antisense oligomers at the same condition (96 h, 10 μmol/L), telomerase was completely inactivated, but tumor cells were still partially viable, indicating that antisense human telomerase oligomers inhibit telomerase activity earlier and more effective than cell growth, and antisense oligomers inhibit cell proliferation via inactivation of telomerase. Agents that target telomerase, unlike most conventional chemotherapeutic agents, might not induce cytotoxicity immediately after administration[13,14]. Although many tumors maintained short telomeres, complete inhibition of tumor cell proliferation required a continuous cell division until their telomeres reached a critically short length[15-17].

Light and electron microscopy showed that gastric cancer cells appeared to be the characteristic signs of apoptosis

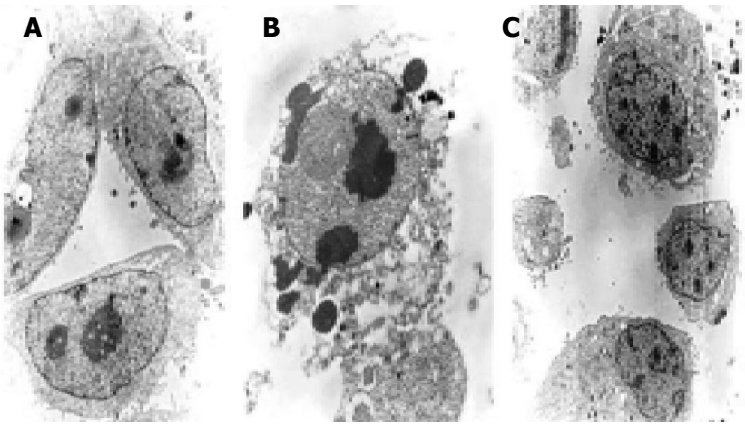

Figure 6 Electron microscopy investigation of cell apoptosis of MKN-45 and SGC-7901 cells after *in vitro* treatment with different oligomers (10 μmol/L, 96 h). **A**: contrast group (×2 300); **B**: antisense group (×6 400); **C**: non-antisense group (×3 800).

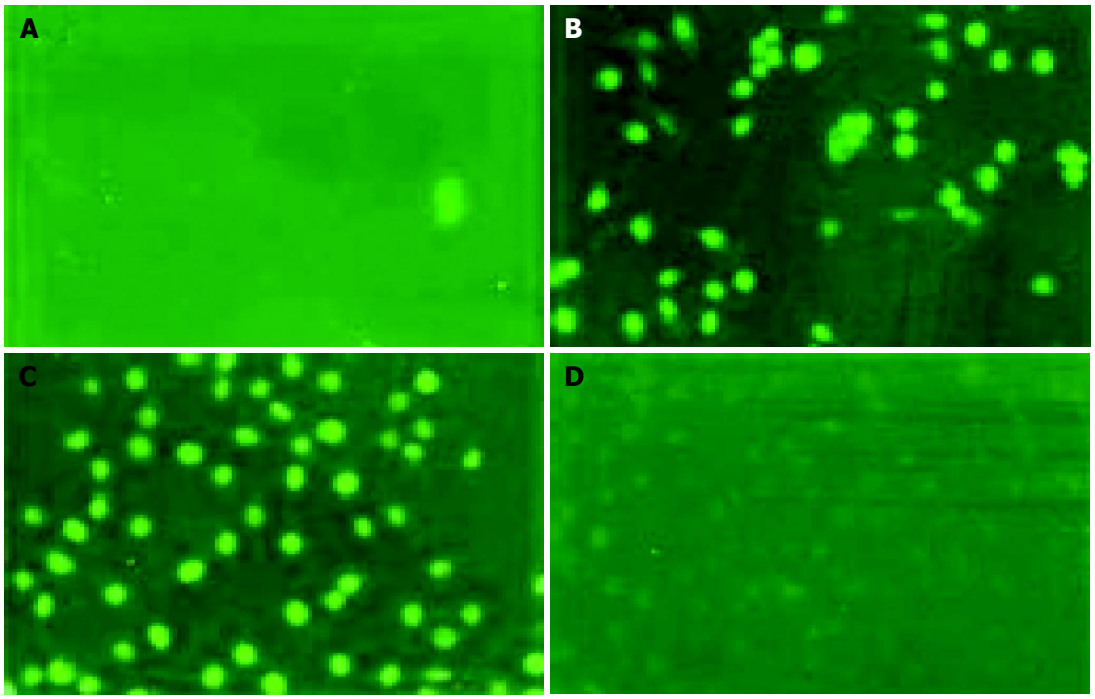

Figure 7 TUNEL test of cell apoptosis of SGC-7901 and MKN-45 gastric cancer cells after *in vitro* treatment with different oligomers (10 μmol/L, 96 h). **A**: negative control (20×15); **B**: positive control (20×15); **C**: antisense group (20×15); **D**: non-antisense group (20×15).

and cell growth inhibition after treatment with antisense oligomers. Flow cytometry also confirmed the same outcome as antisense oligomers that induced cell apoptosis by arresting cells at G0/G1, decreasing the percentage of cells at S and G2/M phases, and reducing the cell growth-rate, but the cells in missense group did not have this effect. These data suggest that inhibition of telomerase could enhance cell inviability and apoptosis in some subpopulations without telomerase activity.

However, antisense oligomers could lead to apoptosis of gastric cancer cells ($P<0.05$, compared to missense group), but the apoptosis ratio was no more than 30-50%, suggesting that other subpopulations during the treatment with antisense oligomers continued to grow and escaped from apoptosis. In agreement with our results, Kondo *et al*[18] has furthermore attested in their therapeutic experiment of neuroglioma that treatment with antisense human telomerase oligomers could not induce apoptosis of all neuroglioma cells, and surviving cells demonstrated an increased expression of more differentiated states, such as decreased motility, invasive ability and tumorigenicity. So they concerned that inhibition of telomerase in tumor cells could trigger two distinct pathways, apoptosis and differentiation. We also found that antisense human telomerase oligomers could significantly inhibit the growth and viability of gastric cancer cells. The main mechanism of which is the inhibition of telomerase activity and the induction of cell apoptosis. Further study is needed to approve the possible mechanism of cell differentiation.

In this study, we found that antisense oligomers of sequence specificity inhibited efficiently the proliferation of poorly-differentiated gastric cancer cells (MKN-45) and moderately-differentiated gastric cancer cells (SGC-7901) at specific conditions, but the inhibitory action on MKN-28 was restricted and not reasonable. Furthermore, antisense oligmers could control the growth rate of moderately-differentiated gastric cancer cells (SGC-7901) more effective than that of poorly-differentiated gastric cancer cells (MKN-45), indicating that antisense oligomers have the capability of inhibiting cell growth, but they do not enhance or weaken their inhibiting efficiency according to the malignant grades of gastric cancer. These results suggest that the mechanism of the growth inhibition by antisense oligomers has little correlation with malignancy or its pathologic differentiation of gastric cancer.

These data also suggest that the inhibition effect of antisense oligomers on the viability of gastric cancer cell lines is not only correlated well with the inhibition effect of telomerase activity by specifically combining the human telomerase RNA, but also determined by the different biologic traits of gastric cancer cell lines. Since a variety of stimuli are known to induce or suppress apoptosis, we believe that after telomerase activity is inhibited by antisense oligomers of sequence specificity, the unique signal transmission channel is activated in different gastric cancer cell lines, thus starting up a new pass of controlling tumor growth, resulting in some cell types undergoing apoptosis, some types undergoing differentiation and others continuing to grow. It has been demonstrated that tumors undergoing apoptosis via p53-dependent pathways after treatment with antisense telomerase are easily inhibited compared to those via p53-independent pathways after treatment with antitelomerase. MKN-28 cells, unlike most gastric cancer cells (including MKN-45, and SGC-7901), instead of containing wild-type *p53* gene, they harbor a missense mutation at codon 257 binding domain, inducing cell apoptosis in a unique way[19]. These studies give some assumption why antisense human telomerase oligomers in our study significantly inhibited cell growth and induced apoptosis in MKN-45 and SGC-7901 gastric cancer cells, but not in MKN-28 cells. So the inhibiting mechanism of antisense telomerase oligomer is not only determined by the sequence specialty, but also correlated with the biologic traits due to the cell lines themselves. Since different cell lines from the same tumor origin may have variant biologic mechanisms in tumorigenesis, they maintain their immortal proliferation in a particular way after overexpression of telomerase activity. Therefore once telomerase activity is inhibited, the response is different to cell apoptosis and growth inhibition.

In agreement with our results, Kondo *et al*[18]and Taggart *et al*[20] have confirmed in their studies that the effect of telomerase inhibitors appears in their own way, and is decided by tumor related genes and different cancer cell subtypes. Though telomerase inactivity may lead to cell apoptosis via telomere shortening, it has been proved that a small proportion of tumor cells could synthesize repetitive sequences of telomere to maintain an effective length via selectively stimulating some unknown bypasses[21,22]. It has been found that antisense oligomers could induce apoptosis via upregulating p53, Rb, or induce differentiation via activation of p21 and p27. It has also been approved that treatment with surviving nonapoptotic cells with antisense oligonucleotides against p27 could induce cell death[18]. To confirm our hypothesis, further study is needed to investigate the real mechanism after telomerase inhibition according to cell lines and cell biology.

In conclusion, antisense oligomers targeting on telomerase RNA can inhibit cell immortalization and proliferation of well-, moderately- and poorly-differentiated gastric cell lines. The main mechanism of which is the specific inactivity of telomerase, and induction of cell apoptosis.

REFERENCES

1 **Greenwood MJ,** Lansdorp PM. Telomeres, telomerase, and hematopoietic stem cell biology. *Arch Med Res* 2003; **34**: 489-495

2 **Karayan-Tapon L**, Menet E, Guilhot J, Levillain P, Larsen CJ, Kraimps JL. Topoisomerase II alpha and telomerase expression in papillary thyroid carcinomas. *Eur J Surg Oncol* 2004; **30**: 73-79

3 **Shen ZY**, Xu LY, Li EM, Cai WJ, Chen MH, Shen J, Zeng Y. Telomere and telomerase in the initial stage of immortalization of esophageal epithelial cell. *World J Gastroenterol* 2002; **8**: 357-362

4 **Usselmann B**, Newbold M, Morris AG, Nwokolo CU. Telomerase activity and patient survival after surgery for gastric and oesophageal cancer. *Eur J Gastroenterol Hepatol* 2001; **13**: 903-908

5 **Tang DQ**. Oncology of the Time. 2nd edition. Shanghai: *Shanghai Medical University* 2000: 695

6 **Zhang RG**, Wang XW, Yuan JH, Guo LX, Xie H. Using a non-radioisotopic, quantitative TRAP-based method detecting telomerase activities in human hepatoma cells. *Cell Res* 2000;

10: 71-77
7 **Zhang RG**, Wang XW, Yuan JH, Xie H. Human hepatoma cell telomerase activity inhibition and cell cycle modulation by its RNA component antisense oligodeoxyribonucleotides. *Acta Pharmacol Sin* 2000; **21**: 742-746
8 **Wang ES**, Wu K, Chin AC, Chen-Kiang S, Pongracz K, Gryaznov S, Moore MA. Telomerase inhibition with an oligonucleotide telomerase template antagonist: *in vitro* and *in vivo* studies in multiple myeloma and lymphoma. *Blood* 2004; **103**: 258-266
9 **Yatabe N**, Kyo S, Kondo S, Kanaya T, Wang Z, Maida Y, Takakura M, Nakamura M, Tanaka M, Inoue M. 2-5A antisense therapy directed against human telomerase RNA inhibits telomerase activity and induces apoptosis without telomere impairment in cervical cancer cells. *Cancer Gene Ther* 2002; **9**: 624-630
10 **Kubo T**, Bakalova R, Ohba H, Fujii M. Antisense effects of DNA-peptide conjugates. *Nucleic Acids Res Suppl* 2003; **3**: 179-180
11 **Kosciolek BA**, Kalantidis K, Tabler M, Rowley PT. Inhibition of telomerase activity in human cancer cells by RNA interference. *Mol Cancer Ther* 2003; **2**: 209-216
12 **Jansen B**, Zangemeister-Wittke U. Antisense therapy for cancer-the time of truth. *Lancet Oncol* 2002; **3**: 672-683
13 **Mo Y**, Gan Y, Song S, Johnston J, Xiao X, Wientjes MG, Au JL. Simultaneous targeting of telomeres and telomerase as a cancer therapeutic approach. *Cancer Res* 2003; **63**: 579-585
14 **Rezler EM**, Bearss DJ, Hurley LH. Telomere inhibition and telomere disruption as processes for drug targeting. *Annu Rev Pharmacol Toxicol* 2003; **43**: 359-379
15 **Odago FO**, Gerson SL. Telomerase inhibition and telomere erosion: a two-pronged strategy in cancer therapy. *Trends Pharmacol Sci* 2003; **24**: 328-331
16 **Ibanez de Caceres I**, Frolova N, Varkonyi RJ, Dulaimi E, Meropol NJ, Broccoli D, Cairns P. Telomerase is frequently activated in tumors with microsatellite instability. *Cancer Biol Ther* 2004; **3**: 289-292
17 **Fukazawa T**, Maeda Y, Sladek FM, Owen-Schaub LB. Development of a cancer-targeted tissue-specific promoter system. *Cancer Res* 2004; **64**: 363-369
18 **Kondo S**, Tanaka Y, Kondo Y, Hitomi M, Barnett GH, Ishizaka Y, Liu J, Haqqi T, Nishiyama A, Villeponteau B, Cowell JK, Barna BP. Antisense telomerase treatment: induction of two distinct pathways, apoptosis and differentiation. *FASEB J* 1998; **12**: 801-811
19 **Naka K**, Yokozaki H, Yasui W, Tahara H, Tahara E, Tahara E. Effect of antisense human telomerase RNA transfection on the growth of human gastric cancer cell lines. *Biochem Biophys Res Commun* 1999; **255**: 753-758
20 **Taggart AK**, Teng SC, Zakian VA. Est1p as a cell cycle-regulated activator of telomere-bound telomerase. *Science* 2002; **297**: 1023-1026
21 **Wong SC**, Yu H, Moochhala SM, So JB. Antisense telomerase induced cell growth inhibition, cell cycle arrest and telomerase activity down-regulation in gastric and colon cancer cells. *Anticancer Res* 2003; **23**: 465-469
22 **Shammas MA**, Shmookler Reis RJ, Li C, Koley H, Hurley LH, Anderson KC, Munshi NC. Telomerase inhibition and cell growth arrest after telomestatin treatment in multiple myeloma. *Clin Cancer Res* 2004; **10**: 770-776

Science Editor Wang XL and Li WZ **Language Editor** Elsevier HK

PO Box 2345, Beijing 100023, China
www.wjgnet.com
wjg@wjgnet.com

ELSEVIER

World J Gastroenterol 2005;11(15):2238-2243
World Journal of Gastroenterology ISSN 1007-9327

Hepatitis B virus genotypes and hepatocellular carcinoma in Thailand

Pisit Tangkijvanich, Varocha Mahachai, Piyawat Komolmit, Juthatip Fongsarun, Apiradee Theamboonlers, Yong Poovorawan

Pisit Tangkijvanich, Department of Biochemistry, Faculty of Medicine, Chulalongkorn University, Bangkok 10330, Thailand
Varocha Mahachai, Piyawat Komolmit, Department of Medicine, Faculty of Medicine, Chulalongkorn University, Bangkok 10330, Thailand
Juthatip Fongsarun, The National Blood Center, Thai Red Cross, Bangkok 10330, Thailand
Apiradee Theamboonlers, Yong Poovorawan, Viral Hepatitis Research Unit, Department of Pediatrics, Faculty of Medicine, Chulalongkorn University, Bangkok 10330, Thailand
Supported by the Thailand Research Fund and Center of Excellence, Viral Hepatitis Research Unit, Chulalongkorn University
Correspondence to: Professor. Yong Poovorawan, MD, Viral Hepatitis Research Unit, Department of Pediatrics, Faculty of Medicine, Chulalongkorn University, Bangkok 10330, Thailand. yong.p@chula.ac.th
Telephone: +662-256-4909 Fax: +662-256-4929
Received: 2004-08-30 Accepted: 2004-10-06

Abstract

AIM: The role of hepatitis B virus (HBV) genotypes on the clinical features and prognosis of patients with hepatocellular carcinoma (HCC) is currently unknown. The aim of the present study was to evaluate the distribution of HBV genotypes and their clinical relevance in Thai patients.

METHODS: HBV genotypes were determined by PCR-RFLP in stored sera of 93 asymptomatic carriers, 103 patients with chronic hepatitis, 60 patients with cirrhosis and 76 patients with HCC. The clinical data were analyzed in relation to the HBV genotype.

RESULTS: HBV genotypes C and B were predominant in Thailand, accounting for 73% and 21%, respectively. The distributions of genotypes B and C were similar in HCC patients compared to the other groups. Genotype C was significantly more common in HCC patients who were under 40 years old than genotype B (18% *vs* 0%, $P = 0.03$), but was significantly less common in patients older than 60 years (26% *vs* 56.5%, $P = 0.01$). The positive rate of hepatitis B e antigen (HBeAg) in patients with genotype C was significantly higher than that in patients with genotype B (71.6% *vs* 44.4%, $P = 0.03$ in chronic hepatitis; 56.8% *vs* 11.1%, $P = 0.01$ in cirrhosis). There were no differences between HCC patients with genotypes B and C regarding tumor staging by CLIP criteria and the overall median survival. Multivariate analyses showed that HBV genotype was not an independent prognostic factor of survival in HCC patients.

CONCLUSION: Patients with genotype C had a higher positive rate of HBeAg and exhibited earlier progression of cirrhosis and HCC than those with genotype B. However, there were no differences in the risk of developing HCC and its prognosis between patients with these genotypes.

Key words: HBV; Genotype; Hepatocellular carcinoma

Tangkijvanich P, Mahachai V, Komolmit P, Fongsarun J, Theamboonlers A, Poovorawan Y. Hepatitis B virus genotypes and hepatocellular carcinoma in Thailand. *World J Gastroenterol* 2005; 11(15): 2238-2243
http://www.wjgnet.com/1007-9327/11/2238.asp

INTRODUCTION

Hepatitis B virus (HBV) infection is associated with a diverse clinical spectrum of liver damage ranging from asymptomatic carrier, chronic hepatitis, cirrhosis and hepatocellular carcinoma (HCC)[1]. HBV, a member of the hepadnaviridae, is a relaxed circular double-stranded DNA virus, and has currently been classified into eight genotypes, designed A-H based on a comparison of entire genomic sequences[2,3]. HBV genotypes appear to show varying geographic patterns in their distribution. For instance, genotypes A and D are predominant in Western countries and India, whereas genotypes B and C prevail in Southeast Asia, China and Japan. Genotype E is restricted to Africa and genotype F is found in Central and South America.

Besides the differences in geographical distribution, there is growing evidence that the viral genotypes may influence the clinical outcomes of patients with chronic HBV infection. Among Asian patients who constitute approximately 75% of HBV carriers worldwide, it has been shown that HBV genotype C is more commonly associated with severe liver diseases and the development of cirrhosis compared to genotype B[4-7]. Genotype C is also associated with a lower rate of hepatitis B e antigen (HBeAg) seroconversion and a lower response rate to alpha interferon therapy compared to genotype B[8,9]. However, the association between HBV genotype and the risk of developing HCC is still controversial[4,10-12]. In addition, the impact of HBV genotype on clinical features and prognosis of patients with HCC remains unclear. Thus, the aim of this study was to determine the role of HBV genotypes on clinical severity of patients with chronic liver disease, particularly those with HCC.

MATERIALS AND METHODS

Subjects

Serum samples were obtained from 470 patients with chronic

HBV infection who had undergone long-term follow-up at Chulalongkorn Memorial Hospital (Bangkok, Thailand), and the National Blood Center, Thai Red Cross, between August 1997 and August 2003. All patients were positive for Hepatitis B s antigen (HBsAg), as determined by the use of a commercially available enzyme-linked immunosorbent assay kit (Abbott Laboratories, Chicago, IL). Of these, patients who were positive for hepatitis C virus antibody (anti-HCV) and those who had another potential cause of chronic liver disease were excluded. Patients who had previously been treated with antiviral therapy were excluded. The patients were clinically classified into four groups including asymptomatic carrier, chronic hepatitis, cirrhosis and HCC. Asymptomatic carrier was diagnosed by periodical examination of normal serum alanine aminotransferase (ALT) level for at least 1 year. Chronic hepatitis was diagnosed by the presence of prolonged elevation of serum ALT level, and confirmed by histologic examinations. The degree of hepatic inflammation and fibrosis was graded according to modified Knodell histology index[13]. Cirrhosis was diagnosed based on histologic examinations and/or imaging studies, and its severity was subsequently classified based on Child's criteria. HCC was established by histopathology and/or a combination of mass lesions in the liver on hepatic imaging and serum alpha-fetoprotein (AFP) levels above 400 IU/mL. The staging of HCC was classified according to CLIP criteria[14].

Serum samples were collected from each patient at the time of their clinical evaluation and stored at -70 ℃ until further tests were performed. All patients were informed regarding the purpose of exterminating the etiologies of liver disease and their written consent were obtained. The study was approved by the Ethics Committee, Faculty of Medicine, Chulalongkorn University.

HBV-DNA extractions

DNA was extracted from 100 μL serum with proteinase-K/SDS in Tris buffer, followed by phenol/chloroform extraction and ethanol precipitation. The pellet was dissolved in 30 μL sterile water and directly subjected to PCR-based amplification.

HBV-DNA detection

HBV-DNA was amplified in an automated thermocycler (Perkin Elmer Cetus, Branchburg, NJ), using the primer sequences previously described[15]. The forward primer was P1 (nt 2823-2845: 5'-TCACCATATTCTTGGGAACAAGA); the reverse primer was P2 (nt 80-61: 5'-TTCCTGAACTGGAGCCACCA). The primers were located in conserved genomic regions to ensure a high sensitivity for the amplification of all HBV genotypes. Two microliters of DNA sample were combined with a reaction mixture containing 20 μL of 2.5×Eppendorf MasterMix (Hamburg, Germany), 1 μmol/L P1, 1 μmol/L P2 and sterile water, in a final volume of 50 μL. PCR was performed under the following conditions: After an initial 2-min denaturation step at 94 ℃, 35 cycles of amplification were performed, each including 30-s denaturation at 94 ℃, 30-s annealing at 55 ℃ and 30-s extension at 72 ℃, followed by a final 10-min extension at 72 ℃. Each amplified DNA sample (10 μL) was added to a loading buffer and run on a 2% agarose gel (FMC Bioproducts, Rockland, ME) at 100 V for 60 min. The 479-bp product stained with ethidium bromide on preparation was visualized on a UV transilluminator.

PCR-RFLP analysis for genotyping

PCR products were subjected to RFLP analysis, using restriction endonuclease *Ava*II and *Dpn*II (New England Biolabs, Beverly, MA) to determine the HBV genotype. Briefly, 10 μL of PCR product was mixed with 1.5 μL of 10×buffer, 3 μL of sterile water and 0.5 μL (5U) of *Ava*II and *Dpn*II, respectively, in separate reactions and incubated at 37 ℃ for 3.5 h. After incubation, the samples were run on a composite gel containing 2% NuSieve agarose (FMC BioProducts, Rockland, ME) and 1% standard agarose. The sizes of the RFLP products, visible under UV light as a result of prior ethidium bromide staining, served to identify the various HBV genotypes based on the polymorphism patterns[15].

Serological and virological assays

HBeAg was determined using commercially available enzyme-linked immunosorbent assay kit (Abbott Laboratories, Chicago, IL). Serum HBV-DNA level was quantified using a commercial kit (Amplicor HBV Monitor, Roche Diagnostics, Tokyo, Japan). The detection range of this assay was from 2.7 to 8.7 log genome equivalents/mL (LGE/mL).

Statistical analysis

Data were presented as percentage, mean and standard deviation. χ^2 test, unpaired *t* test, and ANOVA were used to assess the statistical significance of the difference between groups where appropriate. Survival curves were established using the Kaplan-Meier method and differences between curves were verified using the log-rank test. Cox regression analysis was performed to identify which indepe-ndent variables would have a significant influence on the overall survival. *P* values below 0.05 were considered statis-tically significant. All statistical analyses were performed using SPSS 10.0 software for Windows (SPSS, Inc., Chicago, IL).

RESULTS

Distribution of HBV genotypes in patients with chronic HBV infection

Of the 470 patients enrolled in this study, HBV-DNA was detected in 332 patients (70.6%). Our data showed that the most common HBV genotypes were genotypes C and B, which were found in 243 (73.2%) and 69 (20.8%) patients, respectively. The remaining 20 cases included 11 (3.3%) with genotype A and 9 (2.7%) with unclassified genotype. The demographic and clinical data of 332 patients with different stages of chronic HBV infection are shown in Table 1. Male-to-female ratio of asymptomatic carriers was significantly lower than the other groups ($P = 0.002$). Mean age was significantly higher in patients with cirrhosis and HCC than in the other two groups ($P = 0.001$), and positive HBeAg rate was significantly higher in patients with chronic hepatitis than in other groups ($P = 0.001$). Although genotype C was the most common genotype in each group, no significant differences were observed with respect to the distribution

Table 1 **Demographic and clinical data of 332 patients with chronic HBV infection**

Diagnosis	*n*	Sex (m/f)	Age (yr)	ALT (U/L)	HBeAg positive	Genotype			
						A	B	C	U
Carrier	93	57/36	30.9±10.6	27.5±4.5	42/82 (51.2)	2 (2.2)	16 (17.2)	73 (78.4)	2 (2.2)
CH	103	84/19	36.2±10.1	157.4±103.8	61/92 (66.3)	5 (4.9)	20 (19.4)	76 (73.8)	2 (1.9)
Cirrhosis	60	47/13	48.8±13.8	135.0±90.9	26/53 (49.1)	2 (3.3)	10 (16.7)	44 (73.3)	4 (6.7)
HCC	76	60/16	54.4±12.9	107.8±107.4	15/71 (21.1)	2 (2.6)	23 (30.3)	50 (65.8)	1 (1.3)

CH, chronic hepatitis; HCC, hepatocellular carcinoma; U, unclassified genotype. Quantitative variables are expressed as mean±SD; categorical variables are expressed as *n* (%).

of the genotypes in various stages of chronic HBV infection ($P = 0.16$).

Clinicopathologic differences between genotypes B and C in chronic hepatitis

Because the number of patients with genotype A was less, only genotypes B and C were included for further analysis of clinicopathologic differences between genotypes. As shown in Table 2, patients with genotypes B and C were comparable with respect to sex, age and total bilirubin. The rate of positive HBeAg in patients with genotype B was significantly lower than that in patients with genotype C (44.4% *vs* 71.6%, respectively, $P = 0.03$). Mean ALT level was also significantly lower in patients with genotype B than those in patients with genotype C (119.8±58.5 and 159.8±106.4 IU/L, respectively; $P = 0.03$), but HBV-DNA levels were comparable between them (7.25±1.74 and 7.10±1.34 LGE/mL, respectively; $P = 0.78$). Patients with genotype B had a lower score of both necroinflammation activity and fibrosis than those with genotype C, but the differences were not statistically significant (5.8±2.1 and 1.5±1.0 *vs* 6.7±2.1 and 1.8±0.9, $P = 0.51$ and 0.47, respectively).

Clinical differences between genotypes B and C in cirrhosis

There were no significant differences in gender, total bilirubin, serum albumin, and child classification between groups of patients, as shown in Table 3. The mean age of patients with genotype B tended to be older than those with genotype C (54.7±9.2 *vs* 47.4±14.4 years, respectively, $P = 0.06$). The positive rate of HBeAg in patients with genotype B was significantly lower than that in patients with genotype C (11.1% *vs* 56.8%, respectively, $P = 0.01$). Patients with genotype B tended to have lower mean ALT and HBV-DNA levels than those with genotype C, but the difference was not statistically significant (101.5±49.0 IU/L and 6.59±1.20 LGE/mL *vs* 133.7±93.4 IU/L and 7.05±2.50 LGE/mL, $P = 0.14$ and 0.12, respectively).

Clinical differences between genotypes B and C in HCC

The clinical data of 73 patients with HCC were compared according to HBV genotype, as shown in Table 4. Between the two groups, there were no significant differences in gender, total bilirubin, ALT, serum albumin, AFP and HBV-DNA levels, tumor staging according to CLIP criteria. However, the mean age of patients with genotype B was significantly older than those with genotype C (61.1±9.8 *vs* 51.3±13.1 years, respectively, $P = 0.001$). Four of 22 patients (18.1%) with genotype B were positive for HBeAg, whereas 11 of 49 patients (22.4 %) with genotype C were positive for this marker, but the difference was not statistically significant ($P = 0.68$). When patients with HCC were stratified by age (Figure 1), none of the patients with genotype B was younger than 40 years, whereas nine patients (18 %) with genotype C were younger than 40 years ($P = 0.03$). On the contrary, 13 patients (56.5%) with genotype B were older than 60 years, whereas 13 patients (26 %) with genotype C were older than 60 years ($P = 0.01$).

The Kaplan-Meier survival curves demonstrated that the overall median survival for patients with genotypes B and C were 5.5 and 7.3 mo, respectively ($P = 0.81$, using log-rank test) (Figure 2). For patients who were treated with any specific therapeutic modality, the median survival for the genotype B and C groups were 11.5 and 12.4 mo, respectively ($P = 0.97$). In the untreated cases, the median survival of the genotype B and C groups were 4.5 and 4.0 mo,

Table 2 **Demographic and clinical data of patients with chronic hepatitis**

Characteristics	Genotype B (*n* = 20)	Genotype C (*n* = 76)	*P*
Age (yr)	35.1±9.6	36.4±10.3	NS
Sex (male/female)	16/4	65/11	NS
Total bilirubin (mg/dL)	0.8±0.2	0.7±0.3	NS
ALT (IU/L)	119.8±58.5	159.8±106.4	0.03
HBeAg positive	8/18 (44.4)	53/74 (71.6)	0.03
HBV DNA (LGE/mL)	7.25±1.74	7.10±1.34	NS
HAI inflammation	5.8±2.1	6.7±2.1	NS
HAI fibrosis	1.5±1.0	1.8±0.9	NS

Quantitative variables are expressed as mean±SD. Categorical variables are expressed as *n* (%). HAI inflammation, sum of necroinflammatory scores of histology activity index. HAI fibrosis, sum of fibrosis scores of histology activity index.

Table 3 **Demographic and clinical data of patients with cirrhosis**

Characteristics	Genotype B (*n* = 10)	Genotype C (*n* = 44)	*P*
Age (yr)	54.7±9.2	47.4±14.4	0.06
Sex (male/female)	8/2	35/9	NS
Total bilirubin (mg/dL)	1.4±0.8	2.2±1.2	NS
ALT (IU/L)	101.5±49.0	133.7±93.4	NS
Albumin (g/dL)	3.7±0.4	3.8±0.5	NS
HBeAg positive	1/9 (11.1)	25/44 (56.8)	0.01
HBV DNA (LGE/mL)	6.59±1.20	7.05±2.50	NS
Child classification (A/B/C)	7/2/1	24/15/5	NS

Quantitative variables are expressed as mean±SD. Categorical variables are expressed as *n* (%).

respectively ($P = 0.85$).

HBV genotype was entered into Cox regression analysis together with other variables that would influence prognosis. These included sex, age, HBeAg, HBV-DNA level, CLIP stage and therapy for HCC. The multivariate analyses revealed that independent unfavorable factors of overall survival included CLIP stage and lack of therapy for HCC (Table 5). However, the HBV genotype was not selected as an independent predictor of survival.

DISCUSSION

Identification of host and viral factors leading to severe liver damage and to the development of HCC may have important clinical implications in the management of patients with chronic HBV infection. There are now increasing data suggesting that HBV genotypes may play an important role in causing different disease profiles in chronic HBV infection. Most studies on HBV genotype and its clinical relevance have been performed in Asia and restricted to comparisons between genotypes B and C, which are the two most common HBV genotypes in this region accounting for more than 90% of cases[6,16,17]. Current available data from this region demonstrate that HBV genotype C is more commonly associated with severe liver diseases and the development of cirrhosis compared to genotype B[4-7]. In addition, patients with genotype C infection, compared to those with genotype B, are more frequently HBeAg positive and display higher HBV-DNA levels that may contribute to multiple episodes of acute flares and progression of liver disease[18]. Taken together, these data suggest that patients with genotype C have a tendency to exhibit more severe liver disease than those with genotype B.

In agreement with previous studies[17,19], our study demonstrated that genotype C and B were the predominant strains, accounting for approximately 75% and 20% of patients, respectively. In this respect, it would appear that the prevalence of HBV genotypes in Thailand is comparable to that reported from Japan and China[6,16], but differs from the distribution observed in Taiwan, where HBV genotype B is more common than genotype C[4,20]. Interestingly, the prevalence of genotype B and C in patients with HCC in our study was comparable to that in asymptomatic carrier, chronic hepatitis and cirrhosis. The equal distribution of genotypes B and C among various stages of chronic liver disease is consistent with previous reports conducted in Japan[6,11], but it contradicts the observations from other studies[4,7,16]. Hence, our data suggest that although genotype C is the most prevalent strain in Thailand, the risk of development of HCC may not be different between genotypes B- and C-related chronic liver disease.

The predominance of HBV genotypes B and C allows the comparison of clinical outcomes of patients who are chro-nically infected with these two HBV strains. Our results showed that the mean ages among asymptomatic carriers and chronic hepatitis were comparable between patients with genotypes B and C. However, the mean age of patients with genotype C tended to be older than those with genotype B in cirrhotic group. Interestingly, the divergence in the mean age of patients with genotypes B and C was more noticeably in those with HCC. Given that the majority of Thai patients acquire HBV infection vertically from their mothers at birth or horizontally during early childhood from carrier family members, their age would probably serve as a reasonable

Table 4 **Demographic and clinical data of patients with HCC**

Characteristics	Genotype B ($n = 23$)	Genotype C ($n = 50$)	*P*
Age (yr)	61.1±9.8	51.3±13.1	0.001
Sex (male/female)	20/3	38/12	NS
Total bilirubin (mg/dL)	2.1±2.0	2.9±4.9	NS
ALT (IU/L)	95.5±102.6	121.4±126.1	NS
Albumin (g/dL)	3.4±0.7	3.5±0.5	NS
HBeAg positive	4/22 (18.1)	11/49 (22.4)	NS
HBV DNA (LGE/mL)	6.71±1.62	6.52±2.63	NS
AFP (IU/mL)	42 485.2±95 590.9	42 032.6±89 382.8	NS
CLIP score (0–1/2–3/4–6)	5/7/11	8/25/17	NS

Quantitative variables are expressed as mean±SD. Categorical variables are expressed as *n* (%).

Table 5 **Multivariate analysis of unfavorable factors of survival in patients with HCC, by using Cox regression analysis**

Factors	Risk ratio	95%CI	*P*
CLIP stage	4.63	1.70–12.62	0.003
No therapy	6.22	2.54–15.22	0.001

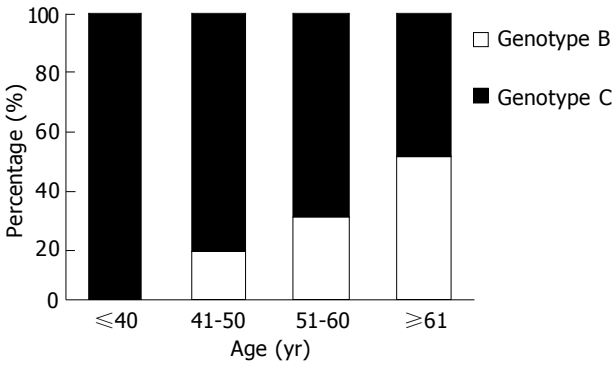

Figure 1 HBV genotypes B and C in 73 patients with HCC.

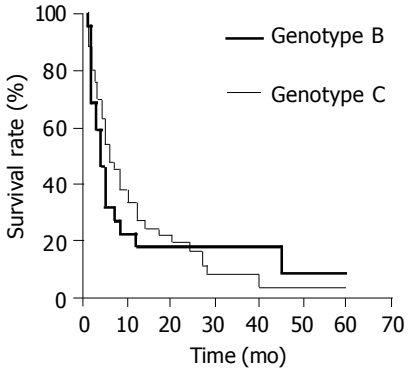

Figure 2 Overall survival of HCC patients with HBV genotypes B and C.

surrogate for the duration of HBV infection, regardless of the viral genotype. Our results also showed that patients with genotype C had a tendency of higher ALT, necroinflammatory scores and HBV-DNA levels than patients with genotype B. Moreover, patients with genotype C had a significantly higher prevalence of HBeAg positivity, particularly among patients with chronic hepatitis and cirrhosis, but the difference seemed to be disappearing upon the disease progression to HCC. Although HBeAg is a marker of active viral replication, the disappearance of HBeAg with or without seroconversion of antibody to HBeAg during the course of chronic infection does not always imply disease remission[21]. Collectively, it is reasonable to speculate that, at least in our populations, patients with genotype C have a trend for delayed HBeAg seroconversion and more prolonged necroinflammatory process causing earlier development of cirrhosis and HCC. Nonetheless, it would appear that there is no difference in the risk between patients with genotypes B and C in the progression to liver cancer.

Indeed, it is currently unclear whether a certain HBV genotype is associated with a greater risk for progression of cirrhosis to HCC. Studies from Taiwan and Japan have demonstrated an increase in HCC development among patients with HBV genotype C compared to genotype B[4,6,12,20]. Similarly, a study conducted in China has suggested that genotype C may predispose to HCC, whereas genotype B has a relatively better prognosis[16]. On the contrary, recent studies from Hong Kong and Japan have shown that there is no difference in the risk of developing HCC between patients with genotypes B and C[11,22]. Moreover, a potential correlation between HBV genotype and the age of the patients with HCC has been debated. Intriguingly, the report from northern Taiwan has observed that genotype B is associated with the development of HCC in patients younger than 35 years of age, while those with genotype C more frequently develop cancer after 50 years of age[4]. This observation, however, has not been confirmed by subse-quent studies from southern Taiwan and Japan[6,11,20]. In southern Taiwan, for example, there is no significant difference in the mean age between HCC patients with genotypes B and C[20]. By remarkable contrast, the mean age of Japanese patients with genotype B is approximately 70 years compared to 55 years of those with genotype C[6]. In the present report, the mean age of HCC patients with genotype B was significantly older than those with genotype C (61 and 51 years, respectively). Thus, the age distribution of HBV genotypes in Thai patients with HCC seems to correspond with the report from Japan, but differs from those studies from Taiwan.

The molecular virological factors responsible for this discrepancy among countries remain largely unknown. It has been postulated that the difference in the mean age between Taiwanese and Japanese patients with HCC may be partially influenced by the divergence of HBV subtypes distributed among different geographic areas[23]. Recently, two subtypes of HBV genotype B, namely Ba and Bj, have been identified based on the phylogenetic analysis. It has shown that genotype Ba consists of the recombination with the precore/core region originating from genotype C, whereas genotype Bj does not[24]. Genotype Bj is exclusively found in Japan, while genotype Ba is ubiquitous in other countries in Asia, including Thailand[25]. Based on our data, however, this postulation could not clarify the similarity in the mean age between Thai and Japanese patients with HCC, and the diversity between Thai and Taiwanese patients. Thus, it is likely that other as yet unrecognized virological factors might act as potential variables influencing the development of HCC in patients with chronic liver disease, even though they are infected with HBV of the same genotype. In addition, discrepancies regarding the role of HBV genotype might be related to variability of host and environmental factors in different geographic areas, such as genetic polymorphism and aflatoxin exposure.

Regarding the impact of HBV genotypes on the prognosis of HCC, a prospective study in Japan demonstrates that patients with genotype C tend to have relatively poor clinical outcomes after transcatheter arterial embolization (TACE) therapy compared with those with genotype B[26]. This finding is consistent with a recent report from Taiwan indicating that patients with genotype C exhibit a greater recurrent rate after curative resection of the tumor compared with those with genotype B[27]. However, our findings showed that the clinical features at presentation and overall survival of patients with HCC did not depend on the HBV genotype. The similarity of the tumor characteristics and clinical outcome of patients with genotypes B and C in this study was supported by the data of a recent case-control report conducted in Hong Kong[28]. Therefore, it would appear that in Thai populations, once HCC has developed, the course of the disease might be independent of the underlying HBV infection because the proportion of surviving patients is similar, irrespective of the infecting genotype. It should also be noted that overall median survival observed in this study was much shorter compared to other reports. The low survival rates in Thai patients with HCC in this study in part resulted from advanced stages of the cancer at the time of the diagnosis, while only minorities had an early detection in the course of follow-up programs.

In summary, our study demonstrated that patients with HBV genotype C, compared to those with genotype B, had a higher positive rate of HBeAg and exhibited earlier progression of cirrhosis and HCC. Genotype by itself, however, might not be responsible for an increased oncogenic effect because there was no difference in the risk of developing HCC and its prognosis between patients with genotypes B and C. Further large-scale prospective studies, which offer advantages over cross-sectional investigations, are needed to establish the existence of these observations in the future.

ACKNOWLEDGMENTS

This study was supported by the Thailand Research Fund [Research Scholar (PT), and Senior Research Scholar (YP)], and Center of Excellence, Viral Hepatitis Research Unit, Chulalongkorn University.

REFERENCES

1 **Ganem D,** Prince AM. Hepatitis B virus infection-natural history and clinical consequences. *N Engl J Med* 2004; **350**: 1118-1129

2 **Kidd-Ljunggren K,** Miyakawa Y, Kidd AH. Genetic variability in hepatitis B viruses. *J Gen Virol* 2002; **83**: 1267-1280
3 **Arauz-Ruiz P,** Norder H, Robertson BH, Magnius LO. Genotype H: a new Amerindian genotype of hepatitis B virus revealed in Central America. *J Gen Virol* 2002; **83**: 2059-2073
4 **Kao JH,** Chen PJ, Lai MY, Chen DS. Hepatitis B genotypes correlate with clinical outcomes in patients with chronic hepatitis B. *Gastroenterology* 2000; **118**: 554-559
5 **Lindh M,** Hannoun C, Dhillon AP, Norkrans G, Horal P. Core promoter mutations and genotypes in relation to viral replication and liver damage in East Asian hepatitis B virus carriers. *J Infect Dis* 1999; **179**: 775-782
6 **Orito E,** Ichida T, Sakugawa H, Sata M, Horiike N, Hino K, Okita K, Okanoue T, Iino S, Tanaka E, Suzuki K, Watanabe H, Hige S, Mizokami M. Geographic distribution of hepatitis B virus (HBV) genotype in patients with chronic HBV infection in Japan. *Hepatology* 2001; **34**: 590-594
7 **Chan HL,** Wong ML, Hui AY, Hung LC, Chan FK, Sung JJ. Hepatitis B virus genotype C takes a more aggressive disease course than hepatitis B virus genotype B in hepatitis B e antigen-positive patients. *J Clin Microbiol* 2003; **41**: 1277-1279
8 **Kao JH,** Wu NH, Chen PJ, Lai MY, Chen DS. Hepatitis B genotypes and the response to interferon therapy. *J Hepatol* 2000; **33**: 998-1002
9 **Wai CT,** Chu CJ, Hussain M, Lok AS. HBV genotype B is associated with better response to interferon therapy in HBeAg (+) chronic hepatitis than genotype C. *Hepatology* 2002; **36**: 1425-1430
10 **Orito E,** Mizokami M, Sakugawa H, Michitaka K, Ishikawa K, Ichida T, Okanoue T, Yotsuyanagi H, Iino S. A case-control study for clinical and molecular biological differences between hepatitis B viruses of genotypes B and C. Japan HBV Genotype Research Group. *Hepatology* 2001; **33**: 218-223
11 **Sumi H,** Yokosuka O, Seki N, Arai M, Imazeki F, Kurihara T, Kanda T, Fukai K, Kato M, Saisho H. Influence of hepatitis B virus genotypes on the progression of chronic type B liver disease. *Hepatology* 2003; **37**: 19-26
12 **Fujie H,** Moriya K, Shintani Y, Yotsuyanagi H, Iino S, Koike K. Hepatitis B virus genotypes and hepatocellular carcinoma in Japan. *Gastroenterology* 2001; **120**: 1564-1565
13 **Desmet VJ,** Gerber M, Hoofnagle JH, Manns M, Scheuer PJ. Classification of chronic hepatitis: diagnosis, grading and staging. *Hepatology* 1994; **19**: 1513-1520
14 A new prognostic system for hepatocellular carcinoma: a retrospective study of 435 patients: the Cancer of the Liver Italian Program (CLIP) investigators. *Hepatology* 1998; **28**: 751-755
15 **Lindh M,** Gonzalez JE, Norkrans G, Horal P. Genotyping of hepatitis B virus by restriction pattern analysis of a pre-S amplicon. *J Virol Methods* 1998; **72**: 163-174
16 **Ding X,** Mizokami M, Yao G, Xu B, Orito E, Ueda R, Nakanishi M. Hepatitis B virus genotype distribution among chronic hepatitis B virus carriers in Shanghai, China. *Intervirology* 2001; **44**: 43-47
17 **Theamboonlers A,** Jantaradsamee P, Kaew-In N, Tangkijvanich P, Hirsch P, Poovorawan Y. The predominant genotypes of hepatitis B virus in Thailand. *Ann Trop Med Parasitol* 1999; **93**: 737-743
18 **Kao JH,** Chen PJ, Lai MY, Chen DS. Genotypes and clinical phenotypes of hepatitis B virus in patients with chronic hepatitis B virus infection. *J Clin Microbiol* 2002; **40**: 1207-1209
19 **Sugauchi F,** Chutaputti A, Orito E, Kato H, Suzuki S, Ueda R, Mizokami M. Hepatitis B virus genotypes and clinical manifestation among hepatitis B carriers in Thailand. *J Gastroenterol Hepatol* 2002; **17**: 671-676
20 **Lee CM,** Chen CH, Lu SN, Tung HD, Chou WJ, Wang JH, Chen TM, Hung CH, Huang CC, Chen WJ. Prevalence and clinical implications of hepatitis B virus genotypes in southern Taiwan. *Scand J Gastroenterol* 2003; **38**: 95-101
21 **Lee WM.** Hepatitis B virus infection. *N Engl J Med* 1997; **337**: 1733-1745
22 **Yuen MF,** Sablon E, Yuan HJ, Wong DK, Hui CK, Wong BC, Chan AO, Lai CL. Significance of hepatitis B genotype in acute exacerbation, HBeAg seroconversion, cirrhosis-related complications, and hepatocellular carcinoma. *Hepatology* 2003; **37**: 562-567
23 **Orito E,** Mizokami M. Hepatitis B virus genotypes and hepatocellular carcinoma in Japan. *Intervirology* 2003; **46**: 408-412
24 **Sugauchi F,** Orito E, Ichida T, Kato H, Sakugawa H, Kakumu S, Ishida T, Chutaputti A, Lai CL, Ueda R, Miyakawa Y, Mizokami M. Hepatitis B virus of genotype B with or without recombination with genotype C over the precore region plus the core gene. *J Virol* 2002; **76**: 5985-5992
25 **Sugauchi F,** Orito E, Ichida T, Kato H, Sakugawa H, Kakumu S, Ishida T, Chutaputti A, Lai CL, Gish RG, Ueda R, Miyakawa Y, Mizokami M. Epidemiologic and virologic characteristics of hepatitis B virus genotype B having the recombination with genotype C. *Gastroenterology* 2003; **124**: 925-932
26 **Tsubota A,** Arase Y, Ren F, Tanaka H, Ikeda K, Kumada H. Genotype may correlate with liver carcinogenesis and tumor characteristics in cirrhotic patients infected with hepatitis B virus subtype adw. *J Med Virol* 2001; **65**: 257-265
27 **Chen JD,** Liu CJ, Lee PH, Chen PJ, Lai MY, Kao JH, Chen DS. Hepatitis B genotypes correlate with tumor recurrence after curative resection of hepatocellular carcinoma. *Clin Gastroenterol Hepatol* 2004; **2**: 64-71
28 **Yuen MF,** Tanaka Y, Mizokami M, Yuen JC, Wong DK, Yuan HJ, Sum SM, Chan AO, Wong BC, Lai CL. Role of hepatitis B virus genotypes Ba and C, core promoter and precore mutations on hepatocellular carcinoma: a case control study. *Carcinogenesis* 2004; **25**: 1593-1598

Science Editor Li WZ **Language Editor** Elsevier HK

PO Box 2345, Beijing 100023, China
www.wjgnet.com
wjg@wjgnet.com

ELSEVIER

World J Gastroenterol 2005;11(15):2244-2248
World Journal of Gastroenterology ISSN 1007-9327

Ornithine decarboxylase gene is overexpressed in colorectal carcinoma

Hai-Yan Hu, Xian-Xi Liu, Chun-Ying Jiang, Yi Lu, Shi-Lian Liu, Ji-Feng Bian, Xiao-Ming Wang, Zhao Geng, Yan Zhang, Bing Zhang

Hai-Yan Hu, Xian-Xi Liu, Yi Lu, Shi-Lian Liu, Ji-Feng Bian, Xiao-Ming Wang, Zhao Geng, Yan Zhang, Bing Zhang, Experimental Center of Medical Molecular Biology, Biochemistry and Molecular Biology Institute, School of Medicine, Shandong University, Jinan 250012, Shandong Province, China
Chun-Ying Jiang, Department of Colo-proctology, The Affiliated Hospital of Shandong University of Tradition Chinese Medicine, Jinan 250012, Shandong Province, China
Supported by the Scientific Research Fund of National Ministry of Health, No. 98-1-173
Correspondence to: Xian-Xi Liu, Experimental Center of Medical Molecular Biology, School of Medicine, Shandong University, Jinan 250012, Shandong Province, China. xianxi@sdu.edu.cn
Telephone: +86-531-8382346
Received: 2004-05-25 Accepted: 2004-06-18

Abstract

AIM: To investigate the ornithine decarboxylase (ODC) gene expression in colorectal carcinoma, ODC mRNA was assayed by RT-PCR and ODC protein was detected by a monoclonal antibody against fusion of human colon ODC prepared by hybridoma technology.

METHODS: Total RNA was extracted from human colorectal cancer tissues and their normal counterpart tissues. ODC mRNA levels were examined by RT-PCR. ODC genes amplified from RT-PCR were cloned into a prokaryotic vector pQE-30. The expressed proteins were purified by chromatography. Anti-ODC mAb was prepared with classical hybridoma techniques and used to determine the ODC expression in colon cancer tissues by immunohistochemical and Western blotting assay.

RESULTS: A cell line, which could steadily secrete anti-ODC mAb, was selected through subcloning four times. Western blotting reconfirmed the mAb and ELISA showed that its subtype was IgG2a. RT-PCR showed that the ODC mRNA level increased greatly in colon cancer tissues ($P<0.01$). Immunohistochemical staining showed that colorectal carcinoma cells expressed a significantly higher level of ODC than normal colorectal mucosa (98.6±1.03% *vs* 5.26±5%, $P<0.01$).

CONCLUSION: ODC gene overexpression is significantly related to human colorectal carcinoma. ODC gene expression may be a marker for the gene diagnosis and therapy of colorectal carcinoma.

Key words: Ornithine decarboxylase; RT-PCR; Colorectal Cancer

Hu HY, Liu XX, Jiang CY, Lu Y, Liu SL, Bian JF, Wang XM, Geng Z, Zhang Y, Zhang B. Ornithine decarboxylase gene is overexpressed in colorectal carcinoma. *World J Gastroenterol* 2005; 11(15): 2244-2248
http://www.wjgnet.com/1007-9327/11/2244.asp

INTRODUCTION

Colorectal cancer is one of the most common cancers in the world and the second leading cause of cancer death in the USA[1,2], and the fourth rate of mortality in China[3]. Therefore, efficient diagnostic and therapeutic approaches are important for colorectal carcinoma research. Laboratory testing and screening are potentially favorable to the outcome and survival rate of patients. Studies have been directed on identifying markers for the development of colorectal cancer[4,5]. Among the biochemical alterations found in cancer cells, polyamine content is one of the most consistent changes[6]. Polyamines are highly charged cations found in all living cells. They are essential for the maintenance of cell proliferation and differentiation, and macromolecule biosynthesis by interacting with nucleic acids, proteins and membranes. Polyamine synthesis is one of the early events occurring during the G1 phase of the cell cycle and cell division[7]. Ornithine decarboxylase (ODC) is the first rate-limiting enzyme in the polyamine biosynthesis pathway[8], and plays a critical role in cell transformation[9]. ODC has been implicated as an essential promoter of cell proliferation. It has recently been postulated that the ODC gene may act as an oncogene since overexpression of this gene is essential for cell transformation. Polyamine content as well as ODC activity have been found to be increased significantly in adenocarcinoma tissues compared to paired normal tissues[10,11]. It is, therefore, suggested that ODC activity may be used as a biologic marker for the tumor growth rate and biological aggressiveness[12]. There is, however, little information on the mRNA and protein status of ODC in surgical specimens of adenocarcinoma.

In our previous studies, we constructed the human ODC expression vectors and obtained the expressed proteins[13]. In the current study, we developed an anti-ODC monoclonal antibody using the recombinant human ODC protein. Using the monoclonal antibody, we compared the ODC protein expression level in colon cancer tissues with normal colon tissues. We also compared the ODC mRNA level in colon

cancer tissues with the surrounding uninvolved mucosa. The results indicate that ODC mRNA and protein expressions in cancer tissues are much higher than those in normal tissues.

MATERIALS AND METHODS

Tissue samples

Eighty-eight paraffin colorectal tissue specimens and 62 fresh specimens were collected by colonoscopy or surgical resection. All patients had no radiation therapy or chemotherapy before surgery. Among these, 100 samples were taken from sporadic colorectal carcinoma and 50 samples of normal colon mucosa were taken from 15 cm apart from the neoplasm.

Cloning, expressing and purifying of human ODC protein

ODC cDNA was synthesized by RT-PCR using total RNA template extracted from human colon cancer tissues. An ODC gene expression vector pQE-ODC was established by inserting ODC cDNA into an expression vector pQE-30, which had a 6-His tag. The protein was purified by Ni-NTA affinity chromatography[13].

Preparation of monoclonal antibody

BALB/c female mice were immunized with the prepared ODC protein directly administered into the spleen by about 20 μg/mouse and reimmunized every two weeks intraperitoneally by about 5 μg/mouse and administered intravenously 5 d before the mice were killed. A spleen cell suspension was prepared as shown by Gerhard *et al*[14]. BALB/c (sp2/0-Ag14) myeloma cells were mixed with immune spleen cells at 1∶10. The antibodies in the supernatant of cell clones were tested by ELISA and the positive hybridoma cells were recloned four times in HAT medium by limiting dilution. The subtype of mAb was analyzed with ELISA.

Testing mAb by Western blotting

Standard ODC protein and purified ODC protein were separated by standard SDS-PAGE techniques and transferred to a cation nylon membrane. The proteins were detected using the anti-ODC antibody purified from ascites. Immunoreactive proteins were detected using HRP-goat anti-mouse IgG.

Immunohistochemical test by anti-ODC antibody

Tissues were fixed in 96% ethanol for 6 h at 4 ℃, embedded in paraffin, and cut into 5-μm thick sections. The sections were deparaffinized in xylol, rehydrated through graded ethanol, washed with PBS-Tween, and incubated for 2 h at room temperature in a humidified chamber with 100 μL of the anti-ODC mAb at 1∶1 000 dilution. The slides were washed and incubated with HRP-labeled rabbit anti-mouse IgG (Dako) diluted in PBS with 100 g/L BSA for 1 h at room temperature. After being washed, the HRP was visualized by development with chromogenic agents.

The staining intensity was graded as follows: -, no staining; +, weak staining; ++, moderate staining; and +++, strong staining.

RNA isolation and reverse transcriptase polymerase chain reaction (RT-PCR)

Total RNA was extracted from normal and cancer tissues, respectively. The method of RNA extraction was similar to the TRIzol RNA extraction protocol (Life Technologies Inc.). The concentration of RNA extracted was determined at wavelength of 260 nm using a U-2000 spectrophotometer (HITACH Ltd, Tokyo, Japan). The sequences of ODC primers were as follows: up-stream primer: 5'-GCAGG-ATCCACCATGAACAACTTTGGTAA -3', down-stream primer: 5'- GCCGAGATCTCAGAAGAAGAAACTTC -3'. This pair of primers could span a 120-bp fragment of human ODC exon 3. Human β-actin was used as a control. Ten microliters of each amplification reaction were analyzed by electrophoresis using 1.2% agarose gel in the presence of 5 ng/mL ethidium bromide. DNA was detected under UV light.

RESULTS

Determination of anti-ODC mAb by enzyme linked immunosorbent assay and Western blotting

ELISA showed that the mAb could immunobind to recombinant human ODC and standard ODC protein (Sigma). ELISA showed that the immunoglobulin produced by the positive clone was the IgG2a type.

Western immunoblotting showed that the mAb bound to the ODC protein (Figure 1).

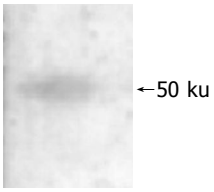

Figure 1 mAb binding to 50 ku ODC protein as shown by Western blotting.

Detection of ODC in colorectal carcinoma by immunohistochemical staining

Tumor histotype and grade of differentiation were defined according to the WHO criteria[15]. Immunohistochemical staining of human colorectal carcinoma using ODC mAb demonstrated staining in cytoplasm. Density staining in deep brown color could be seen in most of the carcinoma tissues while only a few faint stainings were in the normal tissues (Figure 2). The staining intensity showed that ODC protein expression in cancer tissue was much higher than that in normal tissue, but there was no significant difference among different histologic grades of the tumor (Table 1). There was no difference between Duck's stages A/B and C/D.

ODC mRNA expression analysis

RT-PCR showed that the expressed ODC mRNA in colorectal carcinoma tissues was significantly higher than that in normal tissues ($P<0.01$). There was no difference between male and female cases. Among the 27 well-to-moderately differentiated cancer samples, 9 were over-expressed and 18 were highly-expressed. Three of four

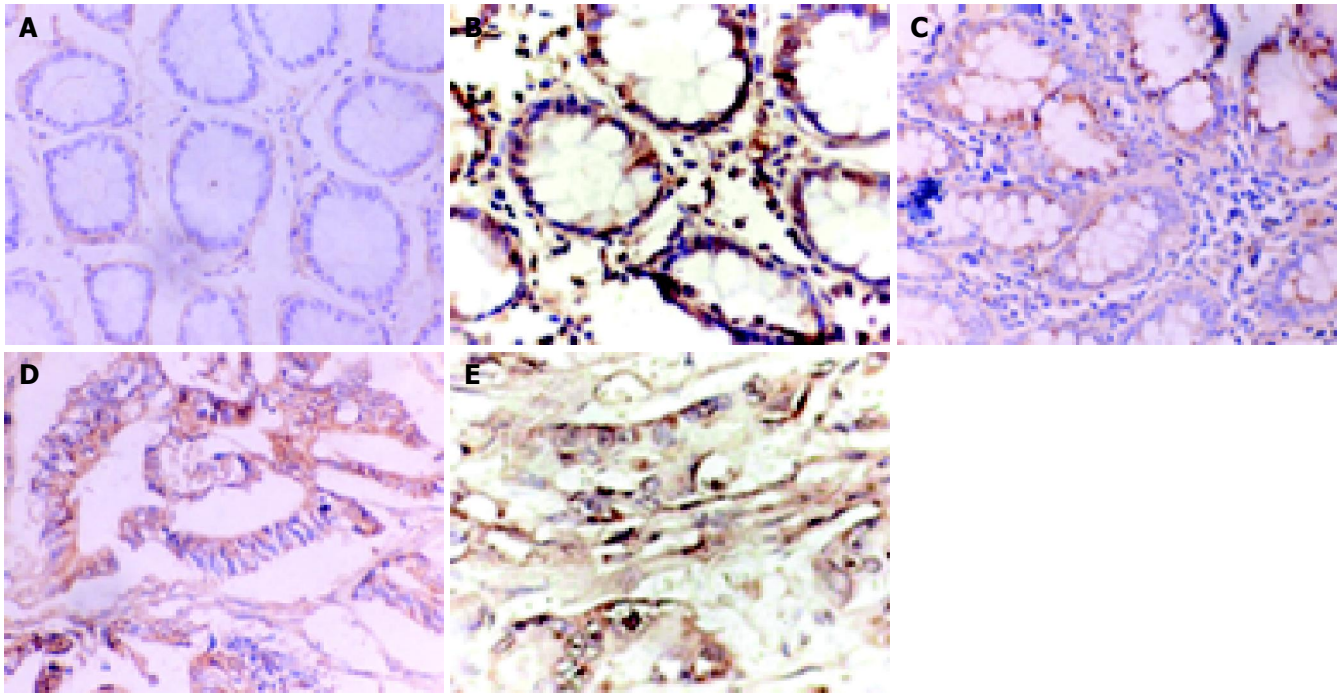

Figure 2 Immunohistochemical staining of colon tissues. **A**: Normal colon tissue obtained 15 cm apart from neoplasm; **B**: Tissue from well-differentiated adenocarcinoma; **C**: Tissue from moderately differentiated adenocarcinoma; **D**: Tissue from poorly differentiated mucinous adenocarcinoma; **E**: Tissue from undifferentiated carcinoma.

Table 1 **Immunohistochemical assay of ODC protein in colorectal carcinoma**

Histological grade and Duck's stage	–	+	++	+++	Total	Positive rate (%)	P^b
Normal	18	1	0	0	19	5	
Grade 1 well differentiated	1	2	4	9	16	93.75	<0.01
Grade 2 moderately differentiated	0	0	7	21	28	100	<0.01
Grade 3 poorly differentiated	0	0	8	7	15	100	<0.01
Grade 4 undifferentiated	0	1	6	3	10	100	<0.01
Duck'SA/B	1	1	11	17	31	96.7	<0.01
Duck'sC/D	0	1	14	23	38	100	<0.01

[b]P<0.01 *vs* normal tissue.

undifferentiated samples were over-expressed (Figure 3 and Table 2). χ^2 test showed that there was no difference among the different histologic grades, but there was a significant difference between Duck's stages AB/CD (P<0.05).

DISCUSSION

Polyamines, such as putrescine, spermidine and spermine, play an important role in cell proliferation, differentiation, and transformation. It has been proposed that urinary or blood measurement might be a useful, non-invasive diagnostic marker of colon cancer[16]. Since the intracellular polyamine pool could be regulated by external factors, such as uptake and excretion, the research outcome was disappointed. As the first and rate-limiting enzyme, ODC is the most extensively studied enzyme in polyamine metabolism. ODC protein is 50 ku as a monomer and about 100 ku when the active dimer is formed. ODC synthesis is dramatically induced by different growth stimuli, such as hormones, growth factors, carcinogens, viruses and oncogenes. The regulation can occur at the levels of transcription, translation and protein degradation. The alterations in enzymes can occur very quickly and change polyamine level in the end. ODC gene is considered as an immediate early gene, and contains response elements for several transacting factors, including a cAMP[17] response element, a possible insulin response element[18] and several Sp1 binding sites. In addition, ODC gene expression has been tightly linked to transformation by activated *ras*, *v-src and myc*[19]. So, recently, ODC gene has been postulated as an oncogene, which is essential for cell transformation[9,20,21]. It has been demonstrated that both ODC and polyamine content analysis in biopsy specimens can be very useful in the diagnosis of malignancy and prognosis of breast cancer[22]. As to colorectal cancer ODC was found in a very limited amount in quiescent cells and its activity was found to be increased significantly in colon adenocarcinoma and prostate tissue compared to normal tissue from the same patients[23,24]. Polyp is a benign neoplasia with a high risk of developing into colorectal cancer. Increased ODC activity and polyamine concentrations have

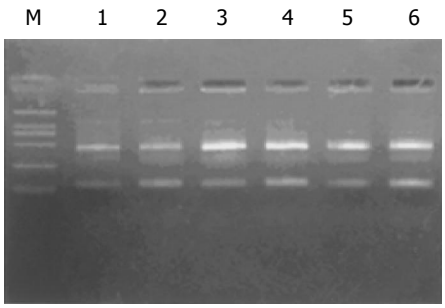

Figure 3 ODC mRNA expression assay by RT-PCR. M: molecular weight marker DL-2000. Lanes 1, 3 and 5: normal mucosa tissues. Lanes 2, 4 and 6: malignant tissue samples. β-actin was amplified as an internal control.

also been observed in the colon of presymptomatic familial adenomatous polyposis patients[22].

In the present study, we compared the ODC gene expression in human colorectal carcinoma with that in normal colon mucosa. ODC mRNA was extracted from human colon cancer tissues and ODC mRNA was detected by RT-PCR. The results showed that the ODC mRNA level in colorectal carcinoma was significantly higher than that in contiguous normal colon mucosa. Furthermore, we found that ODC gene expression was associated with the stage of malignancy. These findings suggest that the increase of ODC mRNA may play an important role in the process of colorectal tumor progression. ODC cDNA was inserted into an expression vector and the ODC gene expression vector pQE-ODC was established. The vector with a 6-His tag, which made the expression of ODC protein with about 95% purity, was used as a good immunogenic agent to immunize the BALB/c mice. Monoclonal anti-ODC antibody was produced by cell hybrids between hypoxanthine phosphoribosyl transferase-deficient myeloma cells and spleen cells of immunized mice. The antibody was the IgG2a type.

ELISA and Western blotting showed that the mAb could combine the standard ODC (EC4.1.1.17) protein. Staining of colorectal tissues with ODC mAb showed a significant difference between normal and tumor mucosae. The deep brown staining could be found in gland cells of the tumor, while there was no staining or weak staining in stoma cells. The results suggested that there was a high concentration of ODC protein in tumor cell cytoplasm. These changes did not correlate with gender, histologic grade or Duck's stage, which confirmed that increase of ODC protein was both an early event and a late event in patients with colon cancer. RT-PCR showed that the ODC mRNA was much higher in colon tumor tissues than in normal tissues. The ODC mRNA expression was higher in Duke's stages C/D than A/B. In conclusion, changes in ODC mRNA and protein content play an important role in the pathology of human colorectal carcinoma, and ODC gene expression may be a diagnosis and therapeutic marker of human colorectal carcinoma.

Table 2 **ODC mRNA expression in normal and colorectal tumor tissues**

Samples	ODC mRNA expression (*n*)			Total (*n*)	*P*
	Low	Over	high		
Normal	31	0	0	31	<0.01
Tumor	0	19	12	31	
Gender					
Male	0	9	6	15	>0.05
Female	0	10	6	16	
Histologic grade					
Well-to-moderately differentiated	0	18	9	27	>0.05
Undifferentiated	0	1	3	4	
Duck's stage					
A/B	0	17	5	22	<0.05
C/D	0	2	7	9	

ACKNOWLEDGMENTS

The authors thank Dr. Jian Zhan, Dr. Jian-Hua Zhan and their colleagues in Shandong Academy of Medical Sciences for their kind help with the preparation of anti-ODC monoclonal antibody.

REFERENCES

1 **Ries LA,** Wingo PA, Miller DS, Howe HL, Weir HK, Rosenberg HM, Vernon SW, Cronin K, Edwards BK. The annual report to the nation on the status of cancer, 1973-1997,with a special section on colorectal cancer. *Cancer* 2000; **88**: 2398-2424
2 **Greenlee RT,** Murray T, Bolden S, Wingo PA. Cancer statistics, 2000. *CA Cancer J Clin* 2000; **50**: 7-33
3 **Shu Z.** Colorectal cancer. In: Jiefu Wang,ed: Gastrointestinal Surgery. Beijing: People's Medical Publishing House,2000: 920-923
4 **McCormick D,** Kibbe PJ, Morgan SW. Colon cancer: prevention, diagnosis, treatment. *Gastroenterol Nurs* 2002; **25**: 204-211; quiz, 211-212
5 **Hamilton SR.** Colon cancer testing and screening. *Arch Pathol Lab Med* 1999; **123**: 1027-1029
6 **Wallace HM,** Caslake R. Polyamines and colon cancer. *Eur J Gastroenterol Hepatol* 2001; **13**: 1033-1039
7 **Rich TA,** Skibber JM, Ajani JA, Buchholz DJ, Cleary KR, Dubrow RA, Levin B, Lynch PM, Meterissian SH, Roubein LD. Preoperative infusional chemoradiation therapy for stage T3 rectal cancer. *Int J Radiat Oncol Biol Phys* 1995; **32**: 1025-1029
8 **Thomas T,** Thomas TJ. Polyamine metabolism and cancer. *J Cell Mol Med* 2003; **7**: 113-126
9 **Auvinen M,** Paasinen A, Andersson LC, Holtta E. Ornithine decarboxylase activity is critical for cell transformation. *Nature* 1992; **360**: 355-358
10 **Rozhin J,** Wilson PS, Bull AW, Nigro ND. Ornithine decarboxylase activity in the rat and human colon. *Cancer Res* 1984; **44**: 3226-3230
11 **Liu XX,** Fu SJ, Zhao CH, Zhang YY, Luo DC, Lin YQ, Jiang CY, Zhang XT, Xuan YJ. ODC activity and polyamine concentration in colon tumor tissue and peratumor tissue. *Zhongguo Gangchangxue Zazhi* 1996; **16**: 11
12 **Canizares F,** Salinas J, de las Heras M, Diaz J, Tovar I, Martinez P, Penafiel R. Prognostic value of ornithine decarboxylase and polyamines in human breast cancer: correlation with clinicopathologic parameters. *Clin Cancer Res* 1999; **5**: 2035-2041
13 **Hu HY,** Liu XX, Jiang CY, Zhang Y, Bian JF, Lu Y, Geng Z, Liu SL, Liu CH, Wang XM, Wang W. Cloning and expression of ornithine decarboxylase gene from human colorectal carcinoma. *World J Gastroenterol* 2003; **9**: 714-716
14 **Gerhard W,** Braciale TJ, Klinman NR The analysis of the monoclonal immune response to influenza virus. I. Production of monoclonal anti-viral antibodies *in vitro*. *Eur J Immunol*

1975; **5**: 720-725
15 WHO. Histological typing of intestinal tumors 2nd ed. In: Jass J. R. Sobin L H. eds. nternational histological classifications of tumors: Berlin: Springer-Verlag, 1989
16 **Russell DH,** Durie BGM. Polyamines and the clinical evauation of patients with cancer. Russell and Durie (editors). New York: Raven Press; 1978: 139-155
17 **Montminy MR,** Bilezikjian LM. Binding of a nuclear protein to the cyclic-AMP response element of the somatostatin gene. *Nature* 1987; **328**: 175-178
18 **Manzella JM,** Rychlik W, Rhoads RE, Hershey JW, Blackshear PJ. Insulin induction of ornithine decarboxylase. Importance of mRNA secondary structure and phosphorylation of eucaryotic initiation factors eIF-4B and eIF-4E. *J Biol Chem* 1991; **266**: 2383-2389
19 **Sistonen L,** Holtta E, Lehvaslaiho H, Lehtola L, Alitalo K. Activation of the neu tyrosine kinase induces the fos/jun transcription factor complex, the glucose transporter and ornithine decarboxylase. *J Cell Biol* 1989; **109**: 1911-1919
20 **Rousseau D,** Kaspar R, Rosenwald I, Gehrke L, Sonenberg N. Translation initiation of ornithine decarboxylase and nucleocytoplasmic transport of cyclin D1 mRNA are increased in cells overexpressing eukaryotic initiation factor 4E. *Proc Natl Acad Sci USA* 1996; **93**: 1065-1070
21 **Pendeville H,** Carpino N, Marine JC, Takahashi Y, Muller M, Martial JA, Cleveland JL. The ornithine decarboxylase gene is essential for cell survival during early murine development. *Mol Cell Biol* 2001; **21**: 6549-6558
22 **Love RR,** Astrow SH, Cheeks AM, Havighurst TC. Ornithine decarboxylase (ODC) as a prognostic factor in operable breast cancer. *Breast Cancer Res Treat* 2003; **79**: 329-334
23 **Linsalata M,** Caruso MG, Leo S, Guerra V, D'Attoma B, Di Leo A. Prognostic value of tissue polyamine levels in human colorectal carcinoma. *Anticancer Res* 2002; **22**: 2465-2469
24 **Giardiello FM,** Hamilton SR, Hylind LM, Yang VW, Tamez P, Casero RA. Ornithine decarboxylase and polyamines in familial adenomatous polyposis. *Cancer Res* 1997; **57**: 199-201

Science Editor Wang XL and Li WZ **Language Editor** Elsevier HK

PO Box 2345, Beijing 100023, China
www.wjgnet.com
wjg@wjgnet.com

ELSEVIER

World J Gastroenterol 2005;11(15):2249-2254
World Journal of Gastroenterology ISSN 1007-9327

Rectosigmoid findings are not associated with proximal colon cancer: Analysis of 6 196 consecutive cases undergoing total colonoscopy

Makoto Okamoto, Takao Kawabe, Yutaka Yamaji, Jun Kato, Tsuneo Ikenoue, Goichi Togo, Haruhiko Yoshida, Yasushi Shiratori, Masao Omata

Makoto Okamoto, Takao Kawabe, Yutaka Yamaji, Jun Kato, Tsuneo Ikenoue, Goichi Togo, Haruhiko Yoshida, Yasushi Shiratori, Masao Omata, Department of Gastroenterology, Faculty of Medicine, University of Tokyo, Japan
Correspondence to: Makoto Okamoto, MD, Department of Gastroenterology, Faculty of Medicine, University of Tokyo, 7-3-1 Hongo, Bunkyo-ku, Tokyo 113-8655, Japan. okamoto-2im@h.u-tokyo.ac.jp
Telephone: +81-3-3815-5411-33056 Fax: +81-3-3814-0021
Received: 2004-05-07 Accepted: 2004-11-30

Abstract

AIM: To review the risk of proximal colon cancer in patients undergoing colonoscopy.

METHODS: We estimated the risk of advanced proximal adenomas and cancers in 6 196 consecutive patients that underwent colonoscopy (mean age 60 years, 65% males, without prior history of colorectal examination). Neoplasms were classified as diminutive adenoma (5 mm or less), small adenoma (6-9 mm), advanced adenoma (10 mm or more, with villous component or high-grade dysplasia) and cancer (invasive adenocarcinoma). The sites of neoplasms were defined as rectosigmoid (rectum and sigmoid colon) and proximal colon (from cecum to descending colon).

RESULTS: The trend of the prevalence of advanced proximal adenoma was to increase with severe rectosigmoid findings, while the prevalence of proximal colon cancer did not increase with severe rectosigmoid findings. Among the 157 patients with proximal colon cancer, 74% had no neoplasm in the rectosigmoid colon. Multivariate logistic-regression analysis revealed that age was the main predictor of proximal colon cancer and existence of rectosigmoid adenoma was not a predictor of proximal colon cancer.

CONCLUSION: Sigmoidoscopy is inadequate for colorectal cancer screening, especially in older populations.

Key words: Colorectal cancer; Advanced adenoma; Rectosigmoid colon; Proximal colon

Okamoto M, Kawabe T, Yamaji Y, Kato J, Ikenoue T, Togo G, Yoshida H, Shiratori Y, Omata M. Rectosigmoid findings are not associated with proximal colon cancer: Analysis of 6 196 consecutive cases undergoing total colonoscopy. *World J Gastroenterol* 2005; 11(15): 2249-2254
http://www.wjgnet.com/1007-9327/11/2249.asp

INTRODUCTION

Colorectal cancer is one of the leading causes of cancer death in the USA and Europe. In USA, it was reported in 1998 that there are 144 300 patients with colorectal cancer and approximately 56 600 deaths per year[1]. Recently, the incidence of colorectal cancer has been increasing remarkably in Japan and China, and nearly 37 000 deaths per year occur in Japan[2,3]. In these countries, there is a proximal shift in the subsite distribution of colorectal cancer[4-6], which is associated with increase in age[7-11].

To reduce the high incidence, screening of colorectal cancer in asymptomatic individuals has been advocated[12-14]. Fecal occult blood testing is widely used in colorectal cancer screening and some prospective cohort studies with large populations have shown that this kind of screening can reduce the mortality of colorectal cancer[15-17]. Sigmoidoscopy is an important screening method that has been proposed as an alternative for fecal occult blood test. Endoscopy has a higher sensitivity than fecal occult blood testing, especially for adenoma. Sigmoidoscopy is simpler, faster, and better tolerable than total colonoscopy, but the scope cannot reach the proximal colon segment and therefore, may miss proximal colon cancer. Previous studies reported that polyps in rectosigmoid colon are associated with advanced proximal neoplasms[18-25]. Thus, examination of the proximal colon is recommended for patients with adenomas detected by sigmoidoscopy[13]. On the other hand, studies have reported that patients with proximal advanced neoplasms may have no rectosigmoid adenoma[26-31].

In the present study, we prospectively collected and analyzed the data from a large cohort of consecutive patients who underwent total colonoscopy for specific reasons. Our aim was to investigate the prevalence of advanced proximal adenoma and cancer according to the findings in rectosigmoid colon, and to find their risk factors.

MATERIALS AND METHODS

Patients

Data were collected from 11 520 consecutive patients who

underwent colonoscopic examinations at the Department of Gastroenterology, University of Tokyo, and its affiliated hospitals between January 1997 and December 2002. Any polyp found during the procedure was removed.

The following data were obtained from all patients: age and gender, indication for colonoscopy, history of colorectal cancer resection or polyp excision, colonoscopic findings such as location and size of polyp or tumor, and histopathology of polyp or tumor.

Excluded from this study were patients with histories of colorectal cancer resection, colorectal polyp excision, hereditary colorectal cancers (familial adenomatous polyposis and hereditary non-polyposis colorectal cancer), inflammatory bowel disease (ulcerative colitis and Crohn's disease), incomplete colonoscopy (unable to reach the cecum), poor bowel preparation, and incomplete polypectomy or unresected polyps. Patients with poor bowel preparation were not included because it was difficult to detect small polyps.

Colonoscopy

Colonoscopy was performed by skilled endoscopists, each with more than 5 years of experience. Examination of the cecum was attempted in each patient. Preparation of colonoscopy consisted of whole-gut lavage with polyethylene glycol-electrolyte solution 3-5 h before the examination. Colonoscopy was performed using a video colonoscope.

Colorectal neoplasms

Histologic diagnosis of adenoma and adenocarcinoma was based on the World Health Organization (WHO) criteria[32] and confirmed by two pathologists. The location and size of all polyps and tumors were recorded at the time of colonoscopy. The location of polyps and tumors was determined by the length of the colonoscope from the anus at the time of examination. The size of polyps was measured with open biopsy forceps at the time of examination.

The location of polyps and tumors was categorized into two groups: rectosigmoid colon (sigmoid colon and rectum) and proximal colon (from cecum to descending colon). In patients with more than one polyp in either the rectosigmoid or proximal segment of the colon, the most advanced lesion in the segment was included in the analysis.

Findings in rectosigmoid and proximal colon were divided into no neoplasm, diminutive, small, and advanced adenomas, and cancer. Diminutive adenoma was defined as tubular adenoma (5 mm or smaller in diameter), small adenoma as tubular adenoma (6-9 mm in diameter), and advanced adenoma as large adenoma (10 mm or larger in diameter) and adenoma with a villous component or high-grade dysplasia[33-35]. Findings such as hyperplastic, inflammatory, and juvenile polyps, or lymphoid aggregation were considered as non-neoplastic lesions and not included in any analyses.

Statistical analysis

Multivariate logistic-regression analysis was used to estimate the odds ratios of proximal advanced adenoma and cancer, categories of age, and gender, indication for colonoscopy, and rectosigmoid findings. Data were analyzed using Bonferroni's method. $P<0.05$ was considered statistically significant.

RESULTS

Patients

During the study period, colonoscopy was performed in 11 520 patients, 5 324 of them were excluded on the basis of the following reasons: history of colorectal polyp excision (n = 3 340), colorectal cancer resection (n = 328), hereditary colorectal cancer (n = 6), inflammatory bowel disease (n = 298), incomplete polypectomy (n = 540), incomplete colonoscopy (n = 490), and poor bowel preparation (n = 322). The remaining 6 196 patients were included in this study (Table 1).

Among these 6 196 patients, 3 999 (64.5%) were males and 2 197 (35.5%) were females. The mean age of the patients was 60.1 years. The indications for colonoscopy were categorized into asymptomatic, positive FOBT, and symptomatic groups. Asymptomatic group was composed of 575 patients who underwent screening colonoscopy without any abdominal symptom and fecal occult blood test. FOBT group was composed of 2 500 patients who had positive fecal occult blood test in mass screening. Symptomatic group was composed of 3 121 patients who complained of abdominal symptoms (lower gastrointestinal bleeding, lower abdominal pain, altered bowel habit, *etc.*).

Table 1 **Characteristics of all included patients (n = 6 196)**

Variable		Value (%)
Gender		
	Male	3 999 (64.5)
	Female	2 197 (35.5)
Age (yr)		
	-49	1 166 (18.8)
	50-59	1 618 (26.1)
	60-69	1 860 (30.0)
	70-	1 552 (25.0)
	mean±SD	60.1 (13.3)
Indications for colonoscopy		
	Asymptomatic	575 (9.3)
	Positive for fecal occult blood	2 500 (40.3)
	Symptomatic	3 121 (50.4)
	Bleeding	922
	Lower abdominal pain	861
	Altered bowel habit	634
	Anemia	261
	Elevated CEA	212
	Other reasons	231

Findings in rectosigmoid colon

Among the 6 196 patients, 1 951 were positive and 4 245 negative for neoplasms in the rectosigmoid colon. Histology of the neoplasms in the rectosigmoid colon showed that 598 patients had diminutive adenomas, 500 patients had small adenomas, 673 patients had advanced adenomas (466 with tubular adenomas, 76 with adenomas with villous histology, and 131 with adenomas with high-grade dysplasia), and 180 had cancer. One thousand three hundred and twenty-nine patients had a single neoplasm and 622 had two or more neoplasms (Table 2).

Table 2 **Findings in rectosigmoid and proximal colon of all patients (*n* = 6 196)**

Findings	Rectosigmoid colon	Proximal colon
	Number of patients (%)	Number of patients (%)
No neoplasm	4 245 (68.5)	3 991 (64.4)
Histology of most advanced lesion		
Diminutive adenoma[1]	598 (9.7)	968 (15.6)
Small adenoma[2]	500 (8.2)	561 (9.1)
Advanced adenoma[3]	673 (10.9)	519 (8.3)
Cancer	180 (2.9)	157 (2.5)
No. of lesions		
One	1 329 (21.4)	1 173 (18.9)
Two or more	622 (10.0)	1 032 (16.7)

[1]Tubular adenoma (5 mm or less in diameter) [2]Tubular adenoma (6–9 mm in diameter) [3]Tubular adenoma (10 mm or more in diameter), villous histology, or severe dysplasia.

Prevalence of advanced proximal adenoma

The prevalence of advanced proximal adenoma was analyzed based on the findings in rectosigmoid colon (Table 3).

The prevalence of advanced proximal adenoma was 6.2% (95% CI, 5.5-6.9) in the 4 245 patients with no rectosigmoid neoplasm, 6.9% (95% CI, 4.8-8.9) in the 598 patients with diminutive rectosigmoid adenomas, 12.0% (95% CI, 9.2-14.8) in the 500 patients with small rectosigmoid adenomas, 18.1% (95% CI, 15.2-21.0) in the 673 patients with advanced rectosigmoid adenomas, and 17.8% (95% CI, 12.2-23.4) in the 180 patients with rectosigmoid cancer.

One hundred and fifty of 1 329 patients with a single neoplasm had advanced proximal adenomas (11.3%, 95% CI, 9.6-13.0), and 105 of 622 patients with two or more rectosigmoid neoplasms had advanced proximal adenomas (16.9%, 95% CI, 13.9-19.8).

The prevalence of advanced proximal adenoma increased with increasingly rectosigmoid findings.

Prevalence of proximal colon cancer

The prevalence of proximal colon cancer was analyzed according to the findings in rectosigmoid colon (Table 3).

The prevalence of proximal cancer was 2.7% (95% CI, 2.2–3.2) in the 4 245 patients without rectosigmoid neoplasm, 1.8% (95% CI, 0.8-2.9) in the 598 patients with diminutive rectosigmoid adenomas, 2.8% (95% CI, 1.4-4.2) in the 500 patients with small rectosigmoid adenomas, 2.2% (95% CI, 1.1-3.3) in the 673 patients with advanced rectosigmoid adenomas, and 0.6% (95% CI, 0.0-1.6) in the 180 patients with rectosigmoid cancer.

Twenty-seven of 1 329 patients with a single neoplasm had proximal cancer (2.0%, 95% CI, 1.3-2.8), and 14 of 622 patients with two or more rectosigmoid neoplasms had proximal cancer (2.3%, 95% CI, 1.1-3.4).

The prevalence of proximal colon cancer was not associated with severe rectosigmoid findings.

Findings in patients with proximal advanced adenoma and cancer

Among the 6 196 patients, 519 patients had proximal advanced adenoma, 264 of these 519 patients had no neoplasm in the rectosigmoid colon (50.9%). Moreover, among 157 patients with proximal colon cancer, 116 had no neoplasm in the rectosigmoid colon (73.9%).

Risk for proximal colon cancer and advanced adenoma

Among the 6 196 patients in this study, multivariate analysis showed that only age was significantly associated with the risk for proximal colon cancer (Table 4). Patients aged 70 years or more showed a markedly increased risk for proximal cancer (odds ratio 35.6; 95% CI 8.7-145.2) compared with patients aged 49 years or less. Gender and rectosigmoid colon findings were not associated with significant differences in the risk for proximal colon cancer.

On the other hand, age and gender were significantly associated with the risk of advanced proximal adenoma. Male patients showed increased risk of advanced proximal adenoma (odds ratio 2.1; 95% CI, 1.7-2.6) compared with female patients, and patients aged 70 years or more showed increased risk for proximal cancer (odds ratio 3.5; 95% CI, 2.4-5.1) compared with patients aged 49 years or less. Patients with diminutive adenomas in the rectosigmoid colon were not associated with significantly increased risk for proximal advanced adenoma (odds ratio 0.9: 95% CI, 0.6-1.3) compared with patients without rectosigmoid neoplasm.

DISCUSSION

In developed countries, the incidence of proximal colon cancer increases with a time trend[4-6]. Furthermore, proximal shift of colorectal cancer is observed in the aged population[7-11]. With the aged population increase in developed countries,

Table 3 **Prevalence of proximal advanced adenoma and cancer**

Rectosigmoid findings	Number of pts	Proximal findings					
		Advanced adenoma			Cancer		
		Number of pts	(%)	(95% CI)	Number of pts	(%)	(95% CI)
No neoplasm	4 245	264	(6.2)	(5.5–6.9)	116	(2.7)	(2.2–3.2)
Histology of most advanced neoplasm							
Diminutive adenoma	598	41	(6.9)	(4.8–8.9)	11	(1.8)	(0.8–2.9)
Small adenoma	500	60	(12.0)	(9.2–14.8)	14	(2.8)	(1.4–4.2)
Advanced adenoma	673	122	(18.1)	(15.2–21.0)	15	(2.2)	(1.1–3.3)
Cancer	180	32	(17.8)	(12.2–23.4)	1	(0.6)	(0.0–1.6)
No. of neoplasms							
One	1 329	150	(11.3)	(9.6–13.0)	27	(2.0)	(1.3–2.8)
Two or more	622	105	(16.9)	(13.9–19.8)	14	(2.3)	(1.1–3.4)

Table 4 **Risk of proximal advanced adenoma and cancer according to gender, age, and rectosigmoid findings (multivariate analysis)**

Variables	No. of pts	Proximal colon					
		Advanced adenoma			Cancer		
		Odds ratio	(95%CI)	*P*	Odds ratio	(95%CI)	*P*
Gender							
Female	2 197	1	(Referent)		1	(Referent)	
Male	3 999	2.1	(1.7–2.6)	<0.0001	0.9	(0.6–1.3)	0.5287
Age (yr)							
–49	1 166	1	(Referent)		1	(Referent)	
50–59	1 618	2.5	(1.7–3.6)	<0.0001	10.0	(2.4–42.4)	0.0018
60–69	1 860	3.1	(2.12–4.5)	<0.0001	13.8	(3.3–57.2)	0.0003
70–	1 552	3.5	(2.4–5.1)	<0.0001	35.6	(8.7–145.2)	<0.0001
Findings of rectosigmoid colon							
No neoplasm	4 245	1	(Referent)		1	(Referent)	
Diminutive adenoma	598	0.9	(0.6–1.3)	0.4995	0.7	(0.3–1.2)	0.1881
Small adenoma	500	1.6	(1.2–2.2)	0.0019	1.0	(0.6–1.8)	0.9731
Advanced adenoma	673	2.5	(2.0–3.2)	<0.0001	0.8	(0.5–1.4)	0.4577
Cancer	180	2.6	(1.7–3.8)	<0.0001	0.2	(0.0–1.2)	0.0726

proximal colon cancer has had more significance. Therefore it is of great significance to review the risk factor for the proximal colon cancer.

Sigmoidoscopy is a vital procedure for screening colorectal cancer[12-14]. If there was a reliable rectosigmoid marker for the presence of clinically important proximal neoplasms or if normal findings in the rectosigmoid colon were a reliable marker for their absence, then sigmoidoscopic examination could determine which patients should undergo total colonoscopy.

The principal findings in this study are as follows: patients with no rectosigmoid adenoma could indeed have proximal colon cancer, which was not associated with rectosigmoid findings. It is clear that a substantial number of colorectal cancers would be missed if only sigmoidoscopy was performed. In addition, old age is an important risk factor for proximal colon cancer.

Studies reported that prevalence of advanced proximal adenoma is related to sigmoidoscopic findings in total colonoscopy[18-31]. According to these studies, the prevalence of advanced proximal adenoma increases with rectosigmoid findings. But the prevalence of proximal colon cancer in association with rectosigmoid findings is rarely reported[28]. Levin *et al*[28], reported that the prevalence of proximal cancer is not associated with rectosigmoid findings. But in their study, the number of proximal cancer cases was less. We used a large number of patients undergoing total colonoscopy and analyzed the prevalence of both advanced proximal adenoma and cancer. We found that the prevalence of advanced proximal adenoma increased in association with rectosigmoid findings. On the other hand, the prevalence of proximal colon cancer did not show such a tendency.

Studies reported that the prevalence of rectosigmoid adenoma in cases of proximal colon cancer is not associated with rectosigmoid neoplasms[36-38]. Rex *et al*[39], carried out a prospective study on the prevalence of distal adenoma in cases of proximal colon cancer, and reported that 66% of the proximal cancer cases have no distal adenoma. In our present study, 74% of the proximal colon cancer cases lacked rectosigmoid adenoma, which is consistent with what was reported in previous studies[36-39]. Moreover, about 3% of the patients with no rectosigmoid adenoma in our cohort had proximal colon cancer.

Imperiale *et al*[27], reported that distal polyps, older age, and male sex were the risk factors of advanced proximal neoplasia including advanced adenoma and invasive cancer. However, the risk for proximal cancer alone was not addressed. In the present study, multivariate logistic-regression analysis revealed that old age, male sex and rectosigmoid small or advanced adenoma were risk factors for advanced proximal adenoma. On the other hand, only old age was a risk factor, but not the male sex or rectosigmoid findings for proximal cancer. These results suggest that sigmoidoscopy is an insufficient screening procedure for detecting proximal cancer, especially in older subjects. Our previous study[7] reported that with advancing age, there is a tendency of a proximal shift of colon cancer, but the distribution of adenoma is not associated with age. This difference between proximal cancer and advanced proximal adenoma may provide some information concerning the carcinogenesis of proximal colon cancer, as it seems that a certain number of proximal colon cancers are not associated with adenoma. This topic, especially from the aspect of molecular biology, requires further extensive studies. Microsatellite instability frequently occurs in the proximal colon cancer, especially in aged patients[40-43], but it is rare in adenoma[44]. This difference between proximal colon cancer and adenoma might be reflected in the difference of the risk factor for proximal colon cancer and adenoma as observed in our study.

Interpretation of our findings requires careful consideration of several methodological issues. First, our data may have been affected by selection bias, because our study population included patients with various indications for colonoscopy To adjust the confounding effect caused by the indications for colonoscopy, multivariate analyses were adjusted according to indications for colonoscopy. Moreover, among the 6 196 patients, 575 asymptomatic patients underwent colonoscopy. Three, of these 575 patients, had proximal colon cancer two patients had no rectosigmoid adenoma, and only one had small adenoma in rectosigmoid colon.

Second, "proximal colon" generally means the colon

proximal to the splenic flexure. But flexible sigmoidoscopy reaches the splenic flexure in only 16% of the cases, and usually reaches up to the sigmoid-descending junction[45]. Thus, in general, neoplasms proximal to the sigmoid colon cannot be visualized by sigmoidoscopy. We defined the proximal colon as proximal to the sigmoid colon in this study.

Third, hyperplastic polyp is a non-neoplastic lesion, and the significance of hyperplastic polyps in the rectosigmoid colon has been controversial. Some studies reported that hyperplastic polyps are a marker of proximal colon neoplasms[23,25,27], whereas other studies showed that hyperplastic polyps in the rectosigmoid colon have no relation with proximal colon neoplasms[24,26,30]. In the present study, patients with hyperplastic polyps in the rectosigmoid colon were considered normal.

Sigmoidoscopy is the method widely used for screening colorectal cancer[12-14], and has led to increased detection of benign diminutive adenomas in the rectosigmoid colon. The need for colonoscopy in individuals with diminutive tubular adenomas found in sigmoidoscopy is an important but controversial issue in screening for colorectal cancer. Some studies reported that adenomas of the rectosigmoid colon, regardless of size, are markers of neoplasms in the colon, and colonoscopy is thus advocated for such patients[13,18,21,22,25,29]. However, other studies reported that the discovery rate of advanced proximal neoplasm in such patients is low and colonoscopy is not indicated[19,28]. According to our study, diminutive adenomas in the rectosigmoid colon might be a useful marker of advanced proximal adenoma, but its prevalence does not differ between patients with no rectosigmoid adenoma and those with rectosigmoid diminutive adenomas. Moreover, neither diminutive adenoma in the rectosigmoid colon nor any other type of rectosigmoid adenoma could be a marker of proximal colon cancer. Even if colonoscopy was performed for any distal adenoma in our study cohort, nearly three-quarters of the patients with proximal invasive cancer and half of the patients with advanced proximal adenoma would have been missed, indicating that a substantial number of proximal cancers and advanced adenomas are not associated with any distal neoplasms.

In conclusion, sigmoidoscopy might be an inadequate method for colorectal cancer screening, especially in older people. The current strategy of deciding who should undergo colonoscopy on the basis of sigmoidoscopy needs to be reconsidered.

REFERENCES

1 **Jemal A,** Thomas A, Murray T, Thun M. Cancer statistics, 2002. *CA Cancer J Clin* 2002; **52**: 23-47
2 Statistics and Information Department. Ministry of Health and Welfare in Japan. Vital statistics of Japan 2001. Tokyo: Kosei Tokei Kyokai, 2003 (in Japanese)
3 **Zhang YL,** Zhang ZS, Wu BP, Zhou DY. Early diagnosis for colorectal cancer in China. *World J Gastroenterol* 2002; **8**: 21-25
4 **Rhodes JB,** Holmes FF, Clark GM. Changing distribution of primary cancers in the large bowel. *JAMA* 1977; **238**: 1641-1643
5 **Levi F,** Randimbison L, La Vecchia C. Trends in subsite distribution of colorectal cancers and polyps from the Vaud Cancer Registry. *Cancer* 1993; **72**: 46-50
6 **Takada H,** Ohsawa T, Iwamoto S, Yoshida R, Nakano M, Imada S, Yoshioka K, Okuno M, Masuya Y, Hasegawa K, Kamano N, Hioki K, Muto T, Koyama Y. Changing site distribution of colorectal cancer in Japan. *Dis Colon Rectum* 2002; **45**: 1249-1254
7 **Okamoto M,** Shiratori Y, Yamaji Y, Kato J, Ikenoue T, Togo G, Yoshida H, Kawabe T, Omata M. Relationship between age and site of colorectal cancer based on colonoscopy findings. *Gastrointest Endosc* 2002; **55**: 548-551
8 **Griffin PM,** Liff JM, Greenberg RS, Clark WS. Adenocarcinomas of the colon and rectum in persons under 40 years old. A population-based study. *Gastroenterology* 1991; **100**: 1033-1040
9 **Nelson RL,** Dollear T, Freels S, Persky V. The relation of age, race, and gender to the subsite location of colorectal carcinoma. *Cancer* 1997; **80**: 193-197
10 **Fante R,** Benatti P, di Gregorio C, De Pietri S, Pedroni M, Tamassia MG, Percesepe A, Rossi G, Losi L, Roncucci L, Ponz de Leon M. Colorectal carcinoma in different age groups: a population-based investigation. *Am J Gastroenterol* 1997; **92**: 1505-1509
11 **Jass JR.** Subsite distribution and incidence of colorectal cancer in New Zealand, 1974-1983. *Dis Colon Rectum* 1991; **34**: 56-59
12 **Winawer S,** Fletcher R, Rex D, Bond J, Burt R, Ferrucci J, Ganiats T, Levin T, Woolf S, Johnson D, Kirk L, Litin S, Simmang C. Colorectal cancer screening and surveillance: clinical guidelines and rationale-Update based on new evidence. *Gastroenterology* 2003; **124**: 544-560
13 **Byers T,** Levin B, Rothenberger D, Dodd GD, Smith RA. American Cancer Society guidelines for screening and surveillance for early detection of colorectal polyps and cancer: update 1997. American Cancer Society Detection and Treatment Advisory Group on Colorectal Cancer. *CA Cancer J Clin* 1997; **47**: 154-160
14 **Rosen L,** Abel ME, Gordon PH, Denstman FJ, Fleshman JW, Hicks TC, Huber PJ, Kennedy HL, Levin SE, Nicholson JD. Practice parameters for the detection of colorectal neoplasms--supporting documentation. The Standards Task Force. AmericanSociety of Colon and Rectal Surgeons. *Dis Colon Rectum* 1992; **35**: 391-394
15 **Mandel JS,** Bond JH, Church TR, Snover DC, Bradley GM, Schuman LM, Ederer F. Reducing mortality from colorectal cancer by screening for fecal occult blood. Minnesota Colon Cancer Control Study. *N Engl J Med* 1993; **328**: 1365-1371
16 **Kronborg O,** Fenger C, Olsen J, Jorgensen OD, Sondergaard O. Randomised study of screening for colorectal cancer with faecal-occult-blood test. *Lancet* 1996; **348**: 1467-1471
17 **Hardcastle JD,** Chamberlain JO, Robinson MH, Moss SM, Amar SS, Balfour TW, James PD, Mangham CM. Randomised controlled trial of faecal-occult blood screening for colorectal cancer. *Lancet* 1996; **348**: 1472-1477
18 **Read TE,** Read JD, Butterly LF. Importance of adenomas 5 mm or less in diameter that are detected by sigmoidoscopy. *N Engl J Med* 1997; **336**: 8-12
19 **Zarchy TM,** Ershoff D. Do characteristics of adenomas on flexible sigmoidoscopy predict advanced lesions on baseline colonoscopy? *Gastroenterology* 1994; **106**: 1501-1504
20 **Papatheodoridis GV,** Triantafyllou K, Tzouvala M, Paspatis G, Xourgias V, Karamanolis DG. Characteristics of rectosigmoid adenomas as predictors of synchronous advanced proximal colon neoplasms. *Am J Gastroenterol* 1996; **91**: 1809-1813
21 **Schoen RE,** Corle D, Cranston L, Weissfeld JL, Lance P, Burt R, Iber F, Shike M, Kikendall JW, Hasson M, Lewin KJ, Appelman HD, Paskett E, Selby JV, Lanza E, Schatzkin A. Is colonoscopy needed for the nonadvanced adenoma found on sigmoidoscopy? The Polyp Prevention Trial. *Gastroenterology* 1998; **115**: 533-541
22 **Wallace MB,** Kemp JA, Trnka YM, Donovan JM, Farraye FA. Is colonoscopy indicated for small adenomas found by screening flexible sigmoidoscopy? *Ann Intern Med* 1998; **129**: 273-278
23 **Blue MG,** Sivak MV, Achkar E, Matzen R, Stahl RR. Hyper-

plastic polyps seen at sigmoidoscopy are markers for additional adenomas seen at colonoscopy. *Gastroenterology* 1991; **100**: 564-566

24 **Provenzale D,** Garrett JW, Condon SE, Sandler RS. Risk for colon adenomas in patients with rectosigmoid hyperplastic polyps. *Ann Intern Med* 1990; **113**: 760-763

25 **Achkar E,** Carey W. Small polyps found during fiberoptic sigmoidoscopy in asymptomatic patients. *Ann Intern Med* 1988; **109**: 880-883

26 **Lieberman DA,** Weiss DG, Bond JH, Ahnen DJ, Garewal H, Chejfec G. Use of colonoscopy to screen asymptomatic adults for colorectal cancer. Veterans Affairs Cooperative Study Group 380. *N Engl J Med* 2000; **343**: 162-168

27 **Imperiale TF,** Wagner DR, Lin CY, Larkin GN, Rogge JD, Ransohoff DF. Risk of advanced proximal neoplasms in asymptomatic adults according to the distal colorectal findings. *N Engl J Med* 2000; **343**: 169-174

28 **Levin TR,** Palitz A, Grossman S, Conell C, Finkler L, Ackerson L, Rumore G, Selby JV. Predicting advanced proximal colonic neoplasia with screening sigmoidoscopy. *JAMA* 1999; **281**: 1611-1617

29 **Sciallero S,** Bonelli L, Aste H, Casetti T, Bertinelli E, Bartolini S, Parri R, Castiglione G, Mantellini P, Costantini M, Naldoni C, Bruzzi P. Do patients with rectosigmoid adenomas 5 mm or less in diameter need total colonoscopy? *Gastrointest Endosc* 1999; **50**: 314-321

30 **Sciallero S,** Costantini M, Bertinelli E, Castiglione G, Onofri P, Aste H, Casetti T, Mantellini P, Bucchi L, Parri R, Boni L, Bonelli L, Gatteschi B, Lanzanova G, Rinaldi P, Giannini A, Naldoni C, Bruzzi P. Distal hyperplastic polyps do not predict proximal adenomas: results from a multicentric study of colorectal adenomas. *Gastrointest Endosc* 1997; **46**: 124-130

31 **Kadakia SC,** Wrobleski CS, Kadakia AS, Meier NJ. Prevalence of proximal colonic polyps in average-risk asymptomatic patients with negative fecal occult blood tests and flexible sigmoidoscopy. *Gastrointest Endosc* 1996; **44**: 112-117

32 **Morson BC,** Sobin LC. Histologic typing of intestinal tumours. In: Intestinal histological classification of tumors. Vol. 15. Geneva: World Health Organization;1976

33 **Grossman S,** Milos ML, Tekawa IS, Jewell NP. Colonoscopic screening of persons with suspected risk factors for colon cancer: II. Past history of colorectal neoplasms. *Gastroenterology* 1989; **96**: 299-306

34 **Stryker SJ,** Wolff BG, Culp CE, Libbe SD, Ilstrup DM, MacCarty RL. Natural history of untreated colonic polyps. *Gastroenterology* 1987; **93**: 1009-1013

35 **DiSario JA,** Foutch PG, Mai HD, Pardy K, Manne RK. Prevalence and malignant potential of colorectal polyps in asymptomatic, average-risk men. *Am J Gastroenterol* 1991; **86**: 941-945

36 **Dinning JP,** Hixson LJ, Clark LC. Prevalence of distal colonic neoplasia associated with proximal colon cancers. *Arch Intern Med* 1994; **154**: 853-856

37 **Lemmel GT,** Haseman JH, Rex DK, Rahmani E. Neoplasia distal to the splenic flexure in patients with proximal colon cancer. *Gastrointest Endosc* 1996; **44**: 109-111

38 **Castiglione G,** Ciatto S, Mazzotta A, Grazzini G. Sensitivity of screening sigmoidoscopy for proximal colorectal tumours. *Lancet* 1995; **345**: 726-727

39 **Rex DK,** Chak A, Vasudeva R, Gross T, Lieberman D, Bhattacharya I, Sack E, Wiersema M, Farraye F, Wallace M, Barrido D, Cravens E, Zeabart L, Bjorkman D, Lemmel T, Buckley S. Prospective determination of distal colon findings in average-risk patients with proximal colon cancer. *Gastrointest Endosc* 1999; **49**: 727-730

40 **Thibodeau SN,** Bren G, Schaid D. Microsatellite instability in cancer of the proximal colon. *Science* 1993; **260**: 816-819

41 **Ionov Y,** Peinado MA, Malkhosyan S, Shibata D, Perucho M. Ubiquitous somatic mutations in simple repeated sequences reveal a new mechanism for colonic carcinogenesis. *Nature* 1993; **363**: 558-561

42 **Togo G,** Toda N, Kanai F, Kato N, Shiratori Y, Kishi K, Imazeki F, Makuuchi M, Omata M. A transforming growth factor beta type II receptor gene mutation common in sporadic cecum cancer with microsatellite instability. *Cancer Res* 1996; **56**: 5620-5623

43 **Togo G,** Shiratori Y, Okamoto M, Yamaji Y, Matsumura M, Sano T, Motojima T, Omata M. Relationship between grade of microsatellite instability and target genes of mismatch repair pathways in sporadic colorectal carcinoma. *Dig Dis Sci* 2001; **46**: 1615-1622

44 **Togo G,** Okamoto M, Shiratori Y, Yamaji H, Kato J, Matsumura M, Sano T, Motojima T, Omata M. Does mutation of transforming growth factor-beta type II receptor gene play an important role in colorectal polyps? *Dig Dis Sci* 1999; **44**: 1803-1809

45 **Lehman GA,** Buchner DM, Lappas JC. Anatomical extent of fiberoptic sigmoidoscopy. *Gastroenterology* 1983; **84**: 803-808

Science Editor Wang XL **Language Editor** Elsevier HK

PO Box 2345, Beijing 100023, China
www.wjgnet.com
wjg@wjgnet.com

ELSEVIER

World J Gastroenterol 2005;11(15):2255-2259
World Journal of Gastroenterology ISSN 1007-9327

In vitro growth inhibition of human colonic tumor cells by Verapamil

Qi-Zhen Cao, Gang Niu, Huan-Ran Tan

Qi-Zhen Cao, Huan-Ran Tan, Department of Pharmacology, Peking University Health Science Center, Peking University, Beijing 100083, China
Gang Niu, Beijing N&N Genetech Company, Beijing 100088, China
Supported by the Foundation of the National New Drug Research of China, No. 96-901-05-197
Correspondence to: Huan-Ran Tan, Department of Pharmacology, Peking University Health Science Center, Peking University, Beijing 100083, China. tanlab@sun.bjmu.edu.cn
Telephone: +86-10-8280-2004 Fax: +86-10-8280-2004
Received: 2004-03-30 Accepted: 2004-05-24

Abstract

AIM: To investigate the effects and mechanisms of Verapamil on cultured human colonic tumor (HCT) cells.

METHODS: HCT cells were treated with different concentrations of Verapamil, and their proliferation was examined by MTT assay. The areas of sub-diploid peak were measured by flow cytometry, and the DNA ladder was found by agarose gel electrophoresis. The characteristic changes in morphology were observed under light microscopy. The cell nuclei (propidium iodide labeled, PI-labeled) and cellular distribution and concentration of calcium (Fluo-3-labeled) were studied by using laser confocal scanning microscope.

RESULTS: The proliferation of HCT cells was inhibited by different concentrations of Verapamil. With the increase in concentration of Verapamil, the percent of G0-G1 phase cells in HCT cells increased and that of S phase cells decreased. After treating with different concentrations of Verapamil, flow cytometry showed that HCT cells were enlarged in areas of sub-diploid in a dose-dependent manner. Gel electrophoresis results displayed a typical DNA ladder. On staining with Wrights-Giemsa, the typical cellular apoptosis morphologic changes were also observed. PI-labeled cell nuclei were found markedly changed. In addition, we inspected that the 100 μmol/L Verapamil could increase the intracellular calcium ion concentration $[Ca^{2+}]_i$ in HCT cells.

CONCLUSION: Verapamil can inhibit proliferation of HCT cells via inducing cell apoptosis.

Key words: HCT; Verapamil

Cao QZ, Niu G, Tan HR. *In vitro* growth inhibition of human colonic tumor cells by Verapamil. *World J Gastroenterol* 2005; 11(15): 2255-2259
http://www.wjgnet.com/1007-9327/11/2255.asp

INTRODUCTION

Due to the critical role of calcium in vital activities, the studies about the impacts of calcium antagonists on the diseases are of practical significance. In the USA, there are about seven million people who use calcium antagonists to treat cardiovascular or cerebrovascular diseases. The uses of these drugs are always considered to have good therapeutic effect[1,2].

Many researchers have demonstrated that the increase of intracellular calcium concentration played an important role in cell apoptosis[3], and the apoptosis of cells is related to the growth of tumor cells[4]. So, it is particularly important to know whether the potential risk of increasing the growth of tumors will exist after the patient takes calcium antagonists orally for a long time. In this study, a series of experiments were carried out aiming at investigating the influence of Verapamil on the tumor cells. Our study demonstrated that the calcium antagonist, Verapamil, might inhibit the proliferation of HCT cells through inducing apoptosis.

MATERIALS AND METHODS

Cell line and drugs

HCT cell line was a generous gift from Professor Cui Jin-Rong (Natural and Imitative Drug Important Laboratory). Verapamil was obtained from Henrini Medical Company in Jiangshu Province, China. MTT (3-(4,5-dimethylthiazol-2-yl)-2,5-diphenyl tetrazolium bromide) was purchased from Amresco (Amresco, USA) Company. PI (Propidium iodide) was purchased from Sigma (Sigma, S. Louis, MO, USA). Trypsin was purchased from Gibco (Gibco BRL, USA).

Cell culture

HCT cells were routinely cultured with RPMI 1640 medium supplemented with 100 mL/L fetal bovine serum at 37 ℃ in a humidified atmosphere containing 50 mL/L CO_2.

HCT cells proliferation assay

Cells were dissociated with 2.5 g/L trypsin and resuspended in tissue culture media to yield a concentration of 1×10^5 cells/mL. Cells were added to 96-well plates (9 000 cells/well), and allowed to attach for 24 h at 37 ℃. Verapamil was added at the concentration 1, 10, 100, 200, 300, 400, 500 μmol/L (10 μL/well), respectively. Control wells contained only

culture medium. After the cells were incubated with these additives for 6, 12, 24 and 48 h cell proliferation was estimated based on the cellular reduction of tetrazolium salt MTT[5] by using a microplate reader (BIO-RAD, Model 550 USA), at a test wavelength of 540 nm.

Detection of cell apoptosis by flow cytometry

The HCT cells were incubated with different concentrations of Verapamil (1, 10, 100 and 500 μmol/L) for 48 h, fixated in 700 mL/L cold ethanol (-20 ℃) after washing twice with PBS (phosphate buffered saline, without Ca^{2+} or Mg^{2+}), and stocked at 4 ℃ overnight. The cells were washed twice with PBS and the cell concentration was adjusted to 1×10^6/mL, and 1 mL of cell suspension was added with 10 μL of 10 g/L RNase A and incubated at 37 ℃ for 30 min. Then, PI was added into the cells at a concentration of 50 mg/L. Cell apoptosis and cell cycle was analyzed with flow cytometry.

DNA isolation and gel electrophoresis

DNA was isolated from cells according to routine protocol[6]. Briefly HCT cells treated with or without Verapamil (100, 200 and 400 μmol/L) were harvested after 48 h incubation. Cells were centrifuged at 800 r/min and washed with PBS. After cells were resuspended at a concentration of 1×10^6 cells/mL in extraction buffer (10 mmol/L Tris-HCl, 0.1 mol/L EDTA, 5 g/mL SDS), they were treated with 20 mg/L RNase A at 37 ℃ for 60 min, followed by incubation with 100 mg/L proteinase K at 37 ℃ for 60 min. Equal volume of phenol:chloroform:isopropyl alcohol (25:24:1) was added to the cells and centrifuged at 13 000 *g* for 10 min. The liquor of supernatant was collected, and then 0.1 volume NaAc (3 mol/L pH 5.2) and 2 volume ethanol (-20 ℃) were added, and stocked at -20 ℃ overnight. The samples were centrifuged at 13 000 *g* for 30 min at 4 ℃. Then the liquor of supernatant was discarded and the pellets were dissolved in 1×TE buffer. The concentration of DNA was detected by UV spectrophotometer (Beckman DU-640, USA). The DNA content (5 μg/tube) was transferred to the 20 g/L agarose gel, horizontal gel electrophoresis was performed at 60 V for 90 min and the DNA in gels was visualized under gel image analysis (BIO-RAD, Gel DOC 2000, USA) after staining with 5 μg/mL ethidium bromide.

Cell morphology observation

In the routine staining with Wrights-Giemsa, the HCT cells were incubated with 100 μmol/L Verapamil for 48 h, the liquor of supernatant was discarded, and cells were fixated and air-dried after washing twice with PBS, and stained with Wrights for 4 min, then with Giemsa for 6 min. Dyestuff was discarded and cells were washed. Then, the cell morphology was observed under microscope.

Cellular concentration of calcium and nuclear shape diversification detected by confocal scanning laser microscopy

Cells were dissociated with 2.5 g/L trypsin and resuspended in tissue culture media to yield a concentration of 1×10^5 cells/mL. Cells were allowed to attach to Petri dish for 24 h at 37 ℃ a humidified 50 mL/L CO_2/950 mL/L air incubator. Verapamil was added at a concentration of 100 μmol/L. An equal volume of PBS was added to the control instead. The cells were incubated with these additives for 12 h. Then the liquor of supernatant was discarded, the cells were treated with Fluo-3/AM at a concentration of 5 μmol/L for marking $[Ca^{2+}]_i$, and PI (50 mg/L) for nuclear (Editor query: is something missing here?) after washing twice with PBS, the cellular concentration of calcium and nuclear shape diversification were analyzed using the confocal scanning laser microscopy (TCS-NT, Leica).

Statistical analysis

All results are expressed as mean±SD. $P<0.05$ was considered statistically significant. All statistical analyses were performed using SPSS 11.0 for Windows.

RESULTS

Effect of Verapamil on cell proliferation and cell cycle

After HCT cells were incubated with different concentrations of Verapamil for 6, 12, 24 or 48 h, we observed a significant inhibition in proliferation of HCT cells in a dose-dependent manner by MTT assay (Figure 1). With the increase in concentration of Verapamil, the percent of G0-G1 phase cells in HCT cells was increased and S phase cells were decreased as detected by flow cytometry. Cell cycle analysis showed that the proliferation of HCT cells was blocked at G0-G1 phase (Figure 2).

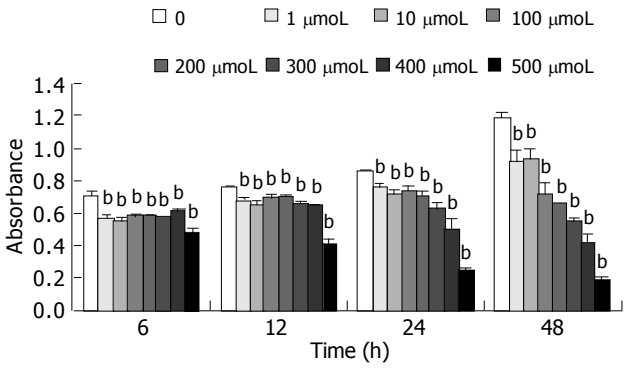

Figure 1 Inhibition of proliferation of HCT cells by Verapamil. Results were expressed as mean±SD $n = 9$ $^bP<0.01$ *vs* control.

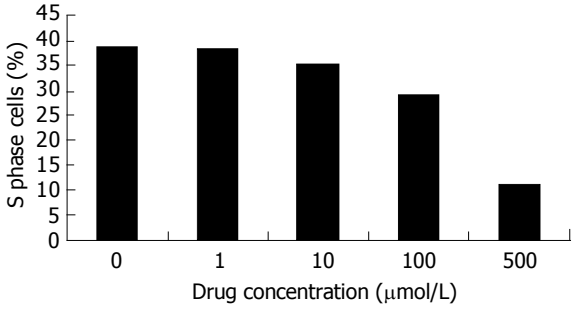

Figure 2 The percentage of S phase HCT cells treated with Verapamil. With increase in Verapamil concentration, the percent of S phase cells was decreased as detected by flow cytometry.

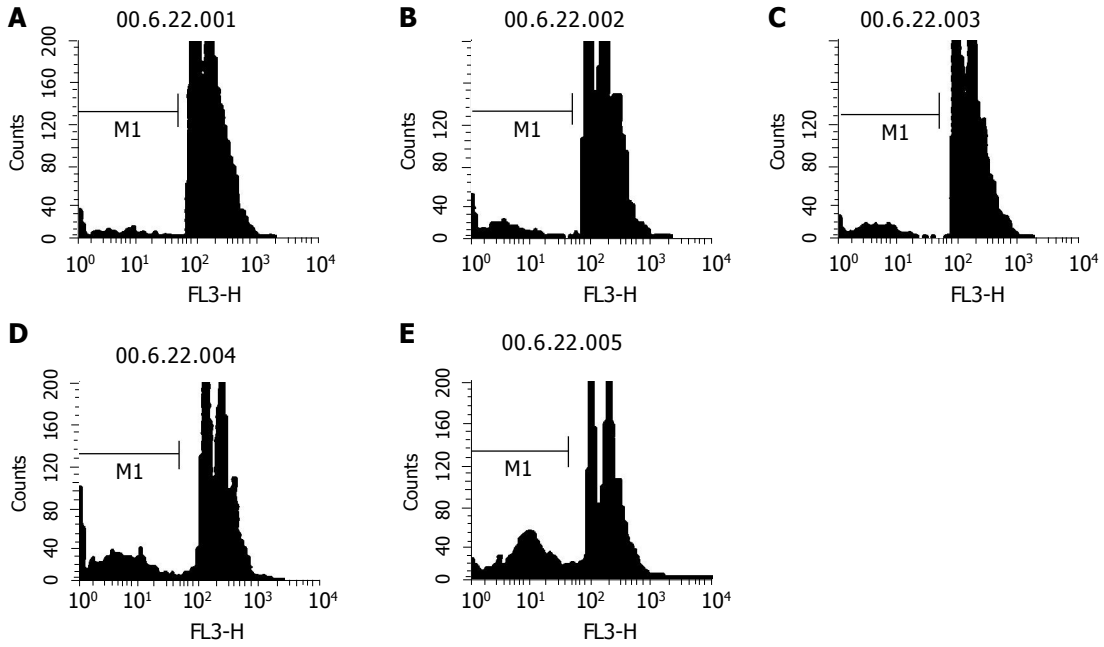

Figure 3 Flow cytometry detection of HCT cells apoptosis. The percentage of apoptotic cells increased as Verapamil concentration increased. **A**: control; **B**: 1 μmol/L Verapamil; **C**: 10 μmol/L Verapamil; **D**: 100 μmol/L Verapamil; **E**: 500 μmol/L Verapamil.

Analysis of cell apoptosis by flow cytometry

HCT cells were treated with different concentrations of Verapamil, and the data from flow cytometry showed the areas of sub-diploid peak that were enlarged in drug-treated HCT cells, suggesting that the percentage of apoptosis cells increased as Verapamil concentration increased (Figure 3).

Induction of HCT cells apoptosis

After HCT cells were treated with different concentrations of Verapamil, a typical DNA ladder was observed, which suggested the induction of apoptosis in Verapamil-treated HCT cells (Figure 4).

Cellular morphological change of apoptosis cell

During routine staining with Wrights-Giemsa, the typical cellular morphologic changes, including cell membrane blebs, and the cytoplasm and nuclear chromatin condensation, were observed (Figure 5). The cell nuclei were marked with fluorescence-probe PI and found markedly changed, most of the cell nuclei were present in reniform and nuclear chromatin condensation (Figure 6).

Change in cytosolic free calcium in HCT cells

The $[Ca^{2+}]_i$ was determined with the laser confocal scanning microscopy, which demonstrated that 100 μmol/L Verapamil could increase the concentration of $[Ca^{2+}]_i$ in HCT cells (Figure 7 and Table 1).

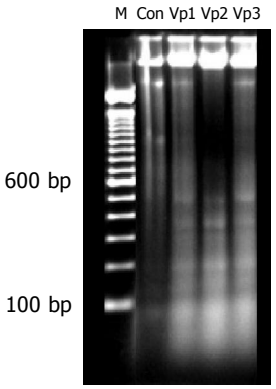

Figure 4 DNA Ladder of HCT cell line treated with Verapamil. M: marker (100 bp DNA Ladder); Con: control; Vp1: 100 μmol/L Verapamil; Vp2: 200 μmol/L Verapamil; Vp3: 400 μmol/L Verapamil.

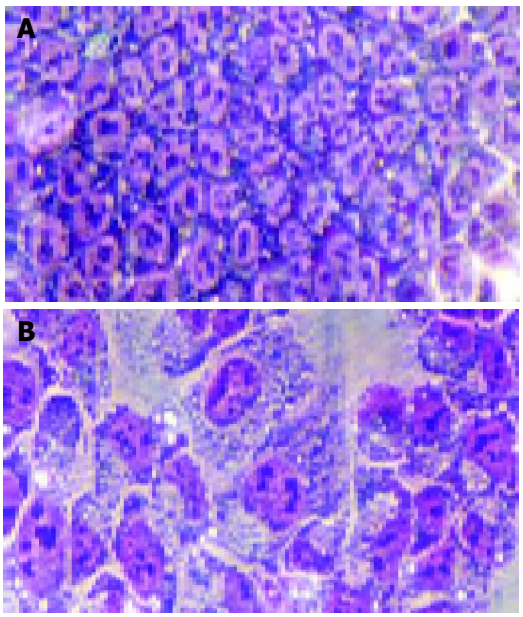

Figure 5 Cellular morphologic changes (400×). Cell membrane blebs and the cytoplasm and nuclear chromatin condensation in HCT cells treated with Verapamil were observed. **A**: control cells; **B**: 100 μmol/L Verapamil.

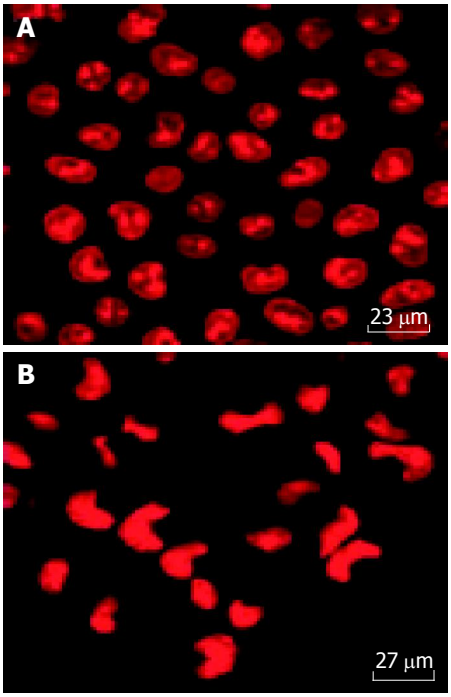

Figure 6 Nuclear model change as reniform and nuclear chromatin condensation in HCT cell line treated with Verapamil and labeled with PI (400×). **A**: Control cells; **B**: 100 μmol/L Verapamil.

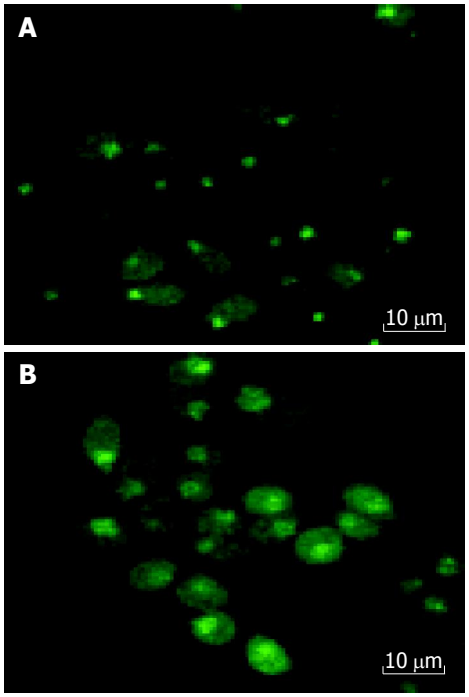

Figure 7 Influence of Verapamil on $[Ca^{2+}]_i$ intensity in HCT cell after 12 h (400×). 100 μmol/L. **A**: Control cells; **B**: 100 μmol/L Verapamil.

Table 1 **$[Ca^{2+}]_i$ intensity in HCT cells treated with Verapamil for 12 h (n = 40, mean±SD)**

Groups	$[Ca^{2+}]_i$ intensity
Control	28.37±11.94
Verapamil (100 μmol/L)	43.34±11.58[b]

[b]P<0.01 *vs* control.

DISCUSSION

A series of experiments have demonstrated that the apoptosis of cells is induced by radiation or drugs and the concentration of free intracellular Ca^{2+} is found to be markedly elevated in the apoptotic cells[7-12]. Intracellular Ca^{2+} is the key-initiating factor during the course of apoptosis of cell line[13]. Now calcium channel antagonists are widely used clinically to treat cardiovascular and cerebrovascular diseases; the routine dosage of these drugs taken orally can improve the symptoms of cardiovascular and cerebral-vascular diseases[14,15]. Do they produce a certain influence on the patients with these diseases complicated by tumors? Are they related to the danger of carcinogenesis and cancer development? And what is the mechanism of their influences on tumors? All of these problems are still of great concern and need to be solved by epidemiologists, clinicians and researchers of basic sciences.

Our study of the effect of Verapamil on cell proliferation demonstrated that Verapamil might inhibit the growth of HCT cells. Results from flow cytometry showed that HCT cells after treating with calcium antagonist, the hypodiploid peak area was increased significantly as the concentrations of Verapamil were increased, which indicated that the proportion of apoptotic cells increased. This result was also proved by cellular morphologic changes, such as cell membrane blebs and the cytoplasm and nuclear chromatin condensation. At the same time, the karyotype of PI-labeled cells was found markedly changed and most of the cell nuclei were present in reniform as detected by confocal scanning microscopy. Our above findings were quite enough to show that the calcium antagonist markedly increased cell apoptosis. Jensen *et al*[16-18] also demonstrated that calcium channel antagonists could inhibit meningioma growth *in vitro* and via interfering with intracellular signaling pathways of cultured meningioma cells. Jensen and Wurster[19] also showed that calcium channel antagonists could decrease but not completely inhibit xenograft meningioma growth over time compared to control groups in nude mice. In this study, flow cytometry showed that as the concentration of Verapamil increased, the percentage of S-phase cells in the whole cycle was lowered, whereas the proportion of G0/G1-phase cells increased, which indicated that Verapamil could block the transformation of HCT cells from G0/G1-phase into S-phase, and interfere with the process of DNA replication in these cells. The proliferation of HCT cells was also inhibited by blocking cell cycle after the use of the calcium antagonist.

In our experiment, when HCT cells were treated with 100 μmol/L Verapamil for 12 h, the intracellular calcium ion concentration $[Ca^{2+}]_i$ detected by Fluo-3AM fluorescence-labeling method, was not surprisingly increased. Why does the intracellular concentration of calcium ions within HCT cells rise after the use of calcium antagonists? Usually, scientists consider that after the use of calcium antagonists, as the entry of extracellular calcium ions is inhibited, the intracellular concentration of calcium ions can then be kept at a relatively low level; but in this experiment we obtained a surprising result. How did the calcium antagonist raise the concentration of calcium ions within the HCT cells? What was the mechanism for that? Did the drug have the tendency to produce only a single effect of preventing the outflow

of calcium ions? These problems need to be further investigated. The more easily accepted theory is that the use of calcium antagonists may destroy the mobile equilibrium between intracellular and extracellular calcium ions, which causes the calcium ions that are stored in the cell organs to be released into the cytoplasm, resulting in the increase of the intracellular concentration of calcium ions.

In conclusion, the use of the calcium antagonist, Verapamil, produces a growth inhibiting effect on HCT cells by increasing the apoptosis of HCT cells and also by blocking cell cycle. The problem whether calcium antagonists can take part in or contribute to the treatment for tumors is to be further studied, and researches should be made through many new relevant subjects.

ACKNOWLEDGMENTS

We thank the members of our laboratory for the stimulating discussions.

REFERENCES

1 **Mason RP**. Effects of calcium channel blockers on cellular apoptosis: implications for carcinogenic potential. *Cancer* 1999; **85**: 2093-2102
2 **Qing SH**, Rao KY, Jiang HY, Wexner SD. Racial differences in the anatomical distribution of colorectal cancer: a study of differences between American and Chinese patients. *World J Gastroenterol* 2003; **9**: 721-725
3 **Ellis RE**, Yuan JY, Horvitz HR. Mechanisms and functions of cell death. *Annu Rev Cell Biol* 1991; **7**: 663-698
4 **Wright SC**, Zhong J, Zheng H, Larrick JW. Nicotine inhibition of apoptosis suggests a role in tumor promotion. *FASEB J* 1993; **7**: 1045-1051
5 **Carmichael J**, DeGraff WG, Gazdar AF, Minna JD, Mitchell JB. Evaluation of a tetrazolium-based semiautomated colorimetric assay: assessment of chemosensitivity testing. *Cancer Res* 1987; **47**: 936-942
6 **Maniatis T,** Fritsch EF, Sambrook J. Molecular cloning: A laboratory manual, 1st edition New York, USA, Cold Spring Haobor Laboratory Press 1982: 280-281
7 **Macho A**, Blanco-Molina M, Spagliardi P, Appendino G, Bremner P, Heinrich M, Fiebich BL, Munoz E. Calcium ionophoretic and apoptotic effects of ferutinin in the human Jurkat T-cell line. *Biochem Pharmacol* 2004; **68**: 875-883
8 **Leger DY**, Liagre B, Corbiere C, Cook-Moreau J, Beneytout JL. Diosgenin induces cell cycle arrest and apoptosis in HEL cells with increase in intracellular calcium level, activation of cPLA2 and COX-2 overexpression. *Int J Oncol* 2004; **25**: 555-562
9 **Groenendyk J,** Lynch J, Michalak M. Calreticulin, Ca2+, and calcineurin - signaling from the endoplasmic reticulum. *Mol Cells* 2004; **17**: 383-389
10 **Sharma AK**, Rohrer B. Calcium-induced calpain mediates apoptosis via caspase-3 in a mouse photoreceptor cell line. *J Biol Chem* 2004; **279**: 35564-35572
11 **Raghupathi R.** Cell death mechanisms following traumatic brain injury. *Brain Pathol* 2004; **14**: 215-222
12 **Lemarie A,** Lagadic-Gossmann D, Morzadec C, Allain N, Fardel O, Vernhet L. Cadmium induces caspase-independent apoptosis in liver Hep3B cells: role for calcium in signaling oxidative stress-related impairment of mitochondria and relocation of endonuclease G and apoptosis-inducing factor. *Free Radic Biol Med* 2004; **36**: 1517-1531
13 **McConkey DJ**, Nicotera P, Hartzell P, Bellomo G, Wyllie AH, Orrenius S. Glucocorticoids activate a suicide process in thymocytes through an elevation of cytosolic Ca^{2+} concentration. *Arch Biochem Biophys* 1989; **269**: 365-370
14 **Xu RX**, Tu YY, Zou CY, Yang ZL, Chen YZ, Cai YQ, Du MX. Reinforcement of Nimodipine to the TK Suicide Gene Therapy of Glioma. *China J Cancer Prev Treat* 2003; **10**: 1129-1133
15 **Li Y,** Wu JZ , Liu B, Duan XH, Li F, Li J. Synergic anti-tumor effect of combination of verapamil with chemotherapy on highly metastatic human mucoepidermoid carcinoma(Mc3) cells. *J Fourth Mil Med Univ* 2003; **24**: 2259-2261
16 **Jensen RL**, Origitano TC, Lee YS, Weber M, Wurster RD. *In-vitro* growth inhibition of growth factor-stimulated meningioma cells by calcium channel antagonists. *Neurosurgery* 1995; **36**: 365-373; discussion 373-374
17 **Jensen RL**, Lee YS, Guijrati M, Origitano TC, Wurster RD, Reichman OH. Inhibition of *in-vitro* meningioma proliferation after growth factor stimulation by calcium channel antagonists Part II--Additional growth factors, growth factor receptor immunohistochemistry, and intracellular calcium measurements. *Neurosurgery* 1995; **37**: 937-946; discussion 946-947
18 **Jensen RL**, Petr M, Wurster RD. Calcium channel antagonist effect on *in vitro* meningioma signal transduction pathways after growth factor stimulation. *Neurosurgery* 2000; **46**: 692-702; discussion 702-703
19 **Jensen RL**, Wurster RD. Calcium channel antagonists inhibit growth of subcutaneous xenograft meningiomas in nude mice. *Surg Neurol* 2001; **55**: 275-283

Science Editor Kumar M **Language Editor** Elsevier HK

PO Box 2345, Beijing 100023, China
www.wjgnet.com
wjg@wjgnet.com

ELSEVIER

World J Gastroenterol 2005;11(15):2260-2263
World Journal of Gastroenterology ISSN 1007-9327

Expression of *Helicobacter pylori* AlpA protein and its immunogenicity

Jing Xue, Yang Bai, Ye Chen, Ji-De Wang, Zhao-Shan Zhang, Ya-Li Zhang, Dian-Yuan Zhou

Jing Xue, Yang Bai, Ye Chen, Ji-De Wang, Ya-Li Zhang, Dian-Yuan Zhou, PLA Institute for Digestive Medicine, Nanfang Hospital, The First Military Medical University, Guangzhou 510515, Guangdong Province, China
Zhao-Shan Zhang, Institute of Biotechnology, Academy of Military Medical Sciences, Beijing 100071, China
Supported by the National Natural Science Foundation of China, No. 30270078
Correspondence to: Dr. Jing Xue, PLA Institute for Digestive Medicine, Nanfang Hospital, The First Military Medical University, Guangzhou 510515, Guangdong Province, China. xj0302@fimmu.com
Telephone: +86-20-61641531
Received: 2003-10-15 Accepted: 2003-12-16

Abstract

AIM: To construct a recombinant strain which expresses adhesin AlpA of *Helicobacter pylori* (*H pylori*) and to study the immunogenicity of adhesin AlpA.

METHODS: Gene Ab, which was amplified from *H pylori* chromosomal DNA by PCR technique, was sequenced and the biological information was analyzed, and inserted into the *Nco* I and *Not* I restriction fragments of the expression vector pET-22b(+) using T4 DNA ligase. The resulting plasmid pET-AlpA was transformed into competent *E.coli* BL21(DE3) cells using ampicillin resistance for selection. Recombinant strains were incubated in 5 mL LB with 100 μg/mL ampicillin overnight at 37 ℃. Sonication of BL21(DE3)pET-22b(+)/AlpA was analyzed by Western blot to detect AlpA immunogenicity.

RESULTS: The gene encoding AlpA protein was amplified by PCR with chromosomal DNA of *H pylori* Sydney strain (SS1) as templates. It revealed that AlpA DNA fragment amplified by PCR had approximately 1 500 nucleotides, compatible with the previous reports. The recombinant plasmid pET-22b(+)/AB was successfully constructed. DNA sequencing showed one open reading frame with the length of 588 bp. It encoded seven conservative regions that showed good antigenicity and hydrophobicity by Parker and Welling method. Furthermore, INTERNET EXPASY, NNPREDICT and ISREC predicted that it was a porin-like structure consisting of β-pleated sheets that were embedded in the outer membrane. BLAST analyzed 836 767 protein sequences and found that the similar sequences were all belonging to *H pylori* OMP sequences. SDS-PAGE and scan analysis showed that the molecular weight of AB was 22.5 ku and recombinant protein amounted to 29% of the total bacterial protein, among which dissolved expression amounted to 21.9% of sonicated supernatant. The rAB purity amounted to 96% through affinity chromatography. Western blot analysis of rAB confirmed that it could be specially recognized by serum form rabbit immunized with AlpA and *H pylori* infected.

CONCLUSION: Adhesin AlpA recombinant protein may be a potential vaccine for control and treatment of *H pylori* infection.

Key words: *H pylori*; Immunogenicity

Xue J, Bai Y, Chen Y, Wang JD, Zhang ZS, Zhang YL, Zhou DY. Expression of *Helicobacter pylori* AlpA protein and its immunogenicity. *World J Gastroenterol* 2005; 11 (15): 2260-2263
http://www.wjgnet.com/1007-9327/11/2260.asp

INTRODUCTION

Helicobacter pylori (*H pylori*) infection is the major cause of chronic active gastritis and peptic ulcer disease[1], and is also closely related with gastric cancers such as adenocarcinomas, mucosa-associated lymphoid tissue lymphoma and primary gastric non-Hodgkin's lymphoma[2]. This organism has been categorized as a class I carcinogen by the World Health Organization, and direct evidence of its carcinogenicity was recently demonstrated in China. In addition, seroprevalence studies indicate that *H pylori* infection is also associated with cardiovascular, respiratory, extra-gastroduodenal digestive, autoimmune diseases. Successful eradication of *H pylori* is thus an important goal. Currently, treatment involves antibiotic therapy, but this has associated problems such as low patient compliance and an increase of resistant strains. An alternative approach is to develop a vaccine, which would not only clear the organism, but also protect against reinfection.

In the development of *H pylori* vaccine, the candidate vaccine antigens adopted currently such as urease, vacuolating cytotoxin and catalase[3] focused basically on blocking toxicity factors of *H pylori*, while few candidate vaccine antigens focused on adhesins, which are closely associated with *H pylori* colonizing in human gastric mucosa by adhering to mucous epithelial cells and the mucus layer lining the gastric epithelium. It is probably a useful attempt to discover protective antigens based on adhesin. Currently, four adhesins have been recognized[4-8], including *H pylori* adhesin BabA[9,10] whose receptor has been determined till date and other three adhesins of AlpA[11], AlpB[11] and HopZ[12].No concerned study has been reported about AlpA in China. So in this study, the recombinant plasmid of *H pylori* AlpA gene was constructed for development of *H pylori* vaccine.

MATERIALS AND METHODS

Materials

Bacterial strain BL21(DE3) and plasmid pET-22b(+) were provided by the Institute of Biotechnology, Academy of

Military Medical Sciences. *H pylori* SS1 was preserved in this research institute. Restriction enzymes *Not* I, *Nco* I and T4 DNA ligase, Vent DNA polymerase and isopropyl-β-D-thiogalactopyranoside (IPTG) were purchased from New England Biolabs. Goat anti-rabbit and goat anti-human IgG-HRP were purchased from Huamei Bioengineering Company, China, and His-Tag precolumn from Invitrogen. The serum from rabbits immunized with AlpA was donated by Odenbreit *et al*[11]. Serum samples were obtained from *H pylori* positive and negative patients who underwent urease test, pathologic examination and germiculture at the Endoscope Center of this institute. Other reagents were analytically pure reagents produced in China.

Recombinant DNA techniques

All restriction enzyme digestions, ligations and other common DNA manipulations, unless otherwise stated, were performed by standard procedures[13]. The genome of *H pylori* was prepared from cells collected from the colonies on the agar plate. The gene of *H pylori* AlpA was amplified from the genome of *H pylori* by PCR (Techne PROGENE) using primers AlpA1 (5'- TG GCC ATG GAT TGC GCT AGC ATA AGT TA -3') as upstream primer and AlpA2 (5'- AG TGC GGC CGC GAA TGA ATA CCC ATA AGA -3') as downstream primer as described in the literature[11]. AlpA1 and AlpA2 contained *Nco* I and *Not* I sites, respectively. PCR was performed with the hot start method. The PCR condition was initial denaturing at 95 ℃ for 30 s, each cycle of amplification consisted of denaturing at 95 ℃ for 30 s, annealing at 55 ℃ for 30 s and polymerization at 72 ℃ for 50 s and further polymerization for 10 min after 35 PCR cycles. The PCR products were harvested from agarose gel, digested with *Nco* I and *Not* I, and inserted into the *Nco* I and *Not* I restriction fragments of the expression vector pET-22b(+) using T4 DNA ligase. The resulting plasmid pET-AlpA was transformed into competent *E.coli* BL21 (DE3) cells using ampicillin resistance for selection. The alkaline lysis method was used for large-scale preparations of the recombinant plasmid and the plasmid was identified by restriction enzymes. DNA sequence was performed with the DNA automatic sequencer.

Induction of expression and SDS-polyacrylamide gel electrophoresis

Recombinant strains were incubated in 5 mL LB with 100 μg/mL ampicillin overnight at 37 ℃. Fifty microliters LB was inoculated and the cells grew until the optical density at 600 nm reached 0.4-0.6. IPTG was added to the cultures at the final concentrations of 0.1, 0.2, 0.4, 0.6, 0.8 and 1.0 mmol/L, respectively. *E.coli* cells were harvested after 3 or 5 h by centrifugation at 12 000 *g* for 10 min. The pellet was resuspended in 1 mL 30 mmol/L Tris buffer (pH 8.0) containing 1 mmol/L EDTA (pH 8.0) and 20% sucrose. The suspension was put on ice for 10 min, then centrifuged for 10 min at 12 000 *g*, and the resulting supernatant contained proteins from the periplasm. The resulting pellet was resuspended in 5 mL 50 mmol/L Tris buffer (pH 8.0) containing 2 mmol/L EDTA, 0.1 mg/mL lysozyme and 1% Triton X-100. The suspension was incubated at 30 ℃ for 20 min and then sonicated on ice until it became clarified. The lysate was centrifuged at 12 000 *g* for 15 min at 4 ℃. Whole-cell lysates, sonicated supernatant, inclusion body, osmotic shock liquid of recombinant strains expressing *H pylori* AlpA were analyzed by electrophoresis in a 10% polyacrylamide gel.

Western blot analysis on sonication of BL21 (DE3) pET-22b (+)/AlpA

Sonication of BL21(DE3)pET-22b(+)/AlpA was analyzed by Western blot to detect AlpA immunogenicity. Protein was separated on 10% SDS-PAGE gel using a mini-gel apparatus (Bio-Rad) and transferred to nitrocellulose membranes using a semi-dry blot system (Biotech Fischer). The polyclonal rabbit antiserum and sera from patients infected with *H pylori* were pre-absorbed with BL21(DE3)pET-22b(+) sonication, to remove non-specific antibodies diluted at 1:50. The membrane was incubated for 90 min at 37 ℃, washed thrice for 15 min with TBS/Tween-20 (TTBS), and then incubated for 1 h with goat-anti rabbit IgG alkaline phosphates conjugate at room temperature. After washing thrice with TTBS, BCIP/NBT was used to visualize bound antibodies.

RESULTS

PCR amplification of H pylori AlpA gene

The gene encoding AlpA protein was amplified by PCR with chromosomal DNA of *H pylori* Sydney strain (SS1) as templates. The cloned products were electrophoresed and visualized on 8 g/L agarose gel (Figure 1). It revealed that AlpA DNA fragment amplified by PCR had approximately 1 500 nucleotides, compatible with the previous reports[11].

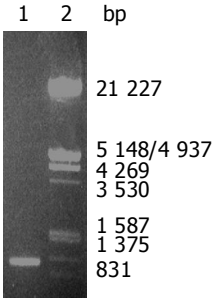

Figure 1 Eight grams per liter agarose gel electrophoreses of AlpA DNA fragment amplified by PCR from *H pylori*. Lane 1: PCR products; Lane 2: nucleotide marker.

Construction of recombinant plasmid and restriction enzyme confirmation

After the PCR products and pET-22b(+) plasmid were cut by *Not* I and *Nco* I, directional cloning was performed, resulting in a recombinant plasmid named pET-22b(+)/AlpA. The recombinant plasmids pET-22b(+)/AlpA were all digested by *Not* I or *Nco* I, and by *Not* I and *Nco* I simultaneously, and then the digestive products were visualized on 8 g/L agarose gel electrophoreses (Figure 2). It demonstrated that recombinant plasmid contained the objective gene.

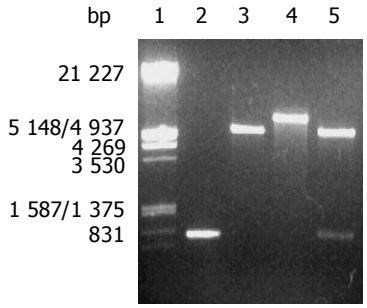

Figure 2 Identification of recombinant plasmid by restriction enzyme digestion. Lane 1: Nucleotide marker; lane 2: PCR products; lane 3: pET22b(+)/*Not* I; lane 4: recombinant plasmid/*Not* I; lane 5: recombinant plasmid/*Not* I and *Nco* I.

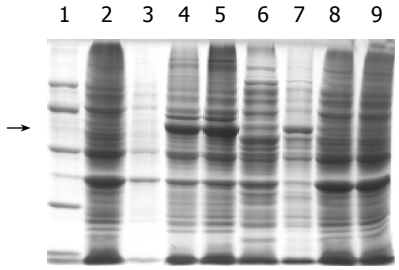

Figure 3 SDS-PAGE analysis of 100 g/L fusion protein expressed in BL21 (DE3). Lane 1: Molecular weight marker (20, 30, 43, 67, 94)×10^3; lane 2: BL21 (pET-AlpA) cells before induction; lane 3: BL21 (pET-AlpA) cells in periplasm protein after 3-h induction with IPTG; lane 4: BL21 (pET-AlpA) cells after 3-h induction with IPTG; lane 5: BL21 (pET-AlpA) cells after 5-h induction with IPTG; lane 6: sonicated supernatant of BL21 (pET-AlpA) cells after 3-h induction with IPTG; lane 7: inclusion body of BL21 (pET-AlpA) cells after 3-h induction with IPTG; lane 8: control strain BL21 (pET) before induction; lane 9: control strain BL21 (pET) after 3-h induction with IPTG.

Sequence analysis of cloned AlpA nucleotide

The nucleotide sequence of cloned genes inserted in pET22b (+) was analyzed by automated sequencing across the cloning junction, using the universal primer T7. The cloned genes contained 1 512 nucleotides coding a putative protein consisted of 504 amino acid residues with a calculated molecular mass of AlpA. The homogenicity was 97.3% between them.

Expression of AlpA gene in Escherichia coli

Whole-cell sonication, sonicated supernatant, osmotic shock liquid of recombinant strains expressing *H pylori* AlpA genes were analyzed by electrophoresis in a 10% polyacrylamide gel for detection of fusion proteins (Figure 3). The result showed that the clearly identifiable band was 56 500 ku highly expressed fusion protein, which was similar to that predicted. Gel automatic scan analysis showed that it was 0.6 at D value and the final concentration of IPTG was 0.1 mmol/L after 3-h induction, and the expression of AlpA increased remarkably, which amounted to 31.9% of the total bacterial protein, 23.7% of the sonicated bacterial supernatant and 64.8% of the bacterial inclusion body.

Antigenicity study of recombinant fusion protein

Western blot analysis on the sonicated BL21(DE3)pET-22b (+)/AlpA using polyclonal rabbit antiserum and patients infected with *H pylori* serum pre-absorbed with sonicated BL21(DE3)pET-22b(+) revealed a protein band, which corresponded to the expected molecular weight (Figure 4). The serum from rabbits without immunization and *H pylori* negative serum from patients were used as a control. Indeed the control serum did not recognize BL21(DE3)pET-22b (+)/AlpA. It showed that anti-AlpA antibody existed in the serum of patients infected with *H pylori* and that rAlpA could enable the organism to generate specific humoral immunity.

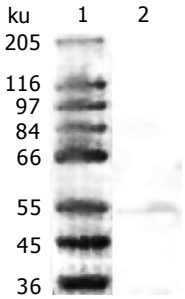

Figure 4 Western blot analysis of AlpA recombinant protein. Lane 1: protein marker; lane 2: AlpA immunogenicity detected using polyclonal rabbit antiserum.

DISCUSSION

In 1996, Odenbreit isolated and characterized a chromosomal locus of *H pylori* previously identified by transposon shuttle mutagenesis as being involved in adhesion of the pathogen to gastric epithelial cells[14]. Afterwards, two close homologous genes were identified, designated as AlpA and AlpB, encoding outer membrane (OM) proteins of 518 amino acids each[11]. They are members of the outer membrane protein supergene family identified in the *H pylori* 26 695 complete genome sequence. Transposon insertion mutagenesis, immunoblotting and primer extension studies indicated that both genes were organized in an operon, but no obvious consensus promoter sequence was found upstream of the transcriptional start site. The C-terminal portion of both proteins was predicted to form a porin-like barrel in the outer membrane, consisting of 14 transmembrane amphipathic strands. Preincubation of *H pylori* with an antiserum raised against the AlpA fusion protein completely blocked binding of *H pylori* to the gastric tissue sections, but an antiserum raised against a *H pylori* urease B fusion protein did not[11]. These data suggested that AlpA might be necessary for specific adhesion of *H pylori* to human gastric tissues and AlpA must be located on the bacterial surface in order to be bound and functionally be impaired by the specific antiserum. Furthermore, the pattern of AlpA-dependent adherence of *H pylori* to gastric epithelial surfaces showed a clear difference to the BabA2-mediated adherence to Lewisb, suggesting that a different receptor is involved. Thus, researches suspected that AlpA played an important role in the mechanism of *H pylori* adherence.

Outer-membrane proteins and porins could form a large family of 32 genes in *H pylori*. These proteins, which are surface exposed and well conserved, might be excellent vaccine candidates[15,16]. AlpA accords with the criteria mentioned above. Furthermore, AlpA as a candidate component of gene engineering vaccines possess the following virtues. AlpA

is a kind of protein so that a gene engineering clone expressing AlpA can be constructed to realize scale-up production and purification. Although AlpA as an adhesion is an important component attending *H pylori* infection and AlpA itself is lack of toxicity and cross-reactivity with human tissue antigens. AlpA exists in *H pylori* isolated from multiple geographic locations. These virtues also fit the criteria for inclusion of an antigen in a final vaccine formulation as Kleanthous *et al*[17], mentioned in 1998. So, to further research, AlpA is helpful in the preparation of *H pylori* gene engineering vaccines.

AlpA carries a functional lipoprotein signal sequence. When we designed specific primers, we discarded the lipoprotein signal sequence. To facilitate the expression and purification at the next stage, we cloned it into a fusion expression vector with six hercynine tails. The restriction enzyme digestion and sequencing result show one open reading frame with 1 512 bp. SDS-PAGE and scanning analysis showed that the molecular weight of AlpA was 56.5 ku and recombinant protein amounted to 31.9% of the total bacterial protein. In this study, the serum from rabbits immunized with purified recombinant protein AlpA could recognize AlpA-specific bands expressed by BL21 (DE3)pET-22b(+)/AlpA, but the serum from rabbits in the control group did not. Serum from patients also showed the same results. These results suggest that AlpA of *H pylori* might be a good candidate as a vaccine component.

REFERENCES

1 **Wang J,** Brooks EG, Bamford KB, Denning TL, Pappo J, Ernst PB. Negative selection of T cells by *Helicobacter pylori* as a model for bacterial strain selection by immune evasion. *J Immunol* 2001; **167**: 926-934

2 **Wang J,** Fan X, Lindholm C, Bennett M, O'Connoll J, Shanahan F, Brooks EG, Reyes VE, Ernst PB. *Helicobacter pylori* modulates lymphoepithelial cell interactions leading to epithelial cell damage through Fas/Fas ligand interactions. *Infect Immun* 2000; **68**: 4303-4311

3 **Bai Y,** Zhang YL, Wang JD, Zhang ZS, Zhou DY. Construction of the non-resistant attenuated Salmonella typhimurium strain expressing *Helicobacter pylori* catalase. *Diyi Junyi Daxue Xuebao* 2003; **23**: 101-105

4 **Bai Y,** Zhang YL, Wang JD, Lin HJ, Zhang ZS, Zhou DY. Conservative region of the genes encoding four adhesins of *Helicobacter pylori*: cloning, sequence analysis and biological information analysis. *Diyi Junyi Daxue Xuebao* 2002; **22**: 869-871

5 **Bai Y,** Dan HL, Wang JD, Zhang ZS, Odenbreit S, Zhou DY, Zhang YL. Cloning, expression, purification and identification of conservative region of four *Helicobacter pylori* adhesin genes in AlpA gene. *Prog Biochen Biophys* 2002; **29**: 922-926

6 **Bai Y,** Zhany YL, Chen Y, Wang JD, Zhou DY. Study of Immunogenicity and Safety and Adherence of Conservative Region of Four *Helicobacter pylori* Adhesin *in vitro*. *Prog Biochen Biophys* 2003; **30**: 422-426

7 **Bai Y,** Zhang YL, Wang JD, Zhang ZS, Zhou DY. Cloning and immunogenicity of conservative region of adhesin gene of Helicobacter pylori. *Zhonghua Yixue Zazhi* 2003; **83**: 736-739

8 **Bai Y,** Wang JD, Zhang ZS, Zhang YL. Construction of the Attenuated Salmonella typhimurium Strain Expressing *Helicobacter pylori* Conservative Region of Adhesin Antigen. *Chin J Biotech* 2003; **19**: 77-82

9 **Ilver D,** Arnqvist A, Ogren J, Frick IM, Kersulyte D, Incecik ET, Berg DE, Covacci A, Engstrand L, Boren T. *Helicobacter pylori* adhesin binding fucosylated histo-blood group antigens revealed by retagging. *Science* 1998; **279**: 373-377

10 **Bai Y,** Chang SH, Wang JD, Chen Y, Zhang ZS, Zhang YL. Construction of the *E.coli* clone expressing adhesin BabA of *Helicobacter pylori* and evaluation of the adherence activity of BabA. *Diyi Junyi Daxue Xuebao* 2003; **23**: 293-295, 309

11 **Odenbreit S,** Till M, Hofreuter D, Faller G, Haas R. Genetic and functional characterization of the alpAB gene locus essential for the adhesion of *Helicobacter pylori* to human gastric tissue. *Mol Microbiol* 1999; **31**: 1537-1548

12 **Peck B,** Ortkamp M, Diehl KD, Hundt E, Knapp B. Conservation, localization and expression of HopZ, a protein involved in adhesion of *Helicobacter pylori*. *Nucleic Acids Res* 1999; **27**: 3325-3333

13 **Sambrook J,** Fritsch EF, Maniatis T. Molecular cloning:a laboratory manual.2nd ed. New York: Cold Spring Harbor Laboratory Press 1989: 35-400

14 **Odenbreit S,** Till M, Haas R. Optimized BlaM-transposon shuttle mutagenesis of *Helicobacter pylori* allows the identification of novel genetic loci involved in bacterial virulence. *Mol Microbiol* 1996; **20**: 361-373

15 **Tomb JF,** White O, Kerlavage AR, Clayton RA, Sutton GG, Fleischmann RD, Ketchum KA, Klenk HP, Gill S, Dougherty BA, Nelson K, Quackenbush J, Zhou L, Kirkness EF, Peterson S, Loftus B, Richardson D, Dodson R, Khalak HG, Glodek A, McKenney K, Fitzegerald LM, Lee N, Adams MD, Hickey EK, Berg DE, Gocayne JD, Utterback TR, Peterson JD, Kelley JM, Cotton MD, Weidman JM, Fujii C, Bowman C, Watthey L, Wallin E, Hayes WS, Borodovsky M, Karp PD, Smith HO, Fraser CM, Venter JC. The complete genome sequence of the gastric pathogen Helicobacter pylori. *Nature* 1997; **388**: 539-547

16 **Doig P,** Trust TJ. Identification of surface-exposed outer membrane antigens of *Helicobacter pylori*. *Infect Immun* 1994; **62**: 4526-4533

17 **Kleanthous H,** Lee CK, Monath TP. Vaccine development against infection with *Helicobacter pylori*. *Br Med Bull* 1998; **54**: 229-241

Science Editor Zhang J Z and Wang XL **Language Editor** Elsevier HK

PO Box 2345, Beijing 100023, China
www.wjgnet.com
wjg@wjgnet.com

ELSEVIER

World J Gastroenterol 2005;11(15):2264-2268
World Journal of Gastroenterology ISSN 1007-9327

• *BASIC RESEARCH* •

Effects of fibril- or fixed-collagen on matrix metalloproteinase-1 and tissue inhibitor of matrix metalloproteinase-1 production in the human hepatocyte cell line HLE

Makoto Nakamuta, Kazuhiro Kotoh, Munechika Enjoji, Hajime Nawata

Makoto Nakamuta, Kazuhiro Kotoh, Munechika Enjoji, Hajime Nawata, Department of Medicine and Bioregulatory Science, Graduate School of Medical Sciences, Kyushu University, Fukuoka 812-8582, Japan
Correspondence to: Makoto Nakamuta, Department of Medicine and Bioregulatory Science, Graduate School of Medical Sciences, Kyushu University, 3-1-1 Maidashi, Higashi-ku, Fukuoka 812-8582, Japan. nakamuta@intmed3.med.kyushu-u.ac.jp
Telephone: +81-92-642-5282 Fax: +81-92-642-5287
Received: 2004-06-15 Accepted: 2004-08-21

Abstract

AIM: Matrix metalloproteinase-1 (MMP-1) and tissue inhibitor of matrix metalloproteinase-1 (TIMP-1) are central to the spontaneous resolution of liver fibrosis. The mechanisms involved have been investigated in hepatic stellate cells (HSC), but not in hepatocytes. We investigated the effects of fibril- and fixed-collagen on MMP-1 and TIMP-1 production in hepatocytes, using the HLE cell line.

METHODS: Fibril type I and IV collagen were prepared by HCl digestion of type I and IV collagen, respectively. For fixed-collagen, culture dishes were coated with fibril type I or IV collagen and fixed by ultraviolet. Type I collagenase activity was measured using fluorescein isothiocyanate-labeled type I collagen. MMP-1 and TIMP-1 in HLE cells were measured by a one-step sandwich enzyme immunoassay.

RESULTS: Both fibril type I and IV collagen significantly increased type I collagenase activity about two-fold compared with no fibril collagen. The effects of the fibril collagen were not affected by the coating condition. There was no significant difference in the effects on collagenase activity between cells cultured in medium containing fibril type I collagen and those cultured in the presence of type IV collagen. Both types of fibril collagen significantly increased MMP-1 production, and showed more than 10-fold higher levels of MMP-1 than the control. The enhanced MMP-1 production by fibril collagens was unaffected by the coating condition. By contrast, TIMP-1 production was not changed by the addition of fibril type I or IV collagen, and neither was it affected by the coating conditions. Coating with type I collagen significantly suppressed MMP-1 production by almost one-tenth compared with no coating. By contrast, TIMP-1 production was not affected by either the absence of a collagen coat or by increasing the concentration of the coating collagen.

CONCLUSION: These results indicated that, in HLE cells, fibril- and fixed-collagen have opposite effects on MMP-1 production without affecting TIMP production. Fibril collagen induced collagenase activity by up-regulation of MMP-1 production without affecting TIMP-1 production. By contrast, fixed collagen reduced MMP-1 production. Our results suggest that hepatocytes might also play an important role in the regulation of the hepatic fibrosis alongside HSC.

Key words: Hepatocyte; Fibril-collagen; Fixed collagen

Nakamuta M, Kotoh K, Enjoji M, Nawata H. Effects of fibril- or fixed-collagen on matrix metalloproteinase-1 and tissue inhibitor of matrix metalloproteinase-1 production in the human hepatocyte cell line HLE. *World J Gastroenterol* 2005; 11 (15): 2264-2268
http://www.wjgnet.com/1007-9327/11/2264.asp

INTRODUCTION

Liver fibrosis, which is characterized by the excess deposition of extracellular matrix components such as collagen I, III, and IV[1,2], is usually the ultimate pathological outcome for the majority of chronic liver injuries e.g., viral and alcoholic hepatitis. Central to the process of liver fibrosis is the activation of the hepatic stellate cells (HSC), which proliferates and stimulates the production and deposition of collagen. The activated HSC also express tissue inhibitors of metalloproteinase-1 (TIMP-1), which inhibit the degradation of interstitial collagens by interstitial collagenase such as matrix metalloproteinase-1 (MMP-1)[3-5].

Advanced fibrosis and cirrhosis were previously considered to be irreversible conditions. However, there is accumulating evidence that this fibrosis is reversible. Recovery, with remodeling of excess collagens, has been demonstrated in experimentally-induced fibrosis in animals[6] and in liver fibrosis in humans[7]. In situations of spontaneous recovery from liver fibrosis, there is a diminution of TIMP expression and an increase in collagenase activity with consequent degradation of the collagen matrix[8]. Furthermore, an additional finding in this and other studies, was that HSC apoptosis was a key process in the resolution of liver fibrosis[8-11]. However, while the loss of activated HSC can explain a decrease in TIMP expression, it is not in itself sufficient to explain the constitutive MMP-1 expression and

continuous increase in collagenase activity, which remodels the existing excess collagens, because the number of activated HSC is dramatically reduced by one-tenth by apoptosis 7 d after peak fibrosis[8]. This cumulative evidence (the loss of HSC, but constitutive MMP-1 expression and an increase in the collagenase activity in the entire liver), suggests that hepatic parenchymal cells, the hepatocytes, might also be contributing to the resolution of liver fibrosis. We previously reported that fibril type I collagen stimulated MMP-1 expression in hepatocellular carcinoma tissue culture cell lines, such as HepG2 and HLE[12]. We have also confirmed that primary hepatocytes express both MMP-1 and TIMP-1 as well as HLE cells. In this study, we used fibril collagen, as a collagen degradation product, while fixed collagen was used to represent immobilized collagen as part of the extracellular matrix in liver fibrosis. We report here on our investigations into the effects of fibril- or fixed-collagen on MMP-1 and TIMP-1 production in HLE cells in order to establish what role liver parenchymal cells may play in the regulation of liver fibrosis.

MATERIALS AND METHODS

Cell culture

HLE cells, a human hepatocellular carcinoma derived cell line, were obtained from the Japanese Cancer Research Resource Bank. The cells were maintained in Dulbecco's modified Eagle's medium (DMEM) (Nissui Pharmaceutical Ltd., Tokyo, Japan) supplemented with 20% fetal calf serum (FCS), 200 units/mL penicillin, and 200 mg/mL streptomycin.

Experiment 1

The first experiment was designed to test the effect of fibril collagen on type I collagenase activity, TIMP-1 production, and MMP-1 production in HLE cells, cultured on a dish with or without collagen coating. To make fibril collagen, type I or type IV collagen (Nitta Gelatin Co. Ltd., Osaka, Japan) were treated with HCl (pH 3.0) at room temperature overnight, and neutralized with phosphate buffered saline (PBS). The procedure for coating the tissue culture dishes with collagen was as follows: 1 mL of fibril collagen solution (10 μg/mL) was placed in a 35 mm dish, and then exposed to ultraviolet (UV) light for 2 h. The coated dish was washed twice with FCS-free DMEM.

HLE cells were plated at a concentration of 5×10^6 and cultured with DMEM, supplemented with 20% FCS, until they reached confluency. They were then washed twice with FCS-free DMEM and cultured with 2 mL of FCS-free DMEM for 12 h. After washing the dishes with PBS, fibril type I or type IV collagen were added to FCS-free DMEM (final concentration: 0, 37.5, 125, 375, or 1 250 μg/mL) and the cells were cultured for a further 24 h. The resulting conditioned (supernatant) medium was concentrated 15-fold for the assay of collagenase activity, and TIMP-1 and MMP-1 production.

Experiment 2

The second experiment was designed to evaluate the effects of coated, fixed collagen on MMP-1 and TIMP-1 production in HLE cells. The cells were prepared as described in experiment 1, and then cultured on dishes coated with 1 mL of several concentration of fibril collagen solution (0, 10, 30, or 100 μg/mL). The concentration of fibril type I or type IV collagen added in FCS-free DMEM was fixed at 37.5 μg/mL.

Measurement of type I collagenase activity

Type I collagenase activity was assayed using fluorescein isothiocyanate (FITC)-labeled type I collagen (0.1%/0.01 mol/L acetic acid) (Cosmo-Bio Co. Ltd, Tokyo, Japan) according to previously described methods[13]. Briefly, after trypsin activation, 50 μL of the concentrated conditioned medium was incubated with 100 μL of FITC-labeled type I collagen for 3 h at 35 ℃. The reaction was terminated by the addition of 80 mmol/L *O*-phenanthrolene. Collagenase activity was estimated by measuring the fluorescent intensity of the supernatant at 495 nm (excitation)/520 nm (emission). A unit of collagenase activity was defined as the amount of enzyme that degraded 1 μg of collagen/min.

Measurement of TIMP-1 and MMP-1

Monoclonal anti-human TIMP-1 antibody, monoclonal anti-human MMP-1, and peroxidase-conjugated Fab' were kindly donated by Fuji Chemical Industries Ltd (Toyama, Japan). TIMP-1 and MMP-1 were measured by a one-step sandwich enzyme immunoassay as previously described[14-16]. Briefly, a sample was mixed with 10 mmol/L sodium phosphate buffer containing 50 ng/mL peroxidase-conjugated Fab', 1% bovine serum albumin, 0.1% Tween 20, 0.1 mol/L NaCl, and 0.005% thimerosal, and then 100 μL of the solution was transferred to a microplate well, coated with the monoclonal antibody. The preparation was allowed to stand for 30 min at room temperature and then washed thrice with PBS. Peroxidase activity was assayed after 20 min incubation with a reaction mixture containing a 0.15 mol/L citric acid phosphate buffer, 0.5 mg/mL *O*-phenylenediamine and 0.02% H_2O_2. Absorbance was measured at 492 nm in a microplate reader.

Statistical analysis

All results were presented as the mean±SE. Data were analyzed by one-way ANOVA, and differences between groups were assessed by Scheffé's test. A level of $P<0.05$ was accepted as statistically significant.

RESULTS

Effects of fibril collagen on type I collagenase activity, MMP-1 production, and TIMP-1 production

At a concentration of 125 μg/mL, fibril type I collagen significantly increased type I collagenase activity about two-fold compared with a concentration of 37.5 μg/mL or no fibril collagen (Figure 1). However, raising the concentration of fibril type I collagen to 375 or 1 250 μg/mL did not further enhance the increased type I collagenase activity. The effects of the fibril collagen type I were not affected by the coating used, as results were similar for cells cultured with or without type I or type IV collagen coating (10 μg/mL) (Figure 1). Fibril type IV collagen had a similar effect on type I collagenase activity, and it was not affected by the coating conditions (Figure 2). There was no significant

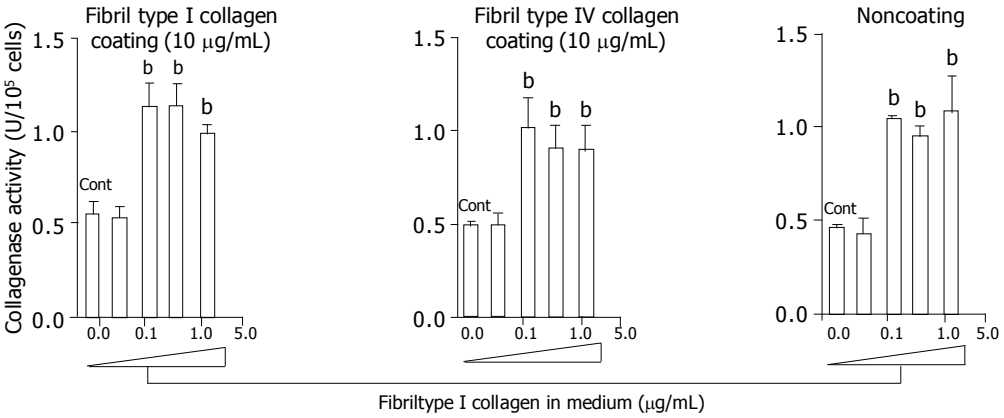

Figure 1 Effects of fibril type I collagen in the culture medium on the collagenase activity for type I collagen. Culture dishes were coated with or without type I collagen (10 μg/mL) and type IV collagen (10 μg/mL). For the control, cells were cultured without fibril collagen. $^{b}P<0.01$ *vs* controls (Cont).

difference in the effects on collagenase activity between cells cultured in medium containing fibril type I collagen and those cultured in the presence of type IV collagen.

In order to investigate the mechanism of this enhanced type I collagenase activity by fibril type I or type IV collagen, the effects of the fibril collagens on MMP-1 production and TIMP-1 production were then evaluated. Both fibril type I and IV collagen significantly increased MMP-1 production, and at a concentration of 375 μg/mL both types showed more than 10-fold higher levels of MMP-1 than the control (Figure 3). The enhanced MMP-1 production by fibril collagens was unaffected by the presence or absence of coating with type I or type IV collagen (Figure 3). By contrast, TIMP-1 production was not changed by the addition of fibril type I or IV collagen, and neither was it affected by the coating conditions (Figure 4).

Effects of the fixed type I collagen on MMP-1 and TIMP-1 production

The effects of the amount of type I collagen coating (fixed collagen) on MMP-1 and TIMP-1 production were also evaluated. Coating with 30 or 100 μg/mL type I collagen significantly suppressed MMP-1 production by almost one-tenth compared with coating with 10 μg/mL type I collagen or no coating (Figure 5A). By contrast, TIMP-1 production was not affected by either the absence of a collagen coat or by increasing the concentration of the coating collagen (Figure 5B).

DISCUSSION

We have demonstrated that fibril type I or IV collagen induced type I collagenase activity, and also increased MMP-1 production. However, neither type had an effect on TIMP-1 production. Type I collagenase activity is regulated by a balance between MMP-1 and TIMP-1, and our data indicated that the enhanced type I collagenase activity was attributable to increased MMP-1 production but not to decreased TIMP-1 production. The fact that the fibril collagens stimulated a 10-fold increase in MMP-1 but only a two-fold increase in the collagenase activity raises questions. One possible explanation is that we measured the whole MMP-1 protein, including pro-MMP1 that does not have any proteinase activity. Another explanation for this apparent discrepancy is that the difference may have been due to the presence of other members of the MMP or TIMP family, such as MMP-2, which is closely related to the process of tumor cell invasion[17]. However, although HLE cells are a hepatocellular carcinoma-derived cell line, in this study the collagenase activity was measured using type I collagen as a substrate, which is a target for MMP-1 not MMP-2. Consequently, the increased collagenase activity was assumed to reflect the up-regulation of MMP-1 activity. In normal

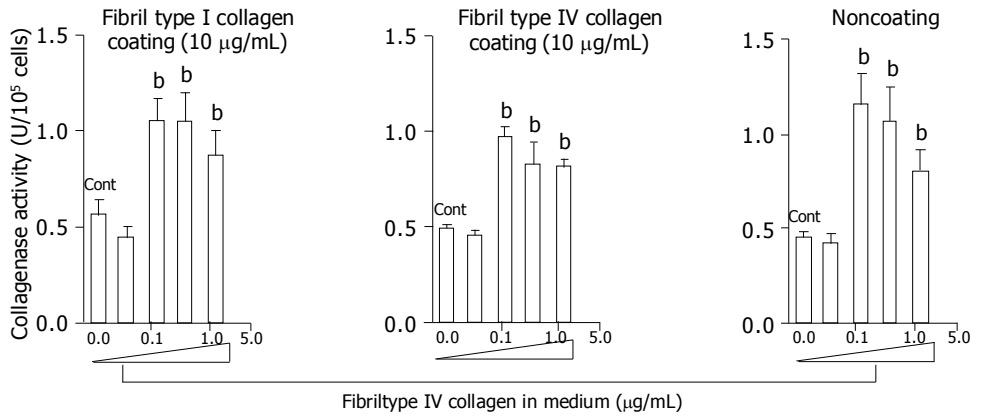

Figure 2 Effects of fibril type IV collagen in the culture medium on collagenase activity for type I collagen. Culture dishes were coated with or without type I collagen (10 μg/mL) and type IV collagen (10 μg/mL). For the control, cells were cultured without fibril collagen. $^{b}P<0.01$ *vs* controls (Cont).

cells, such as keratinocytes, MMP-1 expression is highly elevated after stimulation by type I collagen[18,19]. In this study, we used HLE cells as they are hepatocyte-derived cell lines, and have demonstrated increased MMP-1 production in response to fibril collagen[12]. Although we still need to establish that fibril collagen stimulates collagenase activity and MMP-1 production without affecting TIMP-1 production in primary hepatocytes, we have confirmed that rat primary hepatocytes expressed both MMP-1 and TIMP-1, and preliminarily found that fibril collagen stimulated MMP-1 mRNA expression (unpublished data). Therefore, the evidence from the results reported here, together with preliminary evidence in the rat primary hepatocytes, indicate that the up-regulation of MMP-1 by the fibril collagen is a common feature.

By contrast, fixed (coated) type I collagen down-regulated MMP-1, and did not affect TIMP-1 production. One could assume from this observed decrease in the production of MMP-1 and unchanged TIMP-1 production, that the collagenase activity would be down-regulated. Because collagen encountered *in vivo*, particularly in liver fibrosis, will commonly be immobilized as part of the extracellular matrix, we coated culture dishes with different, increasing concentrations of type I collagen. The precise mechanism behind the opposite effects seen between fibril- and fixed-collagen is unclear. However, it has been suggested that the conformation of fibril collagens interacting with HLE cells might be different from that of the immobilized fixed collagens. Integrins are important trans-cell membrane adhesion glycoproteins, with α and β subunits. They exist in an active and inactive form. The amino acid sequence arginine-glycine-aspartic acid (RGD) is a potent recognition sequence for integrin binding, including the binding of fibronectin to the α5β1 integrin receptor. The α1β1 and α2β1 integrins, both of which are expressed in HLE cells[20], are major cellular receptors for collagens and interact with the triple-helical region of most of the fibril collagen[21,22]. Binding of collagen to integrins is an essential, fundamental step in fibrogenesis and wound healing. We have reported previously that soluble RGD peptide reduced the accumulation of collagen in HSC by stimulating collagenase and MMP-1 activity[23], whereas, conversely, the fibronectin isoform, or EIII A segment, has been shown to increase collagen production[24]. Discoidin domain receptor 2 (DDR2) is another receptor for fibril collagen, and activation of DDR2 has been shown to induce the expression of MMP-1[25]. We have reported previously that HLE cells express the DDR2 receptor, and that fibril collagen stimulated MMP-1 production in these cells, whereas fixed collagen did not[15]. Taken together, all this evidence suggests that fibril collagen might induce MMP-1 production in HLE cells via its activation of DDR2.

Using HLE cells, we tried to evaluate the role of liver parenchymal cells in liver fibrosis and its resolution, although there is limitation of use of HLE cells even which express both MMP-1 and TIMP-1. During the process of liver fibrosis, HSC become active and produce immobilized

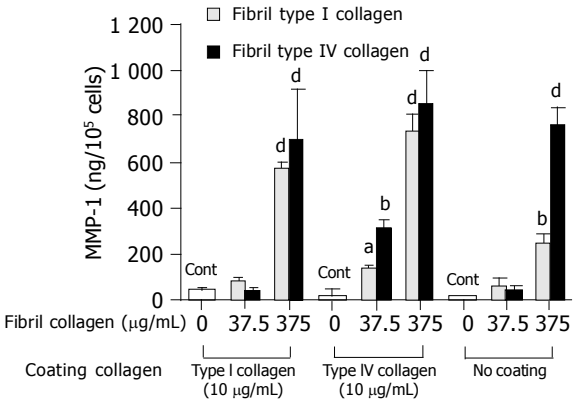

Figure 3 Effects of fibril type I (dotted bar) or type IV (filled bar) collagen on matrix metalloproteinase-1 (MMP-1) production. For the control, cells were cultured without fibril collagen. [a]*P*<0.05; [b]*P*<0.01; [d]*P*<0.001 *vs* controls (Cont).

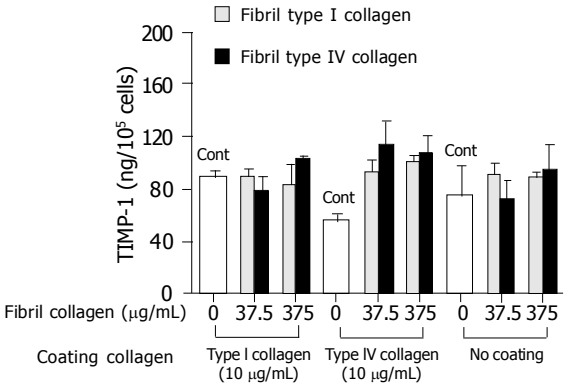

Figure 4 Effects of fibril type I (dotted bar) or type IV (filled bar) collagen on tissue inhibitor of matrix metalloproteinase-1 (TIMP-1) production. For the control(Cont), cells were cultured without fibril collagen.

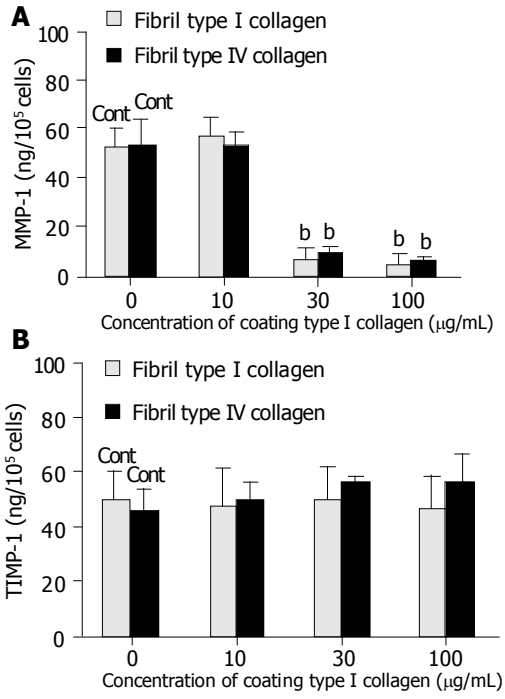

Figure 5 Effect of the coating concentrations of type I collagen on matrix metalloproteinase-1 (MMP-1) (**A**) and tissue inhibitor of matrix metalloproteinase-1 (TIMP-1) (**B**) production. For the control, cells were cultured on non-coating dishes. [b]*P*<0.01 *vs* controls (Cont).

collagens[1]. As shown in Figure 5, immobilized fixed collagen suppressed MMP-1 production but did not affect TIMP-1 production, which would lead to an overall accumulation of collagen in the liver. During the resolution of liver fibrosis, there is a diminution of TIMP expression and an increase in collagenase activity with consequence matrix degradation[11] including the formation of fibril collagen. These fibril collagens act on the hepatocytes to induce MMP-1 production, without affecting TIMP-1 production, resulting in induction of collagenase activity. This link could establish an autocrine-loop for the resolution of fibrosis. Since we know that HSC become apoptotic, and decrease in number by one-tenth within a week of the peak of fibrosis[11], the up-regulation of collagenase activity by hepatocytes could maintain the remodeling and resolution of fibrosis, even after the loss of HSC. Our data implicate hepatocytes as also playing an important role in both liver fibrosis and its resolution alongside HSC. Novel insights into the entire mechanism involved in the regulation of hepatic fibrosis may be obtained by studying the interactions of, or co-operation between, the various types of cells involved, such as HSC and hepatocytes. Furthermore, based on an understanding of the co-operation between various cell functions, such insights might lead to the development of improved therapeutic strategies for the various pathologies which are associated with the process of fibrosis.

REFERENCES

1 **Friedman SL.** Seminars in medicine of the Beth Israel Hospital, Boston. The cellular basis of hepatic fibrosis. Mechanisms and treatment strategies. *N Engl J Med* 1993; **328**: 1828-1835

2 **Du WD,** Zhang YE, Zhai WR, Zhou XM. Dynamic changes of type I, III and IV collagen synthesis and distribution of collagen-producing cells in carbon tetrachloride-induced rat liver fibrosis. *World J Gastroenterol* 1999; **5**: 397-403

3 **Benyon RC,** Iredale JP, Goddard S, Winwood PJ, Arthur MJ. Expression of tissue inhibitor of metalloproteinases 1 and 2 is increased in fibrotic human liver. *Gastroenterology* 1996; **110**: 821-831

4 **Iredale JP,** Benyon RC, Arthur MJ, Ferris WF, Alcolado R, Winwood PJ, Clark N, Murphy G. Tissue inhibitor of metalloproteinase-1 messenger RNA expression is enhanced relative to interstitial collagenase messenger RNA in experimental liver injury and fibrosis. *Hepatology* 1996; **24**: 176-184

5 **Iredale JP,** Murphy G, Hembry RM, Friedman SL, Arthur MJ. Human hepatic lipocytes synthesize tissue inhibitor of metalloproteinases-1. Implications for regulation of matrix degradation in liver. *J Clin Invest* 1992; **90**: 282-287

6 **Abdel-Aziz G,** Lebeau G, Rescan PY, Clements B, Rissel M, Deugnier Y, Campion JP, Guillouzo A. Reversibility of hepatic fibrosis in experimentally induced cholestasis in rat. *Am J Pathol* 1990; **137**: 1333-1342

7 **Lok AS,** Chung HT, Liu VW, Ma OC. Long-term follow-up of chronic hepatitis B patients treated with interferon alfa. *Gastroenterology* 1993; **105**: 1833-1838

8 **Iredale JP,** Benyon RC, Pickering J, McCullen M, Northrop M, Pawley S, Hovell C, Arthur MJ. Mechanisms of spontaneous resolution of rat liver fibrosis. Hepatic stellate cell apoptosis and reduced hepatic expression of metalloproteinase inhibitors. *J Clin Invest* 1998; **102**: 538-549

9 **Gong W,** Pecci A, Roth S, Lahme B, Beato M, Gressner AM. Transformation-dependent susceptibility of rat hepatic stellate cells to apoptosis induced by soluble Fas ligand. *Hepatology* 1998; **28**: 492-502

10 **Issa R,** Williams E, Trim N, Kendall T, Arthur MJ, Reichen J, Benyon RC, Iredale JP. Apoptosis of hepatic stellate cells: involvement in resolution of biliary fibrosis and regulation by soluble growth factors. *Gut* 2001; **48**: 548-557

11 **Wright MC,** Issa R, Smart DE, Trim N, Murray GI, Primrose JN, Arthur MJ, Iredale JP, Mann DA. Gliotoxin stimulates the apoptosis of human and rat hepatic stellate cells and enhances the resolution of liver fibrosis in rats. *Gastroenterology* 2001; **121**: 685-698

12 **Enjoji M,** Kotoh K, Iwamoto H, Nakamuta M, Nawata H. Self-regulation of type I collagen degradation by collagen-induced production of matrix metalloproteinase-1 on cholangiocarcinoma and hepatocellular carcinoma cells. *In Vitro Cell Dev Biol Anim* 2000; **36**: 71-73

13 **Igarashi S,** Hatahara T, Nagai Y, Hori H, Sakakibara K, Katoh M, Sakai A, Sugimoto T. Anti-fibrotic effect of malotilate on liver fibrosis induced by carbon tetrachloride in rats. *Jpn J Exp Med* 1986; **56**: 235-245

14 **Zhang J,** Fujimoto N, Iwata K, Sakai T, Okada Y, Hayakawa T. A one-step sandwich enzyme immunoassay for human matrix metalloproteinase 1 (interstitial collagenase) using monoclonal antibodies. *Clin Chim Acta* 1993; **219**: 1-14

15 **Kodama S,** Iwata K, Iwata H, Yamashita K, Hayakawa T. Rapid one-step sandwich enzyme immunoassay for tissue inhibitor of metalloproteinases. An application for rheumatoid arthritis serum and plasma. *J Immunol Methods* 1990; **127**: 103-108

16 **Hayakawa T,** Yamashita K, Tanzawa K, Uchijima E, Iwata K. Growth-promoting activity of tissue inhibitor of metalloproteinases-1 (TIMP-1) for a wide range of cells. A possible new growth factor in serum. *FEBS Lett* 1992; **298**: 29-32

17 **Stetler-Stevenson WG,** Hewitt R, Corcoran M. Matrix metalloproteinases and tumor invasion: from correlation and causality to the clinic. *Semin Cancer Biol* 1996; **7**: 147-154

18 **Sudbeck BD,** Parks WC, Welgus HG, Pentland AP. Collagen-stimulated induction of keratinocyte collagenase is mediated via tyrosine kinase and protein kinase C activities. *J Biol Chem* 1994; **269**: 30022-30029

19 **Sudbeck BD,** Pilcher BK, Welgus HG, Parks WC. Induction and repression of collagenase-1 by keratinocytes is controlled by distinct components of different extracellular matrix compartments. *J Biol Chem* 1997; **272**: 22103-22110

20 **Masumoto A,** Arao S, Otsuki M. Role of beta1 integrins in adhesion and invasion of hepatocellular carcinoma cells. *Hepatology* 1999; **29**: 68-74

21 **Calderwood DA,** Tuckwell DS, Humphries MJ. Specificity of integrin-I domain-ligand binding. *Biochem Soc Trans* 1995; **23**: 504S

22 **Kühn K.** Conformation-dependent recognition sites. In integrin-ligand interaction, K Kühn and JA Eble, eds. Heidelberg, Germany: Springer, pp.141-155

23 **Iwamoto H,** Sakai H, Kotoh K, Nakamuta M, Nawata H. Soluble Arg-Gly-Asp peptides reduce collagen accumulation in cultured rat hepatic stellate cells. *Dig Dis Sci* 1999; **44**: 1038-1045

24 **Jarnagin WR,** Rockey DC, Koteliansky VE, Wang SS, Bissell DM. Expression of variant fibronectins in wound healing: cellular source and biological activity of the EIIIA segment in rat hepatic fibrogenesis. *J Cell Biol* 1994; **127**: 2037-2048

25 **Vogel W,** Gish GD, Alves F, Pawson T. The discoidin domain receptor tyrosine kinases are activated by collagen. *Mol Cell* 1997; **1**: 13-23

Science Editor Li WZ **Language Editor** Elsevier HK

PO Box 2345, Beijing 100023, China
www.wjgnet.com
wjg@wjgnet.com

ELSEVIER

World J Gastroenterol 2005;11(15):2269-2276
World Journal of Gastroenterology ISSN 1007-9327

• *BASIC RESEARCH* •

Effects of Chinese traditional compound, JinSanE, on expression of TGF-β1 and TGF-β1 type II receptor mRNA, Smad3 and Smad7 on experimental hepatic fibrosis *in vivo*

Shi-Ling Song, Zuo-Jiong Gong, Quan-Rong Zhang, Tuan-Xin Huang

Shi-Ling Song, Zuo-Jiong Gong, Quan-Rong Zhang, Department of Infectious Diseases, Renmin Hospital, Wuhan University, Key Laboratory of Virology of Ministry of Education, Wuhan 430060, Hubei Province, China
Tuan-Xin Huang, Department of Infectious Diseases, Hubei Provincial Corps Hospital, Chinese People's Armed Police Forces, Wuhan 430061, Hubei Province, China
Supported by the Basic Research Program of Hubei Province Education Bureau, No. 2003X113
Correspondence to: Professor Zuo-Jiong Gong, Department of Infectious Diseases, Renmin Hospital, Key Laboratory of Virology for Ministry of Education, Wuhan University, Wuhan 430060, Hubei Province, China. zjgong@163.com
Telephone: +86-27-88041911-8385 Fax: +86-27-88042922
Received: 2004-04-24 Accepted: 2004-05-09

Abstract

AIM: The transforming growth factor-beta (TGF-β)/Smad signaling pathway system plays a prominent role in the control of cell growth and extracellular matrix formation in the progression of liver fibrogenesis. Smad proteins can either positively or negatively regulate TGF-β responses. In this study, the therapeutic effects of Chinese traditional compound decoction, JinSanE, and the changes of TGF-β/Smad signaling pathway system in carbon tetrachloride (CCl_4)-induced rat experimental liver fibrosis were examined.

METHODS: Seventy-two healthy Wistar rats were assigned to groups including normal control group, CCl_4 model group, JinSanE treatment group I and JinSanE treatment group II. Each group contained 18 rats. All groups, except the normal control group, received CCl_4 subcutaneous injection for 8 wk. Rats in JinSanE groups I and II were orally treated with JinSanE daily at the 1st and 5th wk, respectively, after exposure to CCl_4. The expression of TGF-β1 and TGF-β1 type II receptor (TRII) mRNA in the liver was determined by reverse transcription polymerase chain reaction, and the expression of TGF-β1, Smad3 and Smad7 by immunohistochemistry. The liver histopathology was also examined by HE staining and observed under electron microscope. The activities of several serum fibrosis-associated enzymes, alanine aminotransferase (ALT), aspartate aminotransferase (AST), the levels of serum hyaluronic acid (HA) were assayed.

RESULTS: Hepatic fibrosis caused by CCl_4 was significantly inhibited in the JinSanE-treated groups. The degrees of necrosis/degeneration and fibrosis scores were significantly lower in the JinSanE-treated groups than in the model control group. The expression of TGF-β1, TRII and Smad3 was significantly higher in the model group than that in the JinSanE-treated groups, and the active/total TGF-β1 ratio in the JinSanE groups was suppressed. Expression of TRII mRNA and Smad3 proteins showed a distribution pattern similar to that of TGF-β1 with a direct correlation in terms of the degree of hepatic fibrosis. The amount of positive staining Smad7 cells was significantly less in the model group than in the JinSanE-treated groups and the normal group. The contents of ALT, AST and HA were significantly lower in the JinSanE-treated groups than those in the model group.

CONCLUSION: Traditional Chinese medicine, JinSanE, prevents the progression of hepatic damage and fibrosis through the inhibition of TGF-β1, TRII and Smad3 signal proteins, and increases expression of Smad7 signal protein *in vivo*.

Key words: TGF-β; Liver fibrogenesis

Song SL, Gong ZJ, Zhang QR, Huang TX. Effects of Chinese traditional compound, JinSanE, on expression of TGF-β1 and TGF-β1 type II receptor mRNA, Smad3 and Smad7 on experimental hepatic fibrosis *in vivo*. *World J Gastroenterol* 2005; 11(15): 2269-2276
http://www.wjgnet.com/1007-9327/11/2269.asp

INTRODUCTION

Hepatic fibrosis is a common characteristic of the chronic liver disease, which relates to the abnormal accumulation of extracellular matrix (ECM). It is also the major cause of morbidity and mortality due to the development of cirrhosis and its complications including hepatocellular carcinoma[1,2]. Hepatic stellate cells (HSCs) are the primary cell type responsible for matrix deposition in hepatic fibrosis, undergoing a process of transdifferentiation into fibrogenic myofibroblasts (MFBs)[3]. HSCs are a major target of the profibrogenic agent, transforming growth factor-beta (TGF-β). TGF-β has not only multiple profibrogenic, but also anti-inflammatory and immunosuppressive effects[4,5]. In addition to its fibrogenic action leading to transdifferentiation of HSCs into MFBs, TGF-β is also an important negative

regulator of proliferation and an inducer of apoptosis[6]. TGF-β superfamily members signal through transmembrane Ser-Thr kinase receptors that directly regulate the intracellular Smad pathway[7]. Smads are a unique family of signal transduction molecules that can transmit signals directly from the cell surface receptors to the nucleus. In addition, there is recent evidence that Smads can either positively or negatively regulate the transcription of specific genes in response to TGF-β signaling[8,9]. The TGF-β/Smad signaling pathway plays a prominent role in the activation of HSCs and the regulation of the production, degradation, and accumulation of ECM proteins. On the other hand, genetic and biochemical studies in mammals have firmly established the TGF-β/Smad signaling pathway as a pivotal means for the intracellular signaling of TGF-β[10]. Thus, the TGF-β signal transduction pathway has become a new effective target for the prevention and treatment of hepatic fibrosis[11,12].

Chinese herbal medicine has been used for treatment of acute and chronic hepatitis in China and other countries for thousands of years[13-16]. The traditional Chinese compound, JinSanE, is designed to reduce hepatic fibrosis. It is mainly composed of *Radix curcumae*, *Rhizoma sparganii*, and *Rhizoma zedoariae*, which are widely administered to patients with acute or chronic liver diseases in China, and demonstrate therapeutic effects. However, little is known about the effects and mechanism by which JinSanE protects against hepatic fibrosis. We designed this study to investigate whether JinSanE has an inhibitory effect on the development of hepatic fibrosis in a carbon tetrachloride (CCl_4)-induced hepatic fibrosis model in Wistar rats.

MATERIALS AND METHODS

Animals and tissue specimens

Seventy-two Wistar rats, weighting 180-220 g, were obtained from Renmin Hospital of Wuhan University (Wuhan, China). The rats were randomly divided into four groups: normal group, model group, JinSanE group I and JinSanE group II, with 18 rats in each group. Except those in the normal group, all rats were administered with subcutaneous injection of 400 mL/L CCl_4 dissolved in castor oil (Shanghai Changjiang Chemical Plant, Shanghai, China) 3 mL/kg body weight twice per week for 8 wk. The rats in JinSanE groups I and II were treated with traditional Chinese compound decoction, JinSanE, 6 g/kg body weight, daily, via gastrogavage at the 1st and 4th wk, respectively. Once a week, the rats were weighed and the dosage of CCl_4 and JinSanE was adjusted. The rats were maintained under controlled conditions (24 ℃, 58% humidity, and 12-h day/night rhythm) with alternating 12-h dark/light cycles, fed laboratory chow diet, and had free access to food and water. All rats received humane care, and the study protocols comply with the guidelines of Wuhan University. At the end of the 8-wk experimental period, all rats were killed by bleeding from ophthalmic artery and vein. The blood and liver of all rats were collected for further examinations.

Detection of mRNA by reverse-transcription polymerase chain reaction

Isolation of RNA and reverse-transcription polymerase chain reaction (RT-PCR) were performed as described previously[17]. Isolation of total RNA from liver tissue was performed using the Catrimox-14™ RNA Purification kit (Takara BIO Inc., Tokyo, Japan). RNA concentrations were determined by ultraviolet spectrophotometric measurements at wavelengths of 260/280 nm. mRNA was transcribed into complementary DNA using AMV reverse transcriptase (Takara BIO Inc.). Random primers and Taq polymerase for subsequent PCR were also obtained from Takara BIO Inc. Total RNA (1 μg) was reverse transcribed into cDNA. The cDNA was amplified by PCR with the following forward and reverse primers: TGF-β1, 5'-CAC CA T CCATGACATG AACC-3' and 5'-TCATGTTGGACAAC-TGCTCC-3', respectively, with a product size of 404 bp; TGFβ1-type II receptor (TRII), 5'-CTACAAGGCCA-AGCTGAAGC-3' and 5'-A GCCATGGAGTAGACATC CG -3', respectively, with a product size of 580 bp; and GADPH, 5'-T CCCTCAACATTGTCAGCAA-3' and 5'-AGCTCCACAACGGATACATT-3', respectively, with a product size of 309 bp. The 50 μL PCR reaction mix contained 10 mmol/L dNTP, 2.5 mmol/L $MgCl_2$, 20 mmol/L Tris-HCl (pH 8.4), 50 mmol/L KCl, 30 pmol/L levels of sense and antisense primers, and 5 U of Taq DNA Polymerase (Takara BIO Inc.). The thermal profile that was used consisted of denaturation at 94 ℃ for 1 min, annealing at 55 ℃ for 1 min, and extension at 72 ℃ for 1 min for 35 times for TGF-β1, TRII and GAPDH. In all experiments, possible contamination with genomic DNA was excluded by PCR amplification in the absence of reverse transcriptase. The PCR products were electrophoresed on 2% agarose gel electrophoresis. Semiquantitative evaluation was performed using the Gel Doc 2000 System (BioRad Laboratories GmbH, München, Germany). GAPDH was used as a positive internal control, and was equally positive for all specimens. GAPDH expression was used as a correction factor for TGF-β1 and TRII mRNA, thus, the results were expressed as the number of TGF-β1 and TRII cDNA molecules per GAPDH cDNA molecules.

Immunohistochemistry

Rat monoclonal anti-TGF-β1 antibody, rat polyclonal anti-Smad3 antibody and anti-Smad7 antibody were obtained from Santa Cruz (Los Angeles, USA), and the peroxides method was used to stain TGF-β1-positive, Smad3-positive and Smad7-positive cells. The ultrasensitive TM S-P (Rabbit) kit was obtained from Maxin-Bio (Maxin-Bio, Fuzhou, China). Liver tissues were fixed in 40 g/L formaldehyde, embedded in paraffin, and cut into 4-μm thick sections. The sections were deparaffinized, treated with 0.3% endogenous peroxidase blocking solution for 20 min, and treated sequentially with normal nonimmun goat serum for 20 min at room temperature, then incubated with rabbit anti-TGF-β1 antibody at a previously defined optimal dilution of 1:200, or rabbit anti-Smad3 1:100, or rabbit anti-Smad7 1:100 at room temperature for 1.5 h. All antibodies were diluted in PBS with 1% PBS with 1% bovine serum albumin (BSA), and PBS-1% BSA was used as a negative control. The slides were washed thrice with PBS. Primary antibodies were detected with biotin-labeled anti-rabbit immunoglobulin G. Counterstaining was performed

with hematoxylin. Samples were analyzed by confocal microscopy using 40× objective (Olympus, Japan).

Analytical methods for serum samples

Serum content of hyaluronic acid (HA) was assessed by radioimmunoassay (RIA) using a commercial kit (Shanghai NAVY Medical Institute, Shanghai, China). Serum levels of alanine transaminase (ALT), aspartate transaminase (AST), albumin (ALB) and globulin (GLB) were determined by routine laboratory methods using a Hitachi Automatic Analyzer.

Histopathological examination

Liver tissues were fixed in 40 g/L formaldehyde, embedded in paraffin, cut into 4-μm thick sections and stained with hematoxylin-eosin (H&E). The consensus by the Hepatic Fibrosis Study Group of Chinese Liver Diseases Association[18] was used to evaluate hepatic fibrosis degree and necroinflammatory activity by two independent pathologists blindly. Liver tissues fixed in 2% buffer glutaraldehyde were observed with Hitachi H-300 electron microscope.

Statistical analysis

All data were presented as mean±SE. Differences among groups were assessed using unpaired Student's *t* test and one-way ANOVA. A *P* value of less than 0.05 was considered to be statistically significant. Calculations were performed with SPSS11.0 software package of statistical programs.

RESULTS

Detection of TGF-β1 and TRII mRNA by RT-PCR

Detectable levels of TGF-β1 and TRII mRNA were noted in the normal group, but the expression levels in the model group were significantly increased, compared with those in the normal group (both $P<0.01$) (Table 1, Figures 1 and 2). The expression levels of TGF-β1 mRNA (0.590±0.053, 0.693±0.057, respectively) and TRII mRNA (0.462±0.009, 0.539±0.010, respectively) in JinSanE groups I and II were significantly lower compared with the model group livers (1.410±0.094, 0.906±0.03, respectively) (all $P<0.01$) (Table 1). There was no significant difference in the expression level of TGF-β1 mRNA between the normal group (0.401±0.059) and JinSanE group II ($P>0.05$). Similarly, there was no significant difference in the expression level of TRII mRNA between the normal group (0.275±0.027) and JinSanE group I ($P>0.05$). However, the expression level of TRII mRNA in JinSanE group II was significantly greater than that in JinSanE group I ($P<0.01$).

Table 1 **Comparison of semiquantitative RT-PCR results in the four experimental groups (mean±SD)**

Groups	*n*	Expression levels	
		$TGF\beta_1$mRNA	TRII mRNA
Normal	18	0.401±0.059	0.275±0.027
Model	15	1.410±0.094[b]	1.215±0.079[b]
JinSanE I	17	0.590±0.053[d]	0.461±0.029[d]
JinSanE II	16	0.693±0.057[b,d]	0.651±0.035[b,d,f]

[b]$P<0.01$ *vs* compared with the normal group; [d]$P<0.01$ *vs* compared with the model group; and [f]$P<0.01$ *vs* compared with JinSanE group I.

Detection of TGF-β1, Smad3 and Smad7 by immunohistochemistry

The distribution of TGF-β1, Smad3 and Smad7 was observed in cytoplasm of rat livers in all groups, but nuclei were devoid of staining (Figures 3-5). In normal control livers, the cytoplasm of interstitial tissue and liver sinusoidal were positive for TGF-β1, whereas TGF-β1 was scattered along the sinusoidal walls. Smad3 was rarely observed, but intense Smad7 expression was extensively observed in hepatocytes of normal rats. In contrast, many TGF-β1 and Smad3-positive cells were detected in sinus portal, areas fibrous, septum, hepatocytes in pseudolobes and necrotic areas of severe hepatitis in the model rats, and the amount of TGF-β1-positive cells was obviously larger than that of Smad3-positive cells. In fibrotic liver tissues, weak immunostaining for Smad7 was detected in hepatocytes, fibroblasts and occasional mononuclear infiltrates. In contrast, livers of rats fed with JinSanE showed markedly decreased numbers of TGF-β1 and Smad3-positive HSCs and fibroblasts, and these positive cells in livers of the JinSanE group I were less than those in the JinSanE group II. JinSanE also obviously enhanced numbers of Smad7-positive hepatocytes and fibroblasts, and exhibited stronger Smad7 positivity in the livers of JinSanE group I than in JinSanE group II (Figures 3-5). Generally, the staining patterns for TGF-β1 and Smad3 were similarly distributed, but staining for TGF-β1 was much stronger than that for Smad3 (Figures 3 and 4).

Effect of JinSanE on HA and liver function

Serum content of HA was significantly higher in the model group than that in the normal group, but this marker was markedly lowered in two treated groups compared with the model group. Compared with the normal group, the serum levels of ALT and AST in the model group were significantly raised, and serum levels of ALB and ALB/GLB were significantly diminished. Compared with the model group, the levels of ALT and AST were markedly reduced, and ALB and ALB/GLB levels were significantly increased in JinSanE groups I and II (Table 2).

Table 2 **Biochemical data in the four experimental groups (mean±SD)**

Groups	*n*	ALT (IU/L)	AST (IU/L)	ALB (g/L)	A/G	HA (ng/L)
Normal rats	18	50.17±2.37	77.8±13.36	35.4±1.5	1.30±0.09	116.04±17.81
Model rats	15	276.0±45.4[b]	554.8±68.3[b]	24.7±3.15[b]	0.57±0.48[b]	318.65±20.83[b]
JinSanE I rats	17	105.3±15.1[b,d]	331.5±47.9[b,d]	30.1±2.3[b,d]	0.89±0.04[b,d]	138.20±11.39[d]
JinSanE II rats	16	109.5±28.5[b,d]	248.5±9.42[b,d]	32.7±1.8[b,d]	0.94±0.07[b,d]	129.50±17.04[d]

ALT, alanine transaminase; AST, aspartate transaminase; ALB, albumin; A/G, albumin/globulin ratio; and HA, hyaluronic acid. [b]$P<0.01$ *vs* compared with the normal group; [d]$P<0.01$ *vs* compared with the model group.

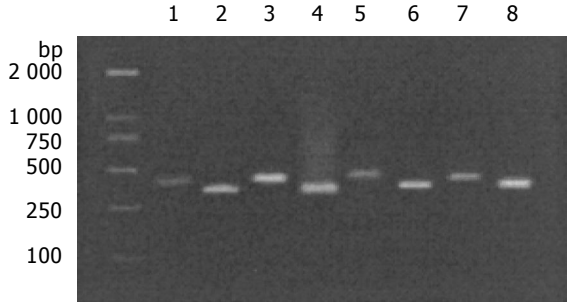

Figure 1 Gel electrophoresis of PCR products for TGF-b1 and GAPDH in rat liver. Total RNA isolated from liver specimens was reverse transcribed and amplified by PCR with specific primers. As a positive control, the housekeeping GAPDH mRNA was also amplified. M (Authors: add M in the photo), Takara markers. Lines 1, 3, 5, 7 are PCR products for TGF-b1, representing the normal, model, JinSanE I and JinSanE II groups, respectively. Lines 2, 4, 6 and 8 are PCR products of GAPDH, representing the normal, model, JinSanE I and JinSanE II groups, respectively.

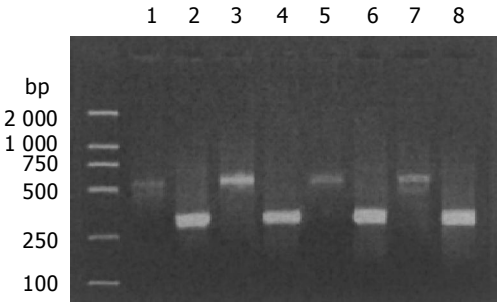

Figure 2 Gel electrophoresis of PCR products for TRII and GAPDH in rat liver. Total RNA isolated from liver specimens was reverse transcribed and amplified by PCR with specific primers. As a positive control, the housekeeping GAPDH mRNA was also amplified. M (Authors: add M in the photo), Takara markers. Lines 1, 3, 5, 7 are PCR products for TRII, representing the normal, model, JinSanE I and JinSanE II groups, respectively. Lines 2, 4, 6 and 8 are PCR products of GAPDH, representing the normal, model, JinSanE I and JinSanE II groups, respectively.

Liver histopathology

The livers in the normal group showed normal lobular architecture with central veins and radiating hepatic cords with irregular sinusoids, and a normal distribution of collagen with a variable amount in portal tracts and a thin rim around central veins. Livers in the model group showed disorderly hepatocyte cords, fatty degeneration, necrosis and infiltration of inflammatory cells and collagen deposition extending from central veins or portal tracts, with thick or thin fibrotic septa and even formation of pseudolobuli. Treatment with JinSanE resulted in apparent amelioration of hepatocyte degeneration, necrosis and infiltration of inflammatory cells, and marked reduction of collagen deposition with no obvious formation of pseudolobuli. Histologic examination revealed that JinSanE-treated rats showed less infiltration of inflammatory cells and less severe progression of liver fibrosis compared with the model rats. Scores of liver necroinflammation and fibrosis are shown in Table 3.

In the livers of the normal rats, the result of electron microscopy showed that HSCs, fat droplet-rich and with pseudopodium, were distributed amongst the hepatocytes. A mass of accumulation of ECM proteins in the Disse's spaces was a prominent finding in fibrotic liver, and the hypertrophied endoplasmic reticulum in HSCs and swollen mitochondrion in hepatocyte were also observed in this group. In the livers of JinSanE-treated rats, the result of electron microscopy showed obviously less accumulation of ECM proteins in the Disse's spaces, fat droplet-rich HSCs, and regenerated and normal hepatocytes.

Table 3 **Effects of JinSanE on liver necroinflammatory scores and fibrosis scores in the four experimental groups (mean±SD)**

Groups	*n*	Necroinflammatory scores	Fibrosis scores
Normal	18	0	0
Model	15	5.28±1.31	7.44±1.59
JinSanE I	17	3.18±0.95[a]	4.40±1.27[a]
JinSanE II	16	4.05±0.92[bc]	5.57±1.20[b]

[b]$P<0.01$ *vs* compared with the model group; [a]$P<0.05$ *vs* compared with the model group; and [c]$P<0.05$ *vs* compared with JinSanE group I.

DISCUSSION

Our study showed that TGF-β1 mRNA and protein increased as fibrosis developed in CCl_4-induced fibrotic liver in a rat model. Our study also demonstrated that ingestion with JinSanE not only suppressed the development of CCl_4-induced hepatic fibrosis, but also decreased the TGF-β1 mRNA and protein levels. The CCl_4-induced hepatic fibrogenesis may be associated with the proliferation of HSCs and ECM accumulation. During the development of chronic liver injury, including inflammation, fibrosis and regeneration, TGF-β1 superfamily plays a prominent role in stimulating liver fibrogenesis by MFBs derived from HSCs[19]. TGF-β1 family regulates many aspects of the cellular function, and consequently exhibits different effects on a variety of cell types and tissues. Hepatocyte apoptosis and HSC activation are both features of chronic liver diseases. TGF-β1 inhibits hepatocyte proliferation and induces hepatocyte apoptosis, and is also the most important cytokine involved in HSC activation, acting via both paracrine and autocrine pathways[20]. TGF-β1 is probably the most decisive cytokine, and HSCs are the most significant cells involved in stimulating ECM synthesis, inhibiting ECM degradation and enhancing accumulation of ECM in the liver[21,22]. Proteolytic release and activation of latent TGF-β by HSCs are key events for pathogenesis of hepatic fibrosis[23]. Cells, such as HSCs, Kupffer cells, MFBs, endothelial cells and invading mononuclear cells, could synthesize and release TGF-β. Many studies have created a strong rationale for an antifibrotic strategy in which the principal objective is blocking TGF-β1.

Active TGF-β binds to specific, high-affinity receptors present on most cells, initiating a signaling cascade that results in biologic effects[24,25]. TGF-β signals through the heteromeric complexes of type I and type II transmembrane Ser/Thr kinase receptors[19,26], which activate the downstream Smad signal transduction pathway. The extracellular domain of the type II receptor binds the ligand, causing formation of heteromeric complexes incorporating type I and type II receptors. The type II receptor then transphosphorylates the type I receptor, activating its kinase and initiating downstream signaling. The type II receptor transmits the

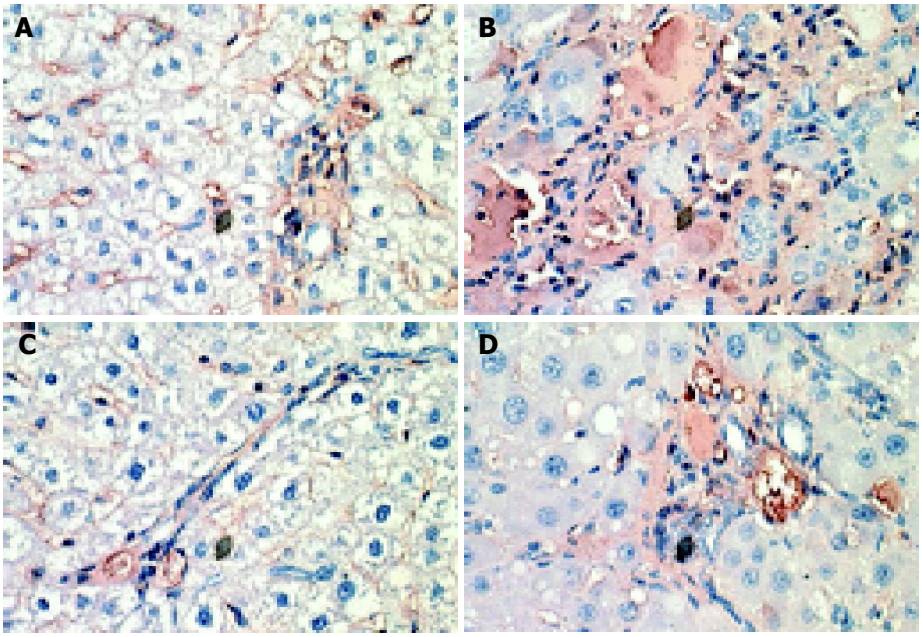

Figure 3 Immunohistochemical staining for TGF-β1 in liver sections. ×400 for **A**, **B**, **C** and **D**. (**A**) TGF-β1 immunoreactivity was evenly distributed within the interstitial tissue and liver sinusoidal in the normal group; (**B**) Stout connective tissue septa were strongly immunoreactive for TGF-β1 in the model group; (**C**) The staining intensity was much weaker in JinSanE group I than that in the model group; and (**D**) The staining positivity in JinSanE group II was stronger than that in the JinSanE group II, but still less than that in the model group.

signal from all isoforms of TGF-β, and it appears to be essential for the biological activity of TGF-β *in vivo*. Thus, its blockade could result in multiple effects[27-32]. Our results indicated that rats treated with JinSanE have reduced expression of TGF-β, TRII mRNA and TGF-β1 protein. This effect may provide an advantage to liver to escape the promoting fibrosis growth signals of TGF-β1, and may be linked to critical steps in the progression of wound repair in liver.

The Smad signaling pathway is critical for TGF-β superfamily signals from the cell surface to the nucleus[33]. Smad proteins are essential components of the intracellular signaling pathways utilized by members of the superfamily. Smad proteins are classified according to their structure and function in signaling by TGF-β family members: the receptor-regulated Smad2 and Smad3 (R-Smads); the common-mediator Smad4 (co-Smads), and the antagonistic or inhibitory Smad6 and Smad7 (I-Smads, part of a negative

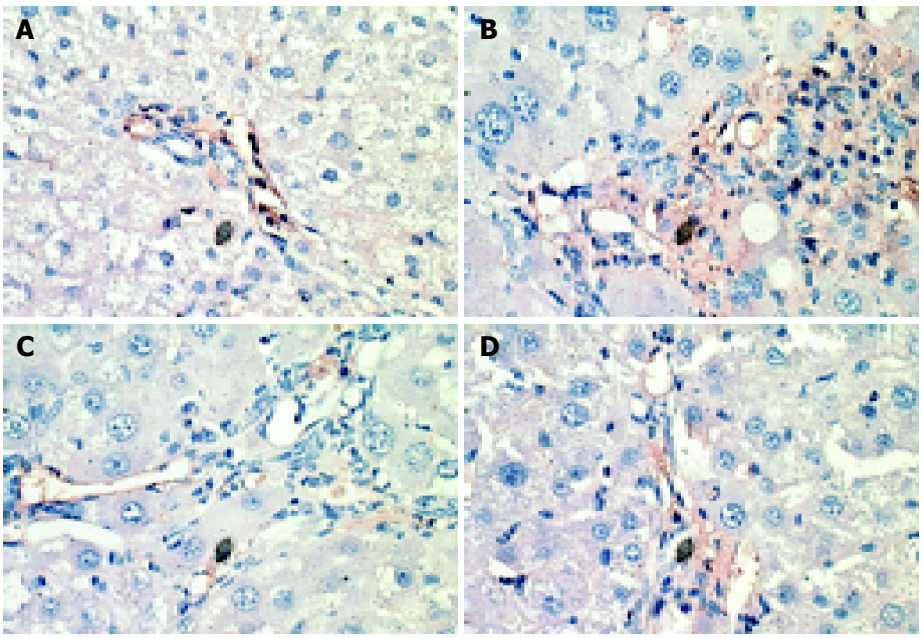

Figure 4 Immunohistochemical staining for Smad3 in liver sections. ×400 for **A**, **B**, **C** and **D**. (**A**) Several cells were positive for Smad3 in the normal group; (**B**) As TGF-β1, similarly increased Smad3 immunoreactivity was detected in the model group, but the staining degree was weak; (**C**) The expression was decreased in JinSanE group I, compared with the model group; and (**D**) Although the staining pattern for Smad3 in JinSanE group II was comparable with that observed for TGF-β1, the staining intensity was much weaker.

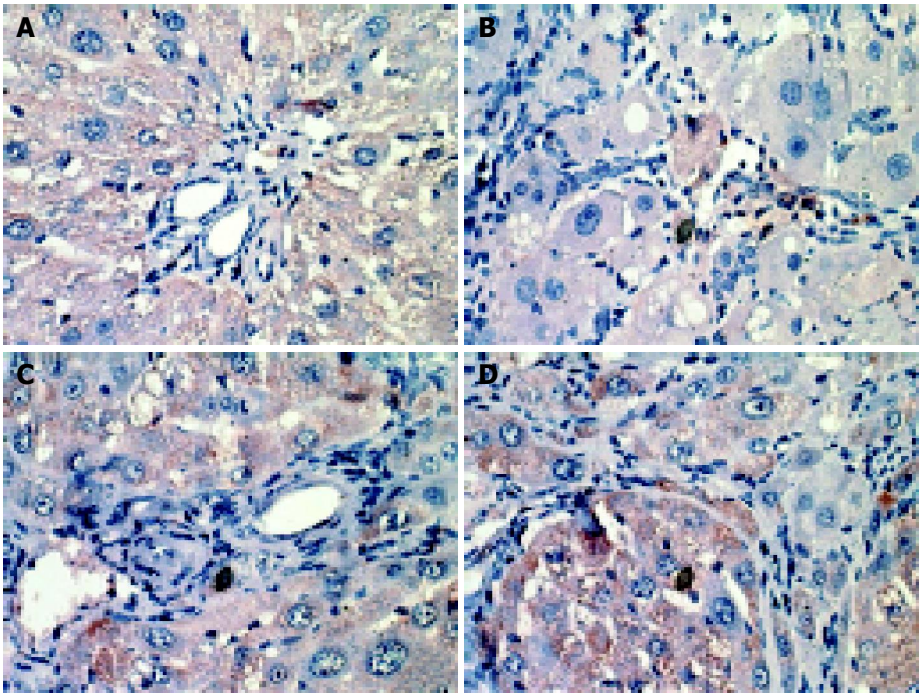

Figure 5 Immunohistochemical staining for Smad7 in liver sections. ×400 for **A**, **B**, **C** and **D**. (**A**) Normal liver displayed ubiquitous and strong staining for Smad7 in hepatocytes; (**B**) Weak staining of Smad7 was observed in the model group, which was in contrast to the abundant expression of TGF-β1 and Smad3 in liver of the group; (**C**) The staining intensity in JinSanE group I was much stronger than that in the model group, and the slender connective tissue septa were strongly immunoreactive; and (**D**) Strong staining for the Smad7 in JinSanE group II was observed.

feedback loop)[34,35]. In quiescent HSCs, TGF-β signaling involves TGF-β type I receptor (TRI)-mediated phosphorylation of serine residues within the conserved SSXS motif at the C-terminus of Smad2 and Smad3, specific R-Smads[9]. Phosphorylation of the R-Smads causes dissociation from the receptor, and induces assembly into complexes with Smad4, a co-Smad. This heteromeric complex then translocates into the nucleus, where the Smads function as transcriptional co-modulators by recruiting co-activators or co-repressors to Smad DNA binding partners[9,19,36]. Thus, Smads transmit signals directly from the receptor kinase into the nucleus, and such a complex accumulates in the nucleus, Smads regulate transcriptional responses by recruiting co-activators and co-repressors to a wide array of DNA-binding partners[37]. In addition, Smad3 phosphorylation mediated by the activated TRI is impaired severely in MFBs during chronic liver injury. Smad3 phosphorylation promotes ECM production in MFBs both *in vitro* and *in vivo*[38]. On the other hand, Smad6 and Smad7 antagonize TGF-β-induced activation of signal-transducing Smads (2 and 3) by preventing the activation of signal-transducing Smad complexes, and participating in a negative feedback loop to control TGF-β responses[19,39-41]. Smad7 interacts stably with activated TRI, thereby preventing R-Smads from binding to and being phosphorylated by these receptors, inhibits the nuclear accumulation of Smad2, and blocks the association, phosphorylation, and activation of Smad2[42,43]. Abnormal expression of anti-sense Smad7 RNA has been found to advance the effect of TGF-β1, supporting the role of Smad7 as a negative regulator in TGF-β signaling[44], thus, ectopic expression of Smad7 in HSCs leads to inhibition of R-Smads and Smad4 phosphorylation and abrogates TGF-β response[45,46]. Smad7 may function as a general inhibitor of TGF-β family signaling, and Smad6 preferentially antagonizes the bone morphogenic protein signaling pathway[47]. In our study, both level and extent of expressions of TGF-β1-inducible Smad7 were remarkably attenuated, whereas Smad3 expression was up-regulated in model fibrotic rats, indicating that Smad7 is a potent *in vivo* inhibitor for signal transduction of the TGF-β superfamily during the development and maintenance of homeostasis of liver tissues. We also observed down-regulation of Smad3 expression and up-regulation of Smad7 expression in JinSanE-treated fibrotic rats, suggesting that JinSanE regulates the balance between Smads3 and Smad7, and thus may decrease activation of an autocrine TGF-β loop that contributes to the HSC change into fibroblasts in hepatic fibrosis.

The advantage of Chinese herbal medicine in treating chronic hepatic diseases has been demonstrated by the results of experimental and clinical studies[2,15,48-50]. Chinese herbal medicine has become of interest to more and more practitioners of western medicine. Fibrosis in the Disse's space may block the exchange of molecules between the sinusoidal space and the hepatocytes[51]. The diminished fibrosis may have led to an attenuation of the hepatic "injury" at a later stage in the disease process, and thus, to a lessening of the liver dysfunction[52]. Our study indicated that traditional Chinese compound decoction, JinSanE, inhibited hepatic fibrosis, which was accompanied by a reduction of liver dysfunction, reduced the serum ALT and AST elevation, and raised the serum levels of ALB and ALB/GLB in rats exposed to CCl_4. Anti-fibrotic therapy with JinSanE is preferentially targeted to the activated mesenchymal cells in the liver that synthesize an excess of

matrix proteins, and resemble the MFBs of healing wounds. Compared with the model rats, there were only slender connective tissue septa and smaller fibrous areas and septum in the livers of rats treated with JinSanE, and the discrimination of liver necroinflammatory scores and fibrosis scores between the rats treated and untreated with JinSanE also demonstrated that JinSanE was effective in protecting against injury. This antifibrotic effect was related to early and long-term use of JinSanE, as confirmed with hepatic histology in our study.

In conclusion, our results demonstrate that TGF-β plays a critical role in the progression of hepatic fibrosis, since TGF-β1, TRII and Smad3 were up-regulated in a rat model of hepatic fibrosis, and the increase in mRNA expression of TGF- β1 and TRII correlated with histological progression to fibrosis. Our study suggests that traditional Chinese compound decoction, JinSanE, should be therapeutic in already-established fibrotic livers *in vivo*. Moreover, our findings demonstrate that the mechanism of antifibrogenic activity of JinSanE is associated with the regulation of ECM proteins, including TGF-β, TRII and Smad expression. The traditional Chinese compound decoction, JinSanE, could inhibit collagen proliferation and facilitate hepatocyte regeneration. Long-term studies in animal models and cells are the next step to establish its safety and clinical potentials.

REFERENCES

1 **Bedossa P,** Paradis V. Liver extracellular matrix in health and disease. *J Pathol* 2003; **200**: 504-515
2 **Shimizu I,** Ma YR, Mizobuchi Y, Liu F, Miura T, Nakai Y, Yasuda M, Shiba M, Horie T, Amagaya S, Kawada N, Hori H, Ito S. Effects of Sho-saiko-to, a Japanese herbal medicine, on hepatic fibrosis in rats. *Hepatology* 1999; **29**: 149-160
3 **Liu C,** Gaca MD, Swenson ES, Vellucci VF, Reiss M, Wells RG. Smads 2 and 3 are differentially activated by transforming growth factor-beta (TGF-beta) in quiescent and activated hepatic stellate cells. Constitutive nuclear localization of Smads in activated cells is TGF-beta-independent. *J Biol Chem* 2003; **278**: 11721-11728
4 **Bissell DM,** Roulot D, George J. Transforming growth factor beta and the liver. *Hepatology* 2001; **34**: 859-867
5 **Galli A,** Crabb DW, Ceni E, Salzano R, Mello T, Svegliati-Baroni G, Ridolfi F, Trozzi L, Surrenti C, Casini A. Antidiabetic thiazolidinediones inhibit collagen synthesis and hepatic stellate cell activation *in vivo* and *in vitro*. *Gastroenterology* 2002; **122**: 1924-1940
6 **Gressner AM,** Weiskirchen R, Breitkopf K, Dooley S. Roles of TGF-beta in hepatic fibrosis. *Front Biosci* 2002; **7**: d793-d807
7 **Tahashi Y,** Matsuzaki K, Date M, Yoshida K, Furukawa F, Sugano Y, Matsushita M, Himeno Y, Inagaki Y, Inoue K. Differential regulation of TGF-beta signal in hepatic stellate cells between acute and chronic rat liver injury. *Hepatology* 2002; **35**: 49-61
8 **Mehra A,** Wrana JL. TGF-beta and the Smad signal transduction pathway. *Biochem Cell Biol* 2002; **80**: 605-622
9 **Wrana JL.** Phosphoserine-dependent regulation of protein-protein interactions in the Smad pathway. *Structure* 2002; **10**: 5-7
10 **Massaguè J.** TGF-beta signal transduction. *Annu Rev Biochem* 1998; **67**: 753-791
11 **Yoshiji H,** Kuriyama S, Yoshii J, Ikenaka Y, Noguchi R, Nakatani T, Tsujinoue H, Fukui H. Angiotensin-II type 1 receptor interaction is a major regulator for liver fibrosis development in rats. *Hepatology* 2001; **34**: 745-750
12 **Dooley S,** Hamzavi J, Breitkopf K, Wiercinska E, Said HM, Lorenzen J, Ten Dijke P, Gressner AM. Smad7 prevents activation of hepatic stellate cells and liver fibrosis in rats. *Gastroenterology* 2003; **125**: 178-191
13 **Zhang M,** Song G, Minuk GY. Effects of hepatic stimulator substance, herbal medicine, selenium/vitamin E, and ciprofloxacin on cirrhosis in the rat. *Gastroenterology* 1996; **110**: 1150-1155
14 **Li J,** Yuan S, Zhao J. Study on the regulatory effect of Chinese herbal medicine on peritoneal lymphatic stomata and in enhancing drainage of ascites in mice with liver fibrosis. *Zhongguo Zhongxiyi Jiehe Zazhi* 2000; **20**: 753-756
15 **Kusunose M,** Qiu B, Cui T, Hamada A, Yoshioka S, Ono M, Miyamura M, Kyotani S, Nishioka Y. Effect of Sho-saiko-to extract on hepatic inflammation and fibrosis in dimethylnitrosamine induced liver injury rats. *Biol Pharm Bull* 2002; **25**: 1417-1421
16 **Li JC,** Ding SP, Xu J. Regulating effect of Chinese herbal medicine on the peritoneal lymphatic stomata in enhancing ascites absorption of experimental hepatofibrotic mice. *World J Gastroenterol* 2002; **8**: 333-337
17 **Okuno M,** Akita K, Moriwaki H, Kawada N, Ikeda K, Kaneda K, Suzuki Y, Kojima S. Prevention of rat hepatic fibrosis by the protease inhibitor, camostat mesilate, via reduced generation of active TGF-beta. *Gastroenterology* 2001; **120**: 1784-1800
18 Hepatic Fibrosis Study Group of Chinese Liver Diseases Association. Consensus on evaluation of the diagnosis and efficacy of hepatic fibrosis. *Chin J Infect Dis* 2002; **10**: 327-328
19 **Tahashi Y,** Matsuzaki K, Date M, Yoshida K, Furukawa F, Sugano Y, Matsushita M, Himeno Y, Inagaki Y, Inoue K. Differential regulation of TGF-beta signal in hepatic stellate cells between acute and chronic rat liver injury. *Hepatology* 2002; **35**: 49-61
20 **Napoli J,** Prentice D, Niinami C, Bishop GA, Desmond P, McCaughan GW. Sequential increases in the intrahepatic expression of epidermal growth factor, basic fibroblast growth factor, and transforming growth factor beta in a bile duct ligated rat model of cirrhosis. *Hepatology 1997*; **26**: 624-633
21 **Le Pabic H,** Bonnier D, Wewer UM, Coutand A, Musso O, Baffet G, Clement B, Theret N. ADAM12 in human liver cancers: TGF-beta-regulated expression in stellate cells is associated with matrix remodeling. *Hepatology* 2003; **37**: 1056-1066
22 **Cui X,** Shimizu I, Lu G, Itonaga M, Inoue H, Shono M, Tamaki K, Fukuno H, Ueno H, Ito S. Inhibitory effect of a soluble transforming growth factor beta type II receptor on the activation of rat hepatic stellate cells in primary culture. *J Hepatol* 2003; **39**: 731-737
23 **Gaca MD,** Zhou X, Issa R, Kiriella K, Iredale JP, Benyon RC. Basement membrane-like matrix inhibits proliferation and collagen synthesis by activated rat hepatic stellate cells: evidence for matrix-dependent deactivation of stellate cells. *Matrix Biol* 2003; **22**: 229-239
24 **Tsunawaki S,** Sporn M, Ding A, Nathan C. Deactivation of macrophages by transforming growth factor-beta. *Nature* 1988; **334**: 260-262
25 **Balza E,** Borsi L, Allemanni G, Zardi L. Transforming growth factor beta regulates the levels of different fibronectin isoforms in normal human cultured fibroblasts. *FEBS Lett* 1988; **228**: 42-44
26 **Roulot D,** Sevcsik AM, Coste T, Strosberg AD, Marullo S. Role of transforming growth factor beta type II receptor in hepatic fibrosis: studies of human chronic hepatitis C and experimental fibrosis in rats. *Hepatology* 1999; **29**: 1730-1738
27 **Tahashi Y,** Matsuzaki K, Date M, Yoshida K, Furukawa F, Sugano Y, Matsushita M, Himeno Y, Inagaki Y, Inoue K. Differential regulation of TGF-beta signal in hepatic stellate cells between acute and chronic rat liver injury. *Hepatology* 2002; **35**: 49-61
28 **Yata Y,** Gotwals P, Koteliansky V, Rockey DC. Dose-dependent inhibition of hepatic fibrosis in mice by a TGF-beta soluble receptor: implications for antifibrotic therapy. *Hepatology* 2002; **35**: 1022-1030
29 **Wrana JL,** Attisano L, Carcamo J, Zentella A, Doody J, Laiho M, Wang XF, Massague J. TGF beta signals through a

heteromeric protein kinase receptor complex. *Cell* 1992; **71**: 1003-1014

30 **Inagaki M,** Moustakas A, Lin HY, Lodish HF, Carr BI. Growth inhibition by transforming growth factor beta (TGF-beta) type I is restored in TGF-beta-resistant hepatoma cells after expression of TGF-beta receptor type II cDNA. *Proc Natl Acad Sci USA* 1993; **90**: 5359-5363

31 **Bhushan A,** Lin HY, Lodish HF, Kintner CR. The transforming growth factor beta type II receptor can replace the activin type II receptor in inducing mesoderm. *Mol Cell Biol* 1994; **14**: 4280-4285

32 **Bassing CH,** Yingling JM, Howe DJ, Wang T, He WW, Gustafson ML, Shah P, Donahoe PK, Wang XF. A transforming growth factor beta type I receptor that signals to activate gene expression. *Science* 1994; **263**: 87-89

33 **Attisano L,** Wrana JL. Signal transduction by the TGF-beta superfamily. *Science* 2002; **296**: 1646-1647

34 **Dong C,** Zhu S, Wang T, Yoon W, Li Z, Alvarez RJ, ten Dijke P, White B, Wigley FM, Goldschmidt-Clermont PJ. Deficient Smad7 expression: a putative molecular defect in scleroderma. *Proc Natl Acad Sci USA* 2002; **99**: 3908-3913

35 **Imamura T,** Takase M, Nishihara A, Oeda E, Hanai J, Kawabata M, Miyazono K. Smad6 inhibits signalling by the TGF-beta superfamily. *Nature* 1997; **389**: 622-626

36 **Carcamo J,** Weis FM, Ventura F, Wieser R, Wrana JL, Attisano L, Massague J. Type I receptors specify growth-inhibitory and transcriptional responses to transforming growth factor beta and activin. *Mol Cell Biol* 1994; **14**: 3810-3821

37 **Zhang Y,** Feng XH, Derynck R. Smad3 and Smad4 cooperate with c-Jun/c-Fos to mediate TGF-beta-induced transcription. *Nature* 1998; **394**: 909-913

38 **Furukawa F,** Matsuzaki K, Mori S, Tahashi Y, Yoshida K, Sugano Y, Yamagata H, Matsushita M, Seki T, Inagaki Y, Nishizawa M, Fujisawa J, Inoue K. p38 MAPK mediates fibrogenic signal through Smad3 phosphorylation in rat myofibroblasts. *Hepatology* 2003; **38**: 879-889

39 **Stopa M,** Benes V, Ansorge W, Gressner AM, Dooley S. Genomic locus and promoter region of rat Smad7, an important antagonist of TGFbeta signaling. *Mamm Genome* 2000; **11**: 169-176

40 **Li X,** Ionescu AM, Schwarz EM, Zhang X, Drissi H, Puzas JE, Rosier RN, Zuscik MJ, O'Keefe RJ. Smad6 is induced by BMP-2 and modulates chondrocyte differentiation. *J Orthop Res* 2003; **21**: 908-913

41 **Ishisaki A,** Yamato K, Hashimoto S, Nakao A, Tamaki K, Nonaka K, ten Dijke P, Sugino H, Nishihara T. Differential inhibition of Smad6 and Smad7 on bone morphogenetic protein- and activin-mediated growth arrest and apoptosis in B cells. *J Biol Chem* 1999; **274**: 13637-13642

42 **Hayashi H,** Abdollah S, Qiu Y, Cai J, Xu YY, Grinnell BW, Richardson MA, Topper JN, Gimbrone MA, Wrana JL, Falb D. The MAD-related protein Smad7 associates with the TGFbeta receptor and functions as an antagonist of TGFbeta signaling. *Cell* 1997; **89**: 1165-1173

43 **Souchelnytskyi S,** Nakayama T, Nakao A, Morén A, Heldin CH, Christian JL, ten Dijke P. Physical and functional interaction of murine and Xenopus Smad7 with bone morphogenetic protein receptors and transforming growth factor-beta receptors. *J Biol Chem* 1998: **273**: 25364-25370

44 **Afrakhte M,** Moren A, Jossan S, Itoh S, Sampath K, Westermark B, Heldin CH, Heldin NE, ten Dijke P. Induction of inhibitory Smad6 and Smad7 mRNA by TGF-beta family members. *Biochem Biophys Res Commun* 1998; **249**: 505-511

45 **Dooley S,** Delvoux B, Streckert M, Bonzel L, Stopa M, ten Dijke P, Gressner AM. Transforming growth factor beta signal transduction in hepatic stellate cells via Smad2/3 phosphorylation, a pathway that is abrogated during *in vitro* progression to myofibroblasts. TGFbeta signal transduction during transdifferentiation of hepatic stellate cells. *FEBS Lett* 2001; **502**: 4-10

46 **Nakao A,** Afrakhte M, Moren A, Nakayama T, Christian JL, Heuchel R, Itoh S, Kawabata M, Heldin NE, Heldin CH, ten Dijke P. Identification of Smad7, a TGFbeta-inducible antagonist of TGF-beta signalling. *Nature* 1997; **389**: 631-635

47 **Datta PK,** Moses HL. STRAP and Smad7 synergize in the inhibition of transforming growth factor beta signaling. *Mol Cell Biol* 2000; **20**: 3157-3167

48 **Yao XX,** Tang YW, Yao DM, Xiu HM. Effects of Yigan Decoction on proliferation and apoptosis of hepatic stellate cells. *World J Gastroenterol* 2002; **8**: 511-514

49 **Zhang M,** Song G, Minuk GY. Effects of hepatic stimulator substance, herbal medicine, selenium/vitamin E, and ciprofloxacin on cirrhosis in the rat. *Gastroenterology* 1996; **110**: 1150-1155

50 **Li MY,** Ryan P, Batey RG. Traditional Chinese medicine prevents inflammation in CCl_4-related liver injury in mice. *Am J Chin Med* 2003; **31**: 119-127

51 **Friedman SL.** Seminars in medicine of the Beth Israel Hospital, Boston. The cellular basis of hepatic fibrosis. Mechanisms and treatment strategies. *N Engl J Med* 1993; **328**: 1828-1835

52 **Qi Z,** Atsuchi N, Ooshima A, Takeshita A, Ueno H. Blockade of type beta transforming growth factor signaling prevents liver fibrosis and dysfunction in the rat. *Proc Natl Acad Sci USA* 1999; **96**: 2345-2349

Science Editor Ma JY **Language Editor** Elsevier HK

PO Box 2345, Beijing 100023, China
www.wjgnet.com
wjg@wjgnet.com

ELSEVIER

World J Gastroenterol 2005;11(15):2277-2282
World Journal of Gastroenterology ISSN 1007-9327

• *BASIC RESEARCH* •

Heterogeneity in predisposition of hepatic cells to be induced into pancreatic endocrine cells by PDX-1

Shun Lu, Wei-Ping Wang, Xiao-Fei Wang, Zong-Mei Zheng, Ping Chen, Kang-Tao Ma, Chun-Yan Zhou

Shun Lu, Wei-Ping Wang, Xiao-Fei Wang, Ping Chen, Kang-Tao Ma, Chun-Yan Zhou, Department of Biochemistry and Molecular Biology, School of Basic Medical Sciences, Peking University, Beijing 100083, China
Zong-Mei Zheng, Peking University Stem Cell Research Center, Beijing 100083, China
Supported by the National Natural Science Foundation of China, No. 30240087; the National High Technology Research and Development Program of China, No. 2003AA205090
Co-first-authors: Shun Lu and Wei-Ping Wang
Correspondence to: Professor Chun-Yan Zhou, Department of Biochemistry and Molecular Biology, School of Basic Medical Sciences, Peking University, 38 Xue Yuan Road, Haidian District, Beijing 100083, China. chunyanzhou@bjmu.edu.cn
Telephone: +86-10-82802417 Fax: +86-10-62015582
Received: 2004-05-12 Accepted: 2004-06-24

Abstract

AIM: The role of Pancreatic and Duodenal Homeobox-1 (PDX-1) as a major regulator of pancreatic development determines the function and phenotype of β cell. In this study, potential plasticity of liver cells into pancreatic endocrine cells induced by PDX-1 was evaluated.

METHODS: Human hepatoma cell line HepG2 was stably transfected with mammalian expression plasmid pcDNA3-PDX encoding human PDX-1 gene. Ectopic expression of PDX-1 and insulin were detected by RT-PCR, Western blot and/or immunostaining. PDX-1$^+$ HepG2 cells were transplanted under renal capsule of STZ-induced diabetic nude mice (n = 16) to examine the inducing effect *in vivo*.

RESULTS: Exogenous PDX-1 transgene was proved to express effectively in HepG2 cell at both mRNA and protein levels. The expression of endogenous insulin and some β cell-specific differentiation markers and transcription factors were not induced in PDX-1$^+$ HepG2 cells. When transplanted under renal capsule of STZ-induced diabetic nude mice, PDX-1$^+$ HepG2 cells did not generate insulin-producing cells. These data indicated that stable transfected PDX-1 could not convert hepatoma cell line HepG2 to pancreatic cells *in vitro* or *in vivo*. Mature hepatocytes might need much more complicated or rigorous conditions to be shifted to insulin-producing cells.

CONCLUSION: The expression of exogenous PDX-1 is not sufficient to induce relatively mature hepatocytes differentiating into insulin-producing cells.

Key words: PDX-1; HepG2, Insulin; Transgene; Diabetes

Lu S, Wang WP, Wang XF, Zheng ZM, Chen P, Ma KT, Zhou CY. Heterogeneity in predisposition of hepatic cells to be induced into pancreatic endocrine cells by PDX-1. *World J Gastroenterol* 2005; 11(15): 2277-2282
http://www.wjgnet.com/1007-9327/11/2277.asp

INTRODUCTION

Insulin-dependent diabetes mellitus (IDDM) is characterized by insulin deficiency due to autoimmune destruction of pancreatic β cells. Gene therapy or cell-replacement therapy might be an optimal strategy[1,2]. Recently, increasing studies focused on inducing non-β-cell derived cells into surrogate β cells that can produce and secrete insulin, by genetic modification in most cases[3-5]. In addition to several types of stem cells[6-8], the most commonly used cell type for this purpose is liver cells[9-11].

Both liver and pancreas emerge from ventral foregut endoderm and specifically at about the same time during embryonic development. Although different set of transcription factors and specialized gene profiles are expressed in liver and pancreas buds, some gene products are common to both tissues[12], including the essential factors in glucose sensing machinery, such as GLUT-2 and glucokinase.

As a regulator located upstream in the insulin gene transcription cascade, pancreatic and duodenal homeobox-1 (PDX-1) is considered as a promising candidate transgene in gene therapy for diabetes. PDX-1 was originally identified as an insulin gene transcription factor[13]. It also activates expression of other islet-enriched genes, including GLUT-2[14], glucokinase[15], islet amyloid polypeptide (IAPP)[16] and somatostatin[17]. PDX-1 knockout mice led to the loss of the whole pancreas[18]. Mice carrying PDX-1 deletion developed diabetes[19]. In humans, patient bearing a mutant PDX-1 gene resulted in agenesis of pancreas at birth[20]. Taking these together, PDX-1 appears to be a major regulator of pancreatic development and determines the function and phenotype of β cell.

Ferber *et al*[21] found that ectopic expression of PDX-1 induced expression of endogenous insulin gene in mouse liver. The same group and another, recently, further demonstrated that PDX-1, as a "master regulator" of directing cell fate, has the sufficient capacity to induce the mature liver cells into pancreatic endocrine cells *in vivo*[22,23]. However, a recent report from Horb *et al*[24] failed to convert liver cells to insulin-producing cells with the transient

expression of wild type PDX-1 alone, but it was achieved when PDX-1 gene was fused with a transcriptional activation domain VP16.

Then the intriguing questions are: if PDX-1 can convert some liver cells to pancreatic cells *in vivo*, what if it is introduced into a hepatocyte-derived or a hepatoma cell line like HepG2 *in vitro*? If transient expression of PDX-1 in HepG2 cannot lead to this kind of conversion, how is it expressed in a constitutive way? What will happen if stably transfected PDX-1$^+$HepG2 cell is further induced by *in vitro* and *in vivo* environment? In order to elucidate these questions, we established a stable PDX-1-expressing HepG2 cell line and transplanted these cells into STZ-induced diabetic nude mice. We found that insulin and other β cell enriched/specific genes were not activated in PDX-1$^+$HepG2 cell line, and no conversion evidence is observed after implantation under renal capsule either.

MATERIALS AND METHODS

Plasmid construction

Human PDX-1 gene coding sequence was amplified by PCR from Human Pancreas Quick-Clone cDNA library (Clontech, Palo Alto, CA) with forward primer 5'-CCATGAACGGCGA GGAGCAGTA and reverse primer 5'-CTGCCTCTCATCGTGGTTCCTG and cloned into pCDNA3 (Invitrogen, Carlsbad, CA), a mammalian expression vector driven by CMV promoter. The construct was designated as pCDNA3-PDX and characterized by restriction analysis and verified by sequencing.

Cell culture and preparation of stable transfectants

HepG2, a human hepatoma-derived cell line, was obtained from ATCC (Rockville, MD) and maintained in Dulbecco's Modified Eagle's Medium (DMEM), supplemented with 10% heat inactivated fetal bovine serum, 100 U/mL penicillin, 100 μg/mL streptomycin. To obtain stable transfectants, HepG2 cells were seeded in 24-well plate 24 h before transfection. A total of 0.8 μg of pCDNA3-PDX plasmid DNA was transfected into cells using lipofectamine 2000 reagent (Invitrogen, Carlsbad, CA) following the manufacturer's recommendation. Forty-eight hours after transfection, the cells were diluted and transferred to 10 cm culture plates, cultured with G418-containing medium (500 μg/mL). The selective medium was changed every 4 d. G418-resistant colonies appeared 3-4 wk after transfection. The single colonies were picked out using clone rings and then subjected to proliferate for further analysis.

RNA isolation and RT-PCR analysis

Total RNA was isolated from single clone derived cells directly from culture plate using TRIzol reagent (Invitrogen, Carlsbad, CA). RNA samples were treated by 10 units of RQ1 Rnase-free Dnase I (Promega, Madison, WI) for 15 min at 37 ℃. Reverse transcription was performed following the manufacturer's instructions (Promega, Madison, WI). Primer sequences and PCR conditions are listed in Table 1. PCR was performed using T-gradient thermocycler (Biometra, Gottingen, Germany) and the product was separated using 1.5% agarose gel and visualized with ethidium bromide. Human fetal pancreas was isolated from a 24-wk gestational age embryo from a natural aborted fetus. Permission to use human embryonic tissues was granted by the Ethics Review Board of Peking University.

Western blot analysis

Expressions of PDX-1 and insulin at protein levels in transfected cells were detected using Western blot analysis as previously

Table 1 **RT-PCR information: Primer sequences and PCR conditions**

Genes	Primer sequences (5′-3′)	Products bp	Annealing		Cycles
			℃	s	
PDX-1	F,GTCCTGGAGGAGCCCAAC	360	58	60	30
	R,GCAGTCCTGCTCAGGCTC				
Insulin	F,GCCTTTGTGAACCAACACCTG	261	62	60	30
	R,GTTGCAGTAGTTCTCCAGCTG				
GLUT-2	F,TGCCACACTCACACAAGAC	260	54	60	30
	R,AGATTGTGGGCAGTTCATC				
Glucokinase	F,CCCGAGGAGAACCACATT	208	56	60	30
	R,GGAACTCTGCCAGGATCT				
IAPP	F,GCTGACATTGAAACATTA	360	56	60	30
	R,TATACAGGAAATCACTAGAA				
Somatostatin	F,TGCGCTGTCCATCGTCCT	258	60	60	30
	R,GCCATAGCCGGGTTTGAGTT				
E47	F,TCAGGCTGGCTTCCTGTCAG	224	62	60	30
	R,CCCTGCCGTATGCCTCACCT				
NeuroD1	F,GCGTTAGCCTTCATGCGTCT	386	60	60	30
	R,GAGGCCCCAGGGTTATGAG				
Isl-1	F,CGGCTTCAGCAAGAACGACT	290	58	60	30
	R,TCTTCTCCGGCTGCTTGTG				
GAPDH	F,GTCAGTGGTGGACCTGACCT	415	55	60	30
	R,AGGGGAGATTCAGTGTGGTG				

PCR conditions: denaturation at 94 ℃ for 30 s; annealing as listed in the table; extension at 72 ℃ for 1 min.

described[25]. The protein concentrations were determined using Bradford assay. Five microgram of cellular lysate were separated by standard SDS-PAGE and then transferred to nitrocellulose membrane. Goat polyclonal anti-PDX-1 or anti-insulin antibodies (Santa Cruz Biotechnology, Santa Cruz, CA) were used to probe the blot.

Under-renal-capsule transplantation into STZ-induced diabetic nude mice

Male BALB/c nude mice at age 8-10 wk were used in this study. The animal experiment conformed to the Guide for the Care and Use of Laboratory Animals published by the US National Institute of Health (NIH Publication No. 85-23, revised 1996). Mice were fasted for 18 h and then treated with STZ (200 mg/kg body weight, i.p., Sigma, St. Louis, MO) freshly dissolved in citrate buffer (pH 4.5). The blood glucose levels were monitored daily by using a Glucotrend® glucose detector (Roche Diagnostics, Mannheim, Germany). Seven days after STZ treatment, the mice with stable hyperglycemia (blood glucose levels >20 mmol/L) were selected for operation. Under pentobarbital sodium (35 mg/kg body weight, i.p.) anesthetization, the left kidney was exposed through a lumbar incision and cells (5×10^6 to 1×10^7) resuspended in PBS were injected into subcapsular cavity by using a 100 μL micro-syringe. The blood glucose level was monitored on 0, 1, 2, 3, 5, 7, 9, 11, 13, 15, 18, 26, 30 d after transplantation. Recipient animals were killed by cervical dislocation 30 d after operation. Kidney and pancreatic tissues were removed and fixed with 10% paraformaldehyde in PBS at 4 ℃ for 5 h and embedded in OCT compound for immunohistochemical staining.

Immunocytochemistry and immunohistochemistry

Cells were cultured on non-coated glass coverslips for 24 h before immunostaining. After rinsing with PBS thrice, the cells were fixed with acetone/methanol at 4 ℃ for 15 min, permeabilized with 10 mL/L Triton X-100 in PBS for 10 min, and incubated sequentially with blocking serum, primary antibodies and TRITC or FITC conjugated secondary antibody. The primary antibodies included goat anti-insulin polyclonal IgG (1∶200 dilution, Santa Cruz), goat anti-PDX-1 polyclonal IgG (1∶100 dilution, Santa Cruz); mouse anti-human nuclei monoclonal antibody (1∶200 dilution, Chemicon, Temecula, CA). Fixed tissue sections (8 μm thick) were also stained with antibodies as mentioned above. The cells and tissue sections were examined under a fluorescence microscope (Olympus, Nagano, Japan).

Statistical analysis

Results are given as mean±SD. The one-way ANOVA was performed by SPSS software (SPSS Science, Chicago, Illinois). $P<0.05$ were considered significant.

RESULTS

Establishment of HepG2 cell line stably expressing PDX-1

To test the feasibility of HepG2 cells differentiating into pancreatic endocrine cell by ectopically expressed PDX-1 gene, HepG2 cells were transfected with pCDNA3-PDX construct and stable transfectants were isolated under G418 selection. A total of 13 individual colonies were isolated and subjected to RT-PCR and Western blot analysis. Five PDX-1 positive colonies were identified. The clone 11 was selected to amplify for further experiments according to its higher expression level of PDX-1 than other clones (data not shown).

There was no obvious difference in the appearance of PDX-1 positive HepG2 cells from their parental cells. The results of RT-PCR and Western blot indicated the expressions of PDX-1 at both mRNA and protein levels in PDX-1$^+$HepG2 cells, but not in wild type HepG2 cells (Figure 1). Although less abundant, the expression level of exogenous PDX-1 gene was comparable to that of human fetal pancreas (Figure 1A). Western blot analysis indicated a 46 ku of PDX-1 protein (Figure 1C). The immunocytochemical staining showed that PDX-1 protein was localized mainly in the nuclei of PDX-1$^+$HepG2 cells (Figure 2C). These results indicate that we established the HepG2 cells ectopically express PDX-1 gene in the nucleus as expected.

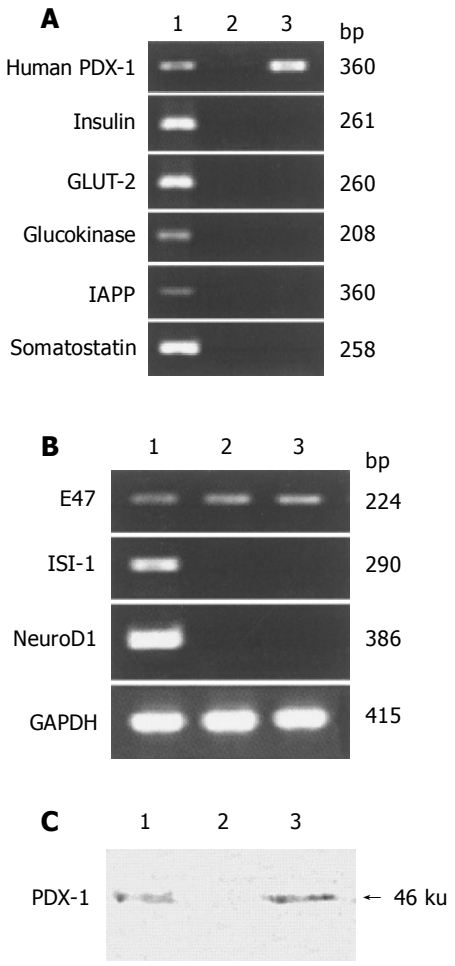

Figure 1 Expression of PDX-1 transgene and other islet-enriched genes in PDX-1$^+$HepG2 cell line. RT-PCR analysis was performed to detect the expression of several islet differentiation markers (**A**) and islet-specific transcriptional factors (**B**). GAPDH mRNA was amplified as an internal control. Western blot analysis was performed to detect the expression of PDX-1 using anti-PDX-1 antibody on total protein lysis (**C**). Lane 1: 24-wk human fetal pancreas (positive control); Lane 2: wild type HepG2 cells (negative control); Lane 3: PDX-1$^+$HepG2 cells. Data are representative of at least three independent experiments.

Examination of islet specific genes' expression in PDX-1⁺HepG2 cells

To examine the possible changes in gene expression patterns caused by exogenous PDX-1 gene in HepG2, we used RT-PCR to detect the presence of mRNA of insulin, glucokinase, GLUT-2, somatostatin and IAPP. None of these genes could be detected in both PDX-1 transfected and wild type HepG2, contrasted to distinct bands from pancreatic tissue (Figure 1A). Absence of insulin was further confirmed by immunocytochemical staining (Figure 2F) and by Western blot analysis (data not shown). To investigate the possible mechanism of silence of these islet marker genes, Isl-1 and neuroD1/beta2, upstream transactivators of insulin gene, were also detected by RT-PCR. They expressed neither in PDX-1⁺HepG2 cells nor in parental HepG2 cells (Figure 1B).

Cell transplantation under renal capsule in diabetic nude mice

Previous studies[26] showed that an *in vivo* microenvironment, such as renal subcapsule, may be advantageous to facilitate the maturation and differentiation of endocrine cells. To examine if PDX-1⁺HepG2 cells could be induced into insulin-producing cells, cell transplantation was performed. BALB/c nude mice were used to exempt implanted cells from immune attack. A total of 5×10^6-1×10^7 PDX-1⁺HepG2 cells or wild type HepG2 cells were implanted to renal subcapsular space of STZ-induced diabetic mice (n = 16 and 7, respectively). The average blood glucose level showed no significant difference between two groups, both at above 20 mmol/L (Figure 3). H&E staining and immunohistochemistry of anti-human nuclei antibody showed that the implanted cells were infiltrated into normal mice nephric tissues (Figure 2), indicating the cell viability and proliferation. The implanted cells displayed stable expression of PDX-1 transgene. No expression of insulin was observed in the kidney sections injected with PDX-1⁺HepG2 cells (Figure 2).

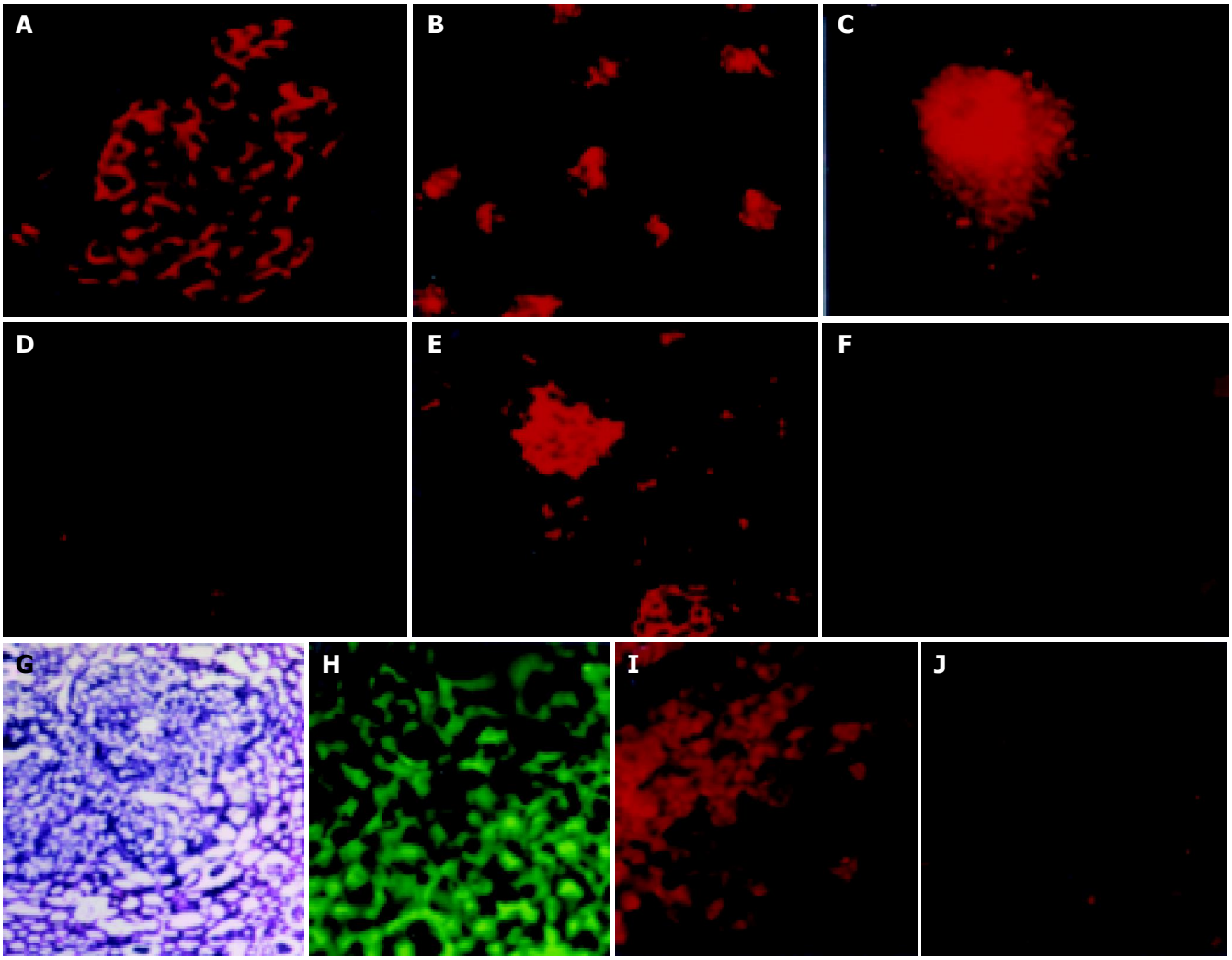

Figure 2 *In situ* immunostaining analysis of PDX-1⁺HepG2 cells in culture and after transplantation into nude mice. Representatives are shown (original magnification 200×, unless otherwise stated). Anti-PDX-1 fluorescence stains cultured PDX-1⁺HepG2 cells (**B**), compared to 24-wk human fetal pancreatic islets (**A**). The ectopically expressed PDX-1 protein locates mainly within nuclear region (**C**, 400×). Parental HepG2 cells serve as a negative control (**D**). Anti-insulin fluorescence immunostaining indicates positive staining in human islet positive control (**E**) but not in PDX-1⁺HepG2 cells (**F**). H&E staining reveals implanted PDX-1⁺HepG2 cells in section of kidney (**G**, 100×), indicating that these cells infiltrated into nephric tissues and underwent proliferation. Anti-human nuclei antibody staining confirmed that these cells were of human origin (**H**, green cells). Anti-PDX-1 staining of mice kidney sections showed consistent expression of PDX-1 transgene in these implanted PDX-1⁺HepG2 cells (**I**), but insulin expression was absent (**J**).

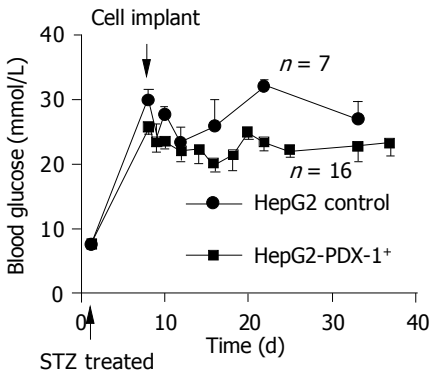

Figure 3 Blood glucose level of STZ-induced diabetic nude mice after implantation of PDX-1$^+$ HepG2 cells under renal capsule. Between 5×10^6 and 1×10^7 PDX-1$^+$HepG2 cells or parental HepG2 cells were injected into subcapsular space. Blood glucose level was measured 0, 1, 2, 3, 5, 7, 9, 11, 13, 15, 18, 26, 30 d after operation. Values are expressed as mean±SD for each time point, PDX-1$^+$HepG2 group (n = 16) *vs* HepG2 group (n = 7).

DISCUSSION

Liver cells seem to contain remarkable potential to convert into pancreatic cells. During embryogenesis, pancreas and liver arise from adjacent areas in the anterior endoderm. The default fate of ventral foregut endoderm is to become pancreas, but a FGF-like signal released from the cardiac mesoderm diverts the fate of some cells into liver[12]. This model implied that pancreas and liver, despite distinct phenotype, may share a similar context of gene expression profile but differ in just a few critical "master regulators". Under certain conditions, the interchange of pancreas and liver then could be possible. Increasing experimental models have been reported to validate this potential. Adult rat hepatic oval stem cells[27] can be induced into pancreatic endocrine hormone producing cells in high-glucose environment without genetic modification. Ferber *et al*[21] found and recently confirmed[22] that ectopic expression of PDX-1 induced mouse a pluripotent population of progenitor liver cells to produce biologically mature insulin *in vivo* and ameliorated STZ-induced diabetes. To evaluate whether PDX-1 is able to reprogram a human hepatocyte-derived cell line HepG2 into such pancreatic endocrine cells, we established a PDX-1$^+$HepG2 stable expression cell line. As expected, the expression of PDX-1 transgene in PDX-1$^+$HepG2 was comparable to that of human pancreas islet. PDX-1 protein was properly translocated into cell nuclei, as demonstrated by immunostaining and Western blot. Unexpectedly, the expressions of pancreatic β cell specific genes including insulin, glucokinase, GLUT-2 and IAPP were detected neither in transfected cells nor in mice with cell transplanted under renal capsule.

It is well established that insulin gene transcription in β cells results from the formation of a transcription complex comprising E47, NeuroD1, Isl-1, PDX-1[28], and more recently, Maf A[29]. In PDX-1$^+$HepG2 cell line, E47 was present as a ubiquitous nuclear factor, but neuroD1 and Isl-1 were absent. Kojima *et al*[30] demonstrated that only combined expressions of Isl-1 and PDX-1 could induce immature rat intestinal crypt cell line IEC-6 to produce insulin, which verified the necessity of Isl-1 in insulin transcription. Recently the same group found that without PDX-1, NeuroD1, or a combination of NeuroD1 and betacellulin gene transfer could induce insulin production in mouse liver and partly or completely reversed diabetes of STZ mice[23], indicating that NeuroD1 is another essential factor for the normal function of pancreatic β cells. The absence of Isl-1 and NeuroD1 in HepG2 cells might account for the silence of insulin and other islet specific genes in our model.

Two independent studies[22,23] confirmed that *in vivo* transfer of PDX-1 by adenovirus into mice unambiguously converted some subpopulation of hepatic cells into pancreatic endocrine and exocrine cells. We intend to specify or narrow down our subject to relatively mature hepatocytes. HepG2 cell line shows a large number of properties of differentiated hepatocytes, including expression of albumin, transferrin and transthyretin[24]. However, the data from our *in vitro* and *ex vivo* models ruled out the possibility of PDX-1-mediated conversion from mature hepatocytes to pancreatic tissues.

There are many different subpopulations of liver stem cells, which stand at various stages of developmental process and express more or less different profiles of transcription factors. We believe that this diversity endows every subpopulation different potential of reacting to stimulus, such as PDX-1 gene transfer, inducing developmental shift to pancreas. Our results proved the stubbornness of mature hepatocytes to PDX-1 induction. Kojima *et al*[23] showed that there were definitely some classes of liver cells that could be converted by PDX-1 transfer and diverse plasticity of these cells were observed under the same manipulation. Combining all these data with ours, we propose that more than one type of subpopulations comprising liver may have the potential to incur liver to pancreas conversion, but they require thresholds fundamentally different from each other to initiate this process. Mature hepatocytes, under this consideration, may also be possible to shift to insulin-producing cells under certain but much more complicated or rigorous conditions, which further needs to be defined.

REFERENCES

1 **Ramiya VK**, Maraist M, Arfors KE, Schatz DA, Peck AB, Cornelius JG. Reversal of insulin-dependent diabetes using islets generated *in vitro* from pancreatic stem cells. *Nat Med* 2000; **6**: 278-282

2 **Bonner-Weir S**, Taneja M, Weir GC, Tatarkiewicz K, Song KH, Sharma A, O'Neil JJ. *In vitro* cultivation of human islets from expanded ductal tissue. *Proc Natl Acad Sci USA* 2000; **97**: 7999-8004

3 **Ianus A**, Holz GG, Theise ND, Hussain MA. *In vivo* derivation of glucose-competent pancreatic endocrine cells from bone marrow without evidence of cell fusion. *J Clin Invest* 2003; **111**: 843-850

4 **Qin XY**, Shen KT, Zhang X, Cheng ZH, Xu XR, Han ZG. Establishment of an artificial beta-cell line expressing insulin under the control of doxycycline. *World J Gastroenterol* 2002; **8**: 367-370

5 **Soria B**, Roche E, Berna G, Leon-Quinto T, Reig JA, Martin F. Insulin-secreting cells derived from embryonic stem cells normalize glycemia in streptozotocin-induced diabetic mice. *Diabetes* 2000; **49**: 157-162

6 **Kahan BW**, Jacobson LM, Hullett DA, Ochoada JM, Oberley TD, Lang KM, Odorico JS. Pancreatic precursors and differ-

entiated islet cell types from murine embryonic stem cells: an *in vitro* model to study islet differentiation. *Diabetes* 2003; **52**: 2016-2024

7 **Efrat S**. Generation of insulin-producing cells from stem cells for cell replacement therapy of type 1 diabetes. *Isr Med Assoc J* 2004; **6**: 265-267

8 **Zorina TD**, Subbotin VM, Bertera S, Alexander AM, Haluszczak C, Gambrell B, Bottino R, Styche AJ, Trucco M. Recovery of the endogenous beta cell function in the NOD model of autoimmune diabetes. *Stem Cells* 2003; **21**: 377-388

9 **Tuch BE**, Szymanska B, Yao M, Tabiin MT, Gross DJ, Holman S, Swan MA, Humphrey RK, Marshall GM, Simpson AM. Function of a genetically modified human liver cell line that stores, processes and secretes insulin. *Gene Ther* 2003; **10**: 490-503

10 **Burkhardt BR**, Loiler SA, Anderson JA, Kilberg MS, Crawford JM, Flotte TR, Goudy KS, Ellis TM, Atkinson M. Glucose-responsive expression of the human insulin promoter in HepG2 human hepatoma cells. *Ann N Y Acad Sci* 2003; **1005**: 237-241

11 **Thule PM**, Liu JM. Regulated hepatic insulin gene therapy of STZ-diabetic rats. *Gene Ther* 2000; **7**: 1744-1752

12 **Deutsch G**, Jung J, Zheng M, Lora J, Zaret KS. A bipotential precursor population for pancreas and liver within the embryonic endoderm. *Development* 2001; **128**: 871-881

13 **Ohlsson H**, Karlsson K, Edlund T. IPF1, a homeodomain-containing transactivator of the insulin gene. *EMBO J* 1993; **12**: 4251-4259

14 **Waeber G**, Thompson N, Nicod P, Bonny C. Transcriptional activation of the GLUT2 gene by the IPF-1/STF-1/IDX-1 homeobox factor. *Mol Endocrinol* 1996; **10**: 1327-1334

15 **Watada H**, Kajimoto Y, Umayahara Y, Matsuoka T, Kaneto H, Fujitani Y, Kamada T, Kawamori R, Yamasaki Y. The human glucokinase gene beta-cell-type promoter: an essential role of insulin promoter factor 1/PDX-1 in its activation in HIT-T15 cells. *Diabetes* 1996; **45**: 1478-1488

16 **Carty MD**, Lillquist JS, Peshavaria M, Stein R, Soeller WC. Identification of cis- and trans-active factors regulating human islet amyloid polypeptide gene expression in pancreatic beta-cells. *J Biol Chem* 1997; **272**: 11986-11993

17 **Leonard J**, Peers B, Johnson T, Ferreri K, Lee S, Montminy MR. Characterization of somatostatin transactivating factor-1, a novel homeobox factor that stimulates somatostatin expression in pancreatic islet cells. *Mol Endocrinol* 1993; **7**: 1275-1283

18 **Jonsson J**, Carlsson L, Edlund T, Edlund H. Insulin-promoter-factor 1 is required for pancreas development in mice. *Nature* 1994; **371**: 606-609

19 **Ahlgren U**, Jonsson J, Jonsson L, Simu K, Edlund H. beta-cell-specific inactivation of the mouse Ipf1/Pdx1 gene results in loss of the beta-cell phenotype and maturity onset diabetes. *Genes Dev* 1998; **12**: 1763-1768

20 **Stoffers DA**, Zinkin NT, Stanojevic V, Clarke WL, Habener JF. Pancreatic agenesis attributable to a single nucleotide deletion in the human IPF1 gene coding sequence. *Nat Genet* 1997; **15**: 106-110

21 **Ferber S**, Halkin A, Cohen H, Ber I, Einav Y, Goldberg I, Barshack I, Seijffers R, Kopolovic J, Kaiser N, Karasik A. Pancreatic and duodenal homeobox gene 1 induces expression of insulin genes in liver and ameliorates streptozotocin-induced hyperglycemia. *Nat Med* 2000; **6**: 568-572

22 **Ber I**, Shternhall K, Perl S, Ohanuna Z, Goldberg I, Barshack I, Benvenisti-Zarum L, Meivar-Levy I, Ferber S. Functional, persistent, and extended liver to pancreas transdifferentiation. *J Biol Chem* 2003; **278**: 31950-31957

23 **Kojima H**, Fujimiya M, Matsumura K, Younan P, Imaeda H, Maeda M, Chan L. NeuroD-betacellulin gene therapy induces islet neogenesis in the liver and reverses diabetes in mice. *Nat Med* 2003; **9**: 596-603

24 **Horb ME**, Shen CN, Tosh D, Slack JM. Experimental conversion of liver to pancreas. *Curr Biol* 2003; **13**: 105-115

25 **Watada H**, Kajimoto Y, Miyagawa J, Hanafusa T, Hamaguchi K, Matsuoka T, Yamamoto K, Matsuzawa Y, Kawamori R, Yamasaki Y. PDX-1 induces insulin and glucokinase gene expressions in alphaTC1 clone 6 cells in the presence of betacellulin. *Diabetes* 1996; **45**: 1826-1831

26 **Gittes GK**, Galante PE, Hanahan D, Rutter WJ, Debase HT. Lineage-specific morphogenesis in the developing pancreas: role of mesenchymal factors. *Development* 1996; **122**: 439-447

27 **Yang L**, Li S, Hatch H, Ahrens K, Cornelius JG, Petersen BE, Peck AB. *In vitro* trans-differentiation of adult hepatic stem cells into pancreatic endocrine hormone-producing cells. *Proc Natl Acad Sci USA* 2002; **99**: 8078-8083

28 **Ohneda K**, Ee H, German M. Regulation of insulin gene transcription. *Semin Cell Dev Biol* 2000; **11**: 227-233

29 **Matsuoka TA**, Zhao L, Artner I, Jarrett HW, Friedman D, Means A, Stein R. Members of the large Maf transcription family regulate insulin gene transcription in islet beta cells. *Mol Cell Biol* 2003; **23**: 6049-6062

30 **Kojima H**, Nakamura T, Fujita Y, Kishi A, Fujimiya M, Yamada S, Kudo M, Nishio Y, Maegawa H, Haneda M, Yasuda H, Kojima I, Seno M, Wong NC, Kikkawa R, Kashiwagi A. Combined expression of pancreatic duodenal homeobox 1 and islet factor 1 induces immature enterocytes to produce insulin. *Diabetes* 2002; **51**: 1398-1408

Science Editor Kumar M and Guo SY **Language Editor** Elsevier HK

PO Box 2345, Beijing 100023, China
www.wjgnet.com
wjg@wjgnet.com

ELSEVIER

World J Gastroenterol 2005;11(15):2283-2290
World Journal of Gastroenterology ISSN 1007-9327

• *BASIC RESEARCH* •

Differential gene expression during capillary morphogenesis in a microcarrier-based three-dimensional *in vitro* model of angiogenesis with focus on chemokines and chemokine receptors

Xi-Tai Sun, Min-Yue Zhang, Chang Shu, Qiang Li, Xiao-Gui Yan, Ni Cheng, Yu-Dong Qiu, Yi-Tao Ding

Xi-Tai Sun, Yi-Tao Ding, Qiang Li, Xiao-Gui Yan, Yu-Dong Qiu, Department of Hepatobiliary Surgery, Affiliated Drum Tower Hospital of Medical College, Hepatobiliary Research Institute, Nanjing University, Nanjing 210008, Jiangsu Province, China
Chang Shu, Ni Cheng, State Key Laboratory of Pharmaceutical Biotechnology, Department of Biochemistry, Nanjing University, Nanjing 210009, Jiangsu Province, China
Min-Yue Zhang, State Key Laboratory of Pharmaceutical Biotechnology, Model Animal Research Center, Department of Biochemistry, Nanjing University, Nanjing 210009, Jiangsu Province, China
Correspondence to: Dr. Yi-Tao Ding, Department of Hepatobiliary Surgery, Affiliated Drum Tower Hospital of Medical College, Hepatobiliary Research Institute, Nanjing University, Nanjing 210008, Jiangsu Province, China. dingyitao@yahoo.com
Telephone: +86-25-83308769 Fax: +86-25-83317016
Received: 2004-03-13 Accepted: 2004-04-13

Abstract

AIM: To globally compare the gene expression profiles during the capillary morphogenesis of human microvascular endothelial cells (HMVECs) in an *in vitro* angiogenesis system with affymetrix oligonucleotide array.

METHODS: A microcarrier-based *in vitro* angiogenesis system was developed, in which ECs migrated into the matrix, proliferated, and formed capillary sprouts. The sprouts elongated, branched and formed networks. The total RNA samples from the HMVECs at the selected time points (0.5, 24, and 72 h) during the capillary morphogenesis were used for microarray analyses, and the data were processed with the softwares provided by the manufacturers. The expression patterns of some genes were validated and confirmed by semi-quantitative RT-PCR. The regulated genes were grouped based on their molecular functions and expression patterns, and among them the expression of chemokines and chemokine receptors was specially examined and their functional implications were analyzed.

RESULTS: A total of 1 961 genes were up- or downregulated two-folds or above, and among them, 468 genes were up- or down-regulated three-folds or above. The regulated genes could be grouped into categories based on their molecular functions, and were also clustered into six groups based on their patterns of expression. As for chemokines and chemokine receptors, CXCL1/GRO-α, CXCL2/GRO-β, CXCL5/ENA-78, CXCL6/GCP2, IL-8/CXCL8, CXCL12/SDF-1, CXCL9/Mig, CXC11/ITAC, CX3CL1/fractalkine, CCL2/MCP-1, CCL3, CCL5/RANTES, CCL7, CCL15, CCL21, CCL23, CCL28, and CCR1, CCR9, CXCR4 were identified. Moreover, these genes demonstrated different changing patterns during the capillary morphogenesis, which implied that they might have different roles in the sequential process. Among the chemokines identified, CCL2/MCP-1, CCL5/RANTES and CX3CL1 were specially up-regulated at the 24-h time point when the sprouting characterized the morphological change. It was thus suggested that they might exert crucial roles at the early stage of angiogenesis.

CONCLUSION: The present study demonstrates a global profile of gene expression during endothelial capillary morphogenesis, and the results provide us much information about the molecular mechanisms of angiogenesis, with which further evaluation of individual genes can be conducted.

Key words: Angiogenesis; *In vitro* model; Endothelial cell; Oligonucleotide array

Sun XT, Zhang MY, Shu C, Li Q, Yan XG, Cheng N, Qiu YD, Ding YT. Differential gene expression during capillary morphogenesis in a microcarrier-based three-dimensional *in vitro* model of angiogenesis with focus on chemokines and chemokine receptors. *World J Gastroenterol* 2005; 11(15): 2283-2290
http://www.wjgnet.com/1007-9327/11/2283.asp

INTRODUCTION

Angiogenesis, the formation of new capillaries from pre-existing blood vessels, plays a crucial role in a wide range of normal and pathologic processes, and is necessary for the continuous growth and invasion of solid tumors. After initial activation by angiogenic mediators such as vascular endothelial growth factor (VEGF) and basic fibroblast growth factor (bFGF), endothelial cells (ECs) degrade the local basement membrane, migrate into the underlying stroma, proliferate, and form capillary sprouts. It is believed that opposing sprouts coalesce and form a new capillary loop[1]. It has become increasingly clear that the angiogenesis is regulated by a balance of pro-and anti-angiogenic forces[2,3], and is a complex sequential process that relies on a controlled cross-talk between ECs and the surrounding environment. In normal adult tissues, anti-angiogenic mediators are dominant and ECs are suppressed and quiescent. During angiog-

enesis, the release of molecules, such as VEGF, overwhelms the inhibitors and ECs undergo the morphological steps necessary to generate a new capillary loop.

The molecular mechanisms underlying these morphological changes are, in large part, unknown. However, the advent of the global analytic techniques of gene expression, such as microarray, differential display, subtraction cDNA cloning and serial analysis of gene expression, has enabled the identification of the crucial angiogenic genes whose expression is regulated under different angiogenic conditions. Using this latter technology, St. Croix *et al*[4], compared the patterns of gene expression in ECs derived from the blood vessels of normal and malignant colorectal tissues. Bell *et al*[5], identified differential gene expressions during capillary morphogenesis in 3-D collagen matrices.

In order to determine the mechanisms controlling the sequential process of angiogenesis, appropriate models are necessary. *In vitro* model represents a rapid, defined and efficient experimental strategy to elucidate the molecular events required for the morphogenesis. Since 2-D angiogenesis models lack the third dimension and obviously do not reflect all physiological steps, the 3-D models are increasingly used for this purpose, because they consider more steps of angiogenesis[6]. In fact, a variety of 3-D angiogenesis models have provided great advances in the understanding of angiogenesis and the investigation of angiogenic and anti-angiogenic factors.

In 3-D angiogenesis models, the ECs are usually reorganized in the following ways: directly overlaid by gels, sandwiched between two gel layers, seeded dispersedly or clustered as spheroids in gels, or attached onto microcarrier (MC) beads. Recently, we have also established an *in vitro* angiogenesis system, which was based on MC, human dermal microvascular endothelial cells (HMVECs) and fibrin matrix[7]. With this system, we have observed all of the angiogenic steps that characterize the *in vivo* angiogenesis, including sprouting, branching, and capillary network formation[7]. The aim of the present study was to identify the gene expression profiles of HMVECs during capillary morphogenesis under stimulation of bFGF in the MC-based *in vitro* angiogenesis system.

MATERIALS AND METHODS

Materials

Dulbecco's modified Eagle's medium (DMEM) was from Gibco Laboratories. Endothelial basal medium (EBM), epidermal growth factor (EGF), bovine brain extract (BBE), hydrocortisone, penicillin and streptomycin were from Clonetics (San Diego, CA). BFGF was from PeproTech EC Ltd (Rocky Hill, NJ). CD31-dynabeads were purchased from Dynal A.S (Oslo, Norway). Immuno-staining kit for factor VIII-related antigens was from Zhongshan Biotechnology Co., Ltd (Beijing, China). Cytodex-3 MCs were purchased from Amersham Pharmacia Biotech (Piscataway, NJ). Fibrinogen was from Raas Blood Product Co., Ltd (Shanghai, China).

Cells isolation and culture

HMVECs were isolated from juvenile foreskin as described[8,9]. Briefly, the foreskin was cut into small pieces, washed with PBS and incubated with 15-20 mL of 0.2% dispase in DMEM overnight (18-24 h) at 4 ℃. The tissue pieces were transferred into fresh DMEM and scratched with a scalpel. The resulting cell suspension was centrifuged and re-suspended in 10-15 mL of EGM, containing EBM supplemented with 10 ng/mL EGF, 12 μg/mL BBE, 1.0 μg/mL hydrocortisone, 100 U/mL penicillin, and 100 mg/mL streptomycin in the presence of 150 mL/L normal human serum, and seeded into a gelatin-coated 75-cm^2 tissue culture flask. Culture medium was changed every 2-3 d. Before the culture reached confluence (normally 5-7 d upon seeding), the HMVECs were separated from the other cells in culture by immuno-magnetic isolation with CD31-dynabeads following the manufacturer's instructions. ECs were characterized and determined to be>99% purity on the basis of the formation of typical cobblestone monolayer in culture and positive immunostaining for factor VIII-related antigens. The purified HMVECs were cultured in EGM at 37 ℃ in a humidified atmosphere containing 50 mL/L CO_2 in air on gelatin-coated cell culture surfaces. All assays were conducted with cells in passages 6 to 8.

Microcarrier cell culture

Gelatin-coated cytodex-3 MCs were prepared according to the recommendations of the supplier. Freshly autoclaved MCs were suspended in EGM, and HMVECs were added to a final density of 50-80 cells/MC. The cells were allowed to attach to the MCs in a 1.5-mL Eppendorf tube for 4 h at 37 ℃. The MCs were then resuspended in a larger volume of medium and cultivated for another 24-48 h at 37 ℃ (50 mL/L CO_2). MCs were gently agitated to prevent aggregation of individual MCs. MCs were used for angiogenesis assay when the ECs on the MCs reached confluence[10,11].

Microcarrier-based fibrin gel angiogenesis system

Microcarrier-based fibrin gel angiogenesis was performed as described[10,11] with some modifications. A working solution of fibrinogen was prepared by dissolving the stock solution of fibrinogens (20 mg/mL in PBS) in EBM to a concentration of 1.0 mg/mL, supplemented with 10 ng/mL of EGF, 1.0 μg/mL of hydrocortisone and 40 ng/mL of bFGF. The 24-well plates were used for the assay. The bottom of each well was first covered with 250 μL of fibrinogen solution, and the clotting was induced by addition of thrombin (0.5 U/mL). After 30 min of polymerization, another 250 μL of fibrinogen solution containing about 250 EC-coated MCs was added. The MCs were evenly distributed in the fibrinogen by gently shaking the plates, and polymerization was induced as described above. After complete polymerization, 1.0 mL of EBM supplemented with 10 ng/mL of EGF, 1.0 μg/mL of hydrocortisone, 40 ng/mL of bFGF and 50 mL/L adult human serum were added. To prevent excess fibrinolysis by fibrin-embedded cells, aprotinin was added to the growth media at 200 kIU/mL.

Total RNA isolation

Medium was aspirated from the surface of fibrin gels, and

the gels were scraped into a 50-mL polypropylene tube. After being centrifugated at 8 000 r/min for 3 min to remove the redundant liquid, two volumes of solution D/β-mercaptoethanol were added. The tube was vortexed vigorously for 5 min to resolve the gels, followed by the addition of 0.1 volume of 2 mol/L sodium acetate, one volume of water-saturated phenol and 0.3 volume of chloroform. After vigorously vortexed for 2 min, the tube was placed on ice for 15 min and then centrifuged at 12 000 *g* for 30 min at 4 ℃. A maximum volume of the upper aqueous phase was transferred to a new tube and equal volume of isopropanol was added. The solution was mixed by reiterative inversion, and incubated at -20 ℃ for at least 2 h. Following centrifugation at 8 000 r/min for 30 min at 4 ℃, the supernatant was removed, 2 mmol/L EDTA+0.1% SDS (1.5 mL/24 gels) were added to resuspend the RNA pellets. The suspension was transferred to 1.5-mL Eppendorf tubes and one volume of water-saturated phenol was added. The tubes were vortexed vigorously for 1 min and centrifuged at 12 000 *g* for 5 min. The upper aqueous phase was transferred to new tubes and 0.5 volume of water-saturated phenol and 0.5 volume of chloroform were added, followed by centrifugation at 12 000 *g* for 5 min. The upper aqueous phases were transferred to new tubes, and 0.1 volume of 3 mol/L sodium acetate and one volume of isopropanol were added. After incubation at -20 ℃ for at least 2 h, the tubes were centrifuged at 12 000 *g* for 15 min. After the supernatant was carefully removed and the pellet was washed twice with 750 mL/L ethanol, the pellets were air desiccated and dissolved in RNase-free H_2O. To determine the concentration and purity of RNA, 1-2 μg of RNA was diluted in 50 mL H_2O, absorption at 260 and 280 nm was checked. The $A_{260\ nm}/A_{280\ nm}$ ratio should be above 1.8. The integrity of total RNA was confirmed by 1% agarose/formaldehyde gel electrophoresis and Northern blotting for fibronectins. The samples of total RNA were eluted in DEPC-H_2O and stored at -80 ℃.

DNA microarray analysis

DNA microarray analyses were used to study the genomic-scale gene expression, the samples at different time points (0.5, 24, and 72 h after the beginning of culture) were compared during capillary morphogenesis. The selection of time points was based on the expression patterns of genes reported to be closely related to angiogenesis, by RT-PCR as described below. Approximately 150 gels for each time point were needed to obtain enough total RNA (about 25 μg for each time point) for this experiment. The total RNA was sent to Gene Company, to perform the hybridization to the Affymetrix GeneChip human genome U133 Sets (including A and B chips) containing 33 000 genes, to compare the RNA samples from the selected time points.

Biotin-labeled cDNAs were used to probe microarray chips and the hybridized probe arrays were stained with streptavidin phycoerythrin conjugate and scanned by the Affymetrix ® G2500A genearray scanner. The amount of light emitted at 570 nm was proportional to the bound target at each location on the probe array and was expressed as the signal value. The signal values from each time point were analyzed automatically by Affymetrix® Microarray suite (version 5.0), Affymetrix® MicroDB (Version 2.0), and Affymetrix® data mining tool (Version 2.0). The system processing methods were found at the manufacturer's web site (www.affymetrix.com).

Validation and confirmation of gene expression by semi-quantitative RT-PCR

To confirm the expression data from cDNA microarrays by an independent technique, gene-specific PCR oligonucleotide primer pairs were designed using Genelooper software (Geneharbor Inc.). Two micrograms of total RNA from each time point was used as the template for production of cDNA. Reverse transcriptions were performed using random primers for first-strand cDNA synthesis. Polymerase chain reactions were performed using samples from each time point to show patterns of expression with gene-specific primers. A GAPDH primer set was utilized to normalize the cDNA over the time course. RT-PCR amplification parameters used were typically 94 ℃ for 30 s, 60 ℃ for 30 s, 72 ℃ for 3 min. This was cycled 30 to 35 times, depending upon the gene, with a final extension at 72 ℃ for 7 min using a PTC-100 thermal cycler (MJ Research, Watertown, MA). Primer sequences used are shown in Table 1.

Table 1 **Primer sequences used for RT-PCR**

Genes	Primer (upstream)	Primer (downstream)	Length (bp) of PCR product	Annealing (temperature)
CYR61	5′-GAATGGAGCCTCGCATCCGATA-3′	5′-GTGGCTGCATTAGTGTCCATCC-3′	703	60
CD31	5′-ATGTGGCTTGGAGTCCTGCTGA-3′	5′-GTGTAGTTGCCACTGTGCTCCA-3′	878	60
RANTES	5′-GGATGGAGAGTCCTTGAACCTG-3′	5′-TTGAGACGGAGTCTCGCTCTGT-3′	441	60
PRSS3	5′-AGCAGCTCACTGCTACAAGACC-3′	5′-AGACCTTGGTGTAGACTCCAGG-3′	518	60
PTGS2	5′-CGGTGAAACTCTGGCTAGACAG-3′	5′-TTGGCTTCCAGTAGGCAGGAGA-3′	941	60
EBI3	5′-CCTTCATTGCCACGTACAGGCT-3′	5′-AGTGACTGGGATTACAGGTGCG-3′	845	60
ANXA1	5′-GTGAAGTCATCCAAAGGTGGTCC-3′	5′-CCTTATGGCGAGTTCCAACACC-3′	811	60
EGR1	5′-AGTGCCATCCAACGACAGCAGT-3′	5′-AGGACTTGGCTCTGAGAACCTC-3′	1 183	60
EDN1	5′-GCTGTTTGTGGCTTGCCAAGGA-3′	5′-GACCTTCGTCAGAAACTCCACC-3′	956	60
ADAM15	5′-TTCCAGCACCTGCTAAACCGCA-3′	5′-CAACTGAGCAGAGACAGGCTGT-3′	708	60
Rac1	5′-TGGTGGGAGACGGAGCTGTA-3′	5′-GGATCGCTTCGTCAAACACTG-3′	791	60
TIMP-1	5′-CACCAGAGAACCCACCATG-3′	5′-GCAGGCTTCAGCTTCCACTC-3′	669	57
TIMP-2	5′-TTTGCAATGCAGATGTAGTG-3′	5′-TCGAGAAACTCCTGCTTGG-3′	534	56
GAPDH	5′-GCCAAAAGGGTCATCATCTC-3′	5′-GTAGAGGCAGGGATGATGTTC-3′	286	60

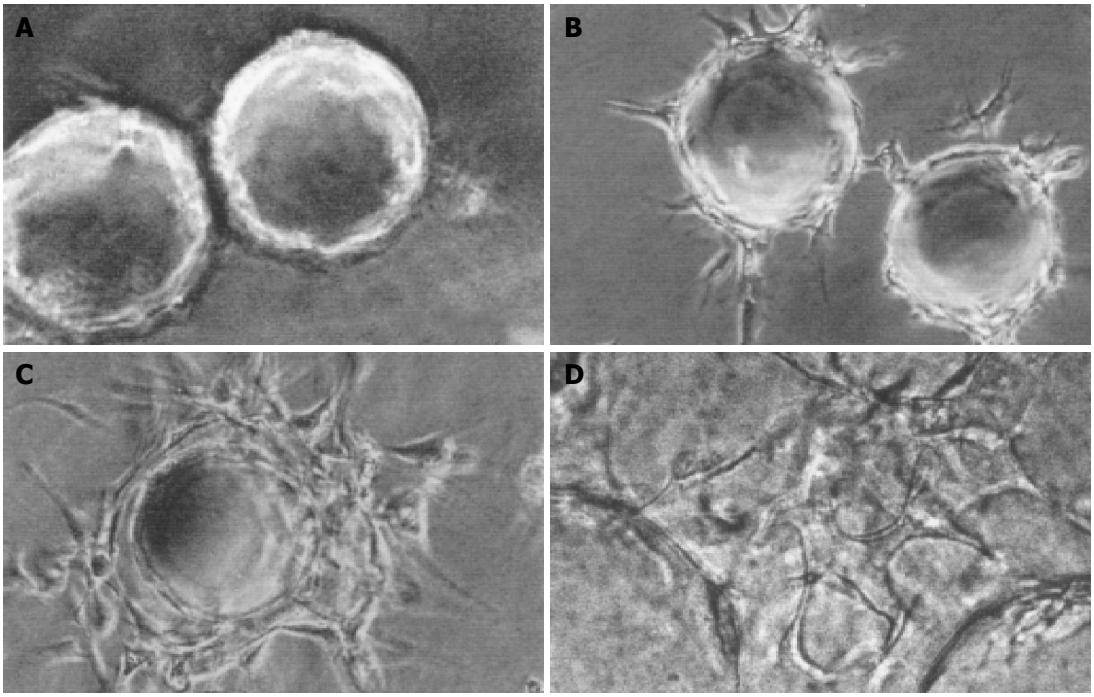

Figure 1 Sequential steps of capillary formation. **A**: MCs coated with HMVECs were embedded in fibrin matrix; **B**: HMVECs on MCs migrated into the matrix and formed sprouts without detectable lumina; **C**: Sprouts elongated, and small intracellular or intercellular lumina formed; **D**: Capillary sprouts anastomosed to each other, and capillary-like network formed (original magnification: A, B, C, ×100; D, ×400).

RESULTS

Sequential steps of capillary formation

In 1995, Nehls and Drenckhan[10] and Bülow[11] described a MC-based *in vitro* model of angiogenesis. In their model, the ECs coated on the MCs invaded the fibrin gel, forming an elongated capillary-like structure as a response to angiogenic factors. However, this model was performed with large vessel ECs of calf pulmonary artery origin[10-12]. In the present study, by modifying the system, we successfully established the MC-based *in vitro* model of angiogenesis with HMVECs in fibrin.

In the early stages of capillary growth (about 16 h after polymerization of the fibrin gel), the HMVECs on MCs migrated into fibrin matrix to form sprouts without detectable lumina. At about 16-48 h, sprouts elongated, and small intracellular or intercellular lumina formed. Usually, broad lumina developed at the base of the sprouts. The lumina frequently contained cellular debris, which could be seen to float by shaking the culture plates, indicating that lumina contents were liquified. The tips of capillary sprouts were generally solid or showed only primitive, slit-like lumina, which in later stages anastomosed to each other, and finally formed capillary-like networks (at about 5-7 d) (Figure 1). This result was not consistent with what was observed by Nehls *et al*[13], who assumed that due to the presence of serum, anastomosis of capillary sprouts occurred rarely. Since our goal was to characterize the gene expression patterns at different steps of angiogenesis including sprouting, branching and networking, our 3-D angiogenesis model gave us a good support.

Determination of the time points for DNA microarray by RT-PCR

From the morphological observation of the model, we found that the angiogenic course in our system could be coarsely divided into three phases as sprouting, branching, and network formation. But this might not give enough information about the changes at gene expression level for our determination of the time points. So some genes such as matrix metalloproteinase-1 (MMP-1), matrix metalloproteinase-2 (MMP-2), tissue inhibitor of metalloproteinase-1 (TIMP1), tissue inhibitor of metalloproteinase-2 (TIMP-2), sprouty, RhoA, Rac1, which were demonstrated to be closely related to angiogenesis by others, were selected and semi-quantitative RT-PCRs were performed to observe their expression patterns during the capillary morphogenesis (9 time points from 0.5 h to 7 d). We demonstrated that the most abrupt changes usually occurred from 24 to 72 h after the beginning of culture. According to the results of RT-PCR (data not shown), we chose 0.5, 24, and 72 h as the time points for the microarray analyses.

DNA microarray analysis of differential gene expression during capillary morphogenesis in the microcarrier-based 3-D fibrin angiogenesis system

Individual genes were represented by 'probe sets' on the Affymetrix oligonucleotide array. To identify differentially regulated genes during the ECs morphogenesis, we performed DNA microarray analyses with the total RNA isolated from cultures at selected time points. Consequently, a total of 1 961 genes were found up- or down-regulated two-folds or above, and among them, 468 genes were regulated three-folds or above. The regulated genes could be grouped into following categories based on their molecular functions such as growth factor and receptor, cell proliferation, extracellular matrix, cell cycle and apoptosis, signaling molecule and transcription factor, EC

Table 2 **Patterns of gene expression observed during capillary morphogenesis in 3-D MC-based angiogenesis system**

Patterns	Gene symbol
1	CDCA8, IRTA2, FLJ23548, ZNF83, ZNF131, ARPC4, COL13A1, LRRFIP1, FLJ90806, FACL4, AZ2, TNFRSF6B, GBP3, FLJ11029, MGC39350, FMO3, POLA2, PLEC1, DHX29, SLC20A1, FLJ21908, WSX1, CIRBP, CDC20, NRCAM, PRC1, LOC85028, TUBGCP5, C1orf33, CDC2, ADAM15
2	LOC51659, CCL5, GLRA3, CCNF, HELLS, WBSCR20A, C14orf80, EBI3, UBD, MCM4, SQLE, CDH2, TAGLN, HYAL3, FLJ22215, CDCA5, S100A3, NAV1, NFKB2, COL22A1, FRA, TP53I5, AURKB, URP2, TRAF1, ARHGDIA, STARD10, C22orf18, CX3CL1, CDT1, PRSS3
3	CAMK2G, PSMD5, MRPL35, RGS4, PXK, UBXD2, CGI-116, NET1, FLJ30707, CPD, DKFZp434L142, TRIP12, MGC11324, MAN2A1, CCL21, PRCP, CDA08, TPK1, SAS10, PTGDS, TRA1, ZNF317, ANGPT2, ADAMTS1, GPR116, GEMIN6, LEREPO4, RBMS1, ANGPT2, CARD10
4	OSR1, SKIL, SPATA1, RASA1, NFATC3, HDAC9, NYD-SP20, MGC8685, DPT, THAP6, BGN, COL4A3, SDCCAG33, KIAA1387, UBE2D3, CHD3, TNRC9, GATM, KERA, KCNF1, LOC90378, AEBP1, MFGE8, WISP3, CDC2L5, FBLN1, KIAA0014, GJA4, CPLX2, KIAA1365
5	FOS, FOSB, DUSP2, EGR4, ATF3, EGR3, EGR1, EGR2, NR4A1, NR4A2, CEBPA, PTGS2, MYLK2, SLC30A3, ZFP36, PTBP2, MYNN, JUNB, CDKN1C, ID2, GADD45B, TM4SF12, GLRA3, KLF4, SOCS5, SKIL, NR4A2, ID2, SUI1, FLJ13615, CYR61, EDN1
6	BHLHB2, KLF4, LOC92906, FXR1, DUSP6, NRP1, MIR, C6orf166, DUSP1, XLKD1, MAF, C11orf15, LRRC1, JUN, DLG1, FLJ90798, SPRY2, NPEPPS, PARVA, MGC9850, DKFZP564B1162, SEPP1, RGS2, HSA9761, ALDH1A1, DKFZP434F0318, LZK1, PDK4, dJ55C23.6, HES1, ANXA1, CD31

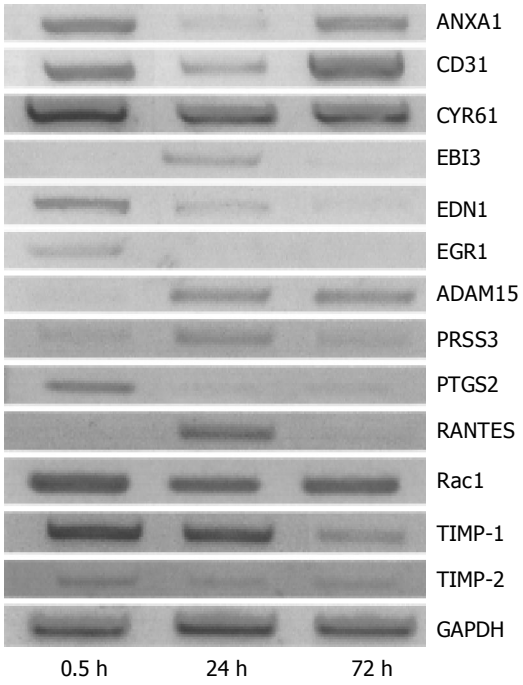

Figure 2 Validation of the expression patterns by RT-PCR.

differen-tiation marker, proteinase inhibitor, *etc*., using the gene ontology mining tool in The NetAffx™ Analysis Center. The regulated genes were also grouped into six patterns based on their changes of expression (Table 2).

To validate the patterns of expression analyzed by the microarrays, some genes were selected and semi-quantitative RT-PCRs were performed. The cDNAs from each time point were normalized to the housekeeping gene GAPDH. As shown in Figure 2, all of the genes evaluated, exhibited alterations in gene expression which was consistent with the data obtained from the oligonucleotide array analyses.

Expression of chemokines and chemokine receptors during the capillary morphogenesis

The chemokines and receptors detected by the oligonucleotide arrays are listed in Table 3, in which the genes were grouped based on their expression patterns (patterns 1-6, pattern 0 represented the genes without significant change during the capillary morphogenesis). Among the genes listed here, CXC and CC group included CXCL1/GRO-α, CXCL2/GRO-β, CXCL5/ENA-78, CXCL6/GCP2, IL-8/CXCL8, CXCL12/SDF-1, CXCL9/Mig, CXC11/ITAC, and CCL2/MCP-1, CCL3, CCL5/RANTES, CCL7, CCL15, CCL21, CCL23, CCL28, respectively. The CX3CL1/fractalkine, a number of CX3C group, were also detected. The expressions of CCL3, CCL28, CXCL9/Mig, and CXC11/ITAC were just detectable level and had no significant change during the process. The chemokine receptors in the list included CCR1, CCR9, CCR10 and CXCR4, but only the significant expression of CXCR4 was detected at all the time points. This implied its critical role in the capillary morphogenesis. Interestingly, by careful perusal of the change of expression, we could find that the CXCR4 ligand CXCL12 was expressed (pattern 4), which was consistent with its hypothetical role in the maintenance of a quiescent endothelium[32].

The different patterns of gene expression in this study gave a complicated context of the chemokines in the angiogenesis process, and implied that different chemokines might have a specific role in the different stages of the capillary morphogenesis. The chemokines that attracted our attention most were of pattern 2, which included CCL2/MCP-1, CCL5/RANTES and CX3CL1/fractalkine. They were specially up-regulated at the 24-h time point, when the sprouting was the morphologic characteristic, and then down-regulated to the basal level. The meaning of the expression in a timely fashion remains to be elucidated.

Since chemokines exerted their roles by recruiting leukocytes, we also examined the expression patterns of adhesion molecules in our assay and found that the adhesion molecules such as intercellular adhesion molecule-1 (ICAM-1) and fibronectin (FN), which could mediate the interaction between ECs and leukocyte cells, were also regulated in the same pattern as that of CCL2/MCP-1, CCL5/RANTES and CX3CL1/fractalkine.

DISCUSSION

Angiogenesis, the formation of new capillaries from pre-existing blood vessels, plays a crucial role in a wide range of normal and pathologic processes, and is necessary for the continuous growth and invasion of solid tumors[1]. Angiogenesis is regulated by the balance between the pro- and anti-angiogenic factors[2,3]. When the net balance was

Table 3 **Chemokines/chemokine receptors detected during capillary morphogenesis**

Sequence derived from	Gene symbol	24 h/0.5 h log ratio	24 h/0.5 h change	24 h/0.5 h change *P*	72 h/24 h log ratio	72 h/24 h change	72 h/24 h change *P*	72 h/0.5 h log ratio	72 h/0.5 h change	72 h/0.5 h change *P*
Pattern 1										
NM_001511.1	CXCL1	1.1	I	0.00004	-0.1	NC	0.5	0.8	I	0.00002
AK026546.1	CXCL5	1.2	I	0.009292	-0.4	NC	0.506476	0.6	I	0.00249
Pattern 2										
U84487	CX3CL1	1.5	I	0.000389	-1.9	D	0.999562	-0.8	NC	0.911062
NM_002985.1	CCL5	3.4	I	0.00002	-3.9	D	0.99998	-0.4	D	0.998799
S69738.1	CCL2	2	I	0.00002	-1.3	D	0.99998	0.5	I	0.00002
Pattern 3										
NM_002989.1	CCL21	-0.1	NC	0.596188	2.8	I	0.00002	2.1	I	0.000023
U58913.1	CCL23	-0.3	NC	0.5	1.4	I	0.000692	0.9	I	0.000147
Pattern 4										
NM_000609.1	CXCL12	0.4	NC	0.118009	-0.8	D	0.999727	-0.4	NC	0.777251
NM_002993.1	CXCL6	0.3	NC	0.088938	-1	D	0.999226	-0.6	NC	0.930187
NM_013246.1	CLC	-0.1	NC	0.5	-0.1	D	0.996959	-1.2	NC	0.98579
Pattern 5										
NM_006273.2	CCL7	-0.6	NC	0.5	-0.8	NC	0.977068	-0.7	D	0.999759
M57731.1	CXCL2	-1	D	0.99288	-0.5	NC	0.900148	-1.5	D	0.995927
Pattern 6										
AF348491.1	CXCR4	-1.7	D	0.99998	1.8	I	0.00002	0.1	NC	0.094279
NM_000584.1	IL8	-0.9	D	0.999965	1.1	I	0.001486	-0.2	NC	0.5
NM_004166.1	CCL15	-1.4	D	0.99998	0.4	I	0.000552	-0.9	D	0.99998
Pattern 0										
NM_016602.1	CCR10	1.1	NC	0.028766	-0.4	NC	0.62112	0.4	NC	0.019624
NM_002416.1	CXCL9	0.1	NC	0.5	-0.4	NC	0.814019	-0.2	NC	0.692594
AF275260.1	CXCL16	0.5	NC	0.5	-0.4	NC	0.5	0.1	NC	0.013078
AF030514.1	CXCL11	-1	NC	0.692594	0.9	NC	0.018128	0.2	NC	0.078937
AF145439.1	CCR9	0.3	NC	0.5	-0.7	NC	0.973302	-0.9	NC	0.938478
NM_001295.1	CCR1	0.4	NC	0.5	-0.8	NC	0.822588	-0.3	NC	0.881991
NM_002983.1	CCL3	0.3	NC	0.5	-0.5	NC	0.506476	-0.5	NC	0.60871
AF266504.1	CCL28	0.3	NC	0.177412	-0.9	NC	0.987976	-0.6	NC	0.854318

D: decrease; I: increase; NC: no change.

tipped in favor of angiogenesis, the "angiogenic switch" was on[14], and the ECs consequently degraded the local basement membrane, migrated into the underlying stroma, proliferated, and formed capillary sprouts[15].

The basal morphologic process of angiogenesis includes sprouting, branching and network formation. The molecular mechanisms underlying these characteristic morphologic changes are now under deep investigation and a variety of *in vitro* 3-D models have been employed. However, because of different systems employed, the results were usually different, or even controversial. Thus, we must keep in mind that any *in vitro* system can only reflect *in vivo* scenario from one respect, and more steps of the process should be considered when we choose the model system for investigation of molecular mechanisms of angiogenesis. In addition, the EC and the 3-D matrix are also the critical factors, which have great effects on the results. It has thus been emphasized that microvascular ECs are mandatory for the angiogenesis investigations[16].

In the present study, we developed an *in vitro* angiogenesis system based on MCs, HMVECs and fibrin matrix. With this system, and under the stimulation of angiogenic factors, such as bFGF and VEGF, we observed all the characteristic steps of *in vivo* angiogenesis, including sprouting, branching and network formation. As shown in a previous study, the morphological changes were dose-dependent on the growth factor used[7]. Thus, we believe that this system has an advantage over the model employed by Bell *et al*[5], for the mechanism investigation of angiogenesis, because in the latter system, the ECs were suspended in the matrix as single cells, and all cells underwent morphologic changes at the same time, which was assumed to be closer to vasculogenesis as discussed by the authors[5].

For the molecular mechanisms, microarray analysis has proved to be an efficient strategy. Using rigorous and tightly controlled experimental conditions, tightly controlled biological replicates, and multiple comparisons, gene expression profiling using microarray technology can yield reliable, highly validated results. For example, Gerritsen *et al*[17,18], identified over 1 000 differentially expressed genes as regulated in a 3-D collagen gel model of endothelial differentiation using the Affymetrix oligonucleotide technology combined with software analysis packages. Several hundred of these genes were selected for further evaluation by an independent method (RT-PCR) and greater than 95% of the genes identified were shown to be regulated in a manner suggested by the results from the oligonucleotide array. In the present study, we also utilized the Affymetrix oligonucleotide array to compare the gene expression profiles during the capillary morphogenesis and the data analyzed were associated with the morphologic changes. We identified discrete subsets of genes that were up-regulated or down-regulated during the process. We also classified the regulated genes into groups according to their changing

patterns, which enabled us to explain their significance in their complicated context.

Among the data obtained from the array, we focused our interest on the chemokines and chemokine receptors. Chemokines are a family of small secreted proteins that, depending on the spacing or presence of four conserved cysteine residues, have been classified into CC, CXC, CX3C and C chemokines[19]. CXC chemokines can be further divided into two groups of molecules (ELR+and non-ELR) according to the presence or absence of an ELR (Glu–Leu-Arg) motif. It has been demonstrated that many types of malignant cells could express chemokines such as RANTES, MCP-1, IL-8, and the expression of these chemokines by tumors were found to be correlated with the tumor angiogenesis and progression[20-22]. It has also been found that ECs are capable of binding and responding to a number of chemokines[23-28]. For example, CXC chemokines, such as CXCL8/IL-8, CXCL1/Gro-α, CXCL2/Gro-β, CXCL4/PF-4 and CXCL10/IP-10 have been implicated in the regulation of EC functions including the stimulation and inhibition of proliferation, angiogenesis and cell migration[29-31]. A proposed theoretical model about the role of chemokines in the angiogenesis is that the chemokines expressed and secreted from malignant cells (or other type of cells) could interact directly with the special receptors on ECs, or recruit leukocytes, which in turn could produce angiogenic factors that then bind to the special receptors on the ECs, exert their specific roles in regulating the EC functions[32].

However, the roles of chemokines and their receptors in angiogenesis still remain to be further elucidated. In fact, many chemokines have been confirmed to be angiogenic or angiostatic, directly or indirectly by regulating other factors. ECs of different origins can express not only chemokine receptors as targets of chemokines from other cells, but also chemokines themselves, which can improve the adhesion of leukocytes to the endothelium, or regulate endothelial functions in autocrine ways[32-36].

In this study, several genes for chemokines were also identified, including CXCL1/GRO-α, CXCL2/GRO-β, CXCL5/ENA-78, CXCL6/GCP2, IL-8/CXCL8, CXCL12/SDF-1, CXCL9/Mig, CXC11/ITAC, and CCL2/MCP-1, CCL3, CCL5/RANTES, CCL7, CCL15, CCL21, CCL23, CCL28, and CX3CL1. The chemokine receptors identified included CCR1, CCR9 and CXCR4. During capillary morphogenesis, these genes underwent different changing patterns. Although the exact roles of these chemokines and chemokine receptors during angiogenesis need further investigation, the changing patterns have given many hints to their possible functions. For example, as described above, the specific up-regulation of CCL2/MCP-1, CCL5/RANTES and CX3CL1/fractalkine in the sprouting process might suggest their important roles at the early stage of angiogenesis.

In conclusion, the present study demonstrates a global profiling of the gene expression during endothelial capillary morphogenesis, and the results provide us much information about the molecular mechanisms of angiogenesis, with which further evaluation of individual genes can be conducted.

REFERENCES

1 **Folkman J.** Tumor angiogenesis. *Adv Cancer Res* 1985; **43**: 175-203

2 **Hanahan D,** Folkman J. Patterns and emerging mechanisms of the angiogenic switch during tumorigenesis. *Cell* 1996; **86**: 353-364

3 **Risau W.** Mechanisms of angiogenesis. *Nature* 1997; **386**: 671-674

4 **St Croix B,** Rago C, Velculescu V, Traverso G, Romans KE, Montgomery E, Lal A, Riggins GJ, Lengauer C, Vogelstein B, Kinzler KW. Genes expressed in human tumor endothelium. *Science* 2000; **289**: 1197-1202

5 **Bell SE,** Mavila A, Salazar R, Bayless KJ, Kanagala S, Maxwell SA, Davis GE. Differential gene expression during capillary morphogenesis in 3D collagen matrices: regulated expression of genes involved in basement membrane matrix assembly, cell cycle progression, cellular differentiation and G-protein signaling. *J Cell Sci* 2001; **114**: 2755-2773

6 **Vailhé B,** Vittet D, Feige JJ. *In vitro* models of vasculogenesis and angiogenesis. *Lab Invest* 2001; **81**: 439-452

7 **Sun XT,** Ding YT, Yan XG, Wu LY, Li Q, Cheng N, Qiu YD, Zhang MY. Angiogenic synergistic effect of basic fibroblast growth factor and vascular endothelial growth factor in an *in vitro* quantitative microcarrier-based 3-dimensional fibrin angiogenesis system. *World J Gastroenterol* 2004; **10**: 2524-2528

8 **Peters K,** Schmidt H, Unger RE, Otto M, Kamp G, Kirkpatrick CJ. Software-supported image quantification of angiogenesis in an *in vitro* culture system: application to studies of biocompatibility. *Biomaterials* 2002; **23**: 3413-3419

9 **Kubota Y,** Kleinman HK, Martin GR, Lawley TJ. Role of laminin and basement membrane in the morphological differentiation of human endothelial cells into capillary-like structures. *J Cell Biol* 1988; **107**: 1589-1598

10 **Nehls V,** Drenckhahn D. A novel, microcarrier-based *in vitro* assay for rapid and reliable quantification of three-dimensional cell migration and angiogenesis. *Microvasc Res* 1995; **50**:311-322

11 **Nehls V,** Drenckhahn D. A microcarrier-based cocultivation system for the investigation of factors and cells involved in angiogenesis in three-dimensional fibrin matrices *in vitro*. *Histochem Cell Biol* 1995; **104**: 459-466

12 **von Bülow C,** Hayen W, Hartmann A, Mueller-Klieser W, Allolio B, Nehls V. Endothelial capillaries chemotactically attract tumour cells. *J Pathol* 2001; **193**: 367-376

13 **Nehls V,** Herrmann R, Hühnken M. Guided migration as a novel mechanism of capillary network remodeling is regulated by basic fibroblast growth factor. *Histochem Cell Biol* 1998; **109**: 319-329

14 **Carmeliet P,** Jain RK. Angiogenesis in cancer and other diseases. *Nature* 2000; **407**: 249-257

15 **Gerwins P,** Skolderberg E, Claesson-Welsh L. Function of fibroblast growth factors and vascular endothelial growth factors and their receptors in angiogenesis. *Crit Rev Oncol Hematol* 2000; **34**: 185-194

16 **Goldbrunner RH,** Wagner S, Roosen K, Tonn JC. Models for assessment of angiogenesis in gliomas. *J Neurooncol* 2000; **50**: 53-62

17 **Gerritsen ME,** Soriano R, Yang S, Zlot C, Ingle G, Toy K, Williams PM. Branching out: a molecular fingerprint of endothelial differentiation into tube-like structures generated by Affymetrix oligonucleotide arrays. *Microcirculation* 2003; **10**: 63-81

18 **Gerritsen ME,** Soriano R, Yang S, Ingle G, Zlot C, Toy K, Winer J, Draksharapu A, Peale, F, Wu TD, Williams PM. In silico data filtering to identify new angiogenesis targets from a large *in vitro* gene profiling data set. *Physiol Genomics* 2002; **10**: 13-20

19 **Rossi D,** Zlotnik A. The biology of chemokines and their receptors. *Annu Rev Immunol* 2000; **18**: 217-242

20 **Luboshits G,** Shina S, Kaplan O, Engelberg S, Nass D, Lifshitz-Mercer B, Chaitchik S, Keydar I, Ben-Baruch A. Elevated expression of the CC chemokine regulated on activation, normal T cell expressed and secreted (RANTES) in advanced

breast carcinoma. *Cancer Res* 1999; **59**: 4681-4687

21 **Ohta M,** Kitadai Y, Tanaka S, Yoshihara M, Yasui W, Mukaida N, Haruma K, Chayama K. Monocyte chemoattractant protein-1 expression correlates with macrophage infiltration and tumor vascularity in human esophageal squamous cell carcinomas. *Int J Cancer* 2002; **102**: 220-224

22 **Azenshtein E,** Luboshits G, Shina S, Neumark E, Shahbazian D, Weil M, Wigler N, Keydar I, Ben-Baruch A. The CC chemokine RANTES in breast carcinoma progression: regulation of expression and potential mechanisms of promalignant activity. *Cancer Res* 2002; **62**: 1093-1102

23 **Biffl WL,** Moore EE, Moore FA, Carl VS, Franciose RJ, Banerjee A. Interleukin-8 increases endothelial permeability independent of neutrophils. *J Trauma* 1995; **39**: 98-102; discussion 102-103

24 **Rot A.** Binding of neutrophil attractant/activation protein-1 (interleukin-8) to resident dermal cells. *Cytokine* 1992; **4**: 347-352

25 **Strieter RM,** Polverini PJ, Kunkel SL, Arenberg DA, Burdick MD, Kasper J, Dzuiba J, Van Damme J, Walz A, Marriott D. The functional role of the ELR motif in CXC chemokine-mediated angiogenesis. *J Biol Chem* 1995; **270**: 27348-27357

26 **Martins-Green M,** Hanafusa H. The 9E3/CEF4 gene and its product the chicken chemotactic and angiogenic factor (cCAF): potential roles in wound healing and tumor development. *Cytokine Growth Factor Rev* 1997; **8**: 221-232

27 **Salcedo R,** Wasserman K, Young HA, Grimm MC, Howard OM, Anver MR, Kleinman HK, Murphy WJ, Oppenheim JJ. Vascular endothelial growth factor and basic fibroblast growth factor induce expression of CXCR4 on human endothelial cells: *In vivo* neovascularization induced by stromal-derived factor-1alpha. *Am J Pathol* 1999; **154**: 1125-1135

28 **Cao Y,** Chen C, Weatherbee JA, Tsang M, Folkman J. gro-beta, a C-X-C-chemokine, is an angiogenesis inhibitor that suppresses the growth of Lewis lung carcinoma in mice. *J Exp Med* 1995; **182**: 2069-2077

29 **Koch AE,** Polverini PJ, Kunkel SL, Harlow LA, DiPietro LA, Elner VM, Elner SG, Strieter RM. Interleukin-8 as a macrophage-derived mediator of angiogenesis. *Science* 1992; **258**: 1798-1801

30 **Tuschil A,** Lam C, Haslberger A, Lindley I. Interleukin-8 stimulates calcium transients and promotes epidermal cell proliferation. *J Invest Dermatol* 1992; **99**: 294-298

31 **Maione TE,** Gray GS, Petro J, Hunt AJ, Donner AL, Bauer SI, Carson HF, Sharpe RJ. Inhibition of angiogenesis by recombinant human platelet factor-4 and related peptides. *Science* 1990; **247**: 77-79

32 **Bernardini G,** Ribatti D, Spinetti G, Morbidelli L, Ziche M, Santoni A, Capogrossi MC, Napolitano M. Analysis of the role of chemokines in angiogenesis. *J Immunol Methods* 2003; **273**: 83-101

33 **Harkness KA,** Sussman JD, Davies-Jones GA, Greenwood J, Woodroofe MN. Cytokine regulation of MCP-1 expression in brain and retinal microvascular endothelial cells. *J Neuroimmunol* 2003; **142**: 1-9

34 **Hillyer P,** Mordelet E, Flynn G, Male D. Chemokines, chemokine receptors and adhesion molecules on different human endothelia: discriminating the tissue-specific functions that affect leucocyte migration. *Clin Exp Immunol* 2003; **134**: 431-441

35 **Salvucci O,** Yao L, Villalba S, Sajewicz A, Pittaluga S, Tosato G. Regulation of endothelial cell branching morphogenesis by endogenous chemokine stromal-derived factor-1. *Blood* 2002; **99**: 2703-2711

36 **Feng L.** Role of chemokines in inflammation and immunoregulation. *Immunol Res* 2000; **21**: 203-210

Science Editor Kumar M and Wang XL **Language Editor** Elsevier HK

PO Box 2345, Beijing 100023, China
www.wjgnet.com
wjg@wjgnet.com

ELSEVIER

World J Gastroenterol 2005;11(15):2291-2295
World Journal of Gastroenterology ISSN 1007-9327

• *BASIC RESEARCH* •

Expression of intestinal trefoil factor, proliferating cell nuclear antigen and histological changes in intestine of rats after intrauterine asphyxia

Ling-Fen Xu, Jun Li, Mei Sun, Hong-Wei Sun

Ling-Fen Xu, Jun Li, Mei Sun, Department of Pediatrics, Second Affiliated Hospital, China Medical University, Shenyang 110004, Liaoning Province, China
Hong-Wei Sun, Department of Pediatrics, Affiliated Central Hospital, Shenyang Medical College, Shenyang 110024, Liaoning Province, China
Supported by the Research Fund of Science and Technology of Liaoning Province, China, No. 20122166
Correspondence to: Dr. Ling-Fen Xu, Department of Pediatrics, Second Affiliated Hospital, China Medical University, Shenyang 110004, Liaoning Province, China. xulingfen@yahoo.com.cn
Telephone: +86-24-83956503
Received: 2004-05-07 Accepted: 2004-08-05

Abstract

AIM: To study the expressions of intestinal trefoil factor (ITF) and proliferating cell nuclear antigen (PCNA) and histologic changes in intestine, to investigate the relationship between ITF and intestinal damage and repair after intrauterine hypoxia so as to understand the mechanism of intestinal injury and to find a new way to prevent and treat gastrointestinal diseases.

METHODS: Wistar rats, pregnant for 21 d, were used to establish animal models of intrauterine asphyxia by clamping one side of vessels supplying blood to uterus for 20 min, another side was regarded as sham operation group. Intestinal tissues were taken away at 0, 24, 48 and 72 h after birth and stored in different styles. ITF mRNA was detected by RT-PCR. PCNA expression was measured by immunohistochemistry. Intestinal tissues were studied histologically by HE staining in order to observe the areas and degree of injury and to value the intestinal mucosa injury index (IMDI).

RESULTS: ITF mRNA appeared in full-term rats and increased with age. After ischemia, ITF mRNA was decreased to the minimum (0.59±0.032) 24 h after birth, then began to increase higher after 72 h than it was in the control group (P<0.01). PCNA positive staining located in goblet cell nuclei. The PCNA level had a remarkable decline (53.29±1.97) 48 h after ischemia. Structure changes were obvious in 48-h group, IMDI (3.40±0.16) was significantly increased. Correlation analyses showed that IMDI had a negative correlation with ITF mRNA and PCNA (r = -0.543, P<0.05; r = -0.794, P<0.01, respectively).

CONCLUSION: Intrauterine ischemia can result in an early decrease of ITF mRNA expression. ITF and PCNA may play an important role in the damage and repair of intestinal mucosa.

Key words: ITF; PCNA

Xu LF, Li J, Sun M, Sun HW. Expression of intestinal trefoil factor, proliferating cell nuclear antigen and histological changes in intestine of rats after intrauterine asphyxia. *World J Gastroenterol* 2005; 11(15): 2291-2295
http://www.wjgnet.com/1007-9327/11/2291.asp

INTRODUCTION

Intestinal trefoil factor (ITF) is a member of the trefoil peptide family[1,2], which is important in maintenance and repair of the intestinal mucosal barrier[3] and was first discovered and named by Suemori *et al*[4], in 1991. Researchers have demonstrated that ITF can protect cells of intestinal mucosa from damage mediated by many kinds of injury factors[5,6]. It can-not only stimulate cell migration and proliferation, promote epithelial cell repair[7,8], but also interact with mucus, stabilize mucus gel by perhaps interacting with intestinal mucin and increasing the viscosity[9]. So it is important in the self-protection mechanism of intestine.

Proliferating cell nuclear antigen (PCNA) is a kind of intranuclear protein, which is an assistant protein of DNase[10]. It has no specificity of species, genus and tissue, exists in the cells, expressing in phages G1 and S, so it has been widely used to mark cells of S phage. In this point PCNA is a perfect marker to evaluate cell proliferation[10].

There are almost 70% neonates with birth asphyxia complicating varied degree damages of organs such as heart, brain, kidney and gastrointestine[11]. Among which the rate of gastrointestinal injury is 33% and even higher than that of brain damage.

Whether the damage of intestine has a relationship with ITF and PCNA remains unknown[12]. In this study, the model of intrauterine asphyxia of rats and the methods of RT-PCR and immunohistochemistry were used to explore the expressions of ITF and PCNA, to observe the histologic changes of intestine so as to understand the mechanism of intestinal injury after asphyxia and to find a new way to prevent and treat gastrointestinal diseases.

MATERIALS AND METHODS

Animal model

Sixty-three Wistar rats (53 females and 10 males, weighing 270±30 and 300±20 g respectively) were provided by the Animal Center of China Medical University No. 2 hospital. According to the methods of Mamoru *et al*, and Terry *et al*[13,14], models of intrauterine acute ischemia were established by clamping one side of vessels supplying blood to uterus of 21-d pregnant Wistar rats for 20 min and the other side was regarded as sham operation group. When the prescribed time was reached, uterus horn was opened rapidly and pups were taken out. A total of 144 surviving baby rats were enrolled in this study, which were fed by other step-mother rats for 0, 24, 48 and 72 h, respectively, then 18 baby rats in each group were killed and 100-200 mg intestinal tissue (taken from 3 to 4 baby rats) was stored at -80 ℃ as samples for ITF mRNA, five samples at each time point. In each intestinal tissue, 0.5-cm intestinal tissue was fixed in 40 g/L formaldehyde for HE staining and PCNA immunohistochemistry study.

RT-PCR for detection of ITF mRNA

Total RNA was isolated from intestine samples using TRIzol reagent (Promega Co., USA). Two microliters of total RNA were used as a template to synthesize cDNA. The resulting cDNA was used as a template for subsequent PCR (TaKaRa Co., Ltd). A 236-bp fragment of ITF was amplified from single-stranded DNA by PCR using two oligonucleotide primers to ITF sequence: sense primer, 5'TTT GAC TCC AGC ATC CCA 3', and antisense primer, 5'CGC AAT TAG AAC AGC CTT G 3' (synthesized by AuGCT Biotechnology Co., Beijing). Meanwhile, amplification of β-actin was performed on the same RNA samples to assess RNA integrity. Reaction mixture for PCR contained cDNA template 4 μL, dd H_2O 11.8 μL, 5× buffer 5 μL, dNTPS 2 μL, TaqE 0.2 μL, primers A and B each 1 μL. Forty-five cycles of PCR were conducted at 94 ℃ for 4 min, at 60.6 ℃ for 1 min, at 72 ℃ for 90 s, at 72 ℃ for 7 min. Agarose gel electrophoresis was used to detect the amplified ITF products. The density of bands was assessed and the amount of ITF mRNA was determined according to the ratio to β-actin[15].

Immunohistochemistry for PCNA

The samples were fixed in 40 g/L formaldehyde and embedded in paraffin. Five-micrometer thick serial sections of paraffin blocks were dewaxed and rehydrated. PCNA monoclonal antibody and SABC correlated reagents were purchased from Zhongshan Biotechnology Co., Beijing. Detection was carried out according to instructions. Five views were randomly selected in each tissue section, measured under a 400× microscope and analyzed with Meta Morph software to assess the average gray density.

Determination of intestinal mucosa damage index (IMDI)

Samples were fixed in 40 g/L formaldehyde and embedded in paraffin, then cut into 5-μm sections and stained with HE. Three sections of each tissue, five sights of each section were selected randomly to observe under a microscope, the areas and degree of injury and IMDI were evaluated by an expert pathologist using double blind. The standard was suggested by Chiu *et al*[17], and Okur *et al*[18].

Grade 0: Normal mucosal villi.

Grade 1: Development of subepithelial Gruenhagen's space, usually at the apex of the villus, often with capillary congestion.

Grade 2: Extension of the subepithelial space with moderate lifting of epithelial layer from the lamina propria.

Grade 3: Massive epithelial lifting down the sides of villi. A few tips might be denuded.

Grade 4: Denuded villi with lamina propria and dilated capillaries exposed. Increased cellularity of lamina propria might be noted.

Grade 5: Digestion and disintegration of lamina propria, hemorrhage and ulceration.

Statistical analysis

Data were expressed as mean±SD. Results were analyzed with *t* test and LSD test (*q* test). Spearman's method was used for correlation analysis by SPSS 10.0 software.

RESULTS

Changes of ITF mRNA expression in intestine after intrauterine asphyxia

RT-PCR showed that expression of ITF mRNA appeared in full-term rats and increased with age. After ischemia, ITF mRNA expression decreased to the minimum (0.59±0.032) 24 h after birth, and then began to increase. It was even higher 72 h after birth than it was in the control group ($P<0.01$) (Figure 1 and Table 1).

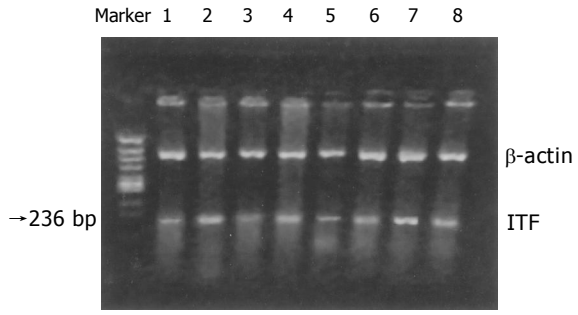

Figure 1 ITF mRNA expression in intestine after intrauterine asphyxia detected by RT-PCR. Lane 1: after intrauterine asphyxia 0-h group; lane 2: control group; lane 3: after intrauterine asphyxia 24-h group; lane 4: control group; lane 5: after intrauterine asphyxia 48-h group; lane 6: control group; lane 7: after intrauterine asphyxia 72-h group; lane 8: control group.

Immunohistochemical results of PCNA after intrauterine asphyxia

Goblet cell nuclei were positively stained in intestinal mucosa of full term rats. The PCNA level had a remarkable decline (53.29±1.97) 48 h after ischemia, then began to increase, but was still lower than that in the control group 72 h after birth. There was a significant difference between ischemic and control groups ($P<0.01$) (Figures 2A and B; Table 1).

Table 1 **Changes of expression of ITF mRNA, PCNA and IMDI after intrauterine asphyxia (*n* = 18, mean±SD)**

Age (h)	ITF mRNA		PCNA		IMDI	
	Experimental	Control	Experimental	Control	Experimental	Control
0	0.86±0.043[a,d]	0.97±0.016	56.75±1.18[a,d]	65.24±2.67	0.67±0.16[b,d]	0
24	0.59±0.032[a,d]	0.98±0.011	55.22±2.14[b,d]	66.17±2.10	2.47±0.17[b,d]	0
48	0.83±0.022[a,d]	0.99±0.025	53.29±1.97[b,d]	72.17±3.19	3.40±0.16[b,d]	0
72	1.19±0.023[a,d]	1.07±0.021	61.80±2.72[b,d]	74.48±1.33	1.60±0.21[b,d]	0

[a]$P<0.05$ *vs* control group; [b]$P<0.01$ *vs* control group; [d]$P<0.01$ *vs* other experimental groups.

Change of histology and IMDI

Histologic examinations of normal newborn rats showed that their intestinal tissues were almost mature. After ischemia, lamina propria hyperemia might be noted 24 h after birth, extension of the subepithelial space with moderate lifting of epithelial layer from the lamina propria could be observed. Structural changes were obvious in 48-h group, denuded villi with lamina propria and dilated capillaries were exposed, cellularity of lamina propria was increased, quantity of villi was declined, IMDI (3.40±0.16) was significantly increased. Seventy-two hours after birth, although the quantity of villi was still less than that in the control group, changes recovered remarkably. The intestinal mucosa of control group had almost no damage (IMDI was 0). Correlation analyses showed that IMDI had a negative correlation with ITF mRNA and PCNA (r = -0.543, $P<0.05$; r = -0.794, $P<0.01$, respectively) (Figures 3A and B; Table 1).

DISCUSSION

Neonatal asphyxia is a common disease during perinatal, which happens in uterus and during labor with a high morbidity and mortality in newborns. Previous studies[18,19] showed that the rate of gastrointestinal injury was 33% and even higher than that of brain damage. However, research has been hardly done on the mechanism of intestinal injury.

Studies have demonstrated that there were changes in levels of blood gastrin and motilin in patients with asphyxia[20,21] and they might suffer from more attacks of gastroesophageal acid reflux than the normal controls[22]. There were also changes of free radicals in intestine after hyperoxia-induction[23]. But it is of great value to discuss the maturity and perfection of intestinal mucosal barrier, whether the barrier is damaged and what happens in the proliferation and repair ability after damage.

A previous study showed that among the growth factors, ITF was most closely associated with intestine and was the initiators of mucosal healing[24]. ITF is a new kind of growth factors secreted by goblet cells[25] into the lumen of the intestinal tract[26] with a characteristic structure of trefoil configuration[1], so it not only has the promoting effect on cell proliferation as a common growth factor, but also could combine with mucin glycoproteins to stabilize the mucus

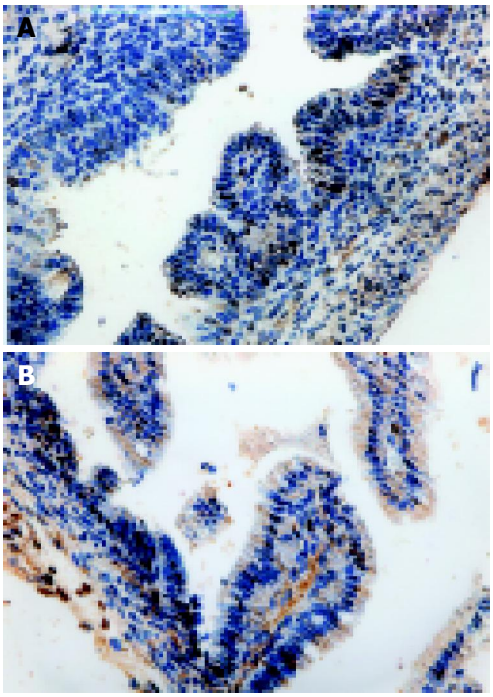

Figure 2 Immunohistochemical results of PCNA (400×). **A**: Positive staining of intestinal mucosal goblet cell nuclei; **B**: Decline of PCNA positive staining 48 h after intrauterine asphyxia.

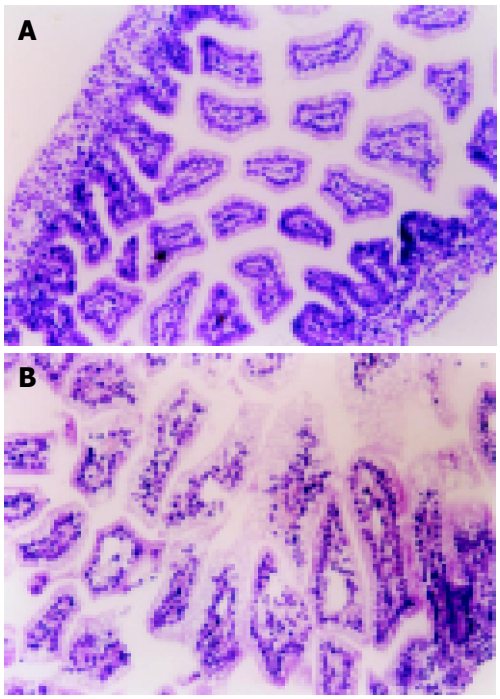

Figure 3 Intestinal tissue HE staining (400×). **A**: Mature intestinal tissue in normal newborn rats; **B**: Obvious structural changes, denuded villi with lamina propria and exposed dilated capillaries increased cellularity of lamina, declined quantity of villi 48 h after intrauterine asphyxia.

gel[3] and prevent the damage caused by proteolytic enzymes and mechanical pressure[27]. In this way, ITF could be looked as a protection factor of intestine[2].

ITF mRNA expression was detected at transcriptional level at different time points after birth in rats with asphyxia in our study. It was found that at birth, the ITF had a certain expression and with time, the expression increased. After asphyxia, ITF mRNA expression decreased. The synthesis ability of ITF of goblet cells decreased and reached the lowest point 24 h after birth, and then increased. It increased more than that in control group 72 h after birth. It was considered as a reflect reaction to injury repair. At this time, the intestinal mucosa began to proliferate fast along with the recovery of intestine function.

The other factor causing damage of the integrity of intestinal mucosal barrier can inhibit intestinal epithelial cell proliferation. Intestinal epithelial cells have the characteristics of short proliferating cycle and strong growth ability, so the intestine could self-repair well. PCNA has no specificity of species, genus, tissue and presense in actively proliferating cells. PCNA is a perfect cell proliferating index in normally proliferating cells and in certain tumor tissues and has already been used as a routing method to test proliferating cells at present[28,29]. It was also demonstrated that the change of PCNA expression increased DNA duplication and cell proliferation[30-32]. The expression of PCNA also increased in intestine of dogs after ischemia and reperfusion[33]. Immunohistochemical technology revealed that the PCNA level had a remarkable decline 48 h after asphyxia, recovered partly after 72 h, but was still lower than that in the control group, suggesting that asphyxia can decrease the proliferating ability of epithelial cells.

At the same time, histologic examination of intestine showed that intestinal mucosa was injured widely and IMDI increased significantly, and then recovered. Correlation analysis showed that IMDI had a negative correlation to ITF mRNA and PCNA. In this way, a low proliferating ability would lead to a low repair ability and perhaps the decline of intestinal mucosa to secrete ITF is associated with dysfunction of mucosal-barrier and the disability of mucosa repair. Whether other factors are involved should be further studied. Feng *et al*[33], studied the relationship between ITF and intestinal damage and repair in rats suffering from severe burns, and found the similar results.

The distinct three-loop secondary structure of ITF could contribute to the remarkable resistance to acid and proteolytic digestion, enabling them to function in the harsh environment of the gastrointestinal tract while maintaining biologic activity[34,35]. It could not affect pH and gastroenteric motility[36], but could stabilize mucus gels so as to protect intestinal mucosa against all kinds of damage factors. Further study should be done to explore whether enteral administration of ITF can prevent and treat intestinal injury caused by asphyxia[37-41].

REFERENCES

1 **Thim L.** Trefoil peptides: from structure to function. *Cell Mol Life Sci* 1997; **53**: 888-903
2 **Thim L.** Trefoil peptides: a new family of gastrointestinal molecules. *Digestion* 1994; **55**: 353-360
3 **Kindon H,** Pothoulakis C, Thim L, Lynch-Devaney K, Podolsky DK. Trefoil peptide protection of intestinal epithelial barrier function: cooperative interaction with mucin glycoprotein. *Gastroenterology* 1995; **109**: 516-523
4 **Suemori S,** Lynch-Devaney K, Podolsky DK. Identification and characterization of rat intestinal trefoil factor: tissue- and cell-specific member of the trefoil protein family. *Proc Natl Acad Sci USA* 1991; **88**: 11017-11021
5 **Andoh A,** Kinoshita K, Rosenberg I, Podolsky DK. Intestinal trefoil factor induces decay-accelerating factor expression and enhances the protective activities against complement activation in intestinal epithelial cells. *J Immunol* 2001; **167**: 3887-3893
6 **Beck PL,** Wong JF, Li Y, Swaminathan S, Xavier RJ, Devaney KL, Podolsky DK. Chemotherapy- and radiotherapy-induced intestinal damage is regulated by intestinal trefoil factor. *Gastroenterology* 2004; **126**: 796-808
7 **Playford RJ,** Marchbank T, Chinery R, Evison R, Pignatelli M, Boulton RA, Thim L, Hanby AM. Human spasmolytic polypeptide is a cytoprotective agent that stimulates cell migration. *Gastroenterology* 1995; **108**: 108-116
8 **Dignass A,** Lynch-Devaney K, Kindon H, Thim L, Podolsky DK. Trefoil peptides promote epithelial migration through a transforming growth factor beta-independent pathway. *J Clin Invest* 1994; **94**: 376-383
9 **Emami S,** Le Floch N, Bruyneel E, Thim L, May F, Westley B, Rio M, Mareel M, Gespach C. Induction of scattering and cellular invasion by trefoil peptides in src- and RhoA-transformed kidney and colonic epithelial cells. *FASEB J* 2001; **15**: 351-361
10 **Prelich G,** Tan CK, Kostura M, Mathews MB, So AG, Downey KM, Stillman B. Functional identity of proliferating cell nuclear antigen and a DNA polymerase-delta auxiliary protein. *Nature* 1987; **326**: 517-520
11 **Perlman JM,** Tack ED, Martin T, Shackelford G, Amon E. Acute systemic organ injury in term infants after asphyxia. *Am J Dis Child* 1989; **143**: 617-620
12 **Lin J,** Holzman IR, Jiang P, Babyatsky MW. Expression of intestinal trefoil factor in developing rat intestine. *Biol Neonate* 1999; **76**: 92-97
13 **Tanaka M,** Natori M, Ishimoto H, Miyazaki T, Kobayashi T, Nozawa S. Experimental growth retardation produced by transient period of uteroplacental ischemia in pregnant Sprague-Dawley rats. *Am J Obstet Gynecol* 1994; **171**: 1231-1234
14 **Hayashi TT,** Dorko ME. A rat model for the study of intrauterine growth retardation. *Am J Obstet Gynecol* 1988; **158**: 1203-1207
15 **Shang YX,** Han XH, Cheng YW, Zhao SQ, Wei KL. Relationship between substance P and asthma. *Zhongguo Dangdai Erke Zazhi* 2003; **5**: 185-188
16 **Chiu CJ,** McArdle AH, Brown R, Scott HJ, Gurd FN. Intestinal mucosal lesion in low-flow states. I. A morphological, hemodynamic, and metabolic reappraisal. *Arch Surg* 1970; **101**: 478-483
17 **Okur H,** Kucukaydin M, Kose K, Kontas O, Dogam P, Kazez A. Hypoxia-induced necrotizing enterocolitis in the immature rat: the role of lipid peroxidation and management by vitamin E. *J Pediatr Surg* 1995; **30**: 1416-1419
18 **McCoy HH,** Berseth CL. Perinatal asphxia alters neonatal intestinal motility in term infants. *Pediatr Res* 1991; **29**: 108
19 **Berseth CL,** McCoy HH. Birth asphyxia alters neonatal intestinal motility in term neonates. *Pediatrics* 1992; **90**: 669-673
20 **Sun M,** Han YK, Zhang H. Blood gastrin and motilin concentration in term newborn infants after asphyxia. *Zhonghua Erke Zazhi* 1997; **35**: 135-137
21 **Lucas A.** Ontogeny of gut hormones and hormone-related substances. *Acta Paediatr Scand Suppl* 1989; **351**: 80-87
22 **Sun M,** Wang WL, Wang W, Wen DL, Zhang H, Han YK. Gastroesophageal manometry and 24-hour double pH monitoring in neonates with birth asphyxia. *World J Gastroenterol* 2001; **7**: 695-697
23 **Fu JH,** Xue XD. Changes of free radical of liver and intestine in

premature rat with hyperoxia-induced chronic lung disease. *Shijie Huaren Xiaohua Zazhi* 2004; **12**: 105-107
24 **Taupin D,** Podolsky DK. Trefoil factors: initiators of mucosal healing. *Nat Rev Mol Cell Biol* 2003; **4**: 721-732
25 **Fernandez-Estivariz C,** Gu LH, Gu L, Jonas CR, Wallace TM, Pascal RR, Devaney KL, Farrell CL, Jones DP, Podolsky DK, Ziegler TR. Trefoil peptide expression and goblet cell number in rat intestine: effects of KGF and fasting-refeeding. *Am J Physiol Regul Integr Comp Physiol* 2003; **284**: R564-R573
26 **Yu K,** Jiang SF, Lin MF, Wu JB, Lin J. Extraction and purification of biologically active intestinal trefoil factor from human meconium. *Lab Invest* 2004; **84**: 390-392
27 **Gibson PR,** Anderson RP, Mariadason JM, Wilson AJ. Protective role of the epithelium of the small intestine and colon. *Inflamm Bowel Dis* 1996; **2**: 279-302
28 **Miyachi K,** Fritzler MJ, Tan EM. Autoantibody to a nuclear antigen in proliferating cells. *J Immunol* 1978; **121**: 2228-2234
29 **Hall PA,** Levison DA, Woods AL, Yu CC, Kellock DB, Watkins JA, Barnes DM, Gillett CE, Camplejohn R, Dover R. Proliferating cell nuclear antigen (PCNA) immunolocalization in paraffin sections: an index of cell proliferation with evidence of deregulated expression in some neoplasms. *J Pathol* 1990; **162**: 285-294
30 **Tsurimoto T.** PCNA binding proteins. *Front Biosci* 1999; **4**: D849-D858
31 **Ioachim E,** Assimakopoulos D, Goussia AC, Peschos D, Skevas A, Agnantis NJ. Glycoprotein CD44 expression in benign, premalignant and malignant epithelial lesions of the larynx: an immunohistochemical study including correlation with Rb, p53, Ki-67 and PCNA. *Histol Histopathol* 1999; **14**: 1113-1118
32 **Feng FC,** Huang W, Wang JD. Clinical significance of P53 protein and PCNA expression in gastric carcinomar tissues. *Xin Xiaohuabingxue Zazhi* 1997; **5**: 624-625
33 **Zhao ZQ,** Liu FL, Zhang L. Expressions of c-fos, PCNA and Bax in intestine after ischemia and reperfusion in dogs. *Shijie Huaren Xiaohua Zazhi* 2001; **9**: 1021-1026
34 **Peng X**, Wang SL, Tao LH, Wang FJ, Zhao Y, Wang P. Relationship of intestinal trefoil factor expression with intestinal damage and reparation in rats after severe burns. *Disan Junyidaxue Xuebao* 2000; **22**: 1023-1025
35 **Taupin DR,** Pang KC, Green SP, Giraud AS. The trefoil peptides spasmolytic polypeptide and intestinal trefoil factor are major secretory products of the rat gut. *Peptides* 1995; **16**: 1001-1005
36 **Kou RQ,** Wang W, Li LY, Ru BG. Precautionary and therapeutic effect of recombinant human intestinal trefoil factor on hydrochloric acid-induced gastric ulcer in rats. *Zhongguo Yaolixue Tongbao* 2000; **16**: 178-181
37 **Chen LP,** Zhang BH, Li Y, Mai GR, Liu ZX. The effect and significance of intestinal trefoil factor IL-8 and MDA for neonatal rat model for hypoxia-induced intestinal injury. *Zhonghua Weichanyixue Zazhi* 2003; **9**: 306-309
38 **Mashimo H,** Wu DC, Podolsky DK, Fishman MC. Impaired defense of intestinal mucosa in mice lacking intestinal trefoil factor. *Science* 1996; **274**: 262-265
39 **Babyatsky MW,** deBeaumont M, Thim L, Podolsky DK. Oral trefoil peptides protect against ethanol- and indomethacin-induced gastric injury in rats. *Gastroenterology* 1996; **110**: 489-497
40 **Poulsom R,** Begos DE, Modlin IM. Molecular aspects of restitution: functions of trefoil peptides. *Yale J Biol Med* 1996; **69**: 137-146
41 **Zhang BH,** Yu HG, Sheng ZX, Luo HS, Yu JP. The therapeutic effect of recombinant human trefoil factor 3 on hypoxia-induced necrotizing enterocolitis in immature rat . *Regul Pept* 2003; **116**: 53-60

Science Editor Wang XL and Li WZ **Language Editor** Elsevier HK

PO Box 2345, Beijing 100023, China
www.wjgnet.com
wjg@wjgnet.com

ELSEVIER

World J Gastroenterol 2005;11(15):2296-2305
World Journal of Gastroenterology ISSN 1007-9327

• *BASIC RESEARCH* •

Identification of expressed genes in regenerating rat liver in 0-4-8-12 h short interval successive partial hepatectomy

Cun-Shuan Xu, Jin-Yun Yuan, Wen-Qiang Li, Hong-Peng Han, Ke-Jin Yang, Cui-Fang Chang, Li-Feng Zhao, Yu-Chang Li, Hui-Yong Zhang, Salman Rahman, Jing-Bo Zhang

Cun-Shuan Xu, Hong-Peng Han, Jin-Yun Yuan, Cui-Fang Chang, Ke-Jin Yang, Li-Feng Zhao, College of Life Science, Henan Normal University, Xinxiang 453002, Henan Province, China
Salman Rahman, Homophilia Research Center, London University, London SE17EH, UK
Wen-Qiang Li, Yu-Chang Li, Hui-Yong Zhang, Jing-Bo Zhang, State Key Laboratory of Cell Differentiation and Regulation of Henan Province and Ministry, Xinxiang 453002, Henan Province, China
Supported by the National Natural Science Foundation of China, No. 30270673 and National Key Laboratory Funds, China
Correspondence to: Professor Cun-Shuan Xu, College of Life Science, Henan Normal University, Xinxiang 453002, Henan Province, China. xucs@x263.net
Telephone: +86-373-3326001 Fax: +86-373-3326524
Received: 2004-03-11 Accepted: 2004-05-29

Abstract

AIM: To identify the genes differentially expressed in the regenerating rat liver of 0-4-8-12 h short interval successive partial hepatectomy (SISPH) and to analyze their expression profiles.

METHODS: Five hundred and fifty-one elements screened from subtractive cDNA libraries were made into a cDNA microarray (cDNA chip). Extensive gene expression analysis following 0-4-8-12 h SISPH was conducted by microarray.

RESULTS: One hundred and eighty-three elements were selected, which were either up- or down-regulated more than 2-fold at one or more time points after SISPH. Cluster analysis and generalization analysis showed that there were five distinct temporal patterns of gene expression. Eighty-six genes were unreported, associated with liver regeneration (LR).

CONCLUSION: Microarray analysis shows that the down regulated genes are much more than the up-regulated ones in SISPH; the numbers of genes expressed consistently are fewer than that expressed immediately; the genes expressed in high abundance are much fewer than that increased 2-5-fold. The comparison of SISPH with partial hepatectomy (PH) shows that the expression trends of most genes in SISPH and in PH are similar, but the expression of 43 genes is specifically altered in SISPH.

Key words: SISPH; Liver regeneration

Xu CS, Yuan JY, Li WQ, Han HP, Yang KJ, Chang CF, Zhao LF, Li YC, Zhang HY, Rahman S, Zhang JB. Identification of expressed genes in regenerating rat liver in 0-4-8-12 h short interval successive partial hepatectomy. *World J Gastroenterol* 2005; 11(15): 2296-2305
http://www.wjgnet.com/1007-9327/11/2296.asp

INTRODUCTION

Liver has a capacity to regain original mass after partial hepatectomy (PH)[1-6]. It was confirmed that a great deal of genes participate in liver regeneration (LR), and the genes expressed in the different phases of LR were various, and that hepatocytes progressing from G_0 phase to G_1 phase occurred in 2-6 h after PH[7,8]. Despite numerous related papers, it is still not thoroughly elucidated how many genes participate in LR and what its molecular mechanism is[9-15]. To get sight into the mechanism of LR, we established the short interval successive partial hepatectomy (SISPH) model[16], which could offer the useful materials for studying specific gene expression at various crucial points of LR[17,18]. To seek some novel differential display genes responsible for LR, the method of subtracted suppression hybridization was used to obtain a bulk of up-regulated and down-regulated expression sequence tags (ESTs) in the regenerating rat liver. With development of cDNA microarray technology, genomewide expression of thousands and thousands of activated or suppressed genes can be simultaneously analyzed under various biological conditions[19-21]. To further explore the genes participating in LR, the present study successfully identified the gene expression profile in regenerating liver following 0-4-8-12 h SISPH by microarray, and some important information was achieved by analyzing the data using Microsoft Excel and GeneSpring.

MATERIALS AND METHODS

Rat model of SISPH

Male and female Sprague-Dawley (SD) rats, aged 10-12 wk, weighting 200-220 g, were raised in Experimental Animal Center of Henan Normal University (HNU). According to Xu *et al*, lobus external sinister, lobus centralis sinister, lobus centralis and lobus dexter were removed one by one at four different time points of 0, 4, 8, 12 h, which is named as 0-4-8-12 h SISPH.

Sample preparation and RNA isolation

The removed liver lobus was rinsed in cold 1×PBS and

immersed and stored in -80 ℃ refrigerator for RNA and protein extraction. Total RNA was isolated from frozen liver lobus according to the manual of TRIzol kit of Invitrogen. In brief, 50-100 mg liver tissue was homogenized in 1 mL TRIzol reagent containing phenol and guanidinium isothiocyanate/cationic detergent, followed by phenol-chloroform extraction and isopropyl alcohol precipitation. The quantity and integrity of total RNA was examined by ultraviolet spectrometer and denaturing formaldehyde agarose electrophoresis stained by ethidium bromide.

Subtracted cDNA library construction and screening

cDNA subtracted libraries were generated from total RNA by PCR-Select™ cDNA Subtraction kit (Clontech) following the manufacturer's instruction. Briefly, total RNA was transcribed into double cDNA strands and digested with restriction enzymes, followed by subtracted hybridization with drivers and testers. Finally with suppression polymerase chain reaction (PCR), differential ESTs were used to construct subtracted cDNA library. The latter was cloned into T/A vector and screened by PCR with nested primer 1 and 2.

cDNA microarray construction

cDNA fragments amplified by PCR with nested PCR primers 1 and 2 and purified by NaAc/isopropyl alcohol were spotted onto glass slides (Biostar) with the help of ProSys-5510A spotting machine following designed project. Then the gene chips were ready by hydration and blockage and drying. Totally 1 152 elements (double spot chip) including 50 control system (8 negative control, 12 blank control, 30 internal control) and 551 target genes to be studied comprised 8 submatrixes (12*12) occupying 9 mm×18 mm (Biostar). Then the gene chips were ready by hydration, blockage and drying.

Fluorescence-labeled cDNA preparation

RNA isolated from rat livers before SISPH was ready for a reference for all cDNA microarray analyses. Totally denatured RNA was reversely transcribed with cy3-conjugated dCTP (control group) and cy5-conjugated dCTP (test group) (Amersham-Pharmacia Biotech) using MMLV reverse transcriptase (Promega) with olig (dT) primer. After bath incubation for 2 h, labeled buffer I and II were subsequently added to the reaction. The control group and test group were mingled together symmetrically and stored in the dark until use.

Hybridization and scanning

The glass slices were prehybridized at 42 ℃ for 5-6 h in hybridization buffer containing freshly cooked shared salmon sperm DNA. The labeled denatured probe was hybridized against cDNA microarrays with overnight (16-18 h) incubation at 42 ℃. The slides were then washed twice with 2× SSC containing 0.5% SDS for 5 min at room temperature, once with 0.2× SSC containing 0.5% SDS at 60 ℃ for 10 min, and finally with 0.2× SSC at 60 ℃ for 10 min. The slices were exposed to photographer. Hybridized images were scanned by a fluorescence laser scanning device, Gene Pix 4000A (Axon Instruments, Inc., Foster City, CA). At least two hybridizations were performed at each time point. In addition, a semiquantitative inspection of the hybridization results was performed for (1) green signal (down-regulation); (2) yellow signal (no obvious regulation); (3) red signal (up-regulation).

Data analysis

The cy3 and cy5 signal intensities were quantified by Gene Pix Pro 3.0 software (Axon Instruments, Inc., Foster City, CA). Subsequently, we normalized the obtained numerical data with classical linear regression techniques. In brief, quantified cy3 and cy5 signal intensities were obtained when foreground signal intensities were deducted by background signal intensities and cy5 signal intensities was replaced by 200 when it was <200. When R_i (R_i = cy5/cy3) was between 0.1 and 10, R_i was taken as logarithms base natural to generate R_i'[log (R_i)] and ND was taken by EXP (R) (averaged R_i'). The modified cy3* was generated by ND multiplying cy3 and was replaced by 200 when it was <200. The ratio was expressed by cy5/cy3*. Therefore, we selected genes whose ratio was more than 2 or less than 0.5 representing a 2-fold difference in expression level.

To analyze the selected gene expression data, we applied κ-means cluster analysis, and performed GeneMaths hierarchical clustering to appraise the number of groups. Whole analyses were executed with Microsoft Excel (Microsoft, Redmond, WA) and GeneSpring (Silicon Genetics, San Carlos, CA).

Chromosome location and functional prediction of the novel ESTs

All the clones of ESTs were sequenced by TaKaLa and blasted in NCBI. The unreported ESTs were searched at http://www.ncbi.nlm.nih.gov/genomeguide/rat/index.html/ for gene location in chromosome and gene corresponding whole genome shotgun. In virtue of rat genome database, electronic cloning and chromosome location of the unreported ESTs representing novel cDNA full-length were performed successfully (data not shown). By delivering the clones sequences to http://genes.mit.edu/GENSCAN.html/, we acquired corresponding coding domain sequences (CDS) supported by the ESTs. Compared with known proteins by BLASTP (http://www.ncbi.nlm.nih.gov/BLAST/), their function and accession number were achieved.

RESULTS

Category of genes identified in the 0-4-8-12 h SISPH

One hundred and eighty-three elements altered by more than 2-fold intensity at least at one time point in the 0-4-8-12 h SISPH were identified and selected, of which, 77 were up regulated and 106 were down regulated. Eighty-six of them belonged to the unreported novel genes, and the other 97 were reported, of which quite a few genes had been previously reported to be involved in LR. Following the functions of the reported genes and the time points at which they attained maximum up or down-regulation, they were respectively categorized into 21 groups: the genes involved in stress response, in glycometabolism, in stearoyl metabolism,

in oxidative and reductive response, genes encoding regulation proteins, glycoproteins, lipid-proteins, nucleolar proteins, receptors, factors, hemoglobins, immunological proteises, cytoskelets, marker proteins, amino acid enzymes, proteolytic enzymes, proteinase inhibitors, phosphorylase, phosphatases, synthases and transferases (Table 1).

Table 1 **Genes related to LR altered in SISPH**

No.	Gene description	Fold difference	No.	Gene description	Fold difference
Unreported genes					
1	CH230-206C20	0.3	62	LRRPAb2-132	0.2
2	CH230-403C20	0.5	63	MGC10946	2.8
3	CH230-329D3	2.2	64	MGC38937	2.4
4	CH230-372C24	0.1	65	MGC5178	0.4
5	CH230-7A22	0.1	66	mKIAA0665	2.4
6	CH230-11N5	2.1	67	RIKEN 1300002A08	0.2
7	CH230-4L11	3.5	68	RIKEN 1600027G01	0.3
8	CH230-211F21	0.4	69	RP11-281N10	0.3
9	CH230-155H3	0.5	70	RP11-586K2	2.6
10	CG31759-PA	2.9	71	RP23-100C5	2.0
11	Citb585c7	0.2	72	RP23-165H7	0.5
12	D930042H13	0.3	73	RP23-235O1	0.4
13	DNA segment of Chr 1 (Wsu94)	3.8	74	RP23-28G130	2.3
14	DNA segment of Chr 17 (Wsu94)	2.0	75	RP23-32O9	2.3
15	KIAA0205	0.4	76	RP23-417P22	0.3
16	KIAA1376	0.4	77	RP23-476D16	1.6
17	LOC303588	2.0	78	RP23-480P21	2.9
18	LOC333273	2.9	79	RP23-92K11	2.9
19	LRRP Cc1-27	0.3	80	RP24-347B22	0.3
20	LRRP Aa2-028	3.1	81	Rp32-28p17	0.3
21	LRRP Aa2-111	0.2	82	U48828	2.4
22	LRRP Aa2-174	0.3	83	Adult male liver cDNA	0.1
23	LRRP Aa2-258	0.5	84	Mouse mRNA	0.4
24	LRRP Ab1-021	9.1	85	Open reading frame 31	0.5
25	LRRP Ab1-022	0.5	**86**	**13 d embryo liver cDNA**	3.6
26	LRRP Ab1-114	3.5	Stress response		
27	LRRP Ab1-216	3.5	87	Acute-phase protein alpha-1-inhibitor 3	0.3
28	LRRP Ab1-334	4.4	88	alpha-1 major acute phase protein prepeptide	6.8
29	LRRP Ab2-001	0.3	89	Angiotensinogen (Agt)	11.5
30	LRRP Ab2-034	0.3	90	Kininogen	2.5
31	LRRP Ab2-037	0.5	91	T-kininogen (Kng)	5.0
32	LRRP Ab2-051	2.1	Glycometabolism		
33	LRRP Ab2-131	0.3	92	alpha enolase (Enolase 1)	2.7
34	LRRP Ab2-132	0.4	93	Isocitrate dehydrogenase 1 (Idh1)	0.1
35	LRRP Ab2-225	0.3	94	3-Phosphoglycerate dehydrogenase	2.2
36	LRRP Ab2-232	0.2	Fatty and stearoyl metabolism		
37	LRRP Ab2-255	0.2	95	Bile acid CoA ligase	2.0
38	LRRP Ab2-371	0.1	96	Malonyl-CoA decarboxylase	0.4
39	LRRP Ab2-389	0.5	97	Methylmalonate semialdehyde dehydrogenase	0.4
40	LRRP Ab2-402	0.2	98	P450 cholesterol 7-alpha-hydroxylase (P450 VII)	0.1
41	LRRP Ab2-416	0.3	99	NAD (P) dependent steroid dehydrogenase	0.1
42	LRRP Ab2-417	0.2	100	3-alpha-hydroxysteroid dehydrogenase	0.1
43	LRRP Ab2-427	0.5	Oxidation and reduction		
44	LRRP Ab2-440	0.3	101	Acyl-coA oxidase	0.5
45	LRRP Ac1-060	0.3	102	Alcohol dehydrogenase (ADH)	0.1
46	LRRP Ac1-158	2.1	103	Cytochrome b5 (Cyb5)	0.3
47	LRRP Ac1-177	7.3	104	Cytochrome P450	0.3
48	LRRP Ac1-233	5.6	105	Cytochrome P450 15-beta gene (Cyp2c12)	0.4
49	LRRP Ac1-873	4.6	106	Cytochrome P450 2E1	0.2
50	LRRP Ac2-061	6.4	107	Cytochrome P450, 2c39 (Cyp2c39)	0.3
51	LRRP Ac2-067	2.6	108	Cytochrome P450 (PNCN inducible, Cyp3A1)	0.4
52	LRRP Ac2-143	2.0	109	Flavin-containing monooxygenase 1 (Fmo1)	0.1
53	LRRP Ac2-210	2.3	110	Peroxisomal sarcosine oxidase (PSO)	0.1
54	LRRP Ba1-647	3.3	111	Plasma selenoprotein P1 (Sepp1)	0.4
55	LRRP Bm403207	7.7	112	Small subunit precursor of RuBPCase	0.1
56	LRRP Cb1-727	0.4	Regulation proteins		
57	LRRP Cb1-739	2.2	113	G-protein beta polypeptide 2-like 1 (Gnb2l1)	2.1
58	LRRP Cc1-27	0.3	114	II-Protein with tetratricopeptide repeats 3	0.2
59	LRRP Cc1-38	0.1	115	RAKb	0.2
60	LRRP Cc1-9	3.5	Glycoproteins		
61	LRRP zbs559	3.5	116	apha-1-B glycoprotein (A1bg)	0.3

117 Fibronectin 1 (Fn1)	3.0
118 Fibrinogen, gamma polypeptide (Fgg)	8.0
119 Myelin-associated glycoprotein (L-MAG)	8.4
120 UDP-glucuronosyltransferase 2B3 (Udpgt)	0.4
121 TRAM1	0.3
Lipid-proteins	
122 Adipose differentiation-related protein	4.6
123 Solute carrier family 20, mem 1 (Slc20a1)	0.4
Nucleolar proteins	
124 Damage-specific DNA binding protein 1 (Ddb1)	0.5
125 Nuclear protein 1 (Nupr1)	2.9
126 Nucleolar protein family A, mem 2	2.9
127 ORF2 endonuclease and Rnase H	0.5
128 RNase A family 4	0.3
Receptors	
129 ATP-binding cassette, sub-family B	0.5
130 ATP-binding cassette, sub-family C	0.1
131 Interleukin 1 receptor, type I (Il1r1)	7.3
132 Nuclear receptor subfamily 0, member 2 (Nr0b2)	0.4
Factors	
133 Amphoterin	0.5
134 Angiogenin	0.4
135 Eukaryotic translation initiation factor 4A1	3.5
136 Early growth response factor 1 (Egr1)	4.3
137 Neuropeptide Y (Npy)	11.3
138 NF-E2-related factor 2 (Nfe2l2)	0.3
139 Pre-B-cell colony-enhancing factor (Pbef)	5.3
140 ADP-ribosylation factor 3 (Arf3)	0.8
141 Angiopoietin-like 3	0.3
Hemoglobins	
142 Hemoglobin, alpha 1 (Hba1)	2.4
143 Hemoglobin beta chain (Hbb)	2.5
Immunological proteises	
144 Achaete-scute complex homolog-like 1 (Ascl1)	0.4
145 Complement component 5 (C5)	19.4
146 Complement component 6 (C6)	0.4
147 Immunoglobulin C kappa gene	0.3
148 JE/MCP-1	2.5
Cytoskelets	
149 Actin -beta	2.3
150 Actin gamma	5.1
151 Keratin 8 (Krt8)	2.8
Marker proteins	
152 alpha globin	2.4
153 Amyloid a-5 protein	53.9
154 Subchromosomal transferable fragment	0.4
Amino acid enzymes	
155 Arginase 1 (Arg1)	6.4
156 Argininosuccinate lyase (Asl)	5.6
157 Cytosolic aspartate aminotransferase	6.8
158 2-Hydroxyphytanoyl-CoA lyase (Hpcl2)	0.3
Proteolytic enzymes	
159 Cathepsin C (Ctsc)	0.4
160 Cathepsin D (Ctsd)	0.5
161 Coagulation factor 2 (F2)	0.5
162 Neutrophil collagenase (Mmp8)	0.2
Proteinase inhibitors	
163 alpha-2-macroglobulin (A2m)	5.1
164 alpha-trypsin inhibitor heavy chain	0.4
165 Contrapsin-like protease inhibitor related protein	6.1
166 Leuserpin-2 (Serpind1)	0.3
167 Serine protease inhibitor 1	5.6
Phosphorylase	
168 CDK103	1.2
169 Purine-nucleoside phosphorylase	0.3
Phosphatases	
170 Phosphatidylserine-specific phospholipase A1	4.9
171 Pyrophosphatase/phosphodiesterase 1(Enpp1)	3.1
172 Protein phosphatase 1 (GL-subunit)	0.2
Synthase	
173 Carbamyl phosphate synthetase I	2.5
174 Fatty acid elongase 1 (rELO1)	0.1
175 Glutamyl-prolyl-tRNA synthetase (Eprs)	2.2
176 RNA cyclase	2.0
Transferases	
177 Glutathione *S*-transferase, alpha 1 (Gsta1)	0.3
178 Glutathione *S*-transferase, type 3 (Yb3) (Gstm3)	0.5
179 Glutathione *S*-transferase Y(b) subunit	0.5
180 Serine hydroxymethyl transferase 1	0.4
181 Sialyltransferase 1 (Siat1)	0.2
182 Sulfotransferase K2	0.2
183 UDP-glucuronosyltransferase 2, mem 5 (Ugt2b5)	0.5

Gene expression differences at the various time points of the 0-4-8-12 h SISPH

The gene expression differences induced or suppressed at 4, 4-8, 4-12, 8, 8-12 h of SISPH are shown in Figure 1. At 4 h of SISPH, 5 genes expressed up over 2-fold (Figure 1A); at 4-8 h of SISPH, 2 genes expressed up over 2-fold (Figure 1A); at 4-12 h of SISPH, 29 genes expressed up (Figures 1B-E), of which 10 genes up over 5-fold (Figure 1B), and 7 genes up over 10-fold (Figure 1C), and 10 genes expressed down (Figures 1D and E); at 8 h of SISPH, 2 genes expressed up (Figure 1G) and 7 genes down (Figure 1F); at 8-12 h of SISPH, 25 genes expressed down (Figures 1H and I).

Gene expression level in the 0-4-8-12 h SISPH

According to the up- and down-regulated density of genes in the 0-4-8-12 h SISPH, we categorized them into three groups: (1) 106 genes were down-regulated by less than 50% (Figure 2A); (2) 54 genes were up-regulated by 2-5-fold (Figure 2B); (3) 23 genes were strongly up-regulated by more than 5-fold (Figure 2C).

Hierarchical cluster analysis of genes expressed in the 0-4-8-12 h SISPH

The expression profile of the 183 genes altered by more than a 2-fold intensity at least at one time point in the 0-4-8-12 h SISPH was emanative to the last time point, which indicated that LR at 12 h has not been completed yet, quite active on the contrary (Figure 3A). We undertook hierarchical clustering of four time points 0, 4, 8 and 12 h of SISPH using GeneSpring software and discovered that gene expression profiles had no similarity between the four time points (Figure 3B). To facilitate the visualization and interpretation of the gene expression program represented in this very large body of data, we used the method of κ-means to order genes on the basis of similarities in their expression patterns and displayed the results in a compact graphical format, generating seven kinds of ramose gene expression clusters (Figure 3C). We then categorized the 183 elements into five distinct temporal induction or suppression patterns following immediate induction, late induction, consistent induction, late suppression, consistent suppression (Figure 3D).

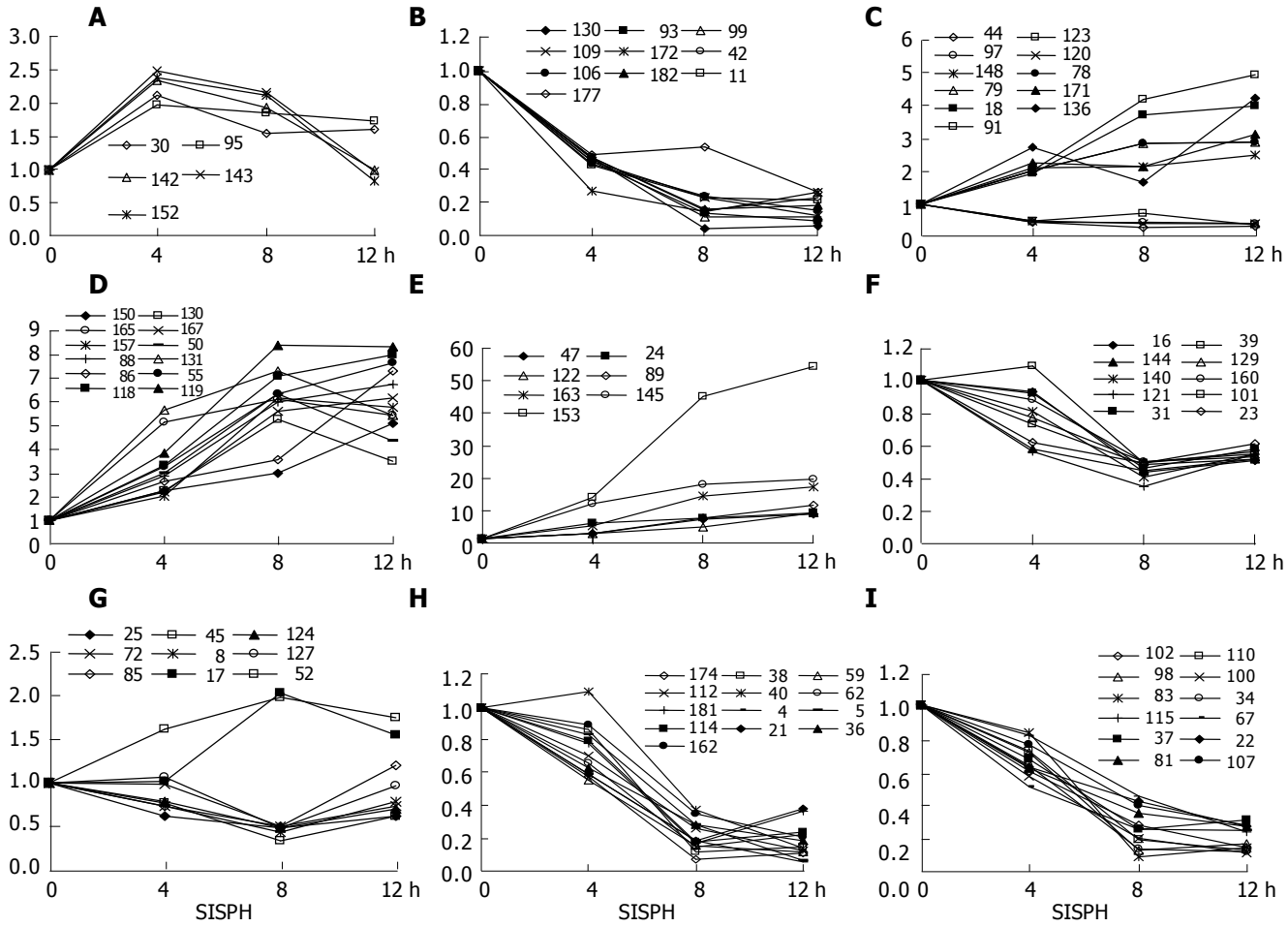

Figure 1 Gene expression differences in 0-4-8-12 SISPH. **A**: 4 h, 4-8 h; **B-E**: 4-12 h; **F** and **G**: 8 h; **H** and **I**: 8-12 h.

Comparison of gene expression in SISPH with that in PH

Comparing gene expression profile in SISPH with that in PH, we discovered that 43 genes were specially induced by SISPH, and the expression of 140 genes were altered simultaneously in both SISPH and PH, but the time points of their expression and extent of up- and down-regulation were different (Table 2).

DISCUSSION

This study found that hemoglobin alpha and beta were immediately induced to synthesize in the residual liver at 4 h in SISPH and after PH and returned to normal level there after, and that the activity peak of bile acid CoA ligase appeared at the same time, indicating a role of hemoglobin and amino acids transport in early phase of LR[22,23].

Thirty-six genes were up-regulated and reached a maximum level at 8 h in SISPH, and then were down regulated, in which 18 were unreported new genes and 18 were reported genes, with little knowledge about their relationship with LR. These results showed that their expression products could be necessary for the initiation of S phase. Myelin-associated glycoprotein-binding activity of novel sulfated GM1b, high-affinity ligands for neural siglecs

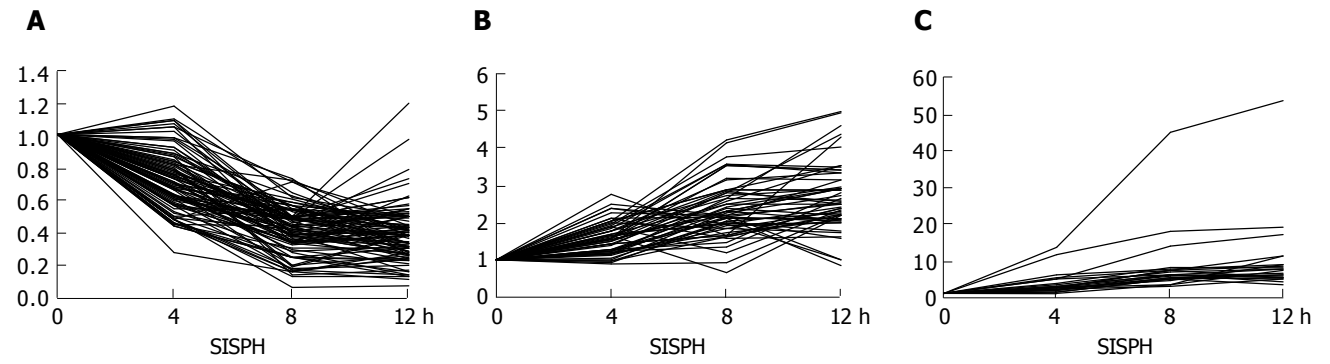

Figure 2 Expression level of genes in the 0-4-8-12 h SISPH. **A**: Down-regulated genes; **B**: up-regulated genes; **C**: strong up-regulated genes.

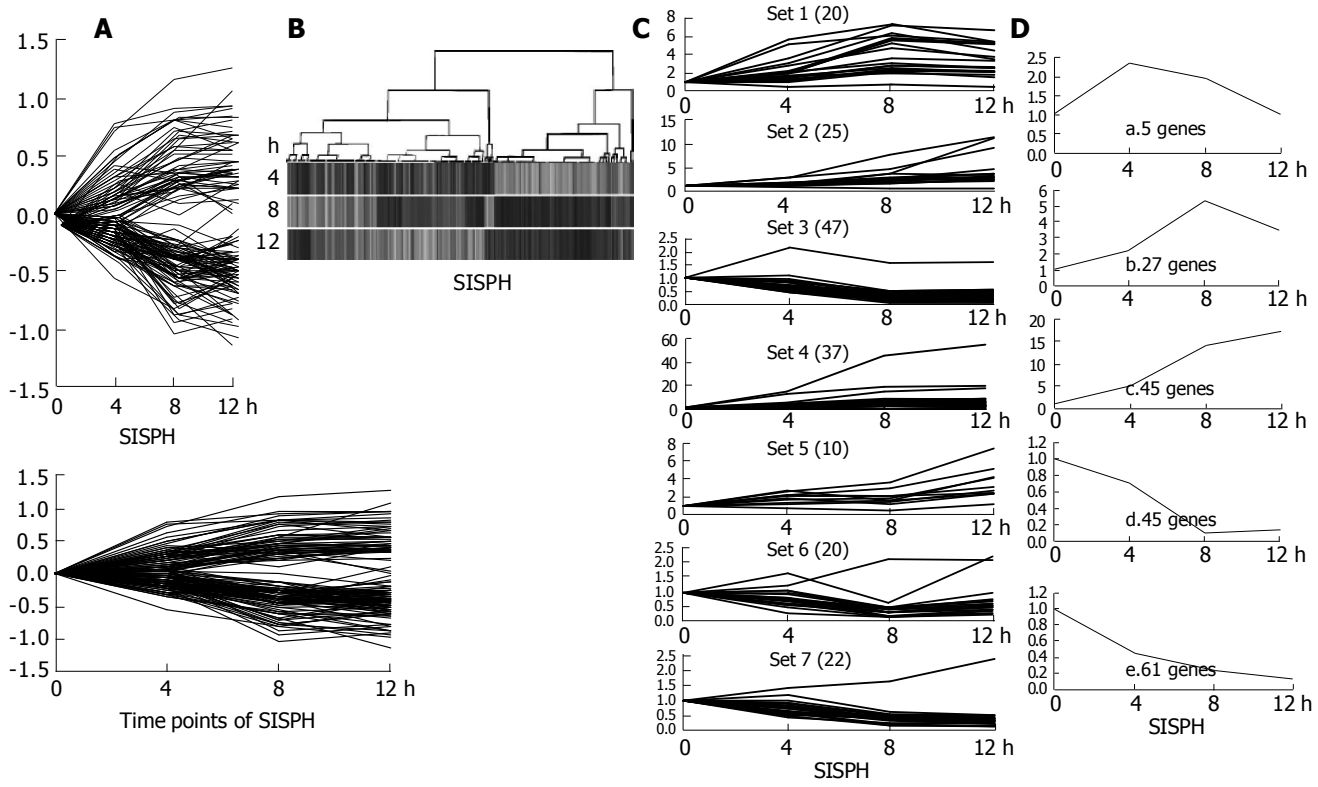

Figure 3 Cluster analysis of 185 elements. **A**: The difference of their intensity was identified more than 2-fold at least at one time point; **B**: A hierarchical clustering of five time points indicated that the genes in these time points hardly had a common expression profile; **C**: The k-means method was used and these genes were classified into seven clusters; **D**: Five distinct temporal patterns were designated. a. Immediate induction; b. Late induction; c. Consistent induction; d. Late suppression; e. Consistent suppression.

is reported important to nerve system regeneration[24]. It may be available to repair liver or hepatocytes damage caused by SISPH. A CPi-21 encoded by contrapsin-like protease inhibitor is found to inhibit the proteolysis of Edman to glycosylation proteins[25]. Abrupt increase of CPi-21 is presumed to be beneficial to cell adherence in SISPH, in which it was severely destroyed. Aspartate amino transformation reaction catalyzed by aspartate aminotransferase is necessary for accommodated purine, indicating liver cells need a great deal of purine for DNA synthesis in SISPH and after PH. Pre-B-cell colony-enhancing factor is known up regulated in the infected fetal membranes[26], which was continuously induced in the early phase of SISPH and PH, and lately suppressed, suggesting that it is associated with recovery of damage in LR. Translation initiation factor eIF-4A1 is reportedly over expressed in human melanoma cells[27], whose abundant expression in SISPH shows that it may participate in protein synthesis in LR.

Forty-five genes were consistently up regulated and reached a maximum level at 12 h in SISPH, in which 21 were unreported new genes, and the others were reported genes, but whether they have relationship with LR is unknown yet. JE/MCP-1 is known as a CC chemokine attracting monocytes, basophils and T-lymphocytes responsible for IL-1β and TNF-α[28,29]. Its consistent induction is assumed to be involved in relinquishing inflammation caused by SISPH. It was confirmed that keratin 8 could form characteristically intermediate filaments of liver and internal epithelia, including derivative cancers, whose consistent induction may help maintain hepatocyte structural and functional integrity following trauma after SISPH. T-kininogen is important in the acute phase response to trauma as a cysteine proteinase inhibitor[30]. IL-6 is confirmed to act as a direct hepatic mitogen and potent liver growth factor with potential clinical utility for increasing liver mass following injury[31]. The augment of T-kininogen and kininogen level in SISPH and PH may reveal that there is an increasing response of kininogen promoter to IL-6 as an LR signal. Serum amyloid α-5 protein, precursor of serum amyloid A, was successively and dramatically up-regulated for more than 50-fold in SISPH and PH, probably on account of IL-6 simulation in LR[32], indicating that they have some positive role in LR, which is worth studying. Angiotensinogen is already known to be induced by TNF-NFκB and the IL-6-STAT3 signaling pathways in PHx[33], whose level was consistently increased by 11-fold in SISPH, implying a role in avoiding excessive loss of hepatic blood in LR. The successive increase of G-protein in SISPH and PH suggests that DNA synthesis by cAMP in hepatocytes are largely activated for LR[34]. The ensuing variations of cAMP levels are supposed to modulate both growth and differentiated functions during LR of SISPH. The advanced transcription level of enolase 1 (α-enolase) is supposed to provide sufficient VEGF for LR of SISPH. Activity and marked content increase of arginase in the previous period of regenerating liver co-ordinated with other urea cycles' enzymes[35,36]. The consistent induction of glutamyl-prolyl-tRNA synthetase (Eprs) may indicate that there is a great demand for glutamyl to induce anti-toxin in LR after SISPH. NPY localized exclusively to hepatic vascular walls is conceived

Table 2 **Comparison of difference of gene expression in SISPH with that in PH**

Gene description	Change		Gene description	Change	
	SISPH	PH		SISPH	PH
Unreported genes					
CH230-206C20	0.3	0.3	Isocitrate dehydrogenase 1 (Idh1)	0.1	0.2
CH230-403C20	0.5	0.2	Fatty and stearoyl metabolism		
CH230-372C24	0.1	0.1	Bile acid CoA ligase	2.0	2.3
CH230-7A22	0.1	0.1	Malonyl-CoA decarboxylase	0.4	0.3
CH230-11N5	2.1	4.5	Methylmalonate semialdehyde dehydrogenase	0.4	0.2
CH230-4L11	3.5	4.5	3-alpha-hydroxysteroid dehydrogenase	0.1	0.2
CG31759-PA	2.9	0.5	Oxidation and reduction		
D930042H13	0.3	0.3	Alcohol dehydrogenase (ADH)	0.1	0.1, 2.4
LRRP Cc1-27	0.3	0.3, 2.1	Cytochrome b5 (Cyb5)	0.3	0.2
LRRP Aa2-028	3.1	3.0	Cytochrome P450	0.3	0.2
LRRP Aa2-174	0.3	0.1	Cytochrome P450 15-beta gene (Cyp2c12)	0.4	0.2
LRRP Ab1-021	9.1	10.0	Cytochrome P450 2E1	0.2	0.1
LRRP Ab1-022	0.5	8.1	Cytochrome P450, 2c39 (Cyp2c39)	0.3	0.1
LRRP Ab1-114	3.5	4.2	Cytochrome P450 (PNCN inducible, Cyp3A1)	0.4	0.2
LRRP Ab1-216	3.5	6.8	Flavin-containing monooxygenase 1 (Fmo1)	0.1	0.1
LRRP Ab1-334	4.4	2.7	Peroxisomal sarcosine oxidase (PSO)	0.1	0.1
LRRP Ab2-001	0.3	0.2	Plasma selenoprotein P1 (Sepp1)	0.4	0.3
LRRP Ab2-132	0.4	0.1	Small subunit precursor of RuBPCase	0.1	0.1, 3.3
LRRP Ab2-225	0.3	0.3	Regulation proteins		
LRRP Ab2-232	0.2	0.2	G-protein beta polypeptide 2-like 1 (Gnb2l1)	2.1	2.4
LRRP Ab2-371	0.1	0.4	II-Protein with tetratricopeptide repeats 3	0.2	0.2
LRRP Ab2-402	0.2	0.1	RAKb	0.2	0.2
LRRP Ab2-417	0.2	0.2	Glycoproteins		
LRRP Ab2-427	0.5	0.4	apha-1-B glycoprotein (A1bg),	0.3	0.3
LRRP Ab2-440	0.3	0.3	Fibronectin 1 (Fn1)	3.0	7.2
LRRP Ac1-060	0.3	0.4, 2.3	Fibrinogen, gamma polypeptide (Fgg)	8.0	5.1
LRRP Ac1-177	7.3	0.5, 4.9	Myelin-associated glycoprotein (L-MAG)	8.4	0.3
LRRP Ac1-233	5.6	4.2	UDP-glucuronosyltransferase 2B3 (Udpgt)	0.4	0.3
LRRP Ac1-873	4.6	0.3	TRAM1	0.3	0.4, 3.3
LRRP Ac2-061	6.4	7.6	Lipid-proteins		
LRRP Ac2-067	2.6	2.5	Adipose differentiation-related protein	4.6	7.3
LRRP Ac2-143	2.0	3.3	Solute carrier family 20, mem1 (Slc20a1)	0.4	0.4
LRRP Ac2-210	2.3	2.4	Nucleolar proteins		
LRRP Ba1-647	3.3	3.2	Damage-specific DNA binding protein 1 (Ddb1)	0.5	0.3
LRRP Bm403207	7.7	2.9	Nuclear protein 1 (Nupr1)	2.9	0.5, 5.1
LRRP Cb1-739	2.2	2.3	Nucleolar protein family A, mem 2	2.9	3.9
LRRP Cc1-27	0.3	0.1, 2.2	ORF2 endonuclease and Rnase H	0.5	0.4
LRRP Cc1-38	0.1	0.2	RNase A family 4	0.3	0.2
LRRP Cc1-9	3.5	3.6	Receptors		
LRRP zbs559	3.5	3.1	ATP-binding cassette, sub-family C	0.1	0.2
LRRPAb2-132	0.2	0.1	Interleukin 1 receptor, type I (Il1r1)	7.3	7.9
MGC10946	2.8	2.8	Nuclear receptor subfamily 0, member 2 (Nr0b2)	0.4	0.2
MGC5178	0.4	0.4	Factors		
RIKEN 1300002A08	0.2	0.3, 2.4	Amphoterin	0.5	0.3
RIKEN 1600027G01	0.3	0.1	Angiogenin	0.4	0.2
RP11-281N10	0.3	0.2	Eukaryotic translation initiation factor 4A1	3.5	3.8
RP23-100C5	2.0	3.0	Early growth response factor 1 (Egr1)	4.3	3.5
RP23-235O1	0.4	0.2	Neuropeptide Y (Npy)	11.3	18.1
RP23-32O9	2.3	2.8	NF-E2-related factor 2 (Nfe2l2)	0.3	0.4
RP23-417P22	0.3	0.1	Pre-B-cell colony-enhancing factor (Pbef)	5.3	3.3
Rp32-28p17	0.3	0.3	Angiopoietin-like 3	0.3	0.2
U48828	2.4	0.2	Hemoglobins		
Open reading frame 31	0.5	0.3, 2.8	Hemoglobin, alpha 1 (Hba1)	2.4	0.3
13 d embryo liver cDNA	3.6	5.9	Hemoglobin beta chain (Hbb)	2.5	0.3
Stress response			Immunological proteises		
alpha-1 major acute phase protein prepeptide	6.8	66.4	Complement component 5 (C5)	19.4	16.5
Angiotensinogen (Agt)	11.5	8.4	Immunoglobulin C kappa gene	0.3	0.3
Kininogen	2.5	5.9	JE/MCP-1	2.5	4.0
T-kininogen (Kng)	5.0	0.2	Cytoskelets		
Glycometabolism			Actin gamma	5.1	4.8
Alpha enolase (Enolase 1)	2.7	3.9	Keratin 8 (Krt8)	2.8	3.8

Marker proteins			Contrapsin-like protease inhibitor related protein	6.1	6.6
Amyloid a-5 protein	53.9	90.4	Leuserpin-2 (Serpind1)	0.3	0.2
Subchromosomaltransferable fragment	0.4	0.3, 2.4	Serine protease inhibitor 1	5.6	5.0
Amino acid enzymes			Phosphatases		
Arginase 1 (Arg1)	6.4	3.5	Phosphatidylserine-specific phospholipase A1	4.9	2.8
Argininosuccinate lyase (Asl)	5.6	4.9	Pyrophosphatase/phosphodiesterase1(Enpp1)	3.1	5.0
Cytosolic aspartate aminotransferase	6.8	7.4	Protein phosphatase1 (GL-subunit)	0.2	0.2
2-Hydroxyphytanoyl-CoA lyase (Hpcl2)	0.3	0.4	Synthase		
Proteolytic enzymes			Carbamyl phosphate synthetase I	2.5	2.9
Cathepsin C (Ctsc)	0.4	0.4	Glutamyl-prolyl-tRNA synthetase (Eprs)	2.2	4.5
Cathepsin D (Ctsd)	0.5	0.3	RNA cyclase	2.0	0.2
Coagulation factor 2 (F2)	0.5	0.2	Transferases		
Neutrophil collagenase (Mmp8)	0.2	0.2	Glutathione *S*-transferase, alpha 1 (Gsta1)	0.3	0.1
Proteinase inhibitors			Glutathione *S*-transferase, type 3 (Yb3) (Gstm3)	0.5	0.3, 2.2
alpha-2-macroglobulin (A2m)	5.1	21.3	Glutathione *S*-transferase Y(b) subunit	0.5	0.3
alpha-trypsin inhibitor heavy chain	0.4	0.2	UDP-glucuronosyltransferase 2 , mem 5 (Ugt2b5)	0.5	0.3

and involved in more complex physiological response[37]. The ascending mRNA level in SISPH was suggested to be correlated to recover damaged vascular walls after hepatectomy. The continuous elevation of nucleolar protein family A and nuclear protein 1 (Nupr1) may ascribe to the need of DNA synthesis for nuclear reconstruction of hepatocytes. The successive induction of alpha 2-macroglobulin, as homotetrimeric protease inhibitor, binding TGF-β family, is premised to participate in restraining protein degradation in SISPH for accumulation of protein and prevention of TGF-β termination for longer LR[38]. Hemoglobin secreted by hepatocytes was replacer of hemachrome in liver without hemachrome[22]. Hemoglobin alpha and beta were always induced by SISPH according to the change in PHx, exerting the same function of hepatocytes nourishment in LR. Fibronectin and fibrinogen gamma polypeptide (Fgg) were all induced abundantly through the process of SISPH for the sake of cell adherence in LR. Compared with normal beta actin which has no obvious change in PHx, mutant beta actin was continuously increased, indicating that house keeping gene is additionally expressed for LR of SISPH.

It was revealed that 45 genes were included in consistent suppression and late induction at 8 h time point, of which 22 are unreported genes and others are reported genes hardly known to be related to LR previously. Trypsin and its substrate are supposed to accelerate hepatocytes regeneration under growth factor, but excessive inhibition by inter alpha-trypsin inhibitor may lead to imbalance of glucose concentration in blood, therefore, there was a late induction at 8 h of SISPH to keep the balance[39]. Commonly, acyl-coA plays many important roles in numerous biochemical reactions, such as tricarboxylic acid cycle, glyoxylate bypass, fatty acid synthesis. As a result, the mRNA level of acyl-coA oxidase is assumed to have dropped to retain the level of fat and glycos vital to LR of SISPH and later ascended to eliminate over expressed acyl-coA. Sialyl is a vital constituent of ganglioside, whose sialyltransferase down-regulation may be intervened to prevent liver from successive injury by SISPH and immigrate to other functional substance in late phase. Mutant glutathione *S*-transferase (GST) mRNA was not always hampered in SISPH, which indicates that its overfull accumulation may lead to opposite reaction in LR. Fatty binding protein is well known to transfer fat from cytoplasm to nuclear or membrane, and fatty acid elongase 1 (rELO1) catalyzes short chain fat transition to long chain fat whose repression of mRNA in SISPH manifested that long chain fat was not badly needed until 12 h in LR. The decrease of purine-nucleoside phosphorylase and phosphatase 1 (GL-subunit) in SISPH may suggest that purine-nucleoside and eser are in demand until 8 h in LR. Nrf2 was reported to lead to antioxidant reaction element to drive gene expression[29], which was suppressed and induced at 8 h, implying that antioxidant reaction was mild in LR of SISPH. Cathepsin D (aspirin endopeptidase) was discovered to participate in basal membrane dissolving, promoting tumor cell migration[40]. The continuous suppression but late induction suggests that basal membrane dissolving was not necessary in early phase of LR of SISPH. Coagulation factor 2 protease inhibitor was supposed to decrease to facilitate blood circulation for LR but at 12-h time point to increase to hamper great loss of blood by SISPH[23]. Damage-specific DNA binding protein was reported to recognize many types of DNA lesions and inducible by DNA damage agent. Its down regulation shows that hepatocytes suffer no severe DNA damage in SISPH, different from other injuries.

Sixty-one genes were consistently suppressed and reached minimum level at 12-h time point of SISPH, of which 22 were novel genes and the others were reported genes that may or may not be related to LR. The genes in the group are presumed to promote LR by various ways. A large number of them are the genes related to energy metabolism, suggesting that the demand for energy in LR of SISPH is not as important as for other demands, differing from partial hepatectomy. The mRNA level of cytochrome P450 2c39 (Cyp2c39), cytochrome P450 2E1, cytochrome b5 (Cyb5), cytochrome P450 15-beta, cytochrome P450, flavin-containing monooxygenase 1 (Fmo1), peroxisomal sarcosine oxidase, malonyl-CoA decarboxylase, methylmalonate semialdehyde dehydrogenase (Mmsdh), alcohol dehydrogenase, microsomal UDP-glucuronosyltransferase 2B3 (Udpgt) are all consistently suppressed from 0 to 12 h of SISPH. The substrate or product of these enzymes related to oxidation and reduction were in urgent need for or toxic to LR, for instance, imine is a cell toxic substance by isocitrate dehydrogenase reaction holding back LR[41]. Angiopoietin-

like protein 3 (Angptl3) is reported to activate lipolysis in adipocytes as a vascular endothelial growth factor by response to the liver X receptor[42]. The sustaining suppression of angiopoietin-like protein 3 mRNA in SISPH suggested that the activity of lipolysis of hepatocytes is very low in LR. Neutrophil collagenase specially degrading type I collagen is generated by osteoblastic progenitors, differentiated osteoblasts, osteocytes, and chondrocytes in the growth plate[43]. The decrease of neutrophil collagenase showed that collagen is in great demand for cell skeletal conformation or osteoblasts, osteocytes and chondrocytes were not distinctly harmed in LR after SISPH. Cathepsin C (dipeptidyl aminopeptidase I) in rat liver was discovered playing significant role in protein degradation and the activation of proenzyme[44]. The decreased mRNA level of cathepsin C was supposed to satisfy requisite of peptide for protein construction in SISPH. 2-Hydroxyphytanoyl-CoA lyase, a peroxisomal pyrophosphate-dependent enzyme, was involved in the carbon-carbon bond cleavage during α-oxidation of 3-methyl-branched fatty acids[45]. 2-Hydroxyphytanoyl-CoA lyase was always repressed through SISPH, implying that degradation of long and branch chain fat by α-oxidation was not important in LR. GST was reported to catalyze nucleophilic addition of tripeptide glutathione to xenobiotics carcinogens and endogenous lipophilic compounds[46]. Different kinds of GST were all reduced in SISPH, implying that xenobiotics carcinogens and endogenous lipophilic compounds may bring some uncertain toxic effect on LR. Leuserpin-2 (Sperpind1) is confirmed to participate in fibrinolysis complement activation and inflammatory response[47], which was continuously repressed in SISPH, suggesting that it can regulate inflammatory response to resume severe injured hepatocytes in LR. In previous research, selenoprotein P can defense against peroxynitrite. Its down-regulation may be the result from activation of vast peroxynitrite in SISPH. Amphoterin is believed to enhance process of extension and migration of embryonic neurons and tumor cells by binding to advanced glycation end products (RAGE)[48], whose down-regulation in SISPH makes clear that LR has not much to do with hepatocytes or other cells' migration.

ACKNOWLEDGMENTS

The authors are very grateful to Dr. JR. Schrock for his correction of and valuable suggestion to the paper. We also thank *BioStar* for microarray.

REFERENCES

1 **Fausto N**. Liver regeneration and repair: hepatocytes, progenitor cells, and stem cells. *Hepatology* 2004; **39**: 1477-1487
2 **Taub R**. Liver regeneration 4: transcriptional control of liver regeneration. *FASEB J* 1996; **10**: 413-427
3 **Fausto N**. Liver regeneration. *J Hepatol* 2000; **32**: 19-31
4 **Zimmermann A**. Liver regeneration: the emergence of new pathways. *Med Sci Monit* 2002; **8**: RA53-RA63
5 **Nagy P**, Bisgaard HC, Schnur J, Thorgeirsson SS. Studies on hepatic gene expression in different liver regenerative models. *Biochem Biophys Res Commun* 2000; **272**: 591-595
6 **Michalopoulos GK**, DeFrances MC. Liver regeneration. *Science* 1997; **276**: 60-66
7 **Fukuhara Y**, Hirasawa A, Li XK, Kawasaki M, Fujino M, Funeshima N, Katsuma S, Shiojima S, Yamada M, Okuyama T, Suzuki S, Tsujimoto G. Gene expression profile in the regenerating rat liver after partial hepatectomy. *J Hepatol* 2003; **38**: 784-792
8 **Gressner AM**. Cytokines and cellular crosstalk involved in the activation of fat-storing cells. *J Hepatol* 1995; **22**: 28-36
9 **Cressman DE**, Diamond RH, Taub R. Rapid activation of the Stat3 transcription complex in liver regeneration. *Hepatology* 1995; **21**: 1443-1449
10 **FitzGerald MJ**, Webber EM, Donovan JR, Fausto N. Rapid DNA binding by nuclear factor kappa B in hepatocytes at the start of liver regeneration. *Cell Growth Differ* 1995; **6**: 417-427
11 **Sato Y**, Igarashi Y, Hakamata Y, Murakami T, Kaneko T, Takahashi M, Seo N, Kobayashi E. Establishment of Alb-DsRed2 transgenic rat for liver regeneration research. *Biochem Biophys Res Commun* 2003; **311**: 478-481
12 **Mars WM**, Kim TH, Stolz DB, Liu ML, Michalopoulos GK. Presence of urokinase in serum-free primary rat hepatocyte cultures and its role in activating hepatocyte growth factor. *Cancer Res* 1996; **56**: 2837-2843
13 **Jensen SA**. Liver gene regulation in rats following both 70 or 90% hepatectomy and endotoxin treatment. *J Gastroenterol Hepatol* 2001; **16**: 525-530
14 **Enami Y**, Kato H, Murakami M, Fujioka T, Aoki T, Niiya T, Murai N, Ohtsuka K, Kusano M. Anti-transforming growth factor-beta1 antibody transiently enhances DNA synthesis during liver regeneration after partial hepatectomy in rats. *J Hepatobiliary Pancreat Surg* 2001; **8**: 250-258
15 **Tang W**, Liang K, Wang J, Du L, Zhang W. Effects of pHGF on hepatocyte DNA synthesis after partial hepatectomy in rats. *J Tongji Med Univ* 1998; **18**: 25-27
16 **Xu CS**, Li YH, Duan RF, Lu AL, Xia M, Ji AL. Effects of the short interval successive partial hepatectomy on rat survival and liver tissue structure. *Dongwu Xuebao* 2001; **47**: 659-665
17 **Li YC**, Lin JT, Li WQ, Zhang HY, Wei MX, Xu CS. Cloning and functional analysis of up-regulated expressed genes in rat liver regeneration following short interval successive partial hepatectomy. *Developmental Reproductive Biol* 2002; **11**: 151-160
18 **Li YC**, Ma ZQ, Xu CS. Change of TNF-α, c-myc, p53, p21, PCNA, Bcl-2, TGF-β related with the cell prolification in rat liver regeneration following short interval successive partial hepatectomy. *Developmental Reproductive Biol* 2002; **11**: 253-260
19 **Yang GP**, Ross DT, Kuang WW, Brown PO, Weigel RJ. Combining SSH and cDNA microarrays for rapid identification of differentially expressed genes. *Nucleic Acids Res* 1999; **27**: 1517-1523
20 **Callow MJ**, Dudoit S, Gong EL, Speed TP, Rubin EM. Microarray expression profiling identifies genes with altered expression in HDL-deficient mice. *Genome Res* 2000; **10**: 2022-2029
21 **Arai M**, Yokosuka O, Chiba T, Imazeki F, Kato M, Hashida J, Ueda Y, Sugano S, Hashimoto K, Saisho H, Takiguchi M, Seki N. Gene expression profiling reveals the mechanism and pathophysiology of mouse liver regeneration. *J Biol Chem* 2003; **278**: 29813-29818
22 **Atha DH**, Riggs A. Tetramer-dimer dissociation in homoglobin and the Bohr effect. *J Biol Chem* 1976; **251**: 5537-5543
23 **Dent SB**, Peterson CT, Brace LD, Swain JH, Reddy MB, Hanson KB, Robinson JG, Alekel DL. Soy protein intake by perimenopausal women does not affect circulating lipids and lipoproteins or coagulation and fibrinolytic factors. *J Nutr* 2001; **131**: 2280-2287
24 **Ito H**, Ishida H, Collins BE, Fromholt SE, Schnaar RL, Kiso M. Systematic synthesis and MAG-binding activity of novel sulfated GM1b analogues as mimics of Chol-1 (alpha-series) gangliosides: highly active ligands for neural siglecs. *Carbohydr Res* 2003; **338**: 1621-1639
25 **Ohkubo K**, Ogata S, Misumi Y, Takami N, Ikehara Y. Molecular cloning and characterization of rat contrapsin-like protease inhibitor and related proteins. *J Biochem* 1991; **109**: 243-250

26 **Ognjanovic S**, Bao S, Yamamoto SY, Garibay-Tupas J, Samal B, Bryant-Greenwood GD. Genomic organization of the gene coding for human pre-B-cell colony enhancing factor and expression in human fetal membranes. *J Mol Endocrinol* 2001; **26**: 107-117

27 **Eberle J**, Fecker LF, Bittner JU, Orfanos CE, Geilen CC. Decreased proliferation of human melanoma cell lines caused by antisense RNA against translation factor eIF-4A1. *Br J Cancer* 2002; **86**: 1957-1962

28 **Ueno M**, Sonoda Y, Funakoshi M, Mukaida N, Nose K, Kasahara T. Differential induction of JE/MCP-1 in subclones from a murine macrophage cell line, RAW 264.7: role of kappaB-3 binding protein. *Cytokine* 2000; **12**: 207-219

29 **Caulin C**, Ware CF, Magin TM, Oshima RG. Keratin-dependent, epithelial resistance to tumor necrosis factor-induced apoptosis. *J Cell Biol* 2000; **149**: 17-22

30 **Cole TJ**, Schreiber G. The structure and expression of the genes for T-kininogen in the rat. *Agents Actions Suppl* 1992; **38 (Pt 1)**: 292-299

31 **Zimmers TA**, Pierce RH, McKillop IH, Koniaris LG. Resolving the role of IL-6 in liver regeneration. *Hepatology* 2003; **38**: 1590-1591; author reply 1591

32 **Ray A**, Schatten H, Ray BK. Activation of Sp1 and its functional co-operation with serum amyloid A-activating sequence binding factor in synoviocyte cells trigger synergistic action of interleukin-1 and interleukin-6 in serum amyloid A gene expression. *J Biol Chem* 1999; **274**: 4300-4308

33 **Sherman CT**, Brasier AR. Role of signal transducers and activators of transcription 1 and -3 in inducible regulation of the human angiotensinogen gene by interleukin-6. *Mol Endocrinol* 2001; **15**: 441-457

34 **Diehl AM**, Yang SQ, Wolfgang D, Wand G. Differential expression of guanine nucleotide-binding proteins enhances cAMP synthesis in regenerating rat liver. *J Clin Invest* 1992; **89**: 1706-1712

35 **Sonoki T**, Nagasaki A, Gotoh T, Takiguchi M, Takeya M, Matsuzaki H, Mori M. Coinduction of nitric-oxide synthase and arginase I in cultured rat peritoneal macrophages and rat tissues *in vivo* by lipopolysaccharide. *J Biol Chem* 1997; **272**: 3689-3693

36 **Garrard LJ**, Bui QT, Nygaard R, Raushel FM. Acid-base catalysis in the argininosuccinate lyase reaction. *J Biol Chem* 1985; **260**: 5548-5553

37 **Ding WG**, Tooyama I, Kitasato H, Fujimura M, Kimura H. Phylogenetic and ontogenetic study of neuropeptide Y-containing nerves in the liver. *Histochem J* 1994; **26**: 453-459

38 **Niemuller CA**, Randall KJ, Webb DJ, Gonias SL, LaMarre J. Alpha 2-macroglobulin conformation determines binding affinity for activin A and plasma clearance of activin A/alpha 2-macroglobulin complex. *Endocrinology* 1995; **136**: 5343-5349

39 **Starzl TE**, Francavilla A, Porter KA, Benichou J, Jones AF. The effect of splanchnic viscera removal upon canine liver regeneration. *Surg Gynecol Obstet* 1978; **147**: 193-207

40 **Bond JS**, Aronson NN. Endocytosis and degradation of native, cathepsin D-degraded, and glutathione-inactivated aldolase by perfused rat liver. *Arch Biochem Biophys* 1983; **227**: 367-372

41 **Zalkin H**, Sprinson DB. An investigation of imine formation in the isocitrate dehydrogenase reaction. *J Biol Chem* 1966; **241**: 1067-1071

42 **Shimamura M**, Matsuda M, Kobayashi S, Ando Y, Ono M, Koishi R, Furukawa H, Makishima M, Shimomura I. Angiopoietin-like protein 3, a hepatic secretory factor, activates lipolysis in adipocytes. *Biochem Biophys Res Commun* 2003; **301**: 604-609

43 **Herman MP**, Sukhova GK, Libby P, Gerdes N, Tang N, Horton DB, Kilbride M, Breitbart RE, Chun M, Schonbeck U. Expression of neutrophil collagenase (matrix metalloproteinase-8) in human atheroma: a novel collagenolytic pathway suggested by transcriptional profiling. *Circulation* 2001; **104**: 1899-1904

44 **Cigic B**, Pain RH. Location of the binding site for chloride ion activation of cathepsin C. *Eur J Biochem* 1999; **264**: 944-951

45 **Foulon V**, Antonenkov VD, Croes K, Waelkens E, Mannaerts GP, Van Veldhoven PP, Casteels M. Purification, molecular cloning, and expression of 2-hydroxyphytanoyl-CoA lyase, a peroxisomal thiamine pyrophosphate-dependent enzyme that catalyzes the carbon-carbon bond cleavage during alpha-oxidation of 3-methyl-branched fatty acids. *Proc Natl Acad Sci USA* 1999; **96**: 10039-10044

46 **Atkins WM**, Wang RW, Bird AW, Newton DJ, Lu AY. The catalytic mechanism of glutathione S-transferase (GST). Spectroscopic determination of the pKa of Tyr-9 in rat alpha 1-1 GST. *J Biol Chem 1*993; **268**: 19188-19191

47 **Ragg H**, Ulshofer T, Gerewitz J. On the activation of human leuserpin-2, a thrombin inhibitor, by glycosaminoglycans. *J Biol Chem* 1990; **265**: 5211-5218

48 **Huttunen HJ**, Kuja-Panula J, Sorci G, Agneletti AL, Donato R, Rauvala H. Coregulation of neurite outgrowth and cell survival by amphoterin and S100 proteins through receptor for advanced glycation end products (RAGE) activation. *J Biol Chem* 2000; **275**: 40096-40105

Science Editor Zhu LH and Guo SY **Language Editor** Elsevier HK

PO Box 2345, Beijing 100023, China
www.wjgnet.com
wjg@wjgnet.com

ELSEVIER

World J Gastroenterol 2005;11(15):2306-2312
World Journal of Gastroenterology ISSN 1007-9327

• *BASIC RESEARCH* •

Vascular contractile response and signal transduction in endothelium-denuded aorta from cirrhotic rats

Han-Chieh Lin, Ying-Ying Yang, Yi-Tsau Huang, Tzung-Yan Lee, Ming-Chih Hou, Fa-Yauh Lee, Shou-Dong Lee

Han-Chieh Lin, Ming-Chih Hou, Fa-Yauh Lee, Shou-Dong Lee, Division of Gastroenterology, Department of Medicine, Taipei Veterans General Hospital and National Yang-Ming University School of Medicine, Taipei, Taiwan, China
Ying-Ying Yang, Institute of Clinical Medicine, National Yang-Ming University School of Medicine and Taipei Chung-Hsiao Municipal Hospital, Taipei, Taiwan, China
Yi-Tsau Huang, Tzung-Yan Lee, Institute of Traditional Medicine, National Yang-Ming University School of Medicine, Taipei, Taiwan, China
Supported by the National Science Council of Taiwan, No. NSC91-2314-B-075-129 and the Taipei Veterans General Hospital of Taiwan, China, No. VGH91-28
Correspondence to: Dr. Han-Chieh Lin, Division of Gastroenterology, Department of Medicine, Taipei Veterans General Hospital, No. 201, Sec. 2, Shih-Pai Road, Taipei 11217, Taiwan, China. hclin1956@yahoo.com
Telephone: +886-2-28757308 Fax: +886-2-28739318
Received: 2004-07-05 Accepted: 2004-08-31

Abstract

AIM: The mechanism of decreased vascular reactivity to vasoconstrictors in portal hypertension is still unclear. In addition to nitric oxide, defects in post-receptor signal transduction pathway have been suggested to play a role. However, substantial evidences observed equivocal changes of vascular reactivity following different agonists that challenged the hypothesis of the post-receptor defect. The current study was to evaluate the vascular reactivity to different agonists and the inositol trisphosphate (IP_3) changes in signal transduction cascade from cirrhotic rats with portal hypertension.

METHODS: The endothelial denuded aortic rings from cirrhotic and sham-operated rats were obtained for *ex vivo* tension study and measurement of the corresponding [^{3}H] IP_3 formation following different receptor and nonreceptor-mediated agonists' stimulation. Additionally, iNOS protein expression was measured in thoracic aorta. The contractile response curves to phenylephrine were performed in endothelial denuded aortic rings with and without preincubation with a specific iNOS inhibitor (L-*N* (6)-(1-iminoethyl)-lysine, L-NIL).

RESULTS: In endothelial denuded aortic rings of cirrhotic rats, the vascular responses were reduced with phenylephrine and arginine vasopressin (AVP) stimulation but were normal with U-46619, NaF/$AlCl_3$, and phorbol esterdibutyrate (PdBU) stimulation. Compared to the corresponding control groups, the degree of the increment of [^{3}H] IP_3 formation from basal level was also decreased with phenylephrine and AVP stimulation, but was normal with U-46619 and NaF/$AlCl_3$ stimulation. The preincubation with L-NIL did not modify the hyporesponsiveness to phenylephrine. Additionally, the iNOS protein expression in thoracic aorta was not different in cirrhotic and sham-operated rats.

CONCLUSION: Without the influence of nitric oxide, vascular hyporeactivity to vasoconstrictors persisted in cirrhotic rats with portal hypertension. However, the decreased vascular reactivity is an agonist-specific phenomenon. In addition, G-protein and phospholipase C pathway associated with the IP_3 productions may be intact in cirrhotic rats with portal hypertension.

Key words: Cirrhosis; Portal hypertension; Inositol trisphosphate; Vascular reactivity; Protein kinase C

Lin HC, Yang YY, Huang YT, Lee TY, Hou MC, Lee FY, Lee SD. Vascular contractile response and signal transduction in endothelium-denuded aorta from cirrhotic rats. *World J Gastroenterol* 2005; 11(15): 2306-2312
http://www.wjgnet.com/1007-9327/11/2306.asp

INTRODUCTION

Peripheral arterial vasodilatation is a characteristic hemodynamic derangement observed in cirrhosis with portal hypertension[1-4]. Increased circulating vasodilators and endothelial-related vasodilatory activity have been suggested to play a role for the development of arterial vasodilatation[5-11]. Additionally, the decreased vascular reactivity to vasoconstrictors also contributes to the arterial vasodilatation in portal hypertension[12-18]. The vasoconstrictors used in those studies to evaluate vascular reactivity were mainly α_1-adrenoceptor agonists, arginine vasopressin (AVP), and angiotensin II. Although increased nitric oxide (NO) production has been shown to play a role, the mechanisms of decreased vascular reactivity have not been completely established and the data on vascular reactivity in portal hypertensive humans and animals are conflicting (for reviews see Hadoke and Hayes[19]).

It has been hypothesized that the presence of a defect in the post-receptor signal transduction cascade plays, in part, a role for the vascular hyporeactivity[14,16,20,21]. Theoretically, if the post-receptor signal transduction cascade is generally impaired in portal hypertension, any vasoconstrictor that leads to a receptor and G-protein-linked stimulation of vascular contraction should lead to a decreased vascular

contractility. However, two recent studies in portal hypertensive patients and animals showed a normal vascular reactivity to the agonist of thromboxane A_2 (TXA_2) receptor[22,23]. In addition, an increased vascular response to 5-hydroxytryptamine stimulation was found in cirrhotic patients[24]. The results from these studies do not support the presence of a defect in the post-receptor signal transduction cascade in portal hypertension. Therefore, the current study was undertaken in cirrhotic rats with portal hypertension to measure the vascular contractile response, without the influence of NO, following administration of different agonists. The inositol trisphosphate (IP_3) formations following agonists' stimulation and the responses to protein kinase C (PKC) activator were also measured to evaluate the post-receptor mechanism of vascular reactivity in cirrhotic portal hypertension.

MATERIALS AND METHODS

Animals

Adult male Sprague-Dawley rats (250-350 g) were used in all experiments. Cirrhosis with portal hypertension was produced by common bile duct ligation (CBL), as previously described[25]. Sham-operated rats had their bile duct exposed but not ligated. All rats were caged at 24 ℃, with a 12-h light-dark cycle, and allowed free access to food and water. Animal studies were approved by the Animal Experiment Committee of the University and conducted humanely.

Hemodynamic measurements

Four to five weeks after surgery, rats were anesthetized with ketamine, 150 mg/kg. The first set of eight cirrhotic and six sham-operated rats were included in this experiment. The ileocolic vein was cannulated with PE-10 tubing for measuring portal venous pressure (PP) and the femoral artery was cannulated with PE-50 tubing for arterial blood pressure (MAP). Pressure and heart rate were monitored by a polygraph (RS 3400, Gould, Valley View, OH, USA) via strain-gauge transducers (P23XL, Viggo-Spectramed, Oxnard, CA, USA). Cardiac output was measured by thermodilution (Columbus Instruments, OH, USA), and cardiac index (CI) and systemic vascular resistance (SVR) were calculated as previously described[26,27].

Ex vivo tension experiments

The second set of CBL and sham-operated rats were used in this study. Rats were killed by an overdose of sodium pentobarbital. Then the thoracic aorta (above the diaphragm and below the aortic arch) was excised and put into aerated (mixture of 95% O_2 5% and CO_2) kreb's Ringer bicarbonate solution (KRBS) and cleaned at room temperature. The composition of the KRBS was in millimolar: NaCl, 118.3; KCl, 4.7; $CaCl_2$, 2.5; $MgSO_4$, 1.2; KH_2PO_4, 1.2; $NaHCO_3$, 25; and glucose, 11.1. The thoracic aorta was cut into 4-mm segments. In order to avoid the effect of endothelium on vascular contractility, the endothelium was removed by gently rubbing the intimal surface of the vessels. Endothelial cell removal was confirmed by the inability of rings pre-contracted with 0.1 μmol/L phenylephrine (PEP) to relax in response to 1 μmol/L acetylcholine. The rings were then suspended horizontally between two stainless steel wires in individual organ chambers filled with 10 mL of KRBS. The solution was continuously bubbled with a mixture of 95% O_2 5% and CO_2 and maintained at 37 ℃ with an outer water jacket and circulating heat pump. One wire was fixed to the chamber and the other was attached to a force displacement transducer (FT 03, Grass Instrument Co., Quincy, MA, USA) with a basic tension of 1.8 g. Tension was recorded on a physiograph (RS 3400, Gould, Valley View, OH, USA). The readiness of tissue indicated by consistent responses induced by three consecutive tests with KCl (30-90 mmol/L) in each group was obtained. The tissue was then rinsed and allowed to recover for 45 min. Segments of aorta from each animal were allocated into five subsets. Then, the cumulative concentration-response curves to PEP (10^{-10} to 10^{-4} mol/L), AVP (10^{-10} to 10^{-4} mol/L), synthetic TXA_2 analog U-46619 (10^{-9} to 10^{-5} mol/L), receptor-independent G-protein activator by NaF (10^{-3} to 1 mol/L)/$AlCl_3$ (30 μmol/L), direct activation of PKC by phorbol esterdibutyrate (PdBU) (10^{-8} to 3×10^{-5} mol/L) were obtained, respectively.

[^{3}H]1,4,5 Inositol trisphosphate assay

The third set of endothelial-denuded aortic segments were weighted (4 mm in length) and incubated in 0.5 mL KRBS containing LiCl (20 mmol/L) and imipramine (4 μmol/L) at 37 ℃ under a mixture of 95% O_2 5% and CO_2 for 10 min. Then, agonists [PEP (10^{-7} to 10^{-5} mol/L), AVP (10^{-7} to 10^{-5} mol/L), U-46619 (10^{-7} and 10^{-6} mol/L), NaF/$AlCl_3$ (0.1 and 1 mol/L)] or vehicle (0.1% ascorbic acid) were added into the tissue bath for 20 min. These concentrations of agonists were chosen according to the concentration-response contractile curve. We used the highest two or three concentrations of agonist to assess their corresponding IP_3 formations under the same experimental condition. The reaction was stopped with 2 mL of CH_3OH-$CHCl_3$-HCl (40:20:1, v/v). The assay method was essentially the same as previously reported[28-30]. To extract inositol phosphates, the tissue was sonicated for 45 min and a mixture of 1.26 mL of H_2O and 0.63 mL of $CHCl_3$ was added to separate the organic and aqueous phases. Tubes were centrifuged at 2 500 r/min for 10 min. The supernatant (aqueous phase containing extracted inositol phosphates) was removed, neutralized to pH 6.8 and 7.2. The neutralized supernatant was added to 300-500 μL of a 1:1 (v/v) mixture of Freon (1, 1, 2-trichlorotrifluoroethane) and tri-*n*-octylamine, and vortex-mix the separate phases. This neutralized mixture was centrifuged for 10 min at 2 000 r/min. Then three separated phases can be found. These three phases are upper phase: neutralized sample plus water soluble components; middle phase: tri-*n*-octylamine perchlorate; lower phase: Freon plus unrecalled tri-*n*-octylamine. Then the upper phase was removed and stored in -70 ℃ for subsequent analysis. The IP_3 formations with or without stimulation of agonist were measured in all samples by the commercial kit of radioimmunoassay (RIA) (PerkinElmer™ Life Sciences, Inc., Boston, MA, USA). The radioactivity of these samples after RIA was counted in a β-counter (LS 6500, Beckman Instruments, Fullerton, CA, USA).

Vascular reactivity with and without [L-N(6)-(1-iminoethyl)-lysine, L-NIL] preincubation and iNOS protein measurement

In order to clarify the role of iNOS on the decreased vascular

Table 1 **Hemodynamic values in sham-operated (sham) and common bile duct-ligated (CBL) rats**

	Sham (n = 6)	CBL (n = 8)
Cardiac index (mL·min/100 g body wt)	29.4±0.6	46.7±0.7[a]
Mean arterial pressure (mmHg)	107±5	97±10
Systemic vascular resistance (dyn·s/cm^5×10^3/100 g body wt)	289±9	167±7[a]
Heart rate (beats/min)	315±6	327±10
Portal pressure (mmHg)	7.9±1.3	19.8±0.6[a]

Values are mean±SE. [a]P<0.05 *vs* sham rats.

Table 2 **Contractile response of different agents to the endothelial-denuded aortic rings from sham and CBL rats**

Vasopressor	Parameter	Sham	CBL
PEP	pEC50	6.41±0.1	6.53±0.8
	R_{max} (g) (10^{-5} mol/L)	3.29±0.37	1.99±0.21[a]
AVP	pEC50	6.51±0.2	7.08±0.9
	R_{max} (g) (10^{-5} mol/L)	3.45±0.28	2.31±0.49[a]
U-46619	pEC50	7.43±0.13	7.81±0.26
	R_{max} (g) (10^{-6} mol/L)	3.18±0.27	3.19±0.17
NaF/AlCl$_3$	pEC50	0.83±0.43	1.01±0.01
	R_{max} (g) (1 mol/L)	3.68±0.13	3.42±0.25
PdBU	pEC50	7.05±0.4	7.05±0.7
	R_{max} (g) (10^{-6} mol/L)	3.87±0.14	3.92±0.22

Values are mean±SE; sham: sham-operated rats; CBL: common bile duct-ligation rats, PEP: phenylephrine, n = 10, in each group with different agonist stimulation, [a]P<0.05 *vs* sham rats.

reactivity, the fourth set CBL and sham-operated rats were killed by an overdose of sodium pentobarbital. The endothelial-denuded aorta segments were prepared as described above. Then, the cumulative concentration-response curves to PEP (10^{-10} to 10^{-4} mol/L) were obtained with and without preincubation with L-NIL (10^{-6} mol/L) in CBL and sham-operated rats. In addition, the iNOS protein expression was measured in the thoracic aorta from CBL and sham-operated rats by Western blot analysis.

Chemicals

All substances were purchased from Sigma Chemical Co. (St. Louis, MO, USA) and added into the organ bath in a volume of 100 μL. PEP was prepared in 0.1% ascorbic acid. U-46619 was dissolved in 10% of methanol. PdBU was dissolved in 10% dimethylsulfoxide. The NaF/AlCl$_3$ acetylcholine chloride, L-NIL (L-*N*(6)-(1-iminoethyl)-lysine) and AVP were dissolved in distilled water. All these solvents had proved not to affect vascular tone in the organ bath.

Statistical analysis

The data are given as mean±SE. Contractile force is expressed in grams (g). Cumulative concentration-response curves to PEP, AVP, U-46619, NaF/AlCl$_3$, and PdBU were obtained. pEC50 (negative logarithm of the concentration producing the half maximum effect) values were calculated from the sigmoid logistic curves in each vessel preparation. Statistical analysis was performed by two-way ANOVA. Additionally, values for maximal contraction (R_{max}) were calculated in absolute values. Statistical analysis of the differences between R_{max} of the aortic rings from rats with cirrhosis and normal were performed with unpaired Student's t test. Dose-response curves were analyzed by repeat measures ANOVA followed by post hoc test (Games and Howell variant of the Tukey and t test) to compare the groups at each dose separately. The tissue (wet) weight of each segment was weighed in each experiment. The signal intensity (integral volume) of the appropriate iNOS protein bands on the autoradiogram was analyzed by use of the ImageQuant software package (Biosoft, Indianapolis, IN, USA). Basal IP_3 formation was calculated as counts per minute per mg wet weight of tissue (cpm/mg). Agonist-stimulated IP_3 formation was calculated as a percentage of cpm in the presence of agonist divided by cpm without agonist (basal formation). For each assay, both basal and agonist-stimulated tubes were prepared in duplicates and the means of duplicates were used for analysis. A P value <0.05 was considered statistically significant. Statistical analysis of the differences was performed with paired or unpaired Student's t test when appropriate.

RESULTS

Hemodynamic studies

About 4 wk after CBL, cirrhotic rats showed jaundice, splenomegaly, mesenteric edema and variable amount of ascites. In Table 1, CBL rats had significantly lower SVR associated with higher CI and PP than sham-operated rats.

Ex vivo contractile responses in thoracic aorta

Both PEP (10^{-10} to 10^{-4} mol/L) and AVP (10^{-10} to 10^{-4} mol/L) induced concentration-dependent contractions in the aorta from CBL and sham-operated rats. Our results demonstrated that the R_{max}, but not pEC50, to PEP and AVP was significantly decreased in the aorta of CBL rats compared to those of sham-operated rats (Table 2). These results showed a decreased vascular reactivity and a normal vascular sensitivity to PEP and AVP of aorta in CBL rats (Figure 1 and Table 2). Similarly, U-46619, NaF/AlCl$_3$, and PdBU also induced the concentration-dependent contractions curve in both study groups (Figure 2). However, neither the R_{max} nor its pEC50 values differed between the two vessel groups (Table 2).

[^{3}H]1,4,5 Inositol trisphosphate (IP_3) formation in aortic rings

The basal IP_3 formation in aortic rings was similar between the CBL and sham-operated rats (385±6 and 402±10 cpm/mg tissue weight, n = 8 in each group with different agonist stimulation). Both PEP (10^{-7} to 10^{-5} mol/L) and AVP (10^{-7} and 10^{-5} mol/L) induced dose-dependent increases of [^{3}H] IP_3 in both groups. In the presence of PEP and AVP, the increments of [^{3}H] IP_3 (% of basal levels) in the CBL rats were significantly lower than that in the sham-operated rats at the concentration of 10^{-6} and 10^{-5} mol/L of PEP and 10^{-7} to 10^{-5} mol/L of AVP, respectively (Figure 3). In contrast, the percentage of increases after U-46619 (10^{-7} and 10^{-6} mol/L) and NaF/AlCl$_3$ (0.1 and 1 mol/L) stimulation were similar between the two groups (Figure 4).

Vascular reactivity with and without L-NIL preincubation and iNOS protein measurement

The effects of selective iNOS inhibition on vascular responses

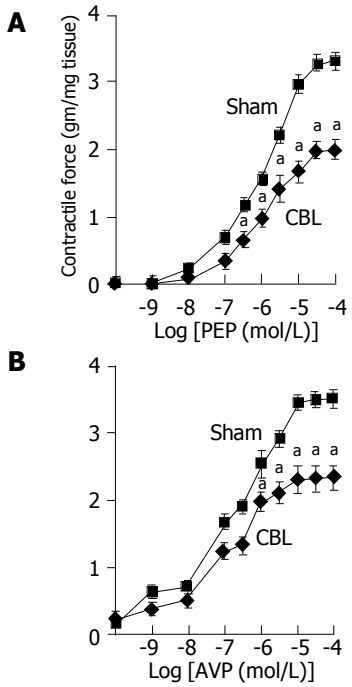

Figure 1 Maximum cumulative concentration-response curves to (**A**) phenylephrine (PEP) (10^{-10} to 10^{-4} mol/L), (**B**) AVP (10^{-10} to 10^{-4} mol/L) in thoracic aorta from CBL (◆) and sham (■) rats. $^aP<0.05$ *vs* sham rats (n = 12 in each group with different agonist stimulation). Sham: sham-operated rats; CBL: common bile duct-ligated rats.

to PEP are shown in Figure 5A. In cirrhotic aortic rings, the vascular hyporeactivity to PEP stimulation still persisted after preincubation with L-NIL. In addition, the iNOS protein expression in the thoracic aorta of BDL rats was not different from sham-operated rats (Figure 5B). These results indicated that iNOS did not play a role in the decreased vascular contractility in portal hypertension.

DISCUSSION

The mechanism of agonists-induced contraction of vascular smooth muscle cells involves both membrane and intracellular changes[31,32]. Agonists bind to surface G-protein-linked transmembrane receptors may activate phospholipase C (PLC). This enzyme hydrolyzes the lipid precursor phosphatidylinositol (4,5)-biphosphate stored in the plasma membrane to give IP_3 and 1,2-diacylglycerol. The IP_3 binds to its receptor located in the membrane of the sarcoplasmic reticulum that lead to open the calcium channels and increases the cytosolic calcium concentration. The agonists have also been shown to open L-type calcium channel located on the plasma membrane to increase cytosolic calcium concentration. On the other hand, diacylglycerol activates PKC with regulation of intracellular calcium concentration. The cytosolic free calcium then binds to calmodulim to form calcium-calmodulim complex, which in turn interact with the contractile proteins that lead to smooth muscle cell contraction. Therefore, any alteration in the G-proteins receptor coupling, transmembrane receptor, or the signal transduction downstream from the transmembrane receptor may play a role in the vascular hyporesponsiveness in portal hypertension.

The mechanisms responsible for the decreased vascular reactivity in cirrhosis are not completely understood. In experimental portal hypertension, the increased nitric oxide production has been suggested to play an important role for the vascular hyporeactivity[7,10,26,33]. Although Vallance and Moncada proposed that the increased activity of iNOS led to NO overproduction and subsequent hyperdynamic circulation[34], substantial studies showed a lack of iNOS expression in the vessels from portal hypertensive animals despite the enhanced NO production[35,36]. It is now generally accepted that eNOS rather than iNOS is the major contributor for the NO overproduction in the hemodynamic derangements in portal hypertension (for review see Wiest and Groszmann[37]), and the role of eNOS is further supported in a recent study using gene-knockout mice[38]. Nevertheless, a persistent vascular hyporeactivity to vasoconstrictor stimulation in portal hypertensive human and animals was still observed in endothelium-free aortic ring or following pre-incubation with NOS inhibitor[13,39]. This observation was further supported in endothelial denuded hepatic artery from cirrhotic patients[22,40]. Therefore, in addition to nitric oxide, other factors are also involved in the pathogenesis of vascular hyporeactivity in portal hypertension. A number of studies have found an attenuated vascular reactivity to vasoconstrictors (such as angiotensin II, vasopressin, and α_1-adrenoceptor agonists), but these receptors were not down regulated or the receptor numbers and affinities were

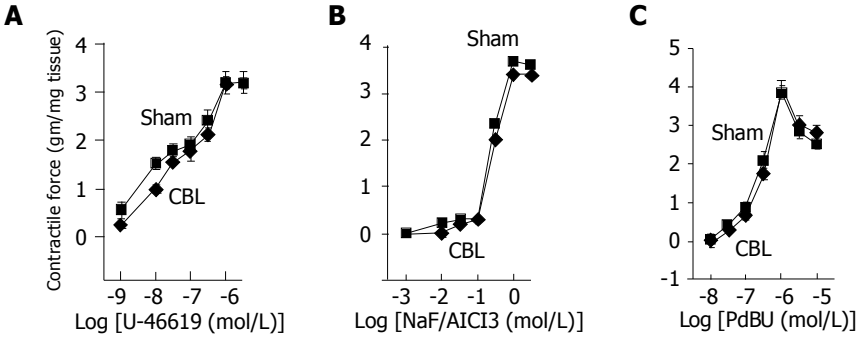

Figure 2 Maximum cumulative concentration-response curves to (**A**) synthetic TXA_2 analog U-46619 (10^{-9} to 10^{-5} mol/L), (**B**) receptor-independent G-protein stimulus NaF (10^{-3}-1 mol/L)/$AlCl_3$ (30 μmol/L), (**C**) direct activation of protein kinase C by PdBU (10^{-8} to 3×10^{-5} mol/L) in thoracic aorta from CBL (◆) and sham-operated (■) rats, n = 10 in each group with different agonist stimulation.

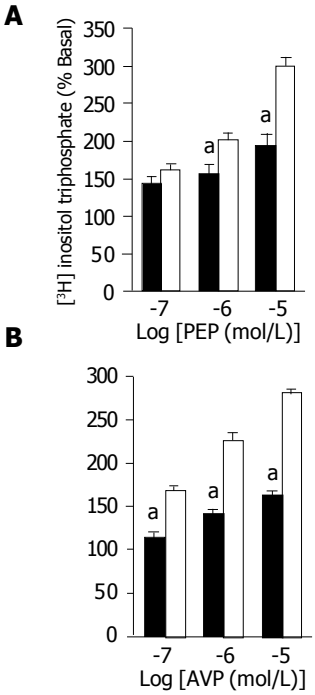

Figure 3 (**A**) Phenylephrine (PEP) (10^{-7} to 10^{-5} mol/L) and (**B**) AVP (10^{-7} to 10^{-5} mol/L)-induced [^{3}H] IP_3 formation in the aortic ring from CBL (black bars) and sham (white bars) rats. [^{3}H] IP_3 formation was expressed as the percentage of counts (cpm) per minute in the presence of agonist divided by the counts without agonist (basal formation). The data are expressed as mean±SE. $^aP<0.05$ *vs* sham rats, $n = 8$ in each group with different agonist stimulation. Sham: sham-operated rats; CBL: common bile duct-ligated rats.

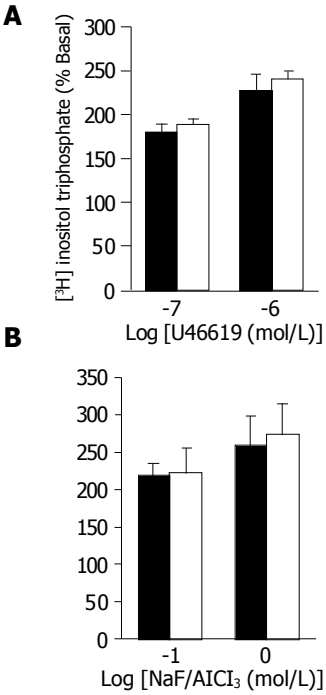

Figure 4 (**A**) U-46619, a synthetic TXA_2 analog (10^{-7} and 10^{-6} mol/L), (**B**) NaF/$AlCl_3$ (0.1 and 1 mol/L)-induced [^{3}H] IP_3 formation in the aortic ring from CBL (black bars) and sham (white bars) rats. [^{3}H] IP_3 formation was expressed as the percentage of counts (cpm) per minute in the presence of agonist divided by the counts without agonist (basal formation). The data are expressed as mean±SE, $n = 8$ in each group with different agonist stimulation.

unchanged[15-18,41]. These studies lead to a hypothesis of a defect in signal transduction cascade in portal hypertension. Accordingly, if the post-receptor defect does exist in portal hypertension, a generalized hyporesponsiveness to any receptor and G-protein linked vasoconstrictors should be observed in cirrhotic human and animals with portal hypertension.

In the current study, we found an expected decrease in contractile responses to PEP (a α_1-adrenoceptor agonist) and AVP (a V_1-AVP receptor agonist) in the endothelium-denuded aortic ring from cirrhotic rats compared to those from sham-operated rats. By contrast, we found a normal contractile response to U-46619 (a TXA_2 receptor agonist) in the aortic rings from cirrhotic rats compared to those from the sham-operated rats. TXA_2 receptor is a G-protein-coupled and PLC-linked transmembrane receptor as well as those of α_1, V_1-AVP or angiotensin II receptors. Van Obbergh *et al*, and Schepke *et al*, have demonstrated similar observations of a normal contractile response to U-46619 in cirrhotic rats and humans[22,23]. In addition, another study in cirrhotic patients also showed an increased vascular response following 5-hydroxytryptamine stimulation[24]. Taken together, it is conceivable that the vascular hyporeactivity to vasoconstrictors in portal hypertension is a selective agonist-mediated phenomenon. In other words, decreased vascular reactivity in portal hypertension may occur in some agonists but do not occur in others. Please note that the vascular reactivity in the current study was performed in endothelium-denuded aortic rings from cirrhotic rats. Similar to previous observations, we also observed a lack of the role of iNOS on the vascular hyporesponsiveness in portal

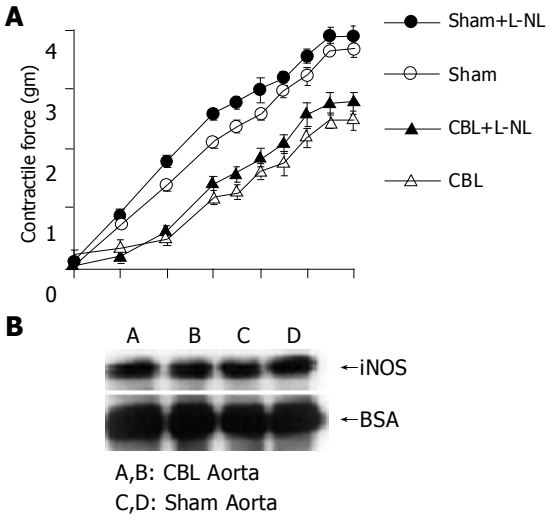

Figure 5 (**A**) Maximum cumulative concentration-response curves to phenylephrine (PEP) (10^{-10} to 10^{-4} mol/L) in thoracic aorta from CBL (◆) and sham (□) rats with and without preincubation with L-NIL (L-*N*(6)-(1-iminoethyl)-lysine, a selective iNOS inhibitor). $n = 10$ in each group with different agonist stimulation. CBL: common bile duct-ligated rats; sham: sham-operated rats. (**B**) Western blot analysis of inducible nitric oxide synthase (iNOS) protein expression from thoracic aorta in CDL and sham-operated rats. Lanes A and B: CBL rats; lanes C and D: sham rats.

hypertension evidenced by both *ex vivo* vascular tension study with L-NIL preincubation and aortic iNOS protein expression[35,36]. Therefore, the role of NO on vascular reactivity has been minimized to the least extent. Moreover, we found a normal contractile response by NaF/$AlCl_3$ from the aortic ring of cirrhotic rats compared to those from sham-operated

rats. A similar observation showing a normal contractile response to NaF/$AlCl_3$ in the endothelium-denuded hepatic artery in cirrhotic patients was reported by Schepke *et al*[22]. Previously, an impairment of contractile response to NaF/$AlCl_3$ had been reported in the intestinal microcirculation of portal hypertensive rats[42]. In that study, vascular contractility was evaluated by perfusion of mesenteric beds with intact endothelium. It is possible that the different vascular preparation and the presence of NO may contribute to such discrepancy. Because NaF/$AlCl_3$ is a direct G protein activator, it produces smooth muscle cells' contraction independent to the receptor and G-protein coupling[31,32]. Our results suggest that the contractile response of aortic smooth muscle cell downstream from G-protein in portal hypertensive humans or animals is similar to that in non-portal hypertensive ones. In other words, it is possible that the signal transduction cascade downstream from G-protein activation may be intact in cirrhotic rats with portal hypertension. However, the current study cannot exclude the minor G-protein-related RhoA/Rho kinase pathway. Further studies are needed to clarify this point.

Phosphoinositide metabolism is important in the signal transduction cascade for receptor-coupled vasoconstriction[31,43]. Its hydrolyzed products, IP_3 and 1,2-diacylglycerol, are crucial second messengers for triggering and maintaining the contractile response of the vascular smooth muscle cells[31,44]. In the current study, we observed that the increased formation of IP_3 after PEP and AVP stimulation in cirrhotic rats was significantly lower than that in sham-operated rats. In contrast, the increased formation of IP_3 after U-46619 and NaF/$AlCl_3$ stimulation was similar between the two experimental groups. The changes in IP_3 formation following different agonists' stimulation were parallel to the corresponding changes of vascular contractile response between cirrhotic and normal rats. In our previous study, we observed that, in portal hypertensive animals, the PEP-stimulated [^{3}H] inositol phosphate formation in tail artery was attenuated, whereas the NaF/$AlCl_3$-mediated [^{3}H] inositol phosphate formation in portal vein was unaltered[21]. On the other hand, Hartleb *et al*[45], observed a lack of vascular hyporesponsiveness to L-type calcium channel activator in cirrhotic rats. Moreover, Castro *et al*[46], found that the intracellular calcium mobilization pathway is preserved in the vascular smooth muscle cells from cirrhotic rats. Together these results strengthened the presence of an intact signal transduction cascade in cirrhosis with portal hypertension that challenged the hypothesis of the post-receptor defect.

PKC plays an essential role in the regulation of vascular smooth muscle cell contraction[47]. In the current study, the PdBU-mediated contractile response was not different between the two experimental groups. The role of PKC in vascular contractility in portal hypertension is controversial. Previous studies have reported that the PdBU-mediated contractile response remains unchanged in aortic rings and mesenteric vascular bed of portal vein stenosed rats, which in line with the findings of the present studies in cirrhotic rats[21,47]. In contrast, other studies have demonstrated that the alteration of PKC plays a partial role for the decreased vascular reactivity in portal hypertension[42,48,49]. However, it has been suggested that overproduction of NO may contribute, in part, a role for the alteration of PKC activity in portal hypertension[50]. Therefore, in the current study, it is possible that a normal PdBU-induced contractile response was observed in endothelial-denuded aortic ring in cirrhotic rats, which suggested a normal PKC activity in cirrhotic rats. All together, the current study suggested that the G-protein and PLC pathway associated with the IP_3 and 1,2-diacylglycerol actions were not impaired in cirrhotic rats with portal hypertension. The decreased vascular reactivity observed in the specific receptors may probably result from a defect in receptor-G-protein coupling. Further studies are needed to clarify this phenomenon.

In summary, this study demonstrated that, without the influence of NO, vascular hyporeactivity persisted in CBL rats with portal hypertension. However, the decreased vascular reactivity is an agonist-specific phenomenon. In addition, the current study is against the presence of a post-receptor defect in vascular hyporeactivity observed in portal hypertension.

REFERENCES

1 **Albillos A,** Colombato LA, Groszmann RJ. Vasodilatation and sodium retention in prehepatic portal hypertension. *Gastroenterology* 1992; **102**: 931-935
2 **Schrier RW,** Arroyo V, Bernardi M, Epstein M, Henriksen JH, Rodés J. Peripheral arterial vasodilation hypothesis: a proposal for the initiation of renal sodium and water retention in cirrhosis. *Hepatology* 1988; **8**: 1151-1157
3 **Vorobioff J,** Bredfeldt JE, Groszmann RJ. Hyperdynamic circulation in portal-hypertensive rat model: a primary factor for maintenance of chronic portal hypertension. *Am J Physiol* 1983; **244**: G52-G57
4 **Vorobioff J,** Bredfeldt JE, Groszmann RJ. Increased blood flow through the portal system in cirrhotic rats. *Gastroenterology* 1984; **87**: 1120-1126
5 **Benoit JN,** Barrowman JA, Harper SL, Kvietys PR, Granger DN. Role of humoral factors in the intestinal hyperemia associated with chronic portal hypertension. *Am J Physiol* 1984; **247**: G486-G493
6 **Tahan V,** Avsar E, Karaca C, Uslu E, Eren F, Aydin S, Uzun H, Hamzaoglu HO, Besisik F, Kalayci C, Okten A, Tozun N. Adrenomedullin in cirrhotic and non-cirrhotic portal hypertension. *World J Gastroenterol* 2003; **9**: 2325-2327
7 **Pizcueta P,** Piqué JM, Fernández M, Bosch J, Rodés J, Whittle BJ, Moncada S. Modulation of the hyperdynamic circulation of cirrhotic rats by nitric oxide inhibition. *Gastroenterology* 1992; **103**: 1909-1915
8 **Silva G,** Navasa M, Bosch J, Chesta J, Pilar Pizcueta M, Casamitjana R, Rivera F, Rodés J. Hemodynamic effects of glucagon in portal hypertension. *Hepatology* 1990; **11**: 668-673
9 **Sitzmann JV,** Li SS, Lin PW. Prostacyclin mediates splanchnic vascular response to norepinephrine in portal hypertension. *J Surg Res* 1989; **47**: 208-211
10 **Sogni P,** Moreau R, Gadano A, Lebrec D. The role of nitric oxide in the hyperdynamic circulatory syndrome associated with portal hypertension. *J Hepatol* 1995; **23**: 218-224
11 **Oberti F,** Sogni P, Cailmail S, Moreau R, Pipy B, Lebrec D. Role of prostacyclin in hemodynamic alterations in conscious rats with extrahepatic or intrahepatic portal hypertension. *Hepatology* 1993; **18**: 621-627
12 **Braillon A,** Cailmail S, Gaudin C, Lebrec D. Reduced splanchnic vasoconstriction to angiotensin II in conscious rats with biliary cirrhosis. *J Hepatol* 1993; **17**: 86-90
13 **Karatapanis S,** McCormick PA, Kakad S, Chin JK, Islam M, Jeremy J, Harry D, McIntyre N, Burroughs AK, Jacobs M.

Alteration in vascular reactivity in isolated aortic rings from portal vein-constricted rats. *Hepatology* 1994; **20**: 1516-1521
14 **Kiel JW,** Pitts V, Benoit JN, Granger DN, Shepherd AP. Reduced vascular sensitivity to norepinephrine in portal-hypertensive rats. *Am J Physiol* 1985; **248**: G192-G195
15 **Liao JF,** Yu PC, Lin HC, Lee FY, Kuo JS, Yang MC. Study on the vascular reactivity and alpha 1-adrenoceptors of portal hypertensive rats. *Br J Pharmacol* 1994; 111: 439-444
16 **MacGilchrist AJ,** Sumner D, Reid JL. Impaired pressor reactivity in cirrhosis: evidence for a peripheral vascular defect. *Hepatology* 1991; **13**: 689-694
17 **Murray BM,** Paller MS. Decreased pressor reactivity to angiotensin II in cirrhotic rats: Evidence for a post-receptor defect in angiotensin action. *Circ Res* 1985; **57**: 424-431
18 **Murray BM,** Paller MS. Pressor resistance to vasopressin in sodium depletion, potassium depletion, and cirrhosis. *Am J Physiol* 1986; **251**: R525-R530
19 **Hadoke PW,** Hayes PC. *In vitro* evidence for vascular hyporesponsiveness in clinical and experimental cirrhosis. *Pharmacol Ther* 1997; **75**: 51-68
20 **Huang YT,** Lin HC, Yu PC, Lee FY, Tsai YT, Lee SD, Yang MC. Decreased vascular reactivity of portal vein in rats with portal hypertension. *J Hepatol* 1996; **24**: 194-199
21 **Huang YT,** Wang GF, Yang MC, Chang SP, Lin HC, Hong CY. Vascular hyporesponsiveness in aorta from portal hypertensive rats: possible sites of involvement. *J Pharmacol Exp Ther* 1996; **278**: 535-541
22 **Schepke M,** Heller J, Paschke S, Thomas J, Wolff M, Neef M, Malago M, Molderings GJ, Spengler U, Sauerbruch T. Contractile hyporesponsiveness of hepatic arteries in humans with cirrhosis: evidence for a receptor-specific mechanism. *Hepatology* 2001; **34**: 884-888
23 **Van Obbergh L,** Leonard V, Chen H, Xu D, Blaise G. The endothelial and non-endothelial mechanism responsible for attenuated vasoconstriction in cirrhotic rats. *Exp Physiol* 1995; **80**: 609-617
24 **Islam MZ,** Williams BC, Madhavan KK, Hayes PC, Hadoke PW. Selective alteration of agonist-mediated contraction in hepatic arteries isolated from patients with cirrhosis. *Gastroenterology* 2000; **118**: 765-771
25 **Kountouras J,** Billing BH, Scheuer PJ. Prolonged bile duct obstruction: a new experimental model for cirrhosis in the rat. *Br J Exp Pathol* 1984; **65**: 305-311
26 **Lee FY,** Albillos A, Colombato LA, Groszmann RJ. The role of nitric oxide in the vascular hyporesponsiveness to methoxamine in portal hypertensive rats. *Hepatology* 1992; **16**: 1043-1048
27 **Lin HC,** Yang MC, Hou MC, Li SM, Huang YT, Yu PC, Tsai YT, Lee SD. Effects of long-term administration of octreotide in portal vein-stenosed rats. *Hepatology* 1996; **23**: 537-543
28 **Bredt DS,** Mourey RJ, Snyder SH. A simple, sensitive, and specific radioreceptor assay for inositol 1,4,5-trisphosphate in biological tissues. *Biochem Biophys Res Commun* 1989; **159**: 976-982
29 **Huang YT,** Yu PC, Lee MF, Lin HC, Hong CY, Yang MC. Decreased vascular contractile and inositol phosphate responses in portal hypertensive rats. *Can J Physiol Pharmacol* 1995; **73**: 378-382
30 **Challiss RA,** Batty IH, Nahorski SR. Mass measurements of inositol (1,4,5) trisphosphate in rat cerebral cortex slices using a radioreceptor assay: effects of neurotransmitters and depolarization. *Biochem Biophys Res Commun* 1988; **157**: 684-691
31 **Hathaway DR,** March KL, Lash JA, Adam LP, Wilensky RL. Vascular smooth muscle: A review of the molecular basis of contractility. *Circulation* 1991: **83**: 382-390
32 **Somlyo AP,** Somlyo AV. Signal transduction and regulation in smooth muscle. *Nature* 1994; **372**: 231-236
33 **Sieber CC,** Groszmann RJ. Nitric oxide mediates hyporeactivity to vasopressors in mesenteric vessels of portal hypertensive rats. *Gastroenterology* 1992; **103**: 235-239
34 **Vallance P,** Moncada S. Hyperdynamic circulation in cirrhosis: a role for nitric oxide? *Lancet* 1991; **337**: 776-778
35 **Fernández M,** García-Pagán JC, Casadevall M, Bernadich C, Piera C, Whittle BJ, Piqué JM, Bosch J, Rodés J. Evidence against a role for inducible nitric oxide synthase in the hyperdynamic circulation of portal-hypertensive rats. *Gastroenterology* 1995; **108**: 1487-1495
36 **Niederberger M,** Ginès P, Martin P, Tsai P, Morris K, McMurtry I, Schrier RW. Comparison of vascular nitric oxide production and systemic hemodynamics in cirrhosis versus prehepatic portal hypertension in rats. *Hepatology* 1996; **24**: 947-951
37 **Wiest R,** Groszmann RJ. The paradox of nitric oxide in cirrhosis and portal hypertension: too much, not enough. *Hepatology* 2002; **35**: 478-491
38 **Theodorakis NG,** Wang YN, Skill NJ, Metz MA, Cahill PA, Redmond EM, Sitzmann JV. The role of nitric oxide synthase isoforms in extrahepatic portal hypertension, studies in geneknockout mice. *Gastroenterology* 2003; **124**: 1500-1508
39 **Michielsen PP,** Boeckxstaens GE, Sys SU, Herman AG, Pelckmans PA. The role of increased nitric oxide in the vascular hyporeactivity to noradrenaline in long-term portal vein ligated rats. *J Hepatol* 1995; **23**: 341-347
40 **Heller J,** Schepke M, Gehnen N, Molderings GJ, Müller A, Erhard J, Spengler U, Sauerbruch T. Altered adrenergic responsiveness of endothelium-denuded hepatic arteries and portal veins in patients with cirrhosis. *Gastroenterology* 1999; **116**: 387-393
41 **MacGilchrist AJ,** Deighton NM, Hamilton CA, Reid JL. Binding studies of platelet alpha 2- and lymphocyte beta 2-adrenoceptors in patients with cirrhosis. *Br J Clin Pharmacol* 1990; **30**: 644-647
42 **Wu ZY,** Benoit JN. Nonreceptor-mediated intestinal vasoconstriction in portal hypertensive rats. *Am J Physiol* 1994; **267**: H370-H375
43 **Heagerty AM,** Ollerenshaw JD. The phosphoinositide signaling system and the pathogenesis of hypertension. In Hypertension: Pathophysiology, diagnosis, and management. Edited by Laragh JH and Brenner BM. *Raven Press New York* 1999: 1601-1615
44 **Rasmussen H,** Takuwa Y, Park S. Protein kinase C in the regulation of smooth muscle contraction. *FASEB J* 1987; **1**: 177-185
45 **Hartleb M,** Moreau R, Gaudin C, Lebrec D. Lack of vascular hyporesponsiveness to the L-type calcium channel activator, Bay K8644, in rats with cirrhosis. *J Hepatol* 1995; **22**: 202-207
46 **Castro A,** Ros J, Jiménez W, Clària J, Llibre J, Leivas A, Arroyo V, Rivera F, Rodés J. Intracellular calcium concentration in vascular smooth muscle cells of rats with cirrhosis. *J Hepatol* 1994; **21**: 521-526
47 **Atucha NM,** Ortiz MC, Martinez C, Quesada T, Garcia-Estan J. Role of protein kinase C in mesenteric pressor responses of rats with portal hypertension. *Br J Pharmacol* 1996; **118**: 277-282
48 **Tazi KA,** Moreau R, Heller J, Poirel O, Lebrec D. Changes in protein kinase C isoforms in association with vascular hyporeactivity in cirrhotic rat aortas. *Gastroenterology* 2000; **119**: 201-210
49 **Trombino C,** Tazi KA, Gadano A, Moreau R, Lebrec D. Protein kinase C alterations in aortic vascular smooth muscle cells from rats with cirrhosis. *J Hepatol* 1998; **28**: 670-676
50 **Chagneau C,** Tazi KA, Heller J, Sogni P, Poirel O, Moreau R, Lebrec D. The role of nitric oxide in the reduction of protein kinase C-induced contractile response in aortae from rats with portal hypertension. *J Hepatol* 2000; **33**: 26-32

Science Editor Guo SY **Language Editor** Elsevier HK

PO Box 2345, Beijing 100023, China
www.wjgnet.com
wjg@wjgnet.com

ELSEVIER

World J Gastroenterol 2005;11(15):2313-2318
World Journal of Gastroenterology ISSN 1007-9327

• *CLINICAL RESEARCH* •

Impact of comorbid anxiety and depression on quality of life and cellular immunity changes in patients with digestive tract cancers

Fu-Ling Zhou, Wang-Gang Zhang, Yong-Chang Wei, Kang-Ling Xu, Ling-Yun Hui, Xu-Sheng Wang, Ming-Zhong Li

Fu-Ling Zhou, Wang-Gang Zhang, Kang-Ling Xu, Department of Hematology and Oncology, Second Hospital of Xi'an Jiaotong University, Xi'an 710004, Shaanxi Province, China
Yong-Chang Wei, Xu-Sheng Wang, Department of Medical Oncology, First Hospital of Xi'an Jiaotong University, Xi'an 710061, Shaanxi Province, China
Ling-Yun Hui, Research Center of Medical Laboratory, First Hospital of Xi'an Jiaotong University, Xi'an 710061, Shaanxi Province, China
Ming-Zhong Li, Department of Radical Oncology, First Hospital of Xi'an Jiaotong University, Xi'an 710061, Shaanxi Province, China
Co-first-authors: Fu-Ling Zhou and Wang-Gang Zhang
Correspondence to: Dr. Wang-Gang Zhang, Department of Hematology and Oncology, Second Hospital of Xi'an Jiaotong University, Xi'an 710004, Shaanxi Province, China. tcdj1971@eyou.com
Telephone: +86-29-87679457 Fax: +86-29-87678599
Received: 2004-06-24 Accepted: 2004-08-30

Abstract

AIM: A study was performed to investigate the impact of comorbid anxiety and depression (CAD) on quality of life (QOL) and cellular immunity changes in patients with digestive tract cancers.

METHODS: One hundred and fifty-six cases of both sexes with cancers of the digestive tract admitted between March 2001 and February 2004 in the Department of Medical Oncology, First Affiliated Hospital of Xi'an Jiaotong University were randomly enrolled in the study. Depressive and anxiety disorder diagnoses were assessed by using the Structured Clinical Interview for DSM-IV. All adult patients were evaluated with the Hamilton depressive scale (HAMD, the 24-item version), the Hamilton anxiety scale (HAMA, a modified 14-item version), quality of life questionnaire-core 30 (QLQ-C30), social support rating scale (SSRS), simple coping style questionnaire (SCSQ), and other questionnaires, respectively. In terms of HAMD $\geqslant$ 20 and HAMA $\geqslant$ 14, the patients were categorized, including CAD (n = 31) in group A, anxiety disorder (n = 23) in group B, depressive disorder (n = 37) in group C, and non-disorder (n = 65) in group D. Immunological parameters such as T-lymphocyte subsets and natural killer (NK) cell activities in peripheral blood were determined and compared among the four groups.

RESULTS: The incidence of CAD was 21.15% in patients with digestive tract cancers. The average scores of social support was 43.67±7.05 for 156 cases, active coping 20.34±7.33, and passive coping 9.55±5.51. Compared with group D, subjective support was enhanced slightly in group A, but social support, objective support, and utilization of support reduced, especially utilization of support with significance (6.16 *vs* 7.80, $P<0.05$); total scores of active coping decreased, while passive coping reversed; granulocytes proliferated, monocytes declined, and lymphocytes declined significantly (32.87 *vs* 34.00, $P<0.05$); moreover, the percentage of CD3, CD4, CD8 and CD56 in T lymphocyte subsets was in lower level, respectively, and CD56 showed a significant decline in group A (26.02 *vs* 32.20, $P<0.05$), however, CD4/CD8 ratio increased. Physical function, role function, fatigue, sleeplessness and constipation had significant changes among different groups by one-way ANOVA, and group A was in poor QOL. It revealed that global health-related quality of life (QL) were positively correlated with active coping and CD56; CAD was negatively correlated with QL, active coping and CD56. Furthermore, the step-wise regression analysis suggested that utilization of support, CD56, active coping, fatigue, sleeplessness and depression were significant factors contributing to QOL.

CONCLUSION: CAD, which can impair QOL and cellular immunity, occurs with a higher incidence in patients with digestive tract cancers. Hence, it is essential to improve mental health for them with specifically tailored interventions.

Key words: Comorbid anxiety and depression; Quality of life; Digestive tract cancers; T lymphocyte subsets; Natural killer cell

Zhou FL, Zhang WG, Wei YC, Xu KL, Hui LY, Wang XS, Li MZ. Impact of comorbid anxiety and depression on quality of life and cellular immunity changes in patients with digestive tract cancers. *World J Gastroenterol* 2005; 11(15): 2313-2318
http://www.wjgnet.com/1007-9327/11/2313.asp

INTRODUCTION

Comorbid anxiety and depression (CAD) occurs at a high rate in primary care, and is costly to both the individual and society. CAD is significantly associated with special conditions, such as severe symptom, chronic course, social functional lesion, suicidal ideation, bad prognosis, and so on. When severe enough, it may cause negative effects on the antitumor therapy, immunological function, as well as the quality of life[1-4]. Distress, social support, and coping style are the most important psychosocial factors in this approach. As a psychotic or neurotic condition, doctors and mental-health professionals have increasingly recognized

the effects of CAD, however, to date, few studies have systematically examined the clinical correlates of CAD or its effect on patients with digestive tract cancers. Cancers of the digestive tract pose complicated public health problems worldwide[5-7]. These cancers are associated with high morbidity and mortality[8-11], in which esophageal, gastric, colorectal and liver cancers are among the top 10 malignant tumors in China and account for 63% of total cancer mortality[12-14]. In this study, we therefore tested the data on the changes of QOL aspects and immunological parameters in patients with digestive tract cancer suffering from CAD. The Hamilton rating scales and other questionnaires, as well as the immunological parameters were investigated in an attempt to provide guidelines for the means of psychological therapy in the clinical practice and for the evaluation, diagnosis, and management of CAD in the primary care setting.

MATERIALS AND METHODS

Patients

One hundred and fifty-six patients, 69 women and 87 men, with newly diagnosed cancers of the digestive tract, were registered to the protocol between March 2001 and February 2004 in the Department of Medical Oncology, First Affiliated Hospital of Xi'an Jiaotong University. Eligibility criteria required that the patients be of age over 18 years and speak Chinese. Patients with known confusion or judged too ill to participate were excluded from the investigation. None of the patients had central nervous system disease, uncontrolled infections, or other malignancies. All cases were finally verified by the histopathologic examination, including 39 esophageal, 45 gastric, 9 liver, 5 duodenal, 5 gall bladder, 4 pancreatic, 42 colonic and 7 rectal cancer cases. The medical records for these patients were reviewed by investigators and abstracted for the case's characteristics such as obvious symptoms. The average age was 58±9 years with education background of 21 graduated from primary school, 58 from junior high school and 77 from senior high school or above. Their performance status (PS) was defined by Eastern Cooperative Oncology Group and social information such as marital and employment status were obtained in the interview. Depressive and anxiety disorder diagnoses were assessed by using the Structured Clinical Interview for DSM-IV. All adult patients were categorized into four groups in terms of the Hamilton scales.

Psychological measurements

Hamilton depressive scale (HAMD) The 24-item HAMD[15-17], a commonly used clinician-rated depression symptom rating scale, includes 24 items rated on a scale of 0-2, 0-3, or 0-4 (total score range: 0-75). The HAMD was administered by experienced clinical raters certified to have a high rate of interrate reliability and level of procedural integrity. HAMD index, equal to or above 20, suggested the presence of depression. It was not meant for HAMD index to offer a strict diagnostic guideline but rather to denote levels of depression in symptomatology that may be of clinical significance.

Hamilton anxiety scale (HAMA) A modified 14-item version[18], just like the HAMD system, includes 14 items rated on a scale of 0-2, 0-3, or 0-4 (total score range: 0-56). The cases were categorized into two levels of psychological conditions. Level 1, the HAMA index below 14, was considered as no significant psychopathology; level 2, the HAMA Index equal to or above 14, suggested the presence of anxiety.

Quality of life questionnaire-core 30 (QLQ-C30) The European Organization of Research and Treatment of Cancer Quality of Life Questionnaire C30 (EORTC QLQ-C30, version 3.0), the most frequently used health-related quality of life (HRQOL) instruments, consists of 30 items that list the functioning and symptoms of cancer patients[19,20]. One is global health-related quality of life (QL), and the other six multi-item function scales are scored: physical function (PF), role function (RF), cognitive functioning (CF), emotional function (EF), and social function (SF). Furthermore, nine single-item symptom scales are assessed: fatigue (FA), pain (PA), nausea and vomiting (NV), dyspnea (DY), sleeplessness (SL), loss of appetite (AP), constipation (CO), diarrhea (DI), and financial difficulties (FI). The scales are linearly transformed according to the EORTC guidelines - all scales range from 0 to 100, in which a higher scale score represents a higher level of functioning. With respect to the single-item scales, a higher score indicates more symptoms or problems. EORTC QLQ C-30 is a cancer-specific questionnaire translated into various languages and validated in several European countries. In this rearrangement of the EORTC, the Cronbach's reliability coefficients are high[21].

Social support rating scale (SSRS) Social support was assessed by the patients' perception of support from their family or social members. The SSRS has ten selective items, which was employed to evaluate total social support, the levels of objective and subjective as well as the utility of this support[22].

Simple coping style questionnaire (SCSQ) There are some relationships between coping and psychosocial adjustment of patients[23,24]. The SCSQ contains 20 items on a two-point scale (active versus passive coping). Overall, the SCSQ active coping index was shown to be relatively valid with a high internal consistency that was exhibited by an alpha coefficient of 0.89, while the SCSQ passive coping index was shown to be relatively valid with a high internal consistency that was exhibited by an alpha coefficient of 0.78.

Study protocols

The study protocol was in accordance with the guidelines for clinical research and was approved by the Institutional Review Board and the Ethical Review Committee of the hospital cancer center. Informed consent was provided according to the Declaration of Helsinki after all subjects had been fully informed of its purpose. In order to make the patients understand and complete the questionnaires correctly, each item for the psychological measurements was explained by the specialist doctors in a quiet environment before the investigation.

On the day of the experiment, 3.5 mL of peripheral blood was drawn from each patient and anticoagulated by ethylenediaminetetra-acetic acid (EDTA), in which 50 μL of blood was quantified with Sysmes KX-21 blood counter

(Japan) for the measurement of lymphocytes, granulocytes and monocytes. The other 3.0 mL of blood sample was used to determine natural killer (NK) cells (CD_{56}) and T lymphocyte subsets with EPICS ELITE flow cytometer (USA) by individuals blinded to the clinical data for the patients in our immunology laboratory.

Statistical analysis

An individual patient was regarded as a unit. Data were expressed as mean±SD of the mean. Demographic variables were analyzed by descriptive statistics to evaluate the clinical and sociodemographic characteristics of the studied samples. Comparisons between experimental groups were performed by One-Way ANOVA. Pearson correlations were adopted to note the correlation among CAD and other variables. Moreover, contributing factors of QOL were assessed by linear regression. For all statistical evaluations, *P* values of 0.05 or less were considered to indicate significance. All data analyses were conducted using SPSS 11.5 for Windows statistical software.

RESULTS

Incidence of CAD in cancer patients

One hundred and fifty-six individuals were categorized into four groups in terms of HAMD and HAMA index scores according to DSM-IV criteria. The patients with CAD (n = 31) in group A, anxiety disorder (n = 23) in group B, depressive disorder (n = 37) in group C, and no disorder (n = 65) in group D. The incidence of CAD was 21.15% in patients with digestive tract cancers. Furthermore, the differences of index scores listed in Table 1 were significant among four groups.

Table 1 **Changes of HAMD and HAMA scores in different group**

Group	Case (%)	DSM-IV	
	156	HAMD	HAMA
A	33 (21.15)	31.92±9.06[b]	21.75±7.96[d]
B	23 (14.74)	18.92±9.14	17.75±5.94[d]
C	35 (22.44)	25.92±8.17[b]	11.92±6.10
D	65 (41.67)	16.33±6.25	8.19±3.70
F		39. 78	35.25
P		0.00	0.00

[b]P<0.01 *vs* group D; [d]P<0.01 *vs* group D.

The comparison of social support, coping style and cellular immunity

The total scores of social support was from 26 to 55 in the 156 cases, active coping from 6 to 35, and passive coping from 1 to 20. Meanwhile, the average of social support was 43.67±7.05 for 156 cases, active coping 20.34±7.33, and passive coping 9.55±5.51. Compared with group D, subjective support was enhanced slightly in group A, but social support, objective support, and utilization of support reduced, especially utilization of support with significance (6.16 *vs* 7.80, P<0.05); total scores of active coping decreased, while passive coping reversed. As for the parameter changes of cell-mediated immunology in peripheral blood, granulocytes proliferated, monocytes declined, and lymphocytes declined significantly (32.87 *vs* 34.00, P<0.05); moreover, the percentage of CD3, CD4, CD8 and CD56 in T lymphocyte subsets was in lower level, respectively, and CD56 showed a significant decline in group A (26.02 *vs* 32.20, P<0.05). The changes of social support, coping style and cellular immunity findings were summarized in Table 2.

Table 2 **Comparison of social support, coping style and cellular immunity in group A, B and C with group D**

Item	Standard scores				*P*		
	A	B	C	D	P1	P2	P3
Social support	43.14	42.25	44.00	44.30	0.62	0.82	0.86
Subjective support	25.00	26.00	25.17	23.50	0.50	0.35	0.48
Objective support	11.50	12.25	12.00	12.00	0.54	0.90	1.00
Utilization of support[a,c]	6.16	5.75	6.83	7.80	0.04	0.03	0.37
Active coping	20.71	20.25	19.50	21.60	0.62	0.53	0.37
Passive coping	11.43	9.75	7.17	9.10	0.12	0.72	0.76
Lymphocyte[a](%)	32.87	29.20	37.20	34.00	0.01	0.33	0.39
Granulocyte (%)	62.70	68.30	58.75	56.90	0.11	0.19	0.81
Monocyte (%)	4.07	2.50	4.14	6.08	0.49	0.18	0.33
CD_3[f] (%)	52.00	52.60	42.50	59.57	0.21	0.25	0.00
CD_4[d] (%)	25.10	37.30	22.85	25.55	0.88	0.00	0.24
CD_8[d,e] (%)	31.30	19.30	34.10	38.12	0.24	0.00	0.03
CD_{56}[a] (%)	26.02	23.20	30.65	32.20	0.02	0.11	0.42

[a]P<0.05 *vs* group D; [c]P<0.05, [d]P<0.01 *vs* group D; [e]P<0.05, [f]P<0.01 *vs* group D.

QOL in patients with digestive tract cancer

The average of global QL were 41.67, 56.67, 35.00, 66.67, respectively, for patients in group A, B, C and D. It indicated that group A was in poor QOL, and the changes of physical function, role function, fatigue, sleeplessness and constipation were significant among different groups by one-way ANOVA (Table 3).

Table 3 **Analysis of QOL in patients with digestive tract cancer**

	Standard scores				*P*		
	A	B	C	D	*P1*	*P2*	*P3*
Global QL	41.67	56.67	35.00	66.67	0.20	0.71	0.12
Function							
PF[a]	61.43	68.33	69.33	74.67	0.04	0.52	0.12
RF[a]	67.62	70.83	70.00	76.67	0.02	0.44	0.15
EF	75.00	47.92	93.33	90.00	0.11	0.24	0.25
CF	66.67	50.00	73.33	86.67	0.36	0.69	0.16
SF	47.62	54.17	63.33	56.67	0.79	0.50	0.65
Symptom							
FA	50.79	16.67	24.44	25.56	0.10	0.17	0.12
NV	21.43	33.33	10.00	20.00	0.57	0.56	0.93
PA	25.67	29.17	23.03	16.67	0.43	0.26	0.52
Single item							
DY	23.33	16.67	23.00	6.00	0.10	0.12	0.10
SL[b,c]	41.00	36.00	18.33	13.33	0.00	0.04	0.36
AP	61.00	41.67	33.33	23.33	0.40	0.23	0.05
CO[a,d]	55.67	16.67	50.00	10.00	0.04	0.76	0.00
DI	22.33	16.67	15.32	12.15	0.05	0.17	0.14
FI	83.33	66.67	41.67	46.67	0.29	0.55	0.26

[a]P<0.05, [b]P<0.01 *vs* group D; [c]P<0.05 *vs* group D; [d]P <0.01 *vs* group D.

Correlation analysis of CAD patients

Pearson correlation analysis was performed among multiple variables in group A (Table 4). It revealed that QL were positively correlated with active coping and CD56 ($P<0.05$); depression was negatively correlated with lymphocyte ($P<0.05$); passive coping was negatively correlated with CD56 ($P<0.05$); CAD was negatively correlated with QL, active coping and CD56.

Table 4 **Pearson correlation analysis among multiple variables in group A**

Variable	QL	Social support	Depression	Anxiety	Active coping	Passive coping
QL	1.00	0.18	–0.28	–0.07	0.42[a]	0.02
Social support	0.18	1.00	–0.06	–0.13	0.17	0.05
Depression	–0.28	–0.06	1.00	0.31	–0.07	–0.15
Anxiety	–0.07	–0.13	0.31	1.00	–0.29	–0.05
Active coping	0.42[a]	0.17	–0.07	–0.29	1.00	0.28
Passive coping	0.02	0.05	–0.15	–0.05	0.28	1.00
Age (yr)	–0.10	–0.28	0.09	0.02	–0.001	0.12
Lymphocyte	0.08	0.07	–0.66[a]	0.21	0.36	0.37
Granulocyte	–0.22	–0.18	0.08	0.06	–0.44	0.39
Monocyte	0.41	0.35	0.14	–0.28	0.37	0.23
CD3	0.18	0.15	–0.32	–0.17	0.09	0.34
CD4	–0.04	–0.22	–0.07	0.31	–0.24	–0.03
CD8	–0.18	–0.03	0.21	–0.05	0.08	–0.06
CD56	0.67[a]	0.24	–0.36	–0.19	0.43	–0.82[b]

[a]$P<0.05$, [b]$P<0.01$.

Factors contributing to QOL

In clinical trials, there were many issues related to QOL, such as social support, active coping, fatigue, depression, monocyte, CD3, CD56, and so on. However, the step-wise regression analysis suggested that utilization of support, CD56, active coping, fatigue, sleeplessness and depression were the significant factors contributing to QOL (Table 5).

Table 5 **Multivariate analysis of contributing factors of QOL with step-wise regression in patients with digestive tract cancer**

Model	Unstandardized coefficients (B)	Standardized coefficients (β)	*t*	*P*
Utilization of support	1.05	1.32	3 245.61	0.000
CD56	0.16	0.69	2 860.22	0.001
Active coping	0.79	0.77	1 288.73	0.011
FA	–0.16	–0.13	–148.03	0.010
SL	–0.04	–0.02	–144.74	0.014
Depression	–0.001	–0.005	–16.67	0.038

DISCUSSION

Increasing evidence suggests that psychosocial factors such as stress and depression may have a harmful impact on the course of many diseases, such as cardiovascular disease[25,26], functional disorder and cancer[27-30], and may heighten susceptibility to infectious diseases[31,32]. As psychosocial stress has been suspected as a risk factor for cancer, an association between mental disorders and cancer has been reported in many clinical studies within patients. In this research, we have used data gathered in a 3-year consecutive study to examine the comorbidity in adult patients. The findings both confirm and extend the previous results.

Cancer of the gastrointestinal tract is a major health problem in China, especially for the elderly. Results indicated that Chinese patients newly diagnosed with gastrointestinal tract cancer experienced a range of symptoms associated with cancer and its treatment that resulted in varying degrees of symptom distress, anxiety and depression[33,34]. More than 20% of the cancer patients have elevated scores on the Hospital Anxiety and Depression Scale (HADS) subscales depression and anxiety in Harter's report[35]. In the present cohort, there were clear and consistent trends that the average age was 58±9 years and the rates of CAD are 21.15% in patients with digestive tract cancers.

High level of social support appears to play a protective role in psychological adjustment of cancer patients[36]. Social networks, including marital/partner status; number of children, relatives, and friends; and the frequency of religious and community participation, may have an important relation with HRQOL-particularly, mental health-among female long-term colorectal cancer survivors[37]. Indeed, social support in the form of marriage, frequent daily contact with others, and the presence of a confidante may all have protective values against cancer progression. The current study showed that utilization of support went down significantly in group A, but the total scores of social support were close in four groups. It is considered that the family pay attention to patients in need and highlight their problems.

Coping with cancer is multidimensional scaling. There is a significant association between patients who scored highly on the HADS and dissatisfaction with the information provided. Young patients, women, patients with advanced tumors and those who had been treated with both surgery and radiotherapy reported worse function. The worse the functional domain, the more likely it was to be associated with anxiety, depression and ineffective coping style[38]. Use of a logistic regression model showed that those patients most likely to be suffering from severe psychological distress had a worse coping style, measured by the Mental Adjustment to Cancer Scale (MACS)[39]. In this study, patients' passive coping of their disease remained relatively stable, whereas their use of active coping strategies decreased remarkably.

Psychosocial factors influence disease-resistance capabilities via the neuroimmune connection. Some immunological parameters such as T lymphocyte subsets and NK cells are thought to play a central role in antitumour immunity[40-42]. For instance, the growth of malignancies was observed to be inhibited by the activated tumor-specific T cells and the depressed activity of NK cells was probably related to the tumor enlargement and dissemination[43,44]. Suppressive effects of CAD on immune function were well documented in our study, providing further evidence for the specificity of immune changes in psychiatric disorders. Granulocytes proliferated, monocytes declined, and lymphocytes declined significantly; moreover, the percentage of CD3, CD4, CD8 and CD56 in T lymphocyte subsets was in lower level. Thus, it is reasonable to hypothesize that CAD may contribute to impairing immunity, and thereby delay

the recovery of immune mechanisms that may be important for cancer resistance.

In the last decade of clinical research, there has been increasing interest in the evaluation of quality of life. Accurate assessment of the QOL of patients can provide important clinical information to physicians, especially in the area of oncology[45-47]. Changes in QOL are important indicators of the impact of a new cytotoxic therapy, which can affect a patient's willingness to continue treatment, and may aid in defining response in the absence of quantifiable endpoints such as tumor regression[48-51]. The results obtained from the validated QLQ-C30 were used to evaluate the physical role, emotional, cognitive and social functioning, global health status as well as energy and sleep[52]. Then, it revealed that QL were positively correlated with active coping and CD56; CAD was negatively correlated with QL, active coping and CD56. Furthermore, use of a step-wise regression model suggested that utilization of support, CD56, active coping, fatigue, sleeplessness and depression were significant factors contributing to QOL. Our findings were consistent with the reports that patients who showed high levels of anxiety or depression had more health problems[53-56].

Quality of life, symptom management, and social support are the traditional foci for the practise of psychosocial oncology. The current paradigm for research in this area primarily assesses patient responses to cancer-related CAD and illuminates the necessity of ameliorating the negative aspects of those responses. Findings from this research provides insight into the importance of ongoing QOL assessment, symptom management, and intervention to improve QOL of Chinese cancer patients. In brief, CAD, which can impair QOL and cellular immunity, occurs with a higher incidence in patients with digestive tract cancers. Hence, it is essential to improve mental health for them with specifically tailored interventions.

REFERENCES

1 **Stein MB**, Barrett-Connor E. Quality of life in older adults receiving medications for anxiety, depression, or insomnia: findings from a community-based study. *Am J Geriatr Psychiatry* 2002; **10**: 568-574
2 **Sekula LK**, DeSantis J, Gianetti V. Considerations in the management of the patient with comorbid depression and anxiety. *J Am Acad Nurse Pract* 2003; **15**: 23-33
3 **Pop-Jordanova N**, Pop-Jordanov J. Psychophysiological comorbidity and computerized biofeedback. *Int J Artif Organs* 2002; **25**: 429-433
4 **Schussler G**, Schubert C. The influence of psychosocial factors on the immune system (psychoneuroimmunology) and their role for the incidence and progression of cancer. *Z Psychosom Med Psychother* 2001; **47**: 6-41
5 **Shibuya K**, Mathers CD, Boschi-Pinto C, Lopez AD, Murray CJ. Global and regional estimates of cancer mortality and incidence by site: II. Results for the global burden of disease 2000. *BMC Cancer* 2002; **2**: 37
6 **Mitry E**, Benhamiche AM, Couillault C, Roy P, Faivre-Finn C, Clinard F, Faivre J. Effect of age, period of diagnosis and birth cohort on large bowel cancer incidence in a well-defined French population, 1976-1995. *Eur J Cancer Prev* 2002; **11**: 529-534
7 **Ogimoto I**, Shibata A, Fukuda K. World Cancer Research Fund/American Institute of Cancer Research 1997 recommendations: applicability to digestive tract cancer in Japan. *Cancer Causes Control* 2000; **11**: 9-23
8 **Mohandas KM**, Jagannath P. Epidemiology of digestive tract cancers in India. VI. Projected burden in the new millennium and the need for primary prevention. *Indian J Gastroenterol* 2000; **19**: 74-78
9 **Le Vu B**, de Vathaire F, de Vathaire CC, Paofaite J, Roda L, Soubiran G, Lhoumeau F, Laudon F. Cancer incidence in French Polynesia 1985-95. *Trop Med Int Health* 2000; **5**: 722-731
10 **Adanja B**, Gledovic Z, Pekmezovic T, Vlajinac H, Jarebinski M, Zivaljevic V, Pavlovic M. Mortality trends of malignant tumours of digestive organs in Belgrade, Yugoslavia, 1975-1997. *Dig Liver Dis* 2000; **32**: 386-391
11 **Tsukuma H**, Ajiki W, Oshima A. Time-trends in cancer incidence and mortality in Japan. *Gan To Kagaku Ryoho* 2001; **28**: 137-141
12 **Ke L**. Mortality and incidence trends from esophagus cancer in selected geographic areas of China circa 1970-90. *Int J Cancer* 2002; **102**: 271-274
13 **Sun X**, Mu R, Zhou Y, Dai X, Qiao Y, Zhang S, Huangfu X, Sun J, Li L, Lu F. 1990-1992 mortality of stomach cancer in China. *Zhonghua Zhongliu Zazhi* 2002; **24**: 4-8
14 **Pan Y**, Wang J, Liang H. 116 multiple primary cancers in the digestive system. *Zhonghua Zhongliu Zazhi* 2002; **24**: 191-193
15 **Hamilton M**. A rating scale for depression. *J Neurol Neurosurg Psychiatry* 1960; **23**: 56-62
16 **Hamilton M**. Development of a rating scale for primary depressive illness. *Br J Soc Clin Psychol* 1967; **6**: 278-296
17 **Miller IW**, Bishop S, Norman WH, Maddever H. The Modified Hamilton Rating Scale for Depression: reliability and validity. *Psychiatry Res* 1985; **14**: 131-142
18 **Maier W**, Buller R, Philipp M, Heuser I. The Hamilton Anxiety Scale: reliability, validity and sensitivity to change in anxiety and depressive disorders. *J Affect Disord* 1988; **14**: 61-68
19 **Kemmler G**, Holzner B, Kopp M, Dunser M, Greil R, Hahn E, Sperner-Unterweger B. Multidimensional scaling as a tool for analysing quality of life data. *Qual Life Res* 2002; **11**: 223-233
20 **Efficace F**, Bottomley A, Vanvoorden V, Blazeby JM. Methodological issues in assessing health-related quality of life of colorectal cancer patients in randomised controlled trials. *Eur J Cancer* 2004; **40**: 187-197
21 **Chie WC**, Yang CH, Hsu C, Yang PC. Quality of life of lung cancer patients: validation of the Taiwan Chinese version of the EORTC QLQ-C30 and QLQ-LC13. *Qual Life Res* 2004; **13**: 257-262
22 **Nan KJ**, Wei YC, Zhou FL, Li CL, Sui CG, Hui LY, Gao CG. Effects of depression on parameters of cell-mediated immunity in patients with digestive tract cancers. *World J Gastroenterol* 2004; **10**: 268-272
23 **Montgomery C**, Pocock M, Titley K, Lloyd K. Predicting psychological distress in patients with leukaemia and lymphoma. *J Psychosom Res* 2003; **54**: 289-292
24 **Yuet LM**, Alexander M, Chun CJ. Coping and adjustment in Chinese patients with chronic obstructive pulmonary disease. *Int J Nurs Stud* 2002; **39**: 383-395
25 **Barefoot JC**, Burg MM, Carney RM, Cornell CE, Czajkowski SM, Freedland KE, Hosking JD, Khatri P, Pitula CR, Sheps D. Aspects of social support associated with depression at hospitalization and follow-up assessment among cardiac patients. *J Cardiopulm Rehabil* 2003; **23**: 404-412
26 **Schulz R**, Beach SR, Ives DG, Martire LM, Ariyo AA, Kop WJ. Association between depression and mortality in older adults: the Cardiovascular Health Study. *Arch Intern Med* 2000; **160**: 1761-1768
27 **Faller H**, Bulzebruck H, Drings P, Lang H. Coping, distress, and survival among patients with lung cancer. *Arch Gen Psychiatry* 1999; **56**: 756-762
28 **Yang EV**, Glaser R. Stress-induced immunomodulation and the implications for health. *Int Immunopharmacol* 2002; **2**: 315-324
29 **Emmanuel AV**, Mason HJ, Kamm MA. Relationship between psychological state and level of activity of extrinsic gut innervation in patients with a functional gut disorder. *Gut* 2001; **49**: 209-213
30 **Devanand DP**, Adorno E, Cheng J, Burt T, Pelton GH, Roose

SP, Sackeim HA. Late onset dysthymic disorder and major depression differ from early onset dysthymic disorder and major depression in elderly outpatients. *J Affect Disord* 2004; **78**: 259-267

31 **Dunlop SP**, Jenkins D, Neal KR, Spiller RC. Relative importance of enterochromaffin cell hyperplasia, anxiety, and depression in postinfectious IBS. *Gastroenterology* 2003; **125**: 1651-1659

32 **Selwyn PA**, Rivard M, Kappell D, Goeren B, LaFosse H, Schwartz C, Caraballo R, Luciano D, Post LF. Palliative care for AIDS at a large urban teaching hospital: program description and preliminary outcomes. *J Palliat Med* 2003; **6**: 461-474

33 **Lissoni P**, Cangemi P, Pirato D, Roselli MG, Rovelli F, Brivio F, Malugani F, Maestroni GJ, Conti A, Laudon M, Malysheva O, Giani L. A review on cancer - psychospiritual status interactions. *Neuro Endocrinol Lett* 2001; **22**: 175-180

34 **Yan H**, Sellick K. Quality of life of Chinese patients newly diagnosed with gastrointestinal cancer: a longitudinal study. *Int J Nurs Stud* 2004; **41**: 309-319

35 **Harter M**, Reuter K, Schretzmann B, Hasenburg A, Aschenbrenner A, Weis J. Comorbid psychiatric disorders in cancer patients in acute inpatient treatment and medical rehabilitation. *Rehabilitation (Stuttg)* 2000; **39**: 317-323

36 **Barrera M**, Fleming CF, Khan FS. The role of emotional social support in the psychological adjustment of siblings of children with cancer. *Child Care Health Dev* 2004; **30**: 103-111

37 **Sapp AL**, Trentham-Dietz A, Newcomb PA, Hampton JM, Moinpour CM, Remington PL. Social networks and quality of life among female long-term colorectal cancer survivors. *Cancer* 2003; **98**: 1749-1758

38 **Hassanein KA**, Musgrove BT, Bradbury E. Functional status of patients with oral cancer and its relation to style of coping, social support and psychological status. *Br J Oral Maxillofac Surg* 2001; **39**: 340-345

39 **Montgomery C**, Pocock M, Titley K, Lloyd K. Predicting psychological distress in patients with leukaemia and lymphoma. *J Psychosom Res* 2003; **54**: 289-292

40 **Luczynsk W**, Stasiak-Barmuta A, Muszynska-Roslan K, Kasprzycka E. T-lymphocyte and monocyte activation in the course of infection in children with neoplastic disease. *Med Wieku Rozwoj* 2002; **6**: 31-41

41 **Norris S**, Doherty DG, Curry M, McEntee G, Traynor O, Hegarty JE, O'Farrelly C. Selective reduction of natural killer cells and T cells expressing inhibitory receptors for MHC class I in the livers of patients with hepatic malignancy. *Cancer Immunol Immunother* 2003; **52**: 53-58

42 **Pardoll D**. T cells take aim at cancer. *Proc Natl Acad Sci USA* 2002; **99**: 15840-15842

43 **Dudley ME**, Wunderlich JR, Robbins PF, Yang JC, Hwu P, Schwartzentruber DJ, Topalian SL, Sherry R, Restifo NP, Hubicki AM, Robinson MR, Raffeld M, Duray P, Seipp CA, Rogers-Freezer L, Morton KE, Mavroukakis SA, White DE, Rosenberg SA. Cancer regression and autoimmunity in patients after clonal repopulation with antitumor lymphocytes. *Science* 2002; **298**: 850-854

44 **Takeuchi H**, Maehara Y, Tokunaga E, Koga T, Kakeji Y, Sugimachi K. Prognostic significance of natural killer cell activity in patients with gastric carcinoma: a multivariate analysis. *Am J Gastroenterol* 2001; **96**: 574-578

45 **Knobel H**, Loge JH, Brenne E, Fayers P, Hjermstad MJ, Kaasa S. The validity of EORTC QLQ-C30 fatigue scale in advanced cancer patients and cancer survivors. *Palliat Med* 2003; **17:** 664-672

46 **Sherif T**, Jehani T, Saadani M, Andejani AW. Adult oncology and chronically ill patients: comparison of depression, anxiety and caregivers' quality of life. *East Mediterr Health J* 2001; **7**: 502-509

47 **Lutgendorf SK**, Anderson B, Ullrich P, Johnsen EL, Buller RE, Sood AK, Sorosky JI, Ritchie J. Quality of life and mood in women with gynecologic cancer: a one year prospective study. *Cancer* 2002; **94**: 131-140

48 **Blazeby JM**, Conroy T, Hammerlid E, Fayers P, Sezer O, Koller M, Arraras J, Bottomley A, Vickery CW, Etienne PL, Alderson D. Clinical and psychometric validation of an EORTC questionnaire module, the EORTC QLQ-OES18, to assess quality of life in patients with oesophageal cancer. *Eur J Cancer* 2003; **39**: 1384-1394

49 **Nowak AK**, Stockler MR, Byrne MJ. Assessing quality of life during chemotherapy for pleural mesothelioma: feasibility, validity, and results of using the European Organization for Research and Treatment of Cancer Core Quality of Life Questionnaire and Lung Cancer Module. *J Clin Oncol* 2004; **22**: 3172-3180

50 **Wu CW**, Lo SS, Shen KH, Hsieh MC, Lui WY, P'eng FK. Surgical mortality, survival, and quality of life after resection for gastric cancer in the elderly. *World J Surg* 2000; **24**: 465-472

51 **Akechi T**, Okuyama T, Sugawara Y, Nakano T, Shima Y, Uchitomi Y. Suicidality in terminally ill Japanese patients with cancer. *Cancer* 2004; **100**: 183-191

52 **Skarstein J**, Aass N, Fossa SD, Skovlund E, Dahl AA. Anxiety and depression in cancer patients: relation between the Hospital Anxiety and Depression Scale and the European Organization for Research and Treatment of Cancer Core Quality of Life Questionnaire. *J Psychosom Res* 2000; **49**: 27-34

53 **Sarna L**, Evangelista L, Tashkin D, Padilla G, Holmes C, Brecht ML, Grannis F. Impact of respiratory symptoms and pulmonary function on quality of life of long-term survivors of non-small cell lung cancer. *Chest* 2004; **125**: 439-445

54 **Ciaramella A**, Poli P. Assessment of depression among cancer patients: the role of pain, cancer type and treatment. *Psychooncology* 2001; **10**: 156-165

55 **Larsson G**, von Essen L, Sjoden PO. Health-related quality of life in patients with endocrine tumours of the gastrointestinal tract. *Acta Oncol* 1999; **38**: 481-490

56 **Okamoto T**, Shimozuma K, Katsumata N, Koike M, Hisashige A, Tanaka K, Ohsumi S, Saito M, Shikama N, Mitsumori M, Yamauchi C, Watanabe T. Measuring quality of life in patients with breast cancer: a systematic review of reliable and valid instruments available in Japan. *Breast Cancer* 2003; **10**: 204-213

Science Editor Guo SY **Language Editor** Elsevier HK

PO Box 2345, Beijing 100023, China
www.wjgnet.com
wjg@wjgnet.com

ELSEVIER

World J Gastroenterol 2005;11(15):2319-2323
World Journal of Gastroenterology ISSN 1007-9327

• *CLINICAL RESEARCH* •

Nitroester drug's effects and their antagonistic effects against morphine on human sphincter of Oddi motility

Shuo-Dong Wu, Zhen-Hai Zhang, Dong-Yan Li, Jun-Zhe Jin, Jing Kong, Zhong Tian, Wei Wang, Min-Fei Wang

Shuo-Dong Wu, Zhen-Hai Zhang, Dong-Yan Li, Jun-Zhe Jin, Jing Kong, Zhong Tian, Wei Wang, Min-Fei Wang, Department of Hepatobiliary Surgery, the Second Affiliated Hospital, China Medical University, Shenyang 110004, Liaoning Province, China
Correspondence to: Dr. Shuo-Dong Wu, Department of Hepatobiliary Surgery, the Second Affiliated Hospital, China Medical University, Shenyang 110004, Liaoning Province, China. wushuodong@hotmail.com
Telephone: +86-24-83955062
Received: 2004-07-31 Accepted: 2004-09-04

Abstract

AIM: To evaluate the effects of nitroester drugs on human sphincter of Oddi (SO) motility and their antagonistic effects against morphine which shows excitatory effect on Oddi's sphincter motility.

METHODS: The effects of these drugs on SO were evaluated by means of choledochofiberoscopy manometry. A total of 67 patients having T-tubes after cholecystectomy and choledochotomy were involved in the study, they were randomly divided into glyceryl trinitrate (GTN) group, isosorbide dinitrate (ISDN) group, pentaerythritol tetranitrate (PTN) group, morphine associated with GTN group, morphine associated with ISDN group and morphine associated with PTN group. Basal pressure of Oddi's sphincter (BPOS), amplitude of phasic contractions (SOCA), frequency of phasic contractions (SOF), duration of phasic contractions (SOD), duodenal pressure (DP) and common bile duct pressure (CBDP) were scored and analyzed. Morphine was given intramuscularly while nitroester drugs were applied sublingually.

RESULTS: BPOS and SOCA decreased significantly after administration of ISDN and GTN, BPOS reduced from 10.95±7.49 mmHg to 5.92±4.04 mmHg (P<0.05) evidently after application of PTN. BPOS increased from 7.37±5.58 mmHg to 16.60±13.87 mmHg, SOCA increased from 54.09±38.37 mmHg to 100.70±43.51 mmHg, SOF increased from 7.15±3.20 mmHg to 10.38±2.93 mmHg and CBDP increased 3.75±1.95 mmHg to 10.49±8.21 mmHg (P<0.01) evidently after injection of morphine. After associated application of ISDN and GTN, the four indications above decreased obviously. As for application associated with PTN, SOCA and SOF decreased separately from 100.64±44.99 mmHg to 66.17±35.88 mmHg and from 10.70±2.76 mmHg to 9.04±1.71 mmHg (P<0.05) markedly.

CONCLUSION: The regular dose of GTN, ISDN and PTN showed inhibitory effect on SO motility, morphine showed excitatory effect on SO while GTN, ISDN and PTN could antagonize the effect of morphine. Among the three nitroester drugs, the effect of ISDN on SO was most significant.

Key words: Sphincter of Oddi; Nitroester drugs; Glyceryl trinitrate; Isosorbide dinitrate; Pentaerythritol tetranitrate; Morphine; Choledochofiberoscopy manometry

Wu SD, Zhang ZH, Li DY, Jin JZ, Kong J, Tian Z, Wang W, Wang MF. Nitroester drug's effects and their antagonistic effects against morphine on human sphincter of Oddi motility. *World J Gastroenterol* 2005; 11(15): 2319-2323
http://www.wjgnet.com/1007-9327/11/2319.asp

INTRODUCTION

The Oddi's sphincter is the smooth muscle junction connecting the common bile duct and the duodenum which provides regulation of bile flow and hinders duodenobiliary reflux. During phasic contractions the papilla is closed and bile flow stops. Between phasic contractions the papillary muscle is relaxed and the bile flows from the common bile duct to the duodenum. Oddi's sphincter manometry (OSM) is considered as the gold standard method for evaluating the function of Oddi's sphincter. OSM can be directly performed during surgery, or indirectly during ERCP, via a T-tube or percutaneously. A basal pressure and phasic contractions of Oddi's sphincter can be obtained with OSM.

Nitroester drugs are organic nitrates which have been shown to relax the smooth muscle of blood vessels. This effect has been widely accepted for the treatment of angina pectoris. Nitrates also act on a range of smooth muscles and effectively relax muscles of the gallbladder, the bile duct and the SO (SO) not in superscript[1-3]. Morphine can cause excitatory effect on Oddi's sphincter motility and therefore induces upper abdominal pain with characteristics of biliary colic in some patients. Morphine could increase intrabiliary duct pressure[4-6], and delay bile flow to the duodenum[7] So morphine should not be used during ERCP manometry or choledochoscope examination. Few reports have described if nitroester drugs could antagonize the excitatory effect of morphine on Oddi's sphincter motility.

The first aim of this study is to evaluate the effects of three nitroester drugs on human Oddi's sphincter motility by choledochoscope manometry. While the second aim is to assess if nitroester drugs can antagonize morphine's excitatory effect on SO motor function.

Table 1 **Manometric data before and after administration of GTN in 10 patients (mean±SD)**

	Before GTN administration (control)	10 min after GTN administration	20 min after GTN administration
Sphincter of Oddi basal pressure (mmHg)	9.70±2.54	5.71±3.95[a]	5.80±3.42[a]
Amplitude of phasic contractions (mmHg)	88.84±68.77	52.07±23.59[c]	49.78±32.67[c]
Frequency of phasic contractions (n/min)	6.71±2.21	7.32±2.69	5.57±2.05
Common bile duct pressure (mmHg)	5.43±4.40	4.19±4.19	5.43±4.39

[a]$P<0.05$, [c]$P<0.05$ *vs* themselves , $n = 10$ (n represent the number of patients involved in the research).

MATERIALS AND METHODS

Patients

OSM was performed for 67 patients (30 men, 37 women, and mean age 52.5 years, range 37-75 years) with PENTAX LX-750p choledochofiberoscopy at the Second Affiliated Hospital of China Medical University between October 2003 and July 2004. All the patients had undergone cholecystectomy and biliary exploring, T tube drainage at least 1.5 mo (mean 2.5 mo) ago, they were given nothing and kept fasting for 8 h before manometry.

Methods

A triple lumen polyethylene manometry catheter of 200 cm length and 1.7 mm outer diameter was used for manometry. The side holes in the distal end were located 2 mm apart. Each catheter lumen was infused with sterile water at a flow rate of 0.5 mL/min by a minimally compliant hydraulic capillary infusion system. PC polygraph HR (Swedish CTD-Synectics Medical Company) and relevant program were used to record and analyze the tracings. The manometry was performed after removing all the stones in the common bile duct. The catheter was introduced via side-pore of choledochofiberoscopy into duodenum directly, when the tracings of the pressure were stable, duodenal pressure (DP)-curve was recorded. It was then withdrawn in a stepwise fashion, the position of catheter in the sphincter was confirmed by the characteristic pressure changes seen on the screen. It could also be confirmed by direct observation through choledochofiberoscopy. The SO and common bile duct motility tracings were recorded respectively. Drugs were administered sublingually or injected intramuscularly at 10 min intervals. Patients were selected randomly, to receive one of the different schemes of drug administration.

GTN group, ISDN group and PTN group, one of the three nitroester drugs was administered sublingually after the first measurement. GTN was administered in dose of 1 mg while ISDN in doses of 5 mg and PTN in doses of 20 mg. Ten minutes later, the second manometry was performed, and then the third, 20 min after administration.

Morphine associated with GTN group, morphine associated with ISDN group and morphine associated with PTN group. Morphine was administered intramuscularly in doses of 10 mg after the first measurement. Ten minutes later, the second manometry was performed. Then the patient took sublingual administration of 1 mg GTN or 5 mg ISDN or 20 mg PTN. Therefore 10 and 20 min later, the procedure was repeated for the third and the fourth time.

Basal pressure of Oddi's sphincter (BPOS), amplitude of phasic contractions (SOCA), frequency of phasic contractions (SOF), duration of phasic contractions (SOD), DP and common bile duct pressure (CBDP) were recorded and analyzed with a special computer program. Statistical analysis was carried out using the Student's t-test. Data were expressed as mean±SD. A single-tailed P value<0.05 was considered statistically significant.

RESULTS

Sixty-seven patients with T-tube who had no evidence of ampullary abnormality underwent SOM. Clear tracings of pressure and phasic contractions were acquired. Every group had data of three or four times which were compared and contrasted.

Effect of solo nitroester drugs on the SO motility

Ten minutes after sublingual administration of 5 mg ISDN or 1 mg GTN, BPOS and SOCA decreased markedly ($P<0.05$). Even 20 min later, the effects still persisted ($P<0.05$) (Tables 1 and 2). As for the PTN group, BPOS reduced significantly 20 min after administration ($P<0.05$). SOCA and CBD decreased slightly 10 and 20 min after application, but it is not statistically significant (Table 3).

Effects of nitroester drugs antagonize morphine on the SO motility

Morphine at a dose of 10 mg produced an immediate and markedly stimulatory effect on the SO and the common bile duct. Levels of BPOS, SOCA, SOF and CBDP significantly increased 10 min after injection ($P<0.01$) (Table 4). Then 10 min after sublingual application of TPN, the four

Table 2 **Manometric data before and after administration of ISDN in 16 patients (mean±SD)**

	Before ISDN administration (control)	10 min after ISDN administration	20 min after ISDN administration
Sphincter of Oddi basal pressure (mmHg)	10.78±10.79	5.56±3.38[a]	5.40±4.78
Amplitude of phasic contractions (mmHg)	92.06±43.36	60.82±33.64[c]	38.16±18.38[d]
Frequency of phasic contractions (n/min)	7.88±2.58	6.83±3.63	7.13±3.47
Common bile duct pressure (mmHg)	4.49±5.33	3.42±1.56	3.13±2.17

[a]$P<0.05$, [c]$P<0.05$ [d]$P<0.01$ *vs* themselves, $n = 16$ (n represents the number of patients involved in the research).

Table 3 **Manometric data before and after administration of PTN in 11 patients (mean±SD)**

	Before PTN administration (control)	10 min after PTN administration	20 min after PTN administration
Sphincter of Oddi basal pressure (mmHg)	10.95±7.49	8.59±11.90	5.92±4.04[a]
Amplitude of phasic contractions (mmHg)	86.19±42.04	68.08±38.23	59.51±27.35
Frequency of phasic contractions (n/min)	7.04±1.50	5.95±2.79	7.31±2.80
Common bile duct pressure (mmHg)	7.26±4.25	4.83±4.13	5.57±3.49

[a]$P<0.05$ *vs* themselves, $n = 11$ (n represents the number of patients involved in the research).

Table 4 **Manometric data before and after administration of morphine in 30 patients (mean±SD)**

	Before morphine administration (control)	10 min after morphine administration
Sphincter of Oddi basal pressure (mmHg)	7.37±5.58	16.60±13.87[b]
Amplitude of phasic contractions (mmHg)	54.09±38.37	100.70±43.51[d]
Frequency of phasic contractions (n/min)	7.15±3.20	10.38±2.93[f]
Common bile duct pressure (mmHg)	3.75±1.95	10.49±8.21[h]

[b]$P<0.01$, [d]$P<0.01$, [f]$P<0.01$, [h]$P<0.01$ *vs* themselves, $n = 30$ (n represents the number of patients involved in the research).

increased indications decreased markedly to normal levels ($P<0.01$), but the effects were transient. As for 20 min after administration, all the indications had no difference to that of 10 min after morphine injection (Table 5) BPOS, CBDP and SOCA lowered significantly 10 and 20 min after application of ISDN, SOF decreased obviously 20 min after administration ($P<0.05$) (Table 6). BPOS decreased evidently 10 and 20 min after the usage of PTN, SOF slowed down slightly 10 min after administration ($P<0.05$) (Table 7).

DISCUSSION

The advent of OSM in the mid-1970s was the most important development in understanding of the motility of the SO. Prior to that time, the SO motility was evaluated by indirect methods such as cineradiography, contrast media drainage time, and transphincteric flow studies via a T-tube either during or after biliary tract surgery. From then on, OSM has obtained widespread application in the evaluation of patients for SO dysfunction (SOD). OSM could be directly performed during surgery, or indirectly during ERCP, via a T-tube or percutaneously. In this study we studied nitroester drugs' effects and their antagonistic effects against morphine on human SO motility via choledochofiberoscopy manometry.

Nitroester drugs can relax vascular smooth muscles, including that of gastrointestinal tract. They also can effectively relax the muscle of Oddi's sphincter. Among these drugs the effect of glyceryl trinitrate (GTN) on the SO has been well researched. There are relatively few reports about isosorbide dinitrate (ISDN) and no report about pentaerythritol tetranitrate(PTN) on the SO motility. Staritz *et al*[8] first reported that sublingual administration of 1.2 mg of GTN markedly lowered the SO basal tone and phasic contraction amplitude. Later on, Brandstatter *et al*[9] also found a remarkable decrease of the BPOS and the phasic SO contraction frequency, which lasted for many minutes after intravenous administration of nitroglycerine. Furthermore, Staritz *et al*[10] and Uchida *et al*[11] found that sublingual GTN enables the endoscopic extraction of small (6-12 mm)

Table 5 **Antagonism of GTN against morphine on the SO motility in 10 patients (mean±SD)**

	10 min after morphine administration (control)	10 min after GTN associated administration	20 min after GTN associated administration
Sphincter of Oddi basal pressure (mmHg)	12.49±5.40	6.46±6.88[b]	13.47±7.69
Amplitude of phasic contractions (mmHg)	96.56±48.49	56.54±27.19[d]	63.89±34.56
Frequency of phasic contractions (n/min)	8.98±1.34	6.96±1.83[f]	7.66±2.50
Common bile duct pressure (mmHg)	10.99±4.75	4.94±3.27[h]	7.87±4.72

[b]$P<0.01$, [d]$P<0.01$, [f]$P<0.01$, [h]$P<0.01$ *vs* themselves, $n = 10$ (n represents the number of patients involved in the research).

Table 6 **Antagonism of ISDN against morphine on the SO motility in 10 patients (mean±SD)**

	10 min after morphine administration (control)	10 min after ISDN associated administration	20 min after ISDN associated administration
Sphincter of Oddi basal pressure (mmHg)	24.63±19.55	5.43±4.82[a]	5.98±6.02[b]
Amplitude of phasic contractions (mmHg)	112.89±35.04	39.65±21.08[d]	43.45±28.65[d]
Frequency of phasic contractions (n/min)	11.46±3.83	8.82±2.67	8.52±2.21[c]
Common bile duct pressure (mmHg)	11.79±8.21	6.05±4.76[e]	5.75±3.87[e]

[a]$P<0.05$, [c]$P<0.05$, [e]$P<0.05$, [b]$P<0.01$, [d]$P<0.01$ *vs* themselves, $n = 10$ (n represents the number of patients involved in the research).

Table 7 **Antagonism of PTN against morphine on the SO motility in 10 patients (mean±SD)**

	10 min after morphine administration (control)	10 min after PTN associated administration	20 min after PTN associated administration
Sphincter of Oddi basal pressure (mmHg)	13.25±9.63	10.61±11.00	13.12±12.09
Amplitude of phasic contractions (mmHg)	100.64±44.99	75.86±32.16[a]	66.17±35.88[a]
Frequency of phasic contractions (n/min)	10.70±2.76	9.95±1.08	9.04±1.71[c]
Common bile duct pressure (mmHg)	6.99±6.30	6.49±3.66	4.48±4.15

[a]$P<0.05$, [c]$P<0.05$ *vs* themselves , $n = 10$ (*n* represents the number of patients involved in the research).

common bile duct (CBD) stones. Because of its potential side effect, such as severe headache, Luman *et al*[12] recently demonstrated that topical infusion 5 or 10 mg of GTN significantly decreased the basal SO tone and phasic motor function. They stated that local administration of GTN was not accompanied by adverse effects. Wehrmann *et al*[13] found that topical application of GTN or ISDN evoked a profound inhibition of SO motor function, and the effect of ISDN was longer than that of GTN. However, locally administered GTN did not facilitate selective bile-duct access during routine ERCP. Yasuyoshi *et al*[14] described the removal of small common bile duct stones through the combined use of intravenous injection of ISDN and baskets and/or balloons without the use of endoscopic sphincterotomy. Stones were completely removed in 15 of the 18 patients.

We found that both GTN and ISDN could decrease BPOS and SOCA, PTN could reduce SOCA, showed inhibitory effects on SO. Among the three drugs, the effect of ISDN on SO was most significant. Nitroester drugs are nitric oxide (NO) donors, application of NO donors could significantly inhibit SO motor function[15,16] The effect of cholecystokinin, a major hormone with relaxing properties, on the SO was mediated through stimulation of non-adrenergic non-cholinergic (NANC) nerves whose neurotransmitter is NO[17]. Sari *et al*[18] found that nitroglycerin increased the cyclic GMP concentration. Neither tetrodotoxin (TTX) nor vasoactive intestinal polypeptide (VIPa) modified this response. It could also increase the cyclic AMP concentration, which was blocked by both TTX and VIPa. This indicated that relaxation of the SO by NO donors involves a glibenclamide-sensitive mechanism which was closely related to increased formation of cyclic AMP but not of cyclic GMP. So we thought the three nitroester drugs which could provide NO inhibited SO motor function via excitation of NANC nerves.

Narcotic drugs (especially morphine) have already been known to cause spasm of the SO. Nonetheless, they were widely used in the perioperative period in patients with biliary tract disease, both for preoperative analgesia and for supplementation of the anesthetic technique. Unfortunately, spasm of the sphincter may yield a "pseudocalculus" artifact during cholangiography that is indistinguishable from impacted common bile duct stone and may result in unnecessary bile duct exploration. Helm *et al*[19] studied the effect of morphine on SO using OSM during ERCP. In a small cumulative dose of 2.5-5 μg/kg, morphine increased the frequency of phasic contractions to a maximum of 10-12/min, but it did not affect the mean amplitude of phasic contractions and the mean SO basal pressure. As the cumulative dose was increased from 10 to 20 μg/kg, no further increase in the frequency of phasic pressure waves was seen. Instead, the phasic wave amplitude and the mean SO basal pressure increased. Blaut *et al*[20] found that morphine increased the intraductal biliary pressure (IDP) with OSM via a T-tube, but the high IDP caused by morphine could be counteracted by transcutaneous electrical nerve stimulation. We found that morphine could increase the basal pressure of Oddi' sphincter, CBDP, frequency and amplitude of phasic contractions. Morphine showed an excitatory effect on the SO, and might be a cause of Oddi's sphincter dysfunction. Our previous study showed that the effect of morphine on SO lasted more than 20 min[21].

Some reports indicate that the morphine-induced SO spasm, can be reversed by injection of naloxone[22], nalbuphine[23], and glucagon[24]. Nitroglycerin has been used to reverse the spasm induced by narcotic usage[25,26]. But there was no research in manometry evaluated if nitroester drugs can antagonize the excitatory effect of morphine on Oddi's sphincter motility. We found that all the three nitroester drugs could antagonize the excitation induced by morphine. But the mechanism was not well known, and needs to be researched further.

The risk of pancreatitis induced by ERCP cannot be eliminated presently. The etiology of ERCP-induced pancreatitis is multifactorial. Attempts to prevent this complication by using administration of glucagon[27], nifedipine[28,29], hydrocortisone[30] and octreotide[30] have been disappointing. Somatostatin[31,32] is effective in reducing the incidence of pancreatitis after therapeutic ERCP, but the cost is relatively expensive. Sudhindran *et al*[33] found prophylactic treatment with GTN reduced the incidence of pancreatitis following ERCP but did not reduce the extent of hyperamylasemia or the severity of pancreatitis.

In summary, our results indicate that all the three nitroester drugs have inhibitory effects on human SO, they also can antagonize the excitation effect of morphine on SO. Among them the effect of ISDN is most obvious. This action is mediated through stimulation of the NANC nerves. These drugs could be used for several purposes: (1) to remove small- and medium-sized common bile duct stones through intact papillae; (2) to facilitate cannulation of the ampulla in diagnostic ERCP; (3) to relieve the pain caused by biliary colic in patients with SO dysfunction; (4) to reverse the spasm of Oddi's sphincter induced by narcotic usage; and (5) to reduce the incidence of pancreatitis following ERCP.

REFERENCES

1 **Greaves R**, Miller J, O'Donnell L, McLean A, Farthing MJ. Effect of the nitric oxide donor, glyceryl trinitrate, on human gall bladder motility. *Gut* 1998; **42**: 410-413

2 **Chelly J**, Tannieres ML, Tournay D, Franchiset F, Alexandre JH, Passelecq J. Nitroglycerin and amyl nitrite action on common bile duct during operation for vesicular lithiasis (author's transl). *Anesth Analg (Paris)* 1979; **36**: 557-560

3 **Staritz M**. Pharmacology of the sphincter of Oddi. *Endoscopy* 1988; **20** Suppl 1: 171-174

4 **Sarles JC**, Midejean A, Devaux MA. Electromyography of the sphincter of Oddi. Technic and experimental results in the rabbit: Effect of certain drugs. *Am J Gastroenterol* 1975; **63**: 221-231

5 **Dedrick DF**, Tanner WW, Bushkin FL. Common bile duct pressure during enflurane anesthesia. Effects of morphine and subsequent naloxone. *Arch Surg* 1980; **115**: 820-822

6 **Radnay PA,** Duncalf D, Novakovic M, Lesser ML. Common bile duct pressure changes after fentanyl, morphine, meperidine, butorphanol, and naloxone. *Anesth Analg* 1984; **63**: 441-444

7 **Joehl RJ**, Koch KL, Nahrwold DL. Opioid drugs cause bile duct obstruction during hepatobiliary scans. *Am J Surg* 1984; **147**: 134-138

8 **Staritz M**, Poralla T, Ewe K, Meyer zum Buschenfelde KH. Effect of glyceryl trinitrate on the sphincter of Oddi motility and baseline pressure. *Gut* 1985; **26**: 194-197

9 **Brandstatter G**, Schinzel S, Wurzer H. Influence of spasmolytic analgesics on motility of sphincter of Oddi. *Dig Dis Sci* 1996; **41**: 1814-1818

10 **Staritz M**, Poralla T, Dormeyer HH, Meyer zum Buschenfelde KH. Endoscopic removal of common bile duct stones through the intact papilla after medical sphincter dilation. *Gastroenterology* 1985; **88**: 1807-1811

11 **Uchida N**, Ezaki T, Hirabayashi S, Minami A, Fukuma H, Matsuoka H, Yachida M, Kurokohchi K, Morshed SA, Nishioka M, Matsuoka M, Nakatsu T. Endoscopic lithotomy of common bile duct stones with sublingual nitroglycerin and guidewire. *Am J Gastroenterol* 1997; **92**: 1440-1443

12 **Luman W**, Pryde A, Heading RC, Palmer KR. Topical glyceryl trinitrate relaxes the sphincter of Oddi. *Gut* 1997; **40**: 541-543

13 **Wehrmann T**, Schmitt T, Stergiou N, Caspary WF, Seifert H. Topical application of nitrates onto the papilla of Vater: manometric and clinical results. *Endoscopy* 2001; **33**: 323-328

14 **Ibuki Y**, Kudo M, Todo A. Endoscopic retrograde extraction of common bile duct stones with drip infusion of isosorbide dinitrate. *Gastrointest Endosc* 1992; **38**: 178-180

15 **Slivka A**, Chuttani R, Carr-Locke DL, Kobzik L, Bredt DS, Loscalzo J, Stamler JS. Inhibition of sphincter of Oddi function by the nitric oxide carrier S-nitroso-N-acetylcysteine in rabbits and humans. *J Clin Invest* 1994; **94**: 1792-1798

16 **Kaufman HS**, Shermak MA, May CA, Pitt HA, Lillemoe KD. Nitric oxide inhibits resting sphincter of Oddi activity. *Am J Surg* 1993; **165**: 74-80

17 **Behar J**, Biancani P. Pharmacologic characterization of excitatory and inhibitory cholecystokinin receptors of the cat gallbladder and sphincter of Oddi. *Gastroenterology* 1987; **92**: 764-770

18 **Sari R**, Peitl B, Kovacs P, Lonovics J, Palvolgyi A, Hegyi P, Nagy I, Nemeth J, Szilvassy Z, Porszasz R. Cyclic GMP-mediated activation of a glibenclamide-sensitive mechanism in the rabbit sphincter of Oddi. *Dig Dis Sci* 2004; **49**: 514-520

19 **Helm JF**, Venu RP, Geenen JE, Hogan WJ, Dodds WJ, Toouli J, Arndorfer RC. Effects of morphine on the human sphincter of Oddi. *Gut* 1988; **29**: 1402-1407

20 **Blaut U**, Marecik J, Hartwich A, Herman RM, Laskiewicz J, Thor PJ. The effect of transcutaneous nerve stimulation on intraductal biliary pressure in post-cholecystectomy patients with T-drainage. *Eur J Gastroenterol Hepatol* 2003; **15**: 21-26

21 **Wu SD**, Kong J, Wang W, Zhang Q, Jin JZ. Effect of morphine and M-cholinoceptor blocking drugs on human sphincter of Oddi during choledochofiberscopy manometry. *Hepatobiliary Pancreat Dis Int* 2003; **2**: 121-125

22 **Butler KC**, Selden B, Pollack CV Jr. Relief by naloxone of morphine-induced spasm of the sphincter of Oddi in a post-cholecystectomy patient. *J Emerg Med* 2001; **21**: 129-131

23 **Humphreys HK**, Fleming NW. Opioid-induced spasm of the sphincter of Oddi apparently reversed by nalbuphine. *Anesth Analg* 1992; **74**: 308-310

24 **Jones RM**, Detmer M, Hill AB, Bjoraker DG, Pandit U. Incidence of choledochoduodenal sphincter spasm during fentanyl-supplemented anesthesia. *Anesth Analg* 1981; **60**: 638-640

25 **Velosy B**, Madacsy L, Lonovics J, Csernay L. Effect of glyceryl trinitrate on the sphincter of Oddi spasm evoked by prostigmine-morphine administration. *Eur J Gastroenterol Hepatol* 1997; **9**: 1109-1112

26 **Toyoyama H**, Kariya N, Hase I, Toyoda Y. The use of intravenous nitroglycerin in a case of spasm of the sphincter of Oddi during laparoscopic cholecystectomy. *Anesthesiology* 2001; **94**: 708-709

27 **Chang FY**, Guo WS, Liao TM, Lee SD. A randomized study comparing glucagon and hyoscine N-butyl bromide before endoscopic retrograde cholangiopancreatography. *Scand J Gastroenterol* 1995; **30**: 283-286

28 **Sand J**, Nordback I. Prospective randomized trial of the effect of nifedipine on pancreatic irritation after endoscopic retrograde cholangiopancreatography. *Digestion* 1993; **54**: 105-111

29 **Prat F**, Amaris J, Ducot B, Bocquentin M, Fritsch J, Choury AD, Pelletier G, Buffet C. Nifedipine for prevention of post-ERCP pancreatitis: a prospective, double-blind randomized study. *Gastrointest Endosc* 2002; **56**: 202-208

30 **Manolakopoulos S**, Avgerinos A, Vlachogiannakos J, Armonis A, Viazis N, Papadimitriou N, Mathou N, Stefanidis G, Rekoumis G, Vienna E, Tzourmakliotis D, Raptis SA. Octreotide versus hydrocortisone versus placebo in the prevention of post-ERCP pancreatitis: a multicenter randomized controlled trial. *Gastrointest Endosc* 2002; **55**: 470-475

31 **Arvanitidis D**, Anagnostopoulos GK, Giannopoulos D, Pantes A, Agaritsi R, Margantinis G, Tsiakos S, Sakorafas G, Kostopoulos P. Can somatostatin prevent post-ERCP pancreatitis? Results of a randomized controlled trial. *J Gastroenterol Hepatol* 2004; **19**: 278-282

32 **Poon RT**, Yeung C, Liu CL, Lam CM, Yuen WK, Lo CM, Tang A, Fan ST. Intravenous bolus somatostatin after diagnostic cholangiopancreatography reduces the incidence of pancreatitis associated with therapeutic endoscopic retrograde cholangiopancreatography procedures: a randomised controlled trial. *Gut* 2003; **52**: 1768-1773

33 **Sudhindran S**, Bromwich E, Edwards PR. Prospective randomized double-blind placebo-controlled trial of glyceryl trinitrate in endoscopic retrograde cholangiopancreatography-induced pancreatitis. *Br J Surg* 2001; **88**: 1178-1182

Science Editor Guo SY **Language Editor** Elsevier HK

PO Box 2345, Beijing 100023, China
www.wjgnet.com
wjg@wjgnet.com

ELSEVIER

World J Gastroenterol 2005;11(15):2324-2329
World Journal of Gastroenterology ISSN 1007-9327

• *CLINICAL RESEARCH* •

Multi-detector CT enterography with iso-osmotic mannitol as oral contrast for detecting small bowel disease

Lian-He Zhang, Shi-Zheng Zhang, Hong-Jie Hu, Min Gao, Ming Zhang, Qian Cao, Qiao-Wei Zhang

Lian-He Zhang, Shi-Zheng Zhang, Hong-Jie Hu, Ming Zhang, Qiao-Wei Zhang, Department of Radiology, Sir Run Run Shaw Hospital, Zhejiang University, Hangzhou 310016, Zhejiang Province, China
Min Gao, Qian Cao, Department of Gastroenterology, Sir Run Run Shaw Hospital, Zhejiang University, Hangzhou 310016, Zhejiang Province, China
Correspondence to: Lian-He Zhang, Department of Radiology, Sir Run Run Shaw Hospital, Zhejiang University, Hangzhou 310016, Zhejiang Province, China. wujinghzyy@163.com
Telephone: +86-571-86090073-4609
Received: 2004-06-28 Accepted: 2004-07-15

Abstract

AIM: To assess the feasibility and usefulness of multi-detector CT enterography with orally administered iso-osmotic mannitol as negative contrast in demonstrating small bowel disease.

METHODS: Thirteen volunteers and 38 patients with various kinds of small bowel disease were examined. We administered about 1 500 mL iso-osmotic mannitol as negative contrast agent and then proceeded with helical CT scanning on a Siemens Sensation 16 scanner. All volunteers and patients were interviewed about their tolerance of the procedure. Two radiologists post-processed imaging data with MPR, thin MIP, VRT and INSPACE when necessary and then interpreted the scans, and adequacy of luminal distention was evaluated on a four-point scale. Demonstration of features of various kinds of small bowel disease was analyzed.

RESULTS: The taste of iso-osmotic mannitol is good (slightly sweet) and acceptable by all. Small bowel distention was excellent and moderate in most volunteers and patients. CT features of many kinds of diseases such as tumors, Crohn's disease,and small bowel obstruction, *etc.* were clearly displayed.

CONCLUSION: Multi-detector CT enterography with iso-osmotic mannitol as negative contrast to distend the small bowel is a simple, rapid, noninvasive and effective method of evaluating small bowel disease.

Key words: Small bowel; Contrast; Enterography

Zhang LH, Zhang SZ, Hu HJ, Gao M, Zhang M, Cao Q, Zhang QW. Multi-detector CT enterography with iso-osmotic mannitol as oral contrast for detecting small bowel disease. *World J Gastroenterol* 2005; 11(15): 2324-2329
http://www.wjgnet.com/1007-9327/11/2324.asp

INTRODUCTION

The small bowel remains the most challenging segment of the alimentary tube to examine, due to its length, caliber, and overlap of loops. Barium enteroclysis is the conventional radiographic examination method which shows intraluminal lesions, while abdominal CT displays extraintestinal manifestations of small bowel disease. CT enteroclysis (CT-E) is a method of examining the small bowel that combines the advantages of both the the above-mentioned methods[1].

Due to the ability of multidetector CT scanners to scan large volumes at faster speed with the ability to perform reconstruction following the examination, CT-E has become a more feasible extension of the conventional enteroclysis and CT methods of examining the small intestine. A well distended small bowel is mandatory to prevent diagnostic error due to empty loops, so placement of a nasojejunal tube is usually needed which is uncomfortable. The study is to assess the feasibility and usefulness of CT enterography using iso-osmotic mannitol as a orally administered negative contrast agent.

MATERIALS AND METHODS

Materials

Fifty-one subjects (female 21, male 30, mean age 52.3 years, age range = 19-81 years) were included, 13 of which were normal volunteers and 38 were patients with various kinds of diseases proved surgically, endoscopically, pathologically and clinically. There were 15 cases of small-bowel tumors, nine cases of Crohn's disease, four cases of small-bowel adhesions after surgery, five cases of mesenteric ischemia, one case of intussusception, one case of eosinophilic gastroenteroitis, one case of volvulus, one case of duodenal stasis and one case of ileal chronic ulcer with multiple inflammatory polyps.

Protocol

The cleansing preparation usually requires a low-residue diet, ample fluids, and 500 mL 20% mannitol administered orally as laxative on the day prior to the exam, and nothing to eat on the day of the examination. About 1 500 mL of iso-osmotic mannitol was drunk continuously in 40-60 min, and then 20 mg of Raceanisodamine hydrochloride was injected intravenously. Five to ten minutes later began the helical CT

Table 1 **Distension, diameter, wall thickness and enhancement of normal small intestine**

	Distension	Diameter/wall thickness	Plain/artery phase/venous phase enhancement (Hu)
Duodenum	2.52±0.22	19.4±7.01/1.68±0.83	36.65±4.15/70.65±11.95/78.6±12.75
Jejunum	2.33±0.19	20.68±3.47/1.1±0.51	33.26±5.06/65.43±8.15/73.31±11.74
Ileum	2.81±0.31	18.10±4.11/0.90±0.34	6.96±4.51/65.29±8.06/72.17±12.11

scanning on a Siemens Sensation 16 scanner (Siemens, Erlanger, Germany) with CARE DOSE 4D software and the following parameters: 120 KVP, 130 effective mAs, 0.5 S rotation time, 7.0 mm thickness, and Kernel B 20 f smooth. After plain scan, arterial phase and venous phase were scanned 20-30 s and 50-70 s after the start of the intravenous injection of 100 mL Omnipaque (300 mgI/mL) at a rate of 3.5 mL/s. Raw data were retrospectively reconstructed with a thickness of 0.75 mm and a gap of 0.7 mm, which was post-processed into MPR, thin MIP and VRT at a WIZARD workstation, using Inspace when necessary.

Acceptance of the procedure was interviewed, and the cost of the examination was also evaluated.

Image evaluation

Imaging data were independently interpreted by three experienced abdominal radiologists together. Small bowel was divided into three segments: duodenum, jejunum and ileum. Adequacy of luminal distention was assessed with a four-point scale in each segment. A distention score 0, 1, 2, 3 represents less than 30%, 30-50%, 50-80% and more than 80% respectively of the evaluated segment was adequately distended. The maximun outer diameter and wall thickness of duodenum, jejunum and ileum were measured and the CT values of bowel wall in different phase were measured with a ROI of 2 mm^2. The truncated areas of superior mesenteric artery and superior mesenteric vein were measured in front of the unicate of pancreas. The demonstration of mesenteric vasculature was evaluated. MDCT-E features and characteristics of various kinds of diseases were also observed and analyzed including the changes of lumen, wall, vascular, mesenteric and other organs.

Statistical analysis

The results of maximun outer diameter of the small bowel, CT values of bowel wall, and the truncated areas of superior mesenteric artery and superior mesenteric vein were all expressed as mean±SD, and the difference of distension scores among three radiologists was analyzed by χ^2 test. $P<0.05$ was considered statistically significant.

RESULTS

Acceptance of the procedure

All volunteers and patients considered the taste of iso-osmotic mannitol as good or acceptable, and no discomfort and complication were found. In our hospital, it costs about 1 000 yuan RMB, just equal to the charge of the CT examination of the whole abdomen.

Luminal distention and measurements of volunteers

Luminal distention was satisfactory and adequate especially in the ileum in most normal volunteers, the distention score being 2.52±0.22, 2.33±0.19 and 2.81±0.31 in duodenum, jejunum and ileum respectively, and difference of distension scores among three radiologists was not statistically significant ($\chi^2 = 1.464$, $P = 0.486$). The normal outer diameter and wall thickness of small bowel were generally less than 30 and 3 mm in all volunteers (Table 1). The truncated area of superior mesenteric artery (SMA) and superior mesenteric vessel (SMV) were 0.43±0.14 and 1.34±0.31 cm^2. Normal branching of SMA, SMV, and inferior mesenteric artery and inferior mesenteric vein was demonstrated clearly even to the vasa recta (Figure 1).

MDCT-E features of various kinds of diseases

Small bowel tumors Three cases of adenocarcinoma, two in the duodenum and one in jejunum, manifested as lobular small mass and small bowel obstruction (Figures 2 and 3A). The mean diameter of the masses is 3.05±1.23 cm and enhanced markedly (mean CT value being 42.03±8.70,

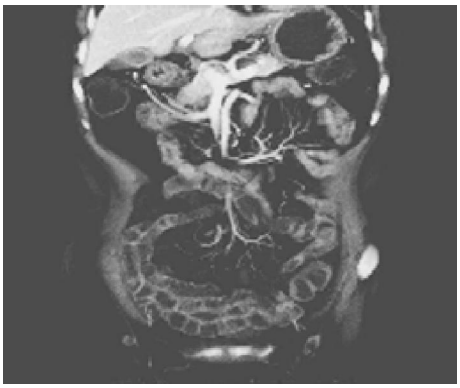

Figure 1 Coronal section shows adequate small bowel luminal distention, uniform wall enhancement and normal superior mesenteric vessels and their branching.

Figure 2 Axial CT-E image of lower abdomen shows an irregular mass at the obstruction point (arrow) which is supposed to be at the ileum.

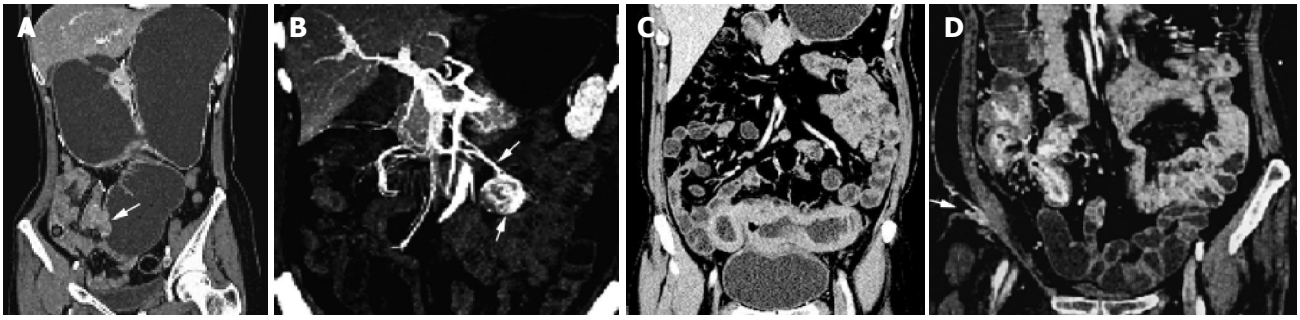

Figure 3 Value of coronal images. **A**: Cronal projection of the same patiet as fig 2 vividly displays the enhanced mass (arrow) at the dilated and elongated proximal jejunum; **B**: Coronal projection of a jejunal GIST clearly exhibits subserously located, markedly enhanced the mass (thin arrow) and its feeding artery and draining vein (thick arrow). **C**: Coronal projection of a MALT lymphoma shows aneurysmal dilatation of a long segment of thickened ileal loop that cannot be seperated from the bladder and multiple mesenteric nodes. **D**: Coronal projection of a patient with Crohn's disease shows segmental ileal wall thickening, mucosal enhancement, prominent perienteric vasculacture and cutaneous orificium fistulae (arrow).

91.30±11.51 and 95.30±9.08 HU at plain scan phase, artery phase and venous phase, respectively). No obviously dilated feeding artery and draining vein were found. Six cases of gastrointestinal stromal tumors (GISTs), one in duodenum and four in jejunum (Figure 3B) and one in ileum, characterized as bigger mass and no bowel obstruction. The masses are larger than adenocarcinoma (mean diameter = 5.13±2.91 cm) and enhanced more significantly (mean CT value being 36.30±12.33, 124.50±12.34, and 136.78±9.12 HU at plain scan phase, artery phase and venous phase, respectively). There were dilated feeding arteries and draining veins in two cases, ring-like calcification in two cases, punctuated calcification in one case, internal necrosis in three cases, hepatic metestasis in one case. All masses are subserously located. One case of T-cell lymphoma demonstrated as thickened wall with ulcer. One case of mucosa associated lymphoid tissue lymphoma in ileum was featured as aneurysmal dilatation of a long segment of thickened ileal loop that cannot be seperated from the bladder and multiple mesenteric nodes (Figure 3C). One case of fibromyxoid sarcoma manifested as a intraluminal mass enhanced markedly combined with retroperitoneal masses. One case of jejunal lipoma displayed as an intraluminal fat density mass with a long stalk. Two cases of peritoneal metastatic adenocarcinoma, which were from pancreatic carcinoma and colon carcinoma respectively, showed peritoneal masses and jejunal obstruction.

Crohn's disease In nine cases of Crohn's disease, 14 segments were involved. The common CT-E signs (Figures 3D and 4) were mucosal enhancement, bowel thickening, luminal stricture and prestenotic dilatation, mesenteric fibrofatty change, prominent perienteric vasculature, mural stratification, enlarged lymph nodes. Other signs include ascites (four cases), abscess anal fistula (one case), enterocutaneous fistula (1 case), gall bladder wall enhancement (two cases) and pelvic bone destruction (one case).

Post-operative adhesions In four cases of post-operative adhesions, common CT-E signs were abnormally distributed loops. Internal hernia and then strangulation (intramural gas) was found in one case. A band and a closed loop were found in the second patient with obstruction. Chronic ulcer in an adhered jejunal loop was displayed clearly in the third patient. Small-bowel loops surrounding a peritoneal catheter was found in the fourth patient.

Mesenteric ischemia In five cases of mesenteric ischemia the common signs were thickened bowel wall and fuzzy mesenteric fat. Two cases were atherosclerotic disease of the superior mesenteric artery (SMA), and luminal narrowing, fewer branching and calcified atherosclerotic plaque were found on the thin MIP. Pneumatosis was found in one patient who combined with pyemia. One case of acute mesenteric ischemia was caused by thrombosis in the SMA which showed the filling defect in the SMA and small bowel mural stratification (Figures 5 and 6). One case of thrombosis in the proximal superior mesenteric vein and one case of hematoma in mesenteric root were clearly

Figure 4 Sagittal projection of the same patient as figure 3D shows a markedly enhanced enterocutaneous fistula (arrow).

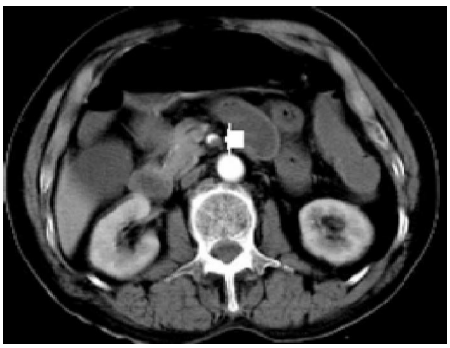

Figure 5 Axial section of an acute mensenteric ischemia caused by thrombosis shows an filling defect in SMA (arrow).

Figure 6 Lower section of the same patient as Figure 5 shows small bowel wall thickening with mural stratification.

demonstrated as intraluminal defect and high density mass around the proximal superior mesenteric vessel.

Others One case of ileum-ileum intussusception looked like sausage-like mass at the obstruction point, the intussuscipiens and intussusceptum being clearly identified. One case of eosinophilic gastroenteritis had diffusely thickened bowel wall that resolved very soon after the administration of cortical hormone. One case of small bowel volvulus after gastric operation showed the whirl sign of the vessels in the mesentery and the mesenteric density increased. One case of duodenal stasis was characterized as dilated proximal duodenum and compressed transverse segment of duodenum by aorta and superior mesenteric artery. One case of chronic ileal ulcer with multiple inflammatory polyps were clearly defined on CT enterography, and the ulcer demonstrated as a regional eccentric thickened bowel wall with irregular inner border and polyps as brightly enhanced nodules.

DISCUSSION

Owing to its length, caliber, and overlap of loops, small bowel remains the most challenging part to be assessed. Barium enteroclysis shows the intraluminal lesion clearly but cannot depict mural and extraintestinal changes, while conventional abdominal CT without adequate distention of the bowel can display the outside of the bowel but usually overlook the intraluminal disease and mural change. MDCT-E combines the advantages of the above two methods and overcomes each other's disadvantages. Currently, data on the technical and clinical application of MDCT-E is fragmentary and preliminary[1]. The adequate distention of small bowel is mandatory to CT-E, and numerous techniques have been designed to optimize visualization of the small bowel[1–3], and the majority of these studies have employed fluoroscopic placement of a nasojejunal tube to infuse contrast material. A few recent reports described CT enterography with orally administered negative contrast, which had satisfactory results[4,5].

Clinical applications of CT-E included: (1) small bowel obstruction - conventional CT has high sensitivity in diagnosing high-grade obstruction and is of value in confirming the presence or absence of strangulation. Contrast examination is not indicated in these cases[6–8]. CT-E has been reported to have greater sensitivity (89%) and specificity (100%) than conventional CT (50% and 94%, respectively) in patients suspected of having a partial small bowel obstruction, and this difference was even greater when abdominal malignancy was known or suspected[1]. The precise localization and classification of adhesions, the most common cause of small bowel obstruction, is readily made with CT-E. Analysis of axial images aided by coronal and sagittal reformatting allows categorization of small bowel adhesions into parietal and visceral adhesions. This ability is especially useful in complicated cases and often increase the confidence of the radiologists[9]. In addition, clinicians and surgeons appreciate the availability of additional planes, which helps them to better understand complex cases[10]. Single or multiple points of obstruction are readily demonstrated similar to barium enteroclysis but their precise location is made easier with CT-E. Obstruction from primary malignancy or metastatic disease is also diagnosed readily with CT-E[11]. (2) Crohn's disease - CT has come to play an increasingly important role in the evaluation of patients with Crohn's disease because of its ability to accurately demonstrate the bowel wall as well as adjacent structures and extraluminal extension of disease[12]. For acutely ill patients, CT is often the only study required, providing crucial information for both the accurate diagnosis and treatment of the many complications associated with Crohn's disease[13-15]. Patients with Crohn's disease often have complex disease that involves multiple bowel loops or adjacent organs. The ability of CT-E to visualize the scan in more than the axial plane is essential for complete understanding of the extent of the disease. Multiplanar reconstructions significantly improved the observer's confidence in their interpretation of the imaging and in their ability to detect the extent of the bowel involvement[16]. We also found that multiplanar reformation is very useful in vividly displaying the complex involvement of Crohn's disease. CT-E can be highly accurate in depicting mucosal abnormalities, bowel thickening, fistulae, and extraintestinal complications. Activity of Crohn's disease was evaluated on CT-E by the presence of mural stratification, mucosal and mural hyperenhancement, edema in the perienteric mesenteric fat, and prominent pericolic or perienteric vasculature[2,17-19]. (3) Neoplasms - CT plays a more active role in detection and staging of small bowel neoplasms. Even subtle adenocarcinomas can be visualized by CT-E, which most frequently appears as eccentric or as circumferential wall thickening involving a short segment of the small bowel and results in "apple core" appearance[20]. Gastrointestinal stromal tumors (GISTs) can be seen as a large mass on CT-E, which may be helpful to define the site of the tumor; benign GISTs cannot be reliably differentiated from malignant ones on CT unless there is obvious metastasis or local extension. GISTs can ulcerate or calcify and usually are not associated with significant adenopathy[20]. In our group, GISTs usually enhanced significantly and have dilated feeding arteries and draining veins. Carcinoid tumor has a propensity for ileum[21], which has not been very successfully detected by traditional CT examinations and now can be visualized when water is given as oral contrast and a good IV contrast bolus is administered and thin-collimation MDCT is performed[22]. Carcinoids that have infiltrated the mesentery demonstrate a characteristic CT appearance as an infiltrating mesenteric mass that contains calcification in upto 70%

of cases. MDCT-E well demonstrate the relationship of the mass to the mesenteric vessels, which is crucial for surgical planning[23]. CT has played an important role in evaluation and follow-up of patients with lymphoma[24]. Primary small bowel lymphoma often appears as focally thickened loop, which usually does not result in obstruction. CT-E offers the advantage of simultaneously assessing adenopathy, extraluminal extent and small bowel lesions. CT-E, because of the large surface rendering with a volume challenge, allows delineation of lesions as small as 0.5 cm in size[25]. (4) Obscure gastrointestinal bleeding - in patients with an obscure gastrointestinal bleeding, the conventional small bowel follow through has no place in clearing the small bowel after negative endoscopy, angiography, or a tagged red cell scan[26,27]. Traditional double-contrast enteroclysis is estimated to be successful in 21% of such cases[28]. CT-E maybe useful in patients with anemia of unknown origin. Arteriovenous malformations are the most common vascular etiology. CT-E using methylcellulose as a neutral luminal contrast material with an IV contrast bolus of 150 mL at 4 mL/s can potentially identify the source of unexplained gastrointestinal bleeding. Vascular malformations have been diagnosed on helical CT with IV contrast material[29,30]. Duodenal varices have been reported to be successfully demonstrated by multislice helical CT[31].

To our knowledge, this is the first report of CT enterography using iso-osmotic mannitol as orally administered negative contrast to distend the small bowel. Iso-osmotic mannitol is slightly sweet and acceptable, which cannot be absorbed by the intestine and a large volume administered orally in a short time can distend the small bowel adequately. This method freed the patients from the placement of nasojejunal tube and acceptable by most patients without important complications. The lumen, wall, extraintestinal structure, and other organs are satisfactorily demonstrated in both volunteers and patients. In our group, adenocarcinoma manifested as small mass with obstruction while GIST as bigger mass enhanced significantly without obstruction. Crohn's disease characterized as thickened wall, enhanced mucosae, fuzzy mesenteric fat, enlarged lymph nodes, prominent perienteric vasculature and extraintestinal complications. Other diseases have also been shown clearly.

With comparison to conventional CT, we found that MDCT-E has many advantages: (1) lesion can be localized more precisely and characterized accurately. Two cases of adenocarcinoma associated with bowel obstruction had been mis-interpreted as distal small bowel obstruction or colon obstruction on conventional axial CT scans, while CT enterography accurately showed the mass causing proximal small bowel obstruction. (2) CT enterography can display mesenteric lymphadenopathy which usually be overlooked at conventional CT. (3) CT enterography with its 3-D display can more precisely explain the relationship between lesions and neighboring structure that is helpful to surgery. (4) CT enterography with its coronal projections that is similar to conventional enteroclysis is much more welcomed by surgeons and physicians.

Although our experience is limited, we believe that CT enterography with iso-osmotic mannitol as orally administered negative contrast is a simple, noninvasive, economic, effective method for assessing small bowel diseases and others, which should be further studied.

REFERENCES

1 **Bender GN**, Maglinte DD, Kloppel VR, Timmons JH. CT enteroclysis: a superfluous diagnostic procedure or valuable when investigating small bowel disease? *AJR Am J Roentgenol* 1999; **172**: 373-378

2 Mako EK, Mester AR, Tarjan Z, Karlinger K, Toth G. Enteroclysis and spiral CT examination in diagnosis and evaluation of small bowel Crohn's disease. *Eur J Radiol* 2000; **35**: 168-175

3 **Bender GN**, Timmons JH, Williard WC, Carter J. Computed tomographic enteroclysis: one methodology. *Invest Radiol* 1996; **31**: 43-49

4 **Doerfler OC**, Ruppert-Kohlmayr AJ, Reittner P, Hinterleitner T, Petritsch W, Szolar DH. Helical CT of the small bowel with an alternative oral contrast material in patients with Crohn disease. *Abdom Imaging* 2003; **28**: 313-318

5 **Wold PB**, Fletcher JG, Johnson CD, Sandborn WJ. Assessment of small bowel Crohn disease: noninvasive peroral CT enterography compared with other imaging methods and endoscopy-feasibility study. *Radiology* 2003; **229**: 275-281

6 **Maglinte DD**, Gage SN, Harmon BH, Kelvin FM, Hage JP, Chua GT, Ng AC, Graffis RF, Chernish SM. Obstruction of the small intestine:accuracy and role of CT in diagnosis. *Radiology* 1993; **188**: 61-64

7 **Megibow AJ**, Balthazar EJ, Cho KC, Medwid SW, Birnbaum BA, Noz ME. Bowel obstruction: evaluation with CT. *Radiology* 1991; **180**: 313-318

8 **Maglinte DD**, Balthazar EJ, Kelvin FM, Megibow AJ. The role of radiology in the diagnosis of small-bowel obstruction. *AJR Am J Roentgenol* 1997; **168**: 1171-1180

9 **Caoili EM**, Paulson EK. CT of small-bowel obstruction: another perspective using multiplanar reformations. *AJR Am J Roentgenol* 2000; **174**: 993-998

10 **Khurana B**, Ledbetter S, McTavish J, Wiesner W, Ros PR. Bowel obstruction revealed by multidetector CT. *AJR Am J Roentgenol* 2002; **178**: 1139-1144

11 **Maglinte DD**, Bender GN, Heitkamp DE, Lappas JC, Kelvin FM. Multidetector-row helical CT enteroclysis. *Radiol Clin North Am* 2003; **41**: 249-262

12 **Fishman EK**, Wolf EJ, Jones B, Bayless TM, Siegelman SS. CT evaluation of Crohn's disease: effect on patient management. *AJR Am J Roentgenol* 1987; **148**: 537-540

13 **Gore RM**, Ghahremani GG. Radiologic investigation of acute inflammatory and infectious bowel disease. *Gastroenterol Clin North Am* 1995; **24**: 353-384

14 **Wills JS**, Lobis IF, Denstman FJ. Crohn disease: state of the art. *Radiology* 1997; **202**: 597-610

15 **Gore RM**, Balthazar EJ, Ghahremani GG, Miller FH. CT features of ulcerative colitis and Crohn's disease. *AJR Am J Roentgenol* 1996; **167**: 3-15

16 **Raptopoulos V**, Schwartz RK, McNicholas MM, Movson J, Pearlman J, Joffe N. Multiplanar helical CT enterography in patients with Crohn's disease. *AJR Am J Roentgenol* 1997; **169**: 1545-1550

17 **Goldberg HI**, Gore RM, Margulis AR, Moss AA, Baker EL. Computed tomography in the evaluation of Crohn disease. *AJR Am J Roentgenol* 1983; **140**: 277-282

18 **Del Campo L**, Arribas I, Valbuena M, Mate J, Moreno-Otero R. Spiral CT findings in active and remission phases in patients with Crohn disease. *J Comput Assist Tomogr* 2001; **25**: 792-797

19 **Meyers MA**, McGuire PV. Spiral CT demonstration of hypervascularity in Crohn disease: "vascular jejunization of the ileum" or the "comb sign". *Abdom Imaging* 1995; **20**: 327-332

20 **Buckley JA**, Jones B, Fishman EK. Small bowel cancer. Imag-

ing features and staging. *Radiol Clin North Am* 1997; **35**: 381-402
21 **Maglinte DT**, Reyes BL. Small bowel cancer. Radiologic diagnosis. *Radiol Clin North Am* 1997; **35**: 361-380
22 **Wallace S**, Ajani JA, Charnsangavej C, DuBrow R, Yang DJ, Chuang VP, Carrasco CH, Dodd GD. Carcinoid tumors: imaging procedures and interventional radiology. *World J Surg* 1996; **20**: 147-156
23 **Horton KM**, Fishman EK. The current status of multidetector row CT and three-dimensional imaging of the small bowel. *Radiol Clin North Am* 2003; **41**: 199-212
24 **Rubesin SE**, Gilchrist AM, Bronner M, Saul SH, Herlinger H, Grumbach K, Levine MS, Laufer I. Non-Hodgkin lymphoma of the small intestine. *Radiographics* 1990; **10**: 985-998
25 **Bender GN**, Maglinte DD, McLarney JH, Rex D, Kelvin FM. Malignant melanoma: patterns of metastasis to the small bowel, reliability of imaging studies, and clinical relevance. *Am J Gastroenterol* 2001; **96**: 2392-2400
26 **Bender GN**. Radiographic examination of the small bowel. An application of odds ratio analysis to help attain an appropriate mix of small bowel follow through and enteroclysis in a working-clinical environment. *Invest Radiol* 1997; **32**: 357-362
27 **Maglinte DD**, Lappas JC, Kelvin FM, Rex D, Chernish SM. Small bowel radiography: how, when, and why? *Radiology* 1987; **163**: 297-305
28 **Moch A**, Herlinger H, Kochman ML, Levine MS, Rubesin SE, Laufer I. Enteroclysis in the evaluation of obscure gastrointestinal bleeding. *AJR Am J Roentgenol* 1994; **163**: 1381-1384
29 **Ettorre GC**, Francioso G, Garribba AP, Fracella MR, Greco A, Farchi G. Helical CT angiography in gastrointestinal bleeding of obscure origin. *AJR Am J Roentgenol* 1997; **168**: 727-731
30 **Mindelzun RE**, Beaulieu CF. Using biphasic CT to reveal gastrointestinal arteriovenous malformations. *AJR Am J Roentgenol* 1997; **168**: 437-438
31 **Weishaupt D**, Pfammatter T, Hilfiker PR, Wolfensberger U, Marincek B. Detecting bleeding duodenal varices with multislice helical CT. *AJR Am J Roentgenol* 2002; **178**: 399-401

Science Editor Guo SY **Language Editor** Elsevier HK

PO Box 2345, Beijing 100023, China
www.wjgnet.com
wjg@wjgnet.com

ELSEVIER

World J Gastroenterol 2005;11(15):2330-2333
World Journal of Gastroenterology ISSN 1007-9327

• *BRIEF REPORTS* •

Effect of ZVAD-fmk on hepatocyte apoptosis after bile duct ligation in rat

Shyr-Ming Sheen-Chen, Hsin-Tsung Ho, Wei-Jen Chen, Hock-Liew Eng

Shyr-Ming Sheen-Chen, Department of Surgery, Chang Gung Memorial Hospital, Kaohsiung, College of Medicine, Chang Gung University, Taiwan China
Hsin-Tsung Ho, Department of Laboratory Medicine, Mackay Memorial Hospital, Taiwan China
Wei-Jen Chen, Hock-Liew Eng, Department of Pathology, Chang Gung Memorial Hospital, Kaohsiung, College of Medicine, Chang Gung University, Taiwan China
Supported by the grant NSC 89-2314-B-182A-165 from the National Science Council of Taiwan China
Correspondence to: Dr. Shyr-Ming Sheen-Chen, Department of Surgery, Chang Gung Memorial Hospital, Kaohsiung, 123, Ta-Pei Road, Niao-Sung Hsiang, Kaohsiung Hsien, Taiwan China. smsheen@yahoo.com
Telephone: +886-7-7317123
Received: 2004-08-14 Accepted: 2004-09-30

Abstract

AIM: Retention and accumulation of toxic hydrophobic bile salts within hepatocyte may cause hepatocyte toxicity by inducing apoptosis. Apoptosis is a pathway of cell death orchestrated by a family of proteases called caspases. Z-Val-Ala-Asp (OMe)-fluoromethyl ketone (ZVAD-fmk) is a cell-permeable irreversible inhibitor of caspase. The purpose of this study was to evaluate the possible effect of ZVAD-fmk on hepatocyte apoptosis after bile duct ligation in the rat.

METHODS: Male Sprague-Dawley rats, weighing 250-300 g, were randomized to five groups of five rats each. Group 1 underwent common bile duct ligation and simultaneous treatment with ZVAD-fmk (dissolved in dimethylsulfoxide (DMSO)). Group 2 underwent common bile duct ligation and simultaneous treatment with Z-Phe-Ala-fluoromethyl ketone (ZFA-fmk, dissolved in DMSO). Group 3 underwent sham operation and simultaneous treatment with the same amount of DMSO. Group 4 underwent sham operation and simultaneous treatment with the same amount of normal saline. Group 5 underwent common bile duct ligation without other manipulation. After three days, liver tissue was harvested for histopathologic analysis and measurements of apoptosis.

RESULTS: When compared with sham operation, common bile duct ligation significantly increased hepatocyte apoptosis ($P = 0.008$) and ductular proliferation ($P = 0.007$). ZVAD-fmk significantly diminished the increased hepatocyte apoptosis and ductular proliferation after common bile duct ligation ($P = 0.008$ and $P = 0.007$, respectively). ZFA did not show the same effects.

CONCLUSION: Hepatocyte apoptosis and ductular proliferation significantly increased after common bile duct ligation. ZVAD-fmk effectively diminished the increased hepatocyte apoptosis and ductular proliferation after common bile duct ligation, whereas ZFA-fmk did not.

Key words: Apoptosis; Obstructive jaundice; ZVAD-fmk; ZFA

Sheen-Chen SM, Ho HT, Chen WJ, Eng HL. Effect of ZVAD-fmk on hepatocyte apoptosis after bile duct ligation in rat. *World J Gastroenterol* 2005; 11(15): 2330-2333
http://www.wjgnet.com/1007-9327/11/2330.asp

INTRODUCTION

Apoptosis is an important process in a wide variety of biological functions, including normal cell turnover, immune responses, embryonic development, metamorphosis and hormone-dependent atrophy, and in chemical-induced cell death[1-3]. Inappropriate apoptosis is implicated in many human diseases[4,5]. Cholestasis, an impairment in bile formation, occurs in many human liver disease[6]. Although the pathogenic events culminating in cholestasis differ in each disease, hepatocellular injury is a consistent feature of cholestasis that causes liver dysfunction, promoting fibrogenesis, and ultimately leads to liver failure[7].

Retention and accumulation of toxic hydrophobic bile salts within hepatocyte may cause hepatocyte toxicity by inducing apoptosis[8-13]. Apoptosis is a pathway of cell death orchestrated by a family of proteases called caspases[14-17]. Z-Val-Ala-Asp (OMe)-fluoromethyl ketone (ZVAD-fmk) is a cell-permeable irreversible inhibitor of caspase and recent data suggest that it might block the processing of many caspases[3,18-20]. The purpose of our study was to evaluate the possible effect of ZVAD-fmk on hepatocyte apoptosis after bile duct ligation in the rat.

MATERIALS AND METHODS

Animal and experimental design

Male Sprague-Dawley rats, weighing 250-300 g, were housed under controlled temperature, humidity and 12-h dark/light cycles living in stainless-steel cages and were allowed free access to water and rat chow before and after operation. The animals were randomized to five groups of five rats each.

Group 1 underwent common bile duct ligation and simultaneous treatment with ZVAD-fmk (dissolved in

dimethylsulfoxide (DMSO), Enzyme Systems Products, Dublin, CA). The first dose of ZVAD-fmk (0.5 mg) was injected into the inferior vena cava immediately after bile duct ligation. Subsequent doses of ZVAD-fmk (0.5 mg twice daily) were given intraperitoneally on the first and second postoperative days. The last dose (0.5 mg) was given on the morning of the third postoperative day.

Group 2 underwent common bile duct ligation and simultaneous treatment with Z-Phe-Ala-fluoromethyl ketone (ZFA-fmk, dissolved in DMSO, Enzyme Systems Products). The first dose of ZFA-fmk (0.5 mg) was injected into the inferior vena cava immediately after bile duct ligation. Subsequent doses of ZFA-fmk (0.5 mg twice daily) were given intraperitoneally on the first and second postoperative days. The last dose (0.5 mg) was given on the morning of the third postoperative day.

Group 3 underwent sham operation and simultaneous treatment with the same amount of DMSO. The first dose of DMSO was injected into the inferior vena cava immediately after sham operation. Subsequent doses of DMSO (the same amount twice daily) were given intraperitoneally on the first and second postoperative days. The last dose was given on the morning of the third postoperative day.

Group 4 underwent sham operation and simultaneous treatment with the same amount of normal saline. The first dose of normal saline was injected into the inferior vena cava immediately after sham operation. Subsequent doses of normal (the same amount twice daily) were given intraperitoneally on the first and second postoperative days. The last dose was given on the morning of the third postoperative day.

Group 5 underwent common bile duct ligation without other manipulation.

Operative procedures

By using sterile techniques, a mid-line incision was made, the common bile duct was identified, double ligated with 5-0 silk and divided between the two ligatures[21-26]. In sham-operated animals, the common bile duct was freed from the surrounding soft tissue without ligation and transection. The operation was performed by using intraperitoneal anesthesia induced with ketamine 80 mg/kg plus xylazine 10 mg/kg.

Harvest of tissues

After three days, the animals were anesthetized, and laparotomy was repeated. Liver tissue was harvested, embedded in optimal cutting temperature compound (Sakura Finetechnical, Tokyo, Japan) and immediately snap-frozen in liquid nitrogen for histopathologic analysis and measurements of apoptosis.

TUNEL assay

Hepatocyte apoptosis was quantitated by using the terminal deoxynucleotidyl transferase-mediated deoxyuridine triphosphate nick-end labeling (TUNEL) assay. This specific assay uses terminal deoxynucleotidyl transferase to attach biotinylated deoxyuridine triphosphate to free 3'-OH DNA ends. All liver tissue specimens about 5 mm in size were fixed in freshly prepared 4% paraformaldehyde in PBS. The tissue blocks were embedded in Enclosed Processing System (Sakura, Tokyo). Tissue sections (5 μm) were prepared using a microtome and placed on glass slides. The sections were deparaffinized in xylene and dehydrated in ethanol. The sections were incubated with 20 μg/mL proteinase K in PBS for 20 min at room temperature. After rinsing the specimen twice with PBS, the sections were processed following the instruction of a commercial kit (DeadEnd Colorimetric Apoptosis Detection System, Promega, Madison, WI). Sections were stained by streptavidin-horseradish peroxidase conjugate, then counterstained with hematoxylin. The peroxidase-positive cells were identified morphometrically by brown staining nuclei. The number of TUNEL-positive cells was counted in 10 random microscopic fields (400×). Each microscopic field contained approximately 913±59 hepatocytes.

Histopathology

H&E and trichrome-stained liver specimens from the rats undergoing bile duct ligation were evaluated by light microscopy for ductal proliferation[7]. The specimens were scored by an experienced hepatopathologist. Ductal proliferation was scored using the following grading system: 0, <10% of portal areas involved; 1, 10-50% of portal areas involved; 2, >50% of portal areas involved; 3, circumferential involvement of at least 50% of the portal area without significant expansion of portal tract; 4, circumferential involvement of at least 50% of the portal area with significant expansion of portal tract; 5, same as 4 plus bridging of the portal tracts in <20% of instances; and 6, same as 4 plus >20% of the portal tracts showing bridging involvement.

Statistical analysis

All the results were analyzed and given as mean±SD. Comparisons were made using the Mann-Whitney *U* test. Differences with a *P* value of less than 0.05 were considered statistically significant.

RESULTS

Tables 1 and 2 and Figures 1 and 2 show the results of TUNEL-positive cells/field and ductular proliferation (grade). Compared with sham operation groups, common bile duct ligation significantly increased hepatocyte apoptosis ($P = 0.008$) and ductular proliferation ($P = 0.007$). After the administration of ZVAD-fmk, the increased hepatocyte apoptosis and ductular proliferation after ligation were significantly diminished ($P = 0.008$ and $P = 0.007$

Table **1 TUNEL-positive cells/field**

OBZVAD ($n = 5$)	OBZFA ($n = 5$)	SDMSO ($n = 5$)	SNS ($n = 5$)	OB ($n = 5$)
2.40±0.55	9.00±1.58	1.40±0.89	1.40±0.89	9.60±1.14

OBZVAD: obstructive jaundice with ZVAD. OBZFA: obstructive jaundice with ZFA. SDMSO: sham operation with DMSO. SNS: sham operation with normal saline. OB: obstructive jaundice. $P = 0.008$ (OBZVAD *vs* OBZFA). $P = 0.008$ (OBZVAD *vs* OB). $P = 0.522$ (OBZFA *vs* OB). $P = 1.000$ (SDMSO *vs* SNS). $P = 0.008$ (SDMSO *vs* OB). $P = 0.008$ (SNS *vs* OB).

Table 2 **Ductular proliferation (grade)**

OBZVAD (n = 5)	OBZFA (n = 5)	SDMSO (n = 5)	SNS (n = 5)	OB (n = 5)
1.20±0.45	4.20±1.30	0.20±0.45	0.20±0.45	4.40±1.14

OBZVAD: obstructive jaundice with ZVAD. OBZFA: obstructive jaundice with ZFA. SDMSO: sham operation with DMSO. SNS: sham operation with normal saline. OB: obstructive jaundice. P = 0.007 (OBZVAD *vs* OBZFA). P = 0.007 (OBZVAD *vs* OB). P = 0.746 (OBZFA *vs* OB). P = 1.000 (SDMSO *vs* SNS). P = 0.007 (SDMSO *vs* OB). P = 0.007 (SNS *vs* OB).

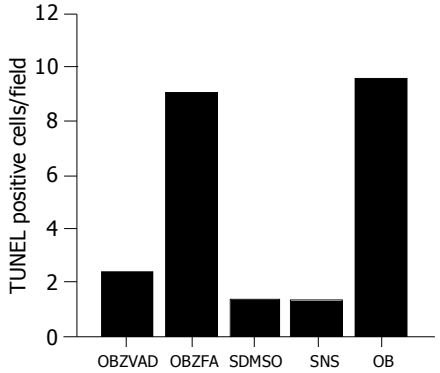

Figure 1 The TUNEL-positive cells/field. OBZVAD: obstructive jaundice with ZVAD. OBZFA: obstructive jaundice with ZFA. SDMSO: sham operation with DMSO. SNS: sham operation with normal saline. OB: obstructive jaundice.

respectively). Moreover, the administration of ZFA failed to show the same effects. Hepatocyte apoptosis (P = 0.008) and ductular proliferation (P = 0.007) significantly differed between OBZVAD and OBZFA groups.

DISCUSSION

Cholestasis, an impairment in bile formation, occurs in a wide variety of human liver diseases[26]. Retention and accumulation of toxic hydrophobic bile salts within hepatocyte may cause hepatocyte toxicity by inducing apoptosis[27-29]. Our study using the bile duct ligation rat as a model of extrahepatic cholestasis demonstrated that increased hepatocyte apoptosis (P = 0.008) and ductular proliferation (P = 0.007) occurred after common bile duct ligation for three days (Tables 1 and 2 and Figures 1 and 2). Without proper treatment, hepatocellular injury is an invariant feature of cholestasis causing liver dysfunction, promoting fibrogenesis, and ultimately leading to liver failure[7]. Our study was therefore designed to examine the effect of hepatocyte apoptosis inhibition with a specific caspase inhibitor after bile duct ligation.

Apoptotic cell death has been recently shown to have a central role in many physiologic and pathophysiologic processes[30-31]. Although the apoptotic cascade is complex and its regulation is not completely understood, it has become clear that a family of cysteine endoproteases called caspases plays a critical role in the execution of apoptotic cell death[32]. ZVAD-fmk is a cell-permeable irreversible inhibitor of caspase and recent data suggest that it might block the processing of many caspases[3,18-20]. In this study, ZVAD-fmk effectively diminished hepatocyte apoptosis and ductular

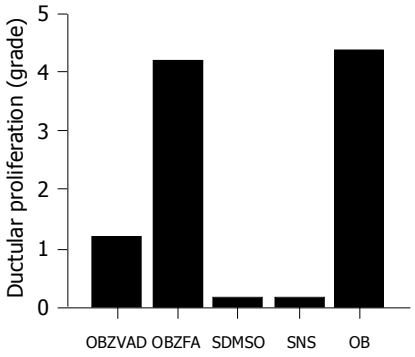

Figure 2 Ductular proliferation (grade). OBZVAD: obstructive jaundice with ZVAD. OBZFA: obstructive jaundice with ZFA. SDMSO: sham operation with DMSO. SNS: sham operation with normal saline. OB: obstructive jaundice.

proliferation after common bile duct ligation, whereas ZFA-fmk, a structurally similar molecule with no anticaspase activity, did not show the same effect (Tables 1 and 2, Figures 1 and 2).

Group 3, which underwent sham operation and simultaneous treatment with the same amount of DMSO, was included to assess whether DMSO used as a vehicle would have a toxic effect *in vivo* and DMSO turned out to be a safe vehicle in this study.

Despite improvements in operative technique and the development of potent, broad-spectrum antibiotics, biliary tract surgery in patients with obstructive jaundice is still associated with high morbidity and mortality rates[33]. In conclusion, our results show that the hepatocyte apoptosis and ductular proliferation were significantly enhanced after bile duct ligation (obstructive jaundice) and the administration of ZVAD-fmk could effectively attenuate this phenomenon. If confirmed in clinical trial, such manipulation may provide a rational adjuvant strategy for the treatment of patients with obstructive jaundice and is expected to reduce the incidence of perioperative mortality and morbidity in obstructive jaundice.

REFERENCES

1 **Kerr JF,** Wyllie AH, Currie AR. Apoptosis: a basic biological phenomenon with wide-ranging implications in tissue kinetics. *Br J Cancer* 1972; **26**: 239-257
2 **Allen RT,** Hunter WJ, Agrawal DK. Morphological and biochemical characterization and analysis of apoptosis. *J Pharmacol Toxicol Methods* 1997; **37**: 215-228
3 **Cohen GM.** Caspases: the executioners of apoptosis. *Biochem J* 1997; **326 (Pt 1)**: 1-16
4 **Siegers CP.** Anthranoid laxatives and colorectal cancer. *Trends Pharmacol Sci* 1992; **13**: 229-231
5 **Branconnier RJ,** Branconnier ME, Walshe TM, McCarthy C, Morse PA. Blocking the Ca(2+)-activated cytotoxic mechanisms of cholinergic neuronal death: a novel treatment strategy for Alzheimer's disease. *Psychopharmacol Bull* 1992; **28:** 175-181
6 **Trauner M,** Meier PJ, Boyer JL. Molecular pathogenesis of cholestasis. *N Engl J Med* 1998; **339**: 1217-1227
7 **Miyoshi H,** Rust C, Roberts PJ, Burgart LJ, Gores GJ. Hepatocyte apoptosis after bile duct ligation in the mouse involves Fas. *Gastroenterology* 1999; **117:** 669-677
8 **Patel T,** Bronk SF, Gores GJ. Increases of intracellular magnesium promote glycodeoxycholate-induced apoptosis in rat hepatocytes. *J Clin Invest* 1994; **94**: 2183-2192
9 **Rodrigues CM,** Fan G, Ma X, Kren BT, Steer CJ. A novel role

for ursodeoxycholic acid in inhibiting apoptosis by modulating mitochondrial membrane perturbation. *J Clin Invest* 1998; **101:** 2790-2799

10 **Webster CR,** Anwer MS. Cyclic adenosine monophosphate-mediated protection against bile acid-induced apoptosis in cultured rat hepatocytes. *Hepatology* 1998; **27**: 1324-1331

11 **Faubion WA,** Guicciardi ME, Miyoshi H, Bronk SF, Roberts PJ, Svingen PA, Kaufmann SH, Gores GJ. Toxic bile salts induce rodent hepatocyte apoptosis via direct activation of Fas. *J Clin Invest* 1999; **103:** 137-145

12 **Benz C,** Angermuller S, Tox U, Kloters-Plachky P, Riedel HD, Sauer P, Stremmel W, Stiehl A. Effect of tauroursodeoxycholic acid on bile-acid-induced apoptosis and cytolysis in rat hepatocytes. *J Hepatol* 1998; **28:** 99-106

13 **Rodrigues CM**, Fan G, Wong PY, Kren BT, Steer CJ. Ursodeoxycholic acid may inhibit deoxycholic acid-induced apoptosis by modulating mitochondrial transmembrane potential and reactive oxygen species production. *Mol Med* 1998; **4:** 165-178

14 **Salvesen GS,** Dixit VM. Caspases: intracellular signaling by proteolysis. *Cell* 1997; **91**: 443-446

15 **Enari M,** Sakahira H, Yokoyama H, Okawa K, Iwamatsu A, Nagata S. A caspase-activated DNase that degrades DNA during apoptosis, and its inhibitor ICAD. *Nature* 1998; **391**: 43-50

16 **Behrns KE,** Schrum LW, Que FG. Apoptosis: cell death by proteolytic scalpel. *Surgery* 1999; **126:** 463-468

17 **Los M,** Van de Craen M, Penning LC, Schenk H, Westendorp M, Baeuerle PA, Droge W, Krammer PH, Fiers W, Schulze-Osthoff K. Requirement of an ICE/CED-3 protease for Fas/APO-1-mediated apoptosis. *Nature* 1995; **375:** 81-83

18 **Piguet PF,** Vesin C, Donati Y, Barazzone C. TNF-induced enterocyte apoptosis and detachment in mice: induction of caspases and prevention by a caspase inhibitor, ZVAD-fmk. *Lab Invest* 1999; **79:** 495-500

19 **Farber A,** Connors JP, Friedlander RM, Wagner RJ, Powell RJ, Cronenwett JL. A specific inhibitor of apoptosis decreases tissue injury after intestinal ischemia-reperfusion in mice. *J Vasc Surg* 1999; **30:** 752-760

20 **Daemen MA,** van 't Veer C, Denecker G, Heemskerk VH, Wolfs TG, Clauss M, Vandenabeele P, Buurman WA. Inhibition of apoptosis induced by ischemia-reperfusion prevents inflammation. *J Clin Invest* 1999; **104:** 541-549

21 **Sheen-Chen SM,** Chau P, Harris HW. Obstructive jaundice alters Kupffer cell function independent of bacterial translocation. *J Surg Res* 1998; **80**: 205-209

22 **Sheen-Chen SM,** Chen HS, Ho HT, Chen WJ, Sheen CC, Eng HL. Effect of bile acid replacement on endotoxin-induced tumor necrosis factor-alpha production in obstructive jaundice. *World J Surg* 2002; **26**: 448-450

23 **Sheen-Chen SM,** Ho HT, Chen WJ, Eng HL, Wu CH. Obstructive jaundice alters CD44 expression in rat small intestine. *Digestion* 2002; **65:** 112-117

24 **Sheen-Chen SM,** Chen HS, Ho HT, Sheen CC, Chen WJ, Eng HL. Obstructive jaundice alters LFA-1alpha expression in rat small intestine. *Dig Dis Sci* 2003; **48:** 1165-1170

25 **Sheen-Chen SM,** Ho HT, Chen WJ, Eng HL. Obstructive jaundice alters proliferating cell nuclear antigen expression in rat small intestine. *World J Surg* 2003; **27:** 1161-1164

26 **Sheen-Chen SM,** Hung KS, Ho HT, Chen WJ, Eng HL. Effect of glutamine and bile acid on hepatocyte apoptosis after bile duct ligation in the rat. *World J Surg* 2004; **28**: 457-460

27 **Trauner M,** Meier PJ, Boyer JL. Molecular pathogenesis of cholestasis. *N Engl J Med* 1998; **339**: 1217-1227

28 **Benz C,** Angermuller S, Tox U, Kloters-Plachky P, Riedel HD, Sauer P, Stremmel W, Stiehl A. Effect of tauroursodeoxycholic acid on bile-acid-induced apoptosis and cytolysis in rat hepatocytes. *J Hepatol* 1998; **28:** 99-106

29 **Faubion WA,** Guicciardi ME, Miyoshi H. Toxic bile salts induce rodent hepatocyte apoptosis via direct activation of Fas. *J Clin Invest* 1999; **103**: 137-145

30 **Hurle JM.** Cell death in developing systems. *Methods Achiev Exp Pathol* 1988; **13**: 55-86

31 **MacDonald HR,** Lees RK. Programmed death of autoreactive thymocytes. *Nature* 1990; **343**: 642-644

32 **Behrns KE,** Schrum LW, Que FG. Apoptosis: cell death by proteolytic scalpel. *Surgery* 1999; **126**: 463-468

33 **Su CH,** P'eng FK, Lui WY. Factors affecting morbidity and mortality in biliary tract surgery. *World J Surg* 1992; **16**: 536-540

Science Editor Guo SY **Language Editor** Elsevier HK

PO Box 2345, Beijing 100023, China
www.wjgnet.com
wjg@wjgnet.com

ELSEVIER

World J Gastroenterol 2005;11(15):2334-2336
World Journal of Gastroenterology ISSN 1007-9327

• *BRIEF REPORTS* •

Influence of various proton pump inhibitors on intestinal metaplasia in noneradicated *Helicobacter pylori* patients

Marinko Marusic, Zarko Babic, Mirjana Nesanovic, Mira Lucijanic-Mlinac, Vesna Stajcar

Marinko Marusic, Zarko Babic, Division of Gastroenterology, Department of Medicine, Sveti Duh General Hospital, Sv. Duh 64, 10000 Zagreb, Croatia
Mirjana Nesanovic, Department of Internal Medicine, General Hospital Karlovac, Croatia
Mira Lucijanic-Mlinac, Vesna Stajcar, Department of Pathology, General Hospital Karlovac, Croatia
Supported by Sveti Duh General Hospital, Zagreb, Croatia, No. UR/P-12/1999
Correspondence to: Assistant Professor Zarko Babic, MD, PhD, Fabkoviceva 3, HR-10000 Zagreb, Croatia. zarko.babic@zg.hinet.hr
Telephone: +3851-3712-111 Fax: +3851-3745550
Received: 2004-02-02 Accepted: 2004-03-02

Abstract

AIM: Intestinal metaplasia (IM) is more often found in patients with *Helicobacter pylori* (*H pylori*) infection, while eradication of *H pylori* results in significant reduction in the severity and activity of chronic gastritis. We aimed to determine in patients with unsuccessful eradication of *H pylori* the role of various proton pump inhibitors (PPIs) having different mechanisms in the resolution of IM.

METHODS: We confirmed endoscopically and pathohistologically (Sydney classification) the IM in 335 patients with gastritis before and after medication for eradication of *H pylori* (Maastricht Protocol 2002). *H pylori* infection was determined by using histology, urease test and culture. Control endoscopy and histology were done after 30 d and thereafter (within 1 year). Unsuccessful eradication was considered if only one of the three tests (histology, urease and culture) was negative after therapy protocol. We used omeprazole, pantoprazole, lansoprazole in therapy protocols (in combination with two antibiotics).

RESULTS: We found no significant difference in resolution of IM by using different PPI between the groups of eradicated and noneradicated patients ($P<0.4821$ and $P<0.4388$, respectively).

CONCLUSION: There is no significant difference in resolution of intestinal metaplasia by different proton pump inhibitors.

Key words: *H pylori*, Intestinal metaplasia

Marusic M, Babic Z, Nesanovic M, Lucijanic-Mlinac M, Stajcar V. Influence of various proton pump inhibitors on intestinal metaplasia in noneradicated *Helicobacter pylori* patients. *World J Gastroenterol* 2005; 11(15): 2334-2336
http://www.wjgnet.com/1007-9327/11/2334.asp

INTRODUCTION

Patients with *Helicobacter pylori* (*H pylori*) infection have been found more frequently with intestinal metaplasia (IM) and atrophic gastritis[1]. Several authors (Asaka *et al* Ohkusa *et al,* and Kokkola *et al,*) have found that eradication of *H pylori* results in significant reduction in the severity and activity of chronic gastritis[2].

We know about different mechanisms of proton pump inhibitors (PPIs). Omeprazole and lansoprazole have effects on Cys 813, and pantoprazole additionally on Cys 822 which is important for irreversible acid blockade. The influence on gastric acid secretion is dose dependent, which means that a higher PPI dose has a stronger acid inhibition[3]. *H pylori* eradication was associated with a histologic improvement of gastric mucosa but in uninfected patients no significant change in inflammation or proliferation occurred during treatment with lansoprazole[4].

The aim of this study was to determine in patients with unsuccessful eradication of *H pylori* the role of various PPIs having different mechanisms in the resolution of IM.

MATERIALS AND METHODS

Patients

We followed up 335 patients with gastritis (142 males and 193 females, mean age 51.3 years, between 18 and 83 years). All patients underwent upper gastrointestinal endoscopy with pathohistologic examination. We used Olympus Q20 and Pentax video endoscopy systems.

Methods

Diagnostic procedures We confirmed endoscopically and pathohistologically (Sydney classification)[5] the IM in patients with gastritis before and after medication for eradication of *H pylori* (Maastricht Protocol 2002)[6]. *H pylori* infection was determined by using histology, urease test and culture in addition to E-test[7-9]. Control endoscopy and histology were done after 30 d and thereafter (within 1 year). Unsuccessful eradication was considered if only one of the three tests (histology, urease and culture) was positive after therapy protocol.

Therapy We used omeprazole 20 mg bid, pantoprazole 40 mg bid, and lansoprazole 30 mg bid in eradication therapy

Table 1 **Influence of various PPIs on intestinal metaplasia in the noneradicated *Helicobacter pylori* infection patients**

Intestinal metaplasia	Omeprazole (*n*)	Pantoprazole (*n*)	Lansoprazole (*n*)
Negative	20	26	14
Positive	16	22	10

$\chi^2 = 2.462$, $\gamma = 3$, $P = 0.4821$.

protocols during 7 d in combination with two antibiotics (amoxicilin 1 g bid and clarithromycin 500 mg bid), and thereafter at the same dose but once a day during the next 4 wk[6]. We included 108 patients on omeprazole protocol, 137 patients on pantoprazole protocol and 90 patients on lansoprazole protocol.

RESULTS

The successful eradication of *H pylori led* to the disappearance of IM in gastric mucosa (208 patients with negative IM *vs* 19 patients with positive IM) ($\chi^2 = 157.36$, $\gamma = 1$, $P<0.001$). The unsuccessful eradication of *H pylori* also led to the disappearance of IM but it was not statistically significant (48 with positive IM *vs* 60 with negative IM; $\chi^2 = 1.33$, $\gamma = 1$, $P<0.1$).

We found no significant difference in resolution of IM by using different PPI in the group of noneradicated patients ($P<0.4821$), as well as in the group of eradicated patients ($P<0.4388$) (Tables 1 and 2).

DISCUSSION

The occurrence of IM was influenced by the presence of *H pylori* infection[1,2].

H pylori modified cellular processes of the host and led to inflammation[1,2]. *H pylori* infection stimulated the infiltration of neutrophils, lymphocytes, plasma cells and macrophages in gastric mucosa[10]. There are several mechanisms by which *H pylori* infection triggers a host response (major histocompatibility complex II, translocation of *H pylori* CagA protein into human gastric epithelial cells using type IV secretion which is ATP-ase dependent)[10]. PPI could influence ATP-ase and glycoprotein[11]. *H pylori* could also influence lamina propria and activate underlying cells[10]. They could influence host response to their presence by regulating prostaglandin production over cyclo-oxgenase-2-expression, activating neutrophils and oxidative stress and mucosal products, and all these processes could result in apoptosis and cell proliferation suppression[10]. Specific gene products synthesized by bacteria or host have been implicated in the inflammatory and IM process (role of cag potency in IM and gastric cancer development)[10].

The gastritis score increased in patients who had no or only mild corpus gastritis before treatment and significantly decreased in those who had moderate or severe gastritis before treatment[12]. We could find similar results in the study of Berstad *et al*[4], with lansoprazole.

Acid secretion decreased dose-dependently in PPI users[13,14]. Reports on endocrine cell changes in the antral mucosa under chronic PPI therapy are controversial and lack clinical relevance[14,15]. Data on the progression of oxintic gastritis under chronic PPI treatment in comparison to untreated controls could not be confirmed in more recent studies including a well-matched control population[14]. The mechanism of PPI action on acid suppression is different. All PPIs bind to and act on Cys 813, which is placed near the curve where TM6 enters the membrane domain. Lansoprazole binds to Cys 321 on ectoplasmatic end TM3, but pantoprazole binds to Cys 822 which is placed deeper in the membrane domain TM6[16]. This can be an explanation for different and irreversible suppressions of Cys 822 by pantoprazole. The recovery of proton pump was measured in rat stomach, and complete recovery of ATP-aze was detected after medication with omeprazole, esomeprazole and rabeprazole but 70% recovery was detected. After medication with pantoprazole no recovery of proton pump was detected after lansoprazole[16]. We wanted to evaluate the influence of PPI on IM in patients with similar conditions (inflammation caused by *H pylori*). Eradication of *H pylori* had no difference on IM disappearance by PPI. We concluded that there was no difference in PPIs between such groups of patients. In the group of patients with unsuccessful eradication of *H pylori*, presence of *H pylori* was constant, and PPI could influence IM, but our results were negative. The explanation can be that *H pylori* disturbs the effect of PPI on IM disappearance in a different way from the mechanism by which it acts on PPI in gastric cells. But it is interesting that in the eradicated group (effect of *H pylori* on gastric cells excluded) the result was the same. Further investigations are needed.

Table 2 **Influence of various PPIs on intestinal metaplasia in the eradicated *Helicobacter pylori* infection patients**

Intestinal metaplasia	Omeprazole (*n*)	Pantoprazole (*n*)	Lansoprazole (*n*)
Negative	64	81	63
Positive	8	8	3

$\chi^2 = 2.702$, $\gamma = 3$, $P = 0.4388$.

REFERENCES

1 **Ohkuma K,** Okada M, Murayama H, Seo M, Maeda K, Kanda M, Okabe N. Association of *Helicobacter pylori* infection with atrophic gastritis and intestinal metaplasia. *J Gastroenterol Hepatol* 2000; **15**: 1105-1112

2 **Kokkola A,** Sipponen P, Rautelin H, Harkonen M, Kosunen TU, Haapiainen R, Puolakkainen P. The effect of *Helicobacter pylori* eradication on the natural course of atrophic gastritis with dysplasia. *Aliment Pharmacol Ther* 2002; **16**: 515-520

3 **Welage LS.** Pharmacocinetic comparison of five proton pump inhibitors. *Gastroenterology* 2002; **122**(Suppl): S1303

4 **Berstad AE,** Hatlebakk JG, Maartmann-Moe H, Berstad A, Brandtzaeg P. *Helicobacter pylori* gastritis and epithelial cell proliferation in patients with reflux oesophagitis after treatment with lansoprazole. *Gut* 1997; **41**: 740-747

5 **Dixon MF,** Genta RM, Yardley JH, Correa P. Classification and grading of gastritis. The updated Sydney System. International Workshop on the Histopathology of Gastritis, Houston 1994. *Am J Surg Pathol* 1996; **20**:1161-1181

6 **Malfertheiner P,** Megraud F, O'Morain C, Hungin AP, Jones R, Axon A, Graham DY, Tytgat G. Current concepts in the

management of Helicobacter pylori infection--the Maastricht 2-2000 Consensus Report. *Aliment Pharmacol Ther* 2002; **16**: 167-180

7 **Megraud F,** Henzel S, Glupczynski Y. Antibiotic susceptibility and resistance in *Helicobacter pylori*: physiology and genetics. *ASM Press* 2001: 511-530

8 **Chaves S,** Gadanho M, Tenreiro R, Cabrita J. Assessment of metronidazole susceptibility in *Helicobacter pylori*: statistical validation and error rate analysis of breakpoints determined by the disk diffusion test. *J Clin Microbiol* 1999; **37**: 1628-1631

9 **Cederbrant G,** Kahlmeter G, Ljungh A. The E test for antimicrobial susceptibility testing of *Helicobacter pylori*. *J Antimicrob Chemother* 1993; **31**: 65-71

10 **Eliot SN,** Ernst PB, Kelly CP. Molecular inflammation. *Current Opinion Gastroenterol* 2001; **17** (Suppl 1): S12-16

11 **Pauli-Magnus C,** Rekersbrink S, Klotz U, Fromm MF. Interaction of omeprazole, lansoprazole and pantoprazole with P-glycoprotein. *Naunyn Schmiedebergs Arch Pharmacol* 2001; **364**: 551-557

12 **Uemura N,** Okamoto S, Yamamoto S, Matsumura N, Yamaguchi S, Mashiba H, Sasaki N, Taniyama K. Changes in Helicobacter pylori-induced gastritis in the antrum and corpus during long-term acid suppressive treatment in Japan. *Aliment Pharmacol Ther* 2000; **14**: 1345-1352

13 **Muller P,** Goksu MA, Fuchs W, Schluter F, Simon B. Initial potency of lansoprazole and omeprazole tablets on pentagastrin-stimulated gastric acid secretion- a placebo-controlled study in healthy volunteers. *Aliment Pharmacol Ther* 2000; **14**: 1225-1229

14 **Stolte M,** Meining A. Changes in Helicobacter pylori gastritis caused by therapy with inhibitors of gastric acid secretion. *Z Gastroenterol* 1999; **37**: 1029-1036

15 **Lamberts R.** Morphological changes of the human gastric mucosa under long-term proton pump inhibitor therapy and their clinical relevance. *Microsc Res Tech* 2000; **48**: 357-366

16 **Shin JM,** Sachs G. Restoration of acid secretion following treatment with proton pump inhibitors. *Gastroenterology* 2002; **123**: 1588-1597

Science Editor Zhu LH, Wang XL and Li WZ **Language Editor** Elsevier HK

PO Box 2345, Beijing 100023, China
www.wjgnet.com
wjg@wjgnet.com

ELSEVIER

World J Gastroenterol 2005;11(15):2337-2339
World Journal of Gastroenterology ISSN 1007-9327

• *BRIEF REPORTS* •

Low gradient ascites: A seven-year course review

Fariborz Mansour-Ghanaei, Afshin Shafaghi, Amir-Hossein Bagherzadeh, Mohammad-Sadegh Fallah

Fariborz Mansour-Ghanaei, Afshin Shafaghi, Amir-Hossein Bagherzadeh, Mohammad-Sadegh Fallah, Gastrointestinal and Liver Diseases Research Center (GLDRC), Guilan University of Medical Sciences, Guilan Province, Iran
Correspondence to: Dr. Fariborz Mansour-Ghanaei, Associate Professor of Medicine and Gastroenterology, Gastrointestinal and Liver Diseases Research Center (GLDRC), Guilan University of Medical Sciences, Razi Hospital, Sardar-e-Jangle Ave, Rasht 41448-95655, Iran. ghanaei@gums.ac.ir
Telephone: +98-131-5535116 Fax: +98-131-5534951
Received: 2003-09-15 Accepted: 2003-12-01

Abstract

AIM: To study the patients with low gradient ascites in hospitals of Guilan Province (northern Iran).

METHODS: Patients admitted in hospitals of Guilan Province with low gradient ascites from 1993 to 2000 were enrolled in the study. Serum and ascitic fluid albumin levels were determined by biochemical reactions. The serum-ascitic albumin gradient (SAAG) less than 1.1 g/dL was considered low. Statistical analysis was performed with SPSS 9.0 software and $P<0.05$ was considered statistically significant.

RESULTS: Of the 148 patients enrolled in the study, 72 (48.6%) were males and 76 (51.4%) were females with a mean age of 59.03±13.54 years. Tuberculous peritonitis was the most frequent cause of low gradient ascites in 68 (45.9%). Other most frequent causes were cancer in 62 (41.9%), nephrotic syndrome in 9 (6%), pancreatitis in 6 (4%). Peritoneal cancer was found in 22 (35%), ovarian and gastric cancers were found in 14 (22.5%) and 12 (19.3%), respectively. All of which were the causes of ascites. The mean SAAG was 0.68±0.19 g/dL. The mean serum and ascitic fluid albumin concentrations were higher in tuberculous patients ($P<0.006$), but lactate dehydrogenase (LDH) level was higher in cancer patients ($P<0.0001$). In peritoneal tuberculosis, mean ascitic glucose concentration was significantly lower than other patients ($P<0.0001$).

CONCLUSION: Tuberculosis should be considered in all patients with low gradient ascites especially in developing countries (like Iran), as the first cause of ascites. In the approach to patients with low gradient ascites, ascitic fluid glucose, and LDH level are useful indicators for decision making.

Key words: Ascites; Tuberculosis; Cancer; Albumin

Mansour-Ghanaei F, Shafaghi A, Bagherzadeh AH, Fallah MS. Low gradient ascites: A seven-year course review. *World J Gastroenterol* 2005; 11(15): 2337-2339
http://www.wjgnet.com/1007-9327/11/2337.asp

INTRODUCTION

Pathologic accumulation of fluid in the peritoneal cavity (ascites) is an important clinical finding and its appropriate treatment depends on correct diagnosis, which can be made by diagnostic abdominal paracentesis, a simple and safe procedure, which can be done at bedside or in the office[1,2].

Serum ascites albumin gradient (SAAG), cell count, bacterial culture, pH, glucose, lactate dehydrogenase (LDH) and amylase are useful in the differential diagnosis of ascites[3,5].

Different diseases can cause different types of ascites. Some of the known low gradient ascites include tuberculous peritonitis-induced ascites, malignancy-induced ascites (for instance, peritoneal carcinomatosis, gastric and ovarian cancer metastases), pancreatic ascites, renal ascites, biliary ascites, bacterial peritonitis and serositis-induced ascites. On the other hand, high gradient ascites are uncomplicated cirrhosis-induced ascites, heart-failure-induced ascites, those induced by extensive liver metastases and other circumstances such as fulminant hepatic failure[4-7].

Like wise, the measurement of SAAG is helpful in the determin-ation of response to treatment of all types of ascites[8].

In the present study, we determined the relative frequency of low gradient ascites in a 7-year period in Guilan Province, northern Iran.

MATERIALS AND METHODS

This survey was done according to the data obtained from the records of admitted patients with primary diagnosis of ascites, from 1993 to 2000 in hospitals of Guilan Province. Serum and ascitic fluid samples were taken for determination of the levels of albumin (blue bromocresol procedure), LDH (LDH specific kits) and glucose (biochemical assays)[9].

In this study, SAAG less than 1.1 g/dL was considered as low gradient ascites[4,6].

Cytological study of ascites and peritoneal biopsy (blind peritoneal biopsy, biopsy with laparoscopy or laparotomy) were used for the diagnosis.

Malignancy-induced ascites included those caused by peritoneal carcinomatosis with unknown origin, ovarian cancer, extensive liver metastases, hepatocellular carcinoma (HCC), lymphoma and gastric cancer[10].

The diagnosis of TB peritonitis required mycobacterial growth in the ascitic fluid culture or the presence of

Table 1 **Comparison of causes of low gradient ascites in age groups**

Causes Age (yr) group	TB		Malignancy		Other causes		Total	
	Frequency	%	Frequency	%	Frequency	%	Frequency	%
35-45	3	11.1	13	48.2	11	40.7	27	100
46-55	11	38	13	44.8	5	17.2	29	100
56-65	21	51.3	19	46.3	1	2.4	41	100
>65	33	64.7	17	33.3	1	2	51	100
Total	68	45.9	62	41.9	18	12.2	148	100

$P<0.0001$, $\chi^2 = 39.3$.

Table 3 **Comparison of the concentration of serum albumin (Alb), ascites Alb, SAAG, ascites, lactate dehydrogenase (LDH) and glucose in TB patients and cancer patients (mean±SD)**

Disease Parameter	TB	Malignancies	Differences
Serum Alb.	4.2±0.49	3.9±0.70	$P<0.005$
Ascitic Alb.	3.5±0.47	3.30±0.50	$P<0.006$
SAAG	0.68±0.17	0.69±0.22	Not significant
Ascitic LDH	327±113	409±106	$P<0.0001$
Ascitic glucose	71±13.82	101.4±17.2	$P<0.001$

granuloma in the biopsy specimen of peritoneum, which was confirmed by laparoscopy[11]. The diagnosis of pancreatic ascites was based on clinical manifestations and at least more than twice the rise of ascitic fluid amylase in proportion to its normal serum level. The diagnosis of renal or nephrotic syndrome ascites was suspected when the patient developed ascites in the presence of nephrotic syndrome (it means urine protein excretion rate more than 3.5 g/1.73 m^2 per 24 h). Connective tissue diseases were considered as a cause of ascites when ascites developed in a known case of connective tissue diseases such as systemic lupus erythematous, scleroderma, rheumatoid arthritis without other causes[4,5].

Data were analyzed with SPSS 9.0 using Friedman's test, Student's *t* test and χ^2 test.

RESULTS

One hundred and forty-eight patients with low gradient ascites admitted into hospitals of Guilan Province from 1993 to 2000 were enrolled in the study. There were 72 (48.6%) males and 76 (51.4%) females with a mean age of 56.03±13.54 years.

Tuberculous peritonitis was the most frequent cause of low gradient ascites in 68 (45.9%). Other frequent causes were cancer in 62 (41.9%), nephrotic syndrome in 9 (6%), pancreatitis in 6 (4%), serositis in 2 (1.3%) and spontaneous bacterial peritonitis (SBP) in 1 (0.7%).

Peritoneal cancer was found in 22 (35%), ovarian and gastric cancers were found in 14 (22.5%) and 12 (19.3%) respectively followed by lymphoma in 8 (12%) and HCC in 6 (10.2%), all of which were the causes of ascites.

Tables 1 and 2 show the frequency of low gradient ascites according to age group and sex.

Age groups had significant differences ($\chi^2 = 39.3$, $P<0.0001$), but type of low gradient ascites did not show any significant difference between male and female groups.

The mean SAAG was 0.68±0.19 g/dL. The mean serum albumin concentration was 3.94±0.76 g/dL and that of ascitic fluid was 3.28±0.68 g/dL. The mean serum and ascitic albumin, LDH and glucose were compared between TB and cancer patients, all differences were significant ($P<0.006$). The mean SAAG did not differ significantly between cancer and TB patients (Table 3).

Moreover, the mean ascitic glucose concentration in TB patients was the lowest in comparison to all other causes of low gradient ascites and the differences were statistically significant ($P<0.001$).

When patients were divided into two groups according to their LDH concentration, the relative frequency of cancer group with LDH >250 u/mL was significantly higher than that of TB group ($P<0.0001$).

Table 2 **Comparison of causes of low gradient ascites in sex groups**

Causes Sex	TB		Malignancy		Other causes		Total	
	Frequency	%	Frequency	%	Frequency	%	Frequency	%
Male	36	50	28	38.9	8	11.1	72	100
Female	32	42.1	34	44.7	10	13.2	76	100
Total	68	45.9	62	41.9	18	12.2	148	100

DISCUSSION

In the present study, the causes of low gradient ascites were found as follows: TB peritonitis, peritoneal carcinomatosis and other malignancies, nephrotic syndrome, pancreatitis, serositis, and SBP.

In a study by Runyon in 1991[3], low gradient ascites include malignancy-induced ascites (peritoneal carcinomatosis), TB peritonitis-induced ascites, pancreatic ascites, biliary ascites, nephrotic ascites, ascites induced by serositis, and intestinal obstruction or infarction.

In contrast, TB was the most frequent cause in our study. Since it is a treatable infectious disease and has a good prognosis, TB should always be considered as the first diagnosis in patients with low gradient ascites. In a survey in United States, 11 of 20 patients with liver cirrhosis died of TB peritonitis, without any suspicion to TB before death[12].

Peritoneal cancer was most frequently found, usually without any evidence of its origin. Prognosis of different cancer-induced ascites was also different. For example, the survival of patients with ovarian cancer was 1-2 years, whereas with gastric cancer, the life span of patients usually was no more than 4 mo[10-13].

In this study, the mean serum and ascitic fluid albumin concentrations were significantly higher in TB patients than in cancer patients.

Ascitic fluid LDH level in cancer patients was higher than that in TB patients, but glucose level was lower in ascitic fluid of TB patients. As reported in the literatures[8,14] measuring LDH and glucose in ascitic fluid would help in the differential diagnosis of low gradient ascites.

The mean SAAG was not significantly different between TB and cancer patients with low gradient ascites, indicating that although SAAG has a good diagnostic value in differential diagnosis of ascites, it does not give much help

in the differentiation of various types of low gradient ascites.

In spite of the moderate prevalence of tuberculosis in Iran[15], more than 45% of low gradient ascites were caused by TB peritonitis followed by cancers. Therefore, we recommend that whenever the diagnosis in low gradient ascites is established by measuring SAAG, LDH and glucose level of ascitic fluid should also be measured as an adjunct for diagnostic approach. Low LDH (<250 u/mL) and glucose levels indicate TB, while high LDH and glucose levels suggest cancer as the major cause.

ACKNOWLEDGEMENTS

We thank Dr. Sara Keihanian, member of Gastrointestinal and Liver Diseases Research Center of Guilan University of Medical Sciences, for helping in the preparation of this manuscript.

REFERENCES

1 **Runyon BA.** Care of patients with ascites. *N Engl J Med* 1994; **330**: 337-342
2 **Habeeb KS,** Herrera JL. Management of ascites, Paracentesis as a guide. *Postgrad Med* 1997; **101**: 191-192
3 **Runyon BA.** Approach to the Patient with ascites. In: Yamada T, Alpers DH, Owyang C, Laine L, Powell DW. Text book of gastroenterology. 3rd Edition. Philadelphia. Lippincott Williams & Wilkins: 1999: 966-991
4 **Glickman RM.** Abdominal swelling and ascites. In: Fauci AS, Braunwald E, Kasper DL, Hauser SL, Longo DL, Jameson JL. Harrison's principles of internal medicine. 15th Edition. McGraw-Hill Companies, Inc 2001: 260-262
5 **Chung RT,** Podolsky DK. Cirrhosis and its Complications. In: Braunwald E, Fausi AS, Kasper DL, Hauser SL, Longo DL, Jameson JL. Harrison's principles of internal medicine. 15th Edition. McGraw-Hill Companies, Inc 2001: 1754-1767
6 **Runyon BA,** Montano AA, Akriviadis EA, Antillon MR, Irving MA, McHutchison JG. The serum-ascites albumin gradient is superior to the exudate-transudate concept in the differential diagnosis of ascites. *Ann Intern Med* 1992;**117**: 215-220
7 **Runyon BA.** Ascites; spontaneous bacterial peritonitis. In: Sleisenger MH, Feldman M, Friedman LS. Sleisenger and Fordtran's Gastrointestinal and Liver Disease, 7th Edition.W. B. *Saunders Company* 2002: 1517-1540
8 **Pare P,** Talbot J, Hoefs JC. Serum-ascites albumin concentration gradient, a physiologic approach to the differential diagnosis of ascites. *Gastroenterology* 1983; **85**: 240-244
9 **Bansal S,** Kaur K, Bansal AK. Diagnosing ascitic etiology on a biochemical basis. *Hepatogastroenterology* 1998; **45**: 1673-1677
10 **Marincola FM,** Schartzentruber DJ. Malignant ascites. In: Devita VT, Hellman S, Rosenberg SA. Cancer principles and practice of oncology. 5th Edition. Philadelphia: 1997: 2598-2605
11 **Aguado JM,** Pons F, Casafont F, San Miguel G, Valle R. Tuberculous peritonitis: a study comparing cirrhotic and noncirrhotic patients. *J Clin Gastroenterol* 1990; **12**: 550-554
12 **Levison ME,** Bush LM. Peritonitis and other intra abdominal infections. In: Mandell GL, Bennett JE, Dolin R. Mandell, Douglas and Bennett's Principles and practice of infectious diseases, 5th Edition.Churchill Livingstone 2000: 821-856
13 **Rector WG,** Reynolds TB. Superiority of the serum-ascites albumin difference over the ascites total protein concentration in separation of "transudative" and "exudative" ascites. *Am J Med* 1984; **77**: 83-85
14 **Spak I.** On the clinical value of chemical analysis of ascites. A study of the main proteins and some enzymes in ascites of differing etiology. *Acta Chir Scand Suppl* 1960; **Suppl 261**: 1-128
15 **Steffen R,** Du Pont HL. Manual of travel medicine and health. Bcdecker Company, Hamilton: 1999

Science Editor Wang XL, Xu JY and Li WZ **Language Editor** Elsevier HK

PO Box 2345, Beijing 100023, China
www.wjgnet.com
wjg@wjgnet.com

ELSEVIER

World J Gastroenterol 2005;11(15):2340-2345
World Journal of Gastroenterology ISSN 1007-9327

• *BRIEF REPORTS* •

Oxidative stress and nitric oxide in rats with alcohol-induced acute pancreatitis

Gülnur Andican, Remisa Gelisgen, Ethem Unal, Osman Baran Tortum, Sergülen Dervisoglu, Tayfun Karahasanoglu, Gülden Burçak

Gülnur Andican, Remisa Gelisgen, Gülden Burçak, Department of Biochemistry, Cerrahpaþa Medical Faculty, Istanbul University, Istanbul, Turkey
Ethem Unal, Osman Baran Tortum, Tayfun Karahasanoglu, Department of Surgery, Cerrahpaþa Medical Faculty, Istanbul University, Istanbul, Turkey
Sergülen Dervisoglu, Department of Pathology, Cerrahpaþa Medical Faculty, Istanbul University, Istanbul, Turkey
Correspondence to: Dr. Gülnur Andican, Ataköy 7-8, Klslm L13 Blok, E kaplsl Da: 45, Istanbul, Turkey. andican@e-kolay.net
Fax:+90-212 559 55 91
Received: 2004-05-25 Accepted: 2004-05-30

Abstract

AIM: Oxygen free radical mediated tissue damage is well established in pathogenesis of acute pancreatitis (AP). Whether nitric oxide (NO) plays a deleterious or a protective role is unknown. In alcohol-induced AP, we studied NO, lipooxidative damage and glutathione in pancreas, lung and circulation.

METHODS: AP was induced in rats (n = 25) by injection of ethyl alcohol into the common biliary duct. A sham laparatomy was performed in controls (n = 15). After 24 h the animals were killed, blood and tissue sampling were done.

RESULTS: Histopathologic evidence confirmed the development of AP. Marked changes were observed in the pulmonary tissue. Compared with controls, the AP group displayed higher values for NO metabolites in pancreas and lungs, and thiobarbituric acid reactive substances in circulation. Glutathione was lower in pancreas and in circulation. Glutathione and NO were positively correlated in pancreas and lungs of controls but negatively correlated in circulation of experimental group. In the experimental group, plasma thiobarbituric acid reactive substances were negatively correlated with pancreas thiobarbituric acid reactive substances but positively correlated with pancreas NO.

CONCLUSION: NO increases in both pancreas and lungs in AP and NO contributes to the pathogenesis of AP under oxidative stress.

Key words: Thiobarbituric acid reactive substances; Glutathione; Nitric oxide; Acute pancreatitis

Andican G, Gelisgen R, Unal E, Tortum OB, Dervisoglu S, Karahasanoglu T, Burçak G. Oxidative stress and nitric oxide in rats with alcohol-induced acute pancreatitis. *World J Gastroenterol* 2005; 11(15): 2340-2345
http://www.wjgnet.com/1007-9327/11/2340.asp

INTRODUCTION

The etiological basis of acute pancreatitis (AP) is multifactorial. However, as in other inflammatory diseases, a final common pathway mediated by reactive oxygen species (ROS) appears to play a role in the associated tissue destruction both in the initiation and progression of AP[1-4]. Augmented production of ROS in a self-perpetuating manner, in excess of antioxidant defenses, occurs predominantly in activated neutrophils. Once produced, ROS could trigger various inflammatory processes. They can directly attack the lipoid matrix of biological membranes, stimulate arachidonic acid metabolism with increased production of prostaglandins, thromboxane, and leukotrienes, thereby enhancing the accumulation and adherence of neutrophils and platelets to the capillary wall[3]. Thus ROS could impair the microcirculation and disturb the microvascular integrity, resulting in decreased perfusion, increased capillary permeability and fluid transudation. Neutrophils infiltrating the pancreas have also been very recently demonstrated to contribute, via ROS, to the pathologic activation of digestive enzymes in acinar cells[1].

Nitric oxide (NO) has also been implicated in the pathogenesis of AP. NO, being a reactive free radical, contributes to the cytotoxicity of neutrophils and macrophages in the inflammatory response. Moreover, under circumstances of oxidative stress, the interaction of NO with superoxide radicals gives rise to peroxynitrite which can cause platelet aggregation, disseminated intravascular coagulation, lipid peroxidation and ubiquitous cell damage[5,6]. On the other hand, NO induces vasodilatation and prevents endothelial damage by inhibiting platelet aggregation and leukocyte adherence. Due to improvement in both pancreatic microcirculation and capillary organ perfusion throughout the body, NO has also been suggested to have a protective role in AP[7-9]. Thus the role of NO in the pathogenesis of AP remains controversial. Accordingly both inhibitors of NOS and NO donors are suggested to be protective in AP[7–11].

AP is known to be often complicated by multiple organ failure. In particular, acute lung injury occurs at an early stage of pancreatitis and significantly contributes to

morbidity and mortality of this disease[12,13]. The etiology of this extrapancreatic disease has not yet been clearly elucidated. The injury in lung and the resulting adult respiratory distress syndrome have been attributed to the release of pancreas-derived proteolytic enzymes into the circulation[14]. There is also evidence of neutrophil related, ROS-mediated microvascular injury. The release of ROS from activated alveolar macrophages (AMs) has also been shown to lead to the progression of lung injury[15]. AM-derived NO was also reported to contribute to lung injury[16].

As alcoholism is the most common etiology in humans and the mechanism of injury remains unknown, we focused our attention on alcohol-induced AP. Only a few studies have been noted on alcohol-induced AP and in most of these, alcohol has not been used alone but in combination with another agent[17-19]. With regard to alcohol usage, an emerging concept is that a single episode of binge drinking may be sufficient to induce an episode of AP[20]. However, the previous dogma was that consistent ingestion of alcohol for a prolonged period was required to prime the pancreas before an episode of pancreatitis.

Thus in this experimental study we aimed to induce AP with a single high dose of alcohol and to assess NO production (stable metabolites of NO, nitrite plus nitrate; NO_x)[21] and oxidative stress as reflected by lipid peroxidation and glutathione depletion in the pancreas, lungs and systemic circulation as far as our literature survey was concerned. In an alcohol-induced AP model these assessments were simultaneously made for the first time.

MATERIALS AND METHODS

Animal treatment

The study was carried out on 40 young adult male (200-320 g) Wistar Albino rats. The rats, cared for in accordance with the Guide for the Care and Use of Laboratory Animals[22], were permitted ad libitum access to standard laboratory chow (20-30 g/rat/d) and tap water for 10 d prior to experimental procedures.

The rats were divided randomly into two groups. The experimental group consisted of 25 rats and control group of 15 rats. Animals were anesthetized with ether to undergo a midline laparotomy and the duodenal portion of the pancreas was exposed. AP was induced by injection of ethyl alcohol (48%, 1 mL) into the common biliary duct. A sham laparotomy was performed in the control group. After 24 h, heparinized blood samples were taken with intracardiac puncture and rats were killed by decapitation under ether anesthesia. Lung and pancreatic tissues were obtained peroperatively and immediately frozen at -80 ℃ for biochemical measurements and fixed in 10% buffered formalin, embedded in paraffin for standard histologic examinations.

Thiobarbituric acid-reactive substances (TBARS), glutathione (GSH) and NO metabolites were measured in the blood and tissue samples. Tissues prepared in cold potassium phosphate buffer 100 g/L were homogenized using a Potter homogenizer. The homogenates were centrifuged at 3 000 r/min for 15 min and the supernatant was used for the biochemical measurements.

Measurement of lipid peroxidation

Lipid peroxidation was determined by measuring the TBARS by the modified method of Buege *et al*[23] in the plasma and by the method of Okhawa *et al*[24] in tissue using 1.56×10^5 mol/L/cm as molar extinction coefficient. TBARS concentration in the supernatant of the tissue homogenates was expressed as μmol/g protein.

Measurement of GSH

GSH concentration in erythrocytes and supernatants of the tissue homogenates was determined according to the method of Buetler *et al*[25] using metaphosphoric acid for protein precipitation and 5'5'-dithiobis-2-nitrobenzoic acid for color development. Erythrocyte GSH concentration was expressed as mg/g Hb using 1.36×10^4 mol/L/cm as molar absorption coefficient. Hemoglobin concentration was determined by the cyanomethemoglobin method[26]. GSH concentration in supernatants of the tissue homogenates was expressed as mg/g protein.

Measurement of nitric oxide metabolites (NO_x)

The stable metabolites of NO, nitrate (NO_3^-) and nitrite (NO_2^-) were measured as an index of NO production. NO colorimetric assay kit (Roche-Boehringer Mannheim) was used. Nitrate was first reduced to nitrite by NADPH in presence of nitrate reductase. Nitrite was reacted with sulfanilamide and naphthyl-ethylenediamine dihydrochloride to give a red-diazo dye. The diazo dye was measured spectrophotometrically at 550 nm. The concentration of NO metabolites was determined by comparison with a standard curve, which was constructed using a set of serial dilutions of nitrate.

Protein concentration was determined according to the method of Lowry (Sigma-Aldrich, Germany).

Histology

For histologic examination, the samples were cut into 4-μm thick sections and stained with hematoxylin and eosin. All slides were evaluated "blindly" by two independent histopathologists for the presence of edema, hyperemia, infiltration by inflammatory cells, hemorrhage and necrosis.

Statistical analysis

All data were presented as mean±SD. Student's *t* test was performed to evaluate significant differences between the groups. Correlation between different variables was studied by Pearson's correlation coefficient. $P<0.05$ was considered statistically significant.

RESULTS

Histopathologic study of the pancreas in the experimental group showed hyperemia, interstitial edema, hemorrhage, inflammatory infiltration of neutrophils and mononuclear cells and focal necrotic areas. Marked changes were also observed in pulmonary histology, with hyperemia and focal atelectasic areas, peribronchial mononuclear and neutrophilic infiltration, early neutrophilic exudation in some alveoli. Some of the cases revealed abscess formation in lung parenchyma. These findings were considered as the evidence of an

Table 1 **Histopathologic lesions observed in pancreas and lung**

	Pancreas					Lung			
	Edema	Hemorrhage	Hyperemia	Necrosis	PMN infiltration	PMN and lymphocytic infiltration	Alveolar neutrophilic exudation	Hyperemia	Focal atelectasia
Control	+/-	-	+	-	-	-	-	+/-	-
AP	+	+	+	++	+	+	+	+	+

The semiquantitative evaluation scale was the mean of the lesions observed in each group evaluated by independent observers: -, no lesion; +/-, minimal lesion; +, mild lesion; ++, moderate lesion; +++, intense lesion. AP: acute pancreatitis.

established AP. They were summarized as semiquantitatively analyzed results in control and AP group (Table 1).

TBARS concentration in the systemic circulation was observed to be higher in the experimental group in comparison to the control (8.992±3.52 *vs* 6.208±0.95, $P<0.05$). However no significant differences were noted between the groups in pancreas or in lung (Figure 1).

GSH concentration was observed to be significantly lower in the pancreas (2.978±1.52 *vs* 5.375±1.38, $P<0.001$) and erythrocytes (1.576±0.44 *vs* 1.947±0.27, $P<0.05$) in the experimental group compared with the control group. No significant difference was noted in GSH concentration in the lung (Figure 2).

NO_x were observed to be higher in both the pancreas (4.079±0.78 *vs* 3.080±0.37, $P<0.01$) and in the lung (1.809±0.89 *vs* 1.023±0.55, $P<0.05$) in the experimental group compared with the control group. No significant difference was noted in the circulation (Figure 3).

The data evaluated by correlation analysis yielded the following results (Table 2). In the control group, GSH and NO were positively correlated both in the pancreas and in the lung ($r = 0.757$, $P<0.001$; $r = 0.533$, $P<0.05$, respectively).

In the experimental group, GSH and NO_x were negatively correlated in the circulation ($r = -0.426$, $P<0.05$). GSH and TBARS were positively correlated in the pancreas ($r = 0.462$, $P<0.05$). Plasma TBARS was negatively correlated with pancreas TBARS ($r = -0.402$, $P<0.05$) but positively correlated with pancreas NO ($r = 0.654$, $P<0.01$). Pancreas TBARS was positively correlated with lung TBARS ($r = 0.650$, $P<0.01$).

DISCUSSION

The pathophysiology of alcohol-related AP is not well understood. The loss in pancreatic duct integrity and/or changes in duct permeability are responsible for the initiation. Elevated intraductal pressure due to increased secretion and/or the sphincter of Oddi spasm and the presence of alcohol are considered necessary for the production of permeable ducts[17,27].

As in experimental animals not adapted to chronic alcohol ingestion ethanol given orally or intravenously had only a weak stimulatory effect on the pancreas[27], we administered alcohol to the common bile duct. Our histopathologic examination showed interstitial edema, infiltration of neutrophils and focal necrotic and hemorrhagic areas in the pancreas 24 h after the administration of alcohol. We considered these findings as lines of evidence of mild-moderate, edematous pancreatitis. Marked changes were

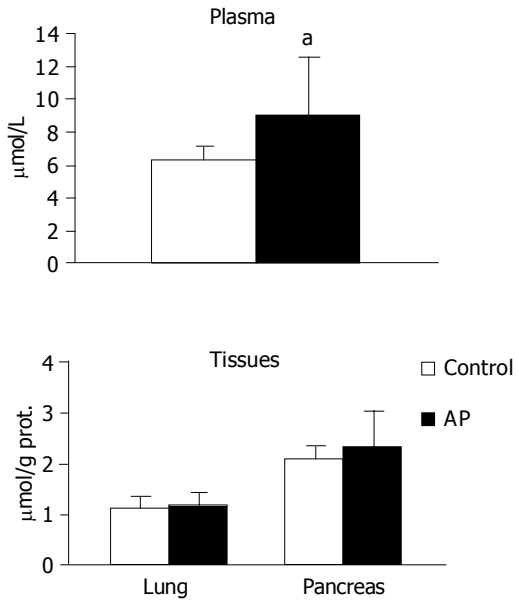

Figure 1 Extent of lipooxidative damage assessed as TBARS in plasma, lung and pancreas in experimental groups. [a]$P<0.05$ *vs* control. AP: acute pancreatitis.

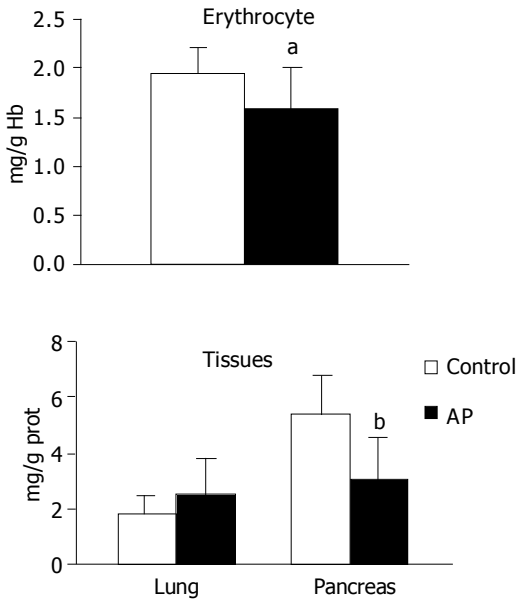

Figure 2 GSH levels in plasma, lung and pancreas in experimental groups. [a]$P<0.05$ *vs* control, [b]$P<0.001$ *vs* control. AP: acute pancreatitis.

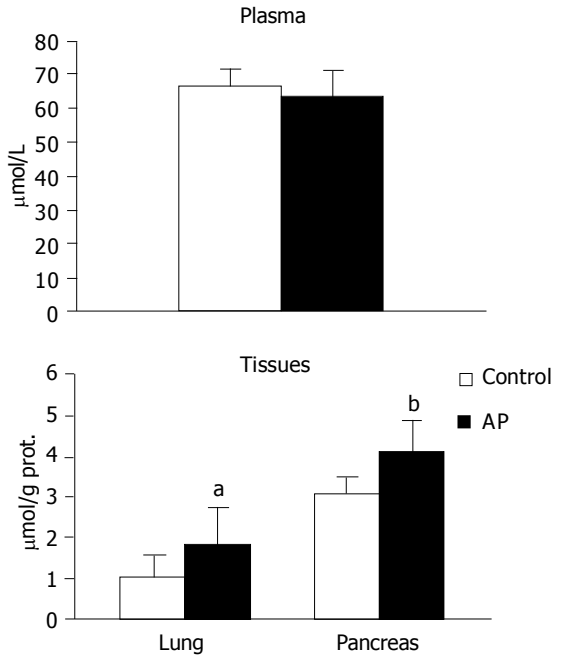

Figure 3 NO_x levels in plasma, lung and pancreas in experimental groups. NO_x: nitrite plus nitrate, AP: acute pancreatitis. $^aP<0.05$ *vs* control, $^bP<0.01$ *vs* control.

Table 2 **Correlation between studied parameters in control and experimental groups**

	Control group ($n = 15$)	AP group ($n = 25$)
GSH_{panc}–NOx_{panc}	$r = 0.757^d$	
GSH_{lung}–NOx_{lung}	$r = 0.533^a$	
GSH_{plasma}–NOx_{plasma}		$r = -0.426^a$
GSH_{panc}–$TBARS_{panc}$		$r = 0.462^a$
$TBARS_{plasma}$–$TBARS_{panc}$		$r = -0.402^a$
$TBARS_{plasma}$–NOx_{panc}		$r = -0.654^b$
$TBARS_{panc}$–$TBARS_{lung}$		$r = 0.650^b$

AP: acute pancreatitis, NO_x: nitrite plus nitrate. $^aP<0.05$, $^bP<0.01$, $^dP<0.001$.

also observed in pulmonary tissue with hyperemia, focal atelectasia, peribronchial mononuclear and neutrophilic infiltration and alveolar neutrophilic exudation resulting in abscess formation in some of the rats with pancreatitis.

High dose of ethanol is known to affect the lipids of cellular membranes and to cause alterations in membranes, permeability and functioning of the integral membrane components[18]. The loss in lysosomal membrane integrity within acinar cells and decompartmentalization of cathepsin B results in pathologic activation of trypsinogen, chymotrypsinogen, proelastase and thus autodigestion of pancreas. Additionally, ethanol affects the antiproteinase components and disturbs the proteinase-antiproteinase balance in pancreatic juice, enabling more effective activation of proteolytic enzymes. Trypsin induced activation of the complement system could contribute to inflammatory interstitial infiltration, parenchymal necrosis, and vacuolization of acinar cells. Activation of proelastase could contribute to damage in microvasculature[19]. There is also growing evidence that ethanol exerts direct toxic effects on pancreatic acinar cells. Certain toxic effects of ethanol have been attributed to both oxidative and nonoxidative metabolites of alcohol, acetaldehyde and fatty acid ethyl ester, respectively[18,28].

As to the pathogenesis of lung injury secondary to AP, it is complex and probably involves pancreatic proteases, phospholipase A_2, activated complements, AMs and neutrophils[16,29]. Ethanol could specifically amplify the effect of phospholipase A_2 which damages pulmonary surfactants, induces AMs to release NO and promotes PAF or eicosanoid production[19].

ROS have been implicated as an important factor in both the initiation and progression of AP in all experimental models. Augmented ROS production could cause lipid peroxidation which induces either apoptosis or necrosis depending on its extent. It has been shown that a short-term, high peak radical attack is more injurious to pancreatic acinar cells than a long lasting, low-level ROS generating system[10]. In our study, under the conditions of neutrophilic infiltration and necrosis in the pancreas, respiratory burst of polymorphonuclear leukocytes, derangement in oxidative phosphorylation, activations of NADPH oxidase, myeloperoxidase, xanthine oxidase and ethanol-catabolizing oxidases all contributed to augmented ROS production[3,30]. The increased TBARS and the decreased GSH that we observed in the circulation of rats 24 h after establishment of alcohol-induced AP reflected oxidative stress on whole body basis. As sham-operated animals served as controls these findings did not reflect laparotomy or bowel-manipulation induced alterations.

Despite an increase of lipid peroxidation in the circulation, we could not demonstrate any increase of lipid peroxidation in tissue samples. The negative correlation of TBARS in pancreatic tissue, with TBARS in circulation suggested the release of lipooxidative damage end-products from the tissue to the circulation. This release might well be due to the autodigestion in the pancreatic tissue. On the other hand, it is also known that injury to the pancreatic tissue during AP was followed by a spontaneous reparative/regenerative process. Accordingly, in several experimental studies, lipid peroxidation, observed to be increased as early as 30 min after induction of pancreatitis was normalized within 12 h[10,31]. Thus, in this respect, lipid peroxidation may perhaps be considered as the sequel of pancreatic inflammation and TBARS in circulation may likely reflect the severity of the systemic inflammatory response, rather than the pancreatic parenchymal damage. Accordingly various reactive aldehydes reflected by TBARS are rather long lived and therefore can diffuse from their site of origin and attack distant targets with some oxidative stress associated pathophysiologic effects. Interestingly we observed that the extent of lipooxidative damage in the lung was correlated with that in the pancreas.

Consumption of GSH as an antioxidant in inflammation and/or its cleavage by the activated carboxypeptidase might account for GSH depletion that we observed in rats with AP. GSH depletion might in turn cause damage to the mitochondria resulting in both ATP loss and increased ROS formation[32,33]. Additionally and importantly, GSH has also roles in acinar stimulus-secretion coupling,

maintenance of the cytoskeleton and appropriate protein folding in the endoplasmic reticulum. Thus GSH depletion may also contribute to impaired zymogen granule transport (secretory block) and premature activation of pancreatic proenzymes[34].

Increased lipid peroxidation and depletion of intracellular GSH in pancreatic tissue in alcohol-induced AP have been reported[17,35,36]. However, it was difficult to compare these data due to the differences in the experimental models and the varying time points of measurements.

Our findings of positively correlated GSH and TBARS in the pancreatic tissues of rats with AP may suggest that depletion of GSH and removal of lipid peroxides occur simultaneously. It may as well be suggested that these are different aspects of the same autodigestive process. As discussed above, lipid peroxide removal might be due to two opposing processes, the detrimental autodigestion and the repair. However, GSH depletion irrespective of the mechanism, represents cellular deterioration and progression of the pathologic process. Relative to earlier repair in the lipoid matrix, long lasting GSH depletion has been reported[10].

In the AP group we observed increased NO production in both of the involved organs, pancreas and lung in comparison to the control. Under prevailing conditions of inflammation and oxidative stress NO became damaging to the tissue, specifically to the endothelium. Specific immunohistochemical staining revealed that the lung and pancreas were important targets of oxidative stress caused by peroxynitrite in AP. The subsequent loss of NO bioactivity further contributed to the endothelial dysfunction[5]. Accordingly, we observed that increased NO production in pancreas was correlated with increased circulatory lipid peroxides in alcohol-induced AP group. The negative correlation of NO and GSH in the circulation of this group suggested that increased NO production was related with GSH depletion in alcohol-induced AP. In accordance to our findings, NO has been reported to compromise the cellular redox state via oxidation of thiols like GSH[10]. In contrast to the AP group, we observed a positive correlation between GSH and NO in both the pancreas and lung in the control group. NO appeared to play an antioxidant role in control rats whereas as a pro-oxidant in alcohol-induced AP rats. These findings clearly indicate that whether NO behaves as an antioxidant or as a pro-oxidant is dependent on the prevailing conditions of oxidative stress[10].

Studies were not in consensus as to whether NO was cytotoxic or cytoprotective in AP[7-11]. Our findings and those reported are in accordance with the well established dual nature of NO. It may act both as a cytotoxic agent and a cytoprotective agent, the main determinants being its concentration and the environment. The action of NO during inflammatory reactions has to be also considered in the context of timing Kröncke *et al*[37].

In conclusion, this experimental study provides biochemical evidence for the cytotoxic role of NO under circumstances of oxidative stress in the pathophysiology of alcohol-induced pancreatitis. Further studies investigating whether modulation of oxidative stress by antioxidant therapy attenuates the cytotoxicity of NO are needed.

REFERENCES

1 **Gough DB,** Boyle B, Joyce WP, Delaney CP, McGeeney KF, Gorey TF, Fitzpatrick JM. Free radical inhibition and serial chemiluminescence in evolving experimental pancreatitis. *Br J Surg* 1990; **77**: 1256-1259

2 **Cuzzocrea S,** Mazzon E, Dugo L, Serraino I, Centorrino T, Ciccolo A, Van de Loo FA, Britti D, Caputi AP, Thiemermann C. Inducible nitric oxide synthase-deficient mice exhibit resistance to the acute pancreatitis induced by cerulein. *Shock* 2002; **17**: 416-422

3 **Tsai K,** Wang SS, Chen TS, Kong CW, Chang FY, Lee SD, Lu FJ. Oxidative stress: an important phenomenon with pathogenetic significance in the progression of acute pancreatitis. *Gut* 1998; **42**: 850-855

4 **Sanfey H,** Bulkley GB, Cameron JL. The role of oxygen-derived free radicals in the pathogenesis of acute pancreatitis. *Ann Surg* 1984; **200**: 405-413

5 **Viola G,** al-Mufti RA, Sohail M, Williamson RC, Mathie RT. Nitric oxide induction in a rat model of selective pancreatic ischemia and reperfusion. *Hepatogastroenterology* 2000; **47**: 1250-1255

6 **Rodeberg DA,** Chaet MS, Bass RC, Arkovitz MS, Garcia VF. Nitric oxide: an overview. *Am J Surg* 1995; **170**: 292-303

7 **Liu X,** Nakano I, Yamaguchi H, Ito T, Goto M, Koyanagi S, Kinjoh M, Nawata H. Protective effect of nitric oxide on development of acute pancreatitis in rats. *Dig Dis Sci* 1995; **40**: 2162-2169

8 **Werner J,** Fernandez-del Castillo C, Rivera JA, Kollias N, Lewandrowski KB, Rattner DW, Warshaw AL. On the protective mechanisms of nitric oxide in acute pancreatitis. *Gut* 1998; **43**: 401-407

9 **Andrzejewska A,** Jurkowska G. Nitric oxide protects the ultrastructure of pancreatic acinar cells in the course of caerulein-induced acute pancreatitis. *Int J Exp Pathol* 1999; **80**: 317-324

10 **Schulz HU,** Niederau C, Klonowski-Stumpe H, Halangk W, Luthen R, Lippert H. Oxidative stress in acute pancreatitis. *Hepatogastroenterology* 1999; **46**: 2736-2750

11 **Sweiry JH,** Mann GE. Role of oxidative stress in the pathogenesis of acute pancreatitis. *Scand J Gastroenterol Suppl* 1996; **219**: 10-15

12 **Tsukahara Y,** Horita Y, Anan K, Morisaki T, Tanaka M, Torisu M. Role of nitric oxide derived from alveolar macrophages in the early phase of acute pancreatitis. *J Surg Res* 1996; **66**: 43-50

13 **Renner IG,** Savage WT, Pantoja JL, Renner VJ. Death due to acute pancreatitis. A retrospective analysis of 405 autopsy cases. *Dig Dis Sci* 1985; **30**: 1005-1018

14 **O'Donovan DA,** Kelly CJ, Abdih H, Bouchier-Hayes D, Watson RW, Redmond HP, Burke PE, Bouchier-Hayes DA. Role of nitric oxide in lung injury associated with experimental acute pancreatitis. *Br J Surg* 1995; **82**: 1122-1126

15 **Guice KS,** Oldham KT, Caty MG, Johnson KJ, Ward PA. Neutrophil-dependent, oxygen-radical mediated lung injury associated with acute pancreatitis. *Ann Surg* 1989; **210**: 740-747

16 **Closa D,** Sabater L, Fernandez-Cruz L, Prats N, Gelpi E, Rosello-Catafau J. Activation of alveolar macrophages in lung injury associated with experimental acute pancreatitis is mediated by the liver. *Ann Surg* 1999; **229**: 230-236

17 **Lüthen RE,** Niederau C, Grendell JH. Glutathione and ATP levels, subcellular distribution of enzymes, and permeability of duct system in rabbit pancreas following intravenous administration of alcohol and cerulein. *Dig Dis Sci* 1994; **39**: 871-879

18 **Rydzewska G,** Jurkowska G, Dzieciol J, Faszczewska A, Wroblewskai E, Gabryelewicz A. Does chronic ethanol administration have influence on pancreatic regeneration in the course of caerulein induced acute pancreatitis in rats. *J Physiol Pharmacol* 2001; **52**: 835-849

19 **Dlugosz JW,** Wroblewski E, Poplawski C, Gabryelewicz A, Andrzejewska A. Does antecedent ethanol intake affect course of taurocholate pancreatitis in rats? *Dig Dis Sci* 1997; **42**: 944-

952
20 **Somogyi L,** Martin SP, Venkatesan T, Ulrich CD. Recurrent acute pancreatitis: an algorithmic approach to identification and elimination of inciting factors. *Gastroenterology* 2001; **120**: 708-717
21 **Upchurch GR,** Welch GN, Fabian AJ, Freedman JE, Johnson JL, Keaney JF, Loscalzo J. Homocyst(e)ine decreases bioavailable nitric oxide by a mechanism involving glutathione peroxidase. *J Biol Chem* 1997; **272:** 17012-17017
22 Guide for the care and use of laboratory animals: Committee on care and use of laboratory animals. Institute of laboratory animal resources, National Research Council 1995: 83
23 **Buege JA,** Aust SD. Microsomal lipid peroxidation. *Methods Enzymol* 1978; **52**: 302-310
24 **Ohkawa H,** Ohishi N, Yagi K. Assay for lipid peroxides in animal tissues by thiobarbituric acid reaction. *Anal Biochem* 1979; **95**: 351-358
25 **Buetler E,** Duran O, Kelly BM. Improved method for the determination of blood glutathione. *J Lab Clin Med* 1963; **51**: 882-888
26 **Fairbanks V,** Klee GG. Biochemical aspects of hematology. In Tietz NW, eds. Textbook of Clinical Chemistry. *Philadelphia: WB Saunders Company* 1986: 1532-1534
27 **Harvey MH,** Cates MC, Reber HA. Possible mechanisms of acute pancreatitis induced by ethanol. *Am J Surg* 1988; **155**: 49-56
28 **Werner J,** Laposata M, Fernandez-Del Castillo C, Saghir M, Iozzo RV, Lewandrowski KB, Warshaw AL. Pancreatic injury in rats induced by fatty acid ethyl ester, a nonoxidative metabolite of alcohol. *Gastroenterology* 1997; **113**: 286-294
29 **Tsukahara Y,** Morisaki T, Horita Y, Torisu M, Tanaka M. Phospholipase A_2 mediates nitric oxide production by alveolar macrophages and acute lung injury in pancreatitis. *Ann Surg* 1999; **229**: 385-392
30 **Schoenberg MH,** Buchler M, Beger HG. Oxygen radicals in experimental acute pancreatitis. *Hepatogastroenterology* 1994; **41**: 313-319
31 **Dabrowski A,** Chwiecko M. Oxygen radicals mediate depletion of pancreatic sulfhydryl compounds in rats with cerulein-induced acute pancreatitis. *Digestion* 1990; **47**: 15-19
32 **Schoenberg MH,** Buchler M, Younes M, Kirchmayr R, Brückner UB, Beger HG. Effect of antioxidant treatment in rats with acute hemorrhagic pancreatitis. *Dig Dis Sci* 1994; **39**: 1034-1040
33 **Kruse P,** Anderson ME, Loft S. Minor role of oxidative stress during intermediate phase of acute pancreatitis in rats. *Free Radic Biol Med* 2001; **30**: 309-317
34 **Gomez-Combronero L,** Camps B, de La Asuncion JG, Cerda M, Pellin A, Pallardo FV, Calvete J, Sweiry JH, Mann GE, Vina J, Sastre J. Pentoxifylline ameliorates cerulein-induced pancreatitis in rats: role of glutathione and nitric oxide. *J Pharmacol Exp Therapeu* 2000; **293**: 670-676
35 **Ozaras R,** Tahan V, Aydin S, Uzun H, Kaya S, Senturk H. N-acetylcysteine attenuates alcohol-induced oxidative stress in the rat. *World J Gastroenterol* 2003; **9:** 125-128
36 **Wittel UA,** Bachem M, Siech M. Oxygen radical production precedes alcohol-induced acute pancreatitis in rats. *Pancreas* 2003; **26**: e74-e80
37 **Kröncke KD,** Suschek CV, Kolb-Bachofen V. Implications of inducible nitric oxide synthase expression and enzyme activity. *Antioxid Redox Signal* 2000; **2**: 585-605

Science Editor Wang XL and Guo SY **Language Editor** Elsevier HK

PO Box 2345, Beijing 100023, China
www.wjgnet.com
wjg@wjgnet.com

ELSEVIER

World J Gastroenterol 2005;11(15):2346-2350
World Journal of Gastroenterology ISSN 1007-9327

• *BRIEF REPORTS* •

Effects of ursodeoxycholic acid and/or low-calorie diet on steatohepatitis in rats with obesity and hyperlipidemia

Jian-Gao Fan, Lan Zhong, Li-Yan Tia, Zheng-Jie Xu, Min-Sheng Li, Guo-Liang Wang

Jian-Gao Fan, Lan Zhong, Li-Yan Tia, Zheng-Jie Xu, Guo-Liang Wang, Department of Gastroenterology, Shanghai First People's Hospital, Jiaotong University, Shanghai 200080, China
Min-Sheng Li, Department of Pathology, Fudan University Medical School, Shanghai 200032, China
Supported by the National Natural Science Foundation of China, No. 3980051; Shanghai Youth Sciences Phosphor Plan, No. 2000QB14010
Correspondence to: Dr. Jian-Gao Fan, Department of Gastroenterology, Shanghai First People's Hospital, Shanghai 200080, China. fanjg@citiz.net
Telephone: +86-21-63240090 Fax: +86-21-63240825
Received: 2004-03-15 Accepted: 2004-04-16

Abstract

AIM: To evaluate the effects of ursodeoxycholic acid (UDCA) and/or low-calorie diet (LCD) on a rat model of nonalcoholic steatohepatitis (NASH).

METHODS: Fifty-five Sprague-Dawley rats were divided into five groups. The control group (n = 9) was fed with standard rat diet for 12 wk, NASH group (n = 10) was fed with high-fat diet consisted of normal diet, 10% lard oil and 2% cholesterol for 12 wk, UDCA group (n = 10) was fed with high-fat diet supplemented with UDCA at a dose of 25 mg/(kg • d) in drinking water for 12 wk, LCD group (n = 10) was fed with high-fat diet for 10 wk and then LCD for 2 wk, and UDCA+LCD group (n = 15) was fed with high-fat diet for 10 wk, followed by LCD+UDCA for 2 wk. At the end of the experiment, body weight, serum biochemical index, and hepatopathologic changes were examined.

RESULTS: Compared with the control group, rats in the NASH group had significantly increased body weight, liver weight, and serum lipid and aminotransferase levels. All rats in the NASH group developed steatohepatitis, as determined by their liver histology. Compared with the NASH group, there were no significant changes in body weight, liver weight, blood biochemical index, the degree of hepatic steatosis, and histological activity index (HAI) score in the UDCA group; however, body and liver weights were significantly decreased, and the degree of steatosis was markedly improved in rats of both the LCD group and the UDCA+LCD group, but significant improvement with regard to serum lipid variables and hepatic inflammatory changes were seen only in rats of the UDCA+LCD group, and not in the LCD group.

CONCLUSION: LCD might play a role in the treatment of obesity and hepatic steatosis in rats, but it exerts no significant effect on both serum lipid disorders and hepatic inflammatory changes. UDCA may enhance the therapeutic effects of LCD on steatohepatitis accompanied by obesity and hyperlipidemia. However, UDCA alone is not effective in the prevention of steatohepatitis induced by high-fat diet.

Key words: UDCA; LCD

Fan JG, Zhong L, Tia LY, Xu ZJ, Li MS, Wang GL. Effects of ursodeoxycholic acid and/or low-calorie diet on steatohepatitis in rats with obesity and hyperlipidemia. *World J Gastroenterol* 2005; 11(15): 2346-2350
http://www.wjgnet.com/1007-9327/11/2346.asp

INTRODUCTION

Nonalcoholic steatohepatitis (NASH) is a hepatic disorder with histologic features of alcoholic hepatitis, occurring in individuals who do not consume significant amount of alcohol. In spite of the high prevalence of hepatic steatosis and of the potential of NASH to progress to fibrosis and cirrhosis, no effective specific treatment is available[1-7]. Management of this condition today is empirical. In NASH patients with comorbid obesity, weight reduction is recommended, chiefly by means of a low-calorie diet (LCD). An inappropriate diet, however, may lead to metabolic disorders, and may even promote portal inflammation, fibrosis, bile stasis or focal necrosis[8-13]. Ursodeoxycholic acid (UDCA) has cytoprotective, anti-apoptotic, membrane stabilizing, anti-oxidant and immunomodulative effects[14]. So UDCA has been recommended in the treatment of NASH and in the prevention of cholelithiasis during weight reduction. Clinical trials of UDCA in NASH therapy, however, have yielded ambiguous results[12-14].

In the present study we determined the effects of UDCA and/or LCD administration on NASH in rats chronically fed with high-fat diet.

MATERIALS AND METHODS

Reagents

Cholesterol was purchased from the Department of Reagents, Huamei Drug Store (Shanghai, China). Lard oil was prepared in our laboratory. UDCA powder (99.9% purity) was kindly provided by the Shanghai 1st Chinese Herb Pharmaceutical Company (Shanghai). Alanine aminotransferase (ALT) and aspartic aminotransferase (AST) assay kits were purchased from Sheneng Company

(Shanghai). Assay kits for free fatty acids (FFA), triglycerides (TG) and total cholesterol (TCH) were from Zhicheng Company (Shanghai), while assay kits for albumin (A) and total proteins (TP) were from the Shanghai Institution of Bio-products (Shanghai). Rabbit polyclonal anti-human lysozyme antibody was purchased from Shanghai Biogenex Company, and mouse anti-human α-smooth muscle actin (α-SMA) was from Dako (Carpinteria, CA). The second antibody for immunochemical assays was from the American Antibody Company (Greenwich, CT).

Animal diet and experimental protocol

All protocols for animal experimentation and maintenance were approved by the Animal Ethics Committee in our university and conformed to the highest international standards of humane care.

Fifty-five male Sprague-Dawley rats weighing 140-160 g were obtained from the Shanghai Experimental Animal Center (Shanghai, China). After being fed with standard rat chow for one week, Sprague-Dawley rats were randomly divided into five groups. Control rats (n = 9) were fed with standard rat diet for 12 wk. Rats of NASH group (n = 10) were fed with high-fat diet (i.e., standard diet supplemented with 10% lard oil and 2% cholesterol) for 12 wk. Animals in the UDCA group (n = 10) were fed with high-fat diet supplemented with UDCA (25 mg/(kg • d) in drinking water) for 12 wk. Rats in the LCD group (n = 10) were fed with high-fat diet for 10 wk and then fed with LCD (70 kcal/(kg • d)) accounting for 1/3 of the daily needs of a healthy rat of that age for 2 wk. Rats in the UDCA+LCD group (n = 15) were fed with high-fat diet for 10 wk and then fed with LCD+UDCA (25 mg/(kg • d)) for 2 wk. Animals were maintained in separate cages and provided with unrestricted amounts of food and water. The cages were kept in temperature-and humidity-controlled rooms, which were maintained on a 12-h light/dark cycle.

The animals were weighed on d 0, 10th wk of the experiment and one day before killing. All rats were killed at the end of wk 12, except for one of the rats in the NASH group, which was killed at the end of wk 10 for the demonstration of hepatopathologic changes. At the time of killing the rats were free from food at least 12 h, blood was obtained by aorta abdominalis puncture, and the resulting serum was stored at -20 ℃ until analysis. Meanwhile, liver sample was rapidly excised and weighed, tissue samples were snap frozen and stored at -70 ℃ until analysis, or were fixed in 4% buffered formaldehyde solution until use.

Blood biochemical analyses

Serum ALT, AST, A, TP, TG, TCH, and FFA were assayed biochemically using an Olympus AU1000 and automated procedures.

Histologic studies

Hepatic sections were stained with hematoxylin and eosin (H&E) for routine histology or with VG carbazotic acid for detection of fibrosis. Ultramicrotomy was performed for transmission electron microscopy (JEM-1200EX, Japan). Hepatocytes associated with fat infiltration into the lobules were counted in H&E stained sections.

The severity of steatosis was graded on the basis of the extent of involved parenchyma. Samples scored as+were those in which fewer than 33% of the hepatocytes were affected; samples scored as ++ were those in which 33-66% of the hepatocytes were affected; samples scored as +++ were those in which more than 66% of the hepatocytes were affected; and samples scored as -- were those in which no hepatocytes were affected[15-17]. Modified Knodell histological activity index (HAI) was used to determine hepatic necroinflammatory activity scored by the severity of portal inflammation (P), intralobular inflammation (L), piecemeal necrosis (PN) and bridging necrosis (BN). The score from 1 to 4 was in accordance with the severity of lesions and the total score was calculated as P+L+2(PN+BN). The number of Kupffer cells and activated hepatic stellate cells was determined immunochemically using lysozyme and α-SMA antibody respectively. All samples were evaluated blindly by the same pathologist.

Statistics

Data were expressed as mean±SD unless otherwise specified. The Student's t test was used to analyze individual differences. Rank samples were analyzed by the Rank-sum test. Rate comparison was analyzed by the U test. A value of $P<0.05$ was considered to be statistically significant.

RESULTS

General information

During the experimental period, the body weight of rats fed on high-fat diet increased quickly. By the end of the 10th wk, the body weight of high-fat fed rats was significantly higher than the controls. At the same time, we randomly harvested one of the high-fat fed rats for hepatopathological examination, which showed liver steatosis with mild nonspecific intralobular inflammation. Biochemical analyses indicated that serum TCH, FFA, ALT, and AST levels in this rat were higher than normal. Rats in the LCD and LCD+UDCA groups were fretful, inflammable, and bellicose, and their weight stopped increasing. No animal died during the experimental period.

Changes in body and liver weight

At the end of the 12-wk experimental period, the rats in the NASH group were 20% heavier than those in the control group ($P<0.05$). Liver index (liver wet weight/body weight×100%) in the NASH group was also significantly higher than in the controls ($P<0.01$). In the UDCA group, the changes in body weight and HAI score were similar to the NASH group. Compared with the NASH group, the body weight ($P<0.01$) and liver index ($P<0.05$) in the LCD group were significantly lower, while the changes in the UDCA+LCD group were similar to those in the LCD group (Table 1).

Changes in serum lipids

After 12 wk, serum TCH ($P<0.05$) and FFA ($P<0.01$) in the NASH group were significantly higher than those in the control group, whereas serum TG levels were equivalent. The changes of blood lipid variables in the UDCA group

Table 1 **Changes of body weight and liver index**

Group	*n*	Body weight (g)	Liver index (%)
Control	9	351.1±43.0	2.957±0.301
NASH	10	423.5±65.2[a]	3.784±0.533[b]
UDCA	10	426.5±26.6	3.476±0.351
LCD	10	329.5±38.4[d]	3.199±0.552[c]
LCD+UDCA	15	310.3±38.6[d]	3.113±0.466[c]

[a]$P<0.05$, [b]$P<0.01$ *vs* control, [c]$P<0.05$, [d]$P<0.01$ *vs* NASH group.

Table 3 **Alterations of some biochemical variables in rat liver function**

Group	*n*	ALT (u/L)	AST (u/L)	A (g/L)	A/G
Control	9	40.2±7.1	98.7±24.8	25.13±4.61	0.71±0.11
NASH	10	75.3±40.21[a]	165.3±59.8[b]	27.40±2.04	0.73±0.08
UDCA	10	66.0±49.4	139.5±54.52	7.49±1.78	0.66±0.09
LCD	10	40.9±14.7[c]	140.4±32.3	24.51±4.69	0.71±0.16
UDCA+LCD	15	40.1±8.8[c]	111.8±22.9[c]	25.3±1.34	0.71±0.07

[a]$P<0.05$, [b]$P<0.01$ *vs* control, [c]$P<0.05$ *vs* NASH group.

were similar to those in the NASH group. Serum TCH in the LCD group was significantly higher than that in the NASH group ($P<0.05$), and FFA in the LCD group was inclined to increase as compared to the NASH group, while TG was significantly decreased ($P<0.001$). Compared with the LCD group, serum lipid disorders in the UDCA+LCD group had a tendency to improve (Table 2).

Changes in liver function

At the end of the 12 wk, serum ALT ($P<0.05$) and AST ($P<0.01$) levels were significantly higher in the NASH group than in the controls. While serum AST was slightly lower in the UDCA group than that in the NASH group, the difference was not statistically significant. In the LCD group, serum ALT level was significantly lower than in the NASH group ($P<0.05$), whereas serum AST level only displayed a decreasing trend in plasma ($P>0.05$). Compared with the LCD group, serum AST level was significantly lower in the UDCA+LCD group ($P<0.05$), while serum ALT level was about the same in the both groups. There were no significant differences in serum albumin levels and albumin-globulin ratio among these groups of rats (Table 3).

Changes in liver histology

At the end of the 12 wk, we observed no specific histologic alterations in the control livers. Under light microscope, sections stained with H&E in the NASH group showed steatosis, which was predominantly macrovesicular and more or less diffusely distributed throughout the liver lobule, and parenchymal inflammation with both acute and chronic inflammatory cells accompanied with focal necrosis. In 80% of the samples, portal inflammation was noted, which was mild compared with lobular inflammation; and 20% samples accompanied with piecemeal necrosis. The score of HAI in the NASH group was significantly higher than in the controls ($P<0.01$). No obvious liver fibrosis was found in VG carbazotic acid-stained tissue sections. Immunohistochemical analysis showed that the number of cells positive for lysozyme and α-SMA was significantly higher in the NASH group than in the controls. Electron microscopic examination showed that, in the NASH group, liver cell nuclei were squeezed to cell ambitus by large lipid droplets, and that there was mitochondrial swelling; proliferation of hepatic stellate cells and Kupffer cells was also found.

Compared with the NASH group, there were no alterations in hepatopathologic findings of rats in the UDCA group. However, the degree of steatosis in the LCD group was significantly reduced ($P<0.05$). Both the degree of steatosis and the score of HAI in the UDCA+LCD group were a little lower than in the LCD group, but obviously lower than the NASH group ($P<0.05$). Significantly fewer cells positive for lysozyme and α-SMA were observed in the UDCA+LCD group than in the NASH group, but these parameters did not differ among the other groups. Histologically, the livers of four rats in the UDCA+LCD group and one in the LCD group were almost normalized, but this difference was not significant (Tables 4 and 5). There still existed mild, nonspecific intralobular inflammation in the rat of the LCD group with hepatic steatosis regressed.

DISCUSSION

Because NASH may lead to progressive hepatic fibrosis and eventually cirrhosis and because its prevalence appears to be increasing, it is necessary to develop effective therapies for NASH. Currently, multiple therapies have been recommended for NASH. However, as is usual in such instance, when many modes of therapy have been proposed, there is no single, well-established consensus regarding effective therapy[1-13].

In our study, while the rats fed on a high-fat diet for 10 wk were overweight and developed hyperlipidemia and fatty liver (this was confirmed by our another study)[18,19], a subsequent 2 wk on LCD made both of their overweight and hyperlipidemia and hepatic steatosis alleviated. In contrast, an additional 2 wk of the high-fat diet led to the development of more severe obesity, hyperlipidemia and steatohepatitis. These findings suggest that altering a high-fat diet to LCD may have markedly positive effects on obesity,

Table 2 **Changes of major plasma lipid parameters**

Group	*n*	TG (mmol/L)	TCH (mmol/L)	FFA (mmol/L)
Control	9	0.63±0.22	1.27±0.17	429.2±96.7
NASH	10	0.62±0.10	1.60±0.41[a]	728.2±178.5[b]
UDCA	10	0.59±0.13	1.60±0.43	629.0±229.6
LCD	10	0.39±0.13[d]	2.04±0.50[c]	771.3±124.4
UDCA+LCD	15	0.51±0.17[e]	1.93±0.27[c]	605.6±152.2

[a]$P<0.05$, [b]$P<0.01$ *vs* control, [c]$P<0.05$, [d]$P<0.01$ *vs* NASH group. [e]$P<0.05$ *vs* LCD group.

Table 4 **Hepatic steatosis in groups of rats**

Group	*n*	-	+	++	+++
Control	9	9			
NASH	10		3	6	1
UDCA	10	1	3	4	2
LCD	10	3	5	2	
UDCA+LCD	15	8	1	4	2

Table 5 HAI in groups of rats

Group	*n*	HAI
Control	9	0.8±0.8
NASH	10	3.4±2.1
UDCA	10	3.0±1.3
LCD	10	2.5±1.0
UDCA+LCD	15	1.9±1.1

hyperlipidemia and combined fatty liver, while continuation on the fat-rich diet may lead to the development of steatohepatitis[20]. Although there was no liver fibrosis, we found activation and proliferation of hepatic stellate cells and Kupffer cells, suggesting that liver fibrosis might be inevitable[18,19]. Subsequent research demonstrated that feeding with a high-fat diet for 24 wk could induce steatohepatitis with liver fibrosis[18,19]. Since the rats in our LCD group developed hypercholesterolemia and hypotriglyceridemia with a trend to increase of serum FFA level, some of their liver samples were still found to have hepatocyte necrosis and inflammatory cell infiltration, indicating that merely short-term LCD therapy may be not quite enough to reverse steatohepatitis and serum lipid disorders[20,21]. Concurrent administration of medications with potential hepatoprotective effects may be reasonable alternatives for the treatment of NASH with obesity.

UDCA is a bile acid with multiple potential mechanisms of action, including immunomodulatory effects, displacement of toxic hydrophobic bile salts from the bile acid pool, lipid-altering properties, and direct cytoprotective effects[22-26]. UDCA was first used as an empiric treatment in NASH in a 66-year-old woman. The patient experienced normalization of serum liver enzyme levels after treatment of UDCA for 1 year[27]. In a pilot study of 40 patients with NASH established by liver biopsy and the exclusion of other causes of hepatitis, 24 patients were treated with UDCA (13-15 mg/(kg • d)) for 1 year. There was no significant change in body weight. There was a statistically significant decrease in levels of ALT, alkaline phosphatase, gamma-glutamyltranspeptidase and in improvement in histologic grade of hepatic steatosis. Sixteen patients with hypertriglyceridemia were placed on clofibrate (2 g/d) for 12 mo and did not have any benefit[28]. Recently, McCullough recommended that until more information is provided, it seems appropriate to treat comorbid diseases in patients with NASH and to implement UDCA[29]. However, our findings suggest that UDCA alone did not have significant effects on rats with NASH induced by high-fat diet. Compared with the NASH group, no alterations in serum biochemistry or liver histology were observed in the UDCA group. This was in accordance with the new results of a randomized, placebo-controlled trial completed by the UDCA/NASH study group of USA, which showed that UDCA (13-15 mg/(kg • d)) was not associated with improved liver biochemistries or liver histology in patients with NASH when compared to placebo, and the weight was stable in the two groups[30,31].

In addition, in our study UDCA was able to ameliorate blood lipid disorders, facilitate regression of hepatic steatosis, inflammation and necrosis, and significantly decrease serum AST level when given together with LCD therapy. So, the addition of UDCA was more efficacious than LCD alone. If this is the case, the following possible mechanisms of UDCA in improving the effects of LCD on steatohepatitis can be proposed in light of the previous study[32-34]. In rats, Tabouy and colleagues showed that the preferential shift of the metabolic pathway of fatty acids from esterification to oxidation due to the ethanol-induced liver mitochondrial damage, and subsequent fat accumulation, may be prevented by UDCA by way of improving ATP synthesis with protection of mitochondrial morphology[32]. In addition to this membrane-protective effect of UDCA, whether this drug directly mediates a shift in fatty acid metabolism from esterification to oxidation is also worth examining. A recent rat study, in which the effect of UDCA on alcohol-induced steatosis and lipid peroxidation was examined, suggests that UDCA might reduce steatosis and lipid peroxidation[33,34].

In summary, our findings suggest that UDCA alone is not effective for the treatment of NASH rats and that short-term LCD alone does not usually resolve NASH. Concurrent administration of UDCA and LCD, however, may enhance the curative effects and reduce the side effects of rapid weight reduction. Thus, while UDCA may not directly reduce or reverse steatohepatitis independently of weight loss, this medication might complement the diet of patients with NASH.

REFERENCES

1 **Tagle Arrospide M.** Non-alcoholic fatty liver. *Rev Gastroenterol Peru* 2003; **23**: 49-57
2 **Alba LM,** Lindor K. Review article: Non-alcoholic fatty liver disease. *Aliment Pharmacol Ther* 2003; **17**: 977-986
3 **Bugianesi E,** Leone N, Vanni E, Marchesini G, Brunello F, Carucci P, Musso A, De Paolis P, Capussotti L, Salizzoni M, Rizzetto M. Expanding the natural history of nonalcoholic steatohepatitis: from cryptogenic cirrhosis to hepatocellular carcinoma. *Gastroenterology* 2002; **123**: 134-140
4 **Shen L,** Fan JG, Shao Y, Zeng MD, Wang JR, Luo GH, Li JQ, Chen SY. Prevalence of nonalcoholic fatty liver among administrative officers in Shanghai: an epidemiological survey. *World J Gastroenterol* 2003; **9**: 1106-1110
5 **Angulo P.** Nonalcoholic fatty liver disease. *N Engl J Med* 2002; **346**: 1221-1231
6 **Neuschwander-Tetri BA,** Caldwell SH. Nonalcoholic steatohepatitis: summary of an AASLD Single Topic Conference. *Hepatology* 2003; **37**: 1202-1219
7 **James O,** Day C. Non-alcoholic steatohepatitis: another disease of affluence. *Lancet* 1999; **353**: 1634-1636
8 **Angulo P.** Current best treatment for non-alcoholic fatty liver disease. *Expert Opin Pharmacother* 2003; **4**: 611-623
9 **Hookman P,** Barkin JS. Current biochemical studies of non-alcoholic fatty liver disease (NAFLD) and non-alcoholic steatohepatitis (NASH) suggest a new therapeutic approach. *Am J Gastroenterol* 2003; **98**: 495-499
10 **Sanyal AJ.** Treatment of non-alcoholic fatty liver disease. *J Gastroenterol Hepatol* 2002; **17** Suppl 3: S385-S388
11 **Oneta CM,** Dufour JF. Non-alcoholic fatty liver disease: treatment options based on pathogenic considerations. *Swiss Med Wkly* 2002; **132**: 493-505
12 **Angulo P,** Lindor KD. Treatment of non-alcoholic steatohepatitis. *Best Pract Res Clin Gastroenterol* 2002; **16**: 797-810
13 **Angulo P,** Lindor KD. Treatment of nonalcoholic fatty liver: present and emerging therapies. *Semin Liver Dis* 2001; **21**: 81-88
14 **Angulo P.** Use of ursodeoxycholic acid in patients with liver disease. *Curr Gastroenterol Rep* 2002; **4**: 37-44
15 **Brunt EM,** Janney CG, Di Bisceglie AM, Neuschwander-Tetri

BA, Bacon BR. Nonalcoholic steatohepatitis: a proposal for grading and staging the histological lesions. *Am J Gastroenterol* 1999; **94**: 2467-2474

16 **Matteoni CA,** Younossi ZM, Gramlich T, Boparai N, Liu YC, McCullough AJ. Nonalcoholic fatty liver disease: a spectrum of clinical and pathological severity. *Gastroenterology* 1999; **116**: 1413-1419

17 **Dixon JB,** Bhathal PS, O'Brien PE. Nonalcoholic fatty liver disease: predictors of nonalcoholic steatohepatitis and liver fibrosis in the severely obese. *Gastroenterology* 2001; **121**: 91-100

18 **Fan JG,** Xu ZJ, Wang GL, Ding XD. Rat model of nonalcoholic steatohepatitis with fibrosis by a fat-rich diet. *Gastroenterology* 2003; **124**: A758

19 **Fan JG,** Xu ZJ, Ding XD, Zheng XY, Tian LY. Changes of Kupffer cell activity in the process of inducing the rat model of nonalcoholic steatohepatitis. *Hepatology* 2003; **36**: A553

20 **Andersen T,** Gluud C, Franzmann MB, Christoffersen P. Hepatic effects of dietary weight loss in morbidly obese subjects. *J Hepatol* 1991; **12**: 224-229

21 **Biourge V,** Groff JM, Fisher C, Bee D, Morris JG, Rogers QR. Nitrogen balance, plasma free amino acid concentrations and urinary orotic acid excretion during long-term fasting in cats. *J Nutr* 1994; **124**: 1094-1103

22 **Laurin J,** Lindor KD, Crippin JS, Gossard A, Gores GJ, Ludwig J, Rakela J, McGill DB. Ursodeoxycholic acid or clofibrate in the treatment of non-alcohol-induced steatohepatitis: a pilot study. *Hepatology* 1996; **23**: 1464-1467

23 **Trauner M,** Graziadei IW. Review article: mechanisms of action and therapeutic applications of ursodeoxycholic acid in chronic liver diseases. *Aliment Pharmacol Ther* 1999; **13**: 979-996

24 **Kumar D,** Tandon RK. Use of ursodeoxycholic acid in liver diseases. *J Gastroenterol Hepatol* 2001; **16**: 3-14

25 **Rudolph G,** Kloeters-Plachky P, Sauer P, Stiehl A. Intestinal absorption and biliary secretion of ursodeoxycholic acid and its taurine conjugate. *Eur J Clin Invest* 2002; **32**: 575-580

26 **Lirussi F,** Okolicsanyi L. Cytoprotection with ursodeoxycholic acid: effect in chronic non-cholestatic and chronic cholestatic liver disease. *Ital J Gastroenterol* 1992; **24**: 31-35

27 **Abdelmalek M,** Ludwig J, Lindor KD. Two cases from the spectrum of nonalcoholic steatohepatitis. *J Clin Gastroenterol* 1995; **20**: 127-130

28 **Laurin J,** Lindor KD, Crippin JS, Gossard A, Gores GJ, Ludwig J, Rakela J, McGill DB. Ursodeoxycholic acid or clofibrate in the treatment of non-alcohol-induced steatohepatitis: a pilot study. *Hepatology* 1996; **23**: 1464-1467

29 **McCullough AJ.** Update on nonalcoholic fatty liver disease. *J Clin Gastroenterol* 2002; **34**: 255-262

30 **Lindor KD.** Ursodeoxycholic acid for treatment of nonalcoholic steatohepatitis: results of a randomized, placbo-controlled trial. *Gastroenterology* 2003; **124**: A708

31 **Vajro P,** Franzese A, Valerio G, Iannucci MP, Aragione N. Lack of efficacy of ursodeoxycholic acid for the treatment of liver abnormalities in obese children. *J Pediatr* 2000; **136**: 739-743

32 **Tabouy L,** Zamora AJ, Oliva L, Montet AM, Beauge F, Montet JC. Ursodeoxycholate protects against ethanol-induced liver mitochondrial injury. *Life Sci* 1998; **63**: 2259-2270

33 **Okan A,** Astarcioglu H, Tankurt E, Sagol O, Altekin E, Astarcioglu I, Gonen O. Effect of ursodeoxycholic acid on hepatic steatosis in rats. *Dig Dis Sci* 2002; **47**: 2389-2397

34 **Oliva L,** Beauge F, Choquart D, Montet AM, Guitaoui M, Montet JC. Ursodeoxycholate alleviates alcoholic fatty liver damage in rats. *Alcohol Clin Exp Res* 1998; **22**: 1538-1543

Science Editor Zhu LH **Language Editor** Elsevier HK

PO Box 2345, Beijing 100023, China
www.wjgnet.com
wjg@wjgnet.com

ELSEVIER

World J Gastroenterol 2005;11(15):2351-2353
World Journal of Gastroenterology ISSN 1007-9327

• *BRIEF REPORTS* •

c-src activating mutation analysis in Chinese patients with colorectal cancer

Ye-Xiong Tan, Han-Tao Wang, Peng Zhang, Zhong-Hua Yan, Guan-Long Dai, Meng-Chao Wu, Hong-Yang Wang

Ye-Xiong Tan, Peng Zhang, Zhong-Hua Yan, Meng-Chao Wu, Hong-Yang Wang, International Co-operational Laboratory on Signal Transduction, Eastern Hepatobiliary Surgery Hospital, Shanghai 200438, China
Han-Tao Wang, Guan-Long Dai, Department of General Surgery, Changhai Hospital, Shanghai 200433, China
Supported by the Major State Basic Research Development Program of China, No. G1998051210
Correspondence to: Dr. Hong-Yang Wang, International Co-operational Laboratory on Signal Transduction, Eastern Hepatobiliary Institute, Shanghai 200438, China. hywangk@online.sh.cn
Telephone: +86-21-25070856 Fax: +86-21-65566851
Received: 2004-04-24 Accepted: 2004-04-29

Abstract

AIM: To investigate the occurrence of cellular src (*c-src*) activating mutation at codon 531 in colorectal cancer patients from Chinese mainland.

METHODS: Polymerase chain reaction-restriction fragment length polymorphism (PCR-RFLP) assay followed by sequencing and single-strand conformation polymorphism analysis were carried out to screen 110 samples of primary colorectal cancer and 20 colorectal liver metastases.

RESULTS: Only one sample showed PCR-RFLP-positive results and carried somatic codon 531 mutations. No additional mutation of *c-src* exon 12 was found.

CONCLUSION: *c-src* codon 531 mutation in colorectal cancer is not the cause of *c-src* activation.

Key words: c-src; Colorectal cancer

Tan YX, Wang HT, Zhang P, Yan ZH, Dai GL, Wu MC, Wang HY. *c-src* activating mutation analysis in Chinese patients with colorectal cancer. *World J Gastroenterol* 2005; 11 (15): 2351-2353
http://www.wjgnet.com/1007-9327/11/2351.asp

INTRODUCTION

Liver metastasis is one of the main causes of death of colorectal cancer patients. Although it is well known that tumor metastasis is a multi-factorial and multi-step process, the exact mechanisms underlying metastasis of colorectal cancer are still largely unclear. Elevated expression and activity of the *src* family tyrosine kinase are often associated with progression and metastasis of human colorectal cancer[1]. As for the mechanism of *src* activation, Irby *et al*[2], reported an activating *c-src* mutation, C-T mutation in codon 531 (located at exon 12), in 12% of advanced human colon cancers[2]. But the following likewise screens of this kind of mutations in four groups all had negative results[3-6]. It is still quite uncertain whether codon 531 activating mutation is a cause of *c-src* activation in advanced colorectal cancers.

In this study, we investigated 110 primary colorectal cancers and 20 colorectal liver metastasis patients from China mainland for this *c-src* specific mutation.

MATERIALS AND METHODS

Tissue specimens

Primary colorectal tumors and corresponding normal tissues and blood samples were obtained from a total of 110 Chinese patients (median age of 52 years, ranging from 36 to 72 years) with primary colorectal cancer during surgery at Changhai Hospital and Changzheng Hospital (both in Shanghai, China) from May 2003 to December 2003. The tumors were classified as Duke stage A in 21, B in 26, C in 38 and D in 25. Twenty liver metastases with colorectal origin were from Shanghai Eastern Hepatobiliary Surgery Hospital. Tissue samples were stored at -80 ℃ until DNA extraction.

PCR amplification and RFLP analysis

Genomic DNA was extracted as previously described[7]. DNAs from all 130 samples served as templates for PCR (Perkin-Elmer) with primers set to amplify exon 12 of *c-src*. The sequences of primers were as follows: forward, 5'-ACAGGGATGGTGAACCGCGA-3' and reverse, 5'-ATCCAAGCCGAGAAGCCGGT-3'.

After DNA extraction (QIAquick PCR purification kit, Qiagen), PCR products were digested with 5 Units of restriction enzyme *Sca* I overnight. Plasmid DNAs bearing *src* 531 mutation created by using overlap extension PCR[8] were used as positive controls. The possible digestion-positive samples were cloned into T-vector (pGEM®-T vector, Promega) and sequenced automatically (Perkin Elmer-Roche, Banchburg, NJ).

SSCP analysis

PCR products of genomic DNA were screened for mutations by single-strand conformational polymorphism (SSCP) analysis exactly as previously described[9].

RESULTS

PCR with primers devised here generated a 266-bp fragment,

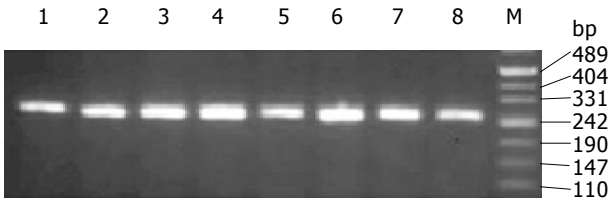

Figure 1 PCR amplification of *src* exon 12 from genomic DNA of colorectal cancer. Lanes 1-8: samples; lane M: marker.

which was confirmed to be exon 12 of *c-src* by direct sequencing (Figure 1). Only one sample (Figure 2) was positive by RFLP analysis among the 110 samples of colorectal cancer and 20 liver metastases in this study. This No. 73 sample could only be partially digested by 5U *Sca* I even after overnight digestion, implying that the corresponding DNA template was a mixture of mutated and wild type clones.

This positive PCR product was cloned into T vector, and 20 transformants were selected for sequencing. The result confirmed the presence of 531 C-T mutation and the ratio of mutated clones *vs* wild type clones was 8:12 (Figure 3). To further know whether it was a somatic or germ line mutation, we analyzed its paired normal samples and blood likewise, but could not find any mutation (Figure 2).

Additionally, SSCP was carried out to screen possible other mutations of *c-src* in exon 12. No aberrant band was found except for No. 73 sample and positive control (Figure 4).

DISCUSSION

Cellular *src* (*c-src*) is a human homolog of the Rous sarcoma viral oncogene, *v-src*. *c-src* has been implicated in the development and progression of numerous human cancers, including colorectal cancer[10]. *c-src* was shown to be dramatically activated in colorectal cancer[11,12]. Irby *et al*[2], reported *src* point mutation at codon 531 truncated *c-src* C-terminal to the negatively regulatory kinase phosphorylation site at Tyr 530 and thereby activated *c-src*. This was the first report of activating *c-src* mutation related to the progression of colorectal cancer. However, no such mutations in Japanese and North European as well as from Italian patients with colorectal cancer were found[3-6].

In this research, 110 primary colorectal cancers (38 in Duke's stage C and 25 in Duke's stage D) and 20 liver metastases were screened by RFLP analysis. Only one sample showed positive results (Figure 2) and was confirmed by direct sequencing, while its adjacent normal intestinal mucosa and blood kept intact. Our results indicated that activating mutation of *c-src* might be only a rare case, which could not explain the *c-src* activation always found in colorectal cancer.

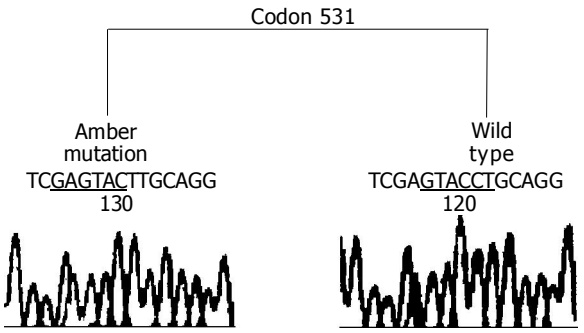

Figure 3 Sequencing of two clones (one wild and the other Amber-mutated) from RFLP-positive PCR products of No. 73 colorectal cancer.

c-src can be activated through various mechanisms, the core of which is to relieve the intramolecular autoinhibition created by binding of its SH2 domain to pY527 in the carboxyl terminus[13]. pY527 is phosphorylated by the protein tyrosine kinase, Csk. Recently, Cam *et al*[14], found that Csk protein and its kinase activity were reduced in colorectal carcinoma and correlated with *c-src* kinase activity. Furthermore, Csk over-expression in mouse NL-17 cells (highly metastatic clone of mouse colon adenocarcinoma) resulted in significant suppression of metastasis, but did not affect its tumorigenicity[15], demonstrating its role in metastatic inhibition. More recently, Rengifo-Cam *et al*[16], found that overexpression of wild-type Csk increased cell-cell contacts, mediated by E-cadherin, could decrease the number of focal contacts and cell adhesion/migration and *in vitro* invasiveness. It is, therefore, worthwhile to detect the activity of Csk in colorectal cancer. However, Be'nistant *et al*[17], reported the existence of autoantibodies to Csk and elevated Csk in colorectal adenocarcinoma. Furthermore, it was found that src was deregulated in all of the tumors tested, suggesting that Csk could not phosphorylate src in transformed cells or that src was activated despite its phosph-

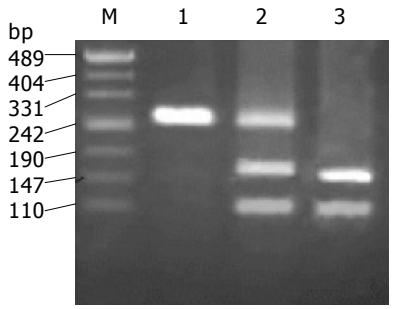

Figure 2 Positive result of No. 73 sample in RFLP analysis. Lane 1: No. 73 para-cancer tissue; lane 2: No. 73 cancer tissue; lane 3: positive control; lane M: DNA marker.

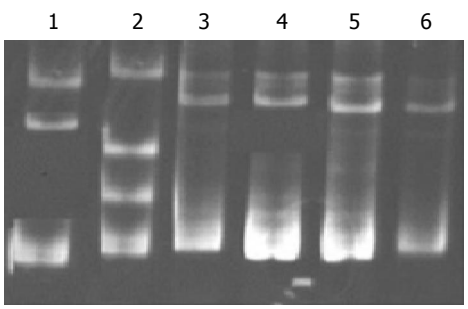

Figure 4 SSCP analysis of *src* exon 12 fragment amplified from colorectal cancer. Lane 1: positive control; lane 2: No. 73; lane 3: negative control; lanes 4-6: three negative samples.

orylation by Csk.

Apart from down-regulation of csk, transcriptional activation might be another mechanism of *c-src* activation in advanced colorectal cancer[18]. Our study demonstrates that activating point mutation in codon 531 may not be the main mechanism of *c-src* activation in colorectal cancer.

REFERENCES

1 **Yeatman TJ.** A renaissance for SRC. *Nat Rev Cancer* 2004; **4**: 470-480

2 **Irby RB,** Mao W, Coppola D, Kang J, Loubeau JM, Trudeau W, Karl R, Fujita DJ, Jove R, Yeatman TJ. Activating SRC mutation in a subset of advanced human colon cancers. *Nat Genet* 1999; **21**: 187-191

3 **Daigo Y,** Furukawa Y, Kawasoe T, Ishiguro H, Fujita M, Sugai S, Nakamori S, Liefers GJ, Tollenaar RA, van de Velde CJ, Nakamura Y. Absence of genetic alteration at codon 531 of the human *c-src* gene in 479 advanced colorectal cancers from Japanese and Caucasian patients. *Cancer Res* 1999; **59**: 4222-4224

4 **Nilbert M,** Fernebro E. Lack of activating *c-SRC* mutations at codon 531 in rectal cancer. *Cancer Genet Cytogenet* 2000; **121**: 94-95

5 **Wang NM,** Yeh KT, Tsai CH, Chen SJ, Chang JG. No evidence of correlation between mutation at codon 531 of src and the risk of colon cancer in Chinese. *Cancer Lett* 2000; **150**: 201-204

6 **Laghi L,** Bianchi P, Orbetegli O, Gennari L, Roncalli M, Malesci A. Lack of mutation at codon 531 of *SRC* in advanced colorectal cancers from Italian patients. *Br J Cancer* 2001; **84**: 196-198

7 **Blin N,** Stafford DW. A general method for isolation of high molecular weight DNA from eukaryotes. *Nucleic Acids Res* 1976; **3**: 2303-2308

8 **Ho SN,** Hunt HD, Horton RM, Pullen JK, Pease LR. Site-directed mutagenesis by overlap extension using the polymerase chain reaction. *Gene* 1989; **77**: 51-59

9 **Orita M,** Suzuki Y, Sekiya T, Hayashi K. Rapid and sensitive detection of point mutations and DNA polymorphisms using the polymerase chain reaction. *Genomics* 1989; **5**: 874-879

10 **Warmuth M,** Damoiseaux R, Liu Y, Fabbro D, Gray N. SRC family kinases: potential targets for the treatment of human cancer and leukemia. *Curr Pharm Des* 2003; **9**: 2043-2059

11 **Talamonti MS,** Roh MS, Curley SA, Gallick GE. Increase in activity and level of pp60 *c-src* in progressive stages of human colorectal cancer. *J Clin Invest* 1993; **91**: 53-60

12 **Iravani S,** Mao W, Fu L, Karl R, Yeatman T, Jove R, Coppola D. Elevated *c-Src* protein expression is an early event in colonic neoplasia. *Lab Invest* 1998; **78**: 365-371

13 **Schlessinger J.** New roles for Src kinases in control of cell survival and angiogenesis. *Cell* 2000; **100**: 293-296

14 **Cam WR,** Masaki T, Shiratori Y, Kato N, Ikenoue T, Okamoto M, Igarashi K, Sano T, Omata M. Reduced C-terminal Src kinase activity is correlated inversely with pp60 (*c-src*) activity in colorectal carcinoma. *Cancer* 2001; **92**: 61-70

15 **Nakagawa T,** Tanaka S, Suzuki H, Takayanagi H, Miyazaki T, Nakamura K, Tsuruo T. Overexpression of the csk gene suppresses tumor metastasis *in vivo*. *Int J Cancer* 2000; **88**: 384-391

16 **Rengifo-Cam W,** Konishi A, Morishita N, Matsuoka H, Yamori T, Nada S, Okada M. Csk defines the ability of integrin-mediated cell adhesion and migration in human colon cancer cells: implication for a potential role in cancer metastasis. *Oncogene* 2004; **23**: 289-297

17 **Be'nistant C,** Bourgaux JF, Chapuis H, Mottet N, Roche S, Bali JP. The COOH-terminal Src kinase Csk is a tumor antigen in human carcinoma. *Cancer Res* 2001; **61**: 1415-1420

18 **Dehm S,** Senger MA, Bonham K. SRC transcriptional activation in a subset of human colon cancer cell lines. *FEBS Lett* 2001; **487**: 367-371

Science Editor Wang XL and Kumar M **Language Editor** Elsevier HK

PO Box 2345, Beijing 100023, China
www.wjgnet.com
wjg@wjgnet.com

ELSEVIER

World J Gastroenterol 2005;11(15):2354-2356
World Journal of Gastroenterology ISSN 1007-9327

• *CASE REPORT* •

Endoscopic findings in a patient with Henoch-Schönlein purpura

Ming-Jen Chen, Tsang-En Wang, Wen-Hsiung Chang, Shu-Jung Tsai, Wen-Shen Liao

Ming-Jen Chen, Tsang-En Wang, Wen-Hsiung Chang, Shu-Jung Tsai, Wen-Shen Liao, Division of Gastroenterology, Department of Internal Medicine, Mackay Memorial Hospital, Mackay Medicine, Nursing and Management College, Taipei, Taiwan, China
Correspondence to: Dr. Ming-Jen Chen, Division of Gastroenterology, Department of Internal Medicine, Mackay Memorial Hospital, No. 92, Sec. 2, Chung-Shan N. Road, Taipei, Taiwan, China. mingjen.ch@msa.hinet.net
Telephone: +886-2-25433535-2260 Fax: +886-2-25433642
Received: 2004-07-12 Accepted: 2005-01-21

Abstract

Henoch-Schönlein purpura (HSP) is a systemic vasculitis of the small vessels of the skin, joints, GI tract, and kidney. It preferentially affects children but may also occur in adults. We report a 60-year-old man with HSP who presented with colicky abdominal pain, bloody diarrhea, arthralgia, and skin rash. The gastrointestinal tract was viewed by upper endoscopy and colonoscopy. We found characteristic endoscopic findings in the stomach, cecum and sigmoid colon, the combination of which has rarely been demonstrated in one patient. Histologic examination of skin biopsy specimens revealed leukocytoclastic vasculitis with positive staining for IgA in the capillaries. Endoscopy appears to have substantial diagnostic utility in patients suspected of having HSP, especially when abdominal symptoms precede the cutaneous lesions.

Key words: Henoch-Schönlein purpura; Purpura; Endoscopy

Chen MJ, Wang TE, Chang WH, Tsai SJ, Liao WS. Endoscopic findings in a patient with Henoch-Schönlein purpura. *World J Gastroenterol* 2005; 11(15): 2354-2356
http://www.wjgnet.com/1007-9327/11/2354.asp

INTRODUCTION

Henoch-Schönlein purpura (HSP) is a systemic vasculitic disorder of the small vessels of the skin, joints, GI tract, and kidney. The clinical manifestations usually include arthralgia, a purpuric skin rash, nephritis, abdominal pain, and GI bleeding. It commonly affects young children, with the peak age of onset between 4 and 7 years. The pathologic changes are mediated by IgA deposition[1], complement activation, granulocyte recruitment, and destruction of endothelial cells. The American College of Rheumatology published diagnostic criteria for HSP in 1990[2] including (1) age less than or equal to 20 years at disease onset, (2) the presence of palpable purpura, (3) GI bleeding, and (4) a biopsy showing granulocytes in the walls of small arterioles or venules. The diagnosis is made when three or more of those criteria are fulfilled.

CASE REPORT

A 60-year-old man presented with three days of colicky abdominal pain with bloody diarrhea, arthralgia in the knees, and ankle edema. His medical history was unremarkable except for a self-limited upper respiratory infection one week previously. Physical examination revealed diffuse lower abdominal rebound tenderness. There was no fever and no skin rash on admission. The initial leukocyte count was 17 830 /mm^3, and the C-reactive protein was 12 mg/dL. A plain abdominal film showed generalized ileus and no evidence of free air. Stool cultures were negative for enteric pathogens, and no ova or parasites were found. Upper endoscopy revealed multiple discrete coin-like petechiae and hemorrhagic erosions in the gastric antrum and lower body (Figure 1). Colonoscopy revealed patches of hyperemic and ecchymotic lesions in the cecum (Figure 2), ileocecal valve, and sigmoid colon. The patient was managed with fasting and intravenous fluids. The day after admission, he developed numerous erythematous, purpuric lesions, predominantly on the lower extremities and buttocks. The lesions rapidly became palpable (Figure 3). A platelet count, prothrombin time and partial thromboplastin time were normal. Based on this constellation of findings, HSP was suspected. Tissue from a skin biopsy of the lesions was compatible with leukocytoclastic vasculitis with deposition of IgA, confirming the diagnosis of HSP. The urinalysis and renal function were normal. Parenteral steroid therapy (5 mg/(kg·d) of hydrocortisone) was instituted initially, resulting in relief of the abdominal pain and arthralgia and gradual resolution of the skin lesions within 5 d. The treatment was switched to oral prednisolone 20 mg/d with gradual tapering over 4 wk. The patient has remained well over 2 years of follow up.

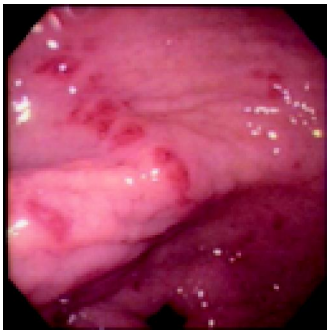

Figure 1 Upper endoscopic view of multiple discrete coin-like petechiae in the lower gastric body.

Figure 2 Colonscopic view of hyperemic and ecchymotic lesions in the cecum.

Figure 3 Numerous erythematous papules and palpable purpura on the lower extremities and buttocks.

DISCUSSION

The above-mentioned patient fulfilled three of four criteria for the diagnosis of HSP. The only exception was his age. The diagnostic sensitivity and specificity of three out of the four criteria are 89.4% and 88.1%, respectively[2]. Although the cause of HSP is unknown, immunizations, certain food allergies, insect bites, infection[3], and some medications[4] may play a role in the development of the disease. It may be that our patient's recent cold predisposed him to HSP. The final diagnosis of HSP was confirmed by histologic examination of a skin biopsy specimen demonstrating a vasculitis with leukocyte infiltration and deposition of IgA.

The diagnosis of HSP can be difficult, especially when abdominal symptoms precede cutaneous lesions. A skin rash is nearly always present, although not necessarily in the earliest stages. Lanzkowsky reported that 14% of patients had abdominal symptoms preceding the skin rash[5]. As in our case, the skin rash is typically on the lower extremities and buttocks, less commonly on the face and trunk. It starts as erythematous papules that quickly become palpable purpura. Normal platelets counts, prothrombin time, and partial thromboplastin time exclude a platelet or hemorrhagic disorder as the cause of purpura. Other laboratory tests are usually not conclusive.

Abdominal symptoms reportedly occur in 50-85% of HSP patients, possibly secondary to edema and hemorrhage within the bowel wall and mesentery. The abdominal pain is always colicky and poorly localized. On physical examination the abdomen may be rigid or distended, occasionally mimicking an acute abdomen and resulting in unnecessary exploratory laparotomy. Signs suggestive of intussusception including an abdominal mass may be present in children. GI bleeding occurs in one-third of cases and may be overt, with hematemesis, melena, or bloody stools[6,7]. While bloody diarrhea is common in HSP, it may also occur in eosinophilic gastroenteritis[8], systemic lupus erythematosus, parasitic infection, and drug-induced vasculitis. Distinguishing between these different vasculitic disorders depends on clinical, serological, hematologic, and histologic findings. Arthralgia is usually symmetrical, with the ankles being the most commonly affected joints. Joint involvement is considered as an indication for systemic steroids. Proteinuria and hematuria indicate renal involvement and generally occur within the first 3 mo after the onset of the disease.

The hallmarks of HSP on computed tomography are multiple focal areas of bowel thickening with skip lesions, mesenteric edema, vascular engorgement, and non-specific lymphadenopathy[9]. However, similar thickening may also be seen in eosinophilic gastroenteritis[8], lymphoma, Crohn's disease, and granulomatous disease. It is thus not a specific sign for HSP. Ultrasound may reveal generalized thickening of the intestinal wall, ascites, and sometimes intussusception.

GI involvement in HSP is seen predominantly in the small bowel[10,11] but may also affect the esophagus, stomach, terminal ileum[12,13] and colon[14]. Our patient had diffuse, poorly localized abdominal pain and bloody diarrhea, prompting us to visualize both the upper and lower GI tract. The endoscopic findings in our patient included discrete coin-like petechiae, hemorrhagic erosions, and skip hyperemic and ecchymotic lesions. These were seen in the gastric antrum, cecum, ileocecal valve, and sigmoid colon. It is important to recognize these characteristic endoscopic findings when a previously healthy patient presents with the sudden onset of an acute abdomen. When encountered, they should suggest the possibility of HSP. Although we did not biopsy the lesions in the GI tract, we expected to find histologic abnormalities similar to those found on skin biopsy. However, endoscopic biopsies often miss the submucosal vessels and only reveal nonspecific inflammation.

HSP is primarily a medical disease and requires only supportive treatment once other acute surgical conditions have been excluded. Simple analgesics or non-steroidal anti-inflammatory drugs are used as first-line therapy for relief of arthralgia. Parenteral steroids have been advocated for more severe abdominal or joint pains, or painful angioedema, but they should be used with caution if there is active GI bleeding. All patients with HSP should have their urine analyzed on several occasions during the initial stages of the disease. Proteinuria and hematuria indicate possible renal involvement which, if it progresses to renal insufficiency, has a poor long-term outcome[15,16]. Our patient's urinalysis was normal, and his renal function has been remained normal over two years of follow up.

In conclusion, the majority of patients with HSP recover fully. The prognosis is best in the absence of renal involvement. The diagnosis of HSP may be difficult, especially when abdominal symptoms precede the characteristic palpable

purpura. Typical endoscopic findings may alert gastroenterologists to consider this disease early and thus avoid unnecessary laparotomy.

REFERENCES

1 **Uchiyama K,** Yoshida N, Mizobuchi M, Higashihara H, Naito Y, Yoshikawa T. Mucosal IgA deposition [correction of depositon] in Henoch-Schonlein purpura with duodenal ulcer. *J Gastroenterol Hepatol* 2002; **17**: 728-729

2 **Mills JA,** Michel BA, Bloch DA, Calabrese LH, Hunder GG, Arend WP, Edworthy SM, Fauci AS, Leavitt RY, Lie JT. The American College of Rheumatology 1990 criteria for the classification of Henoch-Schonlein purpura. *Arthritis Rheum* 1990; **33**: 1114-1121

3 **Gimenez-Esparza Vich JA**, Arguelles BF, Martin IH, Gutierrez Fernandez MJ, Porras Vivas JJ. Recurrence of Henoch-Schonlein purpura in association with colitis. *J Clin Gastroenterol* 2002; **34**: 492-493

4 **Borras-Blasco J**, Enriquez R, Amoros F, Cabezuelo JB, Navarro-Ruiz A, Perez M, Fernandez J. Henoch-Schonlein purpura associated with clarithromycin. Case report and review of literature. *Int J Clin Pharmacol Ther* 2003; **41**: 213-216

5 **Lanzkowsky S,** Lanzkowsky L, Lanzkowsky P. Henoch-Schoenlein purpura. *Pediatr Rev* 1992; **13**: 130-137

6 **Nathan K,** Gunasekaran TS, Berman JH. Recurrent gastrointestinal Henoch-Schonlein purpura. *J Clin Gastroenterol* 1999; **29**: 86-89

7 **Lippl F,** Huber W, Werner M, Nekarda H, Berger H, Weigert N. Life-threatening gastrointestinal bleeding due to a jejunal lesion of Henoch-Schonlein purpura. *Endoscopy* 2001; **33**: 811-813

8 **Chen MJ,** Chu CH, Lin SC, Shih SC, Wang TE. Eosinophilic gastroenteritis: clinical experience with 15 patients. *World J Gastroenterol* 2003; **9**: 2813-2816

9 **Jeong YK,** Ha HK, Yoon CH, Gong G, Kim PN, Lee MG, Min YI, Auh YH. Gastrointestinal involvement in Henoch Schonlein syndrome: CT findings. *AJR Am J Roentgenol* 1997; **168**: 965-968

10 **Esaki M,** Matsumoto T, Nakamura S, Kawasaki M, Iwai K, Hirakawa K, Tarumi K, Yao T, Iida M. GI involvement in Henoch-Schonlein purpura. *Gastrointest Endosc* 2002; **56**: 920-923

11 **Pore G.** GI lesions in Henoch-Schonlein purpura. *Gastrointest Endosc* 2002; **55**: 283-286

12 **Ortego-Centeno N,** Callejas-Rubio JL, Lopez-Manas JG, Troncoso-Garcia E, de la Higuera Torres-Puchol J, Ileitis terminalis in a patient with Henoch-Schonlein purpura. *Dig Dis Sci* 1999; **44**: 1590-1593

13 **Kim HS,** Lee DK, Baik SK, Kwon SO. Ileal vasculitis in Henoch-Schonlein purpura. *Gastrointest Endosc* 2001; **54**: 493-494

14 **Nakasone H,** Hokama A, Fukuchi J, Makishi T, Yamashiro T, Sakugawa H, Kinjo F, Saito A. Colonoscopic findings in an adult patient with Henoch-Schonlein purpura. *Gastrointest Endosc* 2000; **52**: 392

15 **Pillebout E,** Thervet E, Hill G, Alberti C, Vanhille P, Nochy D. Henoch-Schonlein Purpura in adults: outcome and prognostic factors. *J Am Soc Nephrol* 2002; **13**: 1271-1278

16 **Garcia-Porrua C,** Gonzalez-Louzao C, Llorca J, Gonzalez-Gay MA. Predictive factors for renal sequelae in adults with Henoch-Schonlein purpura. *J Rheumatol* 2001; **28**: 1019-1024

Science Editor Guo SY **Language Editor** Elsevier HK

PO Box 2345, Beijing 100023, China
www.wjgnet.com
wjg@wjgnet.com

ELSEVIER

World J Gastroenterol 2005;11(15):2357-2359
World Journal of Gastroenterology ISSN 1007-9327

• *CASE REPORT* •

Pulmonary embolization as primary manifestation of hepatocellular carcinoma with intracardiac penetration: A case report

Elod Papp, Zsuzsanna Keszthelyi, Nagy Karoly Kalmar, Lajos Papp, Csaba Weninger, Tamas Tornoczky, Endre Kalman, Kalman Toth, Tamas Habon

Elod Papp, Zsuzsanna Keszthelyi, 1st Department of Medicine, University of Pecs Medical School, H-7624, Pécs, Ifjusag u. 13. Hungary
Nagy Karoly Kalmar, Department of Surgery, University of Pecs Medical School
Lajos Papp, Heart Institute, University of Pecs Medical School, H-7624, Pécs, Ifjusag u. 13. Hungary
Csaba Weninger, Department of Radiology, University of Pecs Medical School, H-7624, Pécs, Ifjusag u. 13. Hungary
Tamas Tornoczky, Endre Kalman, Department of Pathology, University of Pecs Medical School, H-7624, Pécs, Ifjusag u. 13. Hungary
Kalman Toth, Tamas Habon, 1st Department of Medicine, University of Pecs Medical School, Pecs, Hungary
Correspondence to: Dr. Elod Papp, 1st Department of Medicine, University of Pecs Medical School, H-7624, Pécs, Ifjusag u. 13. Hungary. elod.papp@aok.pte.hu
Telephone: +36-72-536-000 Fax: +36-72-536-148
Received: 2004-09-06 Accepted: 2004-10-08

Abstract

Intracardiac manifestation of hepatocellular carcinoma (HCC) is a rare condition and an uncommon finding even at autopsy. Pulmonary tumor embolism as a presenting feature of HCC has been published only twice previously. In our case report, a 63-year-old man presented with high fever and six episodes of recurrent pneumonias during the last half year. Echocardiography was performed, a solid mass was found in the right atrium. Transesophageal echocardiography proved a tumor mass in the inferior vena cava (IVC) extending into the right atrium, abdominal ultrasound revealed tumor mass in the IVC and a solid tumor in the liver. Combined liver and heart surgery was attempted in order to remove the tumor mass from both the liver and the right atrium. Acute cor pulmonale occurred during tumor removal from the right atrium and the patient expired. In addition to local factors the possibility of embolization should arise in the background of recurrent pneumonia. Occult carcinoma must be included in possible causes of recurrent pulmonary embolism. Searching for primary malignancy should include HCC as frequent cause of hypercoagulability. In case of HCC, echocardiography is suggested because of the possibility of expansion in IVC or right atrium and tumor-embolization.

Key words: Hepatocellular carcinoma; Intracardiac penetration; Pulmonary embolization

Papp E, Keszthelyi Z, Kalmar NK, Papp L, Weninger C, Tornoczky T, Kalman E, Toth K, Habon T. Pulmonary embolization as primary manifestation of hepatocellular carcinoma with intracardiac penetration: A case report. *World J Gastroenterol* 2005; 11(15): 2357-2359
http://www.wjgnet.com/1007-9327/11/2357.asp

INTRODUCTION

Intracardiac manifestation of hepatocellular carcinoma (HCC) is a rare condition, uncommon finding even at autopsy. Pulmonary tumor embolism as a presenting feature of HCC has been published only twice previously[1,2]. In our case recurrent pneumonias and dyspnea were the only symptoms distantly related to HCC.

CASE REPORT

A 63-year-old man presented with high fever, six episodes of recurrent pneumonias during the last half year. His medical history showed pulmonary tuberculosis (30 years ago) and hypertension. There was no hepatitis or any other liver dysfunction in his case history. Only the enlarged liver was a pathologic finding at physical examination.

Two-dimensional transthoracic echocardiography was performed searching for possible infective endocarditis in the background of recurrent fevers. A solid mass was found in the right atrium causing severe inflow obstruction. Transesophageal echocardiography proved a tumor mass in the inferior vena cava (IVC) extending into the right atrium (Figure 1).

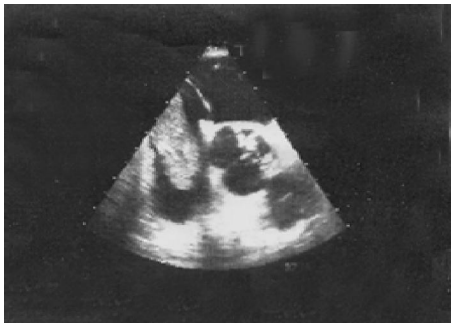

Figure 1 Tumor mass extending into the right atrium (transesophageal echocardiography).

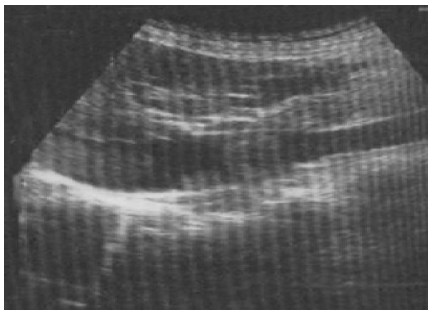

Figure 2 Tumor mass in the inferior vena cava (abdominal ultrasound).

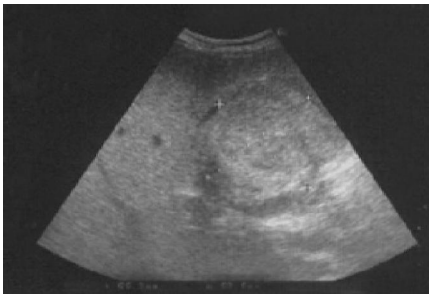

Figure 3 Solid tumor in the fourth segment of the right lobe of the liver (abdominal ultrasound).

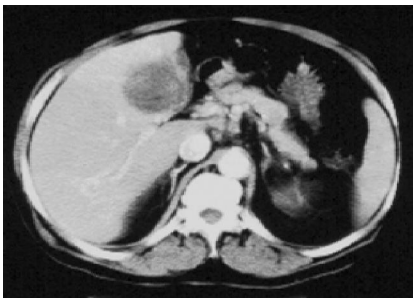

Figure 4 Solid tumor in the fourth segment of the right lobe of the liver (abdominal computerized tomography).

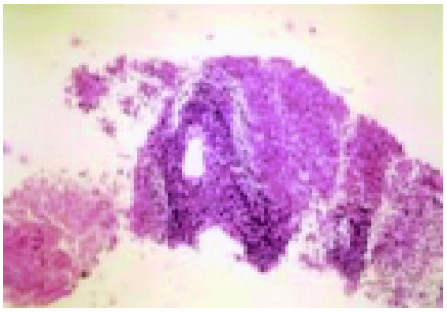

Figure 5 Small round cell HCC (hematoxylin–eosin staining ×10).

Elevated red blood cell sedimentation rate, normal hematocrit, normal transaminase levels and extremely high alfa-fetoprotein (AFP) level (18 184 ng/mL, normal range: <8 ng/mL) were seen in the blood chemistry. No laboratory signs of liver disease were present. Serological examinations disclosed hepatitis B or C viral infection.

Abdominal ultrasound revealed tumor mass in IVC and a solid tumor in the fourth segment of the right lobe of the liver (Figures 2 and 3). Abdominal computerized tomography (CT) scan proved this finding (Figure 4). Fine needle biopsy was performed, which showed small round cell HCC (Figure 5). Combined liver and heart surgery was attempted in order to remove the tumor mass from both the liver and the right atrium. Off pump heart surgery was chosen to avoid an adverse immunocompromised state known to be related to extracorporeal bypass. Acute cor pulmonale occurred during tumor removal from the right atrium and the patient expired. Autopsy revealed fresh pulmonary infarction in the left lung with thrombi in the left main pulmonary artery supplying the infarcted part. Massive embolus was seen in the central part of the right pulmonary artery as a cause of acute cor pulmonale. A tumor mass with a diameter of -7 cm was detected in the right lobe of the liver with no signs of cirrhosis. Histologic examinations proved tumor cells in the thrombus from the IVC (Figure 6), both small round cells and conventional HCC cells in the liver tumor mass with AFP and CD99 positivity (Figure 7).

DISCUSSION

Cancer patients are prone to develop both thrombotic and tumor pulmonary embolism. Although metastatic spread of malignancies to lungs is common, pulmonary tumor embolism is an unusual phenomenon. It remains undetected often and many cases are not recognized until postmortem examination[3].

This case is the third reported one of tumor emboli as

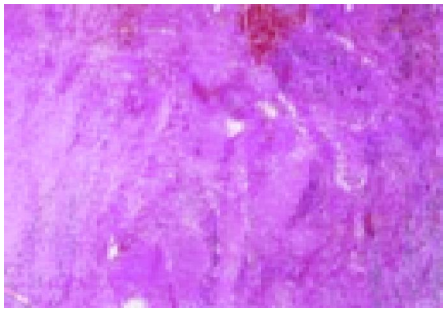

Figure 6 Tumor cells in the thrombus from the inferior vena cava (hematoxylin–eosin staining, ×5).

Figure 7 Both small round cells and conventional HCC cells in the liver tumor mass with AFP and CD99 positivity (hematoxylin–eosin, ×5).

first sign of HCC and the only reported case in which neither the signs of pulmonary embolism nor any of the typical manifestations of HCC but only recurrent pneumonia were present. Autopsy proved tumor emboli in the background of pneumonia.

HCC is one of the most common cancers worldwide but it has a low prevalence in the Western world. More than 70% of patients with HCC have cirrhosis, and more than 80% have elevated alkaline phosphatase or aspartate-aminotransferase serum levels. Epidemiological studies have established that hepatitis B and C viral infections are the main etiologic factors. Patients typically present with abdominal pain and weight loss. None of these were present in the case reported.

Although invasion of the IVC and the right atrium by HCC occurs in less than 2% of the patients with HCC[4], only few cases were reported[4-6]. Pulmonary manifestations vary, the "cannonball" pattern being the most common one[7-9]. Hypercoagulability in malignancy is well known and liver cancer is strongly associated with venous thromboembolism[10]. It is surprising that only two cases with pulmonary embolism have previously been reported.

Intraatrial manifestation of the HCC is a life-threatening condition. The major causes of death are either sudden pulmonary embolism of the thrombus or acute obstruction of the tricuspid valve or both. Resection can provide relatively good long-term survival in this particular clinical situation but not more than 2 years[11]. The surgical approach to IVC and intraatrial masses is difficult. These patients usually die within a short period because of pulmonary embolism, heart failure or cancer progression. The only treatment option is hepatic resection with removal of the tumor thrombus. Most commonly, deep hypothermia and circulatory arrest have been used[12,13]. Georgen *et al*[14], reported a successful removal of HCC from the right atrium without extracorporeal bypass. Optimal decision making in rare cases like this is a complicated task based on intuition rather than scanty information provided by evidence-based medi-cine.

In summary, in addition to local factors the possibility of embolization should arise in the background of recurrent pneumonia. Occult carcinoma must be included in possible causes of recurrent pulmonary embolism. Searching for primary malignancy should include HCC as the frequent cause of hypercoagulability. Regarding the literature review referring to HCC cases, echocardiography is suggested because of the possibility of expansion in IVC or right atrium and tumor-embolization[15]. This case is reported because it describes a rapid clinical progression where the recurrent pneumonia was the first manifestation of a previously undiagnosed neoplastic disease.

REFERENCES

1 **Wilson K,** Guardino J, Shapira O. Pulmonary tumor embolism as a presenting feature of cavoatrial hepatocellular carcinoma. *Chest* 2001; **119**: 657-658
2 **Winterbauer RH,** Elfenbein IB, Ball WC. Incidence and clinical significance of tumor embolization to the lungs. *Am J Med* 1968; **45**: 271-290
3 **Goldhaber SZ,** Dricker E, Buring JE, Eberlein K, Godleski JJ, Mayer RJ, Hennekens CH. Clinical suspicion of autopsy-proven thrombotic and tumor pulmonary embolism in cancer patients. *Am Heart J* 1987; **114**: 1432-1435
4 **Kanematsu M,** Imaeda T, Minowa H, Yamawaki Y, Mochizuki R, Goto H, Seki M, Doi H, Okumura S. Hepatocellular carcinoma with tumor thrombus in the inferior vena cava and right atrium. *Abdom Imaging* 1994; **19**: 313-316
5 **Kojiro M,** Nakahara H, Sugihara S, Murakami T, Nakashima T, Kawasaki H. Hepatocellular carcinoma with intra-atrial tumor growth. A clinicopathologic study of 18 autopsy cases. *Arch Pathol Lab Med* 1984; **108**: 989-992
6 **Atkins KA.** Metastatic hepatocellular carcinoma to the heart. *Diagn Cytopathol* 2000; **23**: 406-408
7 **DeVita VT,** Trujillo NP, Blackman AH, Ticktin HE. Pulmonary manifestations of primary hepatic carcinoma. *Am J Med Sci* 1965; **250**: 428-436
8 **Gasztonyi B,** Par A, Battyany I, Hegedus G, Molnar FT, Horvath L, Mozsik G. Multimodality treatment resulting in long-term survival in hepatocellular carcinoma. *J Physiol Paris* 2001; **95**: 413-416
9 **Gasztonyi B,** Par A, Molnar FT, Cseke L, Horvath OP, Battyany I, Hegedus G, Horvath L, Mozsik Gy. A case report of patient with recurrent hepatocellular carcinoma (HCC): Succesful multimodality treatment. *Eur J Int Med* 1998; 9: 127-129
10 **Sorensen HT,** Mellemkjaer L, Steffensen FH, Olsen JH, Nielsen GL. The risk of a diagnosis of cancer after primary deep venous thrombosis or pulmonary embolism. *N Engl J Med* 1998; **338**: 1169-1173
11 **Fujisaki M,** Kurihara E, Kikuchi K, Nishikawa K, Uematsu Y. Hepatocellular carcinoma with tumor thrombus extending into the right atrium: report of a successful resection with the use of cardiopulmonary bypass. *Surgery* 1991; **109**: 214-219
12 **Donatelli F,** Pocar M, Triggiani M, Moneta A, Lazzarini I, D'Ancona G, Pelenghi S, Grossi A. Surgery of cavo-atrial renal carcinoma employing circulatory arrest: immediate and mid-term results. *Cardiovasc Surg* 1998; **6**: 166-170
13 **Chu MW,** Aboguddah A, Kraus PA, Dewar LR. Urgent heart surgery for an atrial mass: metastatic hepatocellular carcinoma. *Ann Thorac Surg* 2001; **72**: 931-933
14 **Georgen M,** Regimbeau JM, Kianmanesh R, Marty J, Farges O, Belghiti J. Removal of hepatocellular carcinoma extending in the right atrium without extracorporal bypass. *J Am Coll Surg* 2002; **195**: 892-894
15 **Yoshitomi Y,** Kojima S, Sugi T, Matsumoto Y, Yano M, Ozeki Y, Kuramochi M. Echocardiography of a right atrial mass in hepatocellular carcinoma. *Heart Vessels* 1998; **13**: 45-48

Science Editor Guo SY **Language Editor** Elsevier HK

PO Box 2345, Beijing 100023, China
www.wjgnet.com
wjg@wjgnet.com

ELSEVIER

World J Gastroenterol 2005;11(15):2360-2363
World Journal of Gastroenterology ISSN 1007-9327

• *CASE REPORT* •

Multifocal intraportal invasion of breast carcinoma diagnosed by laparoscopy-assisted liver biopsy

Tomoki Nakajima, Satoru Sekoguchi, Taichirou Nishikawa, Hidetaka Takashima, Tadashi Watanabe, Masahito Minami, Yoshito Itoh, Naruhiko Mizuta, Hiroo Nakajima, Takeshi Mazaki, Akio Yanagisawa, Takeshi Okanoue

Tomoki Nakajima, Satoru Sekoguchi, Taichirou Nishikawa, Hidetaka Takashima, Tadashi Watanabe, Masahito Minami, Yoshito Itoh, Takeshi Okanoue, Molecular Gastroenterology and Hepatology, Kyoto Prefectural University of Medicine Graduate School of Medical Science, Kyoto, Japan
Naruhiko Mizuta, Hiroo Nakajima, Endocrine Surgery, Kyoto Prefectural University of Medicine Graduate School of Medical Science, Kyoto, Japan
Takeshi Mazaki, Akio Yanagisawa, Surgical Pathology, Kyoto Prefectural University of Medicine Graduate School of Medical Science, Kyoto, Japan
Correspondence to: Tomoki Nakajima, MD, Molecular Gastroenterology and Hepatology, Kyoto Prefectural University of Medicine Graduate School of Medical Science, Kawaramachi-Hirokoji, Kamigyo-ku, Kyoto 602-8566, Japan. tomnaka@silver.ocn.ne.jp
Telephone: +81-75-251-5519 Fax: +81-75-251-0710
Received: 2004-07-17 Accepted: 2004-09-04

Abstract

Hepar lobatum carcinomatosum (HLC) is defined as an acquired hepatic deformity consisting of an irregularly lobulated hepatic contour caused by intravascular infiltration of metastatic carcinoma. To date, only nine cases of HLC have been reported in the literature. We report a case of a 68-year-old woman showing hepatic metastasis of breast carcinoma in radiologically unidentified form. Initially, she received left partial mastectomy for breast cancer but solid hepatic metastases were identified in S_2 and S_6, 9 mo after surgery. Then, they responded to chemotherapy and radiologically disappeared. After radiological disappearance of the liver tumors, the patient's blood chemistry showed abnormal liver function. A CT scan demonstrated heterogeneous enhancement effect in the liver in the late phase, suggesting uneven hepatic blood supply. Hepatic deformity was not obvious. Laparoscopy revealed a slightly deformed liver surface with multiple indentations and shallow linear depressions. Furthermore, a wide scar was observed on the surface of S_2 possibly at the site where the metastatic tumor existed before chemotherapy. Liver biopsy from the wide scar lesion showed intraportal tumor thrombi with desmoplastic change. Because of its similarity to the histology of the original breast cancer, we concluded that the hepatic functional abnormalities and slightly deformed liver surface were derived from the circulatory disturbance caused by microscopic tumor thrombi. Besides, since the wide scar was located at the site of the pre-existing tumor, it is probable that chemotherapy was an important cause of fibrous scarring as a result of tumor regression. These morphologic findings are compatible with those of HLC. Laparoscopy-assisted liver biopsy was useful to make definite diagnosis, even though the hepatic deformity was radiologically undetectable.

Key words: Metastatic breast cancer; Hepar lobatum carcinomatosum; Laparoscopy

Nakajima T, Sekoguchi S, Nishikawa T, Takashima H, Watanabe T, Minami M, Itoh Y, Mizuta N, Nakajima H, Mazaki T, Yanagisawa A, Okanoue T. Multifocal intraportal invasion of breast carcinoma diagnosed by laparoscopy-assisted liver biopsy. *World J Gastroenterol* 2005; 11(15): 2360-2363
http://www.wjgnet.com/1007-9327/11/2360.asp

INTRODUCTION

Liver metastasis of breast cancer usually presents cancer nodules scattered in the liver and the radiological diagnosis is not difficult. However, rarely, it does not form space-occupying lesions and manifests itself as multifocal occlusion of intrahepatic branches of the portal and/or hepatic veins by tumor thrombi. Such circulatory disturbances can result in deformity of the liver, mimicking cirrhosis[1-4]. In these cases, since radiological findings are uneven hepatic circulation and hepatic deformity, the diagnosis is difficult and sometimes misleading[5-8]. We report a case of hepatic metastasis of breast carcinoma, which diffusely spread in the liver without radiologically detectable lesions or obvious hepatic deformity. It was successfully diagnosed by laparoscopy-assisted liver biopsy. We have discussed its pathogenesis based on the previous reports.

CASE REPORT

A 68-year-old woman was admitted to our hospital complaining of general malaise. She had received left partial mastectomy on August 2, 2002. The tumor was in stage I and was histologically invasive ductal carcinoma of scirrhous type. An enhanced computed tomography (CT) scan on April 2, 2003 revealed a metastatic lesion in liver S_2 (Figure 1A), and an enhanced magnetic resonance image with Ferridex on May 19, 2003 showed metastatic lesions in S_2 and S_6 (Figures 1B and C). From April to December 2003, combination chemotherapy was administered every month, using 900 mg of cyclophosphamide and 110 mg of epirubicin for the first 4 mo and then reducing cyclophosphamide to 500 mg and epirubicin to 60 mg. In February 2004, the

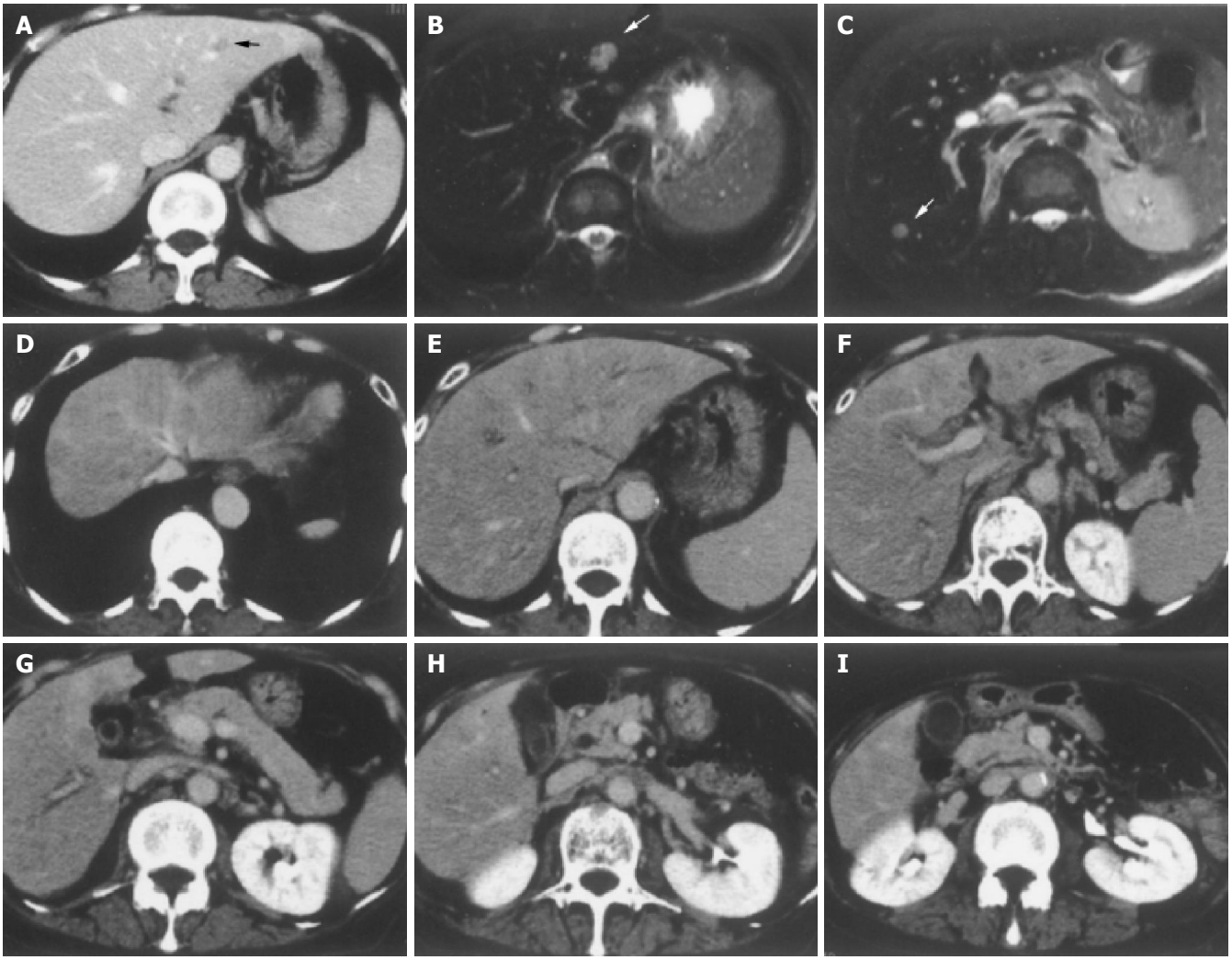

Figure 1 **A:** Enhanced CT scan on April 2, 2003. A metastatic lesion in liver S_2 (arrowhead). **B** and **C**: Enhanced magnetic resonance image with Ferridex on May 19, 2003. Metastatic lesions in S_2 (**B**, arrowhead) and S_6 (**C**, arrowhead). **D-I**: Dynamic study by CT scan on admission. Uneven enhancement effect of the liver in late phase.

patient was admitted to our hospital, complaining of general fatigue and appetite loss and showing abnormal liver function test results. After admission, she also manifested drowsiness, disorientation and insomnia. The patient was 154 cm in height and weighed 54 kg. Visible mucosa showed slight jaundice and no anemia. There was no sign of palmar erythema or vascular spider. Superficial lymph nodes were not palpable. There were two sites of skin eruption at the left anterior chest, which had already been diagnosed as skin metastasis by biopsy. There was leg edema but no hepatosplenomegaly. The blood test showed abnormalities in liver function, coagulation disturbance, and thrombocytopenia. Specifically, the results were as follows: platelet count, $9.3\times10^4/\mu L$; prothrombin time, 82%; fibrin degradation product, 15.4 μg/mL; C-reactive protein, 5.7 mg/dL; lactate dehydrogenase, 810 IU/L; aspartate aminotransferase, 219 IU/L; alanine aminotransferase, 240 IU/L; alkaline phosphatase, 1 826 IU/L; γ-glutamyltranspeptidase, 960 IU/L; total bilirubin 4.97 mg/dL; ammonia, 252 μg/dL; total protein, 5.6 g/dL; albumin, 3.1 g/dL. Dynamic study with CT scan demonstrated uneven enhancement effect in the liver in late phase, suggesting uneven hepatic blood supply. At this time, the metastatic tumors had become undetectable (Figures 1D-I) and hepatic deformity was not obvious. To clarify the exact cause of liver function abnormalities, laparoscopy was performed. It showed an irregular and deformed liver surface with multiple indentations and shallow linear depressions (Figures 2A-D). A wide scar was observed on the surface of S_2 possibly at the site where the metastatic tumor existed before chemotherapy (Figure 2E, arrowheads). Laparoscopic liver biopsy from a wide scar lesion showed residual cancer cells scattered in a wide fibrous band in one area (Figure 3A). In another area intraportal tumor thrombi were clearly demonstrated by CD31 immun-ohistochemical staining (Figures 3B and C). Cancer cells showed desmoplastic change around them (Figure 3D), which extended toward the sinusoids (Figure 3E). Because of its similarity to the histology of original breast cancer (Figure 3F), we concluded that the hepatic functional abnormalities were due to the uneven blood supply caused by intraportal invasion of the breast cancer. Drowsiness, disorientation and insomnia, along with high level of serum ammonia, were suggestive of hepatic encephalopathy. Lactulose and branched-chain amino acid supplement were given but failed to improve the symptoms, and serum ammonia level stayed

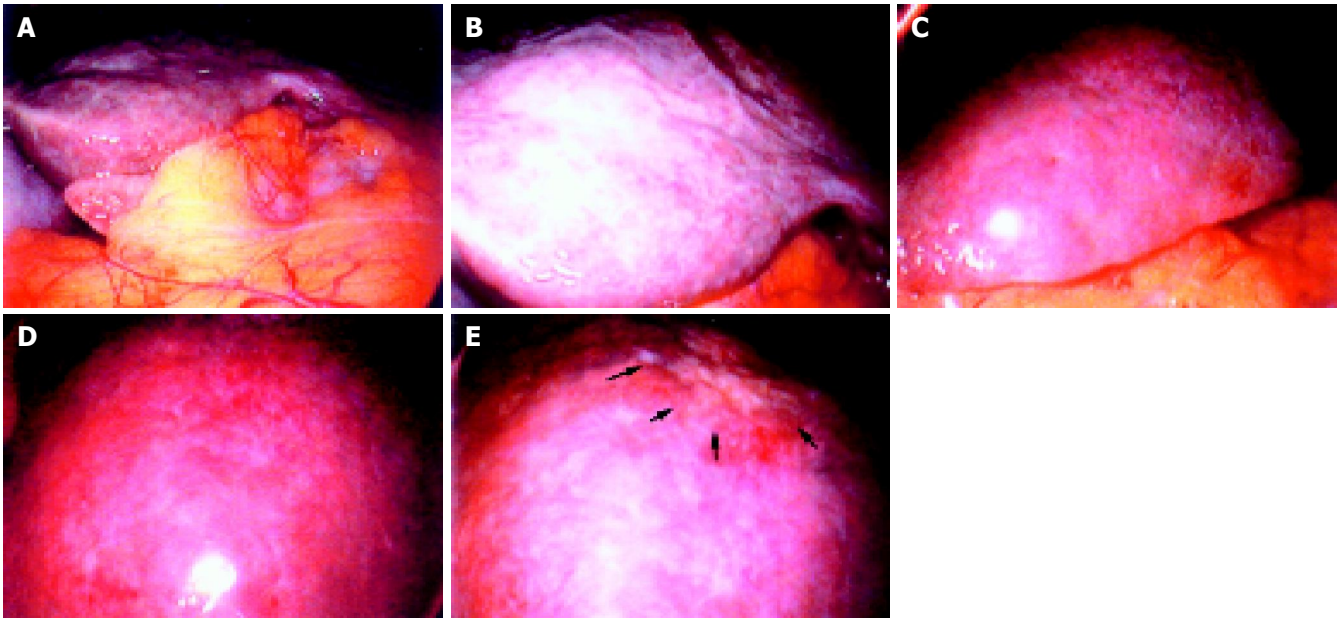

Figure 2 Irregular and deformed liver surface with multiple indentations and shallow linear depressions (**A** and **B**: right lobe, **C** and **D**: left lobe). A wide scar on the surface of S_2 at the site where metastatic tumor existed before chemotherapy (**E**, arrowheads).

over 200 μg/dL. The patient presented a rapid downhill course and died of respiratory failure due to lymphangitis carcinomatosa on March 20, 2004.

DISCUSSION

When metastatic breast carcinoma in the liver does not form space-occupying lesions, its radiological diagnosis is difficult. There are some case reports on diffuse infiltration of breast cancer cells found at autopsy, which was not diagnosed even with the most advanced modalities like CT scan, ultrasonography and magnetic resonance imaging[5-8]. In the present case, radiological diagnosis was difficult because dynamic study by CT scan only demonstrated uneven hepatic blood supply, which is also seen in chronic or acute liver injury. Indeed, definitive diagnosis was made only by laparoscopy-assisted liver biopsy.

Carcinomatous involvement of the liver mimicking cirrhosis is a rare complication of metastatic carcinoma, most frequently observed with scirrhous carcinoma of the breast[1-4]. Borja *et al*[1], reported a case of metastatic breast cancer, which presented various clinical manifestations of liver failure grossly characterized by a distorted liver surface caused by multifocal portal obstruction with cancer cells.

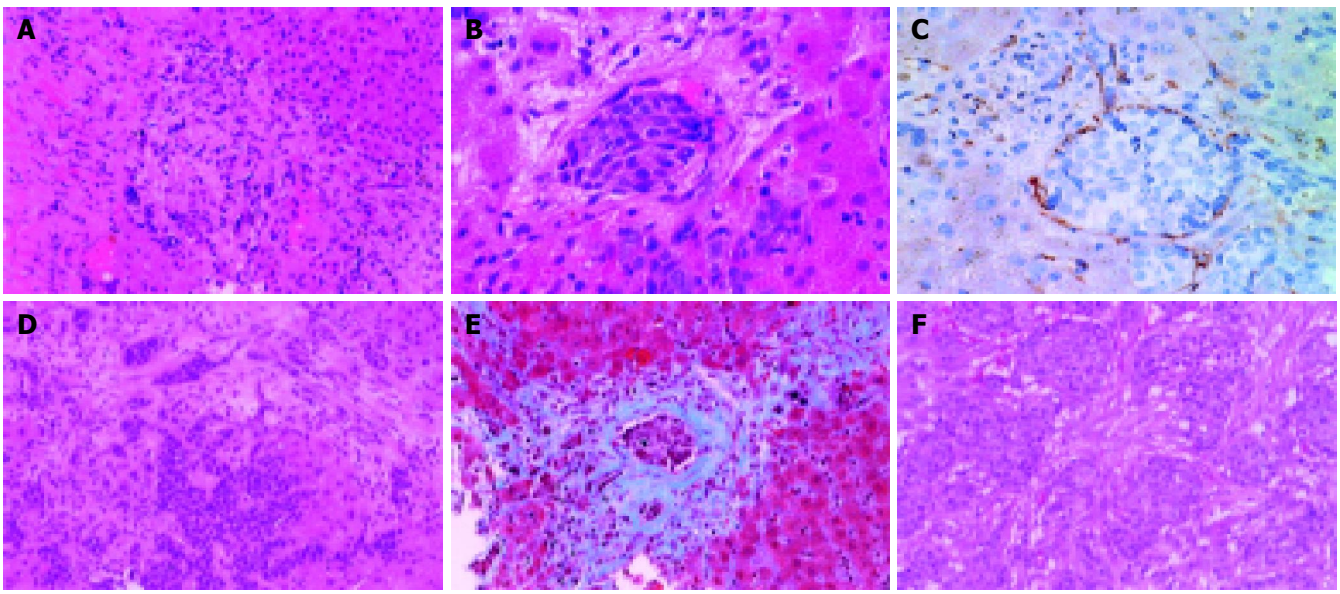

Figure 3 **A**: Laparoscopic liver biopsy from a wide scar lesion showed residual cancer cells scattered in a wide fibrous band in one area (hematoxylin and eosin (HE) stain). **B** and **C**: In another area intraportal tumor thrombi were clearly demonstrated. Endothelial cells were stained brown by CD31 immunohistochemistry (**B**, HE stain, **C**, CD31 immunohistochemical stain). **D** and **E**: Cancer cells showed desmoplastic change around them, which extended toward the sinusoids (**D**, HE stain, **E**, Masson's trichrome stain). **F**: Original breast cancer. Note desmoplastic change around the tumor cells (HE stain).

Busni *et al*[9], first introduced the term hepar lobatum carcinomatosum (HLC), which was defined as an acquired hepatic deformity consisting of an irregularly lobulated hepatic contour caused by intravascular infiltration of metastatic carcinoma. To our knowledge, only nine cases of HLC have been reported in the literature to date[9-13].

In the present case, although radiological examinations revealed neither distorted nor irregularly lobulated liver surface, laparoscopy presented a slightly irregular and deformed liver surface with multiple indentations and shallow linear depressions. A biopsy sample from the wide fibrous scar revealed the intraportal infiltration of cancer cells surrounded by fibrous tissues. As speculated by Gravel *et al*[13], multifocal carcinomatous obstruction of portal veins caused circulatory deficiency leading to multiple scattered and linear depressions on the liver surface, which were interpreted as fibrous scarring. In addition, desmoplastic change caused by carcinoma cells may have also contributed to the formation of fibrous scar tissue. These pathologic conditions are basically the same as those of HLC, and therefore, our case can be categorized as the same entity, though it was not so far advanced in terms of hepatic deformity.

Combination chemotherapy with cyclophosphamide and epirubicin was performed in this case. Various chemotherapeutic agents were given to eight out of the nine previously reported HLC patients, but most of the agents, including cyclophosphamide and doxorubicin (the same group as epirubicin) are not known to induce fibrogenesis by themselves or even synergistically. Hence, some authors[10-14] speculate that fibrosis in HLC is not caused by direct effect of chemotherapeutic agents, but is actually scar contraction after tissue collapse by chemotherapy-induced tumor necrosis or regression. In the present case, this condition occurred after chemotherapy which caused the disappearance of metastatic liver tumors. Furthermore, a wide scar was observed at the site where the metastatic tumor existed before chemotherapy. These findings also support the possibility of chemotherapy as another important but indirect cause of fibrous scarring.

In this case, drowsiness, disorientation and insomnia, and a high level of serum ammonia were suggestive of hepatic encephalopathy. However, lactulose and branched-chain amino acid supplementation were not effective, and serum ammonia level stayed over 200 μg/dL. In addition, leg edema with low serum albumin level mimicked the clinical manifestation of cirrhosis. These clinical symptoms and laboratory data indicate that rapidly progressive and diffuse circulatory disturbance due to carcinomatous obstruction of portal veins can cause some symptoms of hepatic failure[15-18].

REFERENCES

1 **Borja ER,** Hori JM, Pugh RP. Metastatic carcinomatosis of the liver mimicking cirrhosis: case report and review of the literature. *Cancer* 1975; **35**: 445-449
2 **Breitfellner G,** Dirschmid K. Liver cirrhosis due to a breast neoplasm metastasis. So-called metastatic-carcinomatous cirrhosis. *Schweiz Med Wochenschr* 1977; **107**: 241-243
3 **Wallace G,** Conologue TL, Murphy TJ. Metastatic breast carcinoma mimicking macronodular cirrhosis. *Mayo Clin Proc* 2003; **78**: 1431
4 **Mitchell ML,** Filippone MD, Wozniak TF. Metastatic carcinomatous cirrhosis and hepatic hemosiderosis in a patient heterozygous for the H63D genotype. *Arch Pathol Lab Med* 2001; **125**: 1084-1087
5 **Young ST,** Paulson EK, Washington K, Gulliver DJ, Vredenburgh JJ, Baker ME. CT of the liver in patients with metastatic breast carcinoma treated by chemotherapy: findings simulating cirrhosis. *AJR Am J Roentgenol* 1994; **163**: 1385-1388
6 **Nascimento AB,** Mitchell DG, Rubin R, Weaver E. Diffuse desmoplastic breast carcinoma metastases to the liver simulating cirrhosis at MR imaging: report of two cases. *Radiology* 2001; **221**: 117-121
7 **Whitlock JP,** Evans AJ, Jackson L, Chan SY, Robertson JF. Imaging of metastatic breast cancer: distribution and radiological assessment at presentation. *Clin Oncol (R Coll Radiol)* 2001; **13**: 181-186
8 **Burkill GJ,** King LJ, Scurr E, Healy JC. Breast carcinoma metastases to the liver simulating cirrhosis. *Radiology* 2002; **225**: 917; author reply 917-918
9 **Busni NA.** Hepar lobatum carcinomatosum. *Virchows Arch* 1924; **252**: 727-733
10 **Chin NW,** Chapman I, Jimenez FA. Complete chemotherapeutic regression of hepatic metastases with resultant hepar lobatum. *Am J Gastroenterol* 1987; **82**: 149-151
11 **Honma K.** Hepar lobatum carcinomatosum due to metastatic breast carcinoma. *Virchows Arch A Pathol Anat Histopathol* 1987; **410**: 465-469
12 **Uhlmann F,** Martin H, Ringk H, Krocker J. Hepar lobatum carcinomatosum due to chemotherapy of a metastatic breast carcinoma. *Gen Diagn Pathol* 1996; **141**: 279-284
13 **Gravel DH,** Begin LR, Brisson ML, Lamoureux E. Metastatic carcinoma resulting in hepar lobatum. *Am J Clin Pathol* 1996; **105**: 621-627
14 **Shirkhoda A,** Baird S. Morphologic changes of the liver following chemotherapy for metastatic breast carcinoma: CT findings. *Abdom Imaging* 1994; **19**: 39-42
15 **Schneider R,** Cohen A. Fulminant hepatic failure complicating metastatic breast carcinoma. *South Med J* 1984; **77**: 84-86
16 **Martelli O,** Coppola L, De Quarto AL, Palma M, Sarmiento R, Foggi CM. Fulminant hepatic failure caused by diffuse intrasinusoidal metastatic liver disease: a case report. *Tumori* 2000; **86**: 424-427
17 **Agarwal K,** Jones DE, Burt AD, Hudson M, James OF. Metastatic breast carcinoma presenting as acute liver failure and portal hypertension. *Am J Gastroenterol* 2002; **97**: 750-751
18 **Lowenthal A,** Tur-Kaspa R, Brower RG, Almog Y. Acute liver failure complicating ductal breast carcinoma: two cases and literature review. *Scand J Gastroenterol* 2003; **38**: 1095-1096

Science Editor Guo SY **Language Editor** Elsevier HK

PO Box 2345, Beijing 100023, China
www.wjgnet.com
wjg@wjgnet.com

ELSEVIER

World J Gastroenterol 2005;11(15):2364-2366
World Journal of Gastroenterology ISSN 1007-9327

• *CASE REPORT* •

Severe chronic diarrhea and weight loss in cholesteryl ester storage disease: A case report

Uta Drebber, Matthias Andersen, Hans U Kasper, Peter Lohse, Manfred Stolte, Hans P Dienes

Uta Drebber, Hans U Kasper, Hans P Dienes, Institute of Pathology, University of Cologne, Germany
Matthias Andersen, Department of Internal Medicine, St.-Vincenz-Hospital, Datteln, Germany
Peter Lohse, Department of Clinical Chemistry-Grosshadern, University of Munich, Germany
Manfred Stolte, Institute of Pathology, Klinikum Bayreuth, Germany
Correspondence to: Dr. Uta Drebber, Institute of Pathology, University of Cologne, Joseph-Stelzmann-Str. 9, D-59031 Cologne, Germany. u.drebber@uni-koeln.de
Telephone: +49-221-4786370 Fax: +49-221-4786360
Received: 2004-07-08 Accepted: 2004-08-12

Abstract

AIM: An inherited deficiency of human lysosomal acid lipase (LAL) results in the rare conditions of Wolman disease and cholesteryl ester storage disease (CESD). We want to present the rare case of CESD in an adult.

METHODS: We report about an adult female patient with severe chronic diarrhea and weight loss as a consequence of CESD. Clinical examination revealed signs of malabsorption and slightly elevated liver enzymes.

RESULTS: Histopathologic changes in the liver tissue and DNA sequence analysis confirmed the diagnosis of CESD due to homozygosity for the most common CESD mutation, a G934A splice site defect encoded by exon 8 of the lysosomal acid lipase (LIPA) gene.

CONCLUSION: It is the first case in the literature with diarrhea as a putative symptom of CESD in adult patients.

Key words: CESD; Acid esterase; Hydrolase; Liver biopsy; Pathology; Diarrhea

Drebber U, Andersen M, Kasper HU, Lohse P, Stolte M, Dienes HP. Severe chronic diarrhea and weight loss in cholesteryl ester storage disease: A case report. *World J Gastroenterol* 2005; 11(15): 2364-2366
http://www.wjgnet.com/1007-9327/11/2364.asp

INTRODUCTION

Wolman disease and cholesteryl ester storage disease (CESD) are very rare inherited disorders of lipid metabolism. Both are the consequences of autosomal recessive mutations which result in a deficient or severely diminished activity of human lysosomal acid lipase (LAL) acid esterase and cholesteryl ester hydrolase, respectively[1]. The mature 378-amino acid protein with molecular masses of approximately 43-54 ku is encoded by the lysosomal acid lipase (LIPA) gene on chromosome 10q23.2-q23.3 which contains 10 exons dispersed over a 38.8 kb region[2-4].

LAL is essential for the intralysosomal breakdown of cholesteryl esters and triglycerides which are taken up by receptor-mediated endocytosis. An inherited deficiency or low activity results in the intralysosomal storage of the respective lipid substrates. As the enzyme is synthesized by all nucleated cells, lipid-laden cells are found in all organs, particularly in liver, spleen, the adrenal and the hemopoietic system, and in the intestine as well as in the lymph nodes, lungs, testes, and ovaries[5-8].

While Wolman disease has an infaust prognosis and leads to hydrops fetalis and congenital ascites as well as an abnormal neurological development, CESD presents as the milder form due to a residual enzymatic activity of approximately 3% which results in widespread lipid deposition and can induce symptoms at any age[9-13].

CESD is rarely diagnosed. We report about the unusual case of a 41-year-old woman who had been suffering from recurrent diarrhea since early childhood and was referred to the hospital during a severe episode of diarrhea and ensuing weight loss. During the clinical examination, a liver biopsy was taken which led to the tentative diagnosis of CESD. This was confirmed by molecular genetic analysis.

CASE REPORT

A 41-year-old female patient, who had been brought up as a foster-child, was referred to the hospital because of persistent chronic diarrhea which caused deterioration by inducing a weight loss of 10 kg in the last 5 mo (body weight 44 kg, height 168 cm at the time of hospital admission). Clinical examination revealed a reduced level of lipid-soluble vitamins as well as a pathologic lactose tolerance. Abdominal ultrasound showed edema of the small bowel mucosa. Celiac disease was excluded by normal antibody levels against endomysium, tissue-transglutaminase, and gliadin. Other causes of diarrhea-like infection or laxative abuse were excluded as well. The patient had elevated liver enzymes (AST 47 U/L, ALT 57 U/L). There were, however, no signs of a viral hepatitis (HbsAg- and anti-HBc-). Immunoglobulin values were also normal. In order to find a cause for the raised liver enzymes and the diarrhea, biopsies of liver and small intestines were taken.

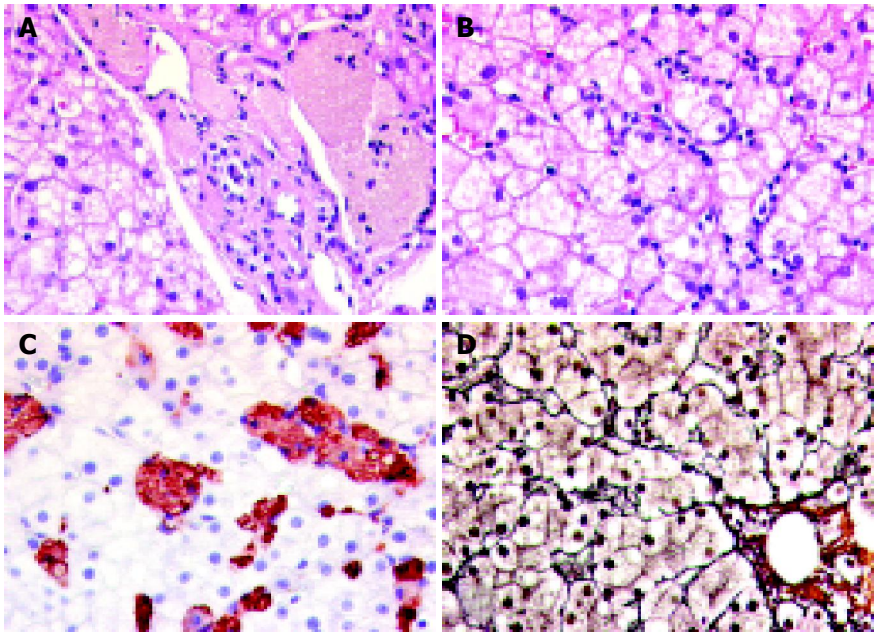

Figure 1 Light microscopic findings in the liver. **A**: A tan-colored foamy material is seen in conspicuous macrophages next to and in a portal tract. HE stain ×400. **B**: Part of an acinus with a prominent intrasinusoidal cellular infiltration and a microvesicular steatosis of hepatocytes. HE stain (×400). **C**: An immunohistochemical staining with CD68 positive macrophages laden with the foamy material. **D**: Reticulin stain (×400). No remarkable fibrosis.

Pathologic findings

Formalin-fixed, paraffin-embedded liver tissue and small bowel biopsies were prepared for histopathologic and immunhistochemical analyses. Ultrastuctural examination was performed on glutaraldehyde-fixed liver tissue under the electron microscope.

Light-microscopy in liver showed an increase of Kupffer cells and macrophages which were found within the sinusoids as well as in the portal tracts. The macrophages were conspicuous with the cytoplasmatic storage of foamy, tan-colored, PAS-positive material. In immunohistochemistry, the described cell population expressed the macrophage-specific marker CD68. The distribution of the CD68-positive population was abundant over the whole acinus without zonal accentuation. Additionally, a discrete parenchymal inflammatory activity with single apoptotic bodies as well as a fine vesicular steatosis in about 40% of the hepatocytes. A discrete pericellular fibrosis was seen in the reticulin stain (Figure 1).

The small bowel biopsies revealed single macrophages with cytoplasmatic storage of PAS-positive foamy, tan-colored material within the apical part of the villi in the lamina submucosa (Figure 2). Ultrastructural examination demonstrated lysosomal lipid storage in the cytoplasm of hepatocytes and macrophages as well as the presence of single cholesteryl ester crystals (Figure 3).

Overall, the histopathologic changes in the liver biopsy were suggestive of CESD. Therefore, a DNA sequence analysis of the proband's LIPA gene was performed. The

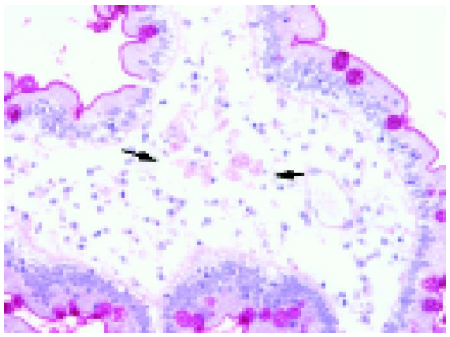

Figure 2 Small bowel biopsy reveals single macrophages with cytoplasmatic storage of PAS-positive foamy, tan-colored material within the apical part of the villi in the lamina submucosa. A PAS stain is demonstrated with PAS-positive macrophages between the arrows (cd) (×400).

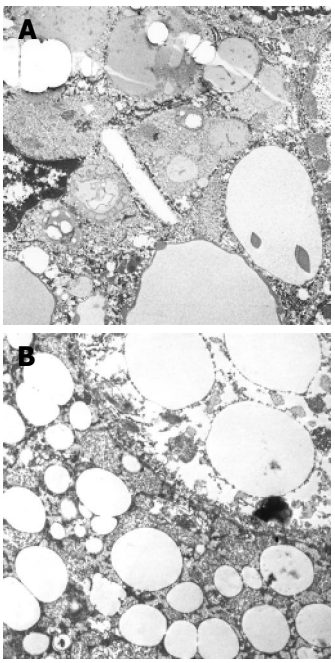

Figure 3 **A**: Electron micrograph of liver tissue demonstrates a single cholesterol crystal in the cytoplasm of a liver cell. **B**: Triglyceride droplets of varied size in the cytoplasm of hepatocytes (×11 000).

patient was found to be a homozygous carrier of the most common CESD mutation, a G934A exchange affecting the last coding base of exon 8, thereby confirming the diagnosis. This genetic defect results in the skipping of exon 8 from the mRNA transcript and in the loss of the internal amino acids 254-277 from the mature enzyme. Despite the presence of the mutation, approximately 3% of normal splicing occurs, which ensures survival of the affected individual[1,3].

DISCUSSION

We present the unusual case of CESD in an adult woman. CESD is a rare condition, which is usually diagnosed during the first or second decade of life due to the accompanying hepatomegaly, often in combination with hypercholesterolemia, but only seldom in later adulthood[7]. Although there is no specific treatment, alleviation can be induced by 3-hydroxy-3-methylglutaryl coenzyme A (HMG CoA) reductase inhibitors such as lovostatin[14-16]. In case of liver cirrhosis, a liver transplantation is indicated[17-19].

The clinical symptoms of our patient, who suffered from severe diarrhea and weight loss, represent a remarkable difference from the typical disease pattern of CESD which normally shows a liver symptomatology with early progression toward cirrhosis[1]. The patient reported about chronic diarrhea with the onset during early childhood, so that CESD seems to play a causal role. Accordingly, laboratory findings showed a reduced level of lipid-soluble vitamins as a sign of chronic malabsorption. The liver symptomatology, in contrast, was discrete. A liver biopsy was taken because of slightly elevated liver enzymes of unknown etiology. Histopathologic changes in the liver were characteristic for CESD, however, a substantial fibrosis had not developed which is reflected by the laboratory findings. This is especially remarkable, because of the long time-period of disease symptoms, and in comparison with other reported cases, where severe fibrosis has been reported to be present as early as childhood[20].

DNA sequence analysis revealed homozygosity for a G934A mutation in exon 8 of the LIPA gene. This nucleotide substitution results in exon skipping and the subsequent loss of 24 amino acids from the mature enzyme. It is the most frequent genetic defect seen in CESD so that the mutation does not explain the unusual clinical presentation[3].

In conclusion, CESD is a very rare metabolic error and presents with an impressing variety of clinical symptoms which make it difficult to establish the correct diagnosis. The patient reported here is the first case in the literature with CESD and chronic diarrhea as the putative symptom of CESD. We therefore conclude that CESD should be taken into account in the differential diagnosis of chronic diarrhea when other causes for diarrhea have been excluded.

REFERENCES

1 **Anderson RA,** Bryson GM, Parks JS. Lysosomal acid lipase mutations that determine phenotype in Wolman and cholesterol ester storage disease. *Mol Genet Metab* 1999; **68**: 333-345

2 **D'Agostino D,** Bay L, Gallo G, Chamoles N. Cholesterol ester storage disease: clinical, biochemical, and pathological studies of four new cases. *J Pediatr Gastroenterol Nutr* 1988; **7**: 446-450

3 **Aslanidis C,** Ries S, Fehringer P, Buchler C, Klima H, Schmitz G. Genetic and biochemical evidence that CESD and Wolman disease are distinguished by residual lysosomal acid lipase activity. *Genomics* 1996; **33**: 85-93

4 **Lohse P,** Maas S, Sewell AC, van Diggelen OP D. Molecular defects underlying Wolman disease appear to be more heterogeneous than those resulting in cholesteryl ester storage disease. *J Lipid Res* 1999; **40**: 221-228

5 **Edelstein RA,** Filling-Katz MR, Pentchev P, Gal A, Chandra R, Shawker T, Guzzetta P, Comly M, Kaneski C, Brady RO. Cholesteryl ester storage disease: a patient with massive splenomegaly and splenic abscess. *Am J Gastroenterol* 1988; 83: 687-692

6 **Elleder M,** Chlumska A, Hyanek J, Poupetova H, Ledvinova J, Maas S, Lohse P. Subclinical course of cholesteryl ester storage disease in an adult with hypercholesterolemia, accelerated atherosclerosis, and liver cancer. *J Hepatol* 2000; 32: 528-534

7 **Elleder M,** Chlumska A, Ledvinova J, Poupetova H. Testis - a novel storage site in human cholesteryl ester storage disease. Autopsy report of an adult case with a long-standing subclinical course complicated by accelerated atherosclerosis and liver carcinoma. *Virchows Arch* 2000; **436**: 82-87

8 **Hanak J,** Elleder M. Cholesterol ester storage disease (CESD). *Cesk Pediatr* 1984; **39**: 721-725

9 **Klima H,** Ullrich K, Aslanidis C, Fehringer P, Lackner KJ, Schmitz G. A splice junction mutation causes deletion of a 72-base exon from the mRNA for lysosomal acid lipase in a patient with cholesteryl ester storage disease. *J Clin Invest* 1993; **92**: 2713-2718

10 **Muntoni S,** Wiebusch H, Funke H, Ros E, Seedorf U, Assmann G. Homozygosity for a splice junction mutation in exon 8 of the gene encoding lysosomal acid lipase in a Spanish kindred with cholesterol ester storage disease (CESD). *Hum Genet* 1995; **95**: 491-494

11 **Aslanidis C,** Klima H, Lackner KJ, Schmitz G. Genomic organization of the human lysosomal acid lipase gene (LIPA). *Genomics* 1994; **20**: 329-331

12 **Pagani F,** Pariyarath R, Garcia R, Stuani C, Burlina AB, Ruotolo G, Rabusin M, Baralle FE. New lysosomal acid lipase gene mutants explain the phenotype of Wolman disease and cholesteryl ester storage disease. *J Lipid Res* 1998; **39**: 1382-1388

13 **Lohse P,** Maas S, Lohse P, Elleder M, Kirk JM, Besley GT, Seidel D. Compound heterozygosity for a Wolman mutation is frequent among patients with cholesteryl ester storage disease. *J Lipid Res* 2000; **41**: 23-31

14 **Levy R,** Ostlund RE, Schonfeld G, Wong P, Semenkovich CF. Cholesteryl ester storage disease: complex molecular effects of chronic lovastatin therapy. *J Lipid Res* 1992; **33**: 1005-1015

15 **Gasche C,** Aslanidis C, Kain R, Exner M, Helbich T, Dejaco C, Schmitz G, Ferenci P. A novel variant of lysosomal acid lipase in cholesteryl ester storage disease associated with mild phenotype and improvement on lovastatin. *J Hepatol* 1997; **27**: 744-750

16 **Rassoul F,** Richter V, Lohse P, Naumann A, Purschwitz K, Keller E. Long-term administration of the HMG-CoA reductase inhibitor lovastatin in two patients with cholesteryl ester storage disease. *Int J Clin Pharmacol Ther* 2001; **39**: 199-204

17 **Leone L,** Ippoliti PF, Antonicelli R, Balli F, Gridelli B. Treatment and liver transplantation for cholesterol ester storage disease. *J Pediatr* 1995; **127**: 509-510

18 **Ferry GD,** Whisennand HH, Finegold MJ, Alpert E, Glombicki A. Liver transplantation for cholesteryl ester storage disease. *J Pediatr Gastroenterol Nutr* 1991; **12**: 376-378

19 **Kale AS,** Ferry GD, Hawkins EP. End-stage renal disease in a patient with cholesteryl ester storage disease following successful liver transplantation and cyclosporine immunosuppression. *J Pediatr Gastroenterol Nutr* 1995; **20**: 95-97

20 **Akcoren Z,** Gogus S, Kocak N, Gurakan F, Ozen H, Yuce A. Cholesteryl ester storage disease: case report during childhood. *Pediatr Dev Pathol* 1999; **2**: 574-576

Science Editor Li WZ **Language Editor** Elsevier HK

PO Box 2345, Beijing 100023, China
www.wjgnet.com
wjg@wjgnet.com

ELSEVIER

World J Gastroenterol 2005;11(15):2367-2369
World Journal of Gastroenterology ISSN 1007-9327

• *CASE REPORT* •

Metastatic low-grade endometrial stromal sarcoma of the sigmoid colon three years after hysterectomy

Yuki Asada, Hajime Isomoto, Fumitaka Akama, Noriko Nomura, Chun-Yang Wen, Haruhiko Nakao, Ikuo Murata, Kan Toriyama, Shigeru Kohno

Yuki Asada, Hajime Isomoto, Noriko Nomura, Ikuo Murata, Shigeru Kohno, Second Department of Internal Medicine, Nagasaki University School of Medicine, 1-7-1 Sakamoto, Nagasaki, Japan
Chun-Yang Wen, Department of Digestive Disease, Nanjing Drum Tower Hospital, Medical School of Nanjing University, Nanjing 210008, Jiangsu Province, China
Fumitaka Akama, Haruhiko Nakao, Department of Surgery, Zeshinkai Hospital, 7-9 Furukawa, Nagasaki, Japan
Kan Toriyama, Department of Pathology, Institute of Tropical Medicine, Nagasaki University School of Medicine, 12-4 Sakamoto, Nagasaki, Japan
Correspondence to: Dr. Hajime Isomoto, Second Department of Internal Medicine, Nagasaki University School of Medicine, 1-7-1 Sakamoto, Nagasaki, Japan. hajimei2002@yahoo.co.jp
Telephone: +81-95-8497567 Fax: +81-95-8497568
Received: 2004-08-12 Accepted: 2004-10-05

Abstract

A 49-year-old woman, who had undergone hysterectomy for low-grade endometrial stromal sarcoma (ESS) 3 years ago, presented with a 2-wk history of lower abdominal pain. Barium enema and sigmoidoscopy disclosed a polypoid submucosal tumor. Histopathologic features of biopsy specimens from the lesion were similar to those of the resected uterine ESS. Under the diagnosis of metastatic ESS of the sigmoid colon, sigmoidectomy was performed. Microscopic examination demonstrated dense proliferation of spindle cells with little nuclear atypia, which were sometimes arranged in whorled pattern around abundant arterioles. Mitotic count is below 1 in 10 high-power fields. Immunohi-stochemically, the neoplastic cells were strongly positive for vimentin, estrogen receptor and progesterone receptor but negative for α-smooth muscle actin, S-100 protein and CD34. Thus, a final diagnosis of low-grade ESS metastasis to the sigmoid colon was made. Her postoperative course was uneventful and hormonal therapy with progestational agents is entertained.

Key words: Endometrial stromal sarcoma; Metastasis; Sigmoidectomy

Asada Y, Isomoto H, Akama F, Nomura N, Wen CY, Nakao H, Murata I, Toriyama K, Kohno S. Metastatic low-grade endometrial stromal sarcoma of the sigmoid colon three years after hysterectomy. *World J Gastroenterol* 2005; 11(15): 2367-2369
http://www.wjgnet.com/1007-9327/11/2367.asp

INTRODUCTION

Endometrial stromal sarcoma (ESS) is a rare neoplasm comprising only 0.2% of all uterine malignancies and 15-26% of primary uterine sarcomas[1-5]. It is classified into two distinct subtypes, low-grade and high-grade, based on differences in morphological atypia and proliferative activity[6]. High-grade ESS has an aggressive nature, whereas low-grade ESS, which was formerly called endolymphatic stromal myosis, is a slowgrowing tumor with much better prognosis[6-8]. However, approximately 50% of cases of low-grade ESS develop recurrent disease and recurrences or metastases are often detected many years after initial treatment[7,9]. The common metastatic sites of low-grade ESS are the vagina, pelvis and peritoneal cavity[10]. Herein, we describe the first case of low-grade ESS metastasized to the sigmoid colon three years after initial surgery.

CASE REPORT

A 49-year-old woman presented with lower abdominal pain of 2-wk duration. She had undergone total hysterectomy for an alleged myoma of the uterus three years before, which was found to be low-grade ESS at postoperative pathologic examination. The family history was unremarkable. Physical examination showed lower abdominal tenderness, but no abdominal mass was palpable. Laboratory tests were normal and her serum carcinoembryonic antigen and CA 125 levels were within normal limits. Barium enema showed an irregular-shaped polypoid lesion in the sigmoid colon. Total colonoscopy disclosed an unusual polypoid tumor covered with normal-appearing mucosa with slight vessel engorgement in the sigmoid colon (Figure 1). Biopsy specimens from the lesion showed diffuse proliferation of spindle-shaped cells with little nuclear atypia, resembling the histology of previously excised uterine ESS. Computed tomograms of the chest, abdomen and pelvis, upper gastrointestinal endoscopy and barium through of the small bowel showed no abnormalities. Thus, the diagnosis was established as metastatic ESS of the sigmoid colon, and sigmoidectomy was performed. Grossly, a well-circumscribed whitish tumor 2 cm in diameter involved all layers of the colonic wall and was associated with overlying polypoid mucosa. Microscopic examination demonstrated that the tumor was composed of short fascicles or sheets of monotonous plump spindle cells with round nuclei and dispersed chromatin, which were sometimes arranged in whorled pattern around abundant arterioles (Figure 2). Mitotic count is below 1 in 10 high-power fields (HPF). Immunohistochemically, the neoplastic cells were strongly positive for vimentin, estrogen and

Figure 1 Colonoscopic picture showing a polypoid tumor in the sigmoid colon. The tumor was covered with normal lining crypts, but had slightly engorged vessels on the surface.

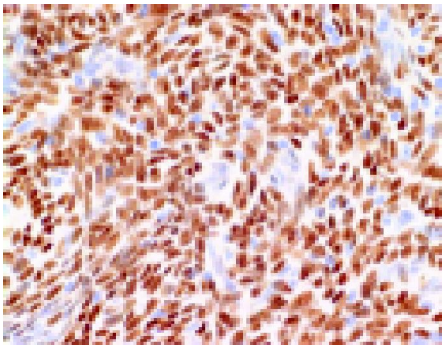

Figure 3 Immunohistochemistry showing strong diffuse immunoreactivity of the nuclei of neoplastic cells for progesterone receptor.

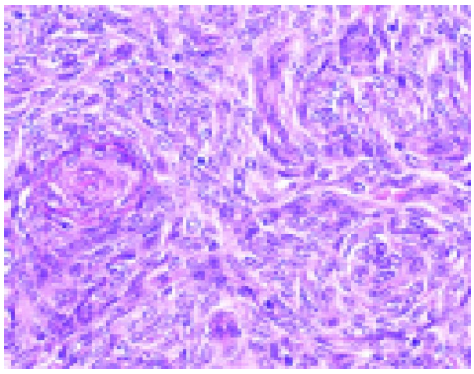

Figure 2 Microscopic picture of the surgical specimen showing dense proliferation of spindle-like cells with ovoid or round nuclei, dispersed chromatin and sparse cytoplasm, arranged in ill-defined whorls centered on small arterioles. These showed features similar to the primary uterine low-grade ESS.

progesterone receptors (Figure 3) but negative for -smooth muscle actin, S-100 protein and CD34. Based on these findings, a final diagnosis of low-grade ESS metastasized to the sigmoid colon was made. Her postoperative course was uneventful. She was free of symptoms at the last follow-up, 4 mo after the abdominal surgery, with no evidence of recurrence.

DISCUSSION

Clinical characteristics of low-grade ESS include a slow growth and indolent disease course with a tendency for late recurrence. One large series, the intervals before recurrence varied from 3 mo to 23 years, with a median interval of 3 years[11]. Styron *et al*[12], reported a patient with recurrent disease of low-grade ESS no less than 29 years after initial treatment. In our case, the metastatic tumor of the sigmoid colon was detected by colonoscopic and radiographic examination three years after hysterectomy. Patients with low-grade ESS almost develop recurrences or metastases in the vagina, pelvis and peritoneal cavity[10]. The less frequent sites were reported to be the lungs, liver, bladder, breast, heart, brain and bones[13-17]. To the best of our knowledge, however, low-grade ESS metastasized to the colon has not been previously documented.

There are two discernible subtypes of ESS, based on differences in mitotic activity: more than 10 mitotic figures for high-grade ESS and less than 10 mitotic figures per 10 HPF for low-grade ESS[6], as observed in our case. Nuclear atypia such as enlargement, increased and/or coarse chromatin and conspicuous nucleoli were absent in both the uterine and colonic lesions, distinguishing our case from high-grade ESS[6,18]. Given the gross appearance of colonic lesion at sigmoidoscopy, one can propose a variety of submucosal tumors as the differential diagnosis. Most of the mesenchymal neoplasms (leiomyoma, fibroma and schwannoma) can be immediately excluded on the basis of the histopathologic features[18]. However, the gastrointestinal stromal tumor (GIST) may be confused with low-grade ESS[18,19]. The presence of short fascicles or sheets of monotonous plump spindle cells, prominent arterioles and perivascular whorl arrangement of the tumor cells should argue against the diagnosis of GIST[18,19]. Finally, immunohistochemical analysis is useful in distinguishing between these entities, as GIST is well known to stain diffusely for CD34 and CD117[20] and ESS exclusively for estrogen receptor and progesterone receptor, reflecting the high sensitivity of low-grade ESS to sex-steroid hormones[2,3,5,18,21,22]. Again, low-grade ESS arising in the gastrointestinal endometriosis has been rarely documented[18,19,23]. According a review in literature by Cho *et al*[19], most of the lesions were located in the rectosigmoid colon, which is an area of bowel having the highest incidence of endometriosis[23]. Our patient has not suffered from endometriosis and there was no evidence of underlying endometriosis in the surgical specimens. Thus, the definite diagnosis of low-grade ESS metastasized to the sigmoid colon was made in this case.

Surgical excision is the major therapeutic procedure for the primary low-grade ESS, but the standard treatment for its recurrent disease including radiotherapy and chemotherapy has not been established[16,24,25]. Some surgeons recommended surgical cytoreduction of the ESS tumors when the extrauterine lesions were present[25,26]. On the other hand, Mansi *et al*[9], asserted that progesterone therapy should be the treatment of first choice for relapsed low-grade ESS, because there was resolution or stabilization of recurrent or metastatic disease in more than 50% of patients treated with progestational agents[12,16,27]. In this regard, immunoreactivity for estrogen receptor and progesterone receptor should be routinely assessed in low-grade ESS, in particular

manifested by recurrence[28]. Adjunct progesterone therapy is now entertained in our patient, since the primary and metastatic tumors showed strong and diffuse staining against anti-estrogen receptor and progesterone receptor antibodies. Considering highly recurrent nature of low-grade ESS, sometimes many years later[7,9,11,12,15,22], a life-long follow-up is necessary for this woman.

REFERENCES

1 **Koss LG,** Spiro RH, Brunschwig A. Endolymphatic stromal sarcoma. *Surg Gynecol Obstet* 1965; **121**: 531-537
2 **Farhood AI,** Abrams J. Immunohistochemistry of endometrial stromal sarcoma. *Hum Pathol* 1991; **22**: 224-230
3 **Gil-Benso R,** Lopez-Gines C, Navarro S, Carda C, Llombart-Bosch A. Endometrial stromal sarcomas: immunohistochemical, electron microscopical and cytogenetic findings in two cases. *Virchows Arch* 1999; **434**: 307-314
4 **Kempson RL,** Bari W. Uterine sarcomas. Classification, diagnosis, and prognosis. *Hum Pathol* 1970; **1**: 331-349
5 **Sabini G,** Chumas JC, Mann WJ. Steroid hormone receptors in endometrial stromal sarcomas. A biochemical and immunohistochemical study. *Am J Clin Pathol* 1992; **97**: 381-386
6 **Norris HJ,** Taylor HB. Mesenchymal tumors of the uterus. I. A clinical and pathological study of 53 endometrial stromal tumors. *Cancer* 1966; **19**: 755-766
7 **Chang KL,** Crabtree GS, Lim-Tan SK, Kempson RL, Hendrickson MR. Primary uterine endometrial stromal neoplasms. A clinicopathologic study of 117 cases. *Am J Surg Pathol* 1990; **14**: 415-438
8 **Gadducci A,** Sartori E, Landoni F, Zola P, Maggino T, Urgesi A, Lissoni A, Losa G, Fanucchi A. Endometrial stromal sarcoma: analysis of treatment failures and survival. *Gynecol Oncol* 1996; **63**: 247-253
9 **Mansi JL,** Ramachandra S, Wiltshaw E, Fisher C. Endometrial stromal sarcomas. *Gynecol Oncol* 1990; **36**: 113-118
10 **Montag TW,** Manart FD. Endolymphatic stromal myosis: surgical and hormonal therapy for extensive venous recurrence. *Gynecol Oncol* 1989; **33**: 255-260
11 **Piver MS,** Rutledge FN, Copeland L, Webster K, Blumenson L, Suh O. Uterine endolymphatic stromal myosis: a collaborative study. *Obstet Gynecol* 1984; **64**: 173-178
12 **Styron SL,** Burke TW, Linville WK. Low-grade endometrial stromal sarcoma recurring over three decades. *Gynecol Oncol* 1989; **35**: 275-278
13 **Yoonessi M,** Hart WR. Endometrial stromal sarcomas. *Cancer* 1977; **40**: 898-906
14 **Hart WR,** Yoonessi M. Endometrial stromatosis of the uterus. *Obstet Gynecol* 1977; **49**: 393-403
15 **Gunhan-Bilgen I,** Memis A, Ustun EE, Ozdemir N. Breast metastasis from low-grade endometrial stromal sarcoma after a 17-year period. *Eur Radiol* 2002; **12**: 3023-3025
16 **Matsuura Y,** Yasunaga K, Kuroki H, Inagaki H, Kashimura M. Low-grade endometrial stromal sarcoma recurring with multiple bone and lung metastases: report of a case. *Gynecol Oncol* 2004; **92**: 995-998
17 **Yokoyama Y,** Ono Y, Sakamoto T, Fukuda I, Mizunuma H. Asymptomatic intracardiac metastasis from a low-grade endometrial stromal sarcoma with successful surgical resection. *Gynecol Oncol* 2004; **92**: 999-1001
18 **Mourra N,** Tiret E, Parc Y, de Saint-Maur P, Parc R, Flejou JF. Endometrial stromal sarcoma of the rectosigmoid colon arising in extragonadal endometriosis and revealed by portal vein thrombosis. *Arch Pathol Lab Med* 2001; **125**: 1088-1090
19 **Cho HY,** Kim MK, Cho SJ, Bae JW, Kim I. Endometrial stromal sarcoma of the sigmoid colon arising in endometriosis: a case report with a review of literatures. *J Korean Med Sci* 2002; **17**: 412-414
20 **Sarlomo-Rikala M,** Kovatich AJ, Barusevicius A, Miettinen M. CD117: a sensitive marker for gastrointestinal stromal tumors that is more specific than CD34. *Mod Pathol* 1998; **11**: 728-734
21 **Chu MC,** Mor G, Lim C, Zheng W, Parkash V, Schwartz PE. Low-grade endometrial stromal sarcoma: hormonal aspects. *Gynecol Oncol* 2003; **90**: 170-176
22 **Satoh Y,** Ishikawa Y, Miyoshi T, Mukai H, Okumura S, Nakagawa K. Pulmonary metastases from a low-grade endometrial stromal sarcoma confirmed by chromosome aberration and fluorescence in-situ hybridization approaches: a case of recurrence 13 years after hysterectomy. *Virchows Arch* 2003; **442**: 173-178
23 **Mostoufizadeh M,** Scully RE. Malignant tumors arising in endometriosis. *Clin Obstet Gynecol* 1980; **23**: 951-963
24 **Pautier P,** Genestie C, Fizazi K, Morice P, Mottet C, Haie-Meder C, Le Cesne A, Lhomme C. Cisplatin-based chemotherapy regimen (DECAV) for uterine sarcomas. *Int J Gynecol Cancer* 2002; **12**: 749-754
25 **Weitmann HD,** Kucera H, Knocke TH, Potter R. Surgery and adjuvant radiation therapy of endometrial stromal sarcoma. *Wien Klin Wochenschr* 2002; **114**: 44-49
26 **Geas FL,** Tewari DS, Rutgers JK, Tewari KS, Berman ML. Surgical cytoreduction and hormone therapy of an advanced endometrial stromal sarcoma of the ovary. *Obstet Gynecol* 2004; **103**: 1051-1054
27 **Tsukamoto N,** Kamura T, Matsukuma K, Imachi M, Uchino H, Saito T, Ono M. Endolymphatic stromal myosis: a case with positive estrogen and progesterone receptors and good response to progestins. *Gynecol Oncol* 1985; **20**: 120-128
28 **Reich O,** Regauer S, Urdl W, Lahousen M, Winter R. Expression of oestrogen and progesterone receptors in low-grade endometrial stromal sarcomas. *Br J Cancer* 2000; **82**: 1030-1034

Science Editor Guo SY **Language Editor** Elsevier HK

PO Box 2345, Beijing 100023, China
www.wjgnet.com
wjg@wjgnet.com

ELSEVIER

World J Gastroenterol 2005;11(15):2370
World Journal of Gastroenterology ISSN 1007-9327

Acknowledgements to Reviewers of *World Journal of Gastroenterology*

Many reviewers have contributed their expertise and time to the peer review, a critical process to ensure the quality of *World Journal of Gastroenterology*. The editors and authors of the articles submitted to the journal are grateful to the following reviewers for evaluating the articles (including those were published and those were rejected in this issue) during the last editing period of time.

Kim Elaine Barrett, Professor
Department of Medicine, UCSD School of Medicine, UCSD Medical Center 8414, 200 West Arbor Drive, San Diego CA 92103, United States

Pelayo Correa, Boyd Professor
Department of Pathology, Louisiana State University Health Science Center, 1901 Perdido St., New Orleans La 70112, United States

Er-Dan Dong, Professor
Department of Life Science, Division of Basic Research in Clinic Medicine, National Natural Science Foundation of China, 83 Shuanqing Road, Haidian District, Beijng 100085, China

Abraham Rami Eliakim, Professor
Gastroenterology, Rambam Medical Center, Technion School of Medicine, P.O.B.9602, Haifa 31096, Israel

Xue-Gong Fan, Professor
Xiangya Hospital, Changsha 410008, Hunan Province, China

Gan-Sheng Feng, M.D.
Huazhong University of Science and Technology, Tongji Medical College, Union Hospital, Wuhan 430032, Hubei Province, China

Jin Gu, Professor
Peking University School of Oncology, Beijing Cancer Hospital, Beijing 100036, China

RG Jakobs, M.D.
Department of Medicine C, Academic Hospital of the University of Mainz, Ludwigshafen, Germany

Dusan M Jovanovic, Professor
Institute of Oncology, Institutski Put 4, Sremska Kamenica 21204, Yugoslavia

Shiu-Ming Kuo, M.D.
University at Buffalo, 15 Farber Hall, 3435 Main Street, Buffalo 14214, United States

Ai-Ping Lu, Professor
China Academy of Traditional Chinese Medicine, Dongzhimen Nei, 18 Beixincang, Beijing 100700, China

You-Yong Lu, Professor
Beijing Molecular Oncology Laboratory, Peking University School of Oncology and Beijing Institute for Cancer Reaearch, #1, Da-Hong-Luo-Chang Street, Western District, Beijing 100034, China

Juan R. Malagelada, M.D.
Hospital General Vall d'Hebron, Digestive Diseases Department Autonomous University of Barcelona, Pg. Vall d'Hebron, 119-129 Barcelona- 08035, Spain

Peter Malfertheiner, M.D.
Clinic of Gastroenterology Hepatology and Ifectious Disease, Otto-von-Guericke-University, Leipziger Str. 44, Magdeburg 39120, Germany

Hiroshi Nakagawa, Assistant Professor
Gastroenterology Division, University of Pennsylvania, 415 Curie Blvd. 638B CRB, Philadelphia 19104, United States

Vasiliy Ivanovich Reshetnyak, Professor
Institute of General Reanimatology, 25-2, Petrovka Str., Moscow 107031, Russian Federation

Tilman Sauerbruch, M.D.
Department of Internal Medicine I, University of Bonn, Sigmund-Freud-Strasse 25, 53105 Bonn, Germany

Qin Su, Professor
Department of Pathology, Cancer Hospital and Cancer Institute, Chinese Academy of Medical Sciences and Peking Medical College, PO Box 2258, Beijing 100021, China

George Y Wu, Professor
Department of Medicine, Division of Gastroenterology-Hepatology University of Connecticut Health Center, 263 Farmington Ave, Farmington, CT 06030, United States

Jia-Yu Xu, Professor
Shanghai Second Medical University, Rui Jin Hospital, 197 Rui Jin Er Road, Shanghai 200025, China

Yuan Yuan, Professor
Cancer Institute of China Medical University, 155 North Nanjing Street, Heping District, Shenyang 110001, Liaoning Province, China

Zhi-Rong Zhang, Professor
West China School of Pharmacy, Sichuan University, 17 South Renmin Road, Chengdu 610041, Sichuan Povince, China

PO Box 2345, Beijing 100023, China
www.wjgnet.com
wjg@wjgnet.com

ELSEVIER

World J Gastroenterol 2005;11(15):Appendix 1
World Journal of Gastroenterology ISSN 1007-9327

Meetings

Major meetings coming up

Digestive Disease Week
106th Annual Meeting of AGA, The American Gastroenterology Association
May 14-19, 2005
www.ddw.org/
Chicago, Illinois

13th World Congress of Gastroenterology
September 10-14, 2005
www.wcog2005.org/
Montreal, Canada

13th United European Gastroenterology Week, UEGW
October 15-20, 2005
www.uegf.org/
Copenhagen, Denmark

American College of Gastroenterology Annual Scientific Meeting
October 28-November 2, 2005
www.acg.gi.org/
Honolulu Convention Center, Honolulu, Hawaii

Events and Meetings in the upcoming 6 months

EASL 2005 the 40th annual meeting
April 13–17, 2005
www.easl.ch/easl2005/
Paris, France

World Congress on Gastrointestinal Cancer
June 15–18, 2005
Barcelona

Digestive Disease Week *DDW 106th Annual Meeting*
May 15–18, 2005
www.ddw.org
Chicago, Illinois

Events and meetings in 2005

Canadian Digestive Disease Week Conference
February 26-March 6, 2005
www.cag-acg.org
Banff, AB

2005 World Congress of Gastroenterology
September 12–14, 2005
Montreal, Canada

International Colorectal Disease Symposium 2005
February 3–5, 2005
Hong Kong

13th UEGW meeting *United European Gastroenterology Week*
October 15–20, 2005
www.webasistent.cz/guarant/uegw2005/
Copenhagen-Malmoe

7th International Workshop on Therapeutic Endoscopy
September 10–12, 2005
www.alfamedical.com
Theodor Bilharz Research Institute

EASL 2005 the 40th annual meeting
April 13–17, 2005
www.easl.ch/easl2005/
Paris, France

Pediatric Gastroenterology, Hepatology and Nutrition
March 13, 2005
Jakarta, Indonesia

21st annual international congress *of Pakistan society of Gastroenterology & GI Endoscopy*
March 25–27, 2005
www.psgc2005.com
Peshawar

8th Congress of the Asian Society of HepatoBiliary Pancreatic Surgery
February 10–13, 2005
Mandaluyong, Philippines

APDW 2005 - Asia Pacific Digestive Week 2005
September 25–28, 2005
www.apdw2005.org
Seoul, Korea

World Congress on Gastrointestinal Cancer
June 15–18, 2005
Barcelona

British Society of Gastroenterology Conference (BSG)
March 14–17, 2005
www.bsg.org.uk
Birmingham

Digestive Disease Week *DDW 106th Annual Meeting*
May 15–18, 2005
www.ddw.org
Chicago, Illinois

70th ACG Annual Scientific Meeting and Postgraduate Course
October 28-November 2, 2005
Honolulu Convention Center, Honolulu, Hawaii

Events and Meetings in 2006

EASL 2006 - THE 41ST ANNUAL MEETING
April 26–30, 2006
Vienna, Austria

Canadian Digestive Disease Week Conference
March 4–12, 2006
www.cag-acg.org
Quebec City

XXX pan-american congress of digestive diseases *XXX congreso panamericano de anfermedades digestivas*
November 25-December 1, 2006
www.gastro.org.mx
Cancun

World Congress on Gastrointestinal Cancer
June 14–17, 2006
Barcelona, Spain

7th World Congress of the International Hepato-Pancreato-Biliary Association
September 3–7, 2006
www.edinburgh.org/conference
Edinburgh

71st ACG Annual Scientific Meeting and Postgraduate Course
October 20–25, 2006
Venetian Hotel, Las Vegas, Neveda

PO Box 2345, Beijing 100023, China
www.wjgnet.com
wjg@wjgnet.com

ELSEVIER

World J Gastroenterol 2005;11(15):Appendix 2-3
World Journal of Gastroenterology ISSN 1007-9327

Instructions to authors

GENERAL INFORMATION

World Journal of Gastroenterology (*WJG,* ISSN 1007-9327 CN 14-1219/R) is a weekly journal of more than 48 000 circulation, published on the 7th, 14th, 21st and 28th of every month.

Original Research, Clinical Trials, Reviews, Comments, and Case Reports in esophageal cancer, gastric cancer, colon cancer, liver cancer, viral liver diseases, *etc*., from all over the world are welcome on the condition that they have not been published previously and have not been submitted simultaneously elsewhere.

Published jointly by
The WJG Press and Elsevier Inc.

SUBMISSION OF MANUSCRIPTS

Manuscripts should be typed double-spaced on A4 (297×210 mm) white paper with outer margins of 2.5 cm. Number all pages consecutively, and start each of the following sections on a new page: Title Page , Abstract, Introduction, Materials and Methods, Results, Discussion, Acknowledgements, References, Tables, Figures and Figure Legends. Neither the Editors nor the Publisher is responsible for the opinions expressed by contributors. Manuscripts formally accepted for publication become the permanent property of The WJG Press and Elsevier Inc., and may not be reproduced by any means, in whole or in part without the written permission of both the Authors and the Publisher. We reserve the right to put onto our website and copy-edit accepted manuscripts. Authors should also follow the guidelines for the care and use of laboratory animals of their institution or national animal welfare committee.

Authors should retain one copy of the text, tables, photographs and illustrations, as rejected manuscripts will not be returned to the author(s) and the editors will not be responsible for the loss or damage to photographs and illustrations.

Online submission
Online submission is strongly advised. Manuscripts should be submitted through the Online Submission System at: http://www.wjgnet.com/index.jsp. Authors are highly recommended to consult the ONLINE INSTRUCTIONS TO AUTHORS (http://www.wjgnet.com/wjg/help/instructions.jsp) before attempting to submit online. Authors encountering problems with the Online Submission System may send an email describing the problem to wjg@wjgnet.com for assistance. If you submit manuscript online, do not make a postal contribution. A repeated online submission for the same manuscript is strictly prohibited.

Postal submission
Send 3 duplicate hard copies of the full-text manuscript typed double-spaced on A4(297×210 mm) white paper together with any original photographs or illustrations and a 3.5 inch computer diskette or CD-ROM containing an electronic copy of the manuscript including all the figures, graphs and tables in native Microsoft Word format or *.rtf format to:

World Journal of Gastroenterology
Apartment 1066 Yishou Garden,
58 North Langxinzhuang Road,
PO Box 2345, Beijing 100023, China
E-mail: wjg@wjgnet.com
http: //www.wjgnet.com

MANUSCRIPT PREPARATION

All contributions should be written in English. All articles must be submitted using a word-processing software. All submissions must be typed in 1.5 line spacing and in word size 12 with ample margins. The letter font is Tahoma. For authors originating from China, one copy of the Chinese translation of the manuscript is also required (excluding references). Style should conform to our house format. Required information for each of the manuscript sections is as follows:

Title page
Full manuscript title, running title, all author(s) name(s), affiliations, institution(s) and/or department(s) where the work was accomplished, disclosure of any financial support for the research, and the name, full address, telephone and fax numbers and email address of the corresponding author should be involved. Titles should be concise and informative (removing all unnecessary words), emphasize what is NEW, and avoid abbreviations. A short running title of less than 40 letters should be provided. List the author(s)' name(s) as follows: initials and/or first name, middle name or initial(s) and full family name.

Abstract
An informative, structured abstract of no more than 250 words should accompany each manuscript. Abstracts for original contributions should be structured into the following sections: AIM: Only the purpose should be included. METHODS: The materials, techniques, instruments and equipments, and the experimental procedures should be included. RESULTS: The observatory and experimental results, including data, effects, outcome, *etc*. should be included. Authors should present *P* value where necessary, and the significant data should accompany. CONCLUSION: Accurate view and the value of the results should be included.

The format of structured abstracts is at: http://www.wjgnet.com/wjg/help/11.doc

Key words
Please list 3-10 key words that could reflect content of the study.

Text
For most article types, the main text should be structured into the following sections: INTRODUCTION, MATERIALS AND METHODS, RESULTS and DISCUSSION, and should include appropriate Figures and Tables. Data should be presented in the body text or Figures and Tables, not both.

Illustrations
Figures should be numbered as 1, 2, 3 and so on, and mentioned clearly in the main text. Provide a brief title for each figure on a separate page. No detailed legend should be involved under the figures. This part should add into the text where the figures are applicable. Digital images: black and white photographs should be scanned and saved in TIFF format at a resolution of 300 dpi; color images should be saved as CMYK (print files) and not RGB (screen-viewing files). Place each photograph in a separate file. Print images: supply images of size no smaller than 126×76 mm printed on smooth surface paper; label the image by writing the Figure number and orientation using an arrow. Photomicrographs: indicate the original magnification and stain in the legend. Digital Drawings: supply files in EPS if created by Freehand and Illustrator, or TIFF from Photoshop. EPS files must be accompanied by a version in native file format for editing purposes. Scans of existing line drawings should be scanned at a resolution of 1200 dpi and as close as possible to the size at which they will appear when printed, not smaller. Please use uniform legends for the same subjects. For example: Figure 1 Pathological changes of atrophic gastritis after treatment. A: ...; B: ...;C: ...; D: ...; E: ...; F: ...; G: ...

Tables
Three-line tables should be numbered as 1, 2, 3 and so on, and mentioned clearly in the main text. Provide a brief title for each table. No detailed legend should be involved under the tables. This part should add into the text where the tables are applicable. The information should complement but not duplicate that contained in the text. Use one horizontal line under the title, a second under the column heads, and a third below the Table, above any footnotes. Vertical and italic lines should be omitted.

Notes in tables and illustrations
Data which is not statistically significant should not be noted. $^{a}P<0.05$, $^{b}P<0.01$ ($P>0.05$ should not be noted). If there are other series of *P* values, $^{c}P<0.05$ and $^{d}P<0.01$ are used; Third series of *P* values can be expressed as $^{e}P<0.05$ and $^{f}P<0.01$. Other notes in tables or under

illustrations should be expressed as ^1F, ^2F, ^3F; or some other symbols with a superscript (Arabic numerals) in the upper left corner. In a multi-curve illustration, each curve should be labeled with ●, ○, ■, □, ▲, △, *etc*. in a certain sequence.

Acknowledgments

Brief acknowledgments of persons who have made genuine contributions to the manuscripts and who endorse the data and conclusions are included. Authors are responsible for obtaining written permission to use any copyrighted text and/or illustrations.

References

Cited references should mainly be drawn from journals covered in the Science Citation Index (http://www.isinet.com) and/or Index Medicus (http://www.ncbi.nlm.nih.gov/PubMed) databases. Mention all references in the text, tables and figure legends, and set off by consecutive, superscripted Arabic numerals. References should be numbered consecutively in the order in which they appear in the text. Abbreviate journal title names according to the Index Medicus style (http://www.ncbi.nlm.nih.gov/entrez/query.fcgi?db=journals). Unpublished observations and personal communications are not listed as references. The style and punctuation of the references conform to ISO standard and the Vancouver style (5th edition); see examples below. Reference lists not conforming to this style could lead to delayed or even rejected publication status. Examples:

Standard jounal article (list all authors and include the PubMed ID [PMID] where applicable)

1 **Das KM,** Farag SA. Current medical therapy of inflammatory bowel disease. *World J Gastroenterol* 2000; 6: 483-489 [PMID: 11819634]
2 **Pan BR**, Hodgson HJF, Kalsi J. Hyperglobulinemia in chronic liver disease: Relationships between *in vitro* immunoglobulin synthesis, short lived suppressor cell activity and serum immunoglobulin levels. *Clin Exp Immunol* 1984; 55: 546-551 [PMID: 6231144]
3 **Lin GZ,** Wang XZ, Wang P, Lin J, Yang FD. Immunologic effect of Jianpi Yishen decoction in treatment of Pixu-diarrhoea. *Shijie Huaren Xiaohua Zazhi* 1999; 7: 285-287 [CMFAID:1082371101835979]

Books and other monographs (list all authors)

4 **Sherlock S,** Dooley J. Diseases of the liver and billiary system. 9th ed. Oxford: Blackwell Sci Pub, 1993: 258-296

Chapter in a book (list all authors)

5 **Lam SK.** Academic investigator's perspectives of medical treatment for peptic ulcer. In: Swabb EA, Azabo S. Ulcer disease: investigation and basis for therapy. New York: Marcel Dekker, 1991: 431-450

Electronic journal (list all authors)

6 **Morse SS.** Factors in the emergence of infectious diseases. Emerg Infect Dis serial online, 1995-01-03, cited 1996-06-05; 1(1):24 screens. Available from: URL: http//www.cdc.gov/ncidod/EID/eid.htm

PMID requirement

From the full reference list, please submit a separate list of those references embodied in PubMed, keeping the same order as in the full reference list, with the following information only: (1) abbreviated journal name and citation (e.g. *World J Gastroenterol* 2003;9(11): 2400-2403; (2) article title (e.g. Epidemiology of gastroenterologic cancer in Henan Province, China; (3) full author list (e.g. Lu JB, Sun XB, Dai DX, Zhu SK, Chang QL, Liu SZ, Duan WJ; (4) PMID (e.g. 14606064). Provide the full abstracts of these references, as quoted from PubMed on a 3.5 inch disk or CD-ROM in Microsoft Word format and send by post to The *WJG* Press. For those references taken from journals not indexed by *Index Medicus*, a printed copy of the first page of the full reference should be submitted. Attach these references to the end of the manuscript in their order of appearance in the text.

Inappropriate references

Authors should always cite references that are relevant to their article, and avoid any inappropriate references. Inappropriate references include those that are linked with a hyphen and the difference between the two numbers at two sides of the hyphen is more than 5. For example, [1-6], [2-14] and [1,3,4-10,22] are all considered as inappropriate references. Authors should not cite their own unrelated published articles.

Statistical data

Present as mean±SD and mean±SE.

Statistical expression

Express *t* test as *t*(in italics), *F* test as *F*(in italics), chi square test as χ^2 (in Greek), related coefficient as *r*(in italics), degree of freedom as γ(in Greek), sample number as *n*(in italics), and probability as *P*(in italics).

Units

Use SI units. For example: body mass, m(B) = 78 kg; blood pressure, p (B)=16.2/12.3 kPa; incubation time, t(incubation)=96 h, blood glucose concentration, c(glucose) 6.4±2.1 mmol/L; blood CEA mass concentration, p(CEA) = 8.6 24.5 μg/L; CO_2 volume fraction, 50 mL/L CO_2 not 5% CO_2; likewise for 40 g/L formaldehyde, not 10% formalin; and mass fraction, 8 ng/g, *etc*. Arabic numerals such as 23,243,641 should be read 23 243 641.

The format about how to accurately write common units and quantum is at: http://www.wjgnet.com/wjg/help/15.doc

Abbreviations

Standard abbreviations should be defined in the abstract and on first mention in the text. In general, terms should not be abbreviated unless they are used repeatedly and the abbreviation is helpful to the reader. Permissible abbreviations are listed in Units, Symbols and Abbreviations: A Guide for Biological and Medical Editors and Authors (Ed. Baron DN, 1988) published by The Royal Society of Medicine, London. Certain commonly used abbreviations, such as DNA, RNA, HIV, LD50, PCR, HBV, ECG, WBC, RBC, CT, ESR, CSF, IgG, ELISA, PBS, ATP, EDTA, mAb, can be used directly without further mention.

Italicization

Quantities: *t* time or temperature, *c* concentration, *A* area, *l* length, *m* mass, *V* volume.
Genotypes: *gyr*A, *arg* 1, *c myc*, *c fos*, *etc*.
Restriction enzymes: *Eco*RI, *Hin*dI, *Bam*HI, *Kbo* I, *Kpn* I, *etc*.
Biology: *Helicobacter pylori, H pylori, E coli, etc*.

SUBMISSION OF THE REVISED MANUSCRIPTS AFTER ACCEPTED

Please revise your article according to the revision policies of *WJG*. The revised version including manuscript and high-resolution image figures (if any) should be copied on a floppy or compact disk. Author should send the revised manuscript, along with printed high-resolution color or black and white photos, copyright transfer letter, the final check list for authors, and responses to reviewers by a courier (such as EMS) (submission of revised manuscript by e-mail or on the WJG Editorial Office Online System is NOT available at present).

Language evaluation

The language of a manuscript will be graded before sending for revision. (1) Grade A: priority publishing; (2) Grade B: minor language polishing; (3) Grade C: a great deal of language polishing; (4) Grade D: rejected. The revised articles should be in grade B or grade A.

Copyright assignment form

It is the policy of WJG to acquire copyright in all contributions. Papers accepted for publication become the copyright of WJG and authors will be asked to sign a transfer of copyright form. All authors must read and agree to the conditions outlined in the Copyright Assignment Form (which can be downloaded from http://www.wjgnet.com/wjg/help/9.doc).

Final check list for authors

The format is at: http://www.wjgnet.com/wjg/help/13.doc

Responses to reviewers

Please revise your article according to the comments/suggestions of reviewers. The format for responses to the reviewers' comments is at: http://www.wjgnet.com/wjg/help/10.doc

Proof of financial support

For paper supported by a foundation, authors should provide a copy of the document and serial number of the foundation.

Publication fee

Authors of accepted articles must pay publication fee.

PO Box 2345, Beijing 100023, China
www.wjgnet.com
wjg@wjgnet.com

ELSEVIER

World J Gastroenterol 2005;11(15):Appendix 4
World Journal of Gastroenterology ISSN 1007-9327

World Journal of Gastroenterology standard of quantities and units

Number	Nonstandard	Standard	Notice
1	4 days	4 d	In figures, tables and numerical narration
2	4 days	four days	In text narration
3	day	d	After Arabic numerals
4	Four d	Four days	At the beginning of a sentence
5	2 hours	2 h	After Arabic numerals
6	2 hs	2 h	After Arabic numerals
7	hr, hrs,	h	After Arabic numerals
8	10 seconds	10 s	After Arabic numerals
9	10 year	10 years	In text narration
10	Ten yr	Ten years	At the beginning of a sentence
11	0,1,2 years	0,1,2 yr	In figures and tables
12	0,1,2 year	0,1,2 yr	In figures and tables
13	4 weeks	4 wk	
14	Four wk	Four weeks	At the beginning of a sentence
15	2 months	2 mo	In figures and tables
16	Two mo	Two months	At the beginning of a sentence
17	10 minutes	10 min	
18	Ten min	Ten minutes	At the beginning of a sentence
19	50% (*V/V*)	500 mL/L	
20	50% (m/*V*)	500 g/L	
21	1 M	1 mol/L	
22	10 μM	10 μmol/L	
23	1N HCl	1 mol/L HCl	
24	1N H_2SO_4	0.5 mol/L H_2SO_4	
25	4rd edition	4^{th} edition	
26	15 year experience	15- year experience	
27	18.5 kDa	18.5 ku,18 500u or M_r18 500	
28	25 $g.kg^{-1}/d^{-1}$	25 g/(kg·d) or 25 g/kg per day	
29	6900	6 900	
30	1000 rpm	1 000 r/min	
31	sec	s	After Arabic numerals
32	1 pg $\cdot L^{-1}$	1 pg/L	
33	10 kilograms	10 kg	
34	13 000 rpm	13 000 *g*	High speed; *g* should be in italic and suitable conversion.
35	1000 *g*	1 000 r/min	Low speed. *g* cannot be used.
36	Gene bank	GenBank	International classified genetic materials collection bank
37	Ten L	Ten liters	At the beginning of a sentence
38	Ten mL	Ten milliliters	At the beginning of a sentence
39	umol	μmol	
40	30 sec	30 s	
41	1 g/dl	10 g/L	10-fold conversion
42	OD_{260}	A_{260}	"OD" has been abandoned.
43	One g/L	One microgram per liter	At the beginning of a sentence
44	*A*260 nm	A_{260}nm	*A* should be in italic.
	^bP<0.05	^aP<0.05	In Table, no note is needed if there is no significance in statistics: ^aP<0.05, ^bP<0.01 (no note if P>0.05). If there is a second set of P value in the same table, ^cP<0.05 and ^dP<0.01 are used for a third set: ^eP<0.05, ^fP<0.01.
45	**F*=9.87, §*F*=25.9, #*F*=67.4	^1F=9.87,^2F=25.9, ^3F=67.4	Notices in or under a table
46	KM	km	kilometer
47	CM	cm	centimeter
48	MM	mm	millimeter
49	Kg, KG	kg	kilogram
50	Gm, gr	g	gram
51	nt	N	newton
52	l	L	liter
53	db	dB	decibel
54	rpm	r/min	rotation per minute
55	bq	Bq	becquerel, a unit symbol
56	amp	A	ampere
57	coul	C	coulomb
58	HZ	Hz	
59	w	W	watt
60	KPa	kPa	kilo-pascal
61	p	Pa	pascal
62	ev	EV	volt (electronic unit)
63	Jonle	J	joule
64	J/mmol	kJ/mol	kilojoule per mole
65	10×10×10cm^3	10 cm×10 cm×10 cm	
66	N·km	KN·m	moment
67	$\bar{x}$±s	mean±SD	In figures, tables or text narration
68	Mean±SEM	mean±SE	In figures, tables or text narration
69	*im*	im	intramuscular injection
70	*iv*	iv	intravenous injection
71	Wang et al	Wang *et al.*	
72	EcoRI	*Eco*RI	*Eco* in italic and RI in positive. Restriction endonuclease has its prescript form of writing.
73	Ecoli	*E.coli*	Bacteria and other biologic terms have their specific expression.
74	Hp	*H pylori*	
75	Iga	*Iga*	writing form of genes
76	*igA*	IgA	writing form of proteins
77	-70 kDa	~70 ku	